THE UNIVERSITY OF AUCKLAND
LIBRARIES AND LEARNING SERVICES

http://researchspace.auckland.ac.nz

ResearchSpace@Auckland

Copyright Statement

The digital copy of this thesis is protected by the Copyright Act 1994 (New Zealand).

This thesis may be consulted by you, provided you comply with the provisions of the Act and the following conditions of use:

- Any use you make of these documents or images must be for research or private study purposes only, and you may not make them available to any other person.
- Authors control the copyright of their thesis. You will recognise the author's right to be identified as the author of this thesis, and due acknowledgement will be made to the author where appropriate.
- You will obtain the author's permission before publishing any material from their thesis.

To request permissions please use the Feedback form on our webpage.
http://researchspace.auckland.ac.nz/feedback

General copyright and disclaimer

In addition to the above conditions, authors give their consent for the digital copy of their work to be used subject to the conditions specified on the Library Thesis Consent Form and Deposit Licence.

Phenotypic analysis of human stem cells and their differentiation potential towards pancreatic cells

Caroline McCulloch

A thesis submitted in fulfilment of the requirements for the degree of
Doctor of Philosophy
The University of Auckland
New Zealand

2013

Abstract

Type 1 diabetes is an autoimmune disorder in which the immune system specifically destroys the insulin-producing β-cells of the pancreas, resulting in a loss of glycemic control. There is no cure for the disease, and patients have the difficult task of managing their blood glucose levels by daily injection of insulin, and monitoring of carbohydrate intake, levels of exercise, and stress. The field of stem cells gives hope to type 1 diabetes patients as stem cells are plastic and can be differentiated into the pancreatic lineage to form insulin-producing β-cell-like cells for transplantation to restore the endocrine function of the pancreas. There are many different stem cell populations described in the published literature that can be easily obtained from the blood, tissues, and organs of adults. They include peripheral blood-insulin producing cells (PB-IPCs) that can be readily isolated due to their unique attachment to hydrophobic surfaces, monocytes that can be dedifferentiated into programmable cells of monocytic origin (PCMOs) and fibroblast-resembling-macrophages (f-MOs), and adipose stem cells (ASCs). There are also other populations of stem cells that can be ethically obtained after childbirth from neonatal tissues that are normally discarded, and include human amniotic stem cells (HASCs) and cord blood hematopoietic stem cells (CB-HSCs). It has been reported in the published literature that each of the above stem cell populations except f-MOs can be induced to form insulin-producing cells. However, in most cases there has been no independent validation of the published data. The aim of this project was to study the phenotype of the above stem cells and determine which stem cell population would be an ideal source from which to derive insulin-producing cells. The published cell differentiation protocols were to be validated, and novel ways of improving upon the protocols were to be examined with the ultimate aim to produce cells that closely resembled pancreatic β-cells.

In this study, the above stem cell populations were either produced from the blood of human donors, or purchased directly from commercial companies. They were phenotyped for stem cell, pancreatic cell, and other cell lineage markers. The stem cells were subjected to a variety of published and novel pancreatic differentiation protocols, and examined for the expression of markers that specify different stages of pancreatic differentiation. The ability to transdifferentiate several of the stem cell populations into other cell lineages including the endothelial, neuronal, and lymphocytic lineages was also examined.

Phenotyping of the stem cell populations revealed that some undifferentiated stem cells already expressed certain markers of pancreatic progenitor cells. Monocytes dedifferentiated into PCMOs expressed SOX-17 and PDX-1, in addition to the monocytic markers CD14 and CD68. A subset of monocytes dedifferentiated into f-MOs expressed PDX-1, while the remaining cells expressed CD14 indicating the presence of two different cell populations. Therefore it appeared that the monocyte-derived stem cell populations are in an intermediate state of transdifferentiation expressing multiple cell lineage markers. Undifferentiated HASCs expressed PDX-1 and SOX-17 whilst also expressing the stem cell markers Nestin and Oct-4. Several CB-HSCs expressed SOX-17, GPR40, and Nestin. ASCs expressed SOX-17, in addition to the characteristic ASC stem cell markers CD29 and CD90. The expression of pancreatic markers by undifferentiated HASCs, CB-HSCs, and ASCs indicates they could have the potential to differentiate towards the pancreatic lineage.

PB-IPCs expressed the pancreatic progenitor cell markers PDX-1, CXCR4, HNF6, and SOX-17 following culture in the absence of additional growth factors other than foetal bovine serum. They highly expressed the dendritic cell marker CD11c and appeared

to be in a state of activation as they strongly expressed HLA-DR. The PB-IPCs were phagocytic. Their function and phenotype therefore suggests they are monocyte-like. Attempts to induce their transdifferentiation towards the pancreatic lineage with previously published protocols and novel combinations of differentiation agents were not successful.

Attempts to differentiate the monocyte-derived PCMOs and f-MOs towards the pancreatic lineage using a published protocol based on an islet cell conditioning medium (ICM) were not successful. Differentiated PCMOs continued to express CD14 and HLA-DR, and differentiated f-MOs retained their expression of PDX-1 or CD14. Thus, these stem cell populations did not show plasticity towards the pancreatic lineage beyond their expression of PDX-1. f-MOs showed plasticity towards the endothelial lineage after treatment with $VEGF_{165}$ resulting in vWF-expressing cells, towards the neuronal lineage after treatment with NGFβ resulting in neuron-specific enolase-expressing cells, and towards the lymphocytic lineage after treatment with IL-2 resulting in an increase in CD3- and CD4-expressing cells. Therefore f-MOs may be a source of cells for the generation of these latter cell types.

Attempts to differentiate CB-HSCs towards the pancreatic lineage with a commercial medium and matrix from Celprogen Inc. resulted in the generation of pancreatic progenitor cells which expressed GIPR, PDX-1, and GPR40, but there was no evidence of further maturation into insulin-producing endocrine cells.

ASCs were subjected to stage-specific differentiation protocols designed to mimic the natural differentiation stages of pancreatic cell formation *in vivo*. The differentiated ASCs showed evidence of differentiation towards the pancreatic lineage as reflected in the upregulation of the posterior foregut markers HNF6 and PDX-1. The highest amount of PDX-1 was expressed after culture of ASCs with a combination of 100 nM IDE-1, followed by KAAD-cyclopamine and fibroblast growth factor (FGF)-10, and then KAAD-cyclopamine, FGF10 and all trans-retinoic acid. These PDX-1-expressing cells represent a source of pancreatic progenitor cells differentiated up to the posterior foregut stage.

HASCs purchased from Celprogen Inc. displayed the greatest potential to be differentiated towards the pancreatic β-cell lineage. They could be transdifferentiated with media and extracellular matrices provided by Celprogen Inc. into cells which expressed PDX-1, SOX-17, Arx, CXCR4, HNF6, glucagon, and PCSK1. However, they did not express insulin. In contrast, ASCs cultured in a published medium on ultra-low attachment plates contained high levels of insulin detectable by a widely used guinea-pig anti-insulin antibody. However, this result is confounded by the fact that insulin expression was not detected by two other anti-insulin antibodies. The differentiated ASCs also did not express proinsulin, amylin, and C-peptide. Therefore the insulin detected by the guinea pig antibody appears not to be genuine, and may result from the previously unreported non-specific binding of the anti-insulin antibody to a related protein.

Phenotyping of the differentiated cells revealed some cells expressed tolerogenic or immunosuppressive markers. Differentiated HASCs and PB-IPCs expressed AIRE suggesting they might serve as tolerogenic antigen presenting cells. However, differentiated PB-IPCs, which expressed AIRE and FOXP3, did not inhibit a mixed lymphocyte response, indicating they were not directly immunosuppressive or potentially tolerogenic. Differentiated CB-HSCs and HASCs expressed the immunosuppressive

marker TGF-β, in accord with the published report that a population of cord blood stem cells selected by hydrophobic surface attachment from whole cord blood are immunosuppressive and can induce the differentiation of naïve mouse splenic T cells into T regulatory cells (Tregs) that are capable of reversing type 1 diabetes in mice and humans.

These studies have independently re-examined protocols for promoting the pancreatic differentiation of a variety of human adult and neonatal stem cells. Only the differentiation of HASCs produced cells that contained detectable levels of pancreatic hormones, in this case glucagon. Most of the published protocols were ineffective at differentiating the stem cell populations to pancreatic hormone-producing cells, contrary to the published data. This raises questions about the reproducibility of stem cell protocols and the need for more robust methods that can be independently replicated.

Acknowledgements

First and foremost I sincerely wish to thank my supervisor, Associate Professor Geoffrey Krissansen. I appreciate the opportunity he has given me to work on this project. I have always appreciated his guidance and advice, while also allowing me to develop my skills as an independent researcher.

I would like to thank my co-supervisor Dr Shiva Reddy. I have appreciated having another person to be able to discuss diabetes and stem cells in depth with, and he has always helped me to see the bigger picture and view my project from other angles.

I am very grateful to the Marsden Fund for their generous support of this project. The Marsden Fund has given me the opportunity to undertake a PhD at the University of Auckland, and provided the resources to allow me to develop my skills as a researcher.

A special thanks to Professor Tim Cundy for providing me with blood samples from patients with type 1 diabetes.

I would also like to thank Yi Yang for sharing her extensive experience in the laboratory, and also for continuously keeping up with my many lab orders for antibodies and differentiation agents.

Special thanks to all the past members of the 'Diabetes' group in our lab, namely Aneta, Glenn, Chris, and Qiliang whose tireless work has further contributed to my understanding of diabetes and stem cells. I appreciate the camaraderie that we had for one another and for the project.

Thanks also to my lab friend Kris who has always been available to be a sounding board for ideas and to discuss methodologies. Thank you to all the remaining members of the Krissansen lab who have provided their assistance, support and friendship.

Finally I wish to thank my partner Geoff, my parents Ian and Katrin, my brother Julian, my sister in-law Rachel, my to-be mother in-law Anne, and Hyde for their continual support and encouragement. To them I dedicate this thesis.

Table of Contents

Abstract II
Acknowledgements V
Table of Contents VI
List of Figures XII
List of Tables XVIII
Abbreviations XIX
Chapter 1 Introduction 25
1.1 Type 1 diabetes mellitus overview 25
1.1.1 Prevalence, health complications and causes of type 1 diabetes 25
1.1.2 Current treatments for patients with type 1 diabetes 25
1.1.3 Type 1 diabetes prevention and treatment 26
1.2 Differentiation of embryonic stem cells into definitive endoderm and then to insulin-producing β-cells 27
1.2.1 The importance of PDX-1 in pancreatic and neural development and function 29
1.3 Factors used to differentiate stem and progenitor cells into insulin-producing cells 30
1.3.1 Factors that induce formation of definitive endoderm 30
1.3.2 Primitive gut tube differentiation 31
1.3.3 Posterior foregut differentiation 31
1.3.4 Differentiation of hESCs into pancreatic endoderm and hormone expressing cells 33
1.3.5 Enhancing the differentiation of stem cells towards the pancreatic β-cell lineage 33
1.3.6 Other differentiation factors that have been trialled for differentiating stem cells towards the pancreatic cell lineage. 34
1.4 The role of Nestin in the differentiation of pancreatic cells 34
1.4.1 Pre-selection of Nestin positive cells 34
1.4.2 Nestin is expressed by pancreatic precursor cells 35
1.5 Similarities between pancreatic and neuronal cell lineages 35
1.5.1 Morphological and physiological similarities shared by pancreatic and neuronal cells 35
1.5.2 Common ancestry of pancreatic and neuronal cells 36
1.5.3 Similarities between pancreatic and neuronal differentiation 36
1.6 Genuine insulin expression by differentiated stem cells 36
1.7 Stem cells found in peripheral blood 37
1.7.1 Peripheral blood insulin-producing cells 37
1.7.2 Monocytes and their subtypes 39
1.8 Cord blood hematopoietic stem cells 44

1.8.1 Transplanted cord blood hematopoietic stem cells (CB-HSCs) differentiate into insulin-producing cells in the pancreas ... 44
1.8.2 Autologous cord blood infusion to treat type 1 diabetes ... 45
1.9 Stem cells from human amniotic fluid and membrane ... 45
1.9.1 Human amniotic epithelial stem cells ... 45
1.9.2 Human amniotic membrane stem cells ... 46
1.9.3 Human amnion-derived fibroblast-like cells ... 46
1.10 Bone marrow hematopoietic stem cells ... 47
1.11 Adipose stem cells ... 47
1.11.1 Differentiation of ASCs into pancreatic cells ... 48
1.11.2 ASCs have anti-inflammatory and angiogenic properties ... 50
1.12 Induced pluripotent stem cells ... 51
1.13 General characteristics of stem cells ... 51
1.13.1 Stem cells express alkaline phosphatase ... 51
1.13.2 Stem cells have a high level of aldehyde dehydrogenase enzyme activity ... 51
1.13.3 Senescence-associated β-galactosidase expression can be used to assay cell senescence ... 52
1.14 Immune tolerance ... 52
1.14.1 Immune regulator lymphocytes - Tregs ... 53
1.14.2 Cord blood stem cells are immunosuppressive ... 54
1.15 Insulin expression outside of the pancreas ... 57
1.16 Objectives of my thesis ... 58
Chapter 2 Materials and Methods ... 59
2.1 Materials ... 59
2.1.1 Suppliers ... 59
2.1.2 Buffers and chemicals ... 60
2.1.3 Tissue culture reagents and cell lines ... 67
2.1.4 Antibodies and protein controls ... 70
2.1.5 DNA plasmids encoding immortalizing transcription factors ... 72
2.1.6 Control pancreatic cell lines ... 75
2.2 Methods ... 83
2.2.1 General cell culture ... 83
2.2.2 Immunocytochemistry ... 86
2.2.3 Cell lysis ... 86
2.2.4 SDS-PAGE and Tris-Tricine gels ... 86
2.2.5 Western blotting ... 87

2.2.6 Dot blot protocol 87
2.2.7 FluoZin™-3 assay 88
2.2.8 CyQUANT® NF Cell Proliferation Assay 88
2.2.9 Alkaline phosphatase activity assay 89
2.2.10 Senescence-associated β-galactosidase (β-gal) assay 89
2.2.11 L-leucine methyl ester treatment of PB-IPCs and monocytes 90
2.2.12 Phagocytosis assay using pHrodo™ Red BioParticles® Conjugates 90
2.2.13 Endotoxin inhibition assay 90
2.2.14 Protein delivery 90
2.2.15 Mixed lymphocyte response 91
2.2.16 Annexin-V-FLUOS staining assay 91
2.2.17 Oil Red O staining 91
2.2.18 Aldehyde dehydrogenase (ALDH) assay 92
2.2.19 Induced pluripotent stem cells (iPSCs) 92
2.2.20 Statistical analysis 94
Chapter 3 Peripheral Blood Insulin-Producing Cells 95
3.1 Introduction 95
3.2 Scope of chapter 95
3.3 Characterization of PBMCs that attach to a hydrophobic surface 95
3.3.1 PBMCs that attach to a hydrophobic surface show a similar morphology to those that attach to a conventional tissue culture surface 95
3.3.2 Cultured PB-IPCs and monocytes have a similar phenotype 97
3.3.3 Validation of PDX-1 expression by Western blot analysis 116
3.3.4 FOXP3 is expressed by cultured monocytes and PB-IPCs 117
3.3.5 Cultured monocytes and PB-IPCs do not express insulin as determined by Western blot analysis 118
3.3.6 Cultured PB-IPCs do not stain with FluoZin™-3 that is used to detect insulin expression 120
3.3.7 PB-IPCs display alkaline phosphatase activity 121
3.4 PB-IPCs and monocytes are not proliferative in the absence of added growth factors 122
3.4.1 Monocytes proliferate in response to stimulation with M-CSF 123
3.5 PB-IPCs rapidly become senescent in culture 125
3.6 PKC activators induce the clustering of PB-IPCs 126
3.6.1 PKC activators induce prolonged clustering of PB-IPCs 126
3.6.2 PKC activation inhibits the senescence of monocytes and PB-IPC 127
3.7 Functional testing of PB-IPCs reveals they retain key properties of monocytes 129
3.7.1 Sensitivity of PB-IPCs to L-leucine methyl ester, a monocytic killing agent 129

3.7.2 PB-IPCs readily take up pHrodo™ Red BioParticles® Conjugates 132
3.8 Various pancreatic differentiation protocols are not able to differentiate PB-IPCs towards the pancreatic cell lineage 133
3.8.1 The protocol devised by Zhao *et al.* (2008) is not able to differentiate PB-IPCs towards the pancreatic cell lineage 135
3.8.2 GLP-1 alone is not able to differentiate PB-IPCs towards the pancreatic cell lineage 138
3.8.3 A combination of nicotinamide, GLP-1, and Ex4 is not able to differentiate PB-IPCs towards the pancreatic cell lineage 140
3.8.4 Preventing the senescence of PB-IPCs with ILV prior to differentiation does not alter their plasticity 143
3.9 Protein transduction of PB-IPCs with recombinant forms of PDX-1 and Pax4 does not induce their differentiation towards the pancreatic lineage 149
3.10 Are PB-IPCs immunosuppressive? 154
3.10.1 Phenotypes of cells present in the mixed lymphocyte response at different time-points 160
3.11 Inhibiting the effects of endotoxins on cell function 172
3.12 Discussion 178
3.12.1 Phenotype of PB-IPCs 178
3.12.2 PB-IPCs are not immunosuppressive 181
3.12.3 PB-IPCs do not proliferate in the absence of growth factors 182
3.12.4 Phenotype of differentiated PB-IPCs 182
3.12.5 Phenotype of spermine-treated PB-IPCs 184
3.12.6 PB-IPCs – a mixed population of cells 184
Chapter 4 Programmable Cells of Monocytic Origin and Fibroblast-resembling-macrophages 185
4.1 Scope of chapter 185
4.2 Generation of PCMOs, and attempts to differentiate them towards the pancreatic cell lineage 185
4.2.1 Dedifferentiation of PBMC to PCMOs 185
4.2.2 Islet cell conditioning medium is not able to differentiate PCMOs into pancreatic cells 188
4.3 Generation of f-MOs, and attempts to differentiate them towards the pancreatic cell lineage 190
4.3.1 Dedifferentiation of PBMCs to f-MOs 190
4.3.2 Islet cell conditioning medium is not able to differentiate f-MOs into pancreatic cells 191
4.3.3 Differentiation of f-MOs to other cell lineages 193
4.4 PCMOs and f-MOs rapidly become senescent 199
4.5 Discussion 201
4.5.1 PCMOs 201
4.5.2 f-MOs 202
4.5.3 Comparison of the shared and unique properties of PCMOs and f-MOs 203
Chapter 5 Human Amniotic Stem Cells 204
5.1 Introduction 204
5.2 Scope of chapter 204

5.3 Characterization of HASCs 205
5.3.1 Phenotyping of HASCs for expression of cell markers 205
5.3.2 HASCs do not display alkaline phosphatase activity 207
5.4 Can HASCs be differentiated into pancreatic cells? 207
5.4.1 Phenotype of HASCs differentiated with pancreatic differentiation matrices 207
5.4.2 Phenotype of HASCs differentiated on tissue culture plates with differentiation agents 214
5.5 Discussion 221
5.5.1 Phenotype of HASCs 221
5.5.2 Phenotype of differentiated HASCs 221
5.5.3 HASCs potential for therapeutic treatment of type 1 diabetics 224
Chapter 6 Cord Blood Hematopoietic Stem Cells 226
6.1 Introduction 226
6.2 Scope of chapter 226
6.3 Characterisation of CB-HSCs 226
6.4 Characterisation of P-HSCs 228
6.4.1 Phenotyping of P-HSCs for cell markers 228
6.4.2 Summary of the phenotyping of CB-HSCs and P-HSCs 230
6.4.3 Western blot analysis confirms that P-HSCs do not express insulin 231
6.5 CB-HSCs and P-HSCs do not display alkaline phosphatase activity 232
6.6 Can CB-HSCs be differentiated into pancreatic cells? 232
6.7 Discussion 235
6.7.1 Phenotype of CB-HSCs 235
6.7.2 Phenotype of differentiated CB-HSCs (dCB-HSCs) 235
6.7.3 Phenotype of P-HSCs 236
6.7.4 Potential of CB-HSCs, dCB-HSCs, and P-HSCs 237
Chapter 7 Adipose Stem Cells 238
7.1 Introduction 238
7.2 Scope of chapter 238
7.3 Characterisation of ASCs for adipose stem cell markers 239
7.4 Induced adipogenesis of ASCs 241
7.4.1 Phenotyping of ASCs for adipose stem cell markers after induced adipogenesis 242
7.5 ASCs display aldehyde dehydrogenase activity 243
7.6 ASCs do not display alkaline phosphatase activity 245
7.7 Trials to differentiate attached ASCs towards the pancreatic lineage 246
7.7.1 Trials to differentiate ASCs into hormone-expressing endocrine cells 246

7.7.2 Stage-specific differentiation of ASCs 256
7.7.3 Differentiation of ASCs that are sorted with respect to expression of ALDH 282
7.8 Differentiation of ASCs cultured in suspension towards the pancreatic lineage 286
7.8.1 Differentiation in Chandra's media 287
7.8.2 Differentiation in Timper's medium 289
7.8.3 Investigation of insulin expression by differentiated ASCs cultured in ultra-low attachment plates using a panel of anti-insulin antibodies 290
7.8.4 Are definitive endoderm markers expressed prior to insulin expression by ASCs cultured in ultra-low attachment plates? 293
7.9 Discussion 298
7.9.1 Phenotype of ASCs 298
7.9.2 Differentiation of attached ASCs 299
7.9.3 Differentiation of ASCs in suspension 303
7.9.4 Differentiation potential of ASCs towards pancreatic cell lineages 305
Chapter 8 Induced Pluripotent Stem Cells 306
8.1 Introduction 306
8.2 Scope of chapter 306
8.3 Selection of a cell line for producing stem cell transcription factors 306
8.4 Optimization of transfection of CHO-K1 cells 307
8.4.1 Oct-4 307
8.4.2 c-Myc 311
8.4.3 KLF4 313
8.4.4 SOX-2 314
8.5 Discussion 316
8.5.1 Production of recombinant stem cell transcription factors 316
8.5.2 Potential uses for the stem cell transcription factors 316
Chapter 9 General Discussion, Conclusions, and Future Directions 317
9.1 General discussion 317
9.2 Conclusions 321
9.3 Future directions 323
Appendix A 325
References 328

List of Figures

Table 1.2 Comparison of the amount of insulin and C-peptide expressed by various cell types 38
Figure 1.1 Schematic diagram of the Stem Cell Educator system. 56
Figure 2.1 Map of the pUNO1-mOCT4::11R expression vector. 73
Figure 2.2 Map of the pUNO1-mcMYC::11R expression vector. 73
Figure 2.3 Map of the pUNO1-mKLF4::11R expression vector. 74
Figure 2.4 Map of the pUNO-mSOX2::11R expression vector. 74
Figure 2.5 Phase contrast image of 1.1B4 cells. 76
Figure 2.6 Phenotyping of 1.1B4 cultures. 77
Figure 2.7 The purchased 1.1B4 cell line does not express insulin. 78
Figure 2.8 Phase contrast image of INS-1E cells. 79
Figure 2.9 Phenotyping of INS-1E cells. 80
Figure 2.10 The RINm5F cell line expresses insulin. 81
Figure 2.11 Phase contrast image of RINm5F cells. 82
Figure 2.12 Phenotyping of RINm5F cells. 83
Figure 2.13 Measurement of the proliferation of the liver cancer cell line HepG2 using the CyQUANT® NF cell proliferation assay. 89
Figure 3.1 Phase contrast images of PB-IPCs (isolated from healthy donors) cultured in hydrophobic and hydrophilic dishes. 96
Figure 3.2 Phase contrast images of cultures of PB-IPCs isolated from a healthy subject and a diabetic patient, and cultured in hydrophobic dishes. 97
Figure 3.3 Phenotyping of adherent PB-IPCs cultured in hydrophobic dishes for 2 h. 100
Figure 3.4 Phenotyping of monocytes cultured in tissue culture dishes for 2 h. 102
Figure 3.5 Phenotyping of adherent PB-IPCs cultured in hydrophobic dishes for 3 days. 104
Figure 3.6 Phenotyping of monocytes cultured in tissue culture dishes for 3 days. 106
Figure 3.7 Phenotyping of adherent PB-IPCs cultured in hydrophobic dishes for 1 week. 108
Figure 3.8 Phenotyping of monocytes cultured in tissue culture dishes for 1 week. 110
Figure 3.9 Phenotyping of adherent PB-IPCs cultured in hydrophobic dishes for 2 weeks. 112
Figure 3.10 Phenotyping of monocytes cultured in tissue culture dishes for 2 weeks. 114
Figure 3.11 PDX-1 is expressed by both cultured monocytes and PB-IPCs. 116
Figure 3.12 Anti-FOXP3 antibody ab20034 detects FOXP3 in the nuclear compartment of monocytes and PB-IPCs. 117
Figure 3.13 Anti-FOXP3 antibody ab36607 detects FOXP3 in the nuclear and cytoplasmic compartments of monocytes and PB-IPCs. 118
Figure 3.14 PB-IPCs cultured for 2 weeks do not express insulin. 119
Figure 3.15 PB-IPCs cultured for 4 weeks do not express insulin. 119
Figure 3.16 PB-IPCs do not stain with FluoZin™-3. 120

Figure 3.17 Cultured PB-IPCs express alkaline phosphatase activity. 121
Figure 3.18 Alkaline phosphatase displayed by PB-IPCs is confined to intracellular vesicles. 121
Figure 3.19 Measurement of the proliferation of monocytes and PB-IPCs cultured in tissue culture dishes and hydrophobic dishes, respectively. 122
Figure 3.20 Proliferation of monocytes in response to stimulation with M-CSF. 123
Figure 3.21 Phase contrast images of monocytes cultured in the presence or absence of M-CSF. 124
Figure 3.22 Senescence-associated β-gal activity of PB-IPCs is detectable as early as 4 days in culture. 125
Figure 3.23 PKC activators (-)-indolactam V and phorbol 12-myristate 13-acetate induce clustering of PB-IPCs. 126
Figure 3.24 PKC delays senescence of PB-IPCs and monocytes for at least 2 weeks. 127
Figure 3.25 Commercial HSC mediums HSC I and HSC II do not prevent the senescence of PB-IPCs. 128
Figure 3.26 Commercial HSC mediums HSC I and HSC II do not prevent the senescence of monocytes. 128
Figure 3.27 Phase contrast images of attached PBMCs treated with increasing concentrations of L-leucine methyl ester prior to seeding in hydrophobic dishes. 130
Figure 3.28 PBMCs that do not attach to hydrophobic dishes and resist toxic concentrations of L-leucine methyl ester are nucleated, and some are undergoing apoptosis. 131
Figure 3.29 Percentage of suspension cells undergoing apoptosis after treatment with increasing concentrations of L-leucine methyl ester. 131
Figure 3.30 PB-IPCs take up pHrodo™ Red BioParticles as efficiently as monocytes. 132
Figure 3.31 Phenotype of PB-IPCs cultured for 2 weeks in control medium. 135
Figure 3.32 Differentiation of PB-IPCs using Zhao's protocol. 137
Figure 3.33 Differentiation of PB-IPCs with GLP-1. 140
Figure 3.34 Differentiation of PB-IPCs using a combination of nicotinamide, GLP-1, and Ex4. 143
Figure 3.35 Pretreatment of PB-IPCs with (-)-indolactam V prior to culture in control media. 145
Figure 3.36 Pretreatment of PB-IPCs with (-)-indolactam V prior to differentiation using Zhao's protocol. 147
Table 3.2 Summary of the phenotypes of differentiated PB-IPCs 148
Figure 3.37 Pro-DeliverIN delivers R-Phycoerythrin into PB-IPCs. 149
Figure 3.38 Phenotype of control PB-IPCs cultured for 1 week. 150
Figure 3.39 Phenotype of PDX-1-treated PB-IPCs. 151
Figure 3.40 Phenotype of Pax4-treated PB-IPCs. 152
Figure 3.41 Diagram detailing the mixed lymphocyte response experimental design. 154
Figure 3.42 PB-IPCs and monocytes do not significantly alter the mixed lymphocyte response at 48 h. 155
Figure 3.43 PB-IPCs and monocytes increased the level of apoptosis in the mixed lymphocyte response at 72 h, but only the effect of the monocytes was significant. 156
Figure 3.44 PB-IPCs significantly increased the mixed lymphocyte response at 96 h, while monocytes did not significantly alter the response. 157
Figure 3.45 PB-IPCs and monocytes increased the level of apoptosis in the mixed lymphocyte response at 120 h, but the results were non-significant. 158

Figure 3.46 Summary of the number of apoptotic cells present at different times during the mixed lymphocyte response. 159
Figure 3.47 Phenotype of cells in the mixed lymphocyte response at 24 h. 162
Figure 3.48 Phenotype of cells in the mixed lymphocyte response at 48 h. 164
Figure 3.49 Phenotype of cells in the mixed lymphocyte response at 72 h. 166
Figure 3.50 Phenotype of cells in the mixed lymphocyte response at 96 h. 168
Figure 3.51 Phenotype of cells in the mixed lymphocyte response at 120 h. 170
Figure 3.52 Summary of the phenotypes of the suspension cells present during the mixed lymphocyte reactions. 171
Figure 3.53 Spermine inhibits the expression of CD68 and HLA-DR by PB-IPCs. 173
Figure 3.54 Control PB-IPC populations cultured in the absence of spermine. 175
Figure 3.55 Pre-treatment of PB-IPCs with spermine inhibits their activation, but does not enhance pancreatic differentiation. 176
Figure 3.56 Inclusion of spermine during pretreatment and differentiation steps does not enhance the pancreatic differentiation of PB-IPCs. 177
Figure 4.1 Dedifferentiation of PBMCs into PCMOs in hydrophobic dishes. 186
Figure 4.2 Dedifferentiation of PBMCs into PCMOs in tissue culture dishes. 187
Figure 4.3 Dedifferentiation of PBMCs into PCMOs, followed by culture in control medium. 189
Figure 4.4 Attempt to differentiate PCMOs into pancreatic cells using islet cell conditioning medium. 189
Table 4.2 Summary of the phenotyping of PCMO differentiated with islet cell conditioning medium (ICM) or control medium[a] 190
Figure 4.5 M-CSF-induced differentiation of PBMCs into f-MOs. 191
Figure 4.6 Differentiation of PBMCs to f-MOs and their culture in control medium. 192
Figure 4.7 Differentiation of f-MOs with islet cell conditioning medium. 192
Figure 4.8 Culture of monocytes for 18 days in control medium. 192
Figure 4.9 Attempt to differentiate f-MOs to endothelial cells with $VEGF_{165}$. 194
Figure 4.10 Attempt to differentiate f-MOs to neural cells with NGFβ. 195
Figure 4.11 Attempt to differentiate f-MOs to T lymphocytes with IL-2. 196
Figure 4.12 Phenotyping of monocytes cultured for 16 days in control medium. 197
Figure 4.13 Phase contrast images of differentiated f-MOs. 199
Figure 4.14 PCMOs and f-MOs are senescent after 4 days of culture. 200
Figure 4.15 PCMOs and f-MOs do not express alkaline phosphatase activity that characterizes stem cells. 200
Figure 5.1 Phase contrast image of a 2 day culture of HASCs. 205
Figure 5.2 Phenotyping of HASCs for stem and pancreatic cell markers. 206
Figure 5.3 HASCs do not display alkaline phosphatase activity. 207
Figure 5.4 Phenotyping of HASCs after differentiation towards the pancreatic lineage by culture on pancreatic cancer stem cell differentiation matrix. 210
Figure 5.5 Phenotyping of HASCs after differentiation towards the pancreatic lineage by culture on pancreatic trans-differentiation stem cell differentiation matrix. 212
Figure 5.6 Phenotyping of HASCs differentiated towards the pancreatic lineage with a medium containing Ex4 and GM-CSF. 215

Figure 5.7 Phenotyping of HASCs differentiated along the pancreatic lineage with a medium containing nicotinamide and high glucose.... 216
Figure 5.8 Phenotyping of HASCs differentiated towards the pancreatic lineage with GLP-1.... 218
Figure 5.9 Phenotyping of HASCs differentiated along the pancreatic lineage with a medium containing GLP-1 and Ex4.... 219
Figure 6.1 Phase contrast image of a culture of CB-HSCs.... 227
Figure 6.2 Phenotyping of CB-HSCs for stem and pancreatic markers.... 228
Figure 6.3 Phase contrast image of a culture of P-HSCs.... 229
Figure 6.4 Phenotyping of P-HSCs for stem and pancreatic markers.... 230
Figure 6.5 Western blot analysis confirms that P-HSCs do not express insulin.... 231
Figure 6.6 CB-HSCs and P-HSCs do not display alkaline phosphatase activity.... 232
Figure 6.7 Phenotyping of dCB-HSCs for stem and pancreatic markers.... 234
Figure 7.1 Phenotyping of ASCs for adipose stem cell markers.... 239
Figure 7.2 Phenotyping of ASCs for stem and pancreatic cell markers.... 240
Figure 7.3 Induced adipogenesis of ASCs.... 241
Figure 7.4 ASCs forced to undergo adipogenesis and phenotyped for the expression of adipose stem cell markers.... 242
Figure 7.5 Phenotyping of ASCs for stem and pancreatic markers after adipogenesis.... 243
Figure 7.6 A subpopulation of ASCs display ALDH activity.... 244
Figure 7.7 ASC retain ALDH enzyme expression for at least 10 passages.... 245
Figure 7.8 ASCs do not display alkaline phosphatase activity.... 245
Figure 7.9 Phenotyping of ASCs cultured for 3 days in tissue culture plates for stem and pancreatic markers.... 247
Figure 7.10 Phenotyping of ASCs cultured for 1 week in tissue culture plates for stem and pancreatic markers.... 248
Figure 7.11 Phenotyping of ASCs cultured for 2 weeks in tissue culture plates for stem and pancreatic markers.... 249
Figure 7.12 Phenotyping of ASCs cultured for 3 days according to the Chandra protocol.... 251
Figure 7.13 Phenotyping of ASCs cultured for 1 week according to the Chandra protocol.... 253
Figure 7.14 Phenotyping of ASCs cultured for 2 weeks according to the Chandra protocol.... 254
Figure 7.15 Phenotyping of ASCs cultured for 3 days in a modified version of the Timper protocol.... 255
Figure 7.16 Phenotyping of ASCs cultured for 10 days in expansion medium.... 258
Figure 7.17 Phenotyping of ASCs differentiated with 100 nM IDE-1 towards definitive endoderm (Stage 1).... 259
Figure 7.18 Phenotyping of ASCs differentiated with 400 nM IDE-1 towards definitive endoderm (Stage 1).... 260
Figure 7.19 Phenotyping of ASCs differentiated with activin A + Wnt3a followed by activin A alone towards definitive endoderm (Stage 1).... 261
Figure 7.20 Phenotyping of ASCs differentiated with activin A + Wnt3a towards definitive endoderm (Stage 1).... 262
Figure 7.21 Phenotyping of ASCs differentiated with 100 nM IDE-1, followed by KAAD-cyclopamine + FGF10 towards the formation of primitive gut tube (Stage 2).... 263
Figure 7.22 Phenotyping of ASCs differentiated with 100 nM IDE-1, followed by KAAD-cyclopamine + FGF10 + BMP-2 towards formation of primitive gut tube (Stage 2).... 264

Figure 7.23 Phenotyping of ASCs differentiated with 400 nM IDE-1, followed by KAAD-cyclopamine + FGF10 towards the formation of primitive gut tube (Stage 2). 265
Figure 7.24 Phenotyping of ASCs differentiated with 400 nM IDE-1, followed by KAAD-cyclopamine + FGF10 + BMP-2 towards the formation of primitive gut tube (Stage 2). 266
Figure 7.25 Phenotyping of ASCs differentiated with activin A + Wnt3a followed by activin A only, followed by KAAD-cyclopamine + FGF10 towards formation of primitive gut tube (Stage 2). 267
Figure 7.26 Phenotyping of ASCs differentiated with activin A + Wnt3a, followed by activin A only, followed by KAAD-cyclopamine + FGF10 + BMP-2 towards the formation of primitive gut tube (Stage 2). 268
Figure 7.27 Phenotyping of ASCs differentiated with activin A + Wnt3a, followed by KAAD-cyclopamine + FGF10 towards formation of primitive gut tube (Stage 2). 269
Figure 7.28 Phenotyping of ASCs differentiated with activin A + Wnt3a, followed by KAAD-cyclopamine + FGF10 + BMP-2 towards formation of primitive gut tube (Stage 2). 270
Figure 7.29 Phenotyping of ASCs differentiated with 100 nM IDE-1, followed with KAAD-cyclopamine + FGF10, and then with KAAD-cyclopamine + FGF10 + all trans-retinoic acid towards formation of posterior foregut (Stage 3). 271
Figure 7.30 Phenotyping of ASCs cultured with 100 nM IDE-1, followed with KAAD-cyclopamine + FGF10 + BMP2, and then with KAAD-cyclopamine + FGF10 + all trans-retinoic acid + BMP-2 towards formation of posterior foregut (Stage 3). 272
Figure 7.31 Phenotyping of ASCs differentiated with 400 nM IDE-1, followed by KAAD-cyclopamine + FGF10, and then with KAAD-cyclopamine + FGF10 + all trans-retinoic acid towards formation of posterior foregut (Stage 3). 273
Figure 7.32 Phenotyping of ASCs differentiated with 400 nM IDE-1, followed by KAAD-cyclopamine + FGF10 + BMP-2, and then with KAAD-cyclopamine + FGF10 + retinoic acid + BMP-2 towards formation of posterior foregut (Stage 3). 274
Figure 7.33 Phenotyping of ASCs differentiated with activin A + Wnt3a, followed by activin A only, followed by KAAD-cyclopamine + FGF10, and then with KAAD-cyclopamine + FGF10 + all trans-retinoic acid towards formation of posterior foregut (Stage 3). 275
Figure 7.34 Phenotyping of ASCs differentiated with activin A + Wnt3a, followed by activin A alone, followed by KAAD-cyclopamine + FGF10 + BMP-2, and then with KAAD-cyclopamine + FGF10 + retinoic acid + BMP-2 towards formation of posterior foregut (Stage 3). 276
Figure 7.35 Phenotyping of ASCs differentiated with activin A + Wnt3a, followed by KAAD-cyclopamine + FGF10, and then with KAAD-cyclopamine + FGF10 + all trans-retinoic acid towards formation of posterior foregut (Stage 3). 277
Figure 7.36 Phenotyping of ASCs differentiated with activin A + Wnt3a, followed by KAAD-cyclopamine + FGF10 + BMP-2, and then with KAAD-cyclopamine + FGF10 + all trans-retinoic acid + BMP-2 towards the formation of posterior foregut (Stage 3).. 278
Figure 7.37 Western blot analysis confirms ASCs express PDX-1 when induced to differentiate to the posterior foregut stage of differentiation. 280
Figure 7.38 Analysis of the expression of PDX-1 by ASCs after differentiation into formation of the primitive gut tube. 281
Figure 7.39 ASCs sorted according to their ALDH activity. 282
Figure 7.40 Phenotyping of ALDH$^+$ ASCs cultured for 4 days in expansion medium. 283
Figure 7.41 Phenotyping of ALDH- ASCs cultured for 4 days in expansion medium. 283
Figure 7.42 Phenotyping of ALDH$^+$ ASCs cultured in the presence of 200 nM IDE-2. 284

Figure 7.43 Phenotyping of ALDH- ASCs cultured in the presence of 200 nM IDE-2. 284
Figure 7.44 Phenotyping of ALDH^{+} ASCs cultured in 200 nM IDE-2 followed by KAAD-cyclopamine + FGF10 + BMP-2. 285
Figure 7.45 Phenotyping of ALDH^{-} ASCs cultured in 200 nM IDE-2 followed by KAAD-cyclopamine + FGF10 + BMP-2. 286
Figure 7.46 Phase contrast images of clustered ASCs after culture in ultra-low attachment plates. 287
Figure 7.47 Phenotyping of ASCs cultured for 2 weeks with Chandra's media in ultra-low attachment plates. 288
Figure 7.48 Phenotyping of ASCs cultured for 2 weeks with Chandra's media in hydrophobic plates. 288
Figure 7.49 Phenotyping of ASCs cultured for 3 days with Timper's medium in ultra-low attachment plates. 289
Figure 7.50 Phenotyping of ASCs cultured for 2 weeks with Chandra's media in ultra-low attachment plates. 290
Figure 7.51 Phenotyping of ASCs cultured for 2 weeks with expansion medium in ultra-low attachment plates. 291
Figure 7.52 The guinea pig anti-human insulin antibody only detects insulin and not insulin homologues. 292
Figure 7.53 Insulin expressed by ASCs differentiated with Chandra's media is not detected by Western blot analysis. 293
Figure 7.54 Phenotyping of ASCs cultured for 2 days in Chandra's SFM-A medium in ultra-low attachment plates for markers of definitive endoderm. 294
Figure 7.55 Phenotyping of ASCs cultured for 2 days in Chandra's SFM-A + mix medium in ultra-low attachment plates for markers of definitive endoderm. 295
Figure 7.56 Phenotyping of ASCs cultured for 2 days in Chandra's SFM-A medium, followed by 2 days in Chandra's SFM-B medium in ultra-low attachment plates for markers of definitive endoderm. 295
Figure 7.57 Phenotyping of ASCs cultured for 2 days in Chandra's SFM-A + mix medium followed by 2 days in Chandra's SFM-B + mix medium in ultra-low attachment plates for markers of definitive endoderm. 296
Figure 7.58 Phenotyping of ASCs cultured for 4 days in Chandra's SFM-A + long-mix medium in ultra-low attachment plates for markers of definitive endoderm. 296
Figure 7.59 Phenotyping of ASCs cultured for 4 days in D'Amour's medium in ultra-low attachment plates for markers of definitive endoderm. 297
Figure 8.1 CHO-K1 cells are more efficiently transfected with Lipofectamine LTX to produce Oct-4 than are 266-6 cells. 307
Figure 8.2 Transfection of CHO-K1 cells with an Oct-4 plasmid using Lipofectamine LTX. 308
Figure 8.3 Transfection of CHO-K1 cells with an Oct-4 plasmid using Polymag. 308
Figure 8.4 Western blot analysis of CHO-K1 cells transfected to express Oct-4 using Lipofectamine LTX. 309
Figure 8.5 Quantification of Oct-4 expression by transfectants. 310
Figure 8.6 Western blot analysis of CHO-K1 cells transfected to express Oct-4 using Polymag. 311
Figure 8.7 Western blot analysis of CHO-K1 cells transfected to express c-Myc using Lipofectamine LTX. 312
Figure 8.8 Quantification of c-Myc expression by transfectants. 312
Figure 8.9 Western blot analysis of CHO-K1 cells transfected to express KLF4 using Lipofectamine LTX. 313
Figure 8.10 Quantification of KLF4 expression by transfectants. 314
Figure 8.11 Western blot analysis of CHO-K1 cells transfected to express SOX-2 using Lipofectamine LTX. 315
Figure 8.12 Quantification of SOX-2 expression by transfectants. 315
Figure A. 1 Phenotyping of monocytes cultured in tissue culture dishes for 3 days. 327

List of Tables

Table 1.1 The 5 stages of differentiation of ESCs to definitive endoderm, and then to insulin-producing β-cells. 28
Table 2.1 List of primary antibodies 70
Table 2.2 List of secondary antibodies 72
Table 2.3 List of control proteins 72
Table 2.4 Summary of the phenotyping of the 1.1B4 cell line 77
Table 2.5 Summary of the phenotyping of the INS-1E cell line 81
Table 2.6 Summary of the phenotyping of the RINm5F cell line 83
Table 3.1 Summary of the phenotypes of adherent PBMCs cultured in either a hydrophobic (PB-IPC) or tissue culture (monocytes, MO) dish 115
Table 4.1 Summary of the phenotyping of PBMCs dedifferentiated into PCMOs 188
Table 4.3 Summary of the phenotype of differentiated f-MOs 198
Table 5.1 Summary of the phenotype of HASCs 206
Table 5.2 Summary of the phenotype of HASCs cultured with two different differentiation media on two different pancreatic differentiation matrices 213
Table 5.3 Summary of the phenotype of HASCs cultured with differentiation agents 220
Table 6.1 Summary of the phenotyping of CB-HSCs and P-HSCs for pancreatic and stem cell markers 230
Table 6.2 Summary of the phenotyping of dCB-HSCs 234
Table 7.1 Summary of markers expressed by ASC after expansion or adipogenesis 243
Table 7.2 Chandra's differentiation protocol and composition of media 250
Table 7.3 Summary of the phenotype of ASCs after differentiation in either expansion media, or according to Chandra's and Timper's (+IGF-2, -pentagastrin) protocols 256
Table 7.5 Summary of the phenotyping of ASCs after their differentiation along embryonic pathways (Stage 1-3) that lead to the formation of the pancreas 279
Table 7.6 Summary of the phenotypes of differentiated $ALDH^+$ and $ALDH^-$ populations of ASCs 286
Table 7.8 Summary of expression by ASCs of markers of definitive endoderm after 2-4 days of differentiation with Chandra and D'Amour's media 297

Abbreviations

°C	Degree Celsius
ABCG2	ATP-binding cassette sub-family G member 2
AIRE	Autoimmune regulator
ALDH	Aldehyde dehydrogenase
APC	Antigen presenting cell
APS	Ammonium persulfate
ASC	Adipose stem cell
ATCC	American Type Culture Collection
β-gal	β-galactosidase
BAAA	Bodipy aminoacetaldehyde
bFGF	Basic fibroblast growth factor
BM	Bone marrow
BMP	Bone morphogenic protein
BSA	Bovine serum albumin
BTC	Betacellulin
C	Cytoplasmic
CB-HSC	Cord blood-hematopoietic stem cell
CB-SC	Cord blood-stem cell
CD	Cluster of differentiation
CMV IE	Cytomegalovirus immediate early
Conc.	Concentration
CPP	Cell-permeable peptide
CTLA-4	Cytotoxic T-lymphocyte antigen 4
CXCR4	Chemokine receptor 4
DAPI	4'6-diamidino-2-phenylindole
DAPT	N-[N-(3,5-Difluorophenacetyl)-L-alanyl]-S-phenylglycine t-butyl ester
DC	Dendritic cell
dCB-HSC	Differentiated cord blood-hematopoietic stem cell
DE	Definitive endoderm
DEAB	Diethylaminobenzaldehyde
dH_2O	Deionized water
DMEM	Dulbecco's modified eagle's medium
DMSO	Dimethyl sulfoxide

DNA	Deoxyribonucleic acid
DTZ	Dithizone
E. coli	*Escherichia coli*
EB	Embryoid body
ECAD	Epithelial cadherin
ECL	Enhanced chemiluminescence
EDTA	Ethylenediaminetetra-acetic acid
EGF	Epidermal growth factor
ELISA	Enzyme-linked immunosorbent assay
EN	Endocrine cell
ESC	Embryonic stem cell
EtOH	Ethanol
Ex4	Exendin-4
FACS	Fluorescence-activated cell sorting
FBS	Foetal bovine serum
FGF	Fibroblast growth factor
FITC	Fluorescein isothiocyanate
f-MO	Fibroblast-resembling-macrophage
FOX	Forkhead box protein
g	Gram
G-CSF	Granulocyte-colony stimulating factor
GAD	Glutamate decarboxylase
GFAP	Glial fibrillary acidic protein
GIPR	Gastric inhibitory polypeptide receptor
GLP	Glucagon-like peptide
Glut	Glucose transporter
GM-CSF	Granulocyte-macrophage colony-stimulating factor
GP	Guinea pig
GPR40	G protein-coupled estrogen receptor 40
GVHD	Graft versus host disease
h	Hour
HADFIL	Human amnion-derived fibroblast-like cells
HAESC	Human amniotic epithelial stem cells
HAMSC	Human amniotic membrane stem cells
HASC	Human amniotic fluid and membrane stem cells
HbA1c	Haemoglobin A1c

HBSS	Hank's balanced salt solution
HEPES	4-(2-hydroxyethyl)-1-piperazineethanesulfonic acid
HGF	Hepatocyte growth factor
HLA	Human leukocyte antigen
HLXB9	Homeobox protein HB9
HNFs	Human newborn fibroblasts
HNF	Hepatocyte nuclear factor
HRP	Horseradish peroxidase
HSC	Hematopoietic stem cell
HSC I/II	Stemline® I/II Hematopoietic Stem Cell Expansion Medium
HUVEC	Human umbilical vein endothelial cells
HY	Hydrophobic
IA-2	Islet antigen-2
ICA	Islet-like cell aggregates
ICC	Immunocytochemistry
ICM	Islet cell conditioning medium
IDDM	Insulin-dependent diabetes mellitus
IDE	Inducer of definitive endoderm
IFN	Interferon
IGF	Insulin-like growth factor
IL	Interleukin
ILV	(-)-Indolactam V
INS	Insulin
INSL3	Insulin-like 3
IPADSC	Insulin-producing adipose-tissue derived stem cells
iPSC	Induced pluripotent stem cell
ISL-1	Islet-1
ITS	Insulin/Transferrin/Selenium
KAAD-CYC	KAAD-cyclopamine
kDa	Kilodalton
KLF4	Kruppel-like factor 4
L	Litre
LIF	Leukaemia inhibitory factor
LPS	Lipopolysaccharide
LB	Luria-Bertani
µ	Micro

M	Molar
mA	Milliamps
MAP-1B	Microtubule associated protein-1B
M-CSF	Macrophage colony-stimulating factor
MDI	Monocyte-derived islet cell
MDSC	Monocyte-derived stem cell
MEF	Mouse embryonic fibroblasts
mg	Milligram
MHC	Major histocompatibility complex
min	Minute
mL	Millilitre
MLR	Mixed lymphocyte response
mM	Millimolar
MO	Monocyte
mRNA	Messenger ribonucleic acid
N	Nuclear
NaCl	Sodium chloride
NEAA	Non-essential amino acids
Neuro	Neurogenic differentiation
NF	Neurofilament
NGF	Nerve growth factor
NGN	Neurogenin
NK cell	Natural killer cell
Nkx	NK homeobox factor
nM	Nanometre
NOD-SCID	Non-obese diabetic/severe combined immunodeficiency
NSE	Neuron specific enolase
Oct-4	Octamer-binding transcription factor 4
P#	Passage #
P-HSC	Pancreatic hematopoietic stem cell
Pax	Paired box
PB-IPC	Peripheral blood insulin-producing cell
PBMC	Peripheral blood mononuclear cell
PBS	Phosphate buffered saline
PC	Prohormone convertase
PCMO	Programmable cell of monocytic origin

PCNA	Proliferating cell nuclear antigen
PCSK1	Proprotein convertase subtilisin/kexin type 1
PDS	Pancreatic ductal stem
PDX-1	Pancreatic and duodenal homeobox 1
PDVF	Polyvinylidene difluoride
PF	Posterior foregut
PG	Primitive gut tube
PHA	Phytohemagglutinin
PI3K	Phosphoinositide 3-kinase
PKC	Protein kinase C
pM	Picomolar
PMA	Phorbol 12-myristate 13-acetate
PMSF	Phenylmethylsulphonyl fluoride
ProINS	Proinsulin
PSG	Penicillin, streptomycin, and L-glutamine
Ptf1a	Pancreas transcription factor 1-α
RA	all trans-retinoic acid
RIA	Radioimmunoassay
RNA	Ribonucleic acid
RPM	Revolutions per minute
RPMI	Roswell Park Memorial Institute (medium)
RT	Room temperature
RT-PCR	Real-time polymerase chain reaction
SA-βgal	Senescence-associated beta-galactosidase
SCF	Stem cell factor
SD	Standard deviation
SDS	Sodium dodecyl sulfate
SDS-PAGE	Sodium dodecyl sulfate polyacrylamide gel electrophoresis
sec	Seconds
SFM	Serum free medium
Shh	Sonic hedgehog
s-MO	Standard macrophage
SOX	Sex determining region Y-box
SSEA	Stage specific embryonic antigen
STI	Soybean trypsin inhibitor
STZ	Streptozotocin

SVF	Stromal vascular fraction
T-TBS	Tween-20 and Tris buffered saline
TC	Tissue culture
tdCB-HSC	Transdifferentiated cord blood-hematopoietic stem cell
TEMED	Tetramethylethylenediamine
TGF-β	Transforming growth factor-β
TLR4	Toll-like receptor 4
TNF	Tumour necrosis factor
TRA	Tumour-rejection antigen
Treg	T regulatory cell
v/v	Volume/volume
VEGF	Vascular endothelial growth factor
vWF	Von Willebrand factor
w/v	Weight/volume
WB	Western blot
wk	Week
X-gal	5-bromo-4-chloro-3-indoyl β-D-galactopyranoside

Chapter 1 Introduction

1.1 Type 1 diabetes mellitus overview

1.1.1 Prevalence, health complications and causes of type 1 diabetes

In the year 2000, it was reported that diabetes affected about 171 million people worldwide, representing 2.8% of the world's population, and including more than 11,000 people in New Zealand (Wild *et al.* 2004). The number of affected individuals worldwide is predicted to rise to 366 million by 2030 (Wild *et al.* 2004). There are two different types of diabetes, namely type 1 and 2. Approximately 5 to 10% of diabetics have type 1 diabetes, with the rest suffering from type 2 (Daneman 2006). Type 1 diabetes is usually diagnosed in childhood (50-60% <18 years old at the time of diagnosis), and is therefore often called "juvenile diabetes", but it can also develop in adulthood (Daneman 2006). Type 1 diabetes is primarily defined by insulin deficiency due to autoimmunity where the immune system specifically destroys the β-cells of the pancreas (Daneman 2006). The β-cell mass in the pancreas maintains normoglycemia and a loss of these cells leads to hypo- or hyperglycemia where the level of blood glucose is uncontrolled (Daneman 2006). Loss of glycemic control can cause serious health complications for the affected individual which can be life-threatening. These complications include microvascular and macrovascular conditions such as retinopathy, neuropathy, nephropathy, limb amputation, hyperlipidemia, hypertension, and cardiovascular disease (Daneman 2006). Therefore, there is a medical need to learn how to replace the lost β-cells in order to treat type 1 diabetes and avoid these severe health complications. Research will also be needed to learn how to tolerize the immune system from attacking the replaced β-cells due to the unrelenting autoimmunity.

Several genes called IDDM (insulin-dependent diabetes mellitus) susceptibility genes are candidates for influencing the onset of the disease (Daneman 2006). They include polymorphic HLA-DR and DQ haplotypes which are inherited (Daneman 2006). People born with the diabetes risk haplotypes have a 1 in 20 risk of developing diabetes, and for those with a family history of diabetes the risk increases to 1 in 5 (Steck and Rewers 2011). There is also an association of type 1 diabetes with the genes encoding solute carrier family 11 A1, protein tyrosine phosphatase non-receptor type 22, cytotoxic T-lymphocyte antigen 4, and ICOS (a member of the CD28/Cytotoxic T-Lymphocyte Antigen 4 (CTLA-4) family) and the immune-regulatory cytokines IL-10, IL-19 and IL-20 (Nichols and Cooke 2009). There is only a 30-50% concordance between genetically identical twins indicating that an unknown environmental component plays a key role in the development of the disease (Adeghate *et al.* 2006). This notion is evidenced by the fact that the incidence of type 1 diabetes is increasing by 3% on average per year in many countries (Onkamo *et al.* 1999).

1.1.2 Current treatments for patients with type 1 diabetes

Sufferers of type 1 diabetes inject a synthetic form(s) of insulin at specified times during the day, particularly just before meals, in order to attempt to maintain normoglycemia (Daneman 2006). Insulin treatment was first applied to a patient in 1922, and the

goal of the procedure remains the same at the present day (Sonksen and Sonksen 2000). Diabetic patients should aim to have a fasting plasma glucose level of between 4-7 mmol/L and a 2 h post-meal plasma glucose level of between 5-11 mmol/L (Daneman 2006). A clinical measurement of the blood glucose control maintained by a diabetic patient over a 3 month period can be obtained by the HbA1c (haemoglobin A1c) test, which measures the level of glycated haemoglobin (Hb) (Daneman 2006). A diabetic patient should aim for an HbA1c level of ≤ 7.0, whereas a non-diabetic individual would expect to have a level of ≤ 6.0 (Daneman 2006).

There is also an option for patients to have a subcutaneous insulin pump which continuously administers a fast-acting form of insulin to help maintain normoglycemia without the need for repeated daily self-injections (Daneman 2006). The pump is designed to allow the patient to self-administer a bolus of insulin before meals if required (Daneman 2006). The insulin pump lowers the risk of episodes of loss of blood glucose control, but many diabetics prefer not to use them as they don't like to be permanently connected to a machine (Daneman 2006).

Neither insulin injections nor insulin pump administration maintain normoglycemia as it is impossible to correctly balance insulin intake with food intake (in particular carbohydrates), exercise, stress and illness (Daneman 2006). This means that all diabetics experience incidences of hypo- and hyperglycemia (Daneman 2006). The patient needs to adjust their administration of insulin according to each of the latter factors. It is preferable for patients to continually monitor their blood glucose concentrations by using the finger prick test in order to ensure they are maintaining normoglycemia, and can intervene before blood glucose levels become too unbalanced (Daneman 2006). Given the above, there is a need for a treatment form that can give a degree of control of blood glucose levels similar to that achieved by the pancreas, where the release of insulin is perfectly matched to increasing blood glucose concentrations without the errors associated with human intervention.

1.1.3 Type 1 diabetes prevention and treatment

Pancreatic β-cell renewal can occur through both residual β-cell proliferation and also from the differentiation of stem cells within the pancreas, such as ductal progenitor cells (Nichols and Cooke 2009). Type 1 diabetics do not make enough β-cells to keep up with the insulin demand due to the continuous immune destruction of newly formed β-cells. Whole pancreas transplants were first performed in the 1960s with the aim of introducing a healthy fully functional pancreas capable of maintaining normoglycemia (Ren *et al.* 2007). Shortly thereafter islets were isolated from human pancreases prior to transplantation with 23,000 human pancreatic islet transplants being performed between 1966 and 2004 (Ren *et al.* 2007). Approximately 85% of transplant patients experience no need for exogenous insulin administration for 1 year after transplantation, and 50% of patients can expect to be able to maintain normoglycemia for 5 years post-transplantation (Ren *et al.* 2007). However, the majority of pancreatic islet transplants fail within 10 years. Further, patients who have received a transplant must take immunosuppressive drugs to prevent graft-rejection which exposes them to infection, and potentially to cancer (Ren *et al.* 2007).

The Edmonton protocol is currently the most successful procedure used to transplant islets (Ren *et al.* 2007). It requires islets isolated from the pancreases of 2 or more donors per recipient (Ren *et al.* 2007). The Edmonton protocol uses an antibody against the IL-2 receptor (daclizumab), together with the drugs sirolimus (rapamycin) and tacrolimus for immunosuppression (Shapiro *et al.* 2006). The viability of the islets was improved pre-transplant by reducing the time prior to isolation and using a collagenase procedure to harvest individual islets (Shapiro *et al.* 2006). In a clinical trial of 36 patients, 44% of patients experienced no severe incidences of hypo- or hyperglycemia for up to 1 year, 28% had partial graft function, and 28% experienced graft loss (Shapiro *et al.* 2006). After 3 years 31% of patients retained at least partial function of the graft and 3% (1 patient) remained insulin-independent (Shapiro *et al.* 2006). There were no reported deaths or cancers associated with the transplantation procedure, however, 38 serious adverse events were recorded (Shapiro *et al.* 2006). These included neutropenia (low number of neutrophils), pneumonia, mouth ulcers and gastrointestinal conditions (Shapiro *et al.* 2006). Prolonged graft maintenance without the need for toxic immunosuppressive regimes remains to be achieved. The requirement for multiple organ donors per patient is also an issue due to the limited number of donors.

Animal models of type 1 diabetes have revealed novel ways to protect transplanted human islets from immune destruction (Ren *et al.* 2007). Encapsulation of pancreatic islets within an ultra-high viscosity clinical-grade alginate cross-linked with Ba^{2+} provides a protective environment, where glucose has entry and pancreatic hormones including insulin produced by the islets can be released from the capsules (Ren *et al.* 2007). In contrast, destructive immune cells such as macrophages and T cells cannot enter the capsule (Ren *et al.* 2007). The encapsulated human islets are capable of responding to external increases in glucose concentration by releasing insulin (Ren *et al.* 2007). Immunocompetent diabetic mice transplanted with 1,800 encapsulated human islets into the peritoneal cavity became normoglycemic within 24 h after transplantation and continued to maintain normoglycemia for >270 days (Ren *et al.* 2007). In comparison, non-encapsulated islets promoted normoglycemia for only ~4-8 days before the graft was rejected (Ren *et al.* 2007). Upon explantation of the alginate-encapsuled islets the mice became hyperglycaemic demonstrating that the normoglycemia was maintained by the transplanted islets (Ren *et al.* 2007).

The shortage of donors has spurred efforts to identify other sources of β-cells. Other potential sources of β-cells include those from xenogeneic sources such as the pig (Elliott *et al.* 2007), and human stem cells which have been differentiated towards the β-cell-lineage and are capable of secreting insulin. There are many different populations of human stem cells which could fill the need for β-cell replacement therapy (see below).

1.2 Differentiation of embryonic stem cells into definitive endoderm and then to insulin-producing β-cells

It is logical to follow the natural developmental stages of human embryonic development in order to differentiate stem cells into insulin-producing pancreatic cells. Different research groups have employed a variety of different approaches to differentiate embryonic stem cells (ESCs) along the pancreatic differentiation pathway in strict stage-specific regimes. There are at least five

stages of differentiation by which ESCs are converted into definitive endoderm and then into insulin-producing cells (D'Amour *et al.* 2006). These are described below and in Table 1.1

Table 1.1 The 5 stages of differentiation of ESCs to definitive endoderm, and then to insulin-producing β-cells.

	Stage 1		Stage 2	Stage 3	Stage 4	Stage 5
	Definitive endoderm		Primitive gut tube	Posterior foregut	Pancreatic endoderm and endocrine precursor	Hormone expressing endocrine cell
Differentiation factors	Activin A + Wnt	Activin A	FGF10 + CYC	FGF10 + CYC + RA	FGF10 + CYC + RA + DAPT + Ex4	FGF10 + CYC + RA + Ex4 + IGF-1 + HGF
	RPMI	RPMI + 0.2% FBS	RPMI + 2% FBS	DMEM + 1% B27	DMEM + 1% B27	CMRL + 1% B27
Stage-specific markers	SOX-17 CER FOXA2 CXCR4		HNF1b HNF4a	PDX-1 HNF6 HLXB9	Nkx6.1 NGN3 Pax4 Nkx2.2	Insulin Glucagon Ghrelin Somatostatin Pancreatic polypeptide

The table illustrates the differentiation factors and cell culture media that some researchers have used to induce each of these stages, and several key differentiation markers expressed at each stage. Abbreviations: FGF10 – fibroblast growth factor 10, CYC – KAAD-cyclopamine, RA – all-trans retinoic acid, DAPT – N-[N-(3,5-difluorophenacetyl)-L-alanyl]-S-phenylglycine t-butyl ester, Ex4 – exendin-4, IGF-1 – insulin-like growth factor 1, HGF – hepatocyte growth factor.

ESCs are defined by expression of the stem cell markers octamer-binding transcription factor 4 (Oct-4), Nanog, sex determining region Y-box 2 (SOX-2) and epithelial cadherin (ECAD) (D'Amour *et al.* 2006). During the first stage of pancreatic differentiation ESCs must form definitive endoderm, which involves two steps (D'Amour *et al.* 2006). In the first step the stem cells exposed to differentiation medium begin to express Brachyury, FGF4, Wnt3 and neural cadherin (D'Amour *et al.* 2006). They then progress along the pancreatic lineage to express the definitive endoderm markers SOX-17, Forkhead box protein A2 (FOXA2) and chemokine receptor 4 (CXCR4) (D'Amour *et al.* 2006). During the second stage the definitive endoderm cells are differentiated into HNF1β and HNF4a expressing cells that make up the primitive gut tube (D'Amour *et al.* 2006). The third stage involves differentiation into the posterior foregut in which cells express the pancreatic posterior foregut markers PDX-1, HNF6 and homeobox HB9 (HLXB9) (D'Amour *et al.* 2006). The development of a pancreas *in vivo* is then mimicked with the formation of pancreatic endoderm-containing endocrine precursor cells expressing Nkx6.1, Nkx2.2, neurogenin3 (NGN3) and Pax4 (D'Amour *et al.* 2006). The fifth and final stage is the differentiation of the cells into a hormone-expressing pancreatic cell type defined by the expression of insulin, glucagon, ghrelin, somatostatin or pancreatic polypeptide, depending on the differentiation protocol.

1.2.1 The importance of PDX-1 in pancreatic and neural development and function

As mentioned above, PDX-1 is expressed after differentiation of stem cells into the posterior foregut (D'Amour *et al.* 2006). In the embryo, PDX-1 expression occurs in the area formed from fusion of the ventral and dorsal walls in the primitive foregut from which the pancreas develops, and later in development PDX-1 is expressed at this site in the duodenum (Ohlsson *et al.* 1993). PDX-1 expression is vital to the development of the pancreas (Jonsson *et al.* 1994). Mice homozygous for a targeted PDX-$1^{-/-}$ mutation do not develop a pancreas (Jonsson *et al.* 1994). They survive foetal development, but die shortly after birth due to insulin insufficiency, other pancreatic hormone deficiencies and a lack of exocrine digestive enzymes (Jonsson *et al.* 1994). Pups with the PDX-$1^{-/-}$ mutation are slightly smaller in size, but have a normal length gastrointestinal tract, and all their other internal organs are normal including the duodenum from which the pancreas branches (Jonsson *et al.* 1994). Thus, the hypothesis is that PDX-1 is specifically required for the determination and maintenance of the pancreas during foetal development (Jonsson *et al.* 1994). Further research showed PDX-$1^{-/-}$ mutant mice form pancreatic buds, but the dorsal bud has poor proliferative potential and forms a small abnormal ductular tree (Offield *et al.* 1996). The ductular tree contains glucagon-expressing cells, but no insulin or amylase positive cells (Offield *et al.* 1996). The duodenal site where normal pancreatic development occurs is also abnormal as it has no epithelial lining, villi or Brunner's glands (Offield *et al.* 1996). Instead, there are glucose transporter-2 (Glut-2) positive cells similar to those seen in the bile duct (Offield *et al.* 1996).

The Cre/LoxP labelling system, where the expression of Cre was driven by the PDX-1 gene promoter, has been utilised to trace the lineage of PDX-1 expressing cells in mice (Gu *et al.* 2003). In a mouse at embryonic day 8.5, pancreas development begins with the endoderm and mesoderm interacting causing some endodermal cells at the mid-foregut junction to start to form the pancreas (Gu *et al.* 2003). Proliferation of these cells results in formation of the pancreatic rudiment and expression of PDX-1 at day 8.5 (Gu *et al.* 2003). The PDX-1-expressing cells are capable of forming all of the different cell types within the pancreas (Gu *et al.* 2003). In the mouse, PDX-1 expression at days 8.5-11.5 promotes the formation of the pancreatic duct, exocrine acini and endocrine islets (Gu *et al.* 2003). NGN3 is only transiently expressed during embryonic development of the pancreas (Gu *et al.* 2003). NGN3 expressing cells differentiate into all of the different cell types that make up the endocrine islets (Gu *et al.* 2003).

PDX-1 also plays a key role within the islet β-cells of the adult pancreas as it binds to the insulin promoter and controls the expression of insulin (Ohlsson *et al.* 1993). In adult rats, PDX-1 is also expressed by islet δ-cells of the pancreas (Leonard *et al.* 1993). It binds a region in the somatostatin gene promoter called the tissue-related elements (I and II), and regulates the expression of somatostatin (Leonard *et al.* 1993). However, PDX-1 is not β- and δ-cell-specific as it is also expressed by other pancreatic and intestinal endocrine cells that do not express somatostatin where its function is unknown (Leonard *et al.* 1993). PDX-1 is expressed by the monocyte cell line THP-1, the cancer cell lines HEK-293 (embryonic kidney) and HeLa (uterine cervical carcinoma), in which it negatively regulates human cytomegalovirus (CMV) immediate early (IE) gene expression (Chao *et al.* 2004). The CMV IE gene is essential for viral replication (Chao *et al.* 2004). In undifferentiated THP-1 cells, PDX-1

specifically binds the CMV IE promoter and represses CMV IE gene expression (Chao *et al.* 2004). However when the THP-1 monocytes differentiate into macrophages with the addition of phorbol 12-myristate 13-acetate (PMA), the expression of the CMV IE gene is no longer repressed despite continued expression of PDX-1 (Chao *et al.* 2004). PDX-1 is also expressed in the forebrain region of the rat central nervous system during embryonic development (Perez-Villamil *et al.* 1999). In the developing rat brain, PDX-1 has the ability to bind the promoter of the glial acidic fibrillary gene via the homeodomain protein DNA-binding site (Perez-Villamil *et al.* 1999). This finding suggests a possible role for PDX-1 in controlling the differentiation of neural cells during the development of the central nervous system (Perez-Villamil *et al.* 1999). Since there are some cells in the brain which express both PDX-1 and somatostatin, it is possible that PDX-1 controls the expression of neuronal somatostatin which serves as a neurotransmitter (Perez-Villamil *et al.* 1999).

1.3 Factors used to differentiate stem and progenitor cells into insulin-producing cells

To date there is not a single protocol which is capable of differentiating stem cells into "β-cell-like cells" that highly express insulin. Most current protocols, such as the one used by D'Amour *et al.* (2006), involve groups of agents which are added at specific stages of cell development to promote differentiation along the pancreatic lineage. The differentiation factors currently used to promote the differentiation of stem and progenitor cells into functional β-cells are discussed below.

1.3.1 Factors that induce formation of definitive endoderm

Factors that induce the formation of definitive endoderm include activin A, inducer of definitive endoderm-1 (IDE-1), and IDE-2 (D'Amour *et al.* 2005; Borowiak *et al.* 2009). hESCs treated with activin A in the presence of low serum (0.5%) for 5 days formed cells expressing SOX-17 and FOXA2 which resembled those found in definitive endoderm (D'Amour *et al.* 2005). Up to 80% of the differentiated hESCs expressed SOX-17 (D'Amour *et al.* 2005). D'Amour *et al.* (2005) discovered that hESCs differentiated into definitive endoderm express the marker CXCR4, which provides a specific biomarker for selecting these cells. Borowiak *et al.* (2009) screened 4,000 small molecules to identify those that can differentiate hESCs into definitive endoderm as defined by expression of SOX-17. They identified two such molecules, designated IDE-1 and IDE-2. The majority of hESCs (62%) treated for 4 days with IDE-1 express SOX-17, similar to the response to treatment with activin A (64%) (Borowiak *et al.* 2009). IDE-2 also induces definitive endoderm differentiation, with 57% of treated cells expressing SOX-17 (Borowiak *et al.* 2009). The addition of activin A and Wnt3a in combination with IDE-1 or IDE-2 increases definitive endoderm formation by only a further 3-5% (Borowiak *et al.* 2009).

The differentiation of ESCs expressing Oct-4 and CD9 to definitive endoderm expressing SOX-17, CXCR4 and FOXA2 can also be promoted by inhibition of phosphatidylinositol 3-kinase (PI3K) (McLean *et al.* 2007). The PI3K inhibitor LY294002 induced ESCs to form definitive endoderm under normal serum culture conditions (McLean *et al.* 2007). Usually the self-renewal of stem cells is promoted with the use of foetal bovine serum (FBS) (McLean *et al.* 2007). However, in low serum conditions there is a

low level of PI3K signalling allowing for differentiation into definitive endoderm (McLean *et al.* 2007). Further, differentiation studies with hESCs have shown that the formation of definitive endoderm can be inhibited by the presence of insulin and insulin-like growth factor (IGF) (McLean *et al.* 2007). Serum contains insulin and IGF in biologically active amounts that will inhibit the formation of definitive endoderm during differentiation (McLean *et al.* 2007). The inhibition by insulin and IGF of differentiation into definitive endoderm was shown by supplementing media with insulin and IGF, which resulted in reduced activin A-induced definitive endoderm differentiation (McLean *et al.* 2007).

1.3.2 Primitive gut tube differentiation

As noted above, the stage of primitive gut tube development is characterised by the expression of the gut tube markers HNF1β and HNF4a (D'Amour *et al.* 2006). The protocol by D'amour *et al.* (2006) uses FGF10 and KAAD-cyclopamine in low serum to differentiate definitive endoderm cells to primitive gut tube cells (D'Amour *et al.* 2006). The differentiation is characterised by changes in definitive endoderm marker expression (D'Amour *et al.* 2006). The expression of CXCR4 is down-regulated whilst SOX-17 is maintained in HNF1β-expressing cells (D'Amour *et al.* 2006). Cyclopamine is a Sonic hedgehog (Shh) inhibitor which promotes pancreatic development (Kim and Melton 1998). The growth factor FGF10 is also used to promote endoderm differentiation and is normally expressed by the pancreatic mesenchyme during the early stages of pancreatic development (Bhushan *et al.* 2001; D'Amour *et al.* 2006). The addition of FGF10 and KAAD-cyclopamine during this differentiation stage eventually results in increased insulin mRNA expression at the final stage of differentiation of definitive endoderm into β-cells (D'Amour *et al.* 2006).

1.3.3 Posterior foregut differentiation

Posterior foregut development is characterized by the expression of PDX-1 and HNF6 (D'Amour *et al.* 2006). D'amour *et al.* (2006) showed that PDX-1 and HNF6 are upregulated in hESCs following incubation with retinoic acid + FGF10 + KAAD-cyclopamine in serum-free (1% B27) DMEM medium. Retinoic acid is required for posterior foregut differentiation and the expression of NGN3, insulin and glucagon during the final stages of pancreatic development when PDX-1 is expressed (D'Amour *et al.* 2006). *In vivo,* the plant-derived chemical cyclopamine expands the region of the gut in which Shh signalling is repressed resulting in a larger area of PDX-1 positive cells becoming foregut endoderm (Kim and Melton 1998). Expression of the primitive gut tube markers HNF1β and HNF4a is maintained during posterior foregut differentiation (D'Amour *et al.* 2006).

1.3.3.1 Increasing the percentage of PDX-1 expressing cells

A high-content screen developed to find molecules that increase the number of PDX-1-expressing endoderm-differentiated (SOX-17 and FOXA2 expressing) ESCs unveiled (-)-Indolactam V (ILV) as a strong inducer of PDX-1 expression and promoter of the β-cell lineage (Chen *et al.* 2009). The expression of PDX-1 was doubled after 4 days of treatment of the endoderm differentiated ESC cell line with ILV (Chen *et al.* 2009). ILV promotes the expression PDX-1 in a protein kinase C-dependent fashion (Chen *et al.* 2009). ILV increased the percentage of PDX-1-expressing cells in a dose-dependent manner, with the

highest increase in the absence of toxicity obtained at 300 nM (Chen *et al.* 2009). ILV in combination with another pancreatic differentiation agent, FGF10, almost doubled the percentage of PDX-1-expressing cells (Chen *et al.* 2009). Substitution of ILV with the PKC agonist, PMA, resulted in a third of cells expressing PDX-1 (Chen *et al.* 2009). Selective inhibition with indolocarbazole Gő 6976, which inhibits Ca^{2+}-dependent isoforms of PKC, inhibited ILV from increasing PDX-1 expression (Chen *et al.* 2009). Importantly, the ILV-treated cells also expressed other pancreatic progenitor markers including HNF6, FOXA2, Nkx6.1 and pancreas transcription factor 1-α (Ptf1a) (Chen *et al.* 2009). The ILV and FGF10 treated cells were further differentiated towards mature endocrine pancreatic cells by culturing them with nicotinamide and bovine FGF for 12 days (Chen *et al.* 2009). The small number of cells expressing insulin and C-peptide increased four-fold after treatment (Chen *et al.* 2009). The cells treated with ILV and FGF10 were also subjected to *in vivo* differentiation by placing them under the kidney capsule of nude mice where the cells began to express insulin, C-peptide (endocrine marker) and amylase (exocrine marker). In contrast, DMSO-treated cells did not express these markers (Chen *et al.* 2009). In accord with the fact that hESCs form teratomas in mice (Prokhorova *et al.* 2009), 8 out of 10 mice transplanted with the DMSO-treated cells developed tumours (Chen *et al.* 2009). In contrast, only 1 of 6 mice given the ILV-treated cells developed tumours, and only 2 of 6 mice given the ILV + FGF10-treated cells developed tumours (Chen *et al.* 2009).

Another research group tested ILV in combination with a modified version of the differentiation protocol devised by D'Amour *et al.* (2006) to promote the endocrine differentiation of induced pluripotent stem cells (iPSC) instead of hESCs (Thatava *et al.* 2010). In this study the combination of FGF10 and KAAD-cyclopamine together with retinoic acid and ILV resulted in expression of PDX-1, NGN3 and NeuroD (Thatava *et al.* 2010). The cells were then further differentiated with HGF, IGF-1 and Ex4, but failed to produce C-peptide (Thatava *et al.* 2010). Therefore the protocol was modified to include glucagon-like peptide-1 (GLP-1) instead of Ex4 to increase the β-cell mass, which resulted in the production of C-peptide-positive islet-like clusters (Thatava *et al.* 2010).

Given the importance of PDX-1 for the formation of the pancreas, it is not surprising that the addition of PDX-1 protein to differentiation protocols promotes the differentiation of stem cells towards the formation of insulin-producing cells (Noguchi *et al.* 2003). Sequencing of the PDX-1 gene sequence revealed the deduced protein contains an antennapedia-like protein transduction domain which enables it to freely enter cells (Noguchi *et al.* 2003). The PDX-1 protein administered to cells was stable for at least 48 hours (Noguchi *et al.* 2003). The PDX-1 protein added to the pancreatic cell line MIN6 drove expression of the insulin promoter (Noguchi *et al.* 2003). Treatment of isolated Sprague-Dawley rat islets and MIN6 cells with PDX-1 increased insulin mRNA expression (Noguchi *et al.* 2003). PDX-1 spontaneously entered rat pancreatic duct cells and promoted the production of mRNA encoding insulin, PDX-1 and Nkx6.1 (Noguchi *et al.* 2003). Thus, addition of the PDX-1 protein to cells can promote insulin transcription and differentiation towards the β-cell lineage (Noguchi *et al.* 2003).

1.3.4 Differentiation of hESCs into pancreatic endoderm and hormone expressing cells

hESCs that have been differentiated into cells that resemble those of the posterior foregut stage of pancreatic differentiation require additional factors to differentiate into pancreatic endoderm cells, as exemplified by the protocol of D'Amour *et al.* (2006). Their incubation with N-[N-(3,5-difluorophenacetyl)-L-alanyl]-S-phenylglycine t-butyl ester (DAPT) and Ex4 for an additional 2-3 days in serum-free medium + 1% B27 results in the expression of pancreatic-specific markers (D'Amour *et al.* 2006). Specifically the cells co-express PDX-1 and Nkx6.1, HNF6 and Nkx6.1 and occasionally Nkx2.2 and PDX-1 or Nkx6.1 or NGN3 (D'Amour *et al.* 2006). The hESCs can then be finally differentiated into hormone-expressing cells by culture with Ex4, HGF and IGF-1 in serum-free medium containing 1% B27 (D'Amour *et al.* 2006). They express the hormones insulin, glucagon, somatostatin, pancreatic polypeptide and ghrelin (D'Amour *et al.* 2006). The differentiating cells co-express PDX-1 and Nkx6.1, a subset of which express Nkx2.2 (D'Amour *et al.* 2006). Nkx2.2-expressing cells also transiently express NGN3 (D'Amour *et al.* 2006). The cells co-express PDX-1 and Nkx2.2 during the early stages of insulin expression where the level of expression is low (not filling the cytoplasm) (D'Amour *et al.* 2006). Prolonged culture of the differentiating cells resulted in co-expression of Pax6 and islet-1 (ISL-1) and insulin expression which filled the cytoplasm (D'Amour *et al.* 2006). The differentiated cells grew in adherent monolayers, and also formed multi-layers (D'Amour *et al.* 2006). The D'Amour *et al.* (2006) protocol on average yielded 7.3% insulin positive and 13.4% somatostatin positive cells.

1.3.5 Enhancing the differentiation of stem cells towards the pancreatic β-cell lineage

Differentiation of stem cells into pancreatic progenitors and insulin-producing cells can be enhanced by treatment with the BMP-2 protein (Talavera-Adame *et al.* 2011). This finding resulted from the discovery that mouse embryoid bodies (EB) cocultured with human microvascular endothelial cells differentiate into PDX-1, NGN3, Nkx6.1, proinsulin, Glut-2 and PTF1A expressing cells at the EB and microvascular endothelial cell junctions (Talavera-Adame *et al.* 2011). However, the expression of Pax4, Pax6, NeuroD1 and MafA remained unchanged (Talavera-Adame *et al.* 2011). Importantly, the expression of mRNA encoding insulin and amylin increased (Talavera-Adame *et al.* 2011). Investigation of the factors involved in EB differentiation induced by the conditioned medium from human microvascular endothelial cells revealed increases in the expression of BMP-2 and its BMP type IA receptor (Talavera-Adame *et al.* 2011). The differentiation of EBs could be partially mirrored by culture of EBs with recombinant human BMP-2 protein for 15 days (Talavera-Adame *et al.* 2011). BMP-2 upregulated the expression of PDX-1, Nkx6.1, insulin, and amylin, however, the expression of NGN3 did not change (Talavera-Adame *et al.* 2011). Thus, BMP-2 is capable of inducing the differentiation of EBs towards the pancreatic lineage, but other factors in human microvascular endothelial cell conditioned medium also play a role.

1.3.6 Other differentiation factors that have been trialled for differentiating stem cells towards the pancreatic cell lineage

Different stem cell populations will differentiate differently in response to the same differentiation factors, as exemplified by the results obtained with hESCs from different laboratories (Cho *et al.* 2008). Cho *et al*. (2008) utilized the earlier published protocol by D'Amour *et al.* (2006), where activin A was used to induce a definitive endoderm phenotype, followed by KAAD-cyclopamine and FGF10 and then all-trans retinoic acid. KAAD-cyclopamine and FGF10 were used to differentiate the hESCs into PDX-1 expressing cells (Cho *et al.* 2008). For the final stage of differentiation DAPT and Ex4 were added, according to the D'Amour *et al.* (2006) protocol, however PDX-1 expression was lost, and C-peptide was absent, whereas the cells expressed glucagon (Cho *et al.* 2008). Betacellulin (BTC) and nicotinamide had to be added for sustained PDX-1 expression and to induce both C-peptide and glucagon expressing clusters, and insulin mRNA expression (Cho *et al.* 2008). However, even with the addition of BTC and nicotinamide, the level of insulin gene expression was much lower than that of pancreatic islets, leaving room for future improvement (Cho *et al.* 2008).

Another research group treated hESCs with activin A and then with a combination of activin A and all-trans retinoic acid, followed by differentiation in DMEM/F12 islet maturation medium containing bFGF for 3 days, and then DMEM/F12 with bFGF and nicotinamide for an additional 3 days (Jiang *et al.* 2007). The cells were then cultured for 5 days in DMEM/F12 with bFGF and nicotinamide on a hydrophobic plate, forming suspended islet-like clusters that expressed mRNAs for PDX-1, Glut-2, insulin and glucokinase (Jiang *et al.* 2007). The clusters which were then seeded onto Matrigel-coated plates variably expressed several pancreatic proteins including PDX-1, C-peptide, glucagon, somatostatin and amylase (Jiang *et al.* 2007). The cells no longer expressed Oct4, a marker of undifferentiated stem cells (Jiang *et al.* 2007). Interestingly this study found that the hESCs differentiated with the above protocol secreted increased insulin and C-peptide in response to glucose challenge when cultured in suspension compared with attachment to plates (Jiang *et al.* 2007).

1.4 The role of Nestin in the differentiation of pancreatic cells

1.4.1 Pre-selection of Nestin positive cells

Stem cell populations can be pre-selected for certain markers to select those more amenable for differentiating towards the β-cell lineage. Primate ESCs express Nestin, stage specific embryonic antigen-4 (SSEA-4) and have alkaline phosphatase activity (Yue *et al.* 2006). They were expanded and selected for Nestin expression, and then treated with or without GLP-1 in serum-free medium for either 10 or 30 days (Yue *et al.* 2006). The Nestin$^+$ cells became mostly insulin$^+$ and C-peptide$^+$, and formed islet-like clusters after 10 and 30 days with or without exposure to GLP-1 (Yue *et al.* 2006). They expressed mRNA for insulin, PDX-1, Glut-2 and NGN3 (Yue *et al.* 2006). Nestin expression began to decrease in islet-like clusters, as insulin expression increased (Yue *et al.* 2006).

1.4.2 Nestin is expressed by pancreatic precursor cells

Nestin is expressed by both adult rat pancreatic ductal stem (PDS) cells and mouse ESCs (Kim *et al.* 2010). PDS cells are isolated from the neogenic ductules after subtotal pancreatectomy (Kim *et al.* 2010). The expression of Nestin in PDS cells increases after cell isolation for up to 3 days, and at the early stage of EB formation by ESCs (Kim *et al.* 2010). Knockdown of Nestin in ESCs by siRNA and culture of the cells in medium containing serum with no added differentiation or growth factors resulted in upregulation of the pluripotent stem cell markers Oct-4, and SSEA-1, and mRNA encoding Nanog (Kim *et al.* 2010). The upregulation of these stem cell markers indicates the cells were inhibited from differentiating after knockdown of Nestin (Kim *et al.* 2010). Mouse ESCs that have been differentiated *in vitro* to form EBs and PDS cells express pancreatic-associated genes (Kim *et al.* 2010). However downregulation of Nestin caused downregulation of the expression of these genes (Kim *et al.* 2010). Messenger RNAs encoding PDX-1, NGN3, and ISL-1 were downregulated, as well as mRNAs of the mature pancreas including those encoding insulin and glucagon (Kim *et al.* 2010). C-peptide and insulin proteins were downregulated, and accordingly insulin secretion was reduced (Kim *et al.* 2010). Therefore it was suggested that Nestin induces the transition of stem cells from a proliferative state to a state of differentiation (Kim *et al.* 2010). Nestin may also play a role in inhibiting the expression of Oct-4 and Nanog (Kim *et al.* 2010). It is important to note that Nestin is not necessarily a marker for pancreatic development. A Nestin progenitor cell can differentiate into either the neuronal or pancreatic cell type (Lumelsky *et al.* 2001). Indeed, it was because of the belief that Nestin was a marker of the pathway towards β-cell development that the stem cell field was misled a decade ago with much effort being made to follow this pathway (Lumelsky *et al.* 2001).

1.5 Similarities between pancreatic and neuronal cell lineages

1.5.1 Morphological and physiological similarities shared by pancreatic and neuronal cells

The cells of the central nervous system and the pancreas share common elements in terms of their morphologies and physiologies (Arntfield and van der Kooy 2011). For instance, neurons and β-cells process insulin and neurotransmitters, respectively, in similar ways which points to a potential common evolutionary pathway (Arntfield and van der Kooy 2011). In particular, the storage of insulin, and the process by which it is released mimics the storage and release of neurotransmitters (Arntfield and van der Kooy 2011). Pancreatic and neuronal cells share the common function of secreting low molecular weight polypeptide hormones, and are termed amino precursor uptake and decarboxylase cells (Arntfield and van der Kooy 2011). Interestingly, both β-cells and neurons do not express repressor element 1 silencing transcription factor which is expressed by non-neuronal cells (Arntfield and van der Kooy 2011). The similarities also extend to gene expression including the expression of the pancreatic transcription factors PDX-1 and Islet-1 by developing neuronal cells (Arntfield and van der Kooy 2011).

1.5.2 Common ancestry of pancreatic and neuronal cells

It is thought that insulin may be conserved through the evolution of species as seen by insulin-like proteins which have been isolated in single-cell bacteria such as *Escherichia coli* (Arntfield and van der Kooy 2011). Other evolutionary distantly related species such as *Aurelia aurita*, a jelly fish, have neuronal cells, but do not express insulin in the gut (Arntfield and van der Kooy 2011). Instead the jelly fish uses neuronal cells to express insulin and regulate blood glucose (Arntfield and van der Kooy 2011). As evolution continued, the nematode *Caenorhabditis elegans*, evolved to express insulin in both the gut and nervous system (Arntfield and van der Kooy 2011). Interestingly the fruit fly *Drosophila melanogaster* does not express insulin in the gut, but instead it expresses insulin in the brain (Arntfield and van der Kooy 2011). The first species to form islet clusters (which also contain somatostatin cells) was the jawless fish, Agnatha, in which glucose levels are controlled by islet clusters within the gut (Arntfield and van der Kooy 2011). These clusters are thought to be the first signs of the evolution of an endocrine pancreas (Arntfield and van der Kooy 2011). The similarities between the early development of neurons and β-cells led to the hypothesis that neuronal stem cell differentiation protocols may help in the differentiation of precursor cells to functional β-cells, and provide insights into how β-cells develop and function (Arntfield and van der Kooy 2011).

1.5.3 Similarities between pancreatic and neuronal differentiation

Both neurons and β-cells develop from an endocrine precursor and respond to notch and NGN to differentiate along the neuronal and endodermal lineages (Arntfield and van der Kooy 2011). NGN-1 and -2 promote neuronal fate specification, whilst NGN3 promotes pancreatic development (Arntfield and van der Kooy 2011). During development *in vivo* the stem cells that create both neurons and pancreatic cells do not originate from the same population of cells (Arntfield and van der Kooy 2011). The pancreas still develops in rats in which the neural tube has been removed, which shows that pancreatic development does not require neuronal stem cells (Arntfield and van der Kooy 2011). Pancreatic precursors can be differentiated into neurons *in vitro* with neuronal differentiation factors by treating the cells as if they were neuronal stem cells (Arntfield and van der Kooy 2011). Insulin-producing cells *in vivo* have also been differentiated into neurons without requiring any additional external differentiation factors (Arntfield and van der Kooy 2011).

1.6 Genuine insulin expression by differentiated stem cells

A functional β-cell is characterised by the ability to release appropriate amounts of insulin in response to a glucose challenge (Hansson *et al.* 2004). Insulin release must be proven to be genuine, and not simply represent uptake of insulin protein from the medium. Typically, C-peptide which is a by-product of the processing of mature insulin is used as a measure of insulin synthesis, and can be quantified by ELISA and radioimmunoassay (RIA) following exposure to incremental increases in glucose concentration (Hansson *et al.* 2004). Some protocols intended to differentiate precursor cells into β-cells lead to uptake of insulin from the medium rather than insulin synthesis, thereby confounding the results and potentially leading to misinterpretation (Hansson *et al.* 2004). In one such example, the human embryonic cell line OS25 was exposed to several different differentiation protocols which produced clusters of cells that were positive for insulin by immunocytochemistry, but were not positive for C-

peptide, PDX-1 or glucagon (Hansson *et al.* 2004). PCR analysis indicated that the cells did not express mRNA transcripts encoding insulin, PDX-1 and prohormone convertase (PC) 2 (Hansson *et al.* 2004). It was also discovered that the insulin positive cells were undergoing apoptosis and necrosis (Hansson *et al.* 2004). In another example, a mouse embryonic cell line, which was grown in the presence of FITC-labelled insulin, became fluorescent indicating that insulin had been taken up into the cells from the medium (Hansson *et al.* 2004). Therefore, an array of evidential proof must be gathered to ascertain that cells express insulin and are β-cell-like, including the presence of C-peptide, insulin and C-peptide mRNA, and the presence of additional β-cell-restricted proteins.

1.7 Stem cells found in peripheral blood

1.7.1 Peripheral blood insulin-producing cells

1.7.1.1 Characteristics of peripheral blood insulin-producing cells (PB-IPCs)

A novel peripheral blood stem cell population was discovered by Zhao *et al.* (Zhao *et al.* 2007a), which spontaneously produces insulin on culture. These cells were termed peripheral blood insulin-producing stem cells (PB-IPCs). They represent an attractive stem cell population for regenerative medicine, as they can be collected relatively non-invasively. PB-IPCs found in the blood are defined as stem cells as they express the stem cell markers Oct-4 and Nanog and show excellent plasticity (Zhao *et al.* 2007a). They can be differentiated into many different cell types including β-cells, other pancreatic lineage cell types, neuronal cells and cardiac cells (Zhao and Mazzone 2008). PB-IPCs are isolated from the Ficoll-fractionated buffy coat of venous blood (Zhao *et al.* 2007a). They are defined by their unique ability to bind to hydrophobic, positively charged surfaces, and can be easily selected from the mononuclear cell population by simple adherence to hydrophobic plastic dishes normally used in microbiology (Zhao *et al.* 2007a). They express a variety of hematopoietic markers including the tetraspanin CD9, stem cell factor receptor CD117, and the leukocyte common antigen CD45, but do not express the HSC marker CD34 (Zhao *et al.* 2007a). PB-IPCs do not express monocyte or macrophage markers including CD14 and CD11b/Mac-2 (Zhao *et al.* 2007a). In comparison with freshly isolated monocytes, they do not express the human leukocyte antigen HLA-DR, CD80 and CD40 (Zhao *et al.* 2007a). However, 10% of PB-IPCs do express HLA-DQ and strongly express HLA-ABC (Zhao *et al.* 2007a). PB-IPCs do not bind to tissue culture dishes, which only bind monocyte/macrophages (Zhao *et al.* 2007a). They appear to have a unique phenotype which suggests they are a novel population of stem cells found in peripheral blood (Zhao *et al.* 2007a).

Zhao *et al.* revealed that mRNA transcripts for the pancreatic transcription factors MafA, Nkx6.1, and HNF6 could be amplified from PBMCs, together with transcripts encoding insulin, somatostatin, ghrelin and the K(ATP) channel proteins Sur-1 and Kir6.2, which are involved in the release of insulin (Zhao *et al.* 2007a). PB-IPCs which attached to hydrophobic surfaces were shown by Western blot analysis to express MafA, Nkx6.1, PDX-1, NeuroD and also the insulin convertases PC1/3 and PC2 (Zhao *et al.* 2007a). PBMCs also express MafA, Nkx6.1, PC1/3 and PC2 proteins, however at much weaker levels than the selected PB-IPC

population (Zhao *et al.* 2007a). PB-IPCs express insulin (0.246 ng/μg cell protein) and C-peptide (35.76 fmol/mg cell protein), as shown by ELISA (Zhao *et al.* 2007a). For a comparison with other cell types see Table 1.2. The expression of insulin mRNA was confirmed by *in situ* hybridization (Zhao *et al.* 2007a). Transmission electron microscopy of PB-IPCs revealed an insulin-specific "halo" structure of granules in the cytoplasm (Zhao *et al.* 2007a). Approximately 70% of PB-IPCs co-express insulin and CD45 (Zhao *et al.* 2007a).

Table 1.2 Comparison of the amount of insulin and C-peptide expressed by various cell types

Cell type	Insulin	C-peptide
Mature beta cell	44 ng/μg protein	
PB-IPCs	0.25 ng/μg protein	35.76 fml/mg protein
PCMO - Neoislets	0.87 ng/μg protein	0.89 ng/μg protein
Chandra differentiated ASCs		582.56 pM
Chandra undifferentiated ASCs		16.88 pM
Rat β-cell	21.5 μg/1x10^6 cells	
INS-1E	2.15 μg/1x10^6 cells	
RINm5f	0.19 pg/cell	

1.7.1.2 Expansion of PB-IPCs

The proliferation of PB-IPCs can be promoted with various agents, but they will also proliferate on their own when attached to hydrophobic plates (Zhao *et al.* 2007a). Zhao and Mazzone (2008) used granulocyte-macrophage colony stimulating factor (GM-CSF), GLP-1 and Ex4 to enhance the proliferation of PB-IPCs. GLP-1 has been shown to increase the proliferation of β-cells via transactivation of the EGF receptor (Buteau *et al.* 2003). Proliferation of PB-IPCs *in vitro* is advantageous as their expansion will mean that a smaller volume of peripheral blood will be required to obtain sufficient cells for the purposes of regenerative medicine.

1.7.1.3 PB-IPCs have the potential to treat patients with type 1 diabetes

The potential of using PB-IPCs for the treatment of type 1 diabetes has been explored in a streptozotocin (STZ)-induced diabetic NOD-SCID mouse model of type 1 diabetes (Zhao *et al.* 2007a). Intraperitoneal injection of 5 million human PB-IPCs per mouse reduced blood glucose levels by 20-30% (Zhao *et al.* 2007a). Human C-peptide was secreted into the serum proving that the transplanted PB-IPCs were functioning (Zhao *et al.* 2007a). One month after transplantation, human C-peptide positive cells could be detected in the mouse pancreas within both the exocrine tissue and residual mouse islets (Zhao *et al.* 2007a). The origin of C-peptide as human was confirmed by fluorescence *in situ* hybridisation with human X/Y chromosome probes (Zhao *et al.* 2007a). The localization of PB-IPCs in the islets of the diabetic mice suggested PB-IPCs might have a homing mechanism

(Zhao *et al.* 2007a). It was discovered that the islets in NOD-SCID diabetic mice express stromal cell-derived factor-1 which is involved in mediating hematopoietic stem cell (HSC) homing (Zhao *et al.* 2007a). Further phenotyping of PB-IPCs showed they strongly express the stromal cell-derived factor-1 receptor CXCR4 providing a possible mechanism for PB-IPCs homing to the pancreas (Zhao *et al.* 2007a).

1.7.1.4 Differentiation of PB-IPCs

PB-IPCs can be differentiated into β-cell-like insulin-producing cells by culture for 3-5 days with differentiating factors (Zhao and Mazzone 2008). The cells are treated with Ex4, GM-CSF, and high glucose (25 mM) in the presence of FBS to enhance their differentiation towards the pancreatic lineage, resulting in the upregulation of mRNAs for insulin, C-peptide, Glut-2, Sur-1 and Kir6.2 (Zhao and Mazzone 2008). The cells form islet-like clusters which stain positive for insulin protein (Zhao and Mazzone 2008).

PB-IPCs can also be differentiated towards other cell lineages, as briefly mentioned above. They can be differentiated into neuronal-like cells by 2 weeks of treatment with nerve growth factor (NGF) (Zhao and Mazzone 2008). About 15% of the treated cells express neuronal markers including synaptophysin, γ-aminobutyric acid and glutamate decarboxylase 65/67 (GAD65/67) (Zhao and Mazzone 2008). They are also capable of differentiating into megakaryocyte-like cells after exposure to thrombopoietin for 10-14 days (Zhao and Mazzone 2008). Approximately 8% of the treated PB-IPCs expressed the megakaryocyte-specific marker CD41b, and exhibited a megakaryocyte morphology with polyploid nuclei (Zhao and Mazzone 2008). The above results illustrate the fact that PB-IPCs are plastic and are able to be differentiated towards a variety of different cell lineages.

1.7.2 Monocytes and their subtypes

Blood monocytes are phagocytes and antigen-presenting cells that form a key part of the innate immune system (Hume 2006). Peripheral blood monocytes differentiate to become macrophages, dendritic cells, and osteoclasts (Varol *et al.* 2009). The main role of a macrophage is to maintain tissue homeostasis by clearing bacteria and foreign material, whereas dendritic cells present antigens to T-cells (Varol *et al.* 2009). Adult tissues also contain macrophage populations which have a role in tissue repair (Varol *et al.* 2009). There are two populations of monocytes in peripheral blood which can be distinguished based on cell size (Wang *et al.* 1992). The larger of the two types is ≥ 98% $CD11b^+CD13^+OKM5^+$ and 47% $CD14^+$, whereas the smaller monocyte population is 61% $CD11b^+$, 35% $CD13^+$ and 23% $CD14^+$ (Wang *et al.* 1992). The larger cell type releases increased levels of IL-1β and TNF-α cytokines in response to lipopolysaccharide (LPS), whereas the smaller cell type produces low levels of these cytokines and remains unresponsive to increased cytokine release upon treatment with LPS (Wang *et al.* 1992).

Monocytes have recently been distinguished based on the morphology they adopt in culture, with standard-macrophages (s-MOs) displaying a rounded, fried egg morphology, and fibroblast-resembling-macrophages (f-MOs) having a fibroblast-like,

spindle-shaped morphology (Zhao *et al.* 2003; Clanchy *et al.* 2006). f-MOs can be induced to proliferate *in vitro* with macrophage-colony stimulating factor (M-CSF) or GM-CSF (Finnin *et al.* 1999). They are characterised by having the phenotype $CD14^{+}CD16^{-}CD64^{+}CD33^{+}c\text{-}FMS^{+}HLA\text{-}DR^{+}$ (Clanchy *et al.* 2006) or by the phenotype $CD14^{+}CD13^{+}CD33^{+}CD11b^{+}CD11c^{+}CD87^{+}HLA\text{-}DR^{+}CD45RO^{+}CD86^{-}CD34^{-}CD80^{-}CD4^{-}CD16^{-}CD56^{-}$ (Finnin *et al.* 1999). About 5% of all monocytes are believed to have these phenotypes (Finnin *et al.* 1999).

1.7.2.1 Monocyte plasticity induced by dedifferentiation

Monocytes can be cultured with certain growth factors such as M-CSF to become remarkably plastic to the extent where they can be differentiated towards a variety of different cell lineages. Dedifferentiated (or partially dedifferentiated) monocytes have been described as Programmable Cells of Monocytic Origin (PCMOs), Monocyte Derived Stem Cells (MDSCs) and f-MOs (Zhao *et al.* 2003).

1.7.2.1.1 Dedifferentiation of monocytes with M-CSF alone

Monocytes cultured with M-CSF (50 ng/mL) alone dedifferentiate into f-MOs, which have a fibroblast-like appearance (Zhao *et al.* 2003). They have an estimated replication time of 3 days, and after 6 days of culture they outnumber the non-proliferative s-MOs (Zhao *et al.* 2003). They proliferate for at least 2 weeks *in vitro* (Zhao *et al.* 2003). Stimulation of monocytes with M-CSF led to the down-regulation of expression of HLA-DR and CD4, whereas the expression of CD3, CD11b, CD14, CD15, and the B1 surface antigen expression was unaffected (Hassan *et al.* 1994; Ruhnke *et al.* 2005; Zangrossi *et al.* 2007). Zhao *et al*. (2003) compared the f-MO and s-MO populations and found that in comparison to s-MOs, f-MOs displayed reduced levels of expression of HLA-DQ, CD1a, IL-10, TNF-α and TNF-RII (Zhao *et al.* 2003). Conversely, the expression of the HSC marker CD34 was upregulated in response to the M-CSF treatment (Zhao *et al.* 2003). f-MOs had reduced levels of expression of lipids, leptin and peroxisome proliferator-activated receptor-γ (Zhao *et al.* 2003).

1.7.2.1.2 Dedifferentiation of monocytes with M-CSF + IL-3

M-CSF can be used in combination with other growth factors or cytokines to dedifferentiate monocytes (Hassan *et al.* 1994). The combination of M-CSF + IL-3 causes an increase in the proliferation of monocytes that exceeds that obtained with just M-CSF alone (Hassan *et al.* 1994). However, monocytes stimulated with M-CSF + IL-3 do not adopt the mostly homogenous spindle-shaped cell morphology seen with M-CSF treatment alone (Hassan *et al.* 1994). Rather, the population consists of mostly rounded cells with only a few spindle-like, fibroblastoid, cells present (Hassan *et al.* 1994). There are fewer cells with the $CD4^{+}HLA\text{-}DR^{+}$ phenotype compared with untreated control monocytes cultured for up to 3 weeks (Hassan *et al.* 1994).

Dedifferentiation of monocytes with M-CSF + IL-3 + β-mercaptoethanol (+ human serum)

Ruhnke *et al.* (2005) treated $CD14^{+}$ monocytes with M-CSF + IL-3 + β-mercaptoethanol and designated the resulting partially dedifferentiated cells as “Programmable Cells of Monocytic Origin” (PCMOs). PCMOs form characteristic colonies after 6 days of

culture (Ruhnke *et al.* 2005). The monopoietic transcription factor gene PRDMI becomes downregulated, particularly during days 2 and 3 of dedifferentiation (Ruhnke *et al.* 2005). The monocyte marker CD14 and the hematopoietic marker CD45 are consistently expressed throughout the dedifferentiation process (Ruhnke *et al.* 2005). The PCMOs exponentially proliferate and increase in size by day 5, and the expression of CD90 and CD115 increase, with the greatest increase occurring during day 2 to 4 of dedifferentiation (Ruhnke *et al.* 2005). The cells express low levels of the HSC markers CD34, CD117 and CD135, whereas CD133 is absent (Ruhnke *et al.* 2005). However, monocytes eventually became macrophages after long-term culture (>20 days) in M-CSF + IL-3 + β-mercaptoethanol (Ruhnke *et al.* 2005).

1.7.2.1.3 Dedifferentiation of monocytes with M-CSF + LIF

Monocytes can also be dedifferentiated with a combination of M-CSF + leukemia inhibitory factor (LIF) for 6 days to form Monocyte Derived Stem Cells (MDSCs) (Winnier *et al.* 2010a). MDSCs formed multinucleated osteoclastic giant cells and also endothelial cells when cultured for longer than 10 days (Winnier *et al.* 2010a). Cell size increased from 9-10 μm to approximately 16 μm after 8 days in culture and then did not increase further (Winnier *et al.* 2010a). MDSCs express low levels of CD4, and high levels of the macrophage markers CD11b (Mac-1) and CD14 (Winnier *et al.* 2010a). Most MDSCs also express CD45 and CD71 (transferrin receptor) (Winnier *et al.* 2010a). They do not express CD3, CD8, CD10, CD15, CD19, CD33, CD34, CD90 (Thy1), CD117 (c-kit receptor) and ATP-binding cassette sub-family G member 2 (ABCG2) (Winnier *et al.* 2010a). MDSCs are positive for CD14 from day 4-8, and become increasingly positive for osteocalcin (Winnier *et al.* 2010a). They are highly positive for HLA-ABC, and become increasingly positive for hairy and enhancer of split-1, and the stem cell marker SSEA-4 (Winnier *et al.* 2010a). The expression of various stem cell markers increased, including Oct-4 (after 10 days), CD117 (after 5 days), and SCF (after 10 days) (Winnier *et al.* 2010a). Importantly monocytes from diabetic patients can also be dedifferentiated using this protocol (Winnier *et al.* 2007), which opens up the option of using diabetic MDSCs for autologous cell therapy should they prove to be plastic enough to be differentiated into pancreatic β-cells.

1.7.2.2 Differentiation of f-MOs, PCMOs, and MDSCs

Monocytes are plastic after dedifferentiation and can be differentiated into a variety of different cell types, including cells of the pancreatic lineage, as discussed below. The results suggest they are promising cells for use in regenerative medicine, and potentially for the future treatment of type 1 diabetes.

1.7.2.2.1 Differentiation of f-MOs

f-MOs have been differentiated into epithelial, lymphoid, neuronal and endothelial cell lineages (Zhao *et al.* 2003). Monocytes dedifferentiated for 12-14 days with M-CSF were differentiated into macrophages with LPS (Zhao *et al.* 2003). LPS treated cells were transformed from an M-CSF-induced elongated f-MO morphology into rounded s-MO cells, which stained for lipid (Zhao *et al.* 2003). The differentiated cells expressed increased HLA-DR, HLA-DQ, TNF-α and IL-10 (Zhao *et al.* 2003). Zhao *et al.* further examined the plasticity of f-MOs by differentiating them into T lymphocytes by the addition of IL-2 for 4 days. In contrast to

untreated control cultures, the majority of cells expressed the T cell markers CD3 and CD8 (Zhao *et al.* 2003). f-MOs have also been differentiated towards the epithelial lineage by treatment for 4 days with EGF (Zhao *et al.* 2003). The cells have an epithelial morphology and phenotype, expressing pan-keratin and ECAD (Zhao *et al.* 2003). Interestingly, f-MOs, but not native monocytes were also able to be differentiated into neuronal cells by culture with NGF (Zhao *et al.* 2003). The cells adopted a neuronal morphology and after 5-8 days most cells expressed the neuronal markers neuronal specific enolase (NSE), neurofilament (NF) and microtubule associated protein-1B (MAP-1B) (Zhao *et al.* 2003). f-MOs have also been shown to be able to differentiate on culture with VEGF into cells with an endothelial morphology expressing the endothelial markers VEGF-R2, VEGF-R3 and von Willebrand Factor (vWF) (Zhao *et al.* 2003). VEGF treatment surprisingly also induced a subset of the cells to adopt a neuronal morphology and to express the neuronal markers NSE, neurofilament and MAP-1B (Zhao *et al.* 2003).

f-MOs can also be transdifferentiated into keratinocyte-like cells and neurons by culturing them in conditioned medium from keratinocytes and neurons (Kodama *et al.* 2006; Medina *et al.* 2009). Those differentiated into keratinocyte-like cells expressed a keratinocyte staining pattern of proteins including stratifin and keratins 5 and 8 (Medina *et al.* 2009). The neuronal cells transdifferentiated from f-MOs after coculture with rat neurons expressed mature neuronal markers including neurofilament, microtubule-associated protein type 2 and hexaribonucleotide binding protein-3 (Kodama *et al.* 2006).

f-MOs have been demonstrated to secrete VEGF (Eubank *et al.* 2003). The conditioned medium from M-CSF-treated monocytes stimulates human umbilical vein endothelial cells (HUVECs) to form endothelial tubes similar to the effect seen when HUVECs are treated with recombinant VEGF (Eubank *et al.* 2003).

1.7.2.2.2 Differentiation of PCMOs to Neoislets and hepatocyte-like cells

PCMOs can be differentiated into pancreatic islet-like cells, designated Neoislets cells, in the presence of EGF, HGF, nicotinamide and low glucose (Ruhnke *et al.* 2005). After only 4 days in culture with Neoislet differentiation medium the newly formed Neoislet cells contained 0.87 ng of insulin and 0.89 ng of C-peptide per μg of cell protein, respectively (Ruhnke *et al.* 2005) (for a comparison with other cell types see Table 1.2). However, this level of insulin expression is over fifty-fold less than that expressed by mature beta cells (44 ng/μg cell protein) (Ruhnke *et al.* 2005). Importantly, Neoislet cells secrete insulin in response to high glucose, however the amount secreted is still ten-fold less than that secreted by mature β-cells (Ruhnke *et al.* 2005). It was suggested that the low level of insulin secreted by Neoislets was because they are likely still immature pancreatic cells (Ruhnke *et al.* 2005).

Neoislet cells form cell aggregates after 4-8 days culture in Neoislet differentiation medium, which are mostly positive for insulin and glucagon (Ruhnke *et al.* 2005). They express mRNA transcripts encoding insulin, glucagon and Glut-2 (Ruhnke *et al.* 2005). They express the pancreatic differentiation factors including NGN3, Nkx6.1, NeuroD, MafA and PDX-1 (Ruhnke *et al.* 2005). Expression of a low level of PDX-1 together with NGN3 led to the conclusion that these cells are α- and β-cell progenitors, as

PDX-1 and NGN3 are only transiently expressed during an early stage of endocrine pancreatic development (Ruhnke *et al.* 2005). Proglucagon genes are also expressed including Pax6, Nkx2.2 and HNF3β (Ruhnke *et al.* 2005).

Transplantation of the Neoislets cells under the kidney capsule of a STZ-induced diabetic Swiss albino mouse corrected hyperglycemia within 2 days of transplantation, and led to persistence of normoglycemia for a further 8 days prior to graft rejection (Ruhnke *et al.* 2005). The transplanted Neoislets showed increased insulin expression, suggesting that the *in vivo* microenvironment may further contribute to their differentiation (Ruhnke *et al.* 2005).

PCMOs are quite plastic as they can also be differentiated along the hepatocyte lineage towards hepatocyte-like cells by culture with FGF-4 ± HGF (Ruhnke *et al.* 2005; Ungefroren and Fandrich 2010). These cells have a hexagonal morphology similar to hepatocytes and express the hepatocyte proteins α-fetoprotein and coagulation factor II (Ruhnke *et al.* 2005), albumin and factor VIII (Ungefroren and Fandrich 2010).

1.7.2.2.3 Differentiation of MDSCs

MDSCs can be differentiated into monocyte-derived islet cells (MDIs) by using a complex pancreatic differentiation medium consisting of Megacell DMEM/F12 (or LDMEM or HDMEM) + L-glutamine, penicillin, streptomyocin, glucose, anti-CD40 antibody, LPS, insulin/transferrin/selenium (ITS), nicotinamide, N2 supplement, EGF, HGF, IGF1, IGF2 and Ex4 (Winnier *et al.* 2010b). The differentiation of the MDSCs can be visualized by morphological changes during culture (Winnier *et al.* 2010b). The cells are fibroblast-like at the start of culture in pancreatic differentiation medium, then appear neuronal, and finally form MDI clusters containing differently sized cells (Winnier *et al.* 2010b). After 6 days in culture the clusters begin to detach from the plate, and insulin, C-peptide, Islet-1 and Glut-2 RNAs become expressed (Winnier *et al.* 2010b). MDIs secrete C-peptide whereas dedifferentiated MDSCs express only very low levels of C-peptide (Winnier *et al.* 2010b). Insulin is detectable in 70% of the cells, and glucagon expression appears in 21 day old MDIs (Winnier *et al.* 2010b). MDIs appear to reflect the relative composition of cells in human pancreatic islets as they are made up of >60% β-cells, 10-25% α-cells and 1-5% δ-cells (Winnier *et al.* 2010b). MDI clusters increase in number and size following exposure to 25 mM glucose, and respond by increasing RNA expression of somatostatin, PDX-1 and NGN3 (Winnier *et al.* 2010b). A high glucose challenge for 24 h revealed that MDIs secreted 28.8 U/mL of active insulin, which is similar to the amount released (30-150 U/mL) by the human pancreas into the plasma during a meal (Winnier *et al.* 2010b). MDIs can be maintained in pancreatic differentiation medium for over a month (Winnier *et al.* 2010b).

Monocytes from type 1 and 2 diabetic patients have also been dedifferentiated into MDSCs and then differentiated into MDIs using the above pancreatic differentiation medium (Winnier *et al.* 2010b). As with control subjects the cells underwent dedifferentiation in 6 days to form MDSCs (Winnier *et al.* 2010b). Then after 6 days in pancreatic differentiation medium the diabetic patients' MDSCs formed MDI clusters and started to detach (Winnier *et al.* 2010b). A similar result was obtained when the MDIs were cultured with high glucose pancreatic differentiation medium (Winnier *et al.* 2010b). Approximately 70% of the

MDIs from both type 1 and 2 diabetic patients expressed C-peptide and PDX-1, and 30% expressed glucagon (Winnier *et al.* 2010b). The MDIs expressed insulin when cultured for 15 to 40 days in high glucose pancreatic differentiation medium (Winnier *et al.* 2010b). The amount of insulin secreted *in vitro* increased over time with 2.5 ng/mL secreted into the medium on day 15 and 3.9 ng/mL on day 40 (Winnier *et al.* 2010b).

MDIs were investigated for their ability to reverse hyperglycemia in the STZ-induced model of diabetes in the NOD/SCID mouse. The MDIs that were transplanted had been differentiated from 6-day-old MDSCs by culture in low glucose pancreatic differentiation medium for 6 days, followed by high glucose pancreatic differentiation medium for an additional 3 (day 15) or 11 (day 23) days (Winnier *et al.* 2010b). The MDIs were injected under the kidney capsule (Winnier *et al.* 2010b). They reversed hyperglycemia to almost wild-type levels, however only the day 15 MDIs, but not the day 23 MDIs, could maintain the decreased blood glucose levels after 6 weeks (Winnier *et al.* 2010b). It was suggested that this may relate to the fact that the day 15 MDIs were more proliferative (Ki-67 positive) than the terminally differentiated day 23 MDIs (Winnier *et al.* 2010b). The transplanted MDIs residing in the kidney capsule expressed insulin and glucagon (Winnier *et al.* 2010b). The results suggest that MDIs formed from blood monocytes can potentially be used to treat the symptoms of diabetes in a mouse model.

1.8 Cord blood hematopoietic stem cells

1.8.1 Transplanted cord blood hematopoietic stem cells (CB-HSCs) differentiate into insulin-producing cells in the pancreas

CB-HSCs used for hematopoietic rescue after high dose chemotherapy can travel to the pancreas to form insulin-expressing cells (Huang *et al.* 2011). In one study, CB-HSCs were located in the pancreases of non-diabetic patients who had received opposite sex cord blood donations and undergone post-mortem (Huang *et al.* 2011). Males who did not receive cord blood donations had 0.32% opposite-sex XX chromosome β-cells whilst those who received cord blood had 3.41% XX chromosome β-cells (Huang *et al.* 2011). Females who did not receive cord blood donations had 0.03% XY chromosome β-cells whilst those who received cord blood had 1.03% XY chromosome β-cells (Huang *et al.* 2011). The insulin-expressing cells originating from the cord blood were found only in the islets of the pancreas and were not randomly distributed throughout the pancreas (Huang *et al.* 2011). They were mostly of normal size indicating they had arisen due to differentiation and not cell fusion with host β-cells (Huang *et al.* 2011). They did not co-express CD68, and therefore phagocytosis of host β-cells by cord blood donor cells is an unlikely reason for insulin expression by the donor cells (Huang *et al.* 2011). It is not known how such a treatment would translate to the treatment of diabetics. For instance, it is not known if CB-HSCs would home to a diabetic pancreas that lacks β-cells, and whether they would be rejected by the immune system once that had differentiated and were producing insulin (Huang *et al.* 2011). However, this evidence of cord blood migration to the pancreas and differentiation into insulin-producing cells is promising and could be developed into a potential therapy for patients with type 1 diabetes.

1.8.2 Autologous cord blood infusion to treat type 1 diabetes

Autologous cord blood infusion in children with type 1 diabetes did not preserve C-peptide expression but it did promote a small increase in the frequencies of T regulatory cells (Tregs) and naïve T cells (Haller *et al.* 2011). The median age of the patients was 5.1 years, and no adverse events were observed as a result of cord blood infusion (Haller *et al.* 2011). The level of C-peptide by the patients was 0.95 ng/mL preinfusion, but declined over time to 0.02 ng/mL at 2 years (Haller *et al.* 2011). Six months postinfusion the total number of Treg ($CD4^+CD25^+FOXP3^+$) cells was increased by 4.4%, and the number of naïve T cells ($CD45RA^+$) increased by 40.5% (Haller *et al.* 2011). The small increase in Treg cell number may help to combat the autoimmune response of type 1 diabetes in these subjects; however, the Tregs may eventually be overcome by memory T cells which will destroy the β-cells regardless (Haller *et al.* 2011).

1.9 Stem cells from human amniotic fluid and membrane

Different types of stem cells can be derived from human amniotic fluid and membrane. They have been called various names including human amniotic fluid and membrane stem cells (HASCs), human amniotic epithelial stem cells (HAESCs), human amniotic membrane stem cells (HAMSCs), and human amnion-derived fibroblast-like (HADFIL) cells (Sharma *et al.* 2003; Miki *et al.* 2007; Tamagawa *et al.* 2009). It is yet to be determined if these cells have the same or similar phenotype(s). The stem cells from human amniotic fluid and membrane are isolated from a full-term human placenta after birth, which poses no ethical issues as the placenta is usually discarded (Miki *et al.* 2007). The amnion is an avascular membrane which is covered with amniotic fluid on the external side and the basal lamina on the internal side (Miki *et al.* 2007). The internal side of the amnion is connected to the mesoderm which contains mesenchymal cells (Miki *et al.* 2007). The isolation of human amniotic fluid and membrane stem cells from the placenta is a simple procedure. Briefly, the amnion membrane is peeled from the chorion layer of the placenta and then digested several times with trypsin to obtain a single cell population (Miki *et al.* 2007). The obtained cells can then be sorted for enrichment of stem cell markers such as SSEA-4 to increase the purity of the stem cell population (Miki *et al.* 2007).

1.9.1 Human amniotic epithelial stem cells

Human amniotic epithelial stem cells (HAESCs) arise from the epiblast just 8 days after fertilization and before gastrulation (Miki *et al.* 2005). HAESCs are extremely plastic and can be differentiated into all 3 germ layers, namely endoderm (pancreas, liver), mesoderm (cardiomyocyte) and ectoderm (neuronal cells) *in vitro* (Miki *et al.* 2007). HAESCs express SSEA-4, SSEA-3, tumour-rejection antigen-1-60 (TRA-1-60) and TRA 1-81, in common with ESCs and germ cells (Miki *et al.* 2007). They also express the pluripotent stem cell markers Oct-4, SOX-2 and Nanog and do not require mouse feeder layers for growth (Miki *et al.* 2007). The expression of the stem cell markers is mostly restricted to HAESCs grown as spheroids *in vitro,* whereas they become diminished in cells grown as a monolayer (Miki *et al.* 2005). HAESCs do not express the hematopoietic stem cell marker CD34, and therefore do not contain HSCs (Miki *et al.* 2005). Freshly isolated HAESCs express PDX-1 RNA (Miki *et al.* 2005). HAESCs do not form tumours when injected into the rear leg muscle, testis (SCID, beige mice), liver or interscapular fat pad (Rag-2 knockout mice), even after 7 months following injection (Miki *et al.* 2005).

HAESCs can be differentiated towards pancreatic, neuronal, hepatic and cardiomyocyte cell lineages (Miki *et al.* 2005). They can be differentiated towards a pancreatic phenotype with retention of PDX-1 RNA expression using a standard medium containing nicotinamide (Miki *et al.* 2005). The differentiated cells express HNF6, Nkx2.2, insulin and glucagon RNA (Miki *et al.* 2005). Glucagon was also detected by immunostaining, however, proinsulin and C-peptide were not detectable (Miki *et al.* 2005).

HAESCs naturally express low levels of RNA for various neuronal markers, including Nestin, and GAD (Miki *et al.* 2005). Neuronal differentiation of HASCs could be achieved by culture of HAESCs for 1 week in standard medium containing all-*trans* retinoic acid + FGF-4 (Miki *et al.* 2005). The cells adopted a neuronal morphology, expressed increased levels of RNA for Nestin and GAD, and were positive by immunostaining for glial fibrillary acidic protein (GFAP) and 2',3'-cyclic-nucleotide 3'-phosphodiesterase indicating they had differentiated into glial and neuronal cells (Miki *et al.* 2005).

1.9.2 Human amniotic membrane stem cells

Human amniotic membrane stem cells (HAMSCs), which can be obtained commercially from Celprogen Inc., express Oct-4 and Nanog (Sharma *et al.* 2003). Sharma *et al.* (2003) cultured HAMSCs in Celprogen Inc.'s human amniotic stem cell undifferentiating complete growth medium and extracellular matrix without mouse feeder layers (Sharma *et al.* 2003). The HAMSCs formed spheroid bodies, which could be differentiated into β-cells, neuronal cells and cardiomyocytes using Celprogen Inc.'s pancreatic, neuronal stem cell and cardiomyocyte differentiation kits, respectively (Sharma *et al.* 2003). HAMSCs cultured using the Celprogen Inc. pancreatic differentiation kit for 1 week expressed Pax6, Nkx2.2, insulin and glucagon RNA (Sharma *et al.* 2003). The plasticity of the HAMSCs was further demonstrated by their expression of the neuronal markers NSE, NF-M, MBP, Nestin and GAD after culture for 1 week in Celprogen Inc.'s neuronal stem cell medium (Sharma *et al.* 2003). HAMSCs cultured for 2 weeks in Celprogen Inc.'s cardiomyocyte differentiation medium expressed the cardiomyocyte markers GATA-4, Nkx2.5, MLC-2A and MLC-2V (Sharma *et al.* 2003). Importantly, HAMSCs transplanted into SCID mice, which were subsequently monitored for up to 6 months, did not form tumours (Sharma *et al.* 2003). Thus, HAMSCs could potentially be a source of non-tumorigenic stem cells for the treatment of type 1 diabetes.

1.9.3 Human amnion-derived fibroblast-like cells

Human amnion-derived fibroblast-like (HADFIL) cells are isolated from the amniotic membrane by mincing the tissue and using collagenase to break down the tissue in order to isolate a single cell population of fibroblast-like cells (Tamagawa *et al.* 2009). The cells are then grown in a medium containing FBS + EGF + LIF (Tamagawa *et al.* 2009). They express HNF3β, which is a transcription factor necessary for endoderm lineage differentiation (Tamagawa *et al.* 2009). HADFIL cells can be differentiated into pancreatic-like cells by first growing the cells on a collagen type I-coated plastic dish until confluent, and then differentiating them using a multiple-step process (Tamagawa *et al.* 2009). Firstly the medium is changed to a high glucose medium containing FBS + retinoic acid for 2 days, then to high glucose medium containing FBS for 2 days, and then they are placed on a Matrigel

matrix for 1 week in low glucose medium containing FBS + nicotinamide + EGF + 1 x N2 supplement (Tamagawa *et al.* 2009). Finally they are incubated for 1 week in a low glucose medium containing Ex4 (Tamagawa *et al.* 2009). When plated on the Matrigel matrix they became rounded and eventually formed islet-like clusters which gradually increased in size (Tamagawa *et al.* 2009). They expressed RNAs for a variety of pancreatic markers including insulin, glucagon, somatostatin, cytokeratin 19, hepatocyte nuclear factor-1α (HNF1α), HNF3β, Islet-1, Glut-2, PDX-1, Pax4, Pax6, Nkx2.2, Nkx6.1, NeuroD and NGN3, as well as the proteins insulin, glucagon and somatostatin (Tamagawa *et al.* 2009). Conversely, the expression of the stem cell marker Nestin, and the definitive endoderm marker SOX-17, and the posterior foregut marker HNF6 were down-regulated (Tamagawa *et al.* 2009).

1.10 Bone marrow hematopoietic stem cells

$CD34^+$ HSCs residing in the bone marrow are responsible for maintaining the vast populations of blood cells within the body, including macrophages, dendritic cells (DCs), T and B cells, granulocytes, mast cells, red blood cells, and platelets amongst others (Bongso and Lee 2005).

Most HSCs mature in the bone marrow, however it is important to note there is also evidence that HSCs circulate in peripheral blood at low levels to provide a surveillance system (Jaiswal and Weissman 2009). HSCs also migrate to tissues where inflammation is occurring to help set up a pool of immune cells to fight infection (Jaiswal and Weissman 2009). The HSCs potentially avoid phagocytosis by resident macrophages by upregulating CD47 which binds to CD47-signal regulatory protein-α on macrophages and inhibits the immune response (Jaiswal and Weissman 2009).

HSCs are retained in the bone marrow by the stromal cell-derived factor-1/CXCR12 which interacts with CXCR4 expressed by HSCs (Levesque and Winkler 2008). HSCs are mobilised into the blood by granulocyte-colony stimulating factor (G-CSF), which causes the release of neutrophil proteases in the bone marrow that cleave CXCR4, thereby causing the release of HSCs (Levesque and Winkler 2008). CXCR4 antagonists synergize with G-CSF to mobilize HSCs (Levesque and Winkler 2008).

1.11 Adipose stem cells

Adipose stem cells (ASCs) are easily recoverable from a lipoaspirate following abdominal liposuction surgery (Locke *et al.* 2011). The lipoaspirate is first washed to remove the red blood cells, digested with collagenase to obtain a single cell suspension, and then centrifuged to collect the cell pellet, known as the stromal vascular fraction (SVF) (Locke *et al.* 2011). The pellet contains multipotent mesenchymal stem cells and endothelial cells (Locke *et al.* 2011).

ASCs (also called adipose mesenchymal stem cells) express mesenchymal stem cell markers such as CD29, CD44, CD71, CD90, CD49d, and CD105 and do not express the HSC markers CD31, CD34 or CD45 (Zuk *et al.* 2002). ASCs are multipotent as they can be differentiated into the adipogenic (fat), osteogenic (bone), myogenic (muscle), chondrogenic (cartilage) and

neuronal (brain) lineages (Zuk *et al.* 2002; Locke *et al.* 2011). ASCs cultured *in vitro* with adipogenic medium undergo differentiation into adipocytes expressing leptin and Glut-4, and stain positive for lipid with Oil Red O, which stains lipid vacuoles within the cells (Zuk *et al.* 2002). ASCs differentiated into osteoblast-like cells that display characteristic alkaline phosphatase activity, and are capable of matrix mineralization (Zuk *et al.* 2002). There have also been reports of ASCs being differentiated into pancreatic cells (Timper *et al.* 2006; Lin *et al.* 2009; Chandra *et al.* 2011; Kang *et al.* 2011).

1.11.1 Differentiation of ASCs into pancreatic cells

1.11.1.1 Differentiation of ASC isolated from lipoaspirate following liposuction surgery

1.11.1.1.1 Multi-step differentiation of lipoaspirate ASCs

Chandra *et al.* (2011) isolated human ASCs from abdominal liposuction surgery and differentiated the cells into islet-like cell aggregates (ICA) (Chandra *et al.* 2011). The cells were seeded at high cell densities (1 x 10^5/cm^2) and grown using a 3-step protocol in serum-free medium on ultra-low attachment plates or glass plates to promote the formation of suspension clusters (Chandra *et al.* 2011).

Initially, the cells were cultured for 2 days in a serum-free medium containing ITS, activin A, sodium butyrate, 2-mercaptoethanol, and bFGF (Chandra *et al.* 2011). They began to express endodermal markers such as HNF3β, transcription factor-2 and SOX-17 (Chandra *et al.* 2011). They were then cultured for 2 days in a medium containing 17.5 mM D-glucose and taurine (Chandra *et al.* 2011).

The final step to differentiate the adipose stem cells into ICAs and promote their survival required the cells to be cultured for 10 additional days in a medium containing taurine, GLP-1 (amide fragment 7-36), nicotinamide, and 1x non-essential amino acids (NEAA) (Chandra *et al.* 2011). RNA transcripts encoding various pancreatic endoderm markers were upregulated including PDX-1, NGN3, NeuroD, Pax-4, Nkx2.2, Nkx6.1, Pax6, ISL-1 and Glut-2 (Chandra *et al.* 2011). The ICAs stained positive with dithizone (DTZ) indicating the presence of insulin (Chandra *et al.* 2011). Importantly, the ICAs expressed mRNAs encoding the pancreatic hormones insulin, glucagon, somatostatin, pan-polypeptide and ghrelin, but at a lower levels than those expressed by the pancreas of a 12-week-old human foetus (Chandra *et al.* 2011). The ICAs were able to respond to increased glucose concentrations by releasing increased levels of C-peptide and insulin, indicating their potential ability for the treatment of diabetes (Chandra *et al.* 2011). The ICAs contained up to 582.86 pM C-peptide, while the undifferentiated ASCs contained 16.88 pM (Chandra *et al.* 2011). For a comparison with other cell types see Table 1.2.

The ICAs were functional when transplanted into the peritoneal cavity of STZ-induced diabetic mice (Chandra *et al.* 2011). They were encapsulated within biocompatible calcium-alginate capsules prior to transplantation (Chandra *et al.* 2011). They induced a marked decrease in blood glucose levels to 180-190 mg/dl after 2-3 weeks, which was maintained for 8 weeks, but did not achieve normoglycemia (Chandra *et al.* 2011). Interestingly, transplantation of undifferentiated adipose stem cells also induced a decrease in blood glucose to 250 mg/dl (Chandra *et al.* 2011). Human C-peptide was detected in the blood serum of mice transplanted with differentiated and undifferentiated ICAs (Chandra *et al.* 2011). Histological sections of the encapsulated ICAs prepared 28 days after transplantation revealed viable cells expressing C-peptide and insulin (Chandra *et al.* 2011).

1.11.1.1.2 PDX-1-directed differentiation of ASCs

ASCs acquired through routine abdominoplasty have been shown to express mRNAs for NeuroD and glucagon (Lin *et al.* 2009). Lentiviral-mediated transfection of the cells to express PDX-1 and culture in DMEM medium containing 23 mM glucose induced the cells to express insulin (Lin *et al.* 2009). The cells were designated "insulin-producing adipose-tissue derived stem cells" (IPADSC). They secreted increasing amounts of insulin on exposure to increasing concentrations of glucose (Lin *et al.* 2009). IPADSCs transplanted under the kidney capsule decreased the blood glucose levels of STZ-induced diabetic rats, whose fur became smoother and the rats suffered from fewer cataracts (Lin *et al.* 2009). Histological examination revealed that the IPADSCs formed tissue-like structures in the subcapsular space and produced insulin (Lin *et al.* 2009).

1.11.1.2 Differentiation of ASCs isolated from eyelid adipose tissue

1.11.1.2.1 Multi-step differentiation of eyelid-derived ASCs

ASCs obtained from eyelid adipose tissue were differentiated into insulin-producing cells using a two-step differentiation protocol over 2 weeks (Kang *et al.* 2011). In the first week ASCs were cultured in a high glucose medium containing FBS, activin A, bFGF, and GLP-1 (Kang *et al.* 2011). For the next 2 weeks they were cultured in a low glucose medium containing FBS, nicotinamide, activin A, GLP-1, and IGF-2 (Kang *et al.* 2011). Undifferentiated ASCs released 1.4 pg/mL of insulin in response to a 25 mM glucose challenge (Kang *et al.* 2011). ASCs differentiated with this medium released 950 pg/mL of insulin (Kang *et al.* 2011). Undifferentiated ASCs expressed mRNA for NeuroD1 and ISL-1 (Kang *et al.* 2011). The above differentiated ASCs expressed NGN3, Nkx2.2, PDX-1 and Glut-2 after the first week of differentiation, followed by Pax6, PC1/3, Nkx6.1 and insulin after the second round of differentiation for 2 weeks (Kang *et al.* 2011). They formed cell colonies and stained strongly with DTZ for the presence of insulin (Kang *et al.* 2011).

1.11.1.3 Adipose stem cells from subcutaneous and visceral tissue after abdominal surgery or mammary reduction

ASCs obtained through abdominal surgery or mammary reduction can be differentiated into insulin-producing cells in ultra-low attachment plates over 3 days in a medium containing glucose, B27 and N2 serum supplements, nicotinamide, activin A, Ex4, HGF and pentagastrin (Timper *et al.* 2006). Freshly harvested ASCs expressed stem cell factor and c-kit, and after expansion in proliferation medium containing bFGF they expressed the stem cell markers Nestin, ABCG2, stem cell factor, Thy-1, and Pax6, and 10% of the ASCs also expressed the pancreatic marker ISL-1 (Timper *et al.* 2006). RNA encoding the stem cell marker ABCG2 was downregulated after differentiation, which correlated with upregulation of pancreatic mRNAs for ISL-1, PDX-1 and NGN3 (Timper *et al.* 2006). Approximately 10% of the cells expressed PDX-1 in their nuclei after 3 days of differentiation (Timper *et al.* 2006). Pax6 mRNA expression decreased, whereas mRNAs for insulin, glucagon and somatostatin were upregulated (Timper *et al.* 2006). The differentiated ASCs expressed C-peptide and secreted somatostatin (Timper *et al.* 2006).

1.11.2 ASCs have anti-inflammatory and angiogenic properties

Culture of PBMCs with an equal number of allogeneic adipose-derived mesenchymal stem cells does not lead to the development of an immune response, as would be evidenced by the proliferation of the T cells (Yanez *et al.* 2006). ASCs inhibit the phytohaemagglutinin (PHA)-induced proliferation of T cells (Yanez *et al.* 2006). They also immunosuppress a T cell proliferative response when stimulator and responder T-cells are incubated with one another (Yanez *et al.* 2006). Direct cell contact was not required for the ASCs to mediate their immunosuppressive effect (Yanez *et al.* 2006). The ASCs inhibited the secretion of pro-inflammatory cytokines by activated T lymphocytes including TNF-α and IFN-γ (Yanez *et al.* 2006).

ASCs prevented graft versus host disease (GVHD) in mice, and increased graft survival (Yanez *et al.* 2006). In this study mice were transplanted with splenocytes and bone marrow cells and treated with ASCs at days 0, 7 and 14 post-transplantation or at days 14, 21 and 28 post-transplantation (Yanez *et al.* 2006). The mice that were treated with ASCs at days 0, 7 and 14 showed little sign of GVHD, whereas those who received the ASCs later showed an increase in GVHD (Yanez *et al.* 2006). Those that did not receive ASCs showed high levels of GVHD.

Importantly, ASCs are also angiogenic (Ohmura *et al.* 2010). Ohmura *et al.* (2010) transplanted 200 islets together with 2×10^5 mouse ASCs into STZ-induced diabetic mice, and discovered that they promoted normoglycemia and increased survival of the graft. It was suggested that the number of islets required to treat type 1 diabetes patients could be reduced by transplanting ASCs together with islets (Ohmura *et al.* 2010). Notably, transplantation of the ASCs alone did not induce normoglycemia (Ohmura *et al.* 2010). Islets transplanted with ASCs had a much higher number of vWF expressing cells present indicating the presence of endothelial cells and graft vascularization, which presumably promoted increased islet survival (Ohmura *et al.* 2010). The anti-inflammatory nature of the ASCs was evidenced by a decrease in the number of $CD4^+$ and $CD8^+$ T-cells and $CD68^+$

macrophages present in islets co-transplanted with ASCs (Ohmura *et al.* 2010). According to this study a mix of undifferentiated and differentiated ASCs could hold the key for the treatment of type 1 diabetes (Ohmura *et al.* 2010).

1.12 Induced pluripotent stem cells

Induced pluripotent stem cells (iPSCs) are somatic cells which have been forced to become stem cells by engineered overexpression of four stem cell protein transcription factors (Takahashi and Yamanaka 2006; Kim *et al.* 2009). One research group established iPSCs by treating human fibroblasts with the essential stem cell transcription factors Oct-4, SOX-2, KLF4 and c-Myc which were rendered cell-permeable by attachment to a cell-permeable peptide (CPP) (Kim *et al.* 2009). Using a CPP means viral-mediated transfection is not necessary as the reprogramming peptides will freely enter the cell during normal cell culture (Kim *et al.* 2009). Human fibroblasts treated with cell-permeable Oct-4, SOX-2, KLF4 and c-Myc adopted a morphology, proliferation characteristics, and phenotype that are in common with hESCs (Kim *et al.* 2009). These iPSCs could be differentiated into all 3 embryonic germ layers (Kim *et al.* 2009). Repeated exposure of a somatic cell line to the reprogramming peptides for approximately 8 weeks was found to be the optimal method for inducing alkaline phosphatase activity and establishing an iPSC cell line (Kim *et al.* 2009). The efficiency of iPSC generation was low with just 0.001% of cells adopting the embryonic state (Kim *et al.* 2009). The iPSCs could be maintained in culture for more than 35 passages (Kim *et al.* 2009). Further proof that an ESC-like fate had been induced was the demonstration of expression of additional stem cell markers including Nanog, TRA-1-60, SSEA-3 and SSEA-4 (Kim *et al.* 2009).

1.13 General characteristics of stem cells

1.13.1 Stem cells express alkaline phosphatase

Human ESCs are pluripotent stem cells derived from the inner cell mass of an embryo which can be maintained in an undifferentiated state, however the point at which the cells begin to differentiate is not always obvious (O'Connor *et al.* 2008). An alkaline phosphatase test is available to show if a population of cells is still undifferentiated (O'Connor *et al.* 2008). Undifferentiated embryonic stem cells are characterised by their high expression of alkaline phosphatase (Pease *et al.* 1990). Human ESCs express the stem cell markers Oct-4, Nanog, SSEA-3, SSEA-4, TRA-1-60 and TRA-1-81 (O'Connor *et al.* 2008). Researchers have discovered that a cell will lose its alkaline phosphatase activity before it loses the expression of Oct-4 and SSEA-3, and therefore alkaline phosphatase activity is an early signal of the start of cellular differentiation (O'Connor *et al.* 2008).

1.13.2 Stem cells have a high level of aldehyde dehydrogenase enzyme activity

Cells displaying high aldehyde dehydrogenase (ALDH) enzyme activity ($ALDH^+$) are considered to be stem cells (Storms *et al.* 1999). Expression of $ALDH^+$ by HSCs correlates with stem cell marker CD34 expression (Storms *et al.* 1999). Neuronal stem cells and ASCs have been reported to be $ALDH^+$ cells (Cai *et al.* 2004; Mitchell *et al.* 2006). Greater than 70% of primary ASCs isolated by liposuction are $ALDH^+$ cells (Mitchell *et al.* 2006). They retain high ALDH activity during passages 0-4, whereas at

passage 9 the percentage of cells which are $ALDH^+$ decreases to 10% of the total cell population (Mitchell *et al.* 2006). The loss of ALDH activity with the increasing number of passages is a sign of the loss of stem cell characteristics (Mitchell *et al.* 2006). Only approximately 50% of ASCs in the SVF are positive for CD34 (Mitchell *et al.* 2006). CD34 expression decreases with increasing passage number such that only 20% of cells are positive by passage 1, followed by a sharp decrease such that less than 10% of cells remain positive at passages 2-4 (Mitchell *et al.* 2006).

1.13.3 Senescence-associated β-galactosidase expression can be used to assay cell senescence

Cell senescence can be induced by cellular or oncogenic stress (Debacq-Chainiaux *et al.* 2009). The expression of senescence-associated β-galactosidase (SA-βgal), a marker of cell senescence, increases with the replicative age of cells. It is not expressed by quiescent (G0 cell cycle phase) or terminally differentiated cells that have not yet become senescent (Debacq-Chainiaux *et al.* 2009). SA-βgal expression can be used to assay the replicative potential of cells, and the effect of compounds on cellular senescence (Debacq-Chainiaux *et al.* 2009). However, there are some exceptions to SA-βgal being expressed only in senescent cells. Adult melanocytes express SA-βgal, despite being healthy and proliferative *in vitro* (Debacq-Chainiaux *et al.* 2009).

1.14 Immune tolerance

It is hoped that one day the autoimmunity associated with type 1 diabetes will be preventable or treatable by inducing immune tolerance. Teplizumab, a humanized anti-CD3 monoclonal antibody, which was trialled for its ability to prevent immune destruction of β-cells by T cells, appears to induce self-tolerance. (Masharani and Becker 2010). Participants with recent onset (4-12 months) type 1 diabetes received daily intravenous doses of teplizumab for 2 weeks while continuing their usual diabetic management routines (Masharani and Becker 2010). After 12 months the teplizumab group's C-peptide response after a meal was 17.7% higher than the placebo group (Masharani and Becker 2010). Teplizumab was more effective on younger (<15 years) participants whose C-peptide response was 31.7% higher than placebo (Masharani and Becker 2010). Treatment benefits were also larger in those individuals with an HbA1c of < 6.5% at entry (Masharani and Becker 2010). The teplizumab group required less exogenous insulin (Masharani and Becker 2010). This study suggests that deterioration in insulin secretion may be improved by administration of teplizumab at the time of disease onset.

Tregs, which help mediate immune tolerance, have been used to successfully inhibit the rejection of skin grafts (Issa *et al.* 2010). Chimeric humanised mice were transplanted with a human skin graft followed by administration of allogeneic Tregs (Issa *et al.* 2010). The Tregs, which had a $CD127^{lo}CD25^+CD4^+$ phenotype, were isolated from human peripheral blood and expanded with IL-2 and anti-CD3/CD28 beads, and administered to the mice 35 days post-transplant (Issa *et al.* 2010). Mice receiving the expanded Tregs maintained a normal appearing graft 100 days post-transplant, and had reduced numbers of infiltrating $CD8^+$ T cells (Issa *et al.* 2010). Thus, the immunosuppressive Tregs ensured the graft's survival for a longer length of time (Issa *et al.* 2010).

As mentioned earlier, type 1 diabetes can be treated with pancreatic islet transplants (Ren *et al.* 2007). In this scenario the patient must take immunosuppressive drugs which as mentioned can increase the risk of infection and cancer (Ren *et al.* 2007). Induction of immune tolerance of the transplant would be the preferred option (Tang *et al.* 2004). In one study donor new-born male pig hepatocytes and splenocytes were given to mice prior to xenotransplantation of donor islets to improve the survival of the graft (Tang *et al.* 2004). The hepatocytes and splenocytes delayed the increase in phagocytosis of the islets by 1 week, and accordingly lymphocyte infiltration and necrosis were reduced (Tang *et al.* 2004).

1.14.1 Immune regulator lymphocytes - Tregs

T lymphocytes are selected in the thymus based on their affinity for MHC-self-antigens (Li and Flavell 2008). Lymphocytes are first positively selected based on their affinity of interaction with the MHC complex expressed on cortical epithelial cells (Starr *et al.* 2003). A T cell which "does not recognise self at all" will undergo "death by neglect" (Kronenberg and Rudensky 2005). Lymphocytes are then negatively selected based on their affinity of interaction with self-antigen-MHC complexes presented by epithelial and dendritic cells at the cortical/medullary junction. A T cell which receives "very strong signals", and hence is potentially autoreactive, will undergo "apoptotic death" (Kronenberg and Rudensky 2005). Autoreactive cells are killed by dendritic cells and bone marrow-derived macrophages. A T cell which receives a "weak signal" will survive and be selected to become a $CD4^+$ or $CD8^+$ effector cell. Even in healthy individuals occasional autoreactive T cells which have a high affinity for MHC-self-antigen are selected and escape into the periphery (Danke *et al.* 2004). They are potentially destructive, therefore regulatory mechanisms exist to control these rogue cells (Danke *et al.* 2004; Li and Flavell 2008). In the development of central tolerance, a T cell which interacts with self-antigen-MHC complexes expressed on medullary epithelial cells, and receives an "intermediate signal" (potentially autoreactive) is destined to become a "natural" T regulatory cell (Treg), an immunosuppressive cell whose job it is to keep autoreactive cells in-check (Kronenberg and Rudensky 2005). Tregs generally have a higher affinity for antigen-MHC, and hence can out-compete autoreactive cells for autoantigen. They are $CD4^+$ T cells which are characterized by expression of the transcription factor FOXP3 which is required for their development, and possess high levels of CD25 (Li and Flavell 2008). After maturation in the thymus T cells relocate to the periphery (Li and Flavell 2008). When a $CD4^+$ helper T cell or $CD8^+$ cytotoxic T cell encounters an antigen it recognizes the cell will proliferate (Li and Flavell 2008). TGF-β, which is expressed by Tregs plays a role in suppressing T cell proliferation and maintaining peripheral tolerance and the homeostasis of the immune system (Li and Flavell 2008). Tregs, via a process called "infectious tolerance", which is partly responsible for peripheral tolerance, are able to transform naive T cells into Tregs in response to inflammation, and thereby enhance the tolerogenic environment (Kronenberg and Rudensky 2005). Tregs exploit a large array of different mechanisms to combat an autoimmune response including the secretion of TGF-β, IL-10, adenosine, cAMP, and indoleamine 2,3-dioxygenase. They sequester IL-2 via high levels of surface expression of CD25, and they express surface CTLA-4 that is a negative regulator of T cell activation (Kronenberg and Rudensky 2005). The T cell antigen receptor expressed on the surface of T cells recognizes foreign peptide antigens presented by the major histocompatibility complex (MHC) I or II expressed on the surface of antigen presenting cells (APCs). The T cell co-receptor CD28 binds to B7 ligands expressed on APCs and initiates co-stimulation to increase the

proliferation of T cells and IL-2 production (June *et al.* 1990; Nestle *et al.* 1994), Conversely, CTLA-4 which is related to CD28 binds B7 ligands on APCs and transmits an inhibitory signal to T cells (Nestle *et al.* 1994).

1.14.2 Cord blood stem cells are immunosuppressive

A population of cells was isolated from cord blood based on their adherence to non-tissue culture treated hydrophobic Petri dishes and found to express the ESC markers Oct-4, Nanog, SSEA-3, SSEA-4 (Zhao *et al.* 2006). These cells, designated cord blood stem cells (CB-SCs), also expressed the hematopoietic cell markers CD9, CD45 and CD117 (Zhao *et al.* 2006). They did not express the macrophage and lymphocyte markers CD11b, CD3 and CD20 (Zhao *et al.* 2006). HLA-ABC was expressed by 5% of the cells, whereas HLA-DR was not expressed (Zhao *et al.* 2006). Thus, CB-SCs express low levels of MHC antigens, and are therefore weakly immunogenic (Zhao *et al.* 2006). Accordingly, they did not stimulate the proliferation of allogeneic lymphocytes in culture (Zhao *et al.* 2006). Human CB-SCs injected into the peritoneal cavity of STZ-induced diabetic mice caused a significant reduction in blood glucose levels, which correlated with the expression of human C-peptide in the sera (Zhao *et al.* 2006). The authors concluded that the CB-SCs had differentiated into insulin-producing cells *in vivo*, and were non-immunogenic raising the possibility that they could be used to treat type 1 diabetes (Zhao *et al.* 2006).

CB-SCs are immunosuppressive as illustrated by their ability to inhibit the proliferation and aggregation of PHA-stimulated and IL-2-stimulated $CD8^+$ lymphocytes (Zhao *et al.* 2007b). CB-SCs stimulate responding $CD4^+$ and $CD8^+$ T cells to upregulate the expression of CD69, a negative regulator of the immune response (Zhao *et al.* 2007b). The lymphocyte migration-associated molecules CD44 and CD62L were down-regulated on $CD4^+$ and $CD8^+$ T cells after coculture with CB-SCs (Zhao *et al.* 2007b). Paradoxically, further investigations showed that CB-SCs also inhibited the IL-2-stimulated proliferation of $CD4^+CD25^+$ Tregs (Zhao *et al.* 2007b). However, CB-SCs cocultured with IL-2/PHA stimulated lymphocytes increased the number of $CD4^-CD8^-$ T cells, and the overall ratio of $CD4^+$ to $CD8^+$ cells was increased (Zhao *et al.* 2007b).

Mouse spleen-derived lymphocytes cocultured with human CB-SCs failed to proliferate (Zhao *et al.* 2009). Coculture of mouse lymphocytes with CB-SCs led to a 5-fold increase in the percentage of $CD4^+CD62L^+$ Treg cells, whereas the percentages of $CD4^+CD25^+$ and $CD4^+FOXP3^+$ Treg were not changed (Zhao *et al.* 2009). A very small number of the $CD4^+CD62L^+$ Treg cells also expressed $CD25^+FOXP3^+$, but the percentage was not different between cocultured cells and non-cocultured cell populations (Zhao *et al.* 2009). IL-4 was significantly downregulated and IL-10, IL-12 and TGF-β1 were significantly upregulated in $CD4^+CD62L^+$ Treg cells exposed to CB-SCs (Zhao *et al.* 2009). The expression of IL-10 and TGF-β1 would be expected to induce immune tolerance *in vivo* (Zhao *et al.* 2009). CB-SC-generated $CD4^+CD62L^+$ Treg cells were termed mCD4CD62L Treg cells (Zhao *et al.* 2009). Treatment of diabetic NOD mice with mCD4CD62L Treg cells induced normoglycemia, whereas treatment with $CD4^+CD62L^+$ Treg cells not generated with CB-SCs did not revert hyperglycemia in the mice (Zhao *et al.* 2009). The level of insulin in the blood was significantly increased in mCD4CD62L-treated NOD mice, which correlated with an increase in total β-cell mass (Zhao *et al.* 2009). Further analysis revealed the presence of small numbers of cells doubly positive for Ki67 and insulin in mice treated with mCD4CD62L Treg cells, which indicated *de novo* proliferation of β cells (Zhao *et al.* 2009). The

investigators found rings of TGF-β-positive cells and TGF-β surrounding the pancreatic islets, perhaps forming a protective immunosuppressive barrier against immune attack from autoreactive T effector cells (Zhao *et al.* 2010). The islet masses of the mice had been destroyed by 80% prior to mCD4CD62L treatment (Zhao *et al.* 2009). After 45 days of treatment, when the study ended, over a third of the islets showed little sign of inflammatory infiltration, 20% showed mild insulitis, 15% showed moderate insulitis, 18% showed severe insulitis and 11% showed profound insulitis (Zhao *et al.* 2009). In comparison, the pancreases of mice treated with $CD4^+CD62L^+$ Treg cells that had not been generated with CB-SCs had islets that were severely infiltrated with immune cells, and few insulin-positive cells were present (Zhao *et al.* 2009). The mCD4CD62L cells appeared to be able to inhibit autoimmunity via expression of IL-10 and TGF-β1, and were able to restore insulin production by promoting β-cell production as evidenced by Ki67 expression by insulin-expressing cells (Zhao *et al.* 2009).

The development of diabetes in transgenic NOD mice, in which the expression of TGF-β in the pancreas could be induced with tetracycline, was prevented by inducing the expression of TGF-β (Peng *et al.* 2004). This effect of TGF-β was due to its ability to expand the population of $CD4^+CD25^+FOXP3^+$ Tregs resulting in immune tolerance (Peng *et al.* 2004). This approach is a way of inducing immune tolerance to protect islet grafts. Zhao *et al.* (2010) hypothesized that CB-SCs or PB-IPCs could be used to introduce and expand β-cells during late stage diabetes when most islets have been destroyed, and to generate $mCD4^+CD62L^+$ Treg to induce self-tolerance of the newly formed pancreatic islets.

1.14.2.1 Cord blood stem cells help patients with type 1 diabetes

Stem Cell Educator (Figure 1.1) is a system developed to expose lymphocytes from patients with type 1 diabetes to CB-SCs *ex vivo* briefly before they re-enter the patient (Zhao *et al.* 2012). In the Stem Cell Educator, allogeneic CB-SCs are attached to discs of a hydrophobic material and the patients' lymphocytes are extracted via the median cubital vein and allowed to flow over the CB-SCs for 2-3 h before the lymphocytes are collected and re-administered to the patient via a dorsal vein in the hand (Zhao *et al.* 2012). Approximately 10 litres of blood is processed in the Stem Cell Educator per patient during two treatments of the lymphocytes (Zhao *et al.* 2012).

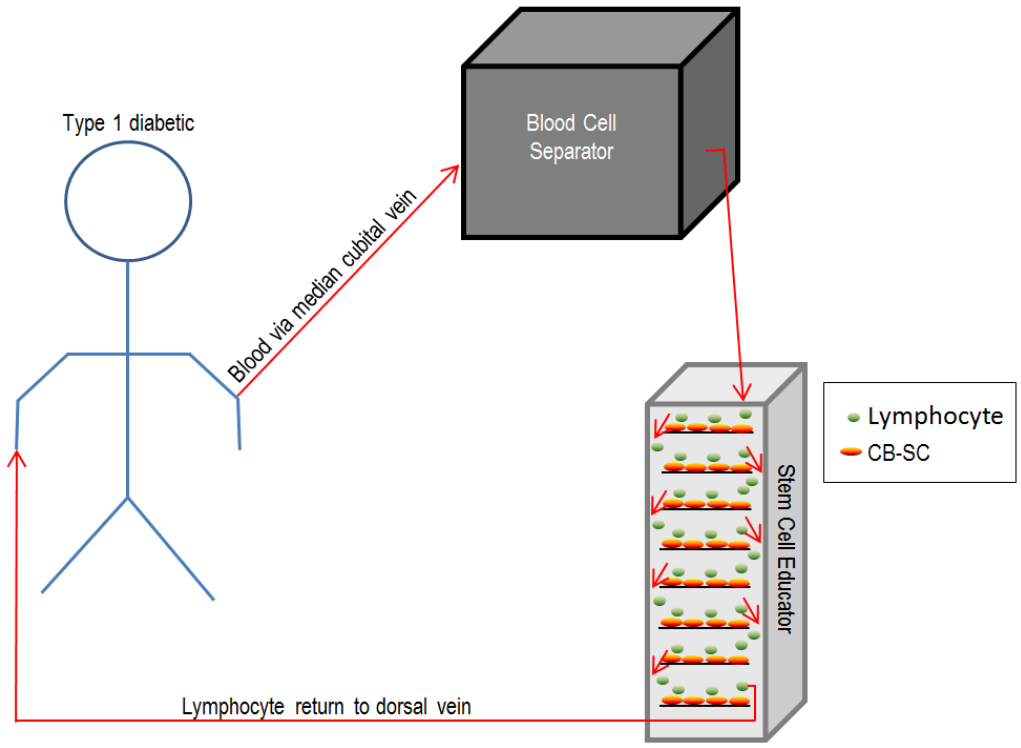


Figure 1.1 Schematic diagram of the Stem Cell Educator system.

Lymphocytes are separated in a Blood Cell Separator and transferred to the Stem Cell Educator system where they are passed over adherent CB-SC. The lymphocytes are then released from the Stem Cell Educator and returned to the patient. Abbreviation: CB-SC – cord blood stem cell.

A clinical trial of Stem Cell Educator was undertaken which involved 15 patients with a median age of 29 years who had suffered from type 1 diabetes for 8.5 ± 6.4 years (Zhao *et al.* 2012). Cells leaving the Stem Cell Educator were tested for the presence of the CB-SC marker SSEA-3 (Zhao *et al.* 2012). It was found that no CB-SCs were transferred to the patients (Zhao *et al.* 2012). Importantly there were no significant adverse events during the trial, and at 24 h and 12 weeks after the treatment no significant difference was noted in white blood cell counts (Zhao *et al.* 2012). The patients with moderate type 1 diabetes showed improved fasting C-peptide levels after 12 and 24 weeks (Zhao *et al.* 2012). The patients trialled with severe type 1 diabetes showed improved fasting C-peptide levels throughout the study (Zhao *et al.* 2012). An oral glucose test showed improvement from weeks 4 to 12 in those patients with moderate type 1 diabetes (Zhao *et al.* 2012). The patients with severe type 1 diabetes initially showed no C-peptide production until 12 weeks after treatment, after which C-peptide production was maintained through 40 weeks (Zhao *et al.* 2012). A control group's lymphocytes were passed through a Stem Cell Educator system that did not contain any CB-SC, and they did not show any difference in C-peptide levels throughout the trial (Zhao *et al.* 2012). Importantly the insulin dose required by the moderate and severe type 1 diabetes patients was reduced by 38% and 25%, respectively, 12 weeks after treatment, and was maintained at 24 weeks (Zhao *et al.* 2012).

The percentage of $CD4^+CD25^+FOXP3^+$ Tregs increased significantly 4 weeks after Stem Cell Educator treatment (Zhao *et al.* 2012). The immunosuppressive cytokines IL-10 and TGF-β1 were analysed 4 weeks after treatment. Those patients receiving the CB-SC-treated lymphocytes showed significantly increased levels of TGF-β1, but no change in IL-10 levels (Zhao *et al.* 2012). CB-SCs were found to express autoimmune regulator (AIRE), which is a transcription factor expressed in the medulla of the thymus that controls immune tolerance (Zhao *et al.* 2012). Knockdown of AIRE led to a decrease in the immune-modulating programmed death ligand-1, and functional knockdown of AIRE in CB-SCs resulted in a decrease in the number of CB-SC-induced Tregs (Zhao *et al.* 2012). Therefore AIRE is deemed to be important for the immune modulation of lymphocytes by CB-SCs (Zhao *et al.* 2012).

1.15 Insulin expression outside of the pancreas

There has been evidence of insulin expression in the brain since the 1970s (Kojima *et al.* 2006). In 1994 Devaskar *et al*. showed that insulin transcripts could be isolated from postnatal rabbit brain. Insulin mRNA was present at higher levels in neurons than in glial cells. Expression increased with the age of the brain in that it was present at higher levels in 10 day-old rabbits compared with 1 day old rabbits (Devaskar *et al.* 1994). Importantly, the sequence of the RT-PCR product obtained from neuronal insulin mRNA was the same as that of pancreatic insulin mRNA transcripts (Devaskar *et al.* 1994). Insulin, as measured by high-performance liquid chromatography, is also expressed by rabbit neurons in culture medium, increasing 3-fold in expression from 24 h to 144 h of culture (Devaskar *et al.* 1994). *In situ* hybridization of insulin mRNA confirmed the expression of insulin mRNA by neuronal cells (Devaskar *et al.* 1994). However, insulin protein expression was absent as determined by immunohistochemistry (Devaskar *et al.* 1994).

The thymus is another organ which shows expression of insulin outside of the pancreas, as first reported in mice in 1994 (Kojima *et al.* 2006). A large number of extra-thymic proteins are expressed by the thymus in its role of inducing central tolerance against potential autoantigens (Pugliese *et al.* 1997). The thymic expression of the diabetes-associated autoantigens insulin, GAD65/67, and Islet antigen-2 (IA-2) was examined during foetal and childhood development in humans (Pugliese *et al.* 1997). Importantly, insulin mRNA was detected in all foetal thymus tissues tested, and several of the thymuses also expressed RNA for the other diabetes associated autoantigens (Pugliese *et al.* 1997). At the protein level, both insulin and proinsulin were detected in the thymus which would lead to exposure of T cells to these proteins to induce self-tolerance (Pugliese *et al.* 1997).

$CD14^+$ DCs originating from the BM have been shown to present proinsulin to APCs (Garcia *et al.* 2005). They play a role in self-tolerance in the thymus (Garcia *et al.* 2005). The $proinsulin^+CD14^+$ cells do not release insulin, express other self-epitopes including GAD65 and IA-2, and commonly express CD11c indicating they are DCs (Garcia *et al.* 2005). Those in peripheral blood also express HLA-DR, CD95, CD40, CD86 and CD123 (Garcia *et al.* 2005).

1.16 Objectives of my thesis

The insulin-producing cells in patients suffering from type 1 diabetes are destroyed by autoimmunity, resulting in a loss of glycemic control. Stem cells have the potential to differentiate into the pancreatic cell type, and can be transplanted to replace the lost cells, and restore a patient to normoglycemia. A variety of adult stem cells have been reported that can be easily and ethically obtained, and show plasticity towards the pancreatic lineage. Peripheral blood insulin-producing cells (PB-IPCs), programmable cells of monocytic origin (PCMOs), and f-macrophages (f-MOs) are obtainable from peripheral blood. Human amniotic stem cells (HASCs) and cord blood hematopoietic stem cells (CB-HSCs) are isolated after childbirth from tissue that is normally discarded. Adipose stem cells (ASCs) can be obtained from fat after liposuction or cosmetic surgery. There is a need to better understand the phenotypes of these stem cell populations to provide a clearer understanding of their stem-ness and plasticity. Many researchers have developed methods to induce the pancreatic differentiation of stem cells. There is a need to perform an independent valuation of these methodologies, and to experiment with ways to enhance pancreatic differentiation as often the resulting cells produce only low levels of insulin. Recent studies have also shown that stem cells can be formed from non-stem cells by treatment with the four induced pluripotent stem cell (iPSC)-inducing transcription factor proteins Oct-4, c-Myc, Kruppel-like factor 4 (KLF4), and SOX-2. Therefore, the overall aim of this project is to provide a clearer understanding of the described stem cell populations, and their differentiation potential towards pancreatic cells, as outlined below.

Specific Objectives:

1. Compare the ability and efficiency of published techniques to create insulin-producing cells from different adult and neonatal tissues.
2. Characterize the cells produced during the different stages of differentiation.
3. Test the functions of insulin-producing cells produced.

Chapter 2 Materials and Methods

2.1 Materials

2.1.1 Suppliers

Abbiotec *(San Diego, CA, USA)*

Abcam Inc. (*Cambridge, MA,* USA)

AbD Serotec *(Oxford, UK)*

American Research Products, Inc. *(Waltham, MA, USA)*

Amersham Bioscience *(Amersham, UK)*

Anaspec *(Fremont, CA, USA)*

BD / BD Biosciences / BD Pharmingen (*Franklin Lakes, NJ*, USA)

Biolegend *(San Diego, CA, USA)*

Bio-Rad Laboratories (*Hercules, CA,* USA)

Celprogen Inc. (*San Pedro, CA,* USA)

Dako *(Glostrup, Denmark)*

Enzo Life Sciences, Inc. (*Farmingdale, NY, USA)*

GE Healthcare (*Chalfont St. Giles,* UK)

GeneTex, Inc. *(San Antonio, TX, USA)*

Gibco/Life Technologies - supplied by Invitrogen (*Carlsbad, CA*, USA)

Hycult Biotech *(Uden, The Netherlands)*

Invitrogen (*Carlsbad, CA*, USA)

INVIVOGEN *(San Diego, CA, USA)*

Jackson ImmunoResearch Europe Ltd *(Suffolk, UK)*

Life Technologies *(Grand Island, NY*, USA)

Linco Research Inc. *(St. Charles, MO, USA)*

Millipore Corp. (*Bedford, MA*, USA)

Miltenyi Biotec *(Bergisch Gladbach, Germany)*

Merck Millipore (*Darmstadt, Germany)*

Novo Nordisk Pharmaceuticals Ltd *(Bagsværd, Denmark)*

Novus Biologicals *(Littleton, CO, USA)*

OZ Biosciences *(Marseille, France)*

PeproTech *(NJ, USA)*

ProSpec-TechnoGene Ltd. (*Rehovot,* Israel)

Proteintech Group, Inc. *(Chicago, IL, USA)*
R&D Systems (*Wiesbaden*, Germany)
Roche Applied Science (Roche; *Mannheim,* Germany)
Santa Cruz Biotechnology Inc. (*Santa Cruz, CA*, USA)
Schleicher & Schuell UK Ltd. (Surrey, UK)
Sigma-Aldrich (*St. Louis, MO*, USA)
Stemgent (*Cambridge, MA*, USA)
STEMCELL™ Technologies Inc. (Vancouver, Canada)
The Developmental Studies Hybridoma Bank *(IA, USA)*
Thermo Fisher Scientific Inc. (*Waltham, MA*, USA)

2.1.2 Buffers and chemicals

Phosphate Buffered Saline (1x PBS)

8 g NaCl
0.2 g KCl
1.44 g Na_2HPO_4
0.24 g KH_2PO_4
Up to 1 L with H_2O
pH 7.4

Fixation solution for cells - all cells except CB-HSC, P-HSC

4% Formaldehyde
Diluted in 1x PBS

Fixation solution for cells - CB-HSC, P-HSC

80% MeOH
Diluted in 1x PBS

Permeabilization solution for cells

0.1% Triton-X-100
Diluted in 1x PBS

Blocking solution for cells

5% (w/v) Casein (C3400, Sigma-Aldrich)

2% Normal horse serum

Diluted in 1x PBS

Antibody dilution buffer

5% (w/v) BSA fraction V IgG free (30063481, Gibco)

Diluted in 1x PBS

Cytoplasmic fraction lysis buffer (25 mL)

1.25 mL Tris.Cl (50 mM)
0.75 mL NaCl (150 mM)
0.25 mL NP40
0.5 mL PMSF (2 mM)
1 mL NaI (20 mM)
20.25 mL H_2O

Nuclear fraction lysis buffer

10 mL Cytoplasmic fraction lysis buffer
6.25 µL STI (5 µg/mL)
100 µL Pepstatin (10 µg/mL)
One tablet of complete EDTA-free protease inhibitor cocktail (11873580001, Roche Applied Science)

Whole cell lysis buffer (1 mL)

125 µL Tris, pH 6.8
100 µL 20% (w/v) SDS
100 µL Glycerol
675 µL H_2O

Whole cell lysis buffer loading dye (reducing) (5x)

0.5 M Dithiothreitol

0.03% Bromophenol blue

Added to whole cell lysis buffer

Protein loading dye solution (non-reducing) (5x)

360 mM Tris-Cl pH 6.8

10% (w/v) SDS

30% (w/v) Glycerol

0.03% Bromophenol blue

Protein loading dye solution (reducing) (5x)

0.5 M Dithiothreitol

Added to non-reducing protein loading dye solution

Tris Buffered Saline with Tween-20 (1x T-TBS)

6 g NaCl

3 g Tris-HCl

0.2 g KCl

1 mL Tween-20

Up to 1 L with dH_2O

Blocking solution for Western blotting

5% (w/v) Skim milk powder

Dissolved in 1x T-TBS

Stripping solution for Western blotting

2% of 10 M NaOH

Diluted in H_2O

Western blot membrane transfer buffer

20% MeOH

80% 1x SDS-PAGE running buffer

SDS-PAGE gel running buffer

1.24 M Tris Base

9.6 M Glycine

5% (w/v) SDS

Diluted in H_2O

30% Acrylamide

30% (w/v) Acrylamide

0.2% Bis-acrylamide

Diluted in H_2O

SDS-PAGE separating gel (12%)

1.7 mL H_2O
2.0 mL 30% Acrylamide
1.3 mL 1.5 M Tris (pH 8.8)
0.05 mL 10% SDS
0.05 mL 10% ammonium persulfate (APS)
0.002 mL TEMED

SDS-PAGE stacking gel

1.4 mL H_2O
0.33 mL 30% Acrylamide
0.25 mL 1.0 M Tris (pH 6.8)
0.02 mL 10% SDS
0.02 mL 10% APS
0.002 mL TEMED

Separating/spacing Tris-tricine buffer

3 M Tris base

0.3% (w/v) SDS

pH 8.9

2x Crosslinker acrylamide

48% (w/v) Acrylamide

3% (w/v) Bis-acrylamide

Diluted in H_2O

Stacking Tris-tricine buffer

1 M Tris-HCl

Diluted in H_2O

pH 6.8

Tris-tricine separating gel

6.7 mL H_2O
10 mL Separating/spacing Tris-tricine buffer
10 mL 2x Crosslinker acrylamide
3.2 mL Glycerol
100 µL 10% (w/v) APS
10 µL TEMED

Tris-tricine spacing gel

6.95 mL H_2O
5 mL Separating/spacing Tris-tricine buffer
3 mL 30% Acrylamide
50 µL 10% (w/v) APS
5 µL TEMED

Tris-tricine stacking gel

10.3 mL H_2O
1.9 mL Stacking Tris-tricine buffer
2.5 mL 30% Acrylamide
150 µL 0.5 M EDTA (pH 8.0)
100 µL 10% (w/v) APS
7.5 µL TEMED

Anode buffer (10x) for Tris-tricine gel

2 M Tris-Cl
Diluted in H_2O
pH 8.9

Cathode buffer (10x) for Tris-tricine gel

1 M Tris Base
1 M Tricine
1% (w/v) SDS
Diluted in H_2O

Protein extraction buffer

100 mM HEPES, pH 8.2

50 mM NaCl

5 mM $MgCl_2$

1 mM Dithiothreitol

1x Complete EDTA-free protease inhibitor cocktail (tablet)

0.1% Gelatin

0.5 g Gelatin (G1890, Sigma)

500 mL H_2O

The resulting solution was autoclaved to dissolve the gelatin and sterilize the solution

60% isopropanol for Oil Red O staining

60 mL Isopropanol

40 mL H_2O

Stock Oil Red O

0.25 g Oil Red O powder (O0625, Sigma-Aldrich)

50 mL Isopropanol

Working Oil Red O solution

3 mL stock Oil Red O solution

2 mL H_2O

Filtered with 0.2 μm filter before use

Alkaline phosphatase rinse buffer

20 mM Tris-HCl, pH 7.4

0.15 M NaCl

0.05% Tween-20

Naphthol/Fast red violet solution

Fast red violet: Naphthol AS-BI phosphate solution: Water

Diluted to 2:1:1

β-galactosidase (β-gal) fixation solution for β-gal staining

2% Formaldehyde

0.2% Glutaraldehyde

Diluted in PBS

Citric acid solution **for β**-gal staining

100 mM $C_6H_8O_7.H_2O$

Dissolved in H_2O

Sodium phosphate (dibasic) solution **for β**-gal staining

200 mM $NaH_2PO_4.H_2O$

Dissolved in H_2O

0.2M Citric acid/Na phosphate buffer **for β**-gal staining

36.85 mL Citric acid solution (100 mM)

63.15 mL Sodium phosphate (dibasic) solution (200 mM)

Checked pH 6.0

Potassium hexacyano-ferrate (II) trihydrate solution **for β**-gal staining

100 mM $K_4[Fe(CN)_6].3H_2O$

Dissolved in H_2O

Potassium hexacyano-ferrate (III) solution **for β**-gal staining

100 mM $K_3[Fe(CN)_6]$

Dissolved in H_2O

Sodium chloride solution **for β**-gal staining

5 M NaCl

Dissolved in H_2O

Magnesium chloride hexahydrate solution **for β**-gal staining

1 M $MgCl_2.6H_2O$

Dissolved in H_2O

X-gal solution for β-gal staining

20 mg/mL X-gal (B4252, Sigma-Aldrich)

Dissolved in N,N-dimethylformamide

β-gal staining solution

40 mM Citric acid/Na phosphate buffer

5 mM $K_4[Fe(CN)_6].3H_2O$

5 mM $K_3[Fe(CN)_6]$

150 mM Sodium chloride

2 mM Magnesium chloride

1 mg/mL X-gal solution

Diluted in H_2O

L-leucine methyl ester solution

10 mM L-leucine methyl ester (L1002, Sigma-Aldrich)

Dissolved in RPMI (11835, Invitrogen)

pH 7.4

2.1.3 Tissue culture reagents and cell lines

2.1.3.1 General tissue culture media

Foetal bovine serum (FBS): FBS (10091-148, Gibco) was heat-inactivated at 56°C for 30 min before supplementing into media.

RPMI 1640: RPMI (11875, Gibco) contains 300 mg/L of L-glutamine and 2000 mg/L D-glucose. The full RPMI medium consisted of RPMI 1640 supplemented with 100 U/mL of penicillin, 100 μg/mL of streptomycin and 0.29 mg/mL of L-glutamine (PSG) (10378-016, Gibco) and 7-10% FBS.

Advanced RPMI 1640: Advanced RPMI (12633, Gibco) contains non-essential amino acids, 2000 mg/L of D-Glucose and 110 mg/L of sodium pyruvate. The full advanced RPMI medium consisted of Advanced RPMI 1640 supplemented with 100 U/mL of penicillin, 100 μg/mL of streptomycin and 0.29 mg/mL of L-glutamine (PSG) and varying amounts of FBS.

DMEM: DMEM (11995, Gibco) contains 4500 mg/L of D-glucose, 110 mg/L of sodium pyruvate and 584 mg/L of L-glutamine. The full DMEM medium consisted of DMEM supplemented with 100 U/mL of penicillin, 100 μg/mL of streptomycin and 0.29 mg/mL of L-glutamine (PSG) and 10% FBS.

DMEM/F12: DMEM/F12 (11320, Gibco) contains 365 mg/L of L-glutamine. This medium is the "expansion medium" which consisted of DMEM/F12 supplemented with 2 ng/mL of bFGF (13256-029, Gibco), 100 U/mL of penicillin, 100 μg/mL of streptomycin and 0.29 mg/mL of L-glutamine (PSG) and 10% FBS.

Hams F-12K (Kaighn's): Hams F12-K (21127, Gibco) contains 292 mg/L of L-glutamine, 1260 mg/L of D-glucose, and 220 mg/L of sodium pyruvate. The full Hams F-12K medium consisted of Hams F-12K supplemented with 100 U/mL of penicillin, 100 μg/mL of streptomycin and 0.29 mg/mL of L-glutamine (PSG) and 10% FBS.

Opti-MEM: Opti-MEM Reduced serum medium (31985, Gibco) contains L-glutamine. This medium was used as a buffer for DNA during cellular transfection.

Freezing Solution: Full medium containing 10% FBS and 1% PSG with 5% DSMO.

2.1.3.2 Mammalian cell lines

The 1.1B4 cell line is a human pancreatic β-cell: PANC-1 hybrid cell line, which is reported to express insulin. It was sourced from Sigma (10012801). The cell line was propagated in full RPMI medium containing 10% FBS at 37°C and 5% CO_2. The experiments in this thesis were conducted using 1 batch of 1.1B4 cells.

The RIN-m5F cell line is a transformed rat pancreatic islet β-cell line. It was kindly donated by Professor Garth Cooper (University of Auckland). The cell line was propagated in full RPMI medium containing 10% FBS at 37°C and 5% CO_2.

The INS-1E cell line is a transformed rat pancreatic islet β-cell tumour cell line. It was kindly donated by Dr Claes Wollheim (Lund University, Sweden). The cell line was propagated in full RPMI medium containing 10% FBS with the addition of 100 mM HEPES (15630-080, Gibco), 50 μM β-mercaptoethanol (21985-023, Gibco) and 1 mM sodium pyruvate (11370-070, Gibco).

StemPro® Human Adipose-Derived Stem Cells (ASCs) were purchased from Life Technologies™ (R7788-110). They were isolated from human adipose tissue during liposuction and then expanded for one passage in MesonPRO RS™ (12746, Gibco) prior to cryopreservation by the supplier. They were propagated in MesonPRO RS™ medium. They are a heterogenous population of cells that express CD29, CD44, CD73, CD90, CD105 and CD166, and not CD14, CD31, CD45, and Lin1 (Life Technologies™). The experiments in this thesis were conducted using 1 batch of ASCs.

Cord blood hematopoietic stem cells (CB-HSCs) derived from human cord blood were sourced from Celprogen Inc. (36001). They were propagated in Human Stem Cell (Cord Blood Derived) Expansion Medium with serum (M36001-02ES, Celprogen Inc.) on plates coated with Human Stem Cell Extra-cellular Expansion Matrix (E36001-02, Celprogen Inc.) at 37°C and 5% CO_2. The experiments in this thesis were conducted using 1 batch of CB-HSCs.

Pancreatic hematopoietic stem cells (P-HSCs) derived from human cord blood by trans-differentiation were sourced from Celprogen Inc. (36004-05). They are reported to express insulin, PDX-1, CD117, and GAD. Cord blood stem cells were differentiated with Human Pancreatic (Trans-Differentiated) Stem Cell Differentiation Media with serum (M36004-05DS, Celprogen Inc.) on plates coated with Human Pancreatic (Trans-Differentiated) Stem Cell Extra-cellular Differentiation Matrix (D36004-05, Celprogen Inc.). The transdifferentiated cells were then maintained in Human Pancreatic (Trans-Differentiated) Stem Cell Media with serum (M36004-05S, Celprogen Inc.) on plates coated with Human Pancreatic Stem Cell Culture Extra-cellular Matrix (E36004-05, Celprogen Inc.). The experiments in this thesis were conducted using 1 batch of P-HSCs.

Human amniotic stem cells (HASCs) derived from human amniotic membrane and amniotic fluid were sourced from Celprogen Inc. (36101-28). They were propagated in Human Embryonic Stem Cell Media with serum (M36101-28S, Celprogen Inc.) on plates coated with Human Embryonic Stem Cell Extra-cellular Matrix (E36101-28, Celprogen Inc.). The experiments in this thesis were conducted using 1 batch of HASCs.

The 266-6 cell line is a pancreatic acinar cell tumour cell line derived from a young adult mouse. The tumour was induced with an elastase I/SV-40 T antigen fusion gene. The cell line was sourced from the ATCC (CRL-2151™), and propagated on 0.1% gelatin-coated flasks in full DMEM medium at 37°C and 5% CO_2.

The CHO-K1 cell line is an ovarian cancer cell line derived from the parental CHO cell line that had in turn been derived from the ovary of a Chinese hamster. The cell line was sourced from the ATCC (CCL-61™), and propagated in full Hams F-12K medium at 37°C and 5% CO_2.

2.1.4 Antibodies and protein controls

Table 2.1 List of primary antibodies

Target antigen (antibody category number)	Host species	Supplier	ICC conc. (µg/mL) used	WB / dot blot dilution used
AIRE (NB100-40799)	Goat	Novus Biologicals	5	
Amylin (250470)	Rabbit	Abbiotec	5	
Arx (sc-98895, H-70)	Rabbit	Santa Cruz Biotechnology Inc.	5	
CD11b/Mac-1 (555386)	Mouse	BD Biosciences	5	
CD11c (550375)	Mouse	BD Pharmingen	5	
CD14 (HM2060)	Mouse	Hycult Biotech	5	
CD154 (310801)	Mouse	Biolegend	5	
CD20 (302320)	Mouse	Biolegend	5	
CD205 (DEC-205)	Mouse	Biolegend	5	
CD25 (MCA2127)	Mouse	AbD Serotec	5	
CD29/Integrin β1 (sc-13590, P5D2)	Mouse	Santa Cruz Biotechnology Inc.	10	
CD3 (550368)	Mouse	BD Pharmingen	5	
CD309	Mouse	Miltenyi Biotec	5	
CD31 (MO823)	Mouse	Dako	5	
CD34 (555820	Mouse	BD Pharmingen	5	
CD4 (555344)	Mouse	BD Pharmingen	5	
CD40/TNFRSF5 (MAB6321)	Mouse	R&D Systems	5	
CD45-FITC (555482)	Mouse	BD Biosciences	1:50	
CD68/EBM11 (MO718)	Mouse	Dako	5	
CD8 (GTX24055)	Rabbit	GeneTex, Inc	5	
CD90/Thy-1 (sc-6071, K-16)	Goat	Santa Cruz Biotechnology Inc.	10	
c-Myc (ab32)	Mouse	Abcam Inc.		1:1000
C-peptide (C-PEP-01, 05-1109)	Mouse	Millipore Corp.	5	
CXCR4 (ab2074)	Rabbit	Abcam Inc.	5	
Fibroblast aka prolyl 4-hydroxylase (β-subunit) (M0877)	Mouse	Dako	5	
FOXA2 (ab40874)	Rabbit	Abcam Inc.	5	
FOXP3 (ab20034)	Mouse	Abcam Inc.	5	1:250
FOXP3 (ab36607)	Mouse	Abcam Inc.	5	1:500
GIPR (sc-69417, Y-15)	Goat	Santa Cruz Biotechnology Inc.	5	
Glucagon (55154A, IN-1)	Rabbit	Anaspec	5	
Glut-1 (sc-7903, H-43)	Rabbit	Santa Cruz Biotechnology Inc.	5	
Glut-2 (sc-9117, H-67)	Rabbit	Santa Cruz Biotechnology Inc.	5	
GPR40 (sc-32905, FL-300)	Rabbit	Santa Cruz Biotechnology Inc.	5	
HLA-DR (NB100-77855)	Mouse	Novus Biologicals	5	
HNF4a (ab41898)	Mouse	Abcam Inc.	5	
HNF6 (sc-13050)	Rabbit	Santa Cruz Biotechnology Inc.	5	
IgG (sc-2025)	Mouse	Santa Cruz Biotechnology Inc.	5-10	
IgG (sc-2027)	Rabbit	Santa Cruz Biotechnology Inc.	5	
IgG (sc-2028)	Goat	Santa Cruz Biotechnology Inc.	5-10	
IgG (sc-2711)	Guinea pig	Santa Cruz Biotechnology Inc.	5	
IgY (sc-2718)	Chicken	Santa Cruz Biotechnology Inc.	5	
IL-2Ralpha (sc-664, C-20)	Rabbit	Santa Cruz Biotechnology Inc.	5	

Target antigen (antibody category number)	Host species	Supplier	ICC conc. (µg/mL) used	WB / dot blot dilution used
Insulin (07-01016)	Chicken	American Research Products, Inc.	5	1:2000
Insulin (4011-01F)	Guinea pig	Linco Research Inc.	5	1:1000
Insulin (I2018)	Mouse	Sigma	5	1:2000
KLF4 (ab75486)	Mouse	Abcam Inc.		1:500
MafA (sc-27138, E-13)	Goat	Santa Cruz Biotechnology Inc.	5	
Nanog (560482)	Mouse	BD Pharmingen	5	
Nestin (AB5922)	Rabbit	Millipore Corp.	5	
Nestin (MAB5326)	Mouse	Millipore Corp.	5	
NeuroD (sc-20805, H-76)	Rabbit	Santa Cruz Biotechnology Inc.	5	
Neurogenin3 (sc-25654, H-80)	Rabbit	Santa Cruz Biotechnology Inc.	5	
Neuron Specific Enolase (AB9698)	Chicken	Millipore Corp.	5	
Nkx2.2 (74.5A5)	Mouse	The Developmental Studies Hybridoma Bank	5	
Nkx6.1 (F55A10)	Mouse	The Developmental Studies Hybridoma Bank	5	
Oct-4 (MAB4401)	Mouse	Millipore Corp.	5	1:2000
Pax4 (ab42450)	Rabbit	Abcam Inc.	5	
Pax6 (09-0075)	Mouse	Stemgent	5	
PCNA (sc-56, PC10)	Mouse	Santa Cruz Biotechnology Inc.	5	
PCSK1 (sc-100578, J-18)	Mouse	Santa Cruz Biotechnology Inc.	5	
PDX-1 (sc-14664, A-17)	Goat	Santa Cruz Biotechnology Inc.	5	
PDX-1 (sc-25403, H-140)	Rabbit	Santa Cruz Biotechnology Inc.	5	1:500
ProINS (GS-9A8)	Mouse	The Developmental Studies Hybridoma Bank	1:100	
PTF1A (AV31839)	Rabbit	Sigma	5	
SOX-17 (ab84990)	Mouse	Abcam Inc.	5	
SOX-17 (sc-17355)	Goat	Santa Cruz Biotechnology Inc.	5	
SOX-2 (MAB4343)	Mouse	Millipore Corp.		1:1000
TGF-beta (MCA797)	Mouse	AbD Serotec	5	
Von Willebrand Factor (ab20435)	Mouse	Abcam Inc.	5	
Wnt-3 (sc-74537)	Mouse	Santa Cruz Biotechnology Inc.	5	
β-actin (ab8227)	Rabbit	Abcam Inc.		1:1000

Abbreviations: ICC - immunocytochemistry, Conc. – concentration, WB - Western blot

Table 2.2 List of secondary antibodies

Secondary antibody (antibody category number)	Host species	Supplier	ICC conc./ WB / dot blot dilution used
Anti-chicken Alexa Fluor 488 (A11039)	Goat	Molecular Probes - Invitrogen	1:500
Anti-chicken horseradish peroxidase (HRP) (AP194P)	Donkey	Millipore	1:40,000
Anti-goat Alexa Fluor 568 (A11057)	Donkey	Molecular Probes - Invitrogen	1:500
Anti-guinea pig Alexa Fluor 568 (A11075)	Goat	Molecular Probes - Invitrogen	1:500
Anti-guinea pig horseradish peroxidase (HRP) (706-035-148)	Donkey	Jackson ImmunoResearch	1:40,000
Anti-mouse Alexa Fluor 488 (A21202)	Donkey	Molecular Probes - Invitrogen	1:500
Anti-mouse Alexa Fluor 568 (A10037)	Donkey	Molecular Probes - Invitrogen	1:500
Anti-mouse horseradish peroxidase (HRP) (A2554)	Goat	Sigma	1:20,000
Anti-rabbit Alexa Fluor 488 (A21206)	Donkey	Molecular Probes - Invitrogen	1:500
Anti-rabbit Alexa Fluor 568 (A10042)	Donkey	Molecular Probes - Invitrogen	1:500
Anti-rabbit horseradish peroxidase (HRP) (711-036-152)	Donkey	Jackson ImmunoResearch	1:20,000
Anti-rat Alexa Fluor 488 (A21208)	Donkey	Molecular Probes - Invitrogen	1:500

Abbreviations: ICC - immunocytochemistry, Conc. – concentration, WB - Western blot

Table 2.3 List of control proteins

Control proteins (category number)	Supplier
Insulin (Novorapid®)	Novo Nordisk Pharmaceuticals Ltd
Insulin-like growth factor-1 (IGF-1) (CYT-216)	ProSpec-TechnoGene Ltd.
Insulin-like growth factor-2 (IGF-2) (CYT-265)	ProSpec-TechnoGene Ltd.
Insulin-like 3 (INSL3) (4544-NS)	R&D Systems
Pancreatic duodenal homeobox-1 (PDX-1, recombinant human) (PRO-415)	ProSpec-TechnoGene Ltd.

2.1.5 DNA plasmids encoding immortalizing transcription factors

The pUNO1 expression vector (INVIVOGEN) is designed for stable and high level gene expression in mammalian cells. It contains the human cytomegalovirus promoter and enhancer, the bacterial EM7 promoter, and the blasticidin resistance gene which allow for amplification in *Escherichia coli* (*E. coli*), and selection of stable clones of mammalian cells. This expression vector was engineered to express the stem cell-related proteins Oct-4, KLF4, SOX2 and c-Myc. The pUNO1-based Oct-4, KLF4, SOX2 and c-Myc expression vectors pUNO1-mOCT4::11R (Figure 2.1), pUNO-mcMYC::11R (Figure 2.2), pUNO1-mKLF4::11R (Figure 2.3), and pUNO-mSOX2::11R (Figure 2.4) were purchased from INVIVOGEN. The inserted genes are fused at the C-terminus with sequences encoding poly-arginine (11R) to render the encoded proteins cell-permeable.

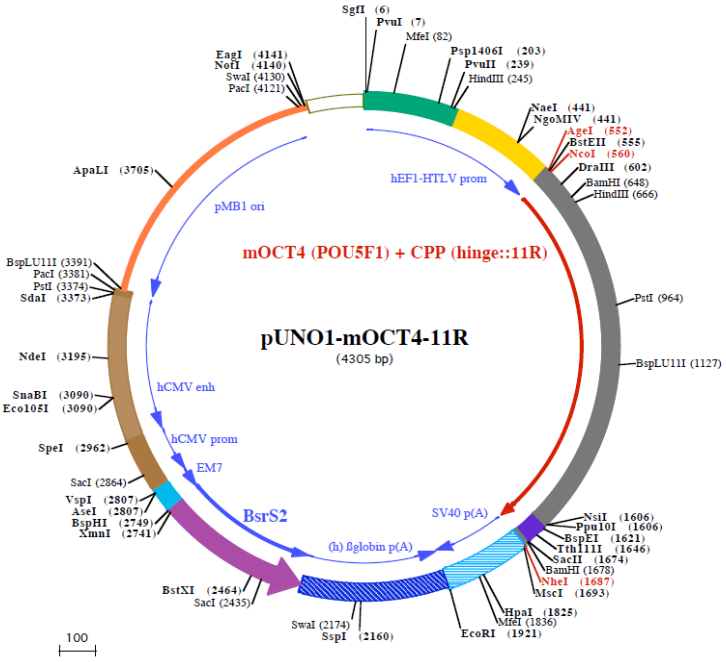


Figure 2.1 Map of the pUNO1-mOCT4::11R expression vector.

Image from INVIVOGEN.com.

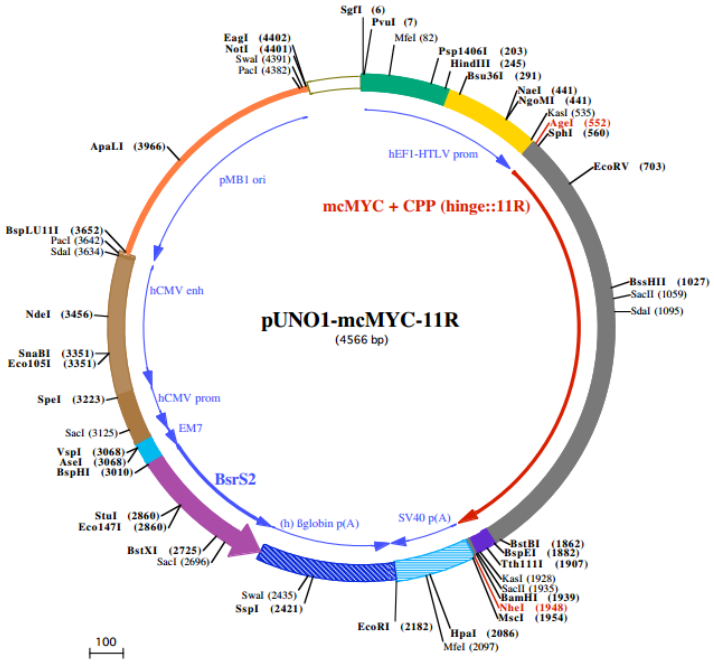


Figure 2.2 Map of the pUNO1-mcMYC::11R expression vector.

Image from INVIVOGEN.com.

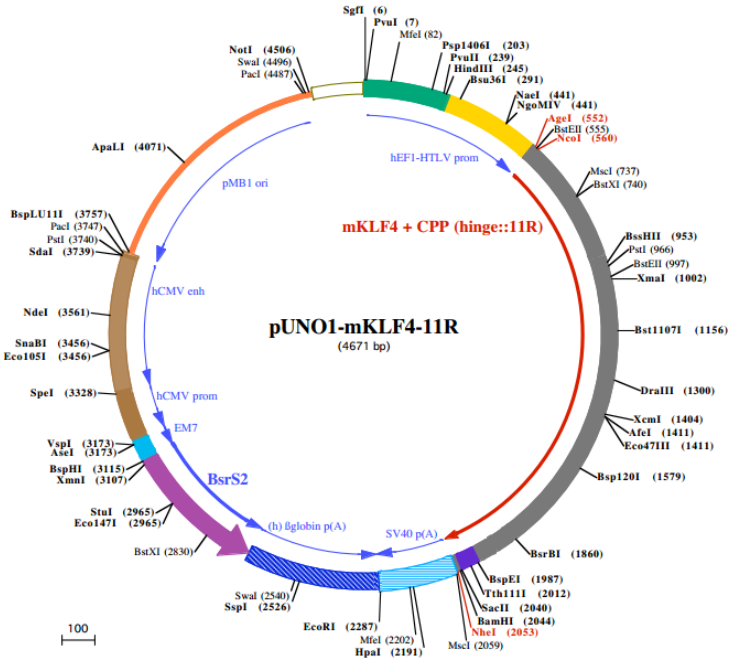


Figure 2.3 Map of the pUNO1-mKLF4::11R expression vector.

Image from INVIVOGEN.com.

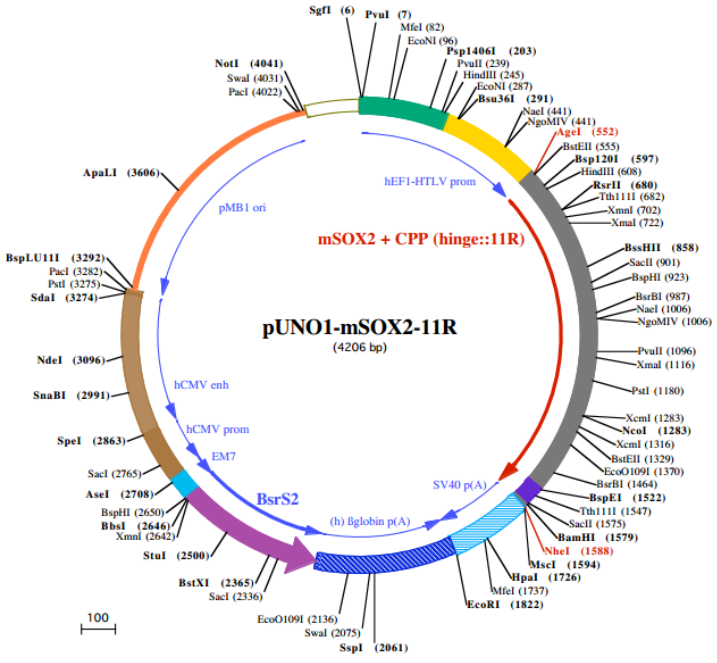


Figure 2.4 Map of the pUNO-mSOX2::11R expression vector.

Image from INVIVOGEN.com.

2.1.6 Control pancreatic cell lines

A panel of pancreatic cell lines including the human pancreatic cell line 1.1B4, and the rat pancreatic cell lines INS-1E and RINm5F, were intended to be used as positive controls for cells that express insulin, and to confirm the specificity of the antibodies used in this study.

2.1.6.1 1.1B4 cell line

The 1.1B4 cell line is a novel human pancreatic cell line that provides a much needed population of functional human insulin-secreting cells for diabetes research (McCluskey *et al.* 2011). The parental cell line was created by electrofusion of freshly isolated human pancreatic islet cells with the hypoxanthine/aminopterin/thymidine-sensitive human PANC-1 epithelial cell line (McCluskey *et al.* 2011). The fused cells were selected by culture with hypoxanthine/aminopterin/thymidine, and the newly formed colonies were tested for secretion of insulin (McCluskey *et al.* 2011). One of the highest insulin-secreting clones isolated was named 1.1B4 (McCluskey *et al.* 2011).

The 1.1B4 cell line grows in monolayers in a pavement pattern and consistently expresses insulin even after a high number of passages (McCluskey *et al.* 2011). Electron micrographs revealed the presence of dark granules in the cytoplasm and at the cell surface, which presumably contain insulin (McCluskey *et al.* 2011). There was reported to be an average of 4.08 ng of insulin per 10^6 1.1B4 cells (McCluskey *et al.* 2011). In addition to insulin, the 1.1B4 cell line expresses C-peptide, amylin, Glut-1, glucokinase (glucose sensor), RNA encoding the prohormone convertases PC1/3 and PC2, and the PC2 binding protein 7B2 (McCluskey *et al.* 2011). It is reported to form pseudo islet-like structures when cultured in suspension on ultra-low attachment plates (McCluskey *et al.* 2011).

The 1.1B4 cell line secretes insulin in response to a glucose challenge (McCluskey *et al.* 2011). STZ-induced diabetic SCID mice were subjected to subscapular implantation of encapsulated 1.1B4 cells. After 28 days they had formed a well vascularized mass (McCluskey *et al.* 2011). Two out of 5 mice were almost normoglycemic at the end of the study, and hyperglycemia in the remaining mice was substantially reduced (McCluskey *et al.* 2011).

2.1.6.2 Phenotyping of 1.1B4 cells

As reported by McCluskey *et al.* (2011), the 1.1B4 cell line grew in monolayers in a pavement pattern (Figure 2.5). Immunocytochemistry confirmed the cell line expressed Glut-1, PDX-1 and MafA, albeit MafA expression was not universal (Figure 2.6). However, in contrast to the previous report by McCluskey *et al.* (2011), the cells did not express insulin or amylin (Figure 2.6). Thus they could not be stained by either the guinea pig or mouse anti-insulin antibodies. A summary of the phenotyping of the 1.1B4 cell line is presented in Table 2.4.

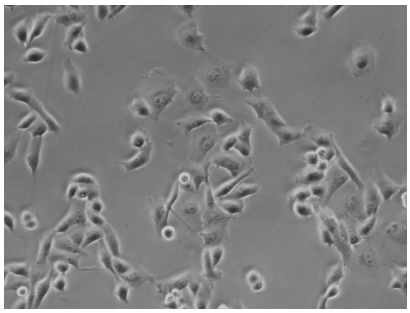
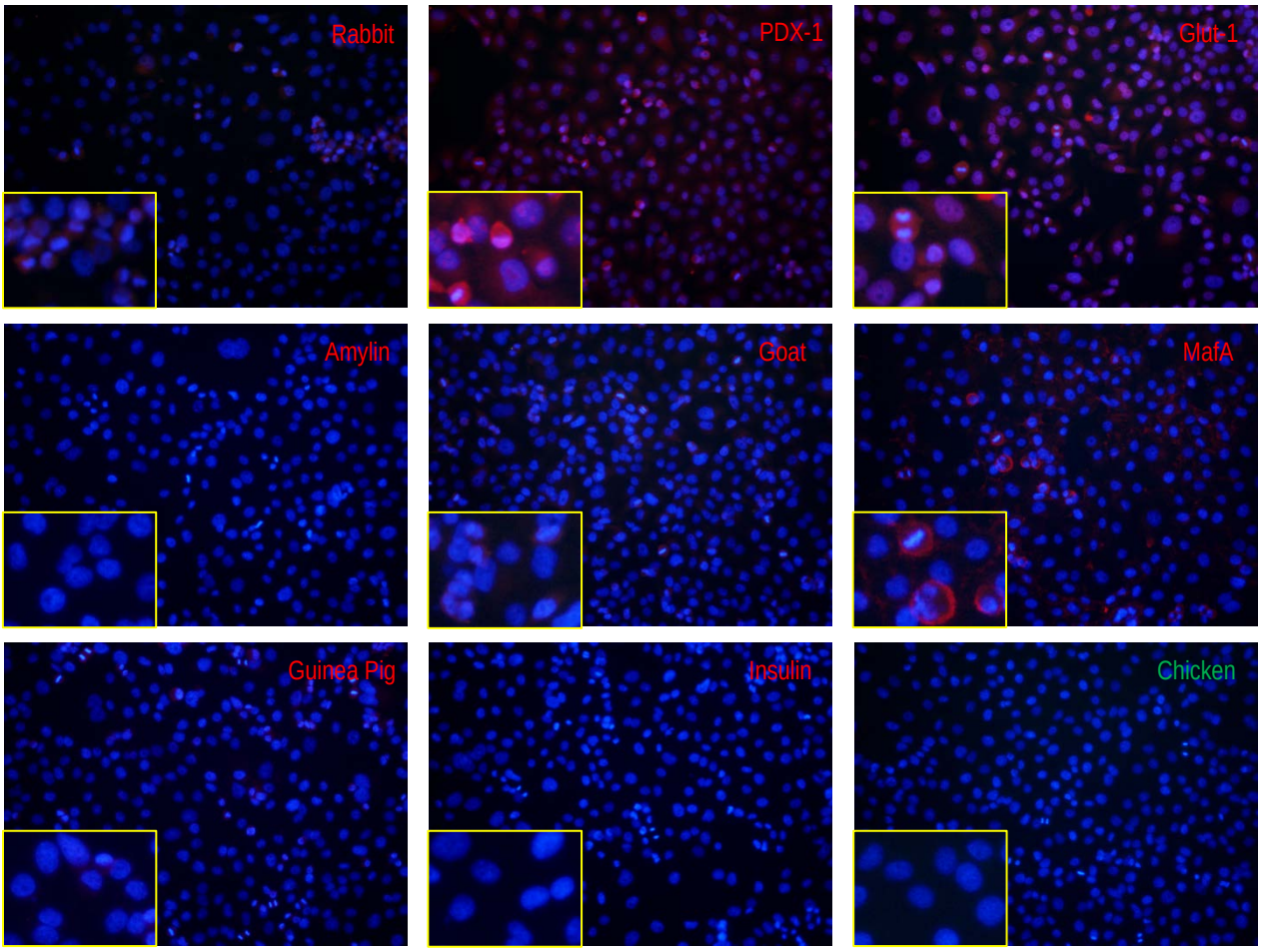


Figure 2.5 Phase contrast image of 1.1B4 cells.

The 1.1B4 cells were cultured for 2 days in RPMI1640 medium containing 10% FBS + 1% PSG. Image was taken at 200x magnification.



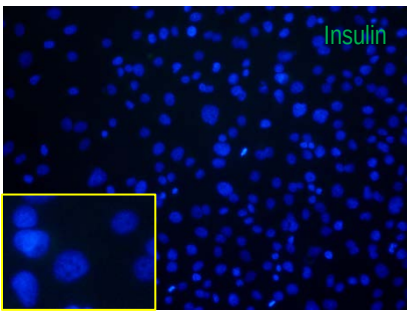


Figure 2.6 Phenotyping of 1.1B4 cultures.

1.1B4 cells were cultured for 1 week in RPMI1640 medium containing 10% FBS + 1% PSG. They were immunostained for the expression of pancreatic cell markers. Immunoreactivity was detected with donkey anti-rabbit (red), donkey anti-goat (red), goat anti-guinea pig (red), and goat anti-chicken (green) antibodies. Cell nuclei were stained blue with DAPI. Images were taken at 200x magnification; inset is a 4x magnification of part of the image. The images are presented so that the staining obtained with each IgG/IgY control immediately precedes stainings with antibodies of the same host species.

Table 2.4 Summary of the phenotyping of the 1.1B4 cell line

	1.1B4
PDX-1	x x x
Glut-1	x x x
MafA	x x x
Amylin	
Insulin	

0	0.1-20	21-40	41-60	61-80	81-100	% Positive

x	x x	x x x	Intensity of staining – weak/moderate/strong

A lysate of 1.1B4 cells was subjected to Western blot analysis to confirm that the cells did not express insulin (Figure 2.7). The cells were cultured for 1 week in RPMI1640 medium containing 10% FBS + 1% PSG, and lysed in cell lysis buffer. The proteins were reduced with β-mercaptoethanol, resolved on a Tris-Tricine gel, transferred to nitrocellulose, and Western blotted with a guinea pig anti-insulin antibody. Recombinant human insulin was used as a control to confirm antibody reactivity. Bands characteristic of the size of insulin (~3 kDa reduced, and 5.8 kDa non-reduced) were not obtained with the 1.1B4 cell lysate (Figure 2.7, left-hand blot). In contrast, the partially reduced recombinant human insulin protein gave bands of the expected size (Figure 2.7). The blot was then re-probed with an antibody against β-actin to confirm that proteins in the lysate had not been proteolytically degraded (Figure 2.7, right-hand blot). The correct-sized β-actin band of 42 kDa was obtained.

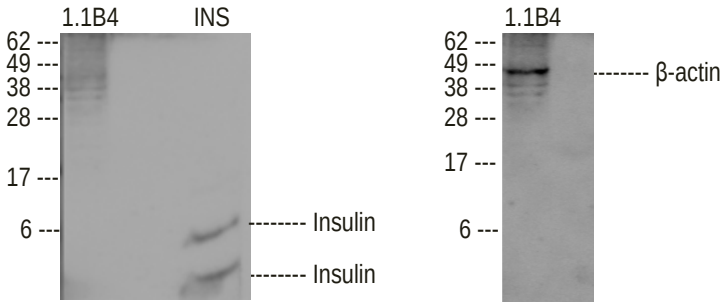


Figure 2.7 The purchased 1.1B4 cell line does not express insulin.

1.1B4 cells were cultured for 1 week in RPMI1640 medium containing 10% FBS + 1% PSG. Left blot: a whole cell lysate of 1.1B4 cells (1 x 10^6), and recombinant human insulin (INS, 1 μg) were Western blotted with a guinea pig antibody against insulin, and immunoreactivity detected with a donkey anti-guinea pig HRP-conjugated antibody. The positions of the ~3 kDa reduced and 5.8 kDa non-reduced bands of insulin are indicated in the right-hand margin. Right blot: the blot was re-probed with an antibody against human β-actin (42 kDa), with immunoreactivity detected with a donkey anti-rabbit HRP-conjugated antibody.

2.1.6.3 INS-1E cell line

The rat INS-1E cell line originated from an x-ray-induced transplantable insulinoma, termed INS-1 (Asfari *et al.* 1992). INS-1 cells contain a variable number of secretory granules, with some granules displaying the same dense centre and clear halo that typifies the granules of normal β-cells (Asfari *et al.* 1992). These cells have maintained cytoplasmic insulin expression for more than 2 years (passage 83) (Asfari *et al.* 1992), and their ability to secrete insulin *in vitro* has been maintained for more than 2 years (116 passages) (Merglen *et al.* 2004). The inclusion of β-mercaptoethanol in the culture medium increases their proliferation and survival (Asfari *et al.* 1992). The INS-1E cell line was selected from INS-1 clones which showed increased insulin secretion in response to 5 to 20 mM glucose (Asfari *et al.* 1992; Merglen *et al.* 2004). INS-1E cells contain on average 2.15 μg of insulin per 10^6 cells, which is just 10% of that produced by normal rat β-cells (Merglen *et al.* 2004) (for a comparison with other cell types see Table 1.2).

2.1.6.4 Phenotyping of INS-1E cells

The rat INS-1E cell line was cultured in tissue culture dishes in which it grew in monolayers (Figure 2.8). The majority of INS-1E cells strongly expressed insulin, HNF6, Glut-2, Arx, Glut-1, FOXA2, HNF4a, SOX-17, AIRE, PDX-1 (cytoplasmic and nuclear), and Nkx6.1 (nuclear) (Figure 2.9). Some cells expressed glucagon, while others expressed both glucagon and insulin, reminiscent of immature precursors of α and β-cells (Figure 2.9). Insulin expression was detectable with both the mouse and guinea pig anti-insulin antibodies. A lysate of INS-1E cells was subjected to dot blot analysis to confirm the expression of insulin (Figure 2.10). The cells were cultured for 1 week in RPMI1640 medium containing 10% FBS + 10 mM HEPES + 50 μM β-mercaptoethanol + 1 mM sodium pyruvate + 1% PSG, and lysed in whole cell lysis buffer. Pure recombinant insulin and cell

lysates were spotted onto a nitrocellulose membrane, and probed with mouse, guinea pig, and chicken anti-insulin antibodies (Figure 2.10). The mouse, guinea pig, and chicken anti-insulin antibodies detected insulin in the INS-1E cell lysate, and also detected pure recombinant insulin protein (Figure 2.10). The antibodies used for immunocytochemistry and dot blot analysis are the same antibodies used to stain populations of human stem cells and progenitors in this study, thereby confirming antibody immunoreactivity. A summary of the phenotype of the INS-1E cell line is presented in Table 2.5.

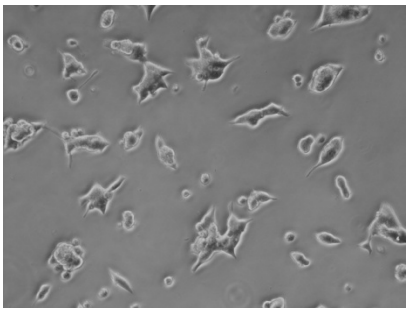
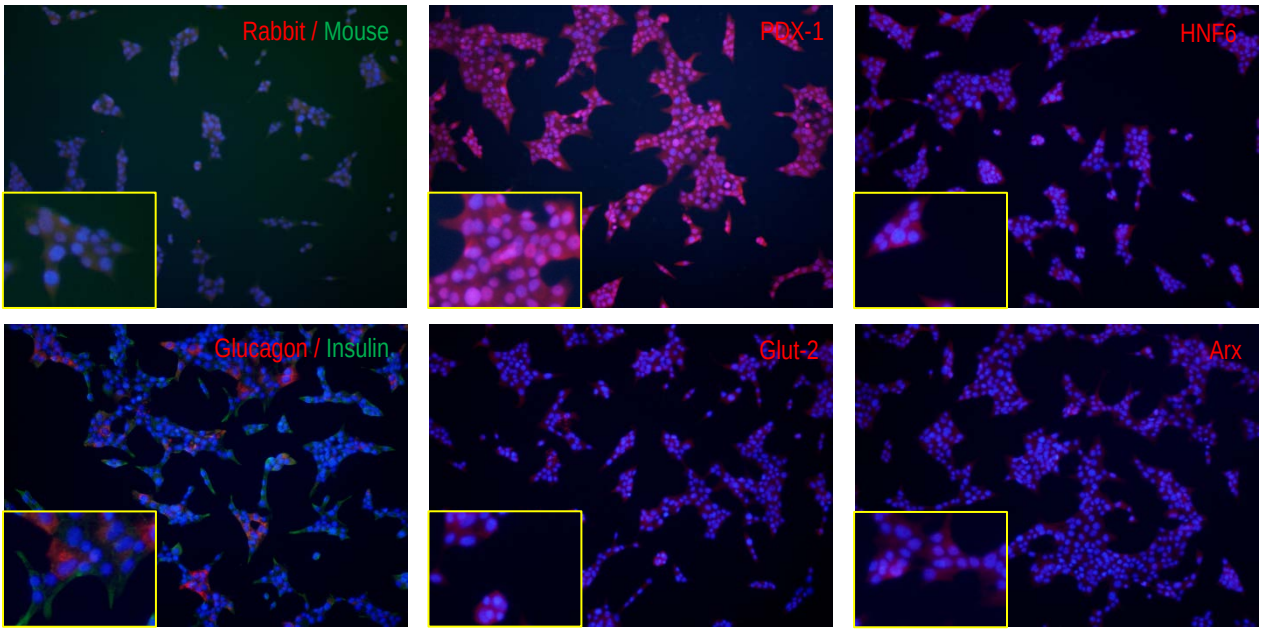


Figure 2.8 Phase contrast image of INS-1E cells.

INS-1E cells were cultured for 2 days in RPMI1640 medium containing 10% FBS + 10 mM HEPES + 50 µM β-mercaptoethanol + 1 mM sodium pyruvate + 1% PSG. Image was taken at 200x magnification.



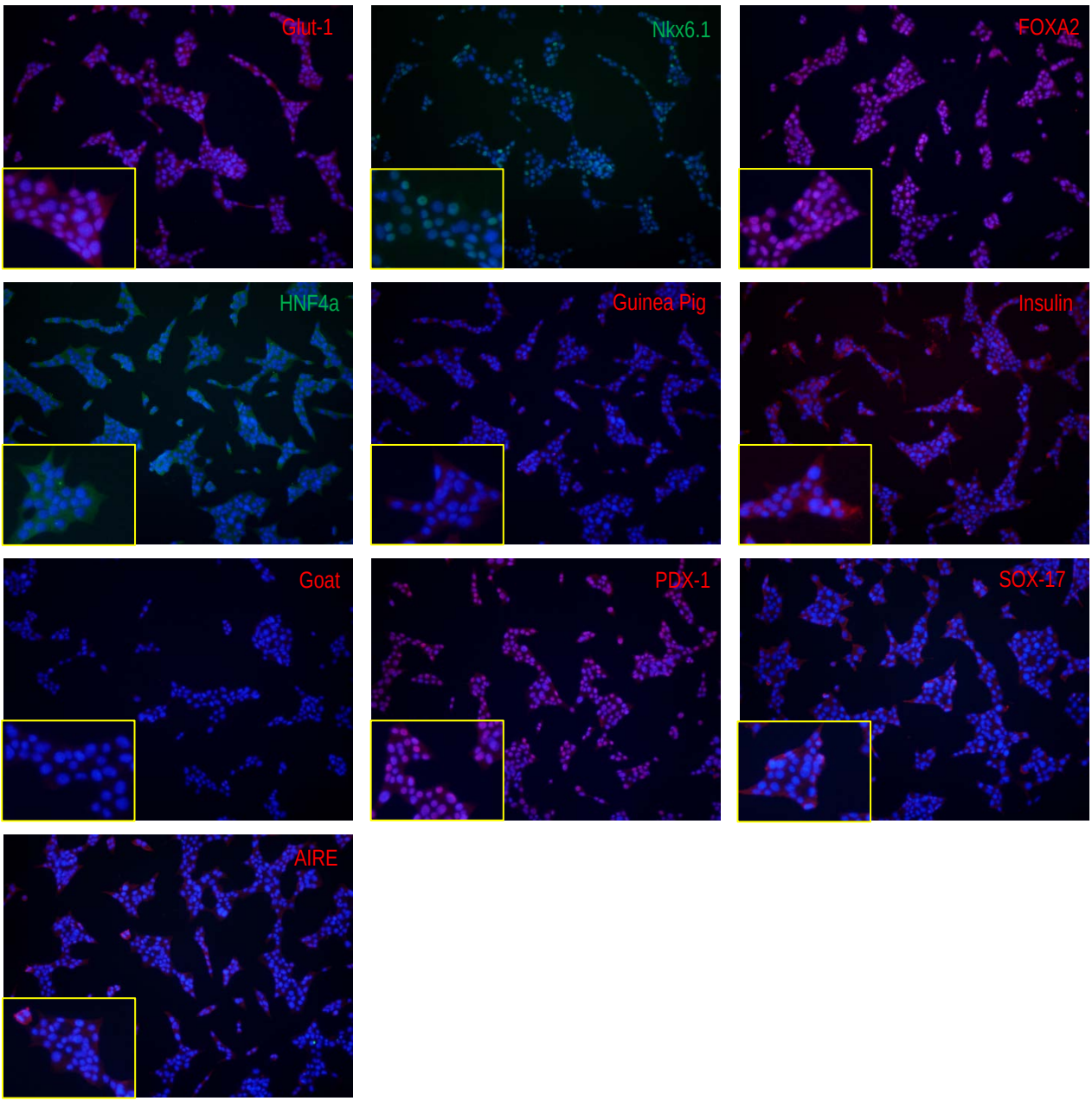


Figure 2.9 Phenotyping of INS-1E cells.

INS-1E cells (passage 79) were cultured for 1 week in RPMI1640 medium containing 10% FBS + 100 mM HEPES + 50 μM β-mercaptoethanol + 1 mM sodium pyruvate + 1% PSG. They were immunostained for the expression of pancreatic cell markers. Immunoreactivity was detected with donkey anti-rabbit (red), donkey anti-mouse (green), goat anti-guinea pig (red), and donkey anti-goat (red) antibodies. Cell nuclei were stained blue with DAPI. Images were taken at 100x magnification; inset is a 4x magnification of part of the image. The images are presented so that the staining obtained with each IgG control immediately precedes stainings with antibodies of the same host species.

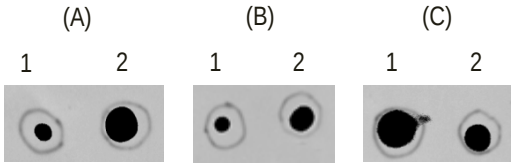


Figure 2.10 The RINm5F cell line expresses insulin.

Pure recombinant insulin (1 μg, spot 1), and whole cell lysates of INS-1E cells (10 μg, spot 2) in PBS were spotted onto nitrocellulose membranes. The position of each protein is denoted by a circle. The dot blots were probed with a chicken anti-insulin antibody (A), mouse anti-insulin antibody (B), and guinea pig anti-insulin antibody (C), respectively, and immunoreactivity was detected with donkey anti-chicken HRP-conjugated, goat anti-mouse HRP-conjugated, and donkey anti-guinea pig HRP-conjugated secondary antibodies, respectively, and developed by chemiluminescence.

Table 2.5 Summary of the phenotyping of the INS-1E cell line

	INS-1E
PDX-1	x x x
HNF6	x x x
Glucagon	x x x
Insulin	x x x
Glut-2	x x x
Arx	x x x
Glut-1	x x x
Nkx6.1	x x x
FOXA2	x x x
HNF4a	x x x
SOX-17	x x x
AIRE	x x x

0	0.1-20	21-40	41-60	61-80	81-100	% Positive

x	x x	x x x	Intensity of staining – weak/moderate/strong

2.1.6.5 RINm5F cell line

Rat RINm5F cells originated from the transplantable radiation-induced insulinoma of a male rat (Chick *et al.* 1977). The original tumours contained both insulin and somatostatin producing cells (Chick *et al.* 1977). Cell lines created from the tumours were transplanted into inbred rats (named RIN-r), or into athymic nude mice (named RIN-m) (Gazdar *et al.* 1980). RIN-m cells cultured in RPMI1640 medium maintained their ability to secrete insulin for more than 400 days, and produce somatostatin, but not glucagon (Gazdar *et al.* 1980). One of the RIN-m cell lines was named RINm5F. It produces 0.19 pg of insulin per cell, which is just 1% of that produced by normal rat β-cells (Praz *et al.* 1983) (for a comparison with other cell types see Table 1.2). RINm5F cells display abnormal insulin secretion in response to glucose as they secrete insulin when the glucose level is increased from 0 to 2.8 mM, but not when it is increased from 2.8 mM to 33.4 mM (Praz *et al.* 1983).

2.1.6.6 Phenotyping of RINm5F cells

RINm5F cells cultured in tissue culture plates grew in monolayers with a cobblestone morphology (Figure 2.11). Phenotyping of RINm5F cells by immunocytochemistry revealed the cells expressed PDX-1, AIRE, and SOX-17 (Figure 2.12). Some of the RINm5F cells strongly expressed insulin, which was detected by the guinea pig anti-insulin antibody used throughout this study (Figure 2.12). The antibodies used to stain the cells are the same antibodies used to stain populations of human stem cells and progenitors in this study, thereby confirming antibody immunoreactivity. A summary of the phenotyping of RINm5F cells is presented in Table 2.6.

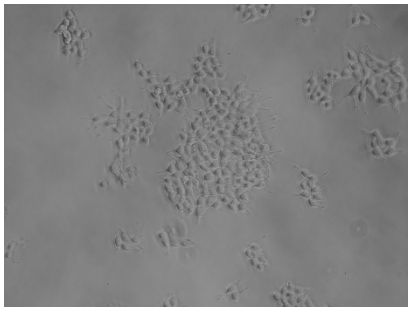
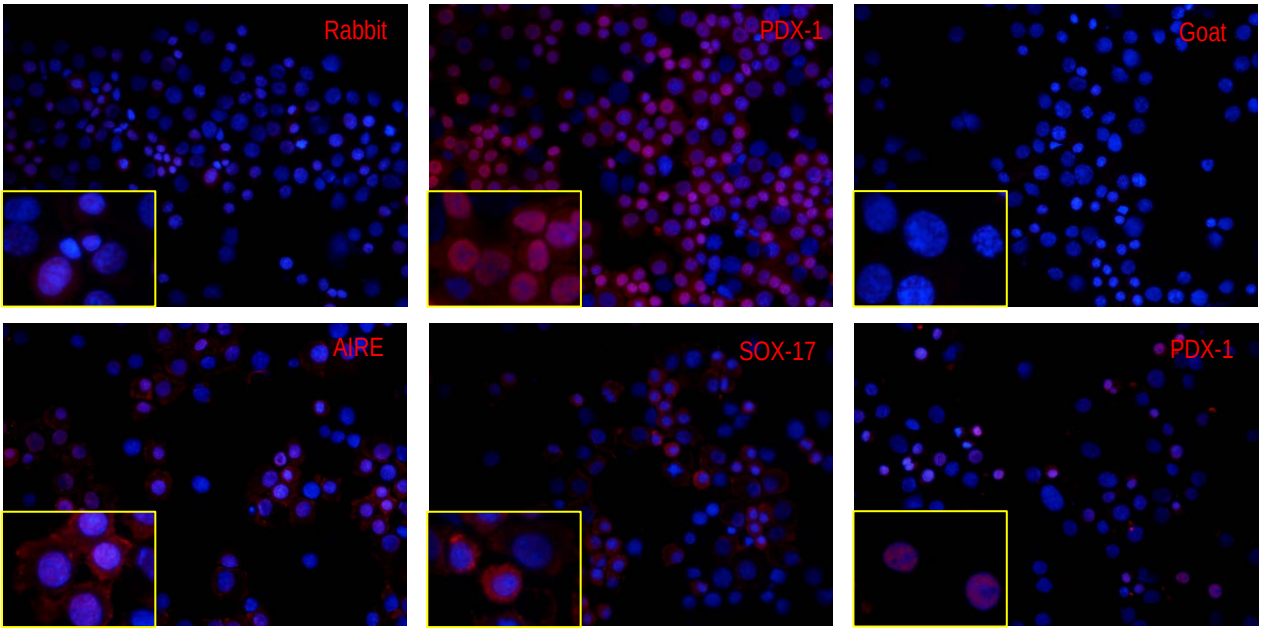


Figure 2.11 Phase contrast image of RINm5F cells.

RINm5F cells were cultured for 1 week in RPMI1640 medium containing 10% FBS + 1% PSG in a tissue culture dish. Image was taken at 100x magnification.



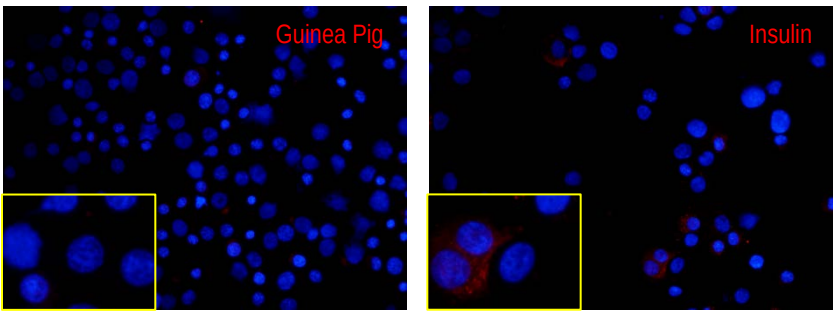


Figure 2.12 Phenotyping of RINm5F cells.

RINm5Fs cells were cultured for 1 week in RPMI1640 medium containing 10% FBS + 1% PSG. They were immunostained for the expression of pancreatic cell markers. Immunoreactivity was detected with donkey anti-rabbit (red), donkey anti-goat (red), and goat anti-guinea pig (red) antibodies. Cell nuclei were stained blue with DAPI. Images were taken at 200x magnification; inset is a 4x magnification of part of the image. The images are presented so that the staining obtained with each IgG control immediately precedes stainings with antibodies of the same host species.

Table 2.6 Summary of the phenotyping of the RINm5F cell line

	RINm5F
PDX-1	x x x
AIRE	x x x
SOX-17	x x x
Insulin	x x x

0	0.1-20	21-40	41-60	61-80	81-100	% Positive

x	x x	x x x	Intensity of staining – weak/moderate/strong

2.2 Methods

2.2.1 General cell culture

All cell types except for PBMC-derived cell populations were split once they reached 80% confluence by removing the media, and washing the cells with PBS, followed by detachment from plates by incubation with 1x trypsin (15400-054, Gibco). They were then collected in the appropriate media containing FBS and centrifuged at 400 g for 5 min. The cells were counted with a haemocytometer and replated for expansion or experimentation. Excess cells were frozen down in freezing solution and stored at -80°C.

2.2.1.1 1.1B4 cultures

1.1B4 cells were cultured in tissue culture treated flasks in full RPMI medium containing 10% FBS at 37°C and 5% CO_2. Culture medium was refreshed twice per week.

2.2.1.2 RINm5F cultures

RINm5F cells were cultured in tissue culture treated flasks in full RPMI medium containing 10% FBS at 37°C, 5% CO_2. Culture medium was refreshed twice per week.

2.2.1.3 INS-1E cultures

INS-1E cells were cultured in tissue culture treated flasks in full RPMI medium containing 10% FBS with the addition of 100 mM HEPES, 50 μM β-mercaptoethanol and 1 mM sodium pyruvate. Culture medium was refreshed twice per week.

2.2.1.4 PBMC isolation and culture

Ethical approval was granted by the Northern X Regional Ethics Committee, Auckland for the isolation of PBMCs from both diabetic and healthy human donors. Consenting adults donated 50 mL of venous blood by collection into heparinized tubes (68480, BD). The blood was diluted 1:1 with PBS and slowly layered on top of 15 mL of Ficoll-paque™ Plus (17-1440-03, GE Healthcare). The layered blood was centrifuged at 400 g for 45 min without applying the brake. The buffy coat layer containing the PBMCs was then collected and resuspended in PBS. The PBMCs were washed thrice by centrifugation for 10 min at 400 g to remove contaminating platelets. Cell numbers were counted with a haemocytometer.

2.2.1.4.1 Peripheral blood insulin-producing cells (PB-IPCs)

PBMCs isolated from peripheral blood were resuspended in full RPMI medium containing 7% FBS and cultured directly in hydrophobic culture dishes (not vacuum gas plasma treated) (351172, BD) at 37°C in 10% CO_2. Cells received fresh medium weekly. The cell seeding concentration was 1-2 x 10^6 cells/mL.

2.2.1.4.2 Monocytes

PBMCs were resuspended in full RPMI medium containing 7% FBS and cultured directly in tissue culture treated dishes (353916, BD) at 37°C in 5% CO_2 to obtain monocytes. Cells received fresh medium weekly. The cell seeding concentration was 1-2 x 10^6 cells/mL.

2.2.1.5 Adipose stem cell (ASC) cultures

Adipose stem cells (ASCs) were cultured in tissue culture treated dishes in expansion medium at 37°C, 5% CO_2. Culture medium was refreshed every 3-4 days. ASCs were cultured in tissue culture plates with a cell seeding concentration of 1 x 10^4 cells/mL. ASCs were cultured in suspension in ultra-low attachment (CORN3471, Merck Millipore) or hydrophobic (351146, BD) 6-well plates with a cell seeding density of 2 x 10^5 cells/cm^2 for the Chandra protocol and 3 x 10^4 cells/cm^2 for the Timper protocol.

2.2.1.6 Cord blood hematopoietic stem cell (CB-HSC) cultures

CB-HSCs at passage 6 were cultured according to Celprogen Inc.'s protocol. Briefly, cells were expanded in Human Stem Cell (Cord Blood Derived) Expansion Medium with serum (M36001-02ES, Celprogen Inc.) at 37°C, 5% CO_2 in flasks coated with Human Stem Cell Extra-cellular Expansion Matrix (E36001-02-T75, Celprogen Inc.). Culture medium was refreshed twice per week. Cells were cultured for a maximum of 12 passages to ensure a uniform cell population was maintained. The cell seeding concentration was 1 x 10^4 cells/mL.

2.2.1.7 Pancreatic hematopoietic stem cell (P-HSC) cultures

P-HSCs at passage 6 were cultured according to Celprogen Inc.'s recommended protocol. They were expanded in Human Pancreatic (Trans-Differentiated) Stem Cell Media with serum (M36004-05S, Celprogen Inc.) at 37°C, 5% CO_2 in plates coated with Human Pancreatic Stem Cell Culture Extra-cellular Matrix (E36004-05-T75, Celprogen Inc.). Culture media was refreshed twice per week. Cells were cultured for a maximum of 12 passages to ensure a uniform cell population was maintained. The cell seeding concentration was 1 x 10^4 cells/mL.

2.2.1.8 Human amniotic stem cell (HASC) cultures

HASCs were cultured according to Celprogen Inc.'s recommended protocol. They were cultured in Human Embryonic Stem Cell Media with serum (M36101-28S, Celprogen Inc.) in dishes coated with Human Embryonic Stem Cell Extra-cellular Matrix (E36101-28, Celprogen Inc.). The cell seeding concentration was 1 x 10^4 cells/mL.

2.2.1.9 266-6 cultures

266-6 cells were cultured in full DMEM medium at 37°C and 5% CO_2 in tissue culture flasks coated with 0.1% gelatin. Culture medium was refreshed twice per week. The cell seeding concentration was 1 x 10^4 cells/mL.

2.2.1.10 CHO-K1 cultures

CHO-K1 cells were cultured in full Hams F-12K medium at 37°C and 5% CO_2 in tissue culture flasks. Culture medium was refreshed twice per week. The cell seeding concentration was 1 x 10^4 cells/mL.

2.2.2 Immunocytochemistry

For immunocytochemistry, 2 x 10^5 cells in suspension were cytospun at 5 RPM for 5 min onto slides using the CytoSpin cytofuge (Thermo Fisher Scientific Inc.). Both cytospun suspension cells and adherent cells attached to plates were fixed with 4% formaldehyde/PBS for 10 min at RT, and then washed thrice with PBS. The only exception was CB-HSCs and P-HSCs, which were fixed with 80% MeOH/PBS for 30 min. Cells were permeabilized with 0.1% Triton-X-100/PBS for 15 min at RT, and then washed thrice with PBS. They were blocked overnight at 4°C or for 2 h at RT with blocking solution. Primary antibodies and IgG matched controls (see Table 2.1 for a list of antibodies and concentrations) were diluted in 2% BSA (Fraction V IgG free, 30063481, Gibco)/PBS and incubated with the cells overnight at 4°C on a rocker, and then the cells were washed thrice with PBS. The secondary antibodies (see Table 2.2) were diluted to 1:500 in 2% BSA/PBS and filtered with a 0.2 μm filter prior to addition to the cells. They were incubated with the cells for 1 h at RT in the dark. The cells were then washed thrice with PBS and covered with ProLong® Gold Antifade reagent with DAPI (P-36931, Invitrogen). Fluorescent, phase contrast, and/or bright field images were viewed with a Leica TE2000 inverted microscope, and photos were taken using Nikon ACT-1 software. Images were combined with Paint.NET (http://www.getpaint.net, dotPDN LLC). In this thesis the results are presented so that an IgG control of each antibody host is presented prior to all antibodies of the same species.

2.2.3 Cell lysis

Cells were lysed with lysis buffers to obtain the cytoplasmic fraction and the nuclear fraction, or they were lysed with whole cell lysis buffer. Cells were directly lysed in the culture dish, or detached with trypsin, pelleted by centrifugation at 400g for 5 min, and then lysed. A total of 1x10^6 cells were lysed per sample and protein levels were quantified with a Nanodrop 2000 spectrophotometer (Thermo Fisher Scientific Inc.). To prepare the cytoplasmic and nuclear fractions the cells were lysed on ice for 10 min in cytoplasmic lysis buffer, followed by centrifugation at 400 g for 5 min. The supernatant which represents the cytoplasmic fraction was collected and stored at -20°C. The pellet containing the cell nuclei was lysed for 10 min at 37°C in the nuclear fraction lysis buffer, and stored at -20°C. To prepare whole cell lysates, the cells were lysed for 15 min on ice with whole cell lysis buffer, and stored at -20°C. All cell lysates were sonicated on ice for 30 sec prior to loading on SDS gels.

2.2.4 SDS-PAGE and Tris-Tricine gels

Samples were diluted in protein loading dye solution or whole cell lysis buffer loading dye, heated at 95°C for 5 min, and loaded into the wells of either a 12% SDS-PAGE or 16% Tris-Tricine polyacrylamide gel. The gels were set up in a Hoefer Mighty small SE250/SE260 mini vertical (Amersham Bioscience) electrophoresis apparatus. SDS-PAGE was used for proteins of >20 kDa and the Tris-Tricine gels were used for low molecular weight proteins of ≤20 kDa. A Precision Plus Protein™ All Blue pre-stained ladder (161-0373, Bio-Rad Laboratories) provided protein standards for the SDS gels, and SeeBlue Plus2 Pre-Stained Standards (LC5925, Life Technologies) were used for Tris-Tricine gels. SDS-PAGE gels were run with 1x SDS-PAGE running buffer, and Tris-Tricine gels were run with 1x anode and 1x cathode buffers. Electrophoresis was carried out at a constant 25 mA/gel. Proteins were electrophoresed under reducing conditions unless otherwise stated.

2.2.5 Western blotting

Proteins separated by SDS-PAGE were transferred onto Hybond-P polyvinylidene difluoride (PDVF) membranes (0.45 μM pore size, Amersham Bioscience) using the semi-dry transfer method. Proteins separated on Tris-Tricine gels were transferred onto nitrocellulose membranes (0.2 μM pore size, Bio-Rad Laboratories). The PDVF membranes were pre-washed in 100% methanol for 5 min, while the nitrocellulose membrane was pre-washed in H_2O for 5 min. The membranes were then soaked for 15 min in Western transfer buffer together with 4 pieces of Whatman® filter paper (Schleicher & Schuell UK Ltd.) per gel. The membrane and gel were sandwiched between the filter papers in a Hoefer TE77 semi-dry transfer unit. Protein transfer was conducted at 50 mA/gel for 1 h. The membrane was then blocked with 5% skim milk powder in T-TBS for 1-2 h at RT. The membrane was incubated overnight at 4°C with a primary antibody diluted in 3 mL of 5% skim milk powder in T-TBS. See Table 2.1 for a list of primary antibodies used and their concentrations. The membrane was then washed six times in 1 h with T-TBS, and incubated for 1 h at RT with a peroxidase-conjugated secondary antibody diluted in 10 mL of 5% skim milk powder in T-TBS. See Table 2.2 for a list of secondary antibodies used and their concentrations. The membrane was then washed again six times in 1 h at RT, and incubated with Enhanced Chemiluminescence (ECL) solution (Amersham Bioscience). Membranes were developed with a Fujifilm LAS-3000 scanner.

2.2.5.1 Stripping of Western blot membranes

Western blot membranes were washed thrice with dH_2O and stripped with 0.2 M NaOH stripping solution for 15 min. The membrane was then washed thrice with dH_2O, followed by two additional washes with T-TBS, and then blocked with 5% skim milk powder in T-TBS for 1 h at RT prior to re-probing with a primary antibody.

2.2.5.2 Densitometry analysis of bands on Western blots

Western blots were scanned using the Fujifilm LAS-3000 scanner and the resulting greyscale images were analysed by ImageJ (http://rsb.info.nih.gov/ij/). Rectangular boxes were drawn around each lane to be analysed and then plotted to reveal the area of intensity in the form of a peak of each gel band. The intensity of each protein band was quantified by drawing a line under the band peak at background level. The software wand tool was then used to generate the area under the curve to give a measure of peak intensity. The intensities of selected bands was compared directly to the corresponding β-actin band to give an indication of the amount of protein expressed relative to the total protein loaded per lane.

2.2.6 Dot blot protocol

Insulin, insulin-like 3, IGF-1, and IGF-2 at 1 μg of protein in 3 μL of PBS were applied to the centre of labelled pencilled circles on a nitrocellulose membrane, and allowed to air dry. In another experiment whole cell lysates of INS-1E cells at 10 μg of protein in 3 μL PBS were applied to a membrane. The membranes were blocked with 5% (w/v) skim milk powder in T-TBS for 1 h at RT. Specificity of the guinea pig, mouse, and chicken anti-insulin antibodies was tested by incubating the membrane for 1 h at RT with the guinea pig anti-insulin antibody (1:1000), mouse anti-insulin antibody (1:2000), or chicken anti-insulin antibody (1:2000)

in 5% (w/v) skim milk powder in T-TBS. The membranes were then washed thrice in 15 min with T-TBS, and incubated for 1 h at RT with either a donkey anti-guinea pig horseradish peroxidase-conjugated antibody (1:40,000), goat anti-mouse horseradish peroxidase-conjugated antibody (1:20,000), or donkey anti-chicken horseradish peroxidase-conjugated antibody (1:40,000), respectively. The membranes were washed thrice in 15 min in T-TBS, and incubated with ECL solution. Membranes were developed with a Fujifilm LAS-3000 scanner.

2.2.7 FluoZin™-3 assay

FluoZin™-3 (F24195, Invitrogen) is a highly sensitive cell-permeable indicator for Zn^{2+} that can detect 1-100 nM Zn^{2+} (Gee *et al.* 2002). β-cell secretory vesicles use Zn^{2+} to create insulin hexamers, and therefore Zn^{2+} is co-secreted with insulin and has sometimes been used as a surrogate marker for insulin (Lukowiak *et al.* 2001). When FluoZin™-3 binds with Zn^{2+} a fluorescent complex is formed which can be detected by fluorescent microscopy (Qian *et al.* 2004). FluoZin™-3 was dissolved in DMSO to a stock concentration of 1 μM and then diluted to 10 nM with PBS. The FluoZin™-3 solution was incubated with cells for 60 min at 37°C, the cells were then rinsed thrice with PBS, and visualized by fluorescence microscopy with a Leica TE2000 inverted microscope. Photos were taken using Nikon ACT-1 software.

2.2.8 CyQUANT® NF Cell Proliferation Assay

The CyQUANT® NF Cell Proliferation Assay Kit (C35007, Invitrogen) which measures DNA content was used to measure cell proliferation. A DNA binding dye which is presented in a permeabilization buffer gives a linear analytical measurement of 100-20,000 cells. The manufacturer's protocol was followed and the length of time of incubation of the dye with the cells was optimised for each of the cell types tested. In brief, the dye binding solution (500x) was diluted to 1x in HBSS. Freshly made CyQUANT® NF dye binding solution was added to the cells at 25 μL/well, followed by incubation at 37°C for 20 min for small cells (e.g. monocytes), and 60 min for larger cells (e.g. 2 week-old macrophages). The fluorescence intensity of the samples was measured at RT using an excitation wavelength at 485 nm and a detection wavelength at 530 nm.

The CyQUANT® NF cell proliferation assay was validated by testing whether it would be able to measure the linear proliferation of the highly proliferative liver cancer cell line, HepG2 (Figure 2.13). A total of 1×10^4 HepG2 cells were allowed to proliferate for up to 3 days with cell fluorescence measured at 2 h, 1, 2 and 3 days. As shown in Figure 2.13, the fluorescent signal doubled in an approximately linear fashion every 24 h.

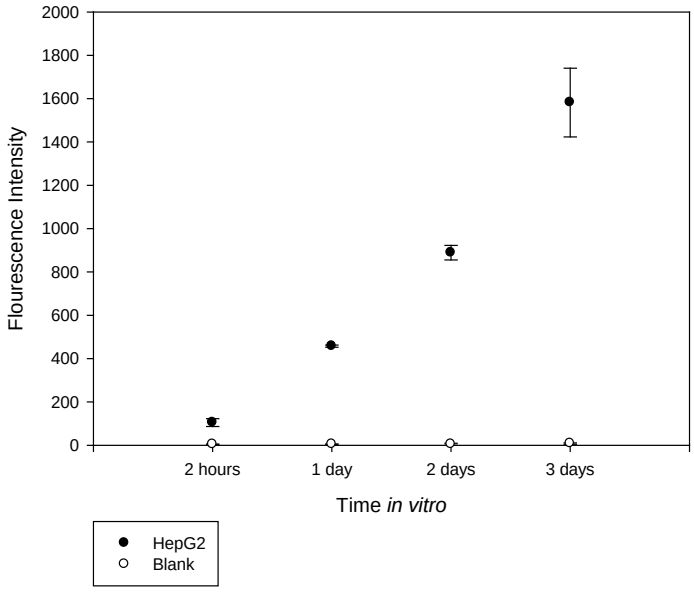


Figure 2.13 Measurement of the proliferation of the liver cancer cell line HepG2 using the CyQUANT® NF cell proliferation assay.

A total of 1 x 10^4 HepG2 cells were allowed to proliferate for up to 3 days with cell fluorescence measured at 2 h, 1, 2 and 3 days. The results are presented as the mean (n=3) ± SD.

2.2.9 Alkaline phosphatase activity assay

Alkaline phosphatase activity is characteristic of undifferentiated stem cells, such as embryonic stem cells (O'Connor *et al.* 2008). It was detected using a sensitive alkaline phosphatase detection kit (SCR004) from Millipore Corp. Cells to be assessed for alkaline phosphatase activity were fixed with 4% formaldehyde for 1-2 min in 96-well plates, washed once with alkaline phosphatase rinse buffer, and 100 µL of Naphthol/Fast Red Violet solution was added to each well. The cells were placed in the dark at RT for 15 min, washed with alkaline phosphatase rinse buffer, and then covered with PBS prior to being viewed by bright field microscopy using a Leica TE2000 inverted microscope. Photos were taken using Nikon ACT-1 software. Undifferentiated stem cells that express alkaline phosphatase stain purple, while differentiated stem cells remain colourless.

2.2.10 Senescence-associated β-galactosidase (β-gal) assay

The state of senescence of cell populations was analysed according to their senescence-associated β-gal activity (Debacq-Chainiaux *et al.* 2009). As cells become senescent they stain blue with an increasing intensity of colour as β-gal activity increases (Debacq-Chainiaux *et al.* 2009). Subconfluent cells to be tested for cellular senescence were washed twice with PBS, fixed with the β-gal fixation solution for 5 min at RT, and washed twice with PBS. They were covered with β-gal staining solution (buffered with a citric acid/sodium phosphate buffer at pH 6.0) for 12 h at 37°C (not in a CO_2 incubator), washed twice with PBS,

once with methanol, and allowed to air dry. Plates were stored in the dark and the cells viewed by bright field microscopy using a Leica TE2000 inverted microscope. Photos were taken using Nikon ACT-1 software.

2.2.11 L-leucine methyl ester treatment of PB-IPCs and monocytes

L-leucine methyl ester is a lysosomotropic compound which selectively kills cells with a high lysosomal content such as monocytes and NK cells (Thiele and Lipsky 1986; Thiele and Lipsky 1990). The L-leucine methyl ester treatment of cells was based on the protocol developed by Thiele *et al*. (1983). A 10 mM L-leucine methyl ester solution without serum (pH 7.4) was sterilised by passing through 0.2 μM filters, and serially diluted to 5, 2.5, 1.25, 0.625, 0.3125 mM concentrations. The control solution was RPMI without serum. Freshly isolated PBMCs were aliquoted at 2.5 x 10^6 cells/mL and resuspended in the L-leucine methyl ester solution or control solution, and left at RT for 40 min. They were centrifuged at 400 g for 5 min, washed twice with excess PBS, and seeded at 1 x 10^6 cells/well into hydrophobic 96-well plates. After 3 days, apoptosis was analysed by the Annexin-V-FLUOS staining assay (see 2.2.16). Separate samples were analysed after 1 week for cell detachment by phase contrast microscopy using a Leica TE2000 inverted microscope. Photos were taken using Nikon ACT-1 software.

2.2.12 Phagocytosis assay using pHrodo™ Red BioParticles® Conjugates

pHrodo™ Red BioParticles® Conjugates (P35361, Life Technologies) are fluorogenic particles which are ingested by phagocytic cells. As the BioParticles are ingested acidification occurs which increases the fluorescence of the conjugated pHrodo™ dye resulting in a strong fluorescent signal. The pHrodo™ Red BioParticles® Conjugates were added to cells as per the manufacturer's recommendations. They were resuspended in PBS at 1 mg/mL, sonicated for 5 min, and a 100 μL aliquot added to cells per well. The plates were incubated for 1.5 h at 37°C, the cells washed thrice with PBS, and BioParticle uptake visualized by fluorescence microscopy using a Leica TE2000 inverted microscope. Photos were taken using Nikon ACT-1 software.

2.2.13 Endotoxin inhibition assay

PB-IPCs were allowed to attach for 2 h, washed thrice with PBS and then incubated for 3 days in full RPMI medium containing 7% FBS in the presence or absence of 35 μM spermine (S4264, Sigma-Aldrich). Alternatively, they were incubated with 100 ng/mL LPS (L4516, Sigma) in full RPMI medium containing 7% FBS in the presence or absence of 35 μM spermine.

2.2.14 Protein delivery

Pro-DeliverIN™ (PI10250, OZ Biosciences) is a lipid based protein delivery reagent that forms non-covalent complexes with proteins. These complexes are delivered into the cell and the protein is released into the cytoplasm without causing toxicity as the lipid is degraded (OZ Biosciences). The reagent is able to deliver proteins to immortalised and primary cell lines such as neuron and glial cells (OZ Biosciences). The manufacturer's recommendations were followed. PBMCs were seeded at 5 x 10^5 cells/well of a hydrophobic 96 well plate, and cultured for 3 h in full RPMI medium containing 7% FBS to allow the cells to attach. Both the R-Phycoerythrin and Pax4 (BC074761, Proteintech Group, Inc.) proteins were diluted in PBS to give a 1 μM solution of

each. The proteins were then mixed with 1 μL/μg Pro-DeliverIN™ and topped up to 120 μL with full RPMI medium containing 7% FBS. The naturally cell-permeable PDX-1 protein was added to cells at 1 μM without needing to add Pro-DeliverIN. A 120 μL aliquot of the medium containing the protein and Pro-DeliverIN, or the protein only in the case of PDX-1, was added to the cells. The medium containing the protein and Pro-DeliverIN or PDX-1 was refreshed on days 3 and 6 prior to fixing the cells on day 7. Uptake of the R-Phycoerythrin protein via Pro-DeliverIN was assessed by microscopy using a Leica TE2000 inverted microscope. Photos were taken using Nikon ACT-1 software.

2.2.15 Mixed lymphocyte response

A total of 5 x 10^5 PBMCs per well were seeded into either hydrophobic or conventional 96-well plates. They were cultured for 1 week in full RPMI medium containing 7% FBS to establish PB-IPC and monocyte cultures. Allogeneic PBMCs obtained from a buffy coat from two different donors (one having donated the PB-IPCs/monocytes) were overlaid onto the PB-IPC/monocyte cultures, or empty plate controls, to determine whether the latter cells could inhibit a mixed lymphocyte response. The mixed lymphocyte response was carried out with 5 x 10^5 PBMCs from each donor in full RPMI medium containing 7% FBS. The suspended lymphocytes were analysed for apoptosis by the Annexin-V-FLUOS assay (see 2.2.16) every 24 h up to 120 h. Each sample was analysed in triplicate. The phenotypes of the suspended cells were analysed by immunocytochemistry (see 2.2.2).

2.2.16 Annexin-V-FLUOS staining assay

Apoptotic cells were detected using an Annexin-V-FLUOS staining kit (11858777001, Roche Applied Science). During the early stages of apoptosis phosphatidylserine is translocated from the inner side to the outside of the plasma membrane (Vermes *et al.* 1995). Annexin-V has high affinity for phosphatidylserine and therefore fluorescently labelled Annexin-V readily binds cells undergoing apoptosis which can then be visualized by fluorescent microscopy (Roche Applied Science). The Annexin-V-FLUOS labelling solution was prepared by adding 20 μL of Annexin-V-FLUOS labelling reagent to 1 mL of incubation buffer. The cells were washed once with incubation buffer and pelleted at 400 g for 5 min, and incubated with 50 μL of Annexin-V-FLUOS labelling solution for 15 min at RT in the dark. They were washed thrice by centrifugation at 400 g for 5 min, and cytospun onto glass slides (2 x 10^5 cells/slide). They were fixed with 4% formaldehyde in PBS for 10 min at RT in the dark, washed twice with PBS, covered with ProLong® Gold Antifade Reagent with DAPI, and overlaid with a coverslip. The cells were then examined for apoptosis by microscopy using a Nikon E600 fluorescent upright microscope, and photos were taken using Nikon ACT-1 software.

2.2.17 Oil Red O staining

Adipocytes contain lipid droplets which can be stained with Oil Red O (Zuk *et al.* 2002). Oil Red O stains lipid droplets red and is viewable by bright field microscopy. Cells were fixed in 4% formaldehyde for 10 min, washed thrice with PBS and stored at 4°C. They were washed with H_2O, followed by 60% isopropanol, and then stained with a 60% Oil Red O working solution for 15 min at RT. They were then washed with 60% isopropanol, and counter-stained with hematoxylin for 10 min. The cells were washed

thrice with H_2O, and glycerol was added to the wells prior to bright field microscopy using a Leica TE2000 inverted microscope. Photos were taken using Nikon ACT-1 software.

2.2.18 Aldehyde dehydrogenase (ALDH) assay

ALDH enzyme expression is characteristic of stem and progenitor cells (Storms *et al.* 1999). ALDH expression was determined with the ALDEFLUOR™ kit (01700, STEMCELL™ Technologies Inc.). ASCs were tested for ALDH activity by incubating them with the uncharged substrate Bodipy aminoacetaldehyde (BAAA) which is taken up by passive diffusion. The substrate is converted by ALDH to the negatively charged green fluorescent product Bodipy-aminoacetate. Efflux of the substrate is inhibited by the assay buffer. The ALDEFLUOR® assay kit also contains diethylaminobenzaldehyde (DEAB) which is used to inhibit the ALDH enzyme as a negative control. The manufacturer's recommended protocol was followed. Briefly, ASCs to be tested for ALDH expression were cultured in expansion medium, washed thrice with PBS, detached from plates with trypsin, and then resuspended in expansion medium. They were centrifuged twice at 300 g for 7 min and resuspended in PBS and then resuspended in 1 mL of ALDEFLUOR™ assay buffer at 1 x 10^6 cells/mL. Negative controls received 10 µL of DEAB. A 5 µL aliquot of activated ALDEFLUOR™ substrate was then added to each sample and the mixture immediately inverted thrice. The samples were incubated for 30 min at 37°C, centrifuged at 4°C for 5 min at 300 g, the solution aspirated, and the pellet resuspended in 0.5 mL of ice-cold ALDEFLUOR™ assay buffer. The samples were immediately placed on ice to further prevent efflux of the fluorescent substrates and analysed by flow cytometry or sorted by FACS. To view ALDH expression microscopically samples were prepared as above and then placed into a 96 well plate, and viewed with a Leica TE2000 inverted microscope. Photos were taken using Nikon ACT-1 software.

2.2.19 Induced pluripotent stem cells (iPSCs)

2.2.19.1 Purification of plasmid DNA

Lyophilised *E. coli* transformed with each of the four iPSC transcription factor plasmids (Oct-4, c-Myc, KLF4, and SOX-2) were resuspended in 1 mL of Luria-Bertani (LB) broth, inverted several times, streaked onto *E. Coli* Fast-Media® Blas blasticidin LB agar plates, and cultured overnight at 37°C. Single bacterial colonies were picked and cultured in 10 mL of Fast-Media® Blas liquid (Terrific Broth supplemented with blasticidin) on a shaker at 37°C overnight to produce a starter culture. The starter cultures were used to make a larger batch culture by combining them with 190 mL of Fast-Media® Blas liquid, followed by incubation overnight at 37°C on a shaker. The culture was centrifuged at 6,000 g for 10 min to obtain a bacterial pellet. The plasmid DNA was extracted using a Qiagen maxiprep kit (Qiagen, Invitrogen) according to the manufacturer's instructions. The bacterial pellet was lysed in the supplied buffers, followed by centrifugation at 20,000 g for 30 min to remove debris. The supernatant containing the DNA was centrifuged at 18,000 g for 15 min and passed through an anion-exchange resin (Qiagen, Invitrogen) to capture the DNA. The DNA was eluted with the provided elution buffer, and then precipitated by adding 10.5 mL of

isopropanol to 15 mL of DNA sample. The solution was centrifuged at 20,000 g for 30 min and the DNA pellet was resuspended in dH_2O. The concentration of DNA in the samples was measured with a nano-drop spectrophotometer (NanoDrop 2000).

2.2.19.2 Sterilisation of plasmid DNA

The plasmid DNA was sterilized prior to transfection to prevent contamination of the recipient CHO-K1 and 266-6 cells. DNA in the solution was precipitated by the addition of NaOAc and EtOH at final concentrations of 0.3 M and 30% (v/v), respectively, and the DNA was placed on ice for 10 min. The DNA was pelleted by centrifugation at 15,000 g for 10 min, and washed with 70% (w/v) ice cold EtOH. Traces of EtOH were removed in a speed-vac, and the DNA was resuspended in dH_2O. The yield of DNA was measured using a nano-drop spectrophotometer (NanoDrop 2000).

2.2.19.3 Transfection of 266-6 and CHO-K1 cells

266-6 and/or CHO-K1 cells in full DMEM and full Hams F12-K media (both without PSG), respectively, were seeded into 6-well plates at 1 x 10^6 cells per well, and cultured overnight at 37°C and 5% CO_2. The medium was then removed, and the cells were washed twice with Opti-MEM medium (containing no FBS or PSG) prior to transfection with either Lipofectamine LTX (Invitrogen™) or Polymag (OZ Biosciences), as below.

2.2.19.3.1 Lipofectamine LTX protocol

Lipofectamine LTX (6, 9, 12, or 15 μL) was diluted in Opti-MEM medium to a total volume of 150 μL. The plasmids encoding Oct-4, c-Myc, SOX-2 or KLF4 (3 μg) were each diluted in Opti-MEM medium to a total volume of 147 μL, followed by the addition of 3 μL of Plus™ Reagent. The lipofectamine and plasmid solutions were mixed together and incubated for 5 min at RT. A total of 250 μL of DNA-lipofectamine solution was added to the cells in 1750 μL of Opti-MEM medium in each well of a 6-well plate followed by incubation for 3 h at 37°C and 5% CO_2. The cells were washed thrice with their respective full media, and cultured for 2 days at 37°C and 5% CO_2.

2.2.19.3.2 Polymag protocol

Polymag solution (3, 6, 9, 12 μL) was mixed with 3 μg of plasmid DNA in 200 μL of Opti-MEM medium and incubated for 20 min at RT. The Polymag/DNA mixture was diluted in 1800 μL of Opti-MEM medium and added to the cells. The plate was placed onto a magnetic plate on a rotating platform for 20 min. The cells were washed thrice, suspended in the appropriate full medium, and cultured for 2 days at 37°C and 5% CO_2.

2.2.19.4 Extraction of immortalizing proteins from transfectants

Immortalizing proteins were extracted from cells transfected with Oct-4, c-Myc, KLF4, and SOX-2 which were to be used to induce pluripotent stem cell formation. Prior to lysis the cell culture medium was removed from the cells which were washed

thrice with PBS. The cells were incubated with protein extraction buffer for 30-45 min on ice in the same dishes they were cultured in and then collected with a cell scraper. The samples were sonicated on ice until all cells were lysed as judged by microscopy and immediately stored at -20°C until required.

2.2.20 Statistical analysis

Results were expressed as mean values ± standard deviation (SD). A Students t-test was used for evaluating statistical significant between groups where significance was indicated by a value less than 0.05 ($p<0.05$).

Chapter 3 Peripheral Blood Insulin-Producing Cells

3.1 Introduction

PBMC that attach to a hydrophobic surface, named peripheral blood insulin-producing cells (PB-IPCs), are a novel population of cells discovered by Zhao *et al.* (2007). PB-IPCs spontaneously produce insulin and therefore provide a potential novel population of cells for the treatment of type 1 diabetes (Zhao *et al.* 2007a). As discussed in Section 1.7.1, Zhao *et al.* (2007) reported that PB-IPCs express Oct-4, Nanog, CD9, CD117, CD45, insulin, C-peptide, MafA, Nkx6.1, PDX-1, NeuroD, HNF6, PC1/3, PC2, and CXCR4 (Zhao *et al.* 2007a). They do not express CD14, CD11b, HLA-DR, CD80, and CD40 (Zhao *et al.* 2007a). The phenotype of this novel population of cells and their ability to differentiate towards the pancreatic cell lineage warranted further investigation.

3.2 Scope of chapter

In this chapter PB-IPCs were isolated from at least 3 different donors by attachment to hydrophobic microbiology petri dishes and characterized for their expression of pancreatic and monocytic cell markers by immunocytochemistry and Western blot analysis. They were phenotyped for the expression of stem cell markers and alkaline phosphatase activity to determine their potential stem cell features. Their phagocytic abilities were tested to determine whether they retained their macrophage character. In addition, the PB-IPCs were tested for their proliferative potential, and their senescence in prolonged culture was determined. The differentiation protocol developed by Zhao *et al.* (2008) to differentiate PB-IPCs towards the pancreatic lineage was replicated here. Novel combinations of differentiation agents were also trialled in an attempt to differentiate PB-IPCs into mature insulin-producing pancreatic cells. The PB-IPC phenotype was compared with that of classic monocytes which were isolated and cultured in conventional tissue culture plates.

3.3 Characterization of PBMCs that attach to a hydrophobic surface

3.3.1 PBMCs that attach to a hydrophobic surface show a similar morphology to those that attach to a conventional tissue culture surface

Phase contrast microscopy was used to examine the morphology of adherent PBMCs isolated from healthy individuals and a diabetic patient that were cultured for 2 weeks in full RPMI media containing 7% FBS in hydrophobic microbiological petri dishes, and conventional hydrophilic tissue culture dishes. Cells isolated by attachment to hydrophobic microbiological petri dishes are here designated PB-IPCs, whereas those isolated by attachment to conventional tissue culture dishes are designated monocytes. The cells were cultured in the same dishes to which they had been attached. The morphology of the adherent PBMCs attached to the two different types of culture dish appeared similar or identical (Figure 3.1). The PBMCs adopted two

distinct morphologies. They were either round and flattened, or were elongated and fibroblast-like. There were also small rounded cells present, which were presumably lymphocytes that had not been completely removed during medium changes.

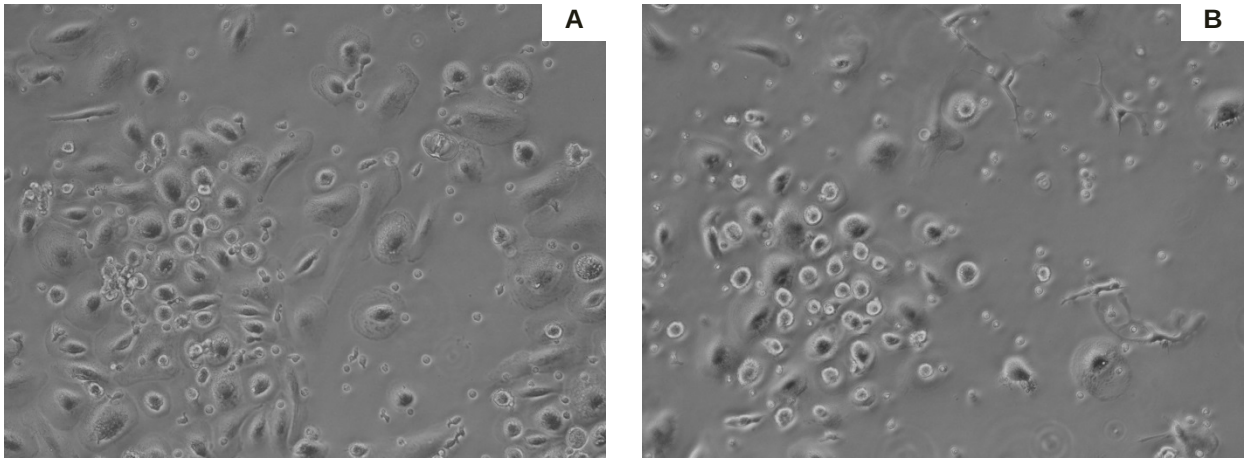


Figure 3.1 Phase contrast images of PB-IPCs (isolated from healthy donors) cultured in hydrophobic and hydrophilic dishes.

PB-IPCs were cultured in full RPMI media containing 7% FBS for 2 weeks in hydrophobic microbiological petri dishes (A) and conventional hydrophilic tissue-culture dishes (B). Images were taken at 200x magnification.

PB-IPCs that were isolated from the blood of a diabetic patient adopted the same morphology as PB-IPCs isolated from a healthy control subject (Figure 3.2). PB-IPCs from diabetic and healthy subjects were small, clustered and rounded after 1 week in culture. After culture for 2 weeks, the cells were still predominantly rounded in shape, but had become larger and had begun to spread over the dish and adopt a flatter shape, potentially indicating they were undergoing terminal differentiation. There were also a few elongated cells present. After 3 weeks of culture, the cells appeared quite flat in appearance and larger still, and after 4 weeks many of the rounded and flattened cells had grown extremely large.

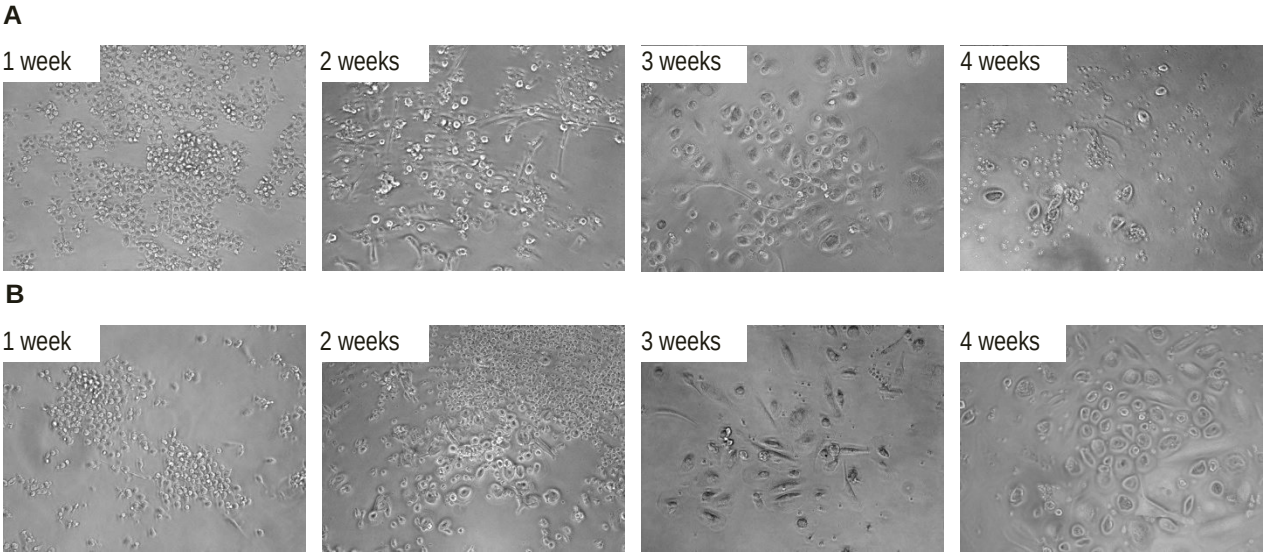


Figure 3.2 Phase contrast images of cultures of PB-IPCs isolated from a healthy subject and a diabetic patient, and cultured in hydrophobic dishes.

PB-IPCs isolated from a diabetic patient (A) and a healthy control subject (B) were cultured in full RPMI media containing 7% FBS in hydrophobic microbiological petri dishes. Images were taken at weekly intervals over 4 weeks. Images were taken at 200x magnification.

3.3.2 Cultured PB-IPCs and monocytes have a similar phenotype

Adherent PB-IPCs and monocytes cultured for 2 h, 3 days, 1 and 2 weeks in hydrophobic petri dishes and tissue culture dishes respectively, were phenotyped by immunostaining with antibodies against a panel of pancreatic, hematopoietic, and Treg cell markers (Figure 3.3 to Figure 3.10). Immunostaining is not a precise measurement of cell marker expression; therefore, the values given are approximate levels of protein expression as seen in visual fields of a microscope from at least 3 donors per time point to give an overall impression of protein expression over time. The cells did not express a number of key pancreatic hormones including amylin, glucagon, insulin and C-peptide, irrespective of which type of dish was used for cell culture (Figure 3.3 to Figure 3.10). Nevertheless, after 1 week of culture both PB-IPCs and monocytes expressed PDX-1, and weakly expressed SOX-17 (Figure 3.7 and Figure 3.8). CXCR4 was weakly expressed by monocytes after 1 week of culture (Figure 3.8) and by PB-IPCs after 2 weeks of culture (Figure 3.9). HNF6 was weakly expressed by monocytes and PB-IPCs after 3 days of culture (Figure 3.5 and Figure 3.6). The cells did not express an array of other pancreatic markers, including Glut-1, GPR40, GIPR, MafA, Pax6, Arx, NGN3, Glut-2, NeuroD, Ptf1a and PCSK1, at any of the time-points (Figure 3.3 to Figure 3.10).

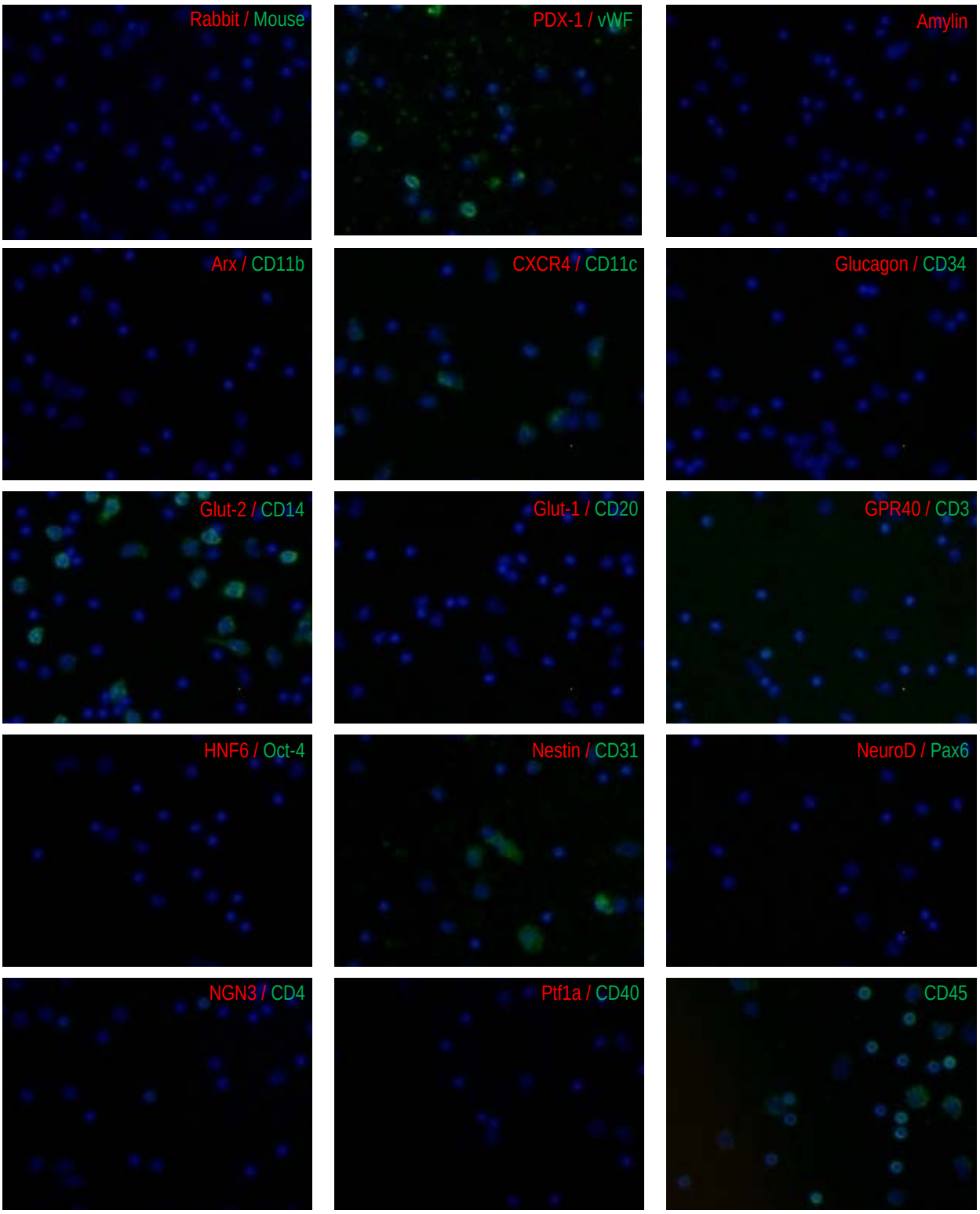
In contrast, immunocytochemistry analysis revealed the majority of cells expressed a variety of monocytic markers, irrespective of which type of dish was used for cell culture. The majority of cells expressed CD11c after 3 days of culture (Figure 3.5 to Figure

3.10). Upregulation of CD11c expression coincided with the expression of CD68 (Figure 3.5 to 10). The MHC class II antigen HLA-DR was expressed by the majority of cells at the start of analysis after 2 h of culture and subsequently for up to 2 weeks (Figure 3.3 to Figure 3.10). The macrophage marker CD11b/Mac-1 was expressed by occasional PB-IPCs and monocytes after 2 weeks of culture (Figure 3.9 and Figure 3.10). In marked contrast, the expression of the monocytic marker CD14 decreased during the 2 weeks of culture, particularly in the latter stages (Figure 3.3 to Figure 3.10). The co-stimulatory protein CD40, which is normally expressed by antigen presenting cells, was weakly expressed by some of cells after 1 week of culture in hydrophobic dishes (Figure 3.7). Its expression was weakly maintained at 2 weeks of culture by a subpopulation of PB-IPCs (Figure 3.9). Expression of the B and T cell markers CD20 (Figure 3.9), CD3 (Figure 3.7 to Figure 3.9) and CD4 (Figure 3.7 to Figure 3.10) was detected on a very small number of cells throughout the time-points tested, reflecting low level contamination with lymphocytes. As expected the majority of the cells expressed the hematopoietic cell marker CD45 reflecting the fact the cells were peripheral leukocytes (Figure 3.3 to Figure 3.10).

AIRE and FOXP3 were expressed by both PB-IPCs and monocytes (Figure 3.3 to Figure 3.10). The platelet endothelial cell adhesion molecule CD31 was expressed by up to 60% of the PBMCs throughout the time-points tested, irrespective of which type of dish was used for cell culture (Figure 3.3 to Figure 3.10, Table 3.1).

Stem cell marker analysis revealed a subpopulation of cells cultured in both types of dishes that expressed Nestin after 3 days of culture (Figure 3.5 and Figure 3.6). The total number of Nestin-positive cells steadily increased throughout the study (Figure 3.5 to Figure 3.10). The stem cell markers CD34 and Oct-4 were not expressed at any time-point tested (Figure 3.3 to Figure 3.10).

The adherent PBMCs expressed other cell lineage markers, including the endothelial cell marker vWF, and fibroblast factor (prolyl 4-hydroxylase or disulphide-isomerase) throughout the time-points tested, irrespective of which type of dish was used for cell culture (Figure 3.3 to Figure 3.10). A comparison of the phenotypes of monocytes versus PB-IPCs is shown in Table 3.1.


Rabbit / Mouse
PDX-1 / vWF
Amylin
Arx / CD11b
CXCR4 / CD11c
Glucagon / CD34
Glut-2 / CD14
Glut-1 / CD20
GPR40 / CD3
HNF6 / Oct-4
Nestin / CD31
NeuroD / Pax6
NGN3 / CD4
Ptf1a / CD40
CD45

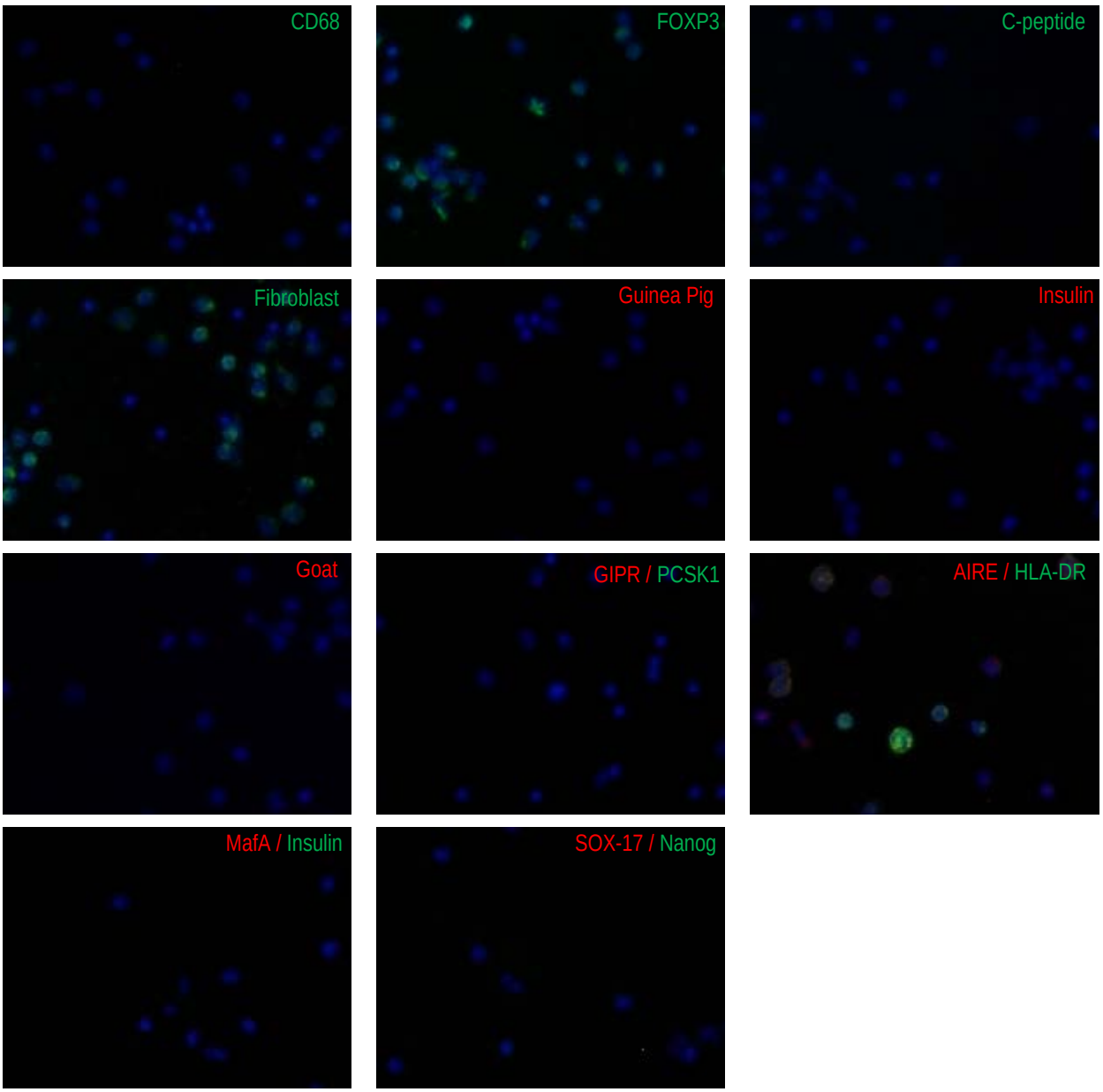
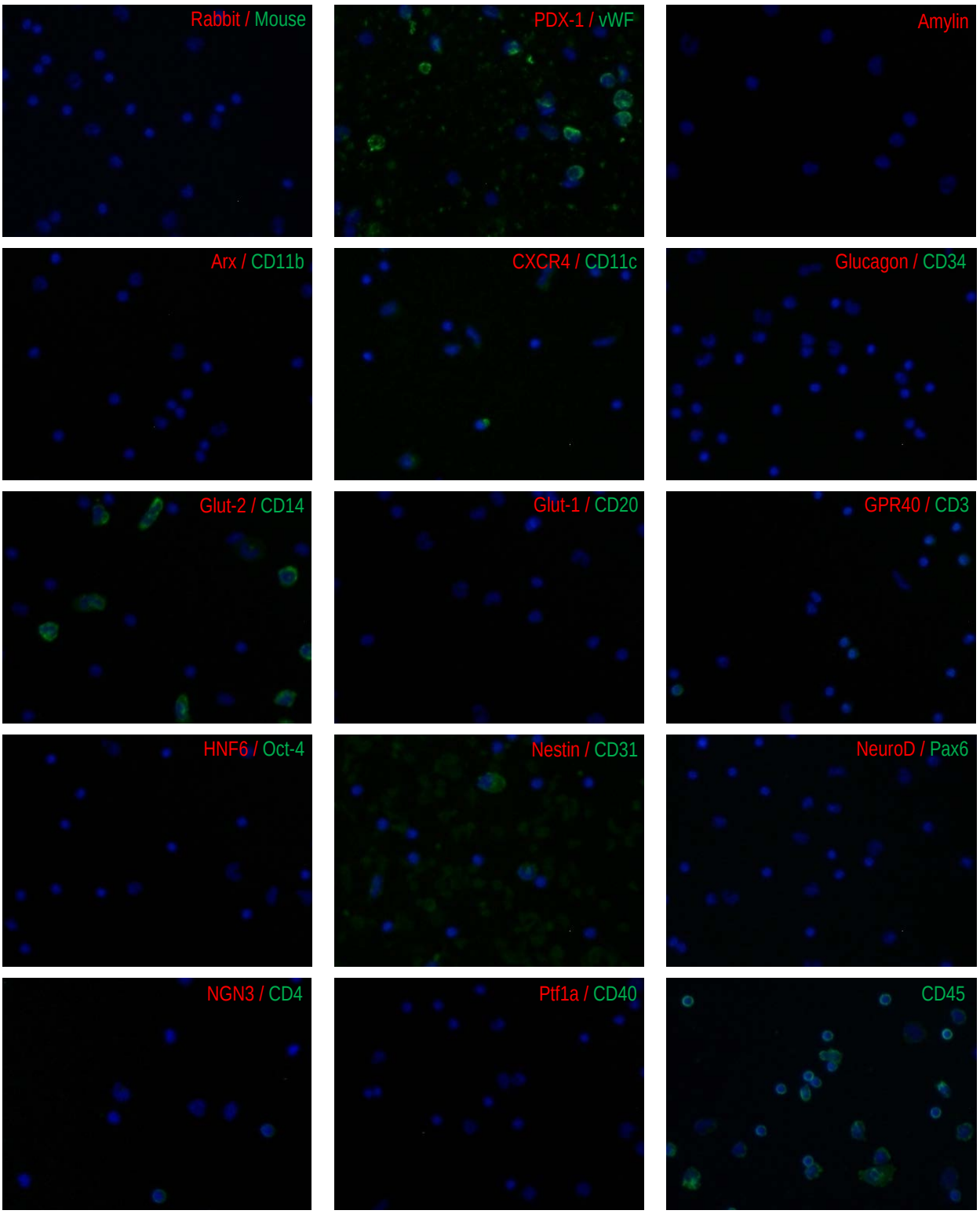


Figure 3.3 Phenotyping of adherent PB-IPCs cultured in hydrophobic dishes for 2 h.

Adherent PB-IPCs were cultured in full RPMI media containing 7%. Cells were stained for the expression of various cell markers. Immunoreactivity was detected with donkey anti-rabbit, goat anti-guinea pig, and donkey anti-goat (red) antibodies and with a donkey anti-mouse antibody (green). Nuclei were stained blue with DAPI. Images were taken at 200x magnification. The images are presented so that the staining obtained with each IgG control immediately precedes stainings with antibodies of the same host species.


Rabbit / Mouse
PDX-1 / vWF
Amylin
Arx / CD11b
CXCR4 / CD11c
Glucagon / CD34
Glut-2 / CD14
Glut-1 / CD20
GPR40 / CD3
HNF6 / Oct-4
Nestin / CD31
NeuroD / Pax6
NGN3 / CD4
Ptf1a / CD40
CD45

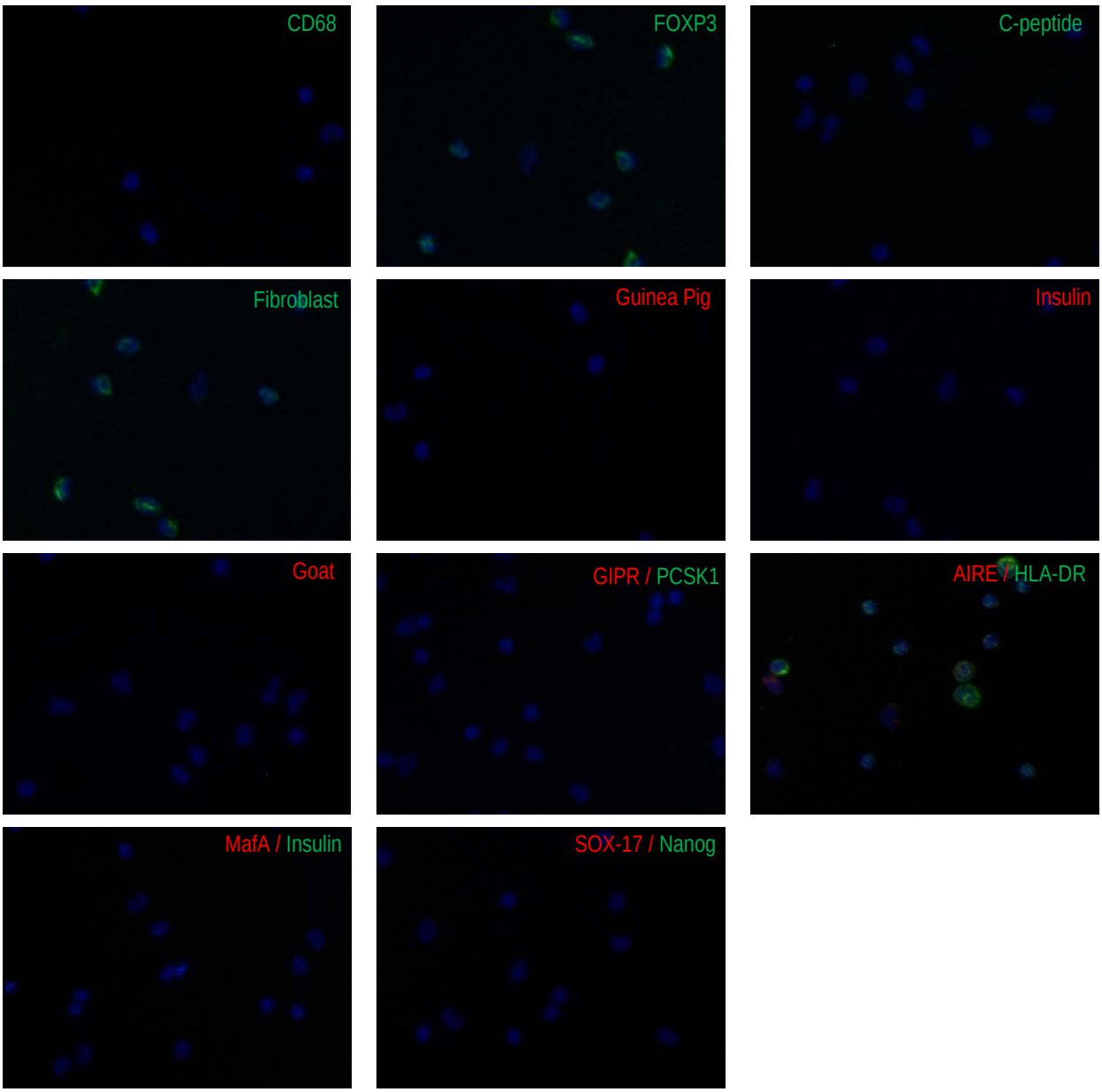
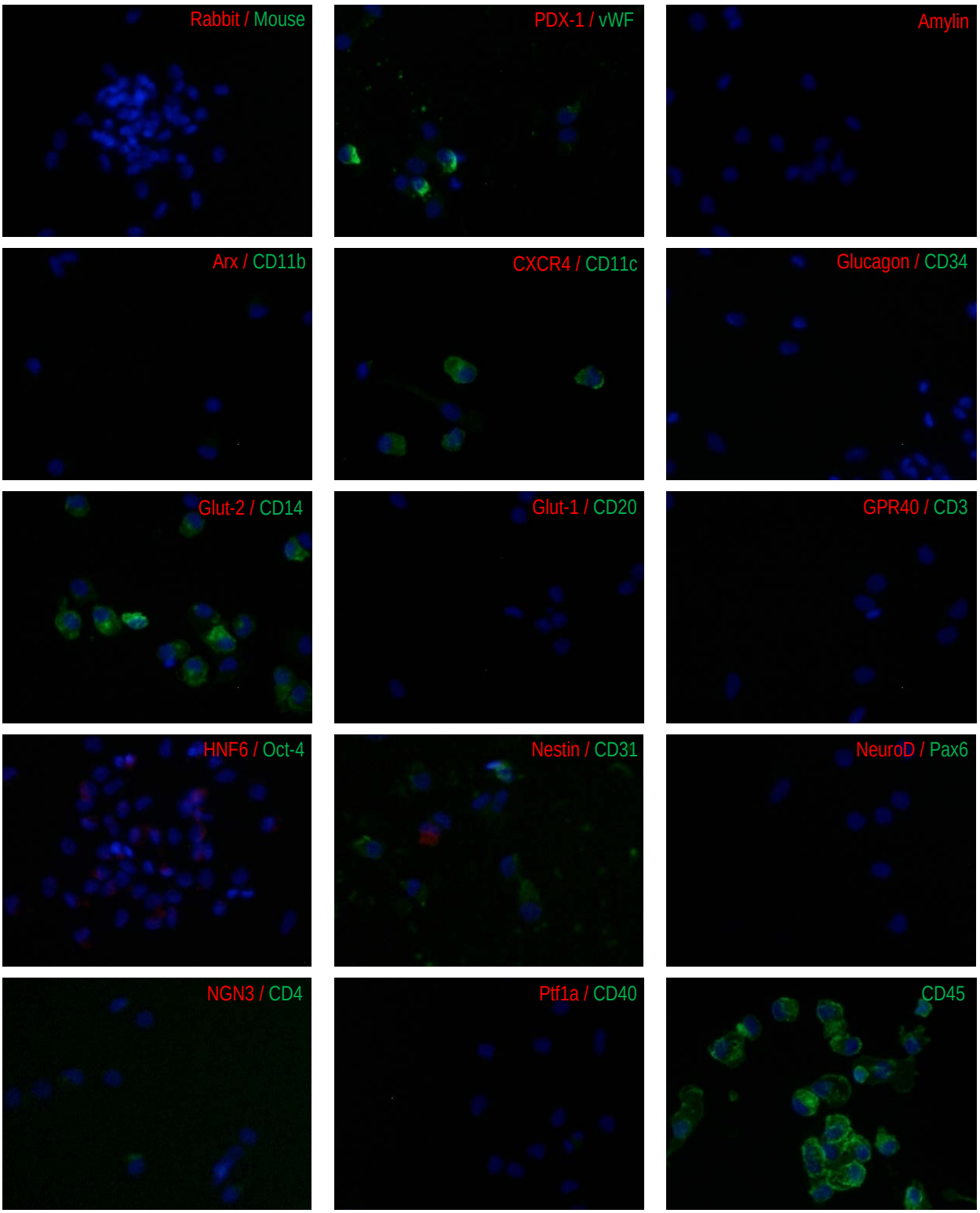


Figure 3.4 Phenotyping of monocytes cultured in tissue culture dishes for 2 h.

Adherent monocytes were cultured in full RPMI media containing 7% FBS. Cells were stained for the expression of various cell markers. Immunoreactivity was detected with donkey anti-rabbit, goat anti-guinea pig, and donkey anti-goat (red) antibodies and with a donkey anti-mouse antibody (green). Nuclei were stained blue with DAPI. Images were taken at 200x magnification. The images are presented so that the staining obtained with each IgG control immediately precedes stainings with antibodies of the same host species.


Rabbit / Mouse
PDX-1 / vWF
Amylin
Arx / CD11b
CXCR4 / CD11c
Glucagon / CD34
Glut-2 / CD14
Glut-1 / CD20
GPR40 / CD3
HNF6 / Oct-4
Nestin / CD31
NeuroD / Pax6
NGN3 / CD4
Ptf1a / CD40
CD45

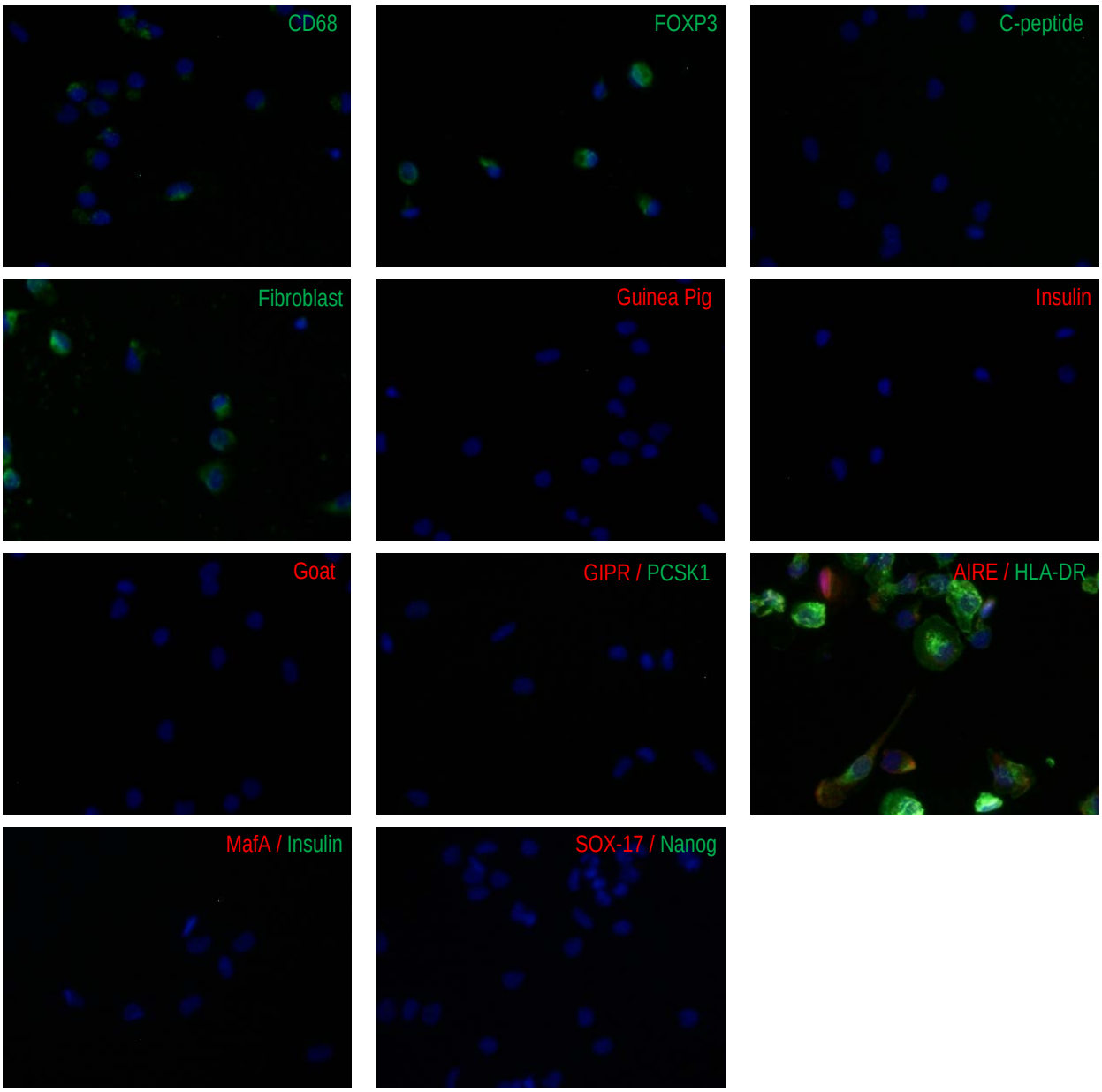
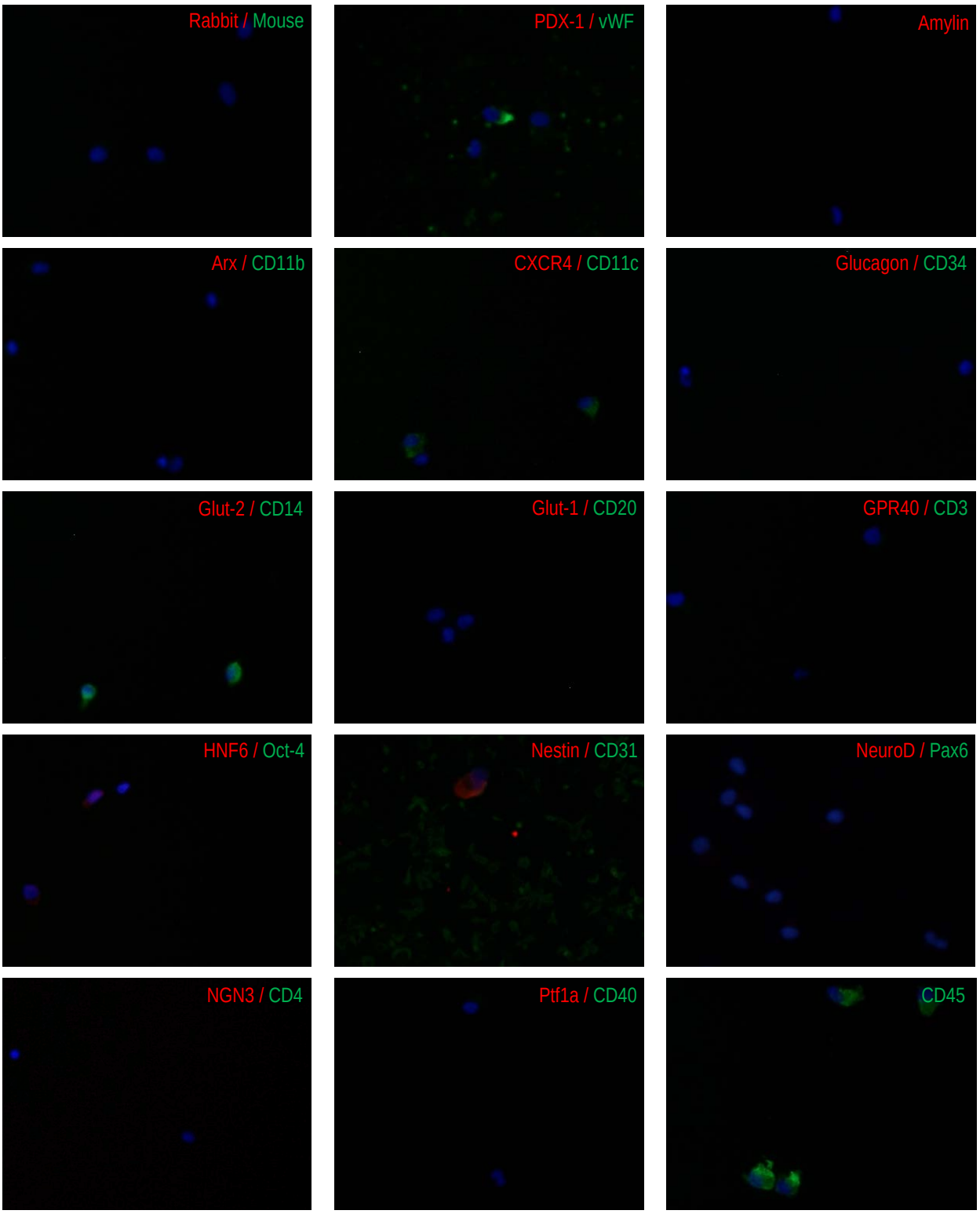


Figure 3.5 Phenotyping of adherent PB-IPCs cultured in hydrophobic dishes for 3 days.

Adherent PB-IPCs were cultured in full RPMI media containing 7% FBS. Cells were stained for the expression of various cell markers. Immunoreactivity was detected with donkey anti-rabbit, goat anti-guinea pig, and donkey anti-goat (red) antibodies and with a donkey anti-mouse antibody (green). Nuclei were stained blue with DAPI. Images were taken at 200x magnification. The images are presented so that the staining obtained with each IgG control immediately precedes stainings with antibodies of the same host species.


Rabbit / Mouse
PDX-1 / vWF
Amylin
Arx / CD11b
CXCR4 / CD11c
Glucagon / CD34
Glut-2 / CD14
Glut-1 / CD20
GPR40 / CD3
HNF6 / Oct-4
Nestin / CD31
NeuroD / Pax6
NGN3 / CD4
Ptf1a / CD40
CD45

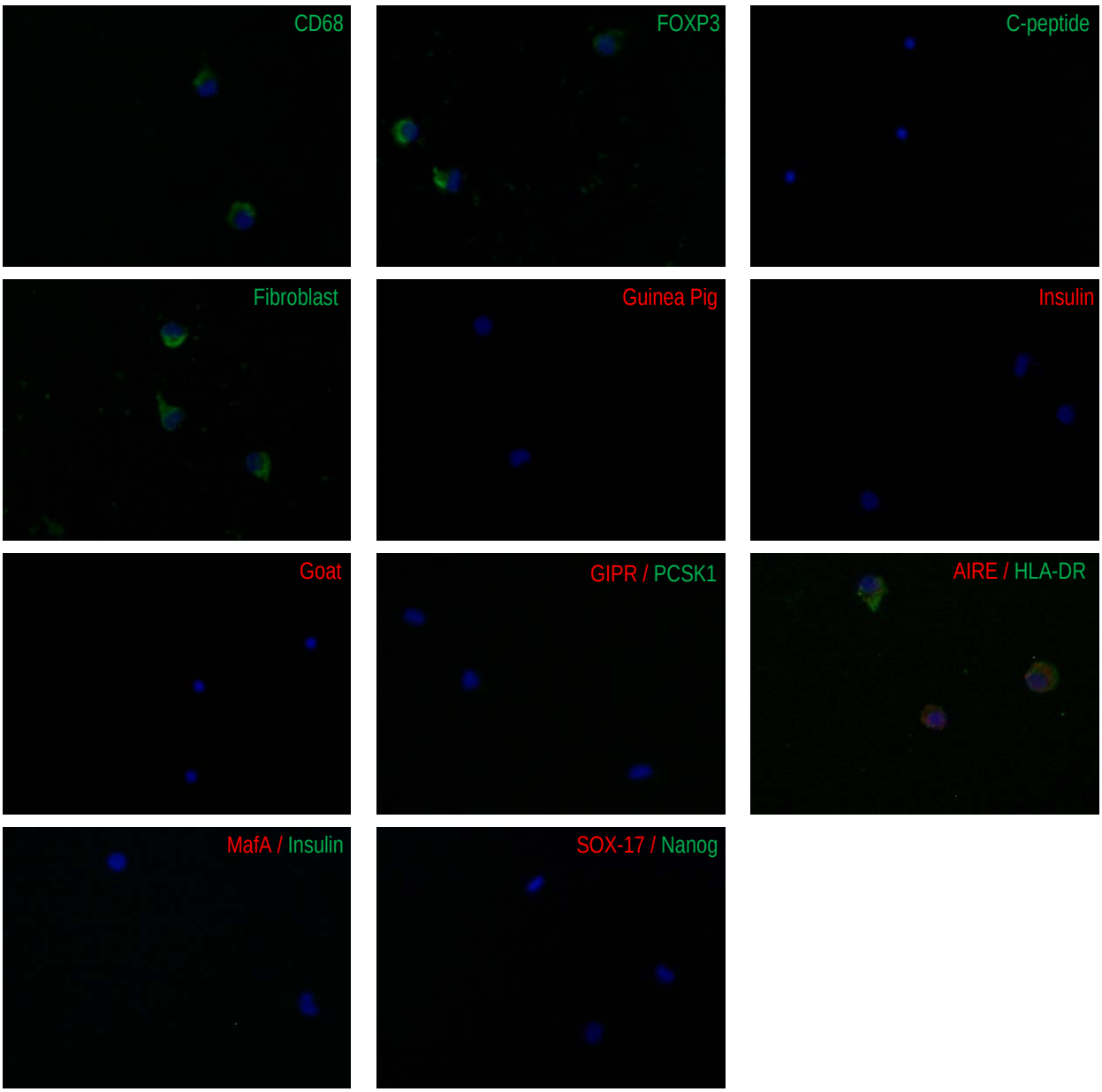
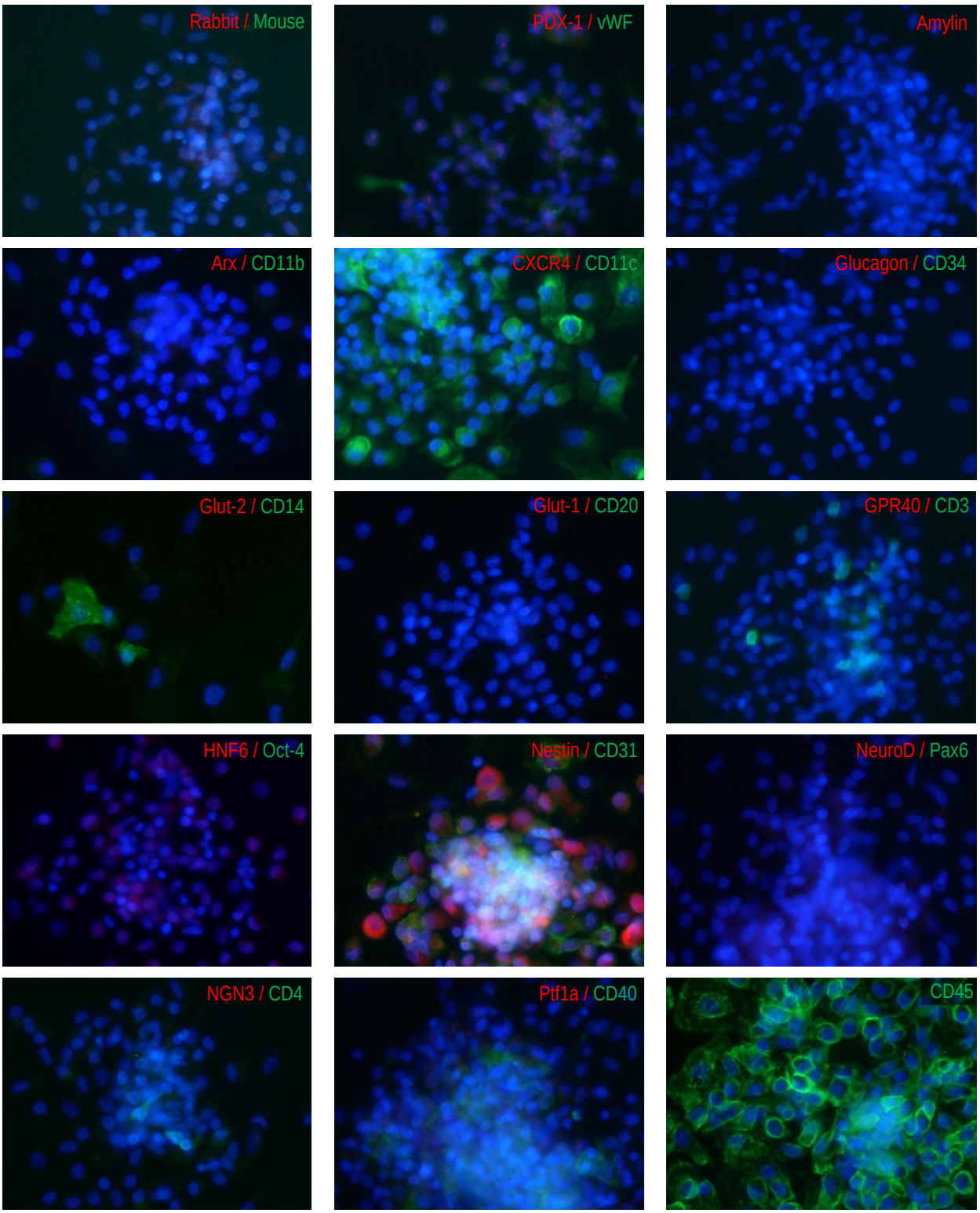


Figure 3.6 Phenotyping of monocytes cultured in tissue culture dishes for 3 days.

Adherent monocytes were cultured in full RPMI media containing 7% FBS. Cells were stained for the expression of various cell markers. Immunoreactivity was detected with donkey anti-rabbit, goat anti-guinea pig, and donkey anti-goat (red) antibodies and with a donkey anti-mouse antibody (green). Nuclei were stained blue with DAPI. Images were taken at 200x magnification. The images are presented so that the staining obtained with each IgG control immediately precedes stainings with antibodies of the same host species. A larger field of these images is presented in Appendix A (Figure A. 1).


Rabbit / Mouse
PDX-1 / vWF
Amylin
Arx / CD11b
CXCR4 / CD11c
Glucagon / CD34
Glut-2 / CD14
Glut-1 / CD20
GPR40 / CD3
HNF6 / Oct-4
Nestin / CD31
NeuroD / Pax6
NGN3 / CD4
Ptf1a / CD40
CD45

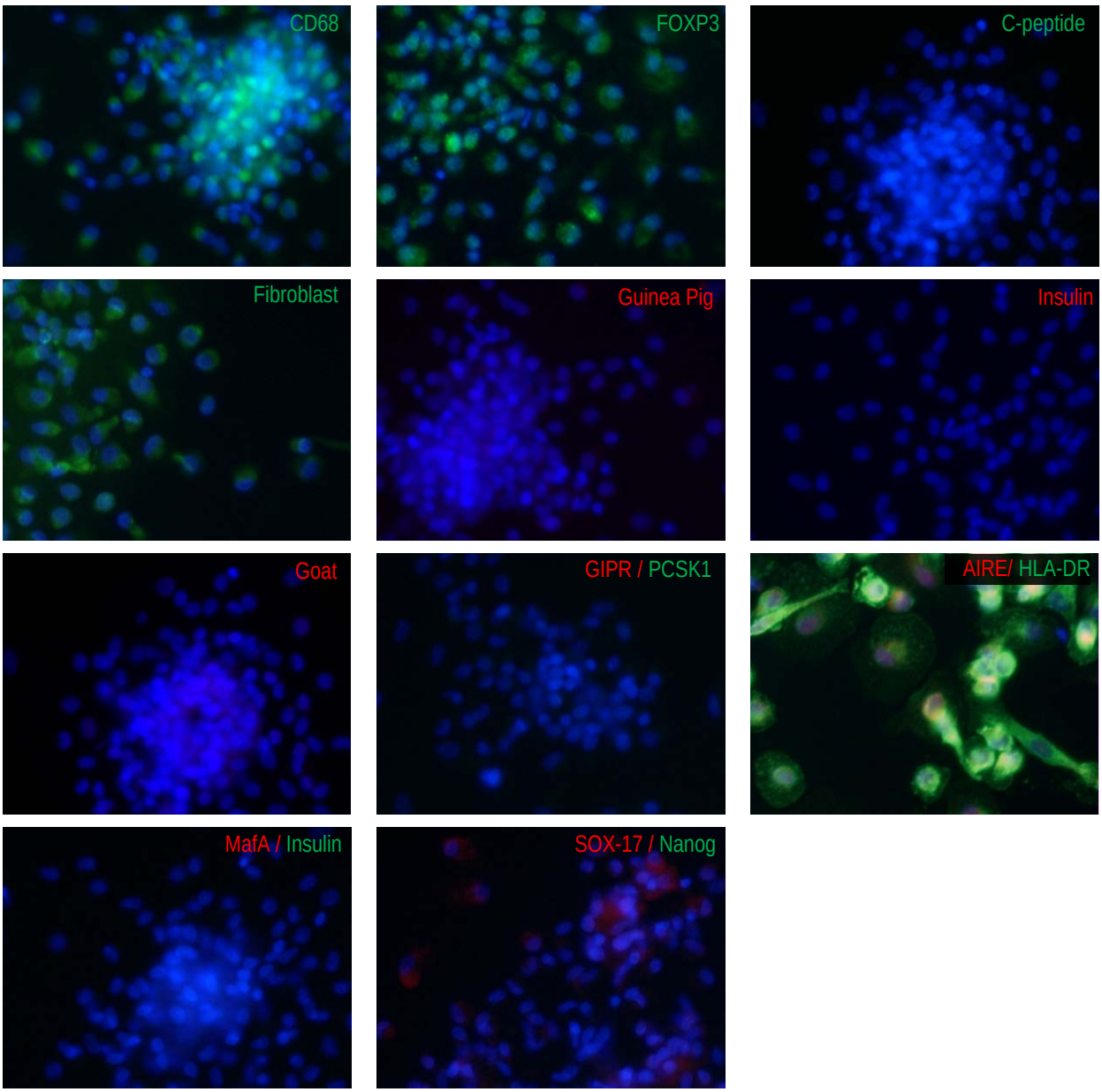
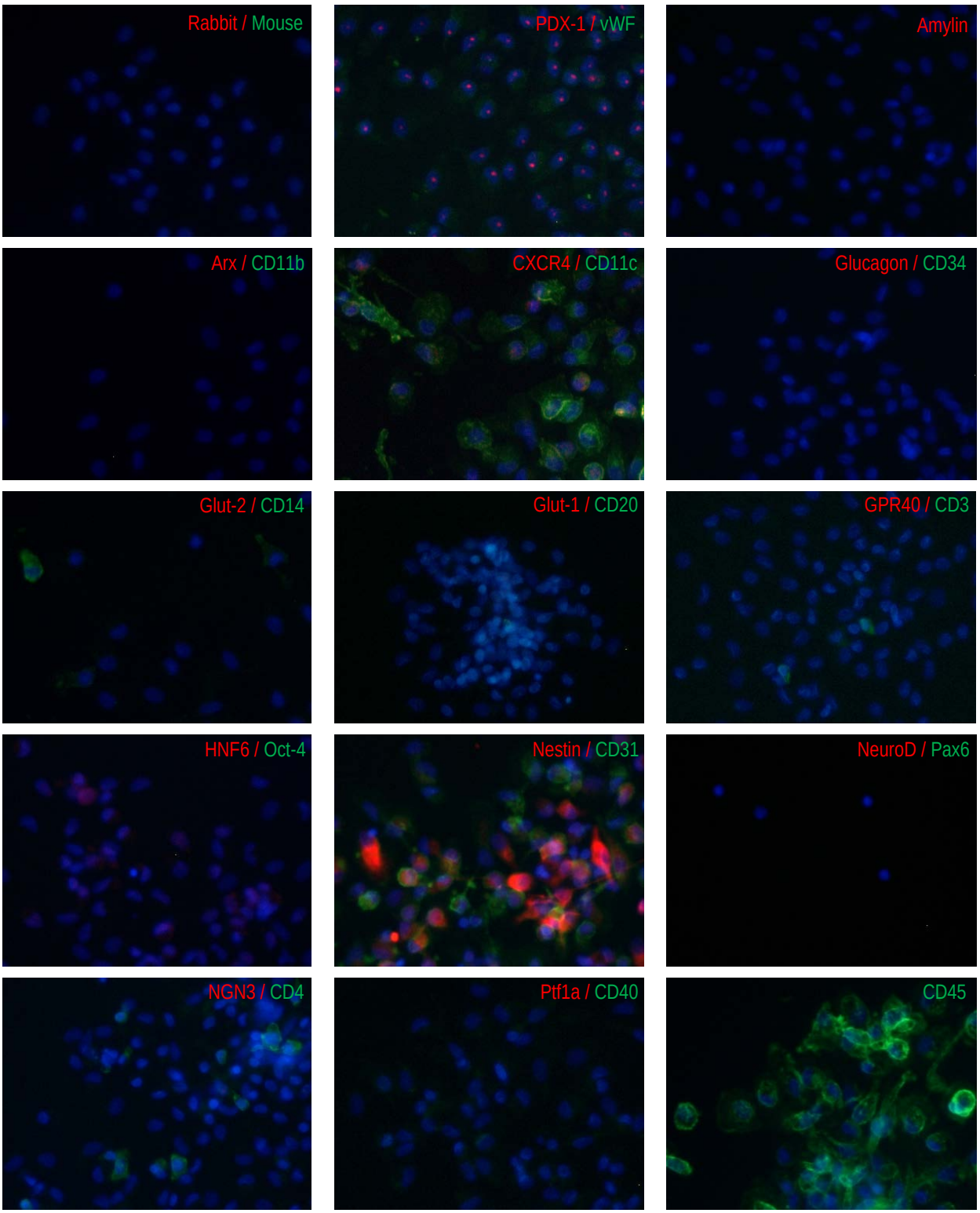


Figure 3.7 Phenotyping of adherent PB-IPCs cultured in hydrophobic dishes for 1 week.

Adherent PB-IPCs were cultured in full RPMI media containing 7% FBS. Cells were stained for the expression of various cell markers. Immunoreactivity was detected with donkey anti-rabbit, goat anti-guinea pig, and donkey anti-goat (red) antibodies and with a donkey anti-mouse antibody (green). Nuclei were stained blue with DAPI. Images were taken at 200x magnification. The images are presented so that the staining obtained with each IgG control immediately precedes stainings with antibodies of the same host species.


Rabbit / Mouse
PDX-1 / vWF
Amylin
Arx / CD11b
CXCR4 / CD11c
Glucagon / CD34
Glut-2 / CD14
Glut-1 / CD20
GPR40 / CD3
HNF6 / Oct-4
Nestin / CD31
NeuroD / Pax6
NGN3 / CD4
Ptf1a / CD40
CD45

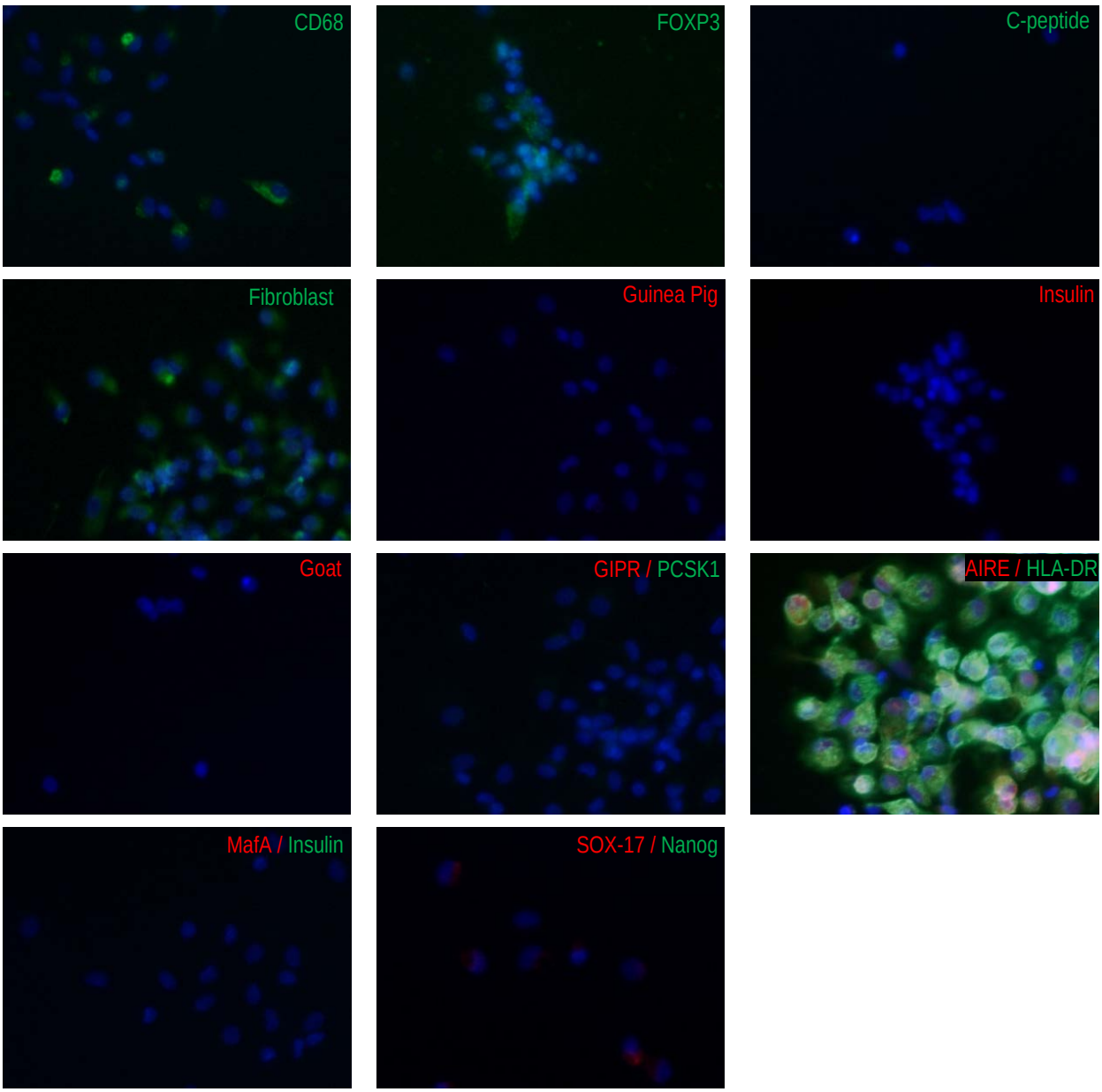
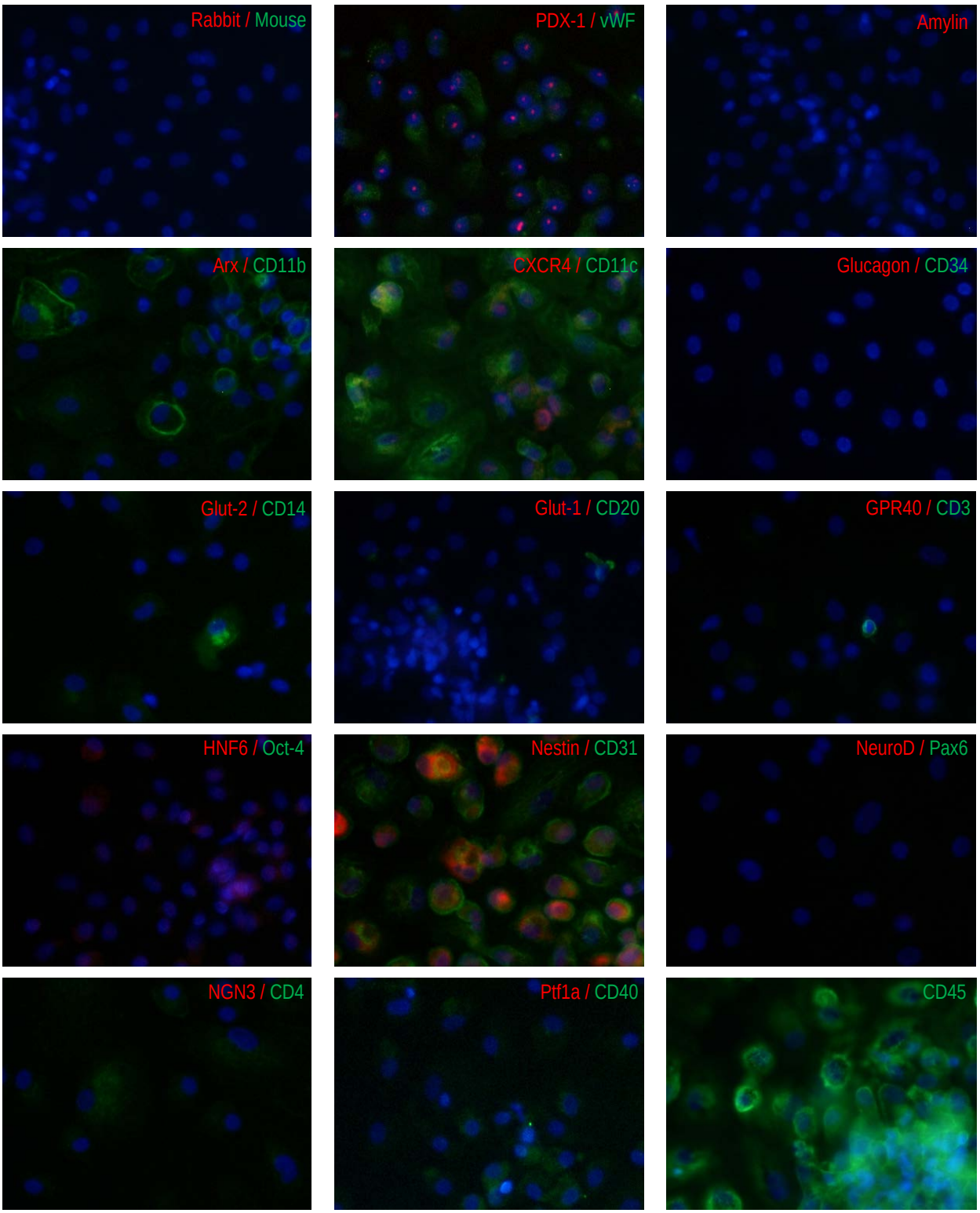


Figure 3.8 Phenotyping of monocytes cultured in tissue culture dishes for 1 week.

Adherent monocytes were cultured in full RPMI media containing 7% FBS. Cells were stained for the expression of various cell markers. Immunoreactivity was detected with donkey anti-rabbit, goat anti-guinea pig, and donkey anti-goat (red) antibodies and with a donkey anti-mouse antibody (green). Nuclei were stained blue with DAPI. Images were taken at 200x magnification. The images are presented so that the staining obtained with each IgG control immediately precedes stainings with antibodies of the same host species.


Rabbit / Mouse
PDX-1 / vWF
Amylin
Arx / CD11b
CXCR4 / CD11c
Glucagon / CD34
Glut-2 / CD14
Glut-1 / CD20
GPR40 / CD3
HNF6 / Oct-4
Nestin / CD31
NeuroD / Pax6
NGN3 / CD4
Ptf1a / CD40
CD45

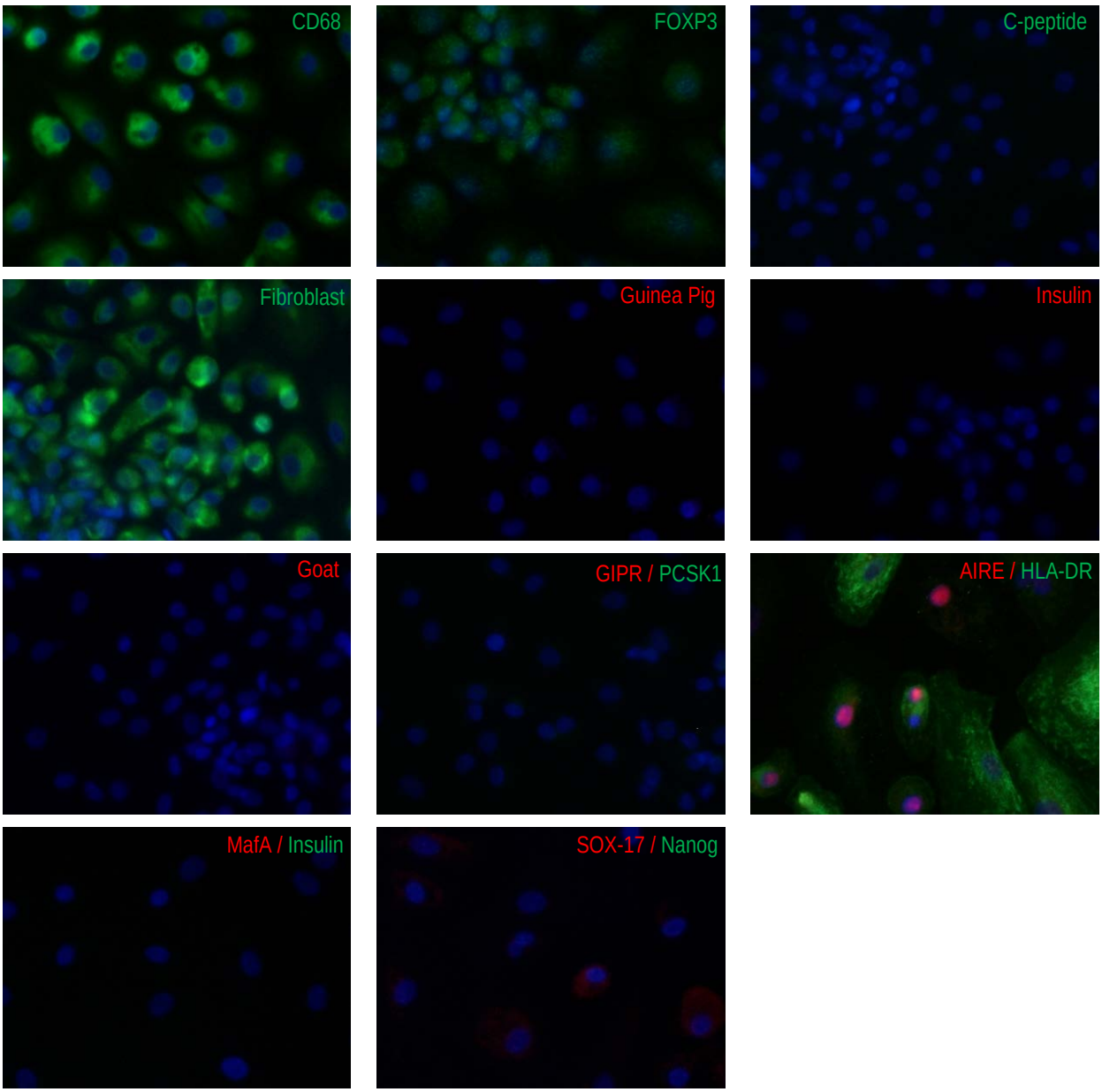
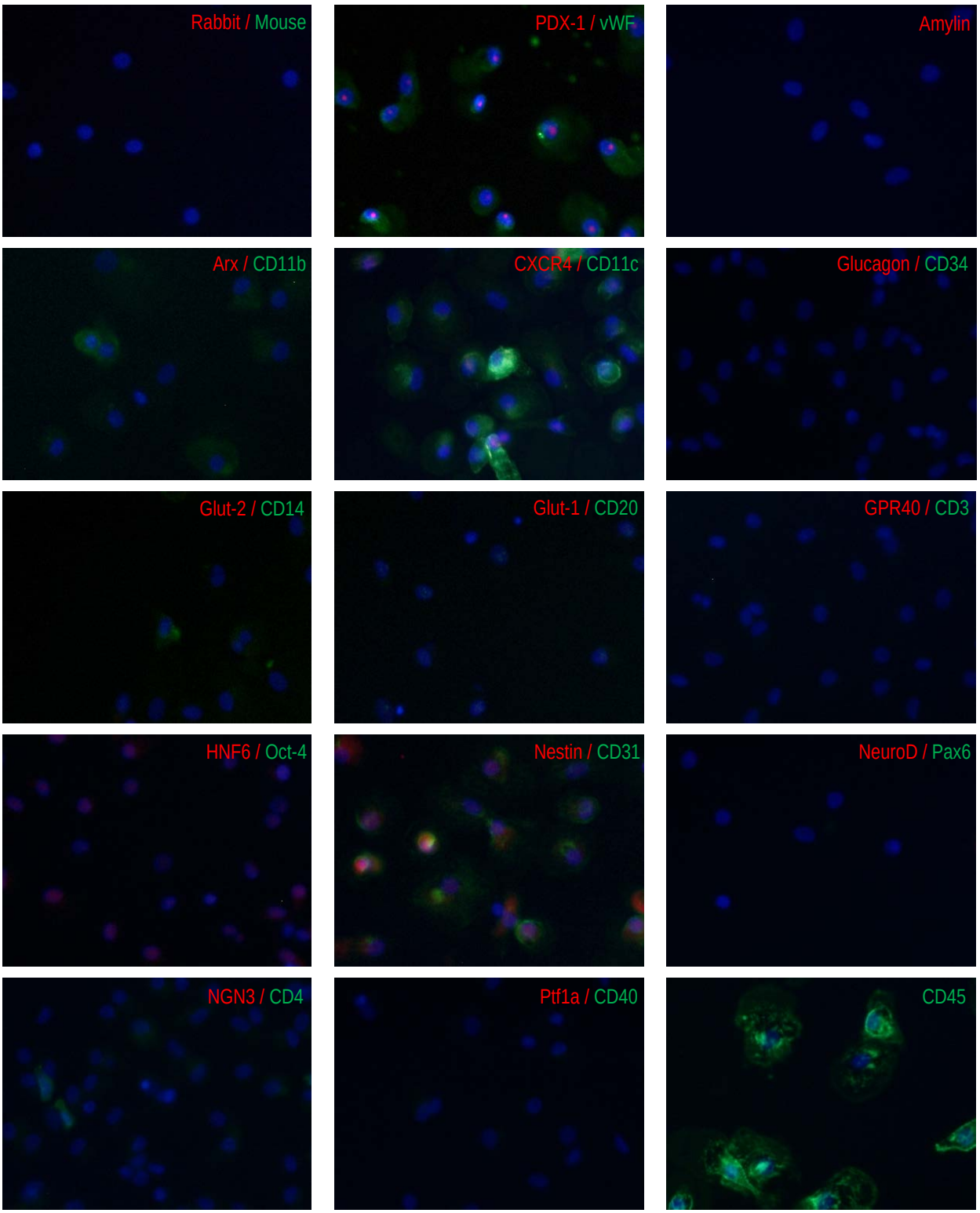


Figure 3.9 Phenotyping of adherent PB-IPCs cultured in hydrophobic dishes for 2 weeks.

Adherent PB-IPCs were cultured in full RPMI media containing 7% FBS. Cells were stained for the expression of various cell markers. Immunoreactivity was detected with donkey anti-rabbit, goat anti-guinea pig, and donkey anti-goat (red) antibodies and with a donkey anti-mouse antibody (green). Nuclei were stained blue with DAPI. Images were taken at 200x magnification. The images are presented so that the staining obtained with each IgG control immediately precedes stainings with antibodies of the same host species.


Rabbit / Mouse
PDX-1 / vWF
Amylin
Arx / CD11b
CXCR4 / CD11c
Glucagon / CD34
Glut-2 / CD14
Glut-1 / CD20
GPR40 / CD3
HNF6 / Oct-4
Nestin / CD31
NeuroD / Pax6
NGN3 / CD4
Ptf1a / CD40
CD45

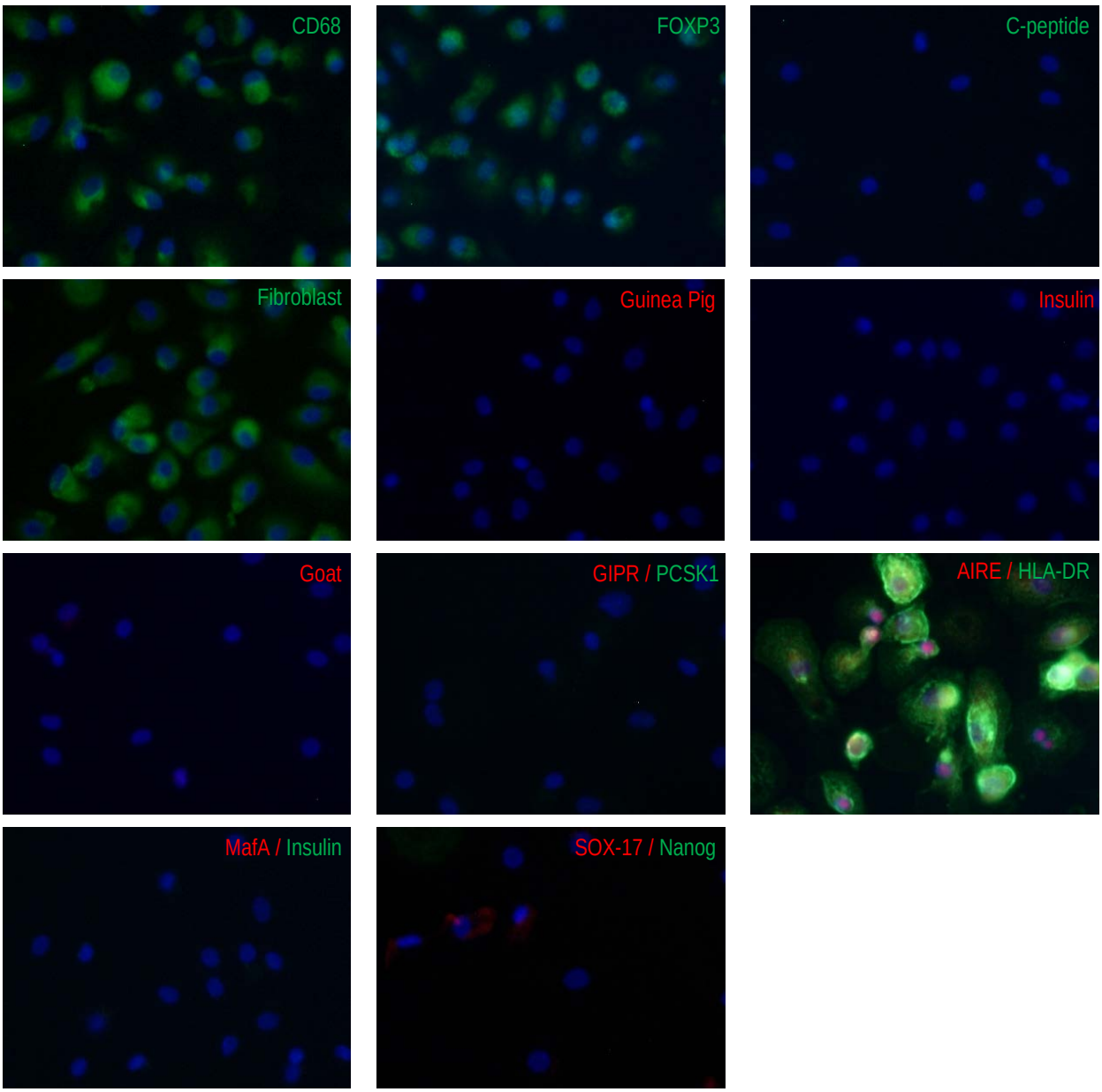


Figure 3.10 Phenotyping of monocytes cultured in tissue culture dishes for 2 weeks.

Adherent monocytes were cultured in full RPMI media containing 7% FBS. Cells were stained for the expression of various cell markers. Immunoreactivity was detected with donkey anti-rabbit, goat anti-guinea pig, and donkey anti-goat (red) antibodies and with a donkey anti-mouse antibody (green). Nuclei were stained blue with DAPI. Images were taken at 200x magnification. The images are presented so that the staining obtained with each IgG control immediately precedes stainings with antibodies of the same host species.

Table 3.1 Summary of the phenotypes of adherent PBMCs cultured in either a hydrophobic (PB-IPC) or tissue culture (monocytes, MO) dish

Cell Type	Marker	Time Course							
		PB-IPC 2 h	MO 2 h	PB-IPC 3 day	MO 3 day	PB-IPC 1 wk	MO 1 wk	PB-IPC 2 wk	MO 2 wk
Pancreatic	PDX-1					x	x x	x x	x x
	CXCR4						x	x	x
	HNF6			x	x	x	x	x	x
	SOX-17					x	x	x	x x
	NeuroD								
	NGN3								
	MafA								
	Pax6								
	Arx								
	GIPR								
	Ptf1a								
	Glut-1								
	GPR40								
	Amylin								
	Glut-2								
	PCSK1								
	Insulin								
	C-peptide								
	Glucagon								
Stem Cell	Nestin			x x	x x	x x x	x x x	x x x	x x x
	CD34								
	Oct-4								
Multi-Lineage	CD31	x x	x	x	x	x x x	x x x	x x x	x x
	Fibroblast	x x	x x	x x	x x	x x	x x	x x x	x x
	vWF	x x x	x x x	x x x	x x x	x	x	x	x x
Blood Cell	AIRE	x	x	x x	x	x x	x x	x x	x x
	FOXP3	x x	x x	x x x	x x x	x x x	x x	x	x x x
	CD20							x	
	CD3					x x	x	x x	
	CD4					x	x x	x	x
	CD11b							x x	x
	CD11c	x	x	x x	x x	x x x	x x x	x x x	x x x
	CD14	x x	x x	x x x	x x x	x x x	x x	x x	x
	CD40					x x		x	
	CD68			x x	x x	x x x	x x x	x x x	x x x
	HLA-DR	x x	x x	x x x	x x	x x x	x x x	x x x	x x x
	CD45	x x	x x	x x x	x x x	x x x	x x x	x x x	x x x

0	0.1-20	21-40	41-60	61-80	81-100	% Positive

x	x x	x x x	Intensity of staining – weak/moderate/strong

3.3.3 Validation of PDX-1 expression by Western blot analysis

The expression of PDX-1 by cultured PBMCs was examined by Western blot analysis to validate the immunocytochemistry results. PBMCs isolated from the same donor were cultured in tissue culture (monocytes) and hydrophobic microbiological (PB-IPC) dishes for 2 weeks in full RPMI media containing 7% FBS. Whole cells (1 x 10^6) were lysed in cell lysis buffer, resolved by SDS-PAGE, transferred to nitrocellulose, and Western blotted with a rabbit anti-PDX-1 antibody. The INS-1E cell line was employed as a positive control as it is known to express PDX-1 (Zhang *et al.* 2012). Recombinant human PDX-1 was also used as a positive control to confirm antibody reactivity. Both the monocytes and PB-IPCs expressed PDX-1 which migrated as major bands of 46 kDa and 31 kDa (Figure 3.11), which represent the sumoylated and unsumoylated forms of PDX1 (Kishi *et al.* 2003). The control INS-1E cells strongly expressed the 46 kDa form of PDX-1 protein, but only weakly expressed the 31 kDa form (Figure 3.11, upper blot). The blot was then re-probed with an antibody against β-actin, which showed that similar amounts of cell protein had been loaded into each lane (Figure 3.11, lower blot).

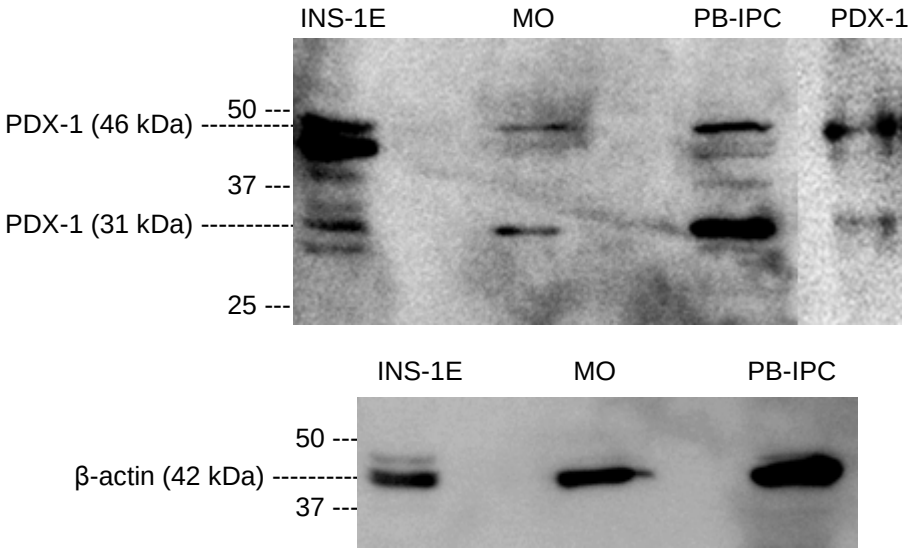


Figure 3.11 PDX-1 is expressed by both cultured monocytes and PB-IPCs.

PBMCs were grown in tissue culture dishes (monocytes; MO) or in hydrophobic dishes (PB-IPCs) for 2 weeks in full RPMI media containing 7% FBS. Upper blot: Whole cell lysates of INS-1E, monocytes (MO), and PB-IPCs, and recombinant human PDX-1 were Western blotted with a rabbit antibody against PDX-1 (46 and 31 kDa), and immunoreactivity detected with a donkey anti-rabbit HRP-conjugated antibody. Lower blot: The blot was stripped and reprobed with an antibody against human β-actin (42 kDa), and immunoreactivity detected with a donkey anti-rabbit HRP-conjugated antibody.

3.3.4 FOXP3 is expressed by cultured monocytes and PB-IPCs

Western blot analysis was also used to validate that monocytes and PB-IPCs express FOXP3. Monocytes and PB-IPCs were cultured for 2 weeks in full RPMI media containing 7% FBS. They were then lysed (1 x 10^6) and the presence of FOXP3 in the cytoplasmic and nuclear compartments analysed by Western blot analysis using two different anti-FOXP3 antibodies (n=1 for each antibody). Antibody ab20034 detected the presence of FOXP3 only in the nuclear fractions of monocytes and PB-IPCs (Figure 3.12), whereas antibody ab36607 detected the presence of FOXP3 in both the cytoplasmic and nuclear fractions (Figure 3.13). The inability to detect FOXP3 in the cytoplasmic fraction with ab20034 may have been due to the fact that less cytoplasmic protein had been loaded, as indicated by reprobing the Western blot with an anti-β-actin antibody. The amounts of nuclear and cytoplasmic protein loaded in the blot probed with the ab36607 anti-FOXP3 antibody were similar, which allowed for quantification of the levels of FOXP3 in the two cellular compartments. Monocytes expressed relatively lower levels of FOXP3 in the cytoplasm (0.6039) versus the nucleus (3.7812), as determined by densitometry analysis of gel bands. In comparison PB-IPCs expressed similar levels of FOXP3 in the cytoplasm (0.3552) and nucleus (0.3968). The results obtained with the ab36607 antibody suggested that monocytes expressed higher levels of FOXP3 in the nucleus than did PB-IPCs. In contrast, densitometry analysis of the protein bands formed with the ab20034 antibody indicated that monocytes (0.6759) and PB-IPCs (0.8134) express similar levels of nuclear FOXP3. The varying results obtained with the two different antibodies suggest caution should be applied when interpreting the levels of proteins by Western blot analysis using different antibodies. Additional repeat experiments to examine the expression of FOXP3 may lead to more reproducible results for the two antibodies trialled.

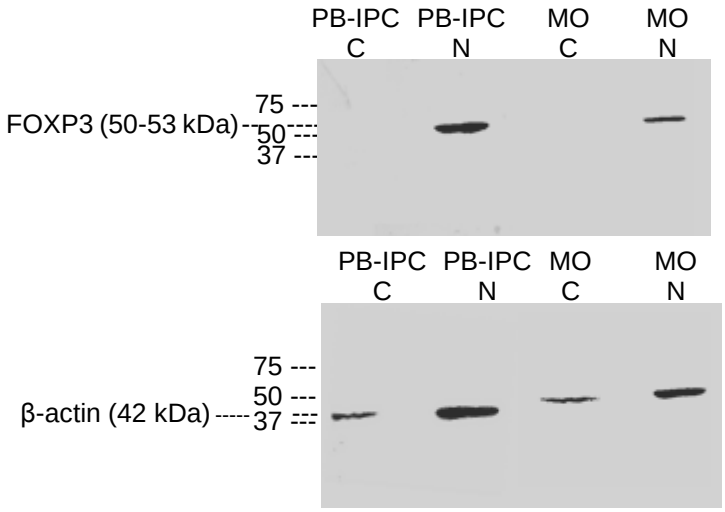


Figure 3.12 Anti-FOXP3 antibody ab20034 detects FOXP3 in the nuclear compartment of monocytes and PB-IPCs.

PBMCs were grown in tissue culture dishes (monocytes; MO) or in hydrophobic dishes (PB-IPCs) for 2 weeks in full RPMI media containing 7% FBS (n=1). Upper blot: Monocytes and PB-IPCs were lysed to obtain the cytoplasmic (C) and nuclear (N) fractions, which were Western blotted with the mouse antibody against FOXP3 ab20034 (50-53 kDa), and immunoreactivity detected with a goat anti-mouse HRP-conjugated antibody. Lower blot: The blot was stripped and reprobed with an antibody against human β-actin (42 kDa), with immunoreactivity detected with a donkey anti-rabbit HRP-conjugated antibody. Expression levels of FOXP3 and β-actin were quantified by densitometry analysis using ImageJ.

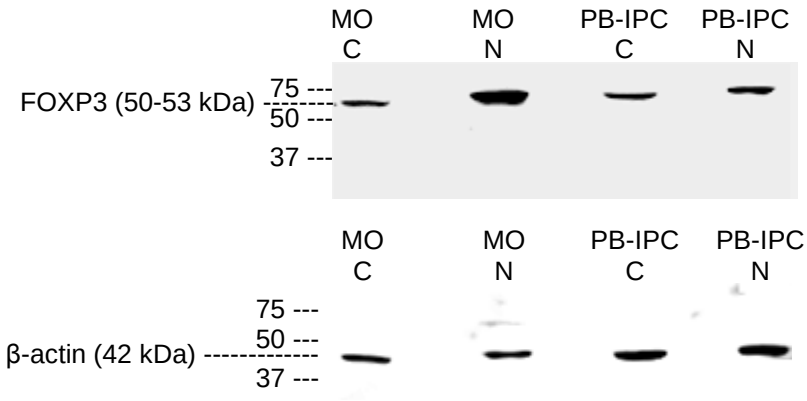


Figure 3.13 Anti-FOXP3 antibody ab36607 detects FOXP3 in the nuclear and cytoplasmic compartments of monocytes and PB-IPCs.

PBMCs were grown in tissue culture dishes (monocytes; MO) or in hydrophobic dishes (PB-IPCs) for 2 weeks in full RPMI media containing 7% FBS (n=1). Upper blot: Monocytes and PB-IPCs were lysed to obtain the cytoplasmic (C) and nuclear (N) fractions, which were Western blotted with the mouse antibody against FOXP3 ab36607 (50-53 kDa), and immunoreactivity detected with a goat anti-mouse HRP-conjugated antibody. Lower blot: The blot was stripped and reprobed with an antibody against human β-actin (42 kDa), and immunoreactivity detected with a donkey anti-rabbit HRP-conjugated antibody. Expression levels of FOXP3 and β-actin were quantified by densitometry analysis using ImageJ.

3.3.5 Cultured monocytes and PB-IPCs do not express insulin as determined by Western blot analysis

Monocytes and PB-IPCs from 2 different donors were cultured for 2 weeks in full RPMI media containing 7% FBS, and examined by Western blot analysis for insulin expression. The rat insulinoma cell line RINm5F was used as an example of a cell that expresses insulin and as a positive control to show the anti-insulin antibody was able to detect insulin (5.8 kDa). Recombinant insulin protein (0.0001 to 1 μg) was used to determine the lowest level of insulin protein detectable by Western blot analysis. The lowest amount of insulin detected by the guinea pig anti-insulin antibody was 100 ng of protein, which indicates that the method was not very sensitive using this antibody (Figure 3.14). A cell lysate of 1 x 10^6 PB-IPCs was loaded per lane of a Tris-tricine gel, and the resolved proteins transferred to nitrocellulose and Western blotted with the anti-insulin antibody. No insulin was detected in either the cytoplasmic or nuclear fractions of PB-IPCs (Figure 3.14). Therefore, 1 x 10^6 PB-IPCs express less than 100 ng of insulin. In contrast, > 1 μg of insulin was detectable in each of the cytoplasmic and nuclear fractions of RINm5F cells (1 x 10^6).

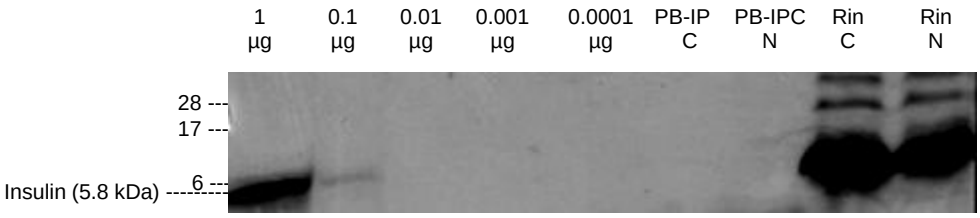


Figure 3.14 PB-IPCs cultured for 2 weeks do not express insulin.

Human PB-IPCs were cultured for 2 weeks in full RPMI media containing 7% FBS in hydrophobic dishes (n=2). The RINm5F (Rin) cell line was included as a positive control. The cells were lysed to obtain the cytoplasmic (C) and nuclear (N) fractions, which were Western blotted with a guinea pig antibody against insulin (5.8 kDa), and immunoreactivity detected with a donkey anti-guinea pig HRP-conjugated antibody. Recombinant insulin protein (1 µg – 0.001 µg) was used as a positive control.

PB-IPCs from 1 donor were cultured for 4 weeks in full RPMI media containing 7% FBS to determine whether they would express insulin after extended culture. The PB-IPCs (1 x 10^6) did not express detectable levels of insulin even after 4 weeks of culture (Figure 3.15, upper blot). Staining for actin showed that the protein samples were not degraded (Figure 3.15, lower blot).

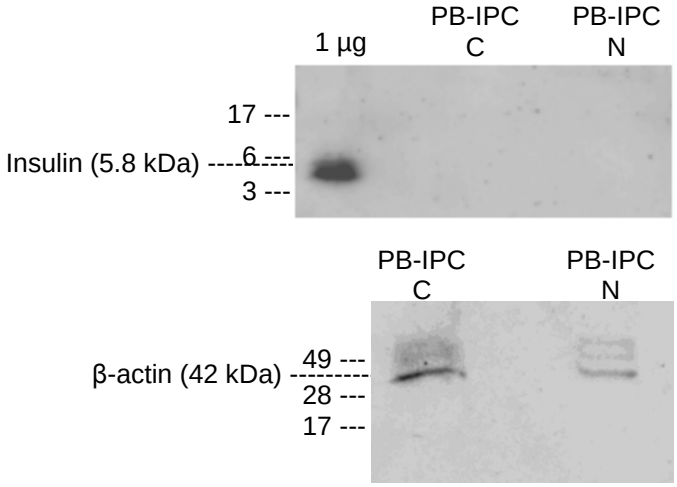


Figure 3.15 PB-IPCs cultured for 4 weeks do not express insulin.

Human PB-IPCs were cultured for 4 weeks in full RPMI media containing 7% FBS in hydrophobic dishes (n=1). The cells were lysed to obtain the cytoplasmic (C) and nuclear (N) fractions, which were Western blotted with a guinea pig antibody against insulin (5.8 kDa; upper blot) or with a rabbit antibody against β-actin (42 kDa; lower blot), and immunoreactivity detected with a donkey anti-guinea pig HRP-conjugated antibody or donkey anti-rabbit HRP-conjugated antibody, respectively. Recombinant insulin protein (1 µg) was used as a positive control.

3.3.6 Cultured PB-IPCs do not stain with FluoZin™-3 that is used to detect insulin expression

PB-IPCs from 2 different donors were further tested for insulin expression by incubation with FluoZin™-3 AM, a cell membrane permeant, fluorogenic, Zn^{2+}-specific indicator (Molecular Probes®). Pancreatic β-cells contain very high levels of Zn^{2+} within secretory vesicles where it is used to package insulin into hexamers (Lukowiak *et al.* 2001). Zn^{2+} is co-stored and co-released with insulin. Zn^{2+} reacts with high affinity with FluoZin™-3, forming a fluorescent complex (Qian *et al.* 2004). PB-IPCs were cultured for 2 weeks in full RPMI media containing 7% FBS in hydrophobic dishes, and stained with FluoZin™-3. No staining was detected, again indicating that PB-IPCs do not express insulin (Figure 3.16). In contrast, the insulin-expressing cell line RINm5F fluoresced bright green after incubation with FluoZin™-3 (Figure 3.16).

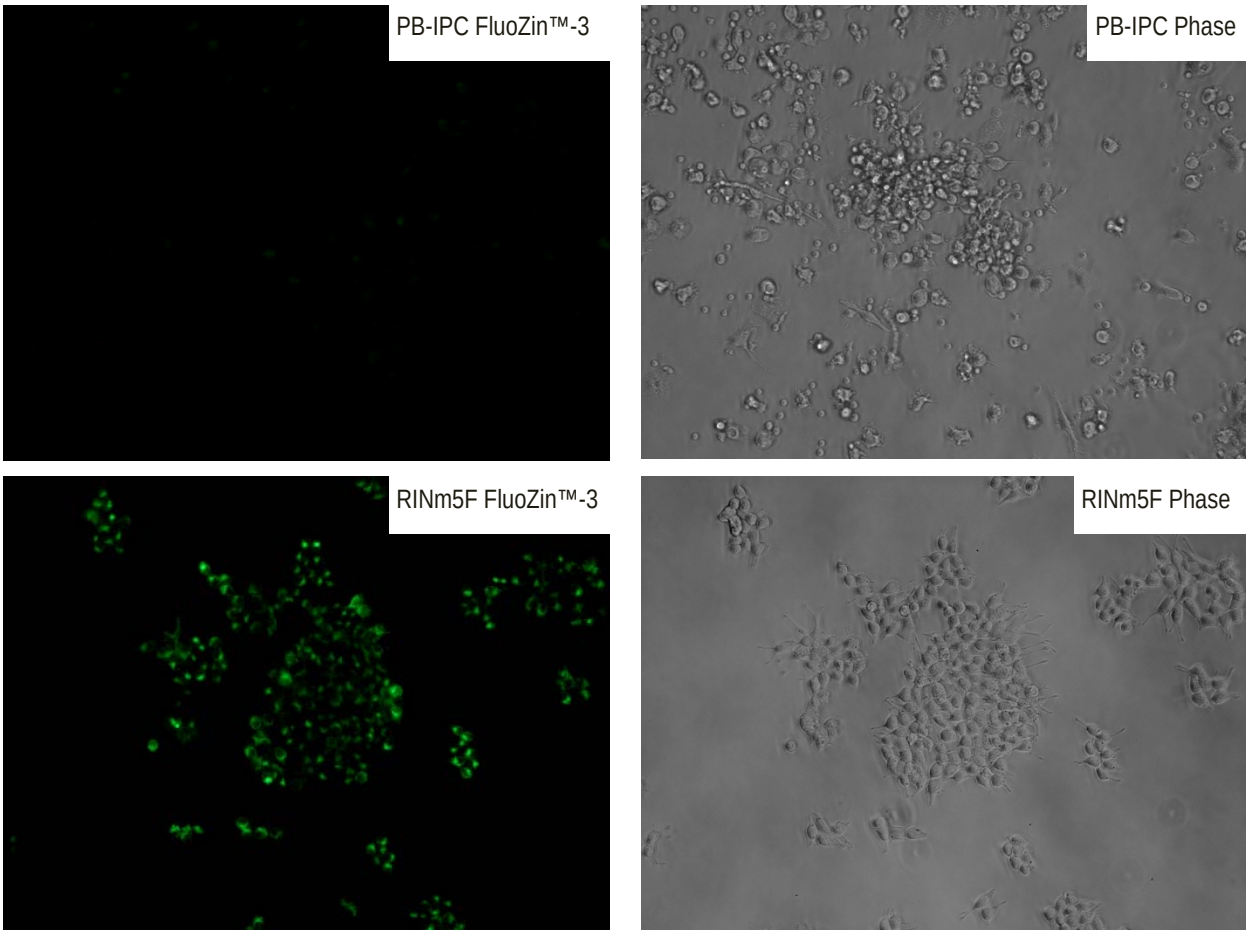


Figure 3.16 PB-IPCs do not stain with FluoZin™-3.

PB-IPCs were cultured for 2 weeks in full RPMI media containing 7% FBS in hydrophobic dishes (n=2). Images were taken at 200x magnification.

3.3.7 PB-IPCs display alkaline phosphatase activity

The finding that cultured monocytes and PB-IPCs express the stem cell marker Nestin led to a study to determine whether these cells had any stem cell functional characteristics. Stem cells characteristically express alkaline phosphatase activity (O'Connor *et al.* 2008), which can be detected using the chromogenic substrate, Fast Red Violet solution in combination with Naphthol, producing a purple coloured product (Millipore). PB-IPCs from 2 different donors were cultured for 1 week in full RPMI media containing 7% FBS in hydrophobic dishes, and were sampled on each day for testing for alkaline phosphatase activity. PB-IPCs cultured for one day had no alkaline phosphatase activity, however, after 2 days a few cells weakly stained purple (Figure 3.17). The intensity of staining of the few cells that expressed alkaline phosphatase peaked at day 3 (Figure 3.17). The percentage of alkaline phosphatase positive cells equated to ≤ 0.1% of the total cell population at day 7. High magnification of the cells revealed that the alkaline phosphatase activity was confined to vesicles within the cell (Figure 3.18).

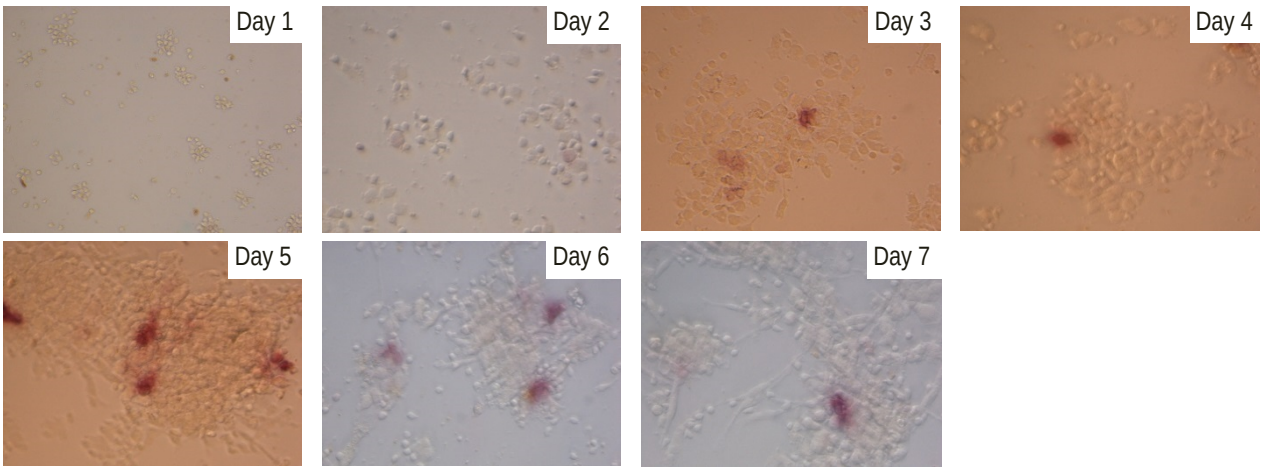


Figure 3.17 Cultured PB-IPCs express alkaline phosphatase activity.

PB-IPCs were cultured for up to 7 days in full RPMI media containing 7% FBS in hydrophobic dishes (n=2). They were tested for alkaline phosphatase activity at pH 6.0 where purple-red staining indicates activity. Day 1: 200 x magnification, Days 2-7: 400x magnification.

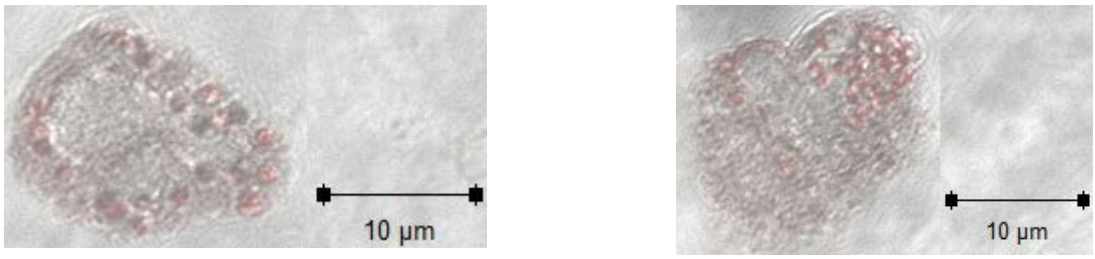


Figure 3.18 Alkaline phosphatase displayed by PB-IPCs is confined to intracellular vesicles.

PB-IPCs were cultured for up to 7 days in full RPMI media containing 7% FBS in hydrophobic dishes. They were tested for alkaline phosphatase activity at pH 6.0. A single cell is shown in each photo. Images were taken at 600x magnification.

3.4 PB-IPCs and monocytes are not proliferative in the absence of added growth factors

Zhao *et al*. (2007) reported that PB-IPCs proliferated in full RPMI media containing 7% FBS for up to 45 days without additional growth factors other than those present in serum. In the present study, PB-IPCs and monocytes were seeded in triplicate into 4 separate hydrophobic or tissue culture dishes in this same medium. Cell culture medium was refreshed weekly, and cell growth was measured using the CyQUANT® NF cell proliferation assay which measures DNA content. The assay established that monocytes and PB-IPCs do not proliferate in the absence of growth factors (Figure 3.19). Rather, there appeared to be a gradual decrease in DNA content, which may be due to loss of cells.

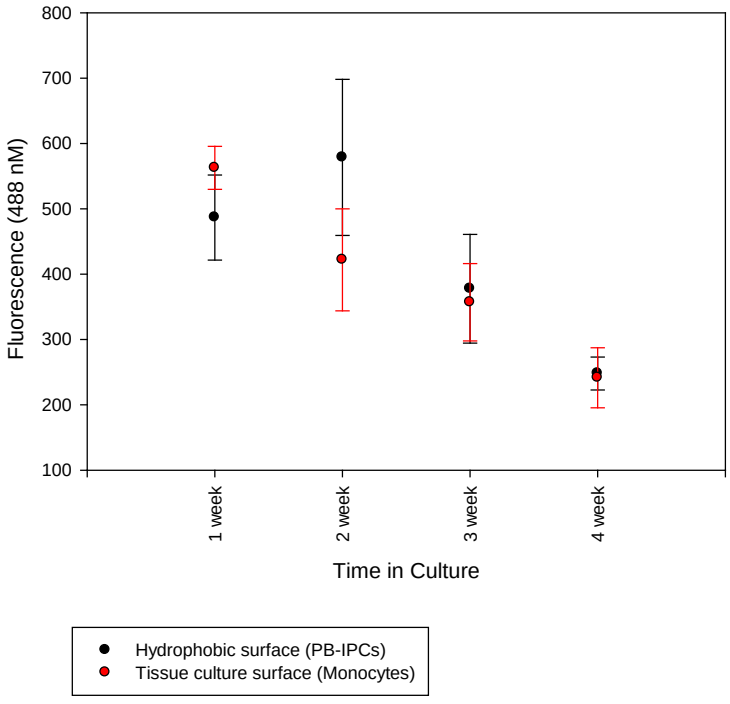


Figure 3.19 Measurement of the proliferation of monocytes and PB-IPCs cultured in tissue culture dishes and hydrophobic dishes, respectively.

Cells were cultured in full RPMI media containing 7% FBS. Cell proliferation was measured by the CyQUANT® NF cell proliferation assay. The results are presented as the mean (n=3) ± SD.

3.4.1 Monocytes proliferate in response to stimulation with M-CSF

Monocytes seeded in triplicate into 6 separate conventional 96-well tissue culture plates were stimulated for up to 16 days with 50 ng/mL M-CSF (216-MC, R&D Systems) in full RPMI media containing 7% FBS to confirm they were viable and capable of proliferating. Untreated control monocytes were cultured in the absence of M-CSF. The medium was refreshed every 3 days. Cell proliferation was measured every third day by the CyQUANT® NF cell proliferation assay. After 10-16 days in culture M-CSF-stimulated monocytes gave an increased fluorescence signal indicating they had increased in cell number (n=3, day 10: p = 0.015, day 13: p = 0.023, day 16: p = 0.010) whereas as before untreated monocytes appeared to decrease in number (Figure 3.20). At day 16, M-CSF-treated cells were largely small and rounded, whereas untreated cells contained numerous elongated fibroblast-like cells (Figure 3.21).

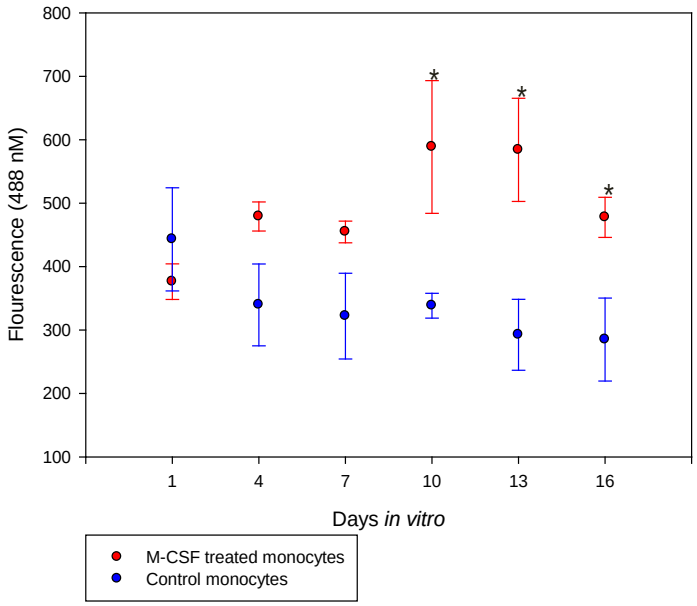


Figure 3.20 Proliferation of monocytes in response to stimulation with M-CSF.

M-CSF treated monocytes were cultured with 50 ng/mL M-CSF in full RPMI media containing 7% FBS in tissue culture dishes. Control monocytes were cultured in the same media without M-CSF. Cell proliferation was measured by the CyQUANT® NF cell proliferation assay. The results are presented as the mean (n=3) ± SD. * Significant difference between M-CSF-treated and untreated cells: day 10: p = 0.015, day 13: p = 0.023, day 16: p = 0.010.

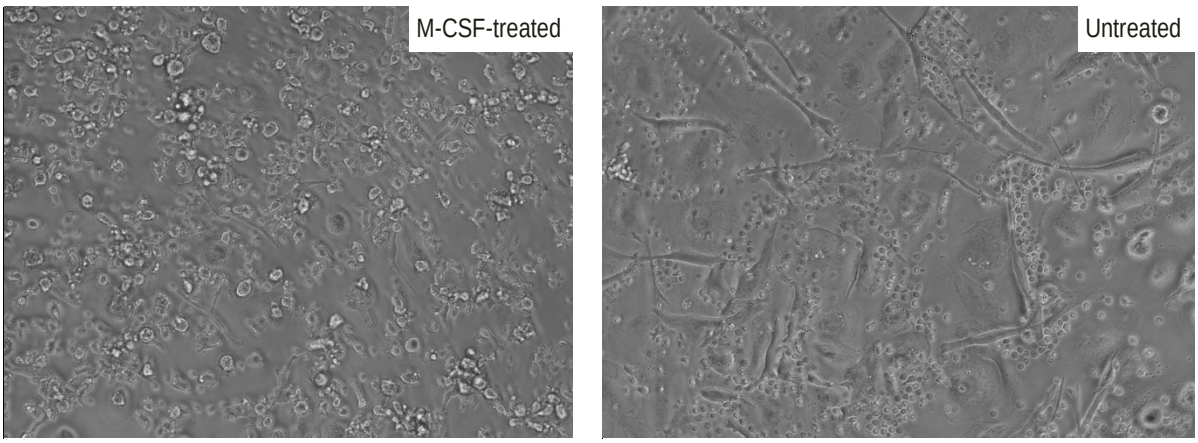


Figure 3.21 Phase contrast images of monocytes cultured in the presence or absence of M-CSF.

Monocytes were cultured in full RPMI media containing 7% FBS in the presence or absence of 50 ng/mL M-CSF in tissue culture dishes (n=3). Images were taken at 200x magnification.

3.5 *PB-IPCs rapidly become senescent in culture*

Senescent cells have alkalinized lysosomes which results in a change in intracellular pH from pH 4.0 to pH 6.0 (Debacq-Chainiaux *et al.* 2009). The assay utilizes the chromogenic β-gal substrate, 5-bromo-4-chloro-3-indoyl β-D-galactopyranoside (X-gal), which is cleaved by β-gal to produce an insoluble blue substrate (Debacq-Chainiaux *et al.* 2009). The senescence of PB-IPCs (from 2 different donors) in culture was detected by measuring the level of senescence-associated β-gal activity at pH 6.0 (Figure 3.22). PB-IPCs were cultured for 2 to 14 days in full RPMI media containing 7% FBS in hydrophobic dishes, respectively. Senescence-associated β-gal activity was weakly expressed by small numbers of PB-IPCs after 4 days of culture (Figure 3.22). The majority of cells strongly expressed senescence-associated β-gal activity at day 7 (Figure 3.22). Thus, PB-IPCs become senescent as early as 4 days in culture and highly senescent after 7 days.

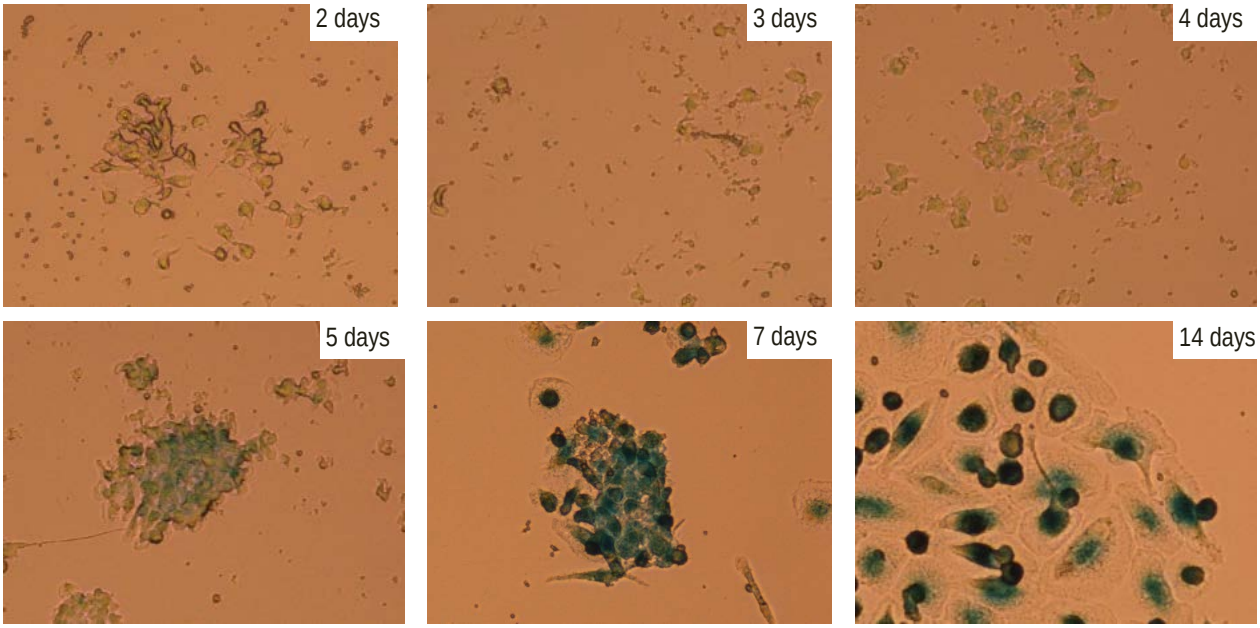


Figure 3.22 Senescence-associated β-gal activity of PB-IPCs is detectable as early as 4 days in culture.

PB-IPCs were cultured in full RPMI media containing 7% FBS in hydrophobic culture dishes in the absence of growth factors (n=2). They were stained with the β-gal substrate X-gal at pH 6. Cells that express senescence-associated β-gal activity are coloured blue. Images were taken at 200x magnification.

3.6 PKC activators induce the clustering of PB-IPCs

3.6.1 PKC activators induce prolonged clustering of PB-IPCs

Treatment of monocytes with PKC activators activates integrin's such as LFA-1 expressed on the surface of monocytes, which results in cell clustering (Xue *et al.* 2012). PB-IPCs from 2 different donors were cultured for 3 days in full RPMI media containing 7% FBS and increasing concentrations of the PKC activators ILV (ALX-420-011, Enzo Life Sciences, Inc.) and phorbol 12-myristate 13-acetate (PMA) (P8139, Sigma) in hydrophobic culture dishes to determine whether the PKC activators would induce cell clustering. Cell clusters formed with ≥ 100 nM ILV and ≥ 1 nM PMA (Figure 3.23).

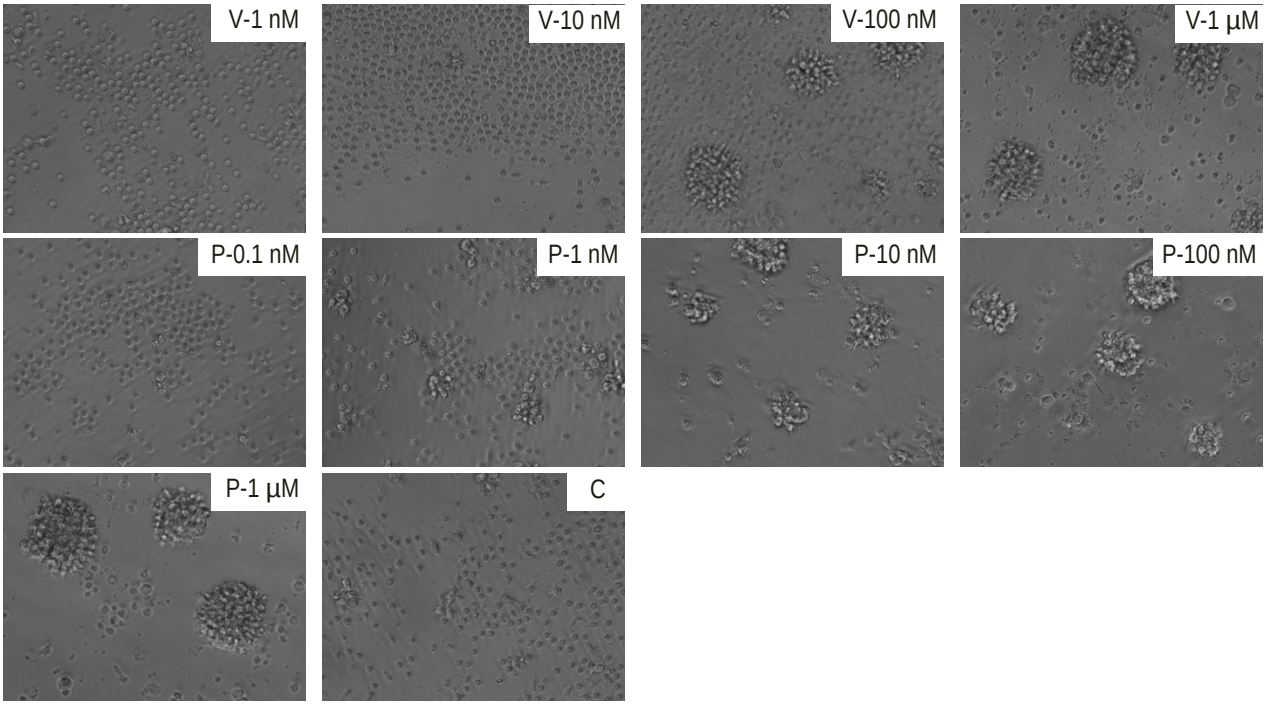


Figure 3.23 PKC activators (-)-indolactam V and phorbol 12-myristate 13-acetate induce clustering of PB-IPCs.

PB-IPCs were cultured for 3 days in full RPMI media containing 7% FBS and increasing concentrations of the PKC activators ILV (V) and phorbol 12-myristate 13-acetate (P) in hydrophobic culture dishes (n=2). C, control medium (full RPMI media containing 7% FBS). Images were taken at 200x magnification.

3.6.2 PKC activation inhibits the senescence of monocytes and PB-IPC

PKC activators have previously been shown to inhibit the senescence of cancer cells (Paget *et al*. 2012). It was hypothesized that inhibition of the senescence of PB-IPCs would promote their differentiation towards the pancreatic lineage if the cells were indeed plastic. Treatment of PB-IPCs with 100 nM ILV inhibited their senescence for at least 2 weeks (Figure 3.24). Monocytes cultured for 1 and 2 weeks in full RPMI media containing 7% FBS also became senescent. Their senescence was also prevented by inclusion of 100 nM ILV in the culture media (Figure 3.24). The cell number increased after the addition of ILV indicating that by inhibiting cell death/scencence the cells have been allowed to proliferate.

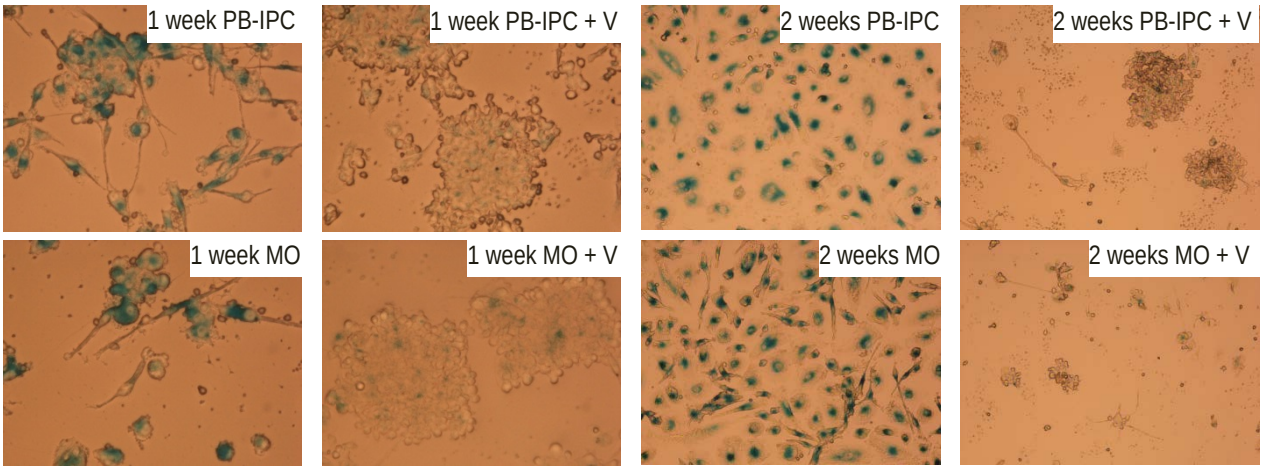


Figure 3.24 PKC delays senescence of PB-IPCs and monocytes for at least 2 weeks.

PB-IPCs and monocytes (MO) were cultured for 1 and 2 weeks in full RPMI media containing 7% FBS with and without 100 nM ILV (V) in hydrophobic and tissue culture dishes, respectively. They were stained with the β-gal substrate X-gal at pH 6 (n=2). Cells that express senescence-associated β-gal activity are coloured blue. C, control medium (full RPMI media containing 7% FBS); V, 100 nM ILV. Images were taken at 200x magnification.

Commercial stem cell media that help maintain HSCs were also trialled to see if they could prevent the senescence of PB-IPCs and monocytes. Commercial stem cell media Stemline® Hematopoietic Stem Cell Expansion Medium (HSC I) (S0189, Sigma) and Stemline® II Hematopoietic Stem Cell Expansion Medium (HSC II) (S0192, Sigma) could not prevent the senescence of PB-IPCs (Figure 3.25) and monocytes (Figure 3.26). In contrast to the results seen with the RPMI medium above, it was found that inclusion of 100 nM ILV in the HSC I and II media was not able to prevent cell senescence (Figure 3.25, Figure 3.26). Further, the PB-IPCs and monocytes cultured in HSC I and HSC II did not aggregate in response to the addition of ILV (Figure 3.25, Figure 3.26). Intriguingly, many of the cells at 2 weeks had become became multinucleated, irrespective of the addition of ILV (Figure 3.25, Figure 3.26).

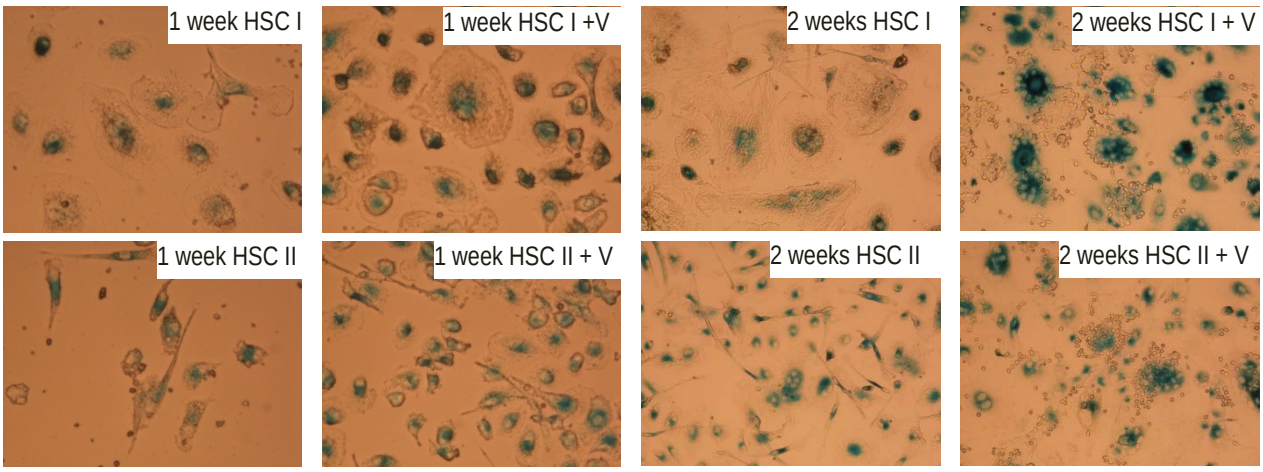


Figure 3.25 Commercial HSC mediums HSC I and HSC II do not prevent the senescence of PB-IPCs.

PB-IPCs were cultured for 1 and 2 weeks in HSC I and HSC II mediums in the presence or absence of 100 nM ILV (V) (n=2). Images were taken at 200x magnification.

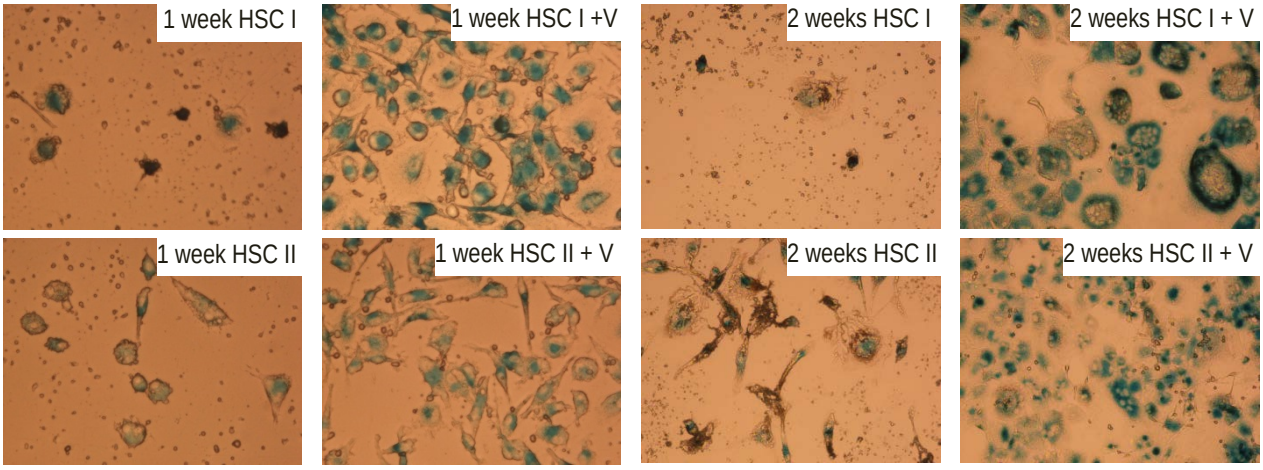


Figure 3.26 Commercial HSC mediums HSC I and HSC II do not prevent the senescence of monocytes.

Monocytes were cultured for 1 and 2 weeks in HSC I and HSC II mediums in the presence or absence of 100 nM ILV (V) (n=2). Images were taken at 200x magnification.

3.7 Functional testing of PB-IPCs reveals they retain key properties of monocytes

3.7.1 Sensitivity of PB-IPCs to L-leucine methyl ester, a monocytic killing agent

L-leucine methyl ester is a lysosomotropic compound which selectively kills monocytes, NK cells and cytotoxic T lymphocytes (Thiele and Lipsky 1986; Thiele and Lipsky 1990). It works by disrupting lysosomes, and therefore specifically kills cells having a high lysosome content (Thiele *et al.* 1983). Specifically, L-leucine methyl ester is internalised into the lysosomes of cells and is metabolised to leucine (Thiele *et al.* 1983). Leucine exits the lysosome more slowly than L-leucine methyl ester enters the cell, resulting in a build-up of L-leucine methyl ester, and within 30 min the lysosome ruptures causing cell death (Thiele *et al.* 1983). Treating PBMCs with ≥ 1 mM L-leucine methyl ester results in an almost complete loss of monocytes whereas some cells will survive at lower concentrations (Thiele *et al.* 1983).

The monocytic-like phenotype of PB-IPCs suggested that PB-IPCs might retain key functional properties of monocytes. Are PB-IPCs sensitive to the monocyte-killing agent L-leucine methyl ester? PBMCs from 2 different donors were treated with increasing concentrations of L-leucine methyl ester, seeded onto hydrophobic dishes, and cultured for 1 week in full RPMI media containing 7% FBS. No cells reminiscent of PB-IPCs were detected when PBMCs were pretreated with L-leucine methyl ester at concentrations ≥ 1.25 mM (Figure 3.27). The only cells present were exceptionally small, were not attached, and may have been contaminating lymphocytes or cells undergoing apoptosis (Figure 3.28). Attached cells exhibiting the typical morphology of PB-IPCs increased in number as the concentration of L-leucine methyl ester was reduced below 1.25 mM, in agreement with Thiele *et al.* (1983) (Figure 3.27).

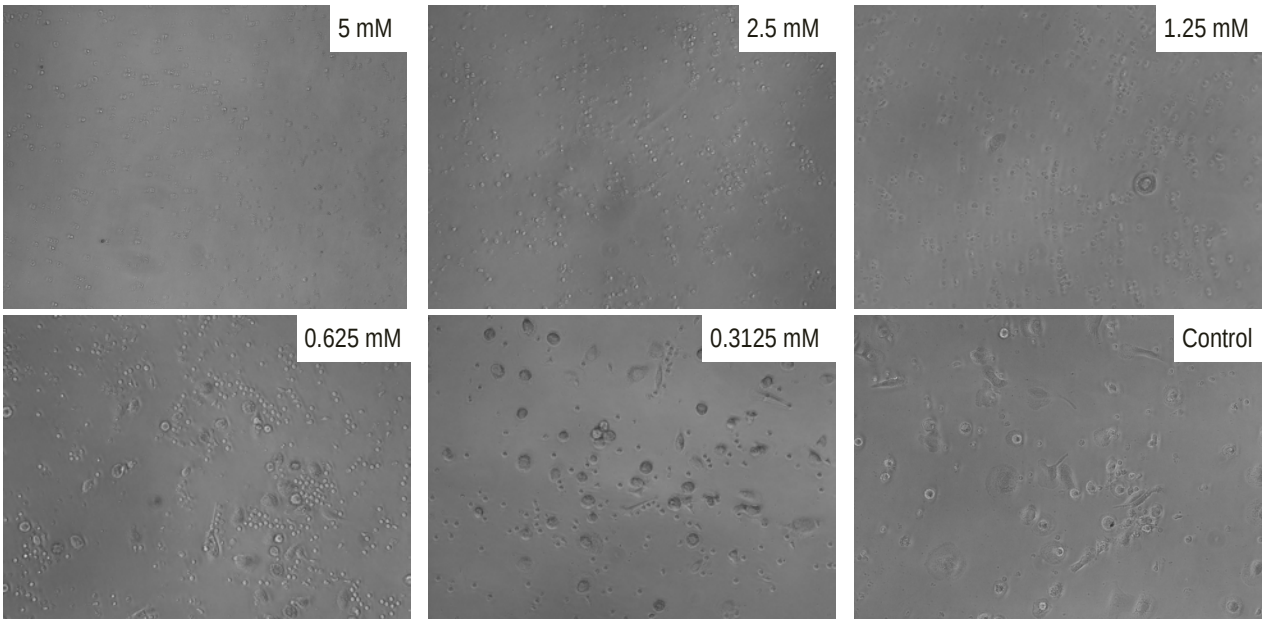


Figure 3.27 Phase contrast images of attached PBMCs treated with increasing concentrations of L-leucine methyl ester prior to seeding in hydrophobic dishes.

PBMCs ($5x10^6$ in 1 mL) were treated with 5 mM - 0.3125 mM L-leucine methyl ester, as indicated, in serum free medium. Control cells were treated in serum free medium only. The cells were then seeded into hydrophobic dishes and cultured for 1 week in full RPMI media containing 7% FBS (n=2).

PBMCs were treated with 0.3125-5 mM L-leucine methyl ester and then cultured for 3 days in hydrophobic dishes. The unattached cells were collected and stained with Annexin-V to determine if any live cells remained (especially at the higher concentrations) (Figure 3.28). Most of the cells stained with DAPI indicating they were nucleated, and therefore not platelets. A small proportion of the cells stained green with Annexin-V indicating they were apoptotic. The percentage of apoptotic cells increased with increasing concentrations of L-leucine methyl ester (Figure 3.29). The remaining live unattached cells that had resisted the toxic concentrations of L-leucine methyl ester must not be monocytes, NK cells or cytotoxic T cells (Figure 3.28). Their identity remains unknown but they did not attach to the hydrophobic surface during the 3 day incubation period hence are not PB-IPCs. They may be helper T cells and B cells which resist the effects of L-leucine methyl ester (Thiele and Lipsky 1990).

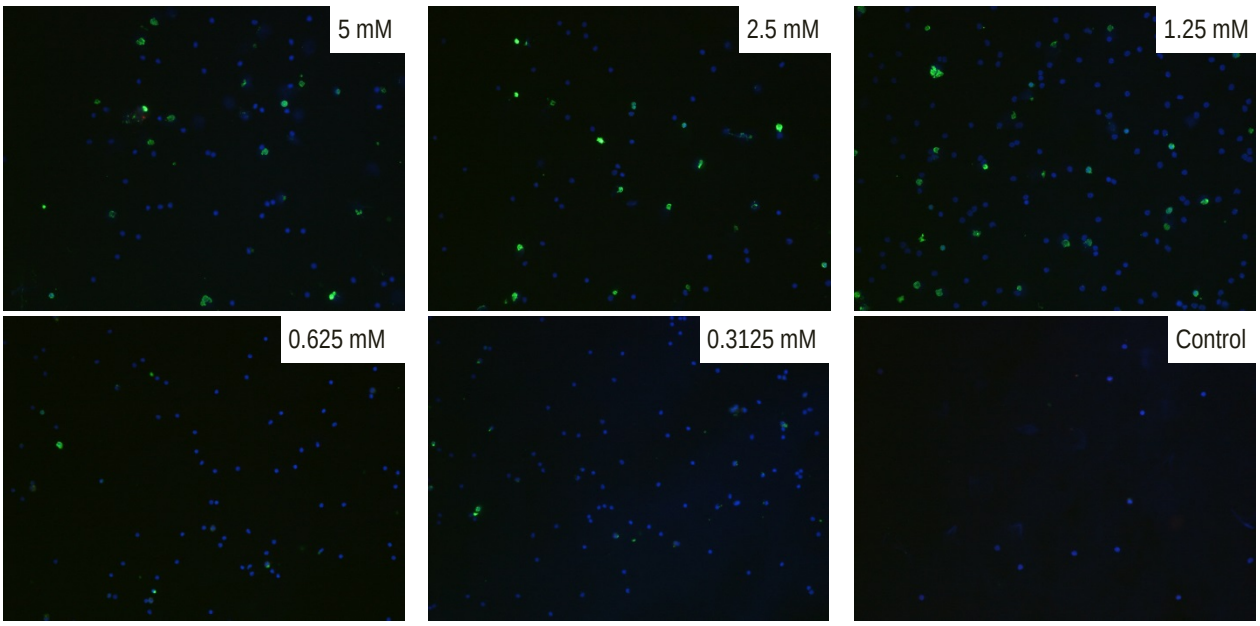


Figure 3.28 PBMCs that do not attach to hydrophobic dishes and resist toxic concentrations of L-leucine methyl ester are nucleated, and some are undergoing apoptosis.

PB-IPCs were cultured for 3 days in full RPMI media containing 7% FBS and 0.3125 to 5 mM L-leucine methyl ester. Cell nuclei were stained blue with DAPI, and apoptotic cells were stained green with Annexin-V.

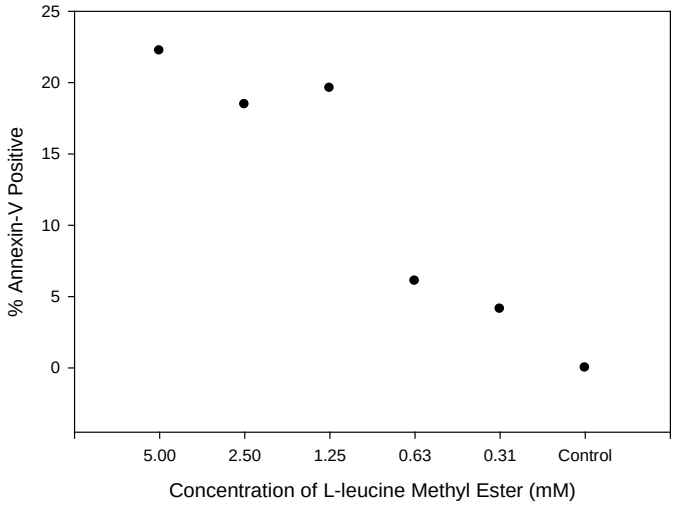


Figure 3.29 Percentage of suspension cells undergoing apoptosis after treatment with increasing concentrations of L-leucine methyl ester.

PBMCs were treated with 0.3125 to 5 mM L-leucine methyl ester and then cultured for 3 days in full RPMI media containing 7% FBS. The percentages of apoptotic cells in suspension that stained green with Annexin-V were plotted.

3.7.2 PB-IPCs readily take up pHrodo™ Red BioParticles® Conjugates

To provide further proof of the monocytic nature of PB-IPCs, the cells were incubated with pHrodo™ Red BioParticles® Conjugates. These particles are characteristically taken up by phagocytic cells such as monocytes via phagocytosis and endocytosis, where acidification occurs which dramatically increases the fluorescence of the conjugated pHrodo dye. The PB-IPCs took up the BioParticles, as efficiently as the monocytes (Figure 3.30). In contrast, the non-phagocytic breast cancer cell line SKBR3, which served as a negative control, did not take up the pHrodo™ Red BioParticles (Figure 3.30).

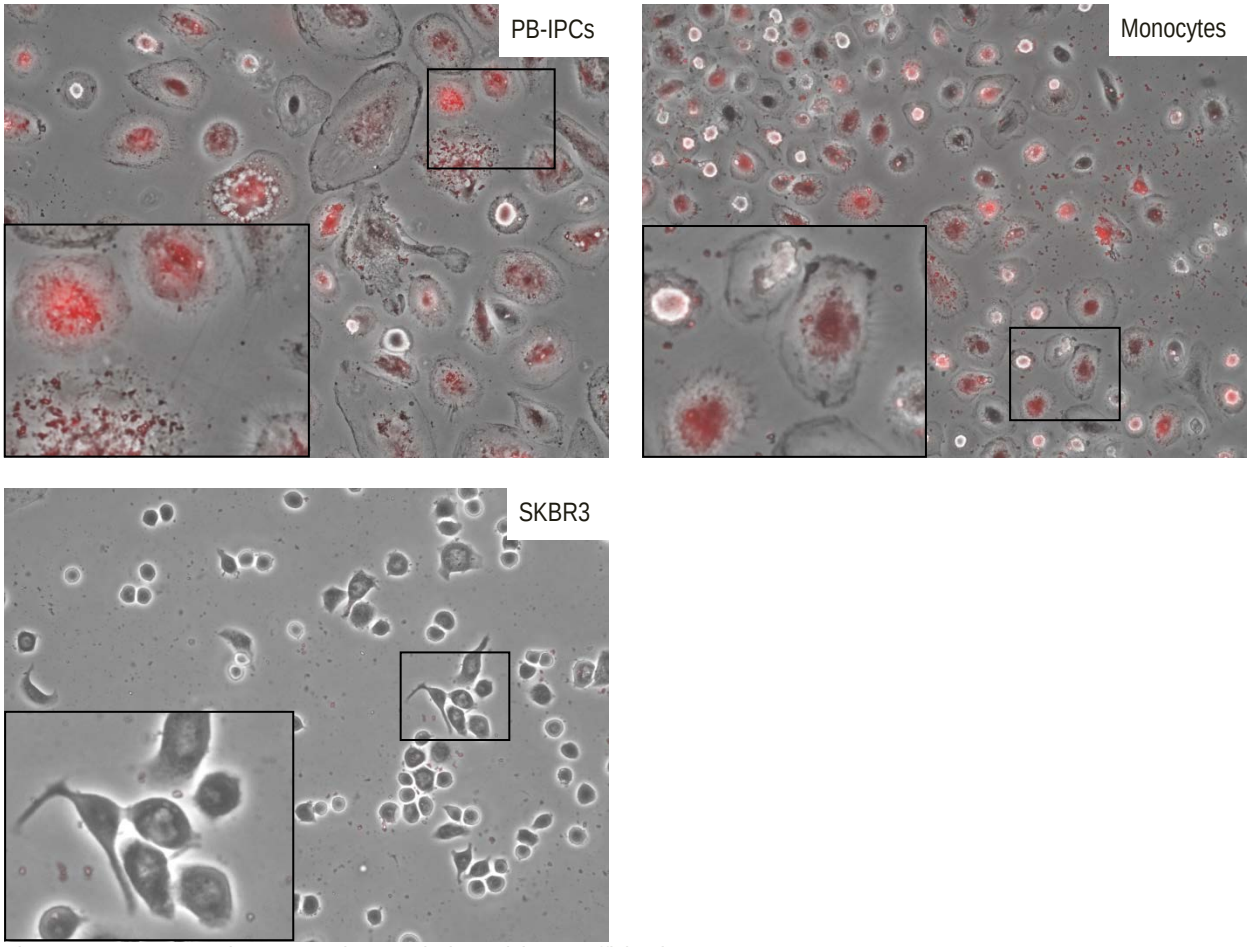
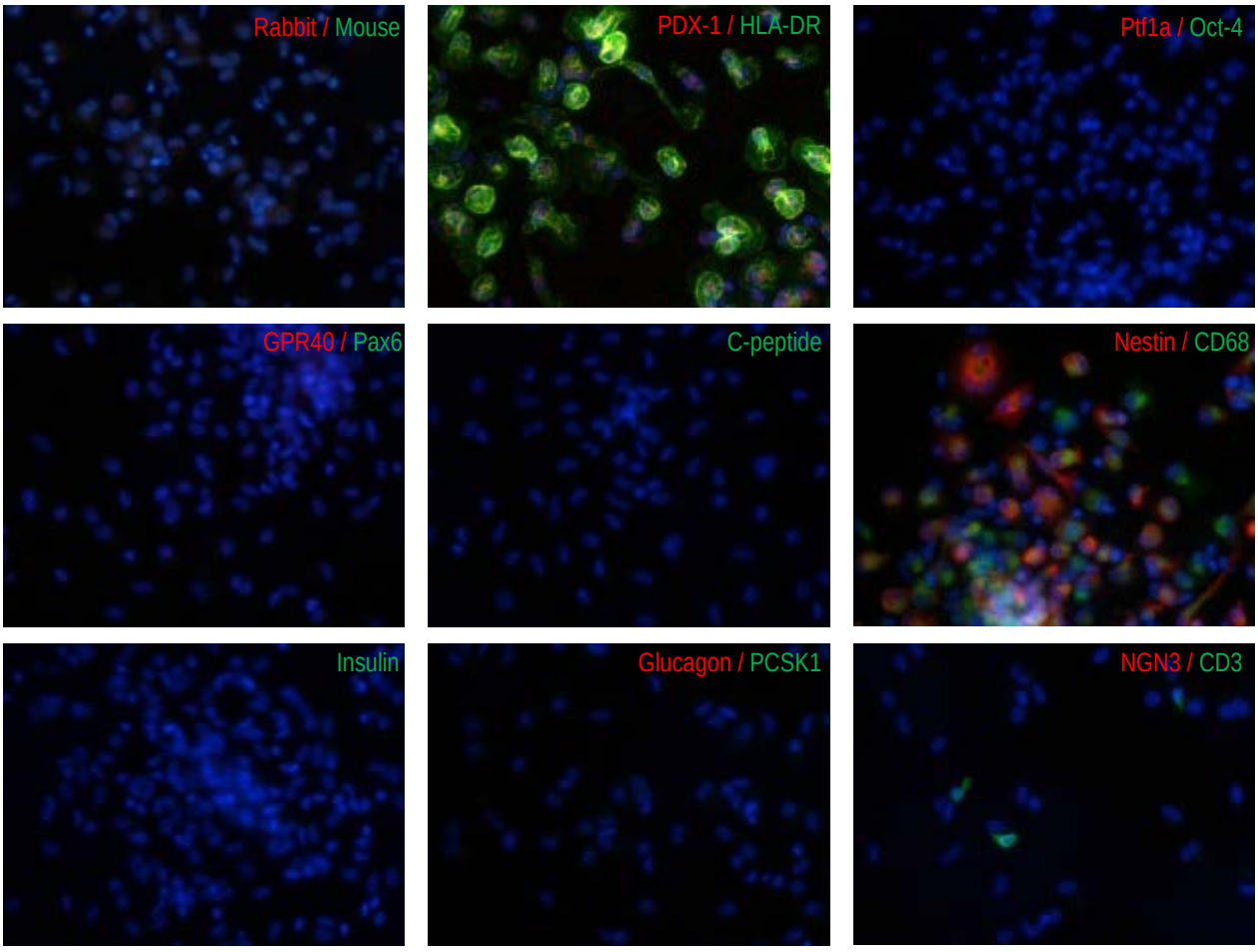


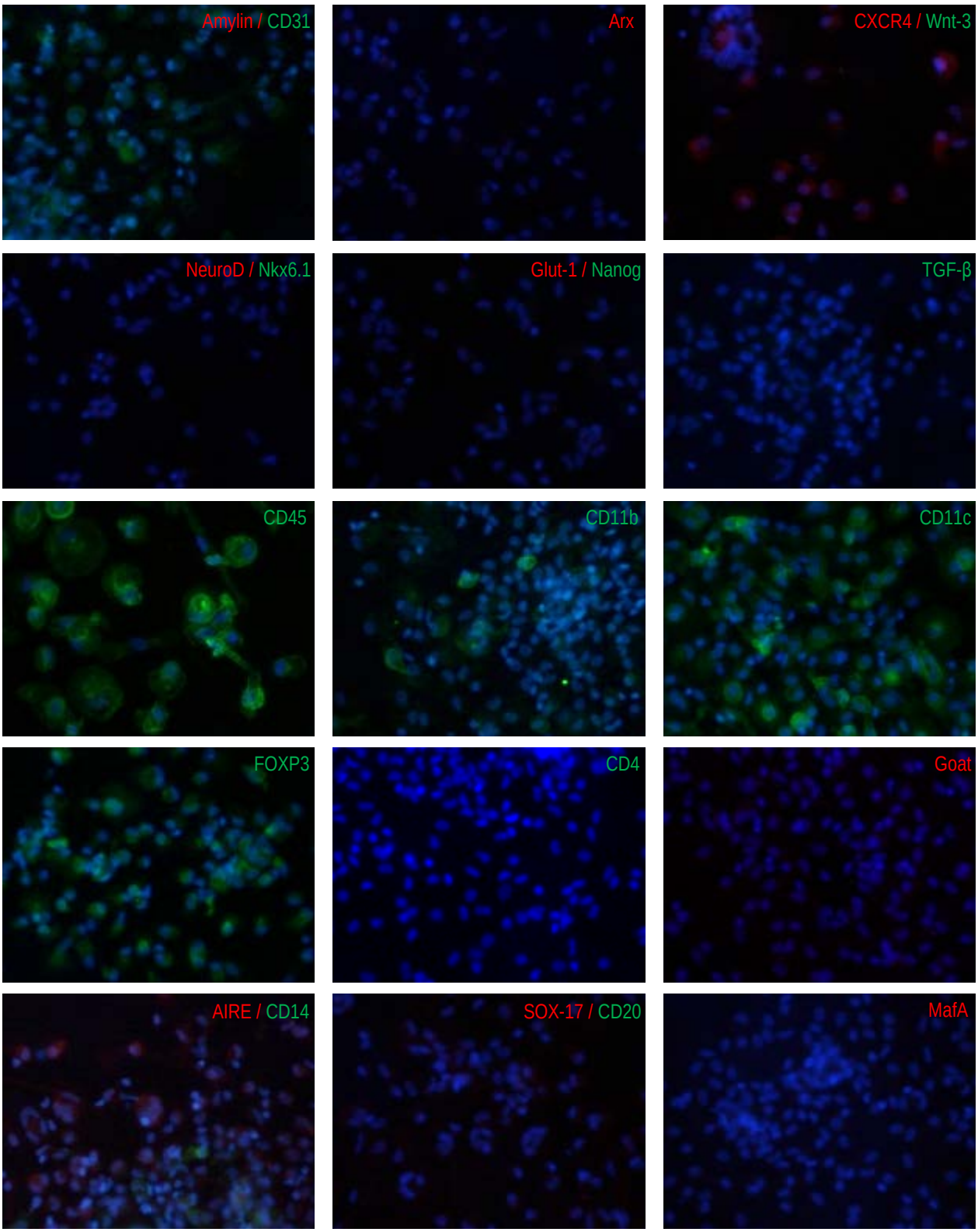
Figure 3.30 PB-IPCs take up pHrodo™ Red BioParticles as efficiently as monocytes.

PB-IPCs and monocytes were cultured for 2 weeks in full RPMI media containing 7% FBS in a hydrophobic dish (top left photograph) and a tissue culture dish (top right photograph), respectively, and then incubated for 1.5 h with 1 mg/mL pHrodo™ Red BioParticles (n=1). The non-phagocytic cell line SKBR3 was used as a negative control. Phase contrast and fluorescence microscopy images of the cells were overlaid. Images were taken at 200x magnification; inset is a higher magnification of each image.

3.8 Various pancreatic differentiation protocols are not able to differentiate PB-IPCs towards the pancreatic cell lineage

In the following set of experiments, PB-IPCs from 2 different donors were cultured for 1 week in full RPMI media containing 7% FBS followed by a further week in a variety of pancreatic differentiation media. A baseline phenotype was established by culturing PB-IPCs for 2 weeks in control medium (full RPMI media containing 7% FBS). The resulting cells had a similar phenotype to those previously described in Figure 3.9. They expressed PDX-1, CXCR4, Nestin, AIRE, CD11c, CD11b, CD14, CD68, CD31, HLA-DR, FOXP3, and CD45 (Figure 3.31). Occasionally CD3 T cells were found but CD4 T cells were absent (Figure 3.31). Several key markers of pancreatic cells and their progenitors were not detected including NeuroD, Wnt-3, Nkx6.1, NGN3, MafA, Pax6, Arx, GIPR, Ptf1a, Glut-1, GPR40, SOX-17, amylin, PCSK1, insulin, C-peptide, and glucagon (Figure 3.31). The cells did not express the stem cell markers Oct-4 and Nanog, the B cell marker CD20, or the growth factor TGF-β (Figure 3.31). A summary of these findings is shown in Table 3.2.




Amylin / CD31
Arx
CXCR4 / Wnt-3
NeuroD / Nkx6.1
Glut-1 / Nanog
TGF-β
CD45
CD11b
CD11c
FOXP3
CD4
Goat
AIRE / CD14
SOX-17 / CD20
MafA

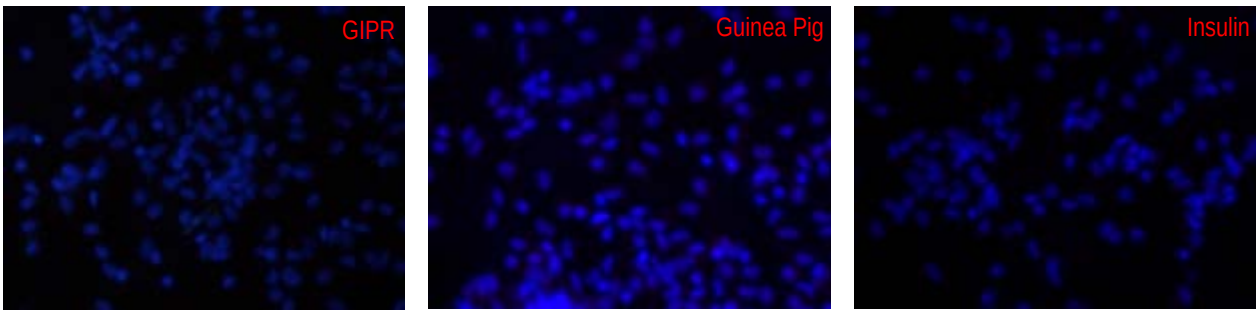


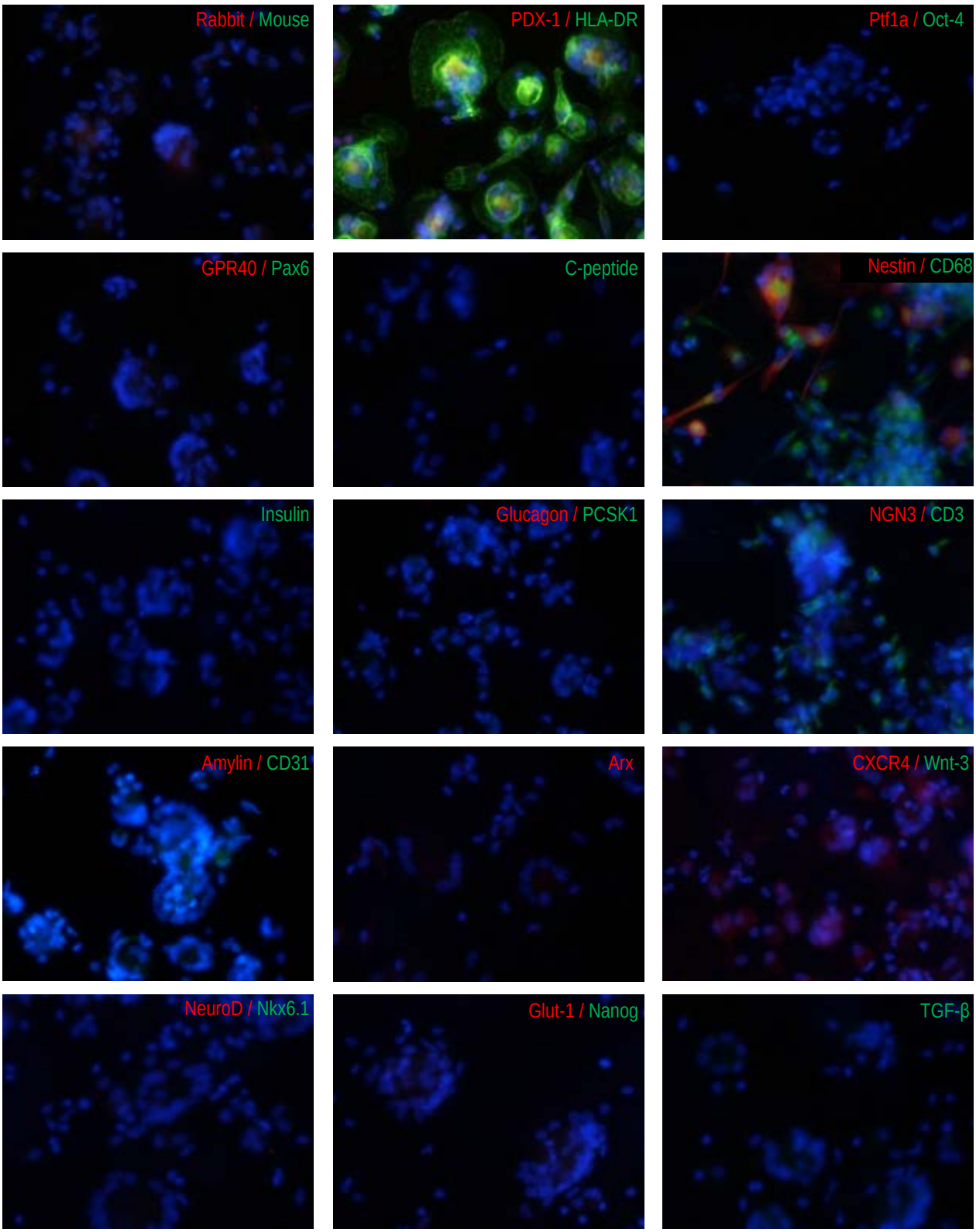
Figure 3.31 Phenotype of PB-IPCs cultured for 2 weeks in control medium.

PB-IPCs were cultured for 2 weeks in full RPMI media containing 7% FBS (n=2). Cells were stained for the expression of various cell markers. Immunoreactivity was detected with a donkey anti-rabbit, rabbit anti-goat, and goat anti-guinea pig antibodies (red) and with a donkey anti-mouse antibody (green). Cell nuclei were stained blue with DAPI. Images were taken at 200x magnification. The images are presented so that the staining obtained with each IgG control immediately precedes stainings with antibodies of the same host species.

3.8.1 The protocol devised by Zhao *et al.* (2008) is not able to differentiate PB-IPCs towards the pancreatic cell lineage

Zhao's protocol was tested for its ability to differentiate PB-IPCs into β-cell-like insulin-producing cells. It was previously reported that the resulting cells produce insulin and C-peptide, and express Glut-2, Sur1, and Kir6.2, and form an islet-like structure (Zhao and Mazzone 2008).

Accordingly, PB-IPCs from 2 different donors were cultured for 1 week in full RPMI media containing 7% FBS in hydrophobic dishes, followed by culture for 1 week in high glucose DMEM medium (11965-09, Gibco) containing 10 nM Ex4 (E7114, Sigma), 10 ng/mL GM-CSF (300-03, PeproTech), 7% FBS, and 1% PSG. The cells were then fixed with 4% formaldehyde and analysed by immunocytochemistry for the expression of pancreatic, blood, and stem cell markers. The resulting cells (Figure 3.32) expressed the same markers, and at the similar levels, as cells that had been cultured for 2 weeks in control medium (full RPMI media containing 7% FBS) (Figure 3.9 and Figure 3.31). They expressed PDX-1, CXCR4, AIRE, CD11c, CD14, CD68, HLA-DR, CD45, and FOXP3 (Figure 3.32). There were a decreased number of cells expressing Nestin, CD31, and CD11b, whereas there was an increase in the number of CD3-expressing T cells (Figure 3.32). Several key markers of pancreatic cells and their progenitors were not detected including NeuroD, Wnt-3, Nkx6.1, NGN3, MafA, Pax6, Arx, GIPR, Ptf1a, Glut-1, GPR40, SOX-17, amylin, PCSK1, insulin, C-peptide, and glucagon (Figure 3.32). The cells did not express the stem cell markers Oct-4 and Nanog, the B cell marker CD20, the T cell marker CD4, or the growth factor TGF-β (Figure 3.32). A summary of these findings is shown in Table 3.2.


Rabbit / Mouse
PDX-1 / HLA-DR
Ptf1a / Oct-4
GPR40 / Pax6
C-peptide
Nestin / CD68
Insulin
Glucagon / PCSK1
NGN3 / CD3
Amylin / CD31
Arx
CXCR4 / Wnt-3
NeuroD / Nkx6.1
Glut-1 / Nanog
TGF-β

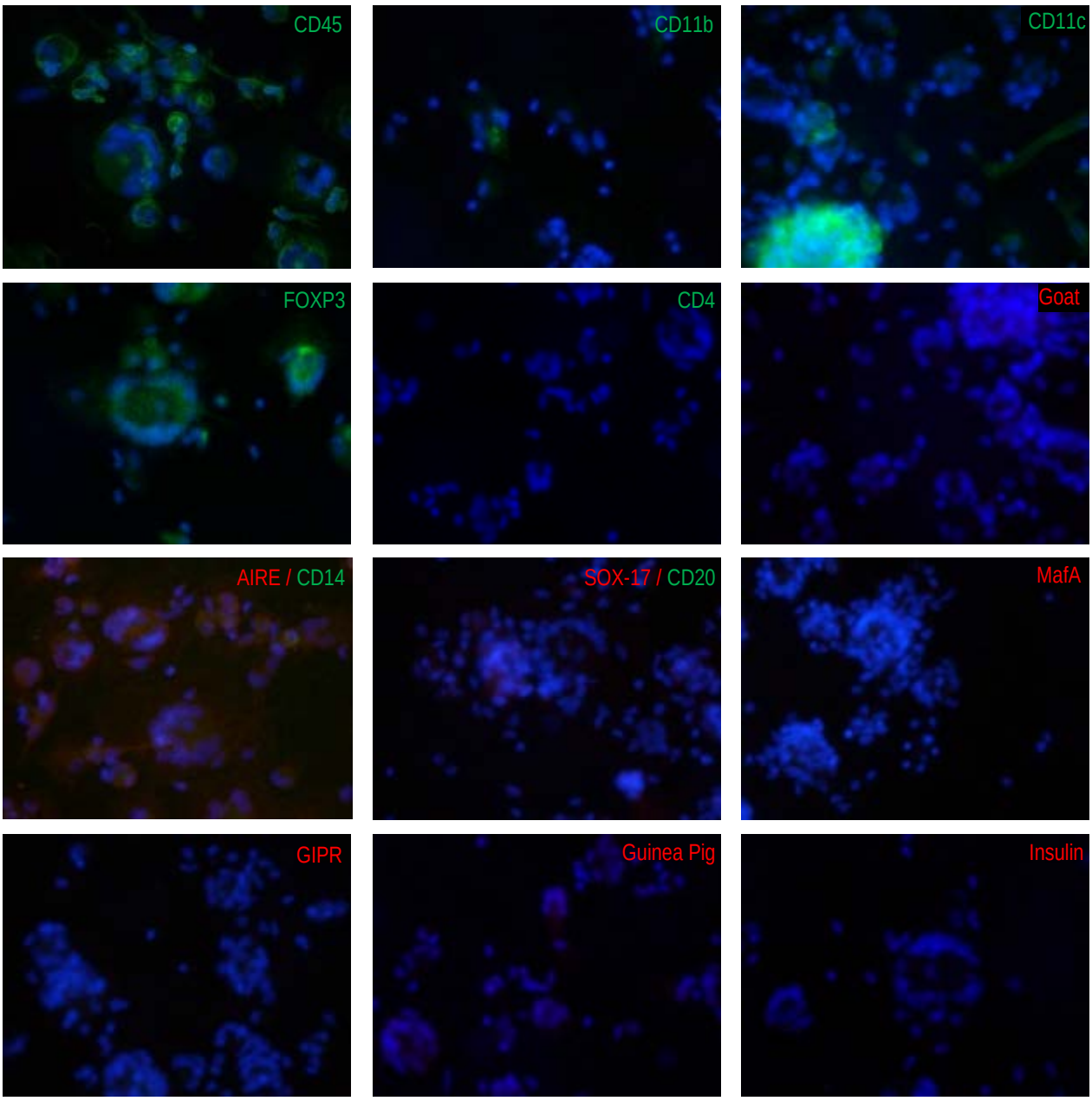


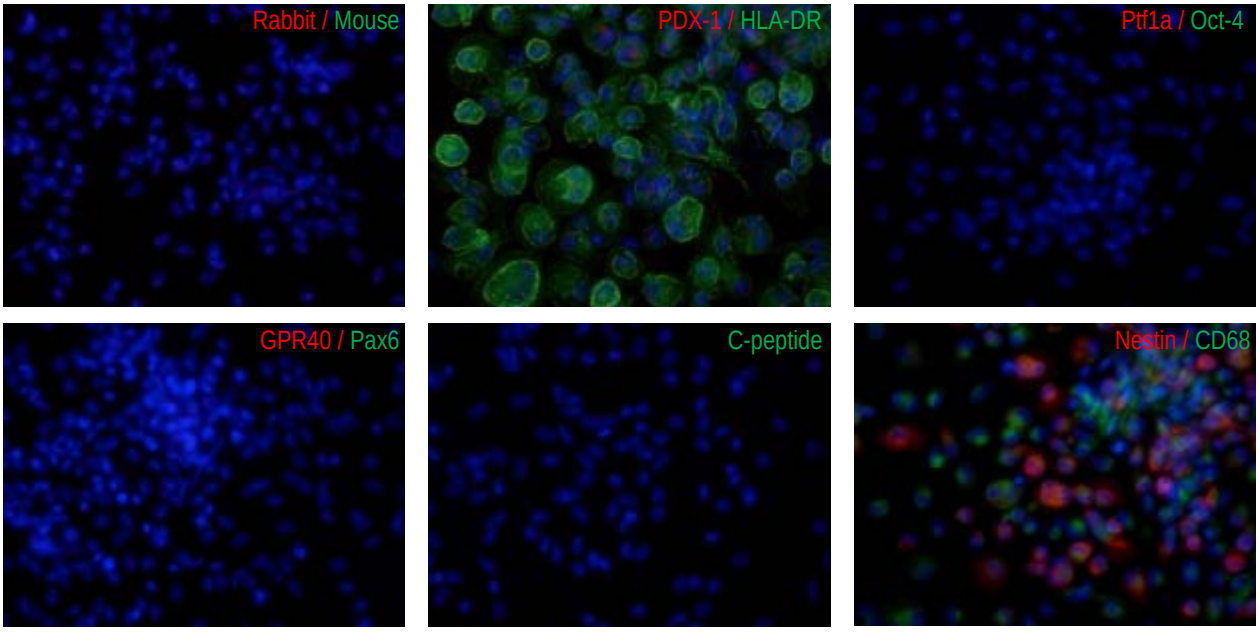
Figure 3.32 Differentiation of PB-IPCs using Zhao's protocol.

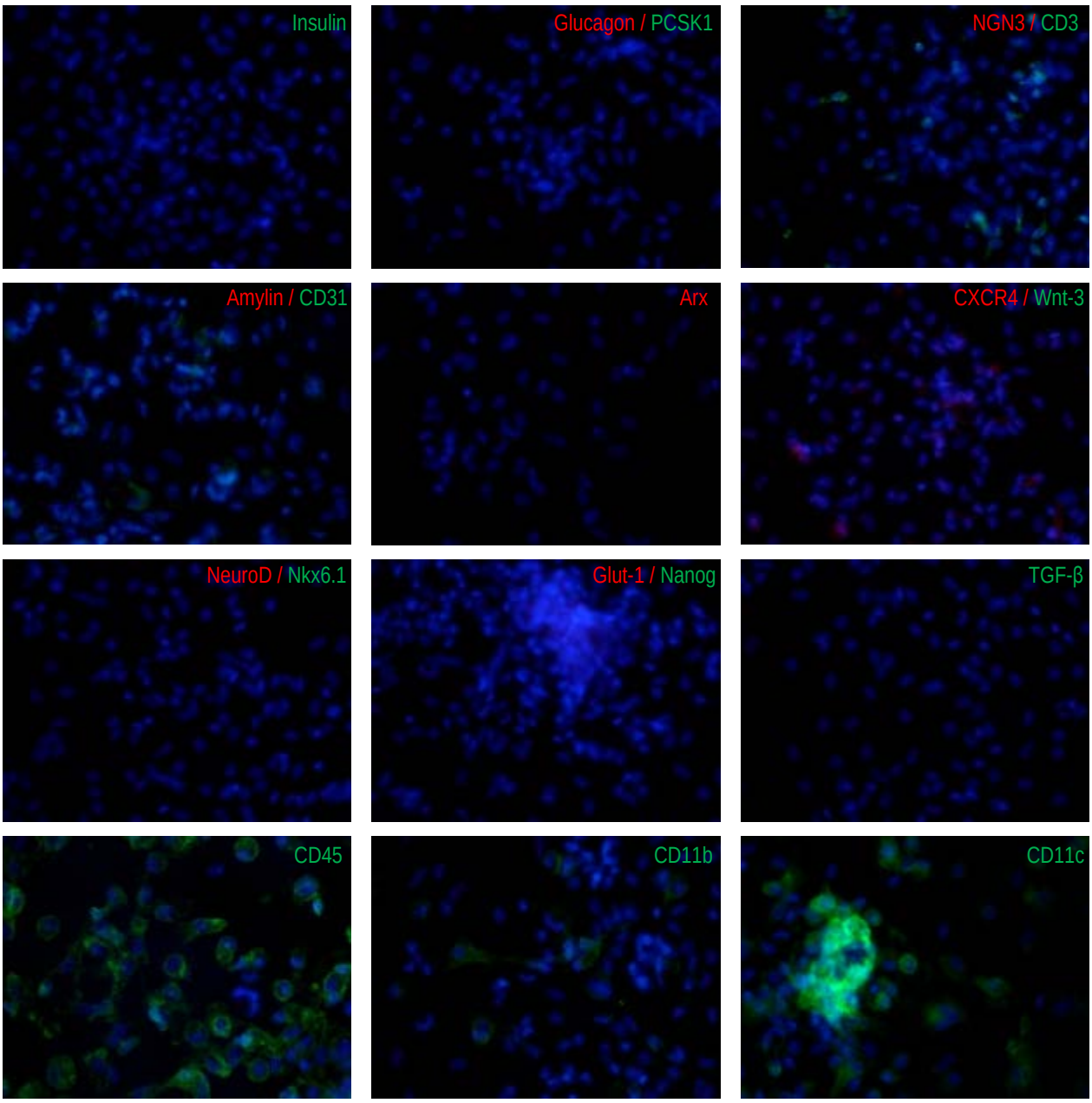
PB-IPCs were cultured for 1 week in full RPMI media containing 7% FBS in hydrophobic dishes, followed by culture for 1 week in DMEM medium containing 10 nM Ex4, 10 ng/mL GM-CSF, 25 mM glucose, 7% FBS, and 1% PSG (n=2). Cells were stained for the expression of various cell markers. Immunoreactivity was detected with a donkey anti-rabbit, rabbit anti-goat, and goat anti-guinea pig antibodies (red) and with a donkey anti-mouse antibody (green). Cell nuclei were stained blue with DAPI. Images were taken at 200x magnification. The images are presented so that the staining obtained with each IgG control immediately precedes stainings with antibodies of the same host species.

3.8.2 GLP-1 alone is not able to differentiate PB-IPCs towards the pancreatic cell lineage

In the next trial PB-IPCs from 2 different donors were cultured for 1 week in full RPMI media containing 7% FBS in hydrophobic dishes, followed by culture for 1 week in the same buffer containing 100 nM GLP-1. GLP-1 induces pancreatic differentiation of Nestin-positive primate embryonic stem cells, as seen by increases in insulin, PDX-1, Glut-2, and NGN3 expression (Yue *et al.* 2006). Here, the inclusion of GLP-1 was trialled to determine if pancreatic differentiation of PB-IPCs could also be induced.

The phenotype of the cells resulting from the addition of GLP-1 was very similar to that induced by Zhao's protocol in that similar numbers of cells expressed PDX-1, Nestin, CD3, CD11c, CD14, CD68, HLA-DR and CD45 (Figure 3.33). There was a decrease in the number of cells expressing CXCR4, CD31, FOXP3 and CD11b, compared to cells cultured in the control medium (Figure 3.31). The cells did not express a number of key markers of pancreatic cells and their progenitors, including NeuroD, Wnt-3, Nkx6.1, NGN3, MafA, Pax6, Arx, GIPR, Ptf1a, Glut-1, GPR40, SOX-17, amylin, PCSK1, insulin, C-peptide, and glucagon. They did not express the stem cell markers Oct-4 and Nanog, or the T cell marker CD4 (Figure 3.33). A summary of these findings is shown in Table 3.2.




Insulin
Glucagon / PCSK1
NGN3 / CD3
Amylin / CD31
Arx
CXCR4 / Wnt-3
NeuroD / Nkx6.1
Glut-1 / Nanog
TGF-β
CD45
CD11b
CD11c

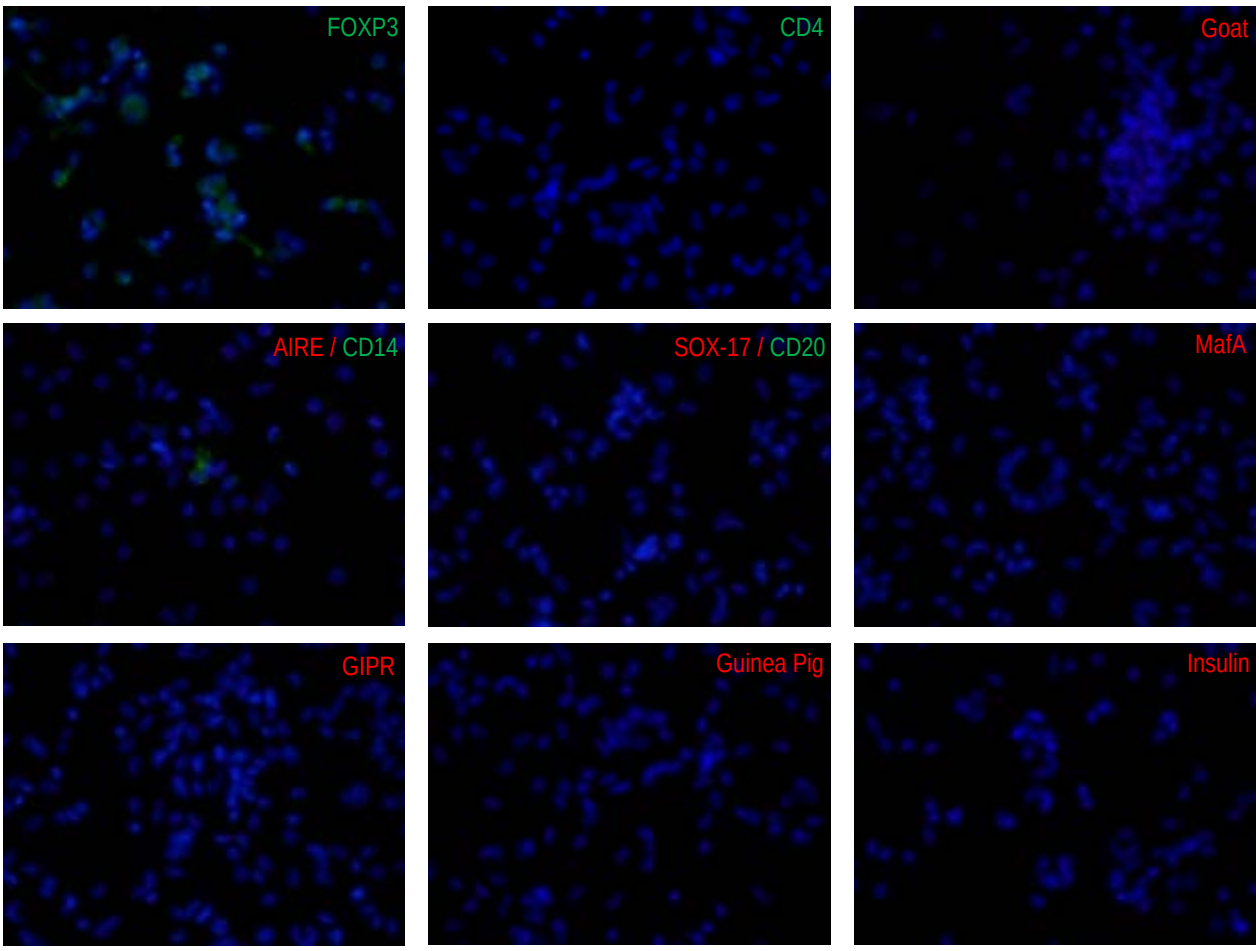


Figure 3.33 Differentiation of PB-IPCs with GLP-1.

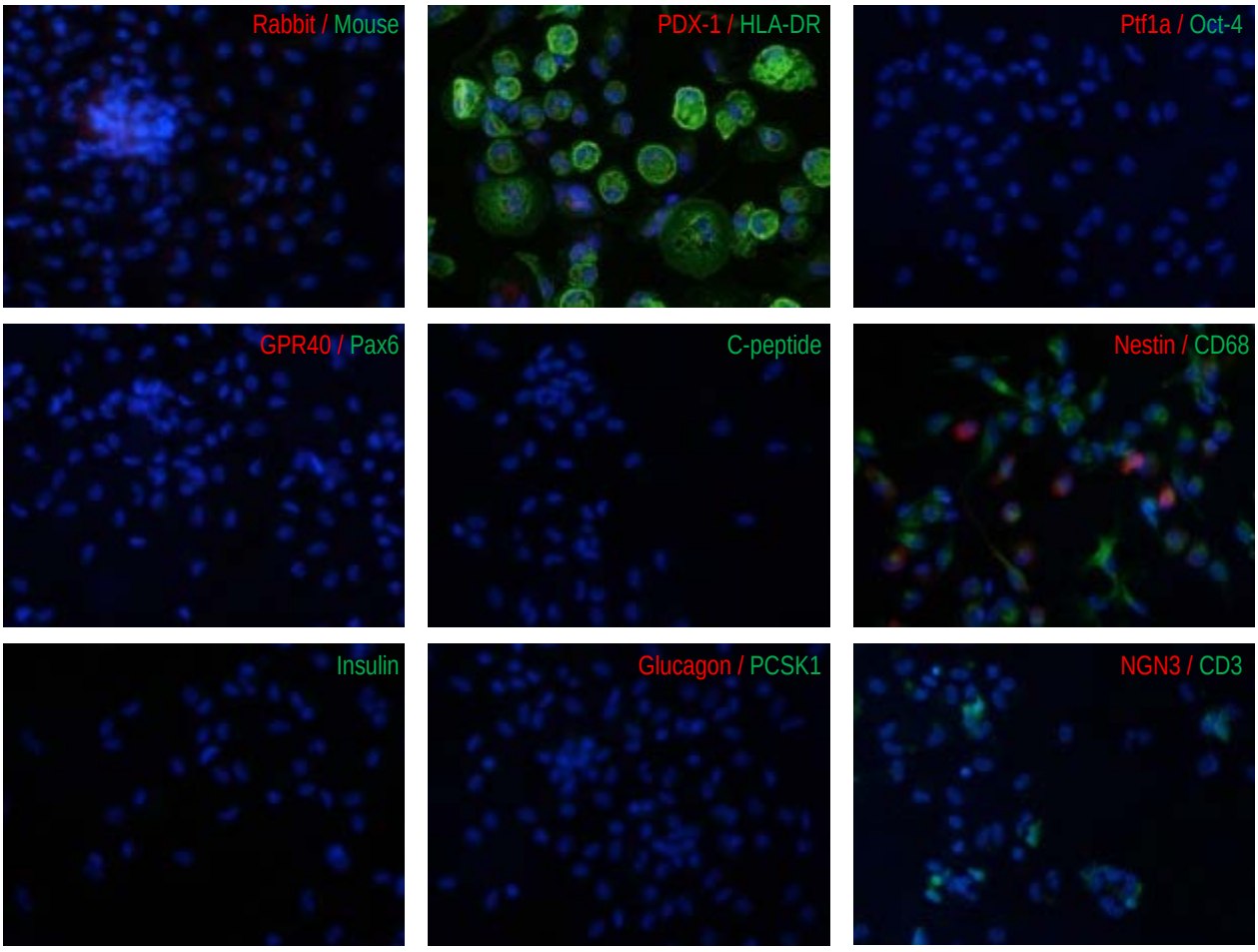
PB-IPCs were cultured for 1 week in full RPMI media containing 7% FBS, followed by 1 week in the same medium containing 100 nM GLP-1 (n=2). Cells were stained for the expression of various cell markers. Immunoreactivity was detected with a donkey anti-rabbit, rabbit anti-goat, and goat anti-guinea pig antibodies (red) and with a donkey anti-mouse antibody (green). Cell nuclei were stained blue with DAPI. Images were taken at 200x magnification. The images are presented so that the staining obtained with each IgG control immediately precedes stainings with antibodies of the same host species.

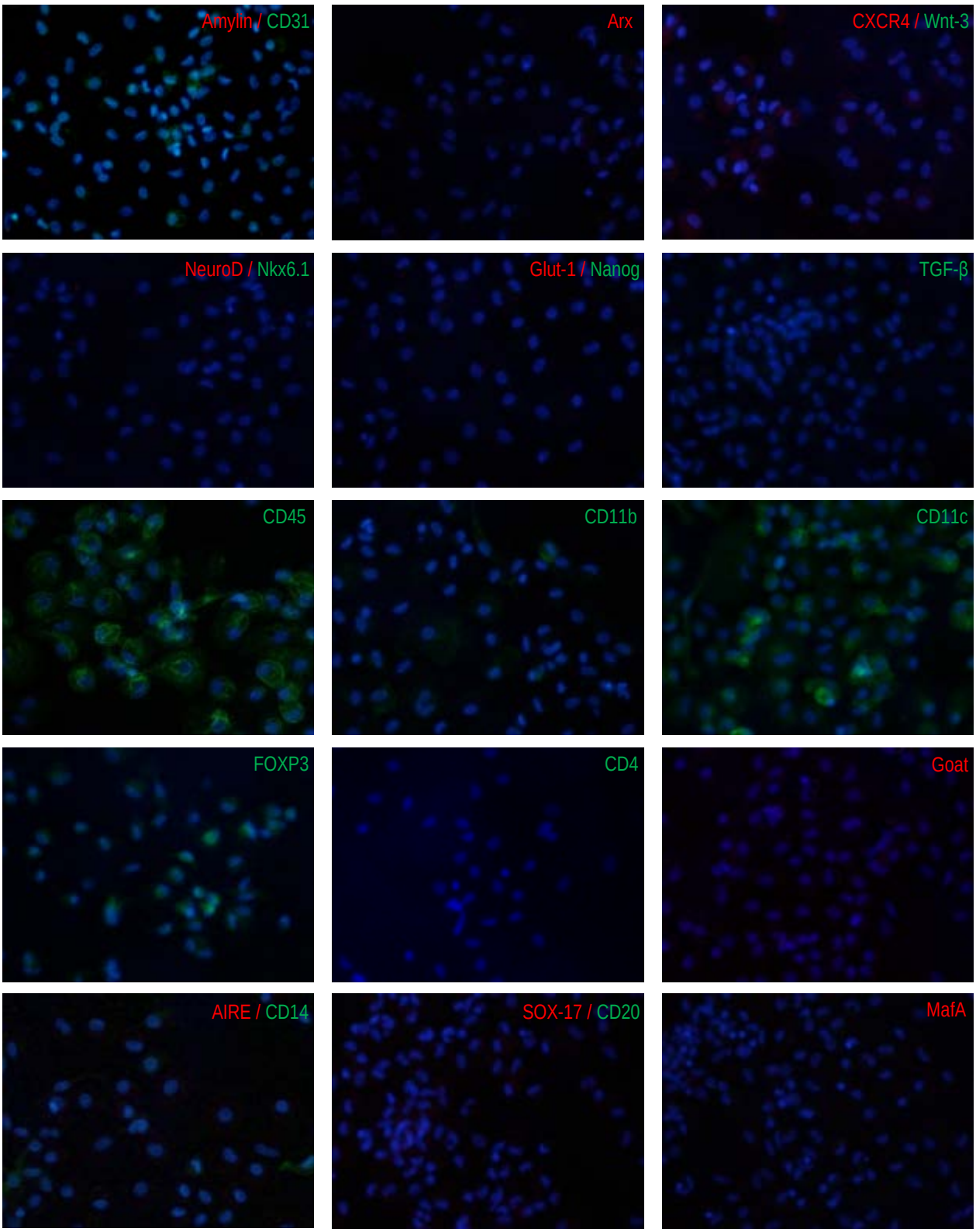
3.8.3 A combination of nicotinamide, GLP-1, and Ex4 is not able to differentiate PB-IPCs towards the pancreatic cell lineage

In the next trial PB-IPCs from 2 different donors were cultured for 1 week in full RPMI media containing 7% FBS in hydrophobic dishes, followed by culture for 1 week in a pancreatic differentiation medium consisting of full RPMI media containing 7% FBS, 10 mM nicotinamide, 100 nM GLP-1, and 10 nM Ex4 (N,G,E). These differentiation agents were chosen in combination as they are common to pancreatic differentiation pathways (Gao *et al.* 2008; Yang *et al.* 2010), and GLP-1 alone was ineffective (Figure 3.33). Nicotinamide, GLP-1, and Ex4 are often used as maturation agents to help promote differentiation towards the pancreatic

endocrine cell lineage (Gao *et al.* 2008; Yang *et al.* 2010). Therefore these agents were included to induce the pancreatic differentiation of the PB-IPCs.

The phenotype of the cells resulting from the N,G,E differentiation protocol was very similar to that induced by Zhao's protocol. Similar numbers of cells expressed PDX-1, CD31, FOXP3, CD4, CD11c, CD14, CD68, HLA-DR, and CD45 (Figure 3.34). A decreased number of cells expressed CXCR4, Nestin and CD11b (Figure 3.34) compared to cells cultured in the absence of the differentiation factors (Figure 3.9 and Figure 3.31). The N,G,E treated cells did not express AIRE, unlike the control cells, and there was an increase in the number of CD3 cells (compare Figure 3.9, Figure 3.31, and Figure 3.34). The cells remained negative for the expression of a number of key markers of pancreatic cells and their progenitors including NeuroD, Wnt-3, Nkx6.1, NGN3, MafA, Pax6, Arx, GIPR, Ptf1a, Glut-1, GPR40, SOX-17, amylin, PCSK1, insulin, C-peptide, and glucagon, and for the stem cell markers Oct-4 and Nanog (Figure 3.34). A summary of these findings is shown in Table 3.2.




Amylin / CD31
Arx
CXCR4 / Wnt-3
NeuroD / Nkx6.1
Glut-1 / Nanog
TGF-β
CD45
CD11b
CD11c
FOXP3
CD4
Goat
AIRE / CD14
SOX-17 / CD20
MafA

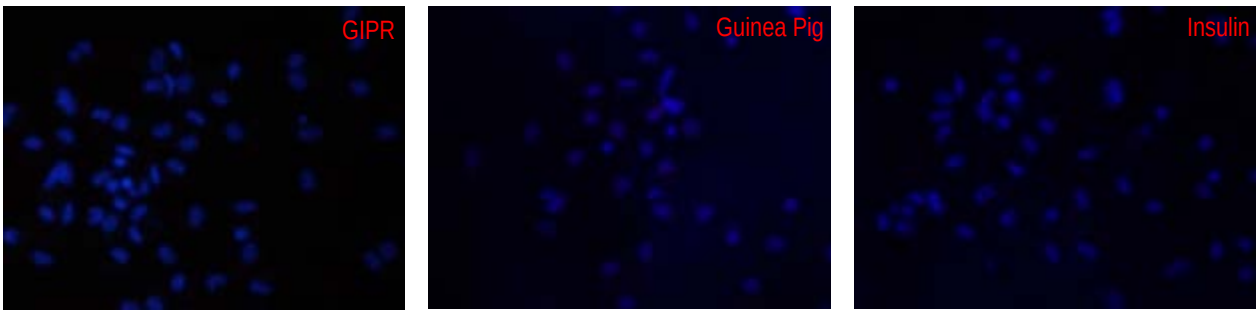
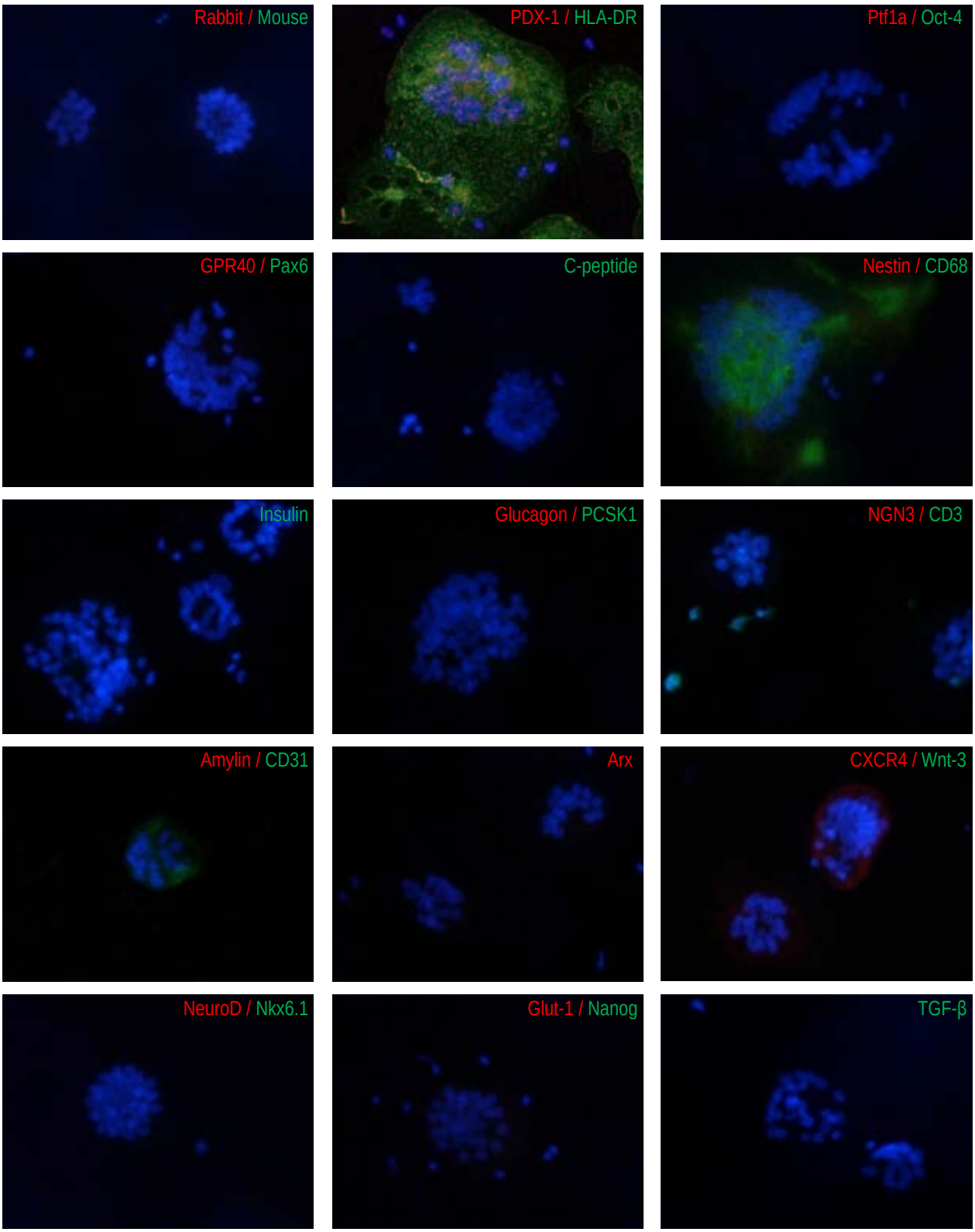


Figure 3.34 Differentiation of PB-IPCs using a combination of nicotinamide, GLP-1, and Ex4.

PB-IPCs were cultured for 1 week in full RPMI media containing 7% FBS in hydrophobic dishes, followed by culture for 1 week in the same medium containing 10 mM nicotinamide, 100 nM GLP-1, and 10 nM Ex4 (N,G,E) (n=2). Cells were stained for the expression of various cell markers. Immunoreactivity was detected with a donkey anti-rabbit, rabbit anti-goat, and goat anti-guinea pig antibodies (red) and with a donkey anti-mouse antibody (green). Cell nuclei were stained blue with DAPI. Images were taken at 200x magnification. The images are presented so that the staining obtained with each IgG control immediately precedes stainings with antibodies of the same host species.

3.8.4 Preventing the senescence of PB-IPCs with ILV prior to differentiation does not alter their plasticity

Earlier experiments showed that ILV prevented the senescence of cultured PB-IPCs (Figure 3.24). Therefore PB-IPCs from 2 different donors were exposed to ILV prior to pancreatic differentiation according to Zhao's protocol to discover whether ILV would promote their responsiveness to differentiating factors. PB-IPCs were cultured for 1 week in full RPMI media containing 7% FBS, and 100 nM ILV in hydrophobic dishes, followed by culture for 1 week in full RPMI media containing 7% FBS (control media) (Figure 3.35) or in DMEM medium containing 10 nM Ex4, 10 ng/mL GM-CSF, 25 mM glucose, 7% FBS and 1% PSG (Figure 3.36). The cells were then analysed by immunocytochemistry for a range of pancreatic, blood, and stem cell markers. There was no change in the number of cells expressing PDX-1, CXCR4, CD31, AIRE, and CD11c, and strong expression of CD68, HLA-DR and CD45 was retained (Figure 3.36), compared to cells cultured in control media following treatment with ILV (Figure 3.35). However, no cells expressed CD4 or CD14, and there was an increase in the number of cells expressing Nestin, FOXP3, and CD11b positive cells (Figure 3.36), compared to cells cultured in control media following treatment with ILV (Figure 3.35). The cells remained clustered following ILV treatment (Figure 3.36 and Figure 3.35). Expression of key markers of pancreatic cells and their progenitors were missing, including NeuroD, Wnt-3, Nkx6.1, NGN3, MafA, Pax6, Arx, GIPR, Ptf1a, Glut-1, GPR40, SOX-17, amylin, PCSK1, insulin, C-peptide, and glucagon, and the stem cell markers Oct-4 and Nanog, in both treatments (compare Figure 3.35 and Figure 3.36). A low number of contaminating CD3 T cells was also present in both conditions (Figure 3.35 and Figure 3.36). A summary of these findings is shown in Table 3.2.


Rabbit / Mouse
PDX-1 / HLA-DR
Ptf1a / Oct-4
GPR40 / Pax6
C-peptide
Nestin / CD68
Insulin
Glucagon / PCSK1
NGN3 / CD3
Amylin / CD31
Arx
CXCR4 / Wnt-3
NeuroD / Nkx6.1
Glut-1 / Nanog
TGF-β

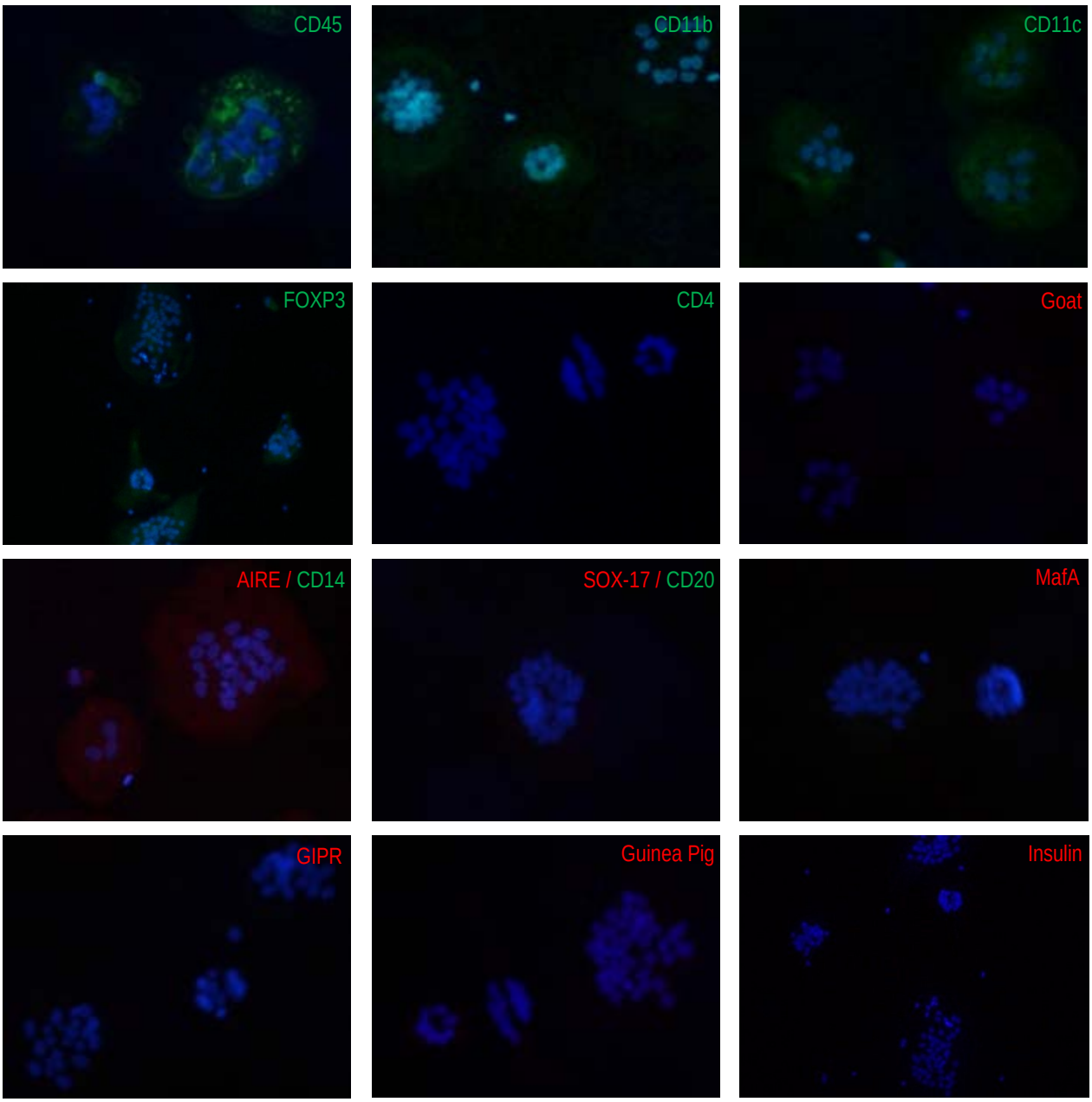
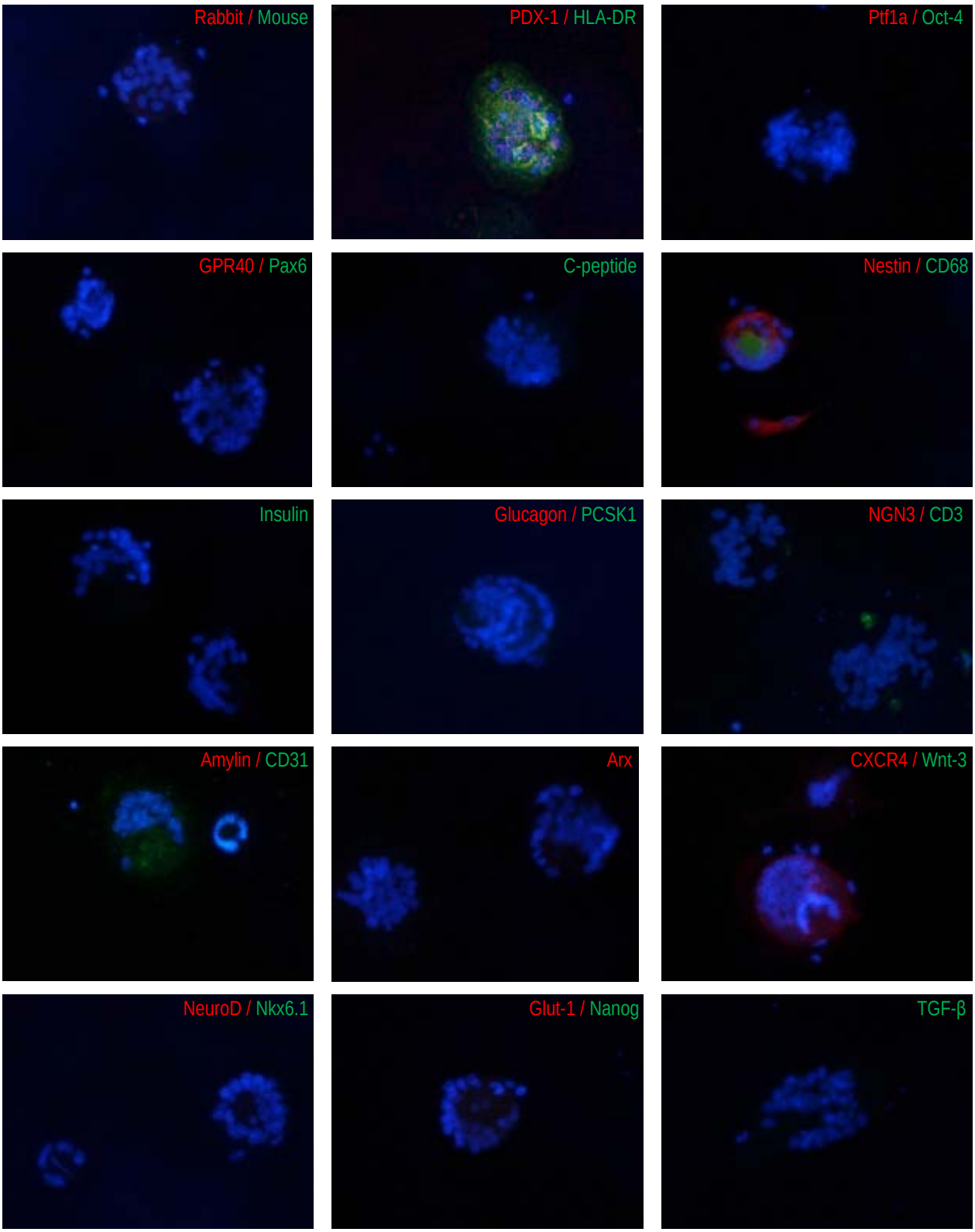


Figure 3.35 Pretreatment of PB-IPCs with (-)-indolactam V prior to culture in control media.

PB-IPCs were cultured for 1 week in full RPMI media containing 7% FBS, and 100 nM ILV in hydrophobic dishes, followed by culture for 1 week in the same media without ILV (n=-2). Cells were stained for the expression of various cell markers. Immunoreactivity was detected with a donkey anti-rabbit, rabbit anti-goat, and goat anti-guinea pig antibodies (red) and with a donkey anti-mouse antibody (green). Cell nuclei were stained blue with DAPI. Images were taken at 200x magnification. The images are presented so that the staining obtained with each IgG control immediately precedes stainings with antibodies of the same host species.


Rabbit / Mouse
PDX-1 / HLA-DR
Ptf1a / Oct-4
GPR40 / Pax6
C-peptide
Nestin / CD68
Insulin
Glucagon / PCSK1
NGN3 / CD3
Amylin / CD31
Arx
CXCR4 / Wnt-3
NeuroD / Nkx6.1
Glut-1 / Nanog
TGF-β

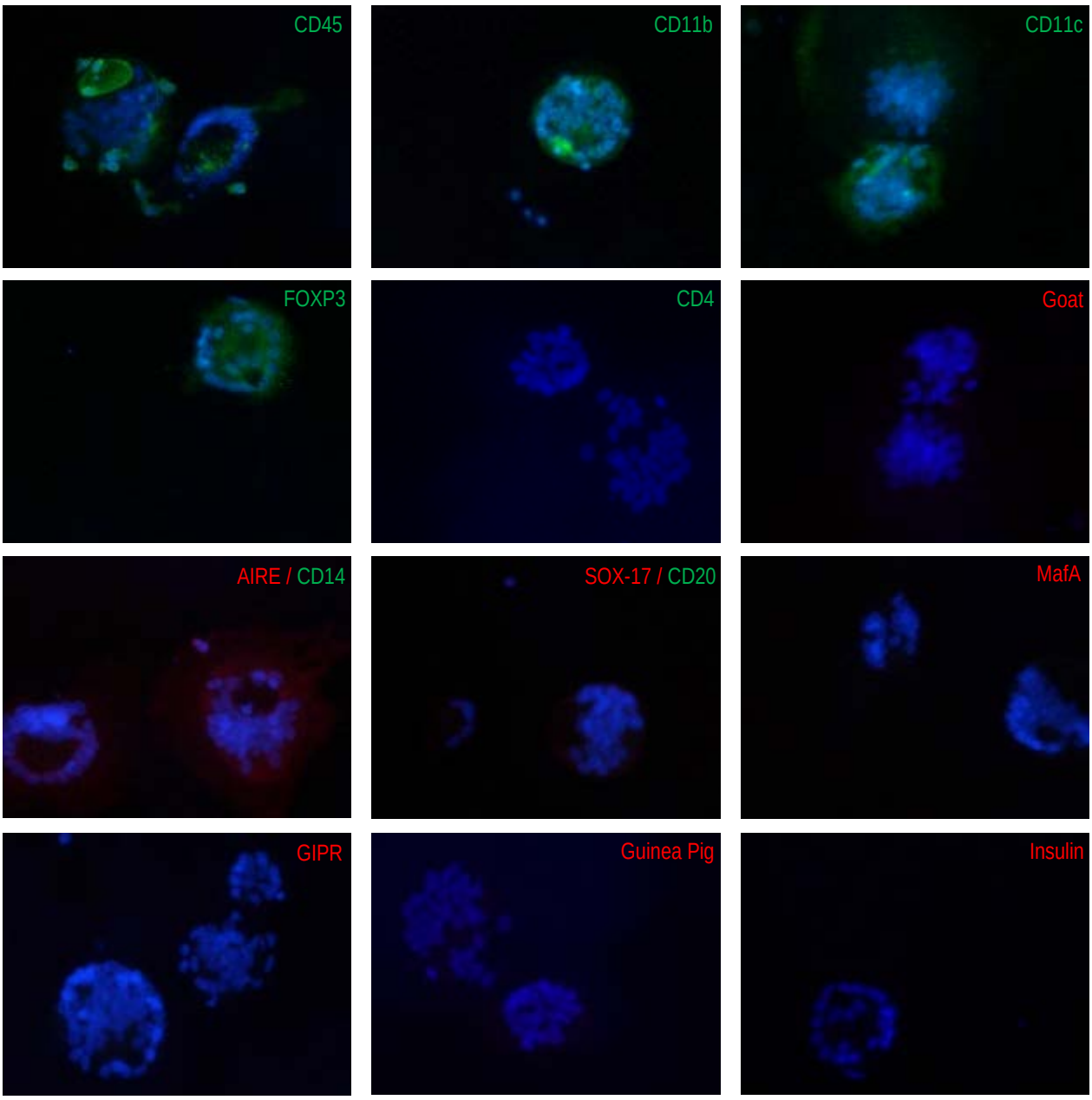


Figure 3.36 Pretreatment of PB-IPCs with (-)-indolactam V prior to differentiation using Zhao's protocol.

PB-IPCs were cultured for 1 week in full RPMI media containing 7% FBS, and 100 nM ILV in hydrophobic dishes, followed by culture for 1 week in DMEM medium containing 10 nM Ex4, 10 ng/mL GM-CSF, 25 mM glucose, 7% FBS and 1% PSG (n=2). Cells were stained for the expression of various cell markers. Immunoreactivity was detected with a donkey anti-rabbit, rabbit anti-goat, and goat anti-guinea pig antibodies (red) and with a donkey anti-mouse antibody (green). Cell nuclei were stained blue with DAPI. Images were taken at 200x magnification. The images are presented so that the staining obtained with each IgG control immediately precedes stainings with antibodies of the same host species.

Table 3.2 Summary of the phenotypes of differentiated PB-IPCs

Cell Type	Marker	Control Control	Control Zhao	Control G	Control N,G,E	Indo V Control	Indo V Zhao	WEEK 1 WEEK 2
Pancreatic	PDX-1	x x	x x	x x	x x	x x	x x	
	CXCR4	x x	x x	x	x	x x	x x	
	SOX-17							
	Wnt-3							
	Nkx6.1							
	NGN3							
	MafA							
	Pax6							
	Arx							
	GIPR							
	Ptf1a							
	Glut-1							
	GPR40							
	Amylin							
	PCSK1							
	Insulin							
	C-peptide							
	Glucagon							
Stem Cell	Nestin	x x x	x x x	x x x	x x x		x x x	
	Oct-4							
	Nanog							
Multi-Lineage	CD31	x	x	x	x	x x	x x	
Blood Cell	AIRE	x x	x			x	x	
	FOXP3	x x x	x x x	x x	x x	x	x x x	
	CD20							
	CD3	x x	x x	x x	x x	x	x x	
	CD4							
	CD11b	x x	x x	x x	x	x	x x	
	CD11c	x x x	x x	x x x	x x x	x	x x	
	CD14	x	x	x	x			
	CD68	x x x	x x x	x x x	x x x	x x x	x x x	
	HLA-DR	x x x	x x x	x x x	x x x	x x x	x x x	
	CD45	x x x	x x x	x x x	x x x	x x x	x x x	
Growth Factor	TGF-β							

0	0.1-20	21-40	41-60	61-80	81-100	% Positive

x	x x	x x x	Intensity of staining – weak/moderate/strong

3.9 Protein transduction of PB-IPCs with recombinant forms of PDX-1 and Pax4 does not induce their differentiation towards the pancreatic lineage

PDX-1 and Pax4 proteins have been used separately to induce pancreatic differentiation (Liew *et al.* 2008; Delisle *et al.* 2009). Previous research by other groups has shown that PDX-1 treatment causes transdifferentiation of rat epithelial stem-like cells into insulin expressing cells (Delisle *et al.* 2009). Another group showed transfection of ESCs with Pax4 causes proinsulin expression (Liew *et al.* 2008). The pancreatic transcription factor PDX-1 is naturally cell-permeable (Noguchi *et al.* 2003). PDX-1 contains an Antennapedia-like protein transduction domain (Noguchi *et al.* 2003). Here the aim was to determine whether protein transduction of PB-IPCs with PDX-1 and Pax4 would direct the differentiation of PB-IPCs towards a pancreatic cell phenotype. Pax4 is not naturally cell-permeable, hence it had to be delivered using the protein delivery agent Pro-DeliverIN. Pro-DeliverIN successfully delivered the red fluorescent control protein R-Phycoerythrin to attached PB-IPCs (Figure 3.37). PB-IPCs from 1 donor were cultured for 7 days in full RPMI media containing 7% FBS, with 1 μM additions of PDX-1 or Pax4 being made on days 0, 3, and 6. Pro-DeliverIN (1 μL/μg of protein) was added together with Pax4. The cells were fixed on day 7 and phenotyped for expression of a panel of cell markers (Figure 3.39 and Figure 3.40). The PDX-1 and Pax4 proteins were not fluorescently tagged; hence the end point of this study was characterization of pancreatic differentiation by a variety of pancreatic markers including PDX-1 (Figure 3.39 and Figure 3.40).

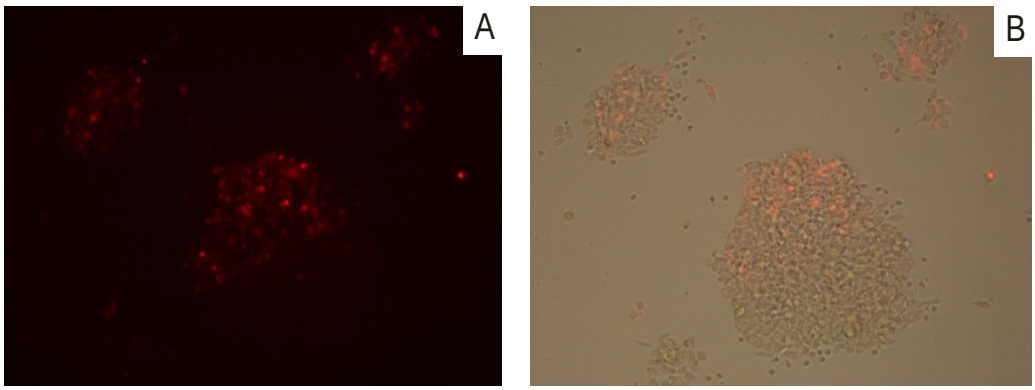


Figure 3.37 Pro-DeliverIN delivers R-Phycoerythrin into PB-IPCs.

PB-IPCs ($5x10^5$ in 200 μL) were incubated for 7 days with full RPMI media containing 7% FBS, with 1 μM additions of R-Phycoerythrin and 1 μL/μg of protein of Pro-DeliverIN being made on days 0, 3, and 6 (n=1). Cells visualized at day 7 by A) fluorescence microscopy, and B) combined fluorescence and phase contrast microscopy. Images were taken at 200x magnification.

Immunocytochemistry analysis showed the PB-IPCs did not differentiate towards the pancreatic lineage after transduction of PDX-1 (Figure 3.39) and Pax4 (Figure 3.40) proteins. Cells cultured in the presence or absence of PDX-1 protein surprisingly showed similar levels of staining with the anti-PDX-1 antibody (compare Figure 3.38 and Figure 3.39). Cells transduced with Pax4 expressed reduced levels of PDX-1 (Figure 3.40). All cell populations expressed similar levels of CXCR4, fibroblast factor

(prolyl 4-hydroxylase or disulphide-isomerase), and CD45 (Figure 3.38, Figure 3.39, and Figure 3.40). Treatment with PDX-1 led to most of the cells very weakly expressing CD31, while with Pax4 protein treatment only half the cells expressed this marker (Figure 3.39 and Figure 3.40). The control cells showed stronger expression of CD31 (compare Figure 3.7, Figure 3.39, and Figure 3.40). The monocytic marker CD14 was expressed by several cells, irrespective of the culture media; however, the greatest level of CD14 expression was seen with Pax4 treatment (Figure 3.40). In contrast, PDX-1 treatment increased the number of cells expressing CD68, whereas Pax4 reduced the number of cells expressing CD68, compared with cells cultured in control media (Figure 3.38, Figure 3.39, and Figure 3.40). None of the other markers tested including Nkx6.1, NeuroD, GPR40, NGN3, Ptf1a, insulin, glucagon, and CD309 (VEGFR-2) were expressed following treatment with PDX-1 or Pax4. A summary of the cell markers expressed by cells treated with PDX-1 and Pax4 is presented in Table 3.3.

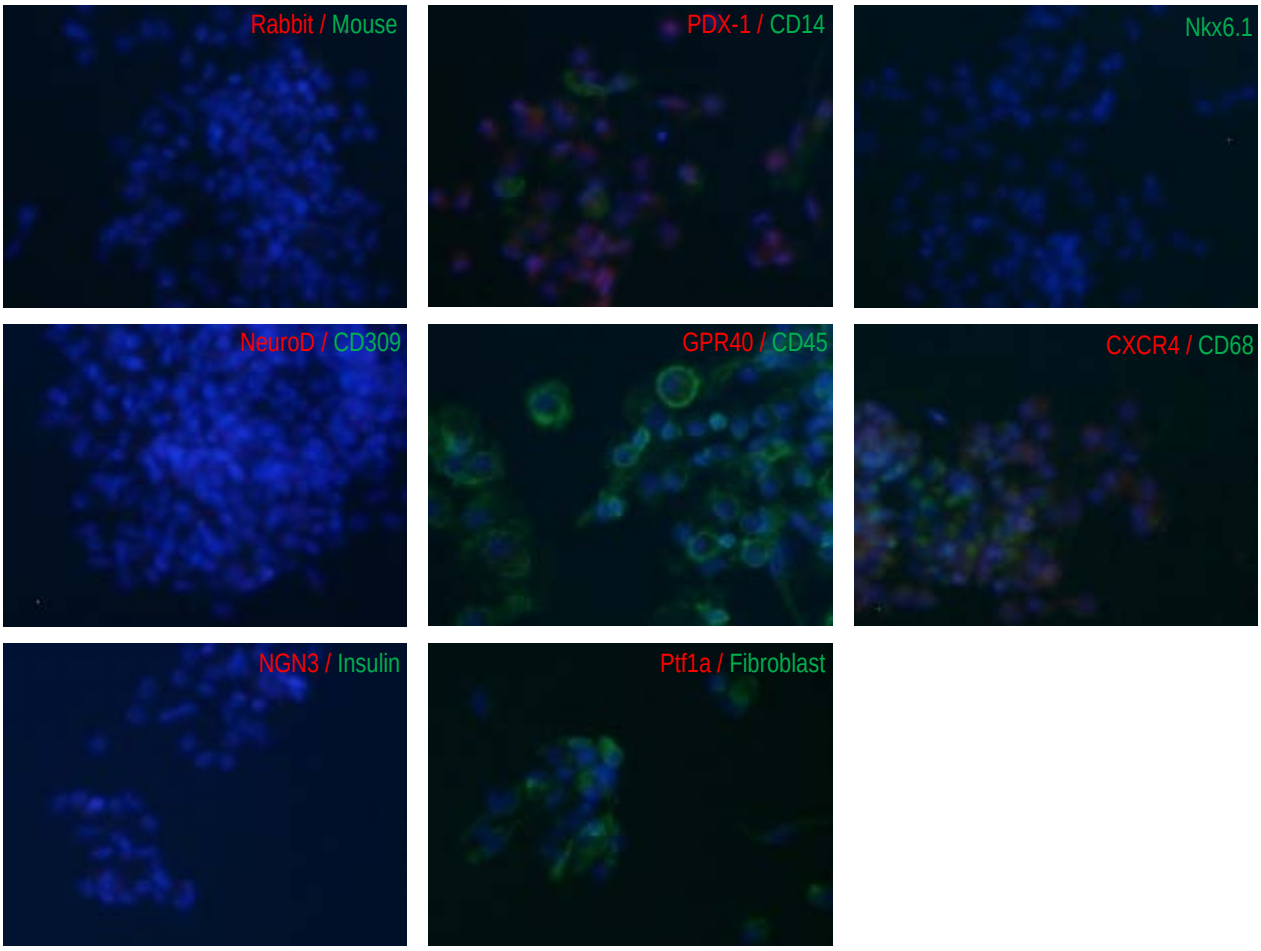


Figure 3.38 Phenotype of control PB-IPCs cultured for 1 week.

PB-IPCs (5 x 10^5 in 200 µL) were cultured for 1 week in full RPMI media containing 7% FBS, and stained with antibodies against various cell markers (n=1). Immunoreactivity was detected with a donkey anti-rabbit antibody (red) and with a donkey anti-mouse antibody (green). Cell nuclei were stained blue with DAPI. Images were taken at 200x magnification. The images are presented so that the staining obtained with each IgG control immediately precedes stainings with antibodies of the same host species.

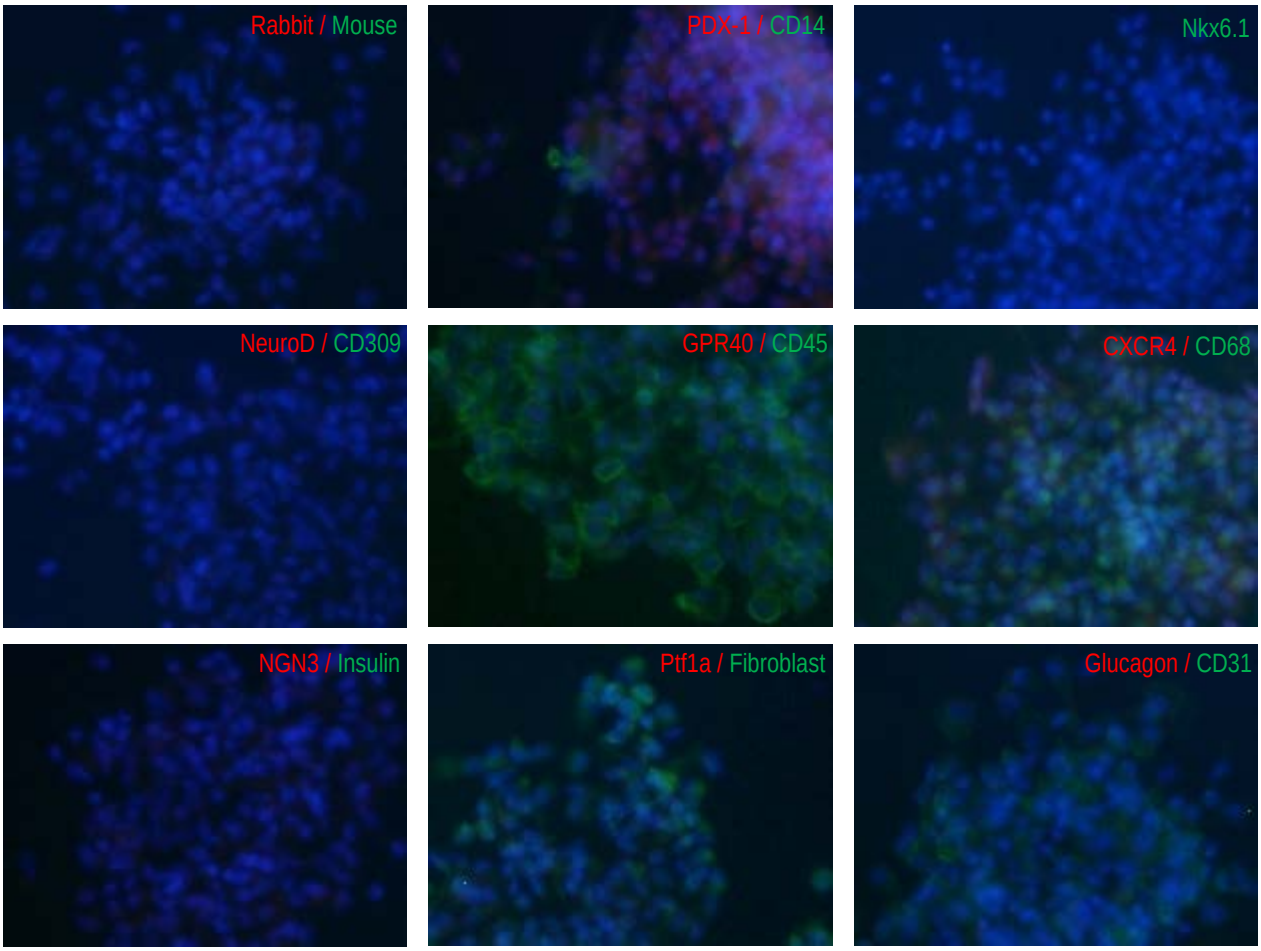


Figure 3.39 Phenotype of PDX-1-treated PB-IPCs.

PB-IPCs (5 x 10^5 in 200 µL) were cultured for 1 week in full RPMI media containing 7% FBS with 1 µM additions of PDX-1 being made on days 0, 3, and 6 (n=1). Cells were stained with antibodies against various cell markers, and immunoreactivity was detected with a donkey anti-rabbit antibody (red) and with a donkey anti-mouse antibody (green). Cell nuclei were stained blue with DAPI. Images were taken at 200x magnification. The images are presented so that the staining obtained with each IgG control immediately precedes stainings with antibodies of the same host species.

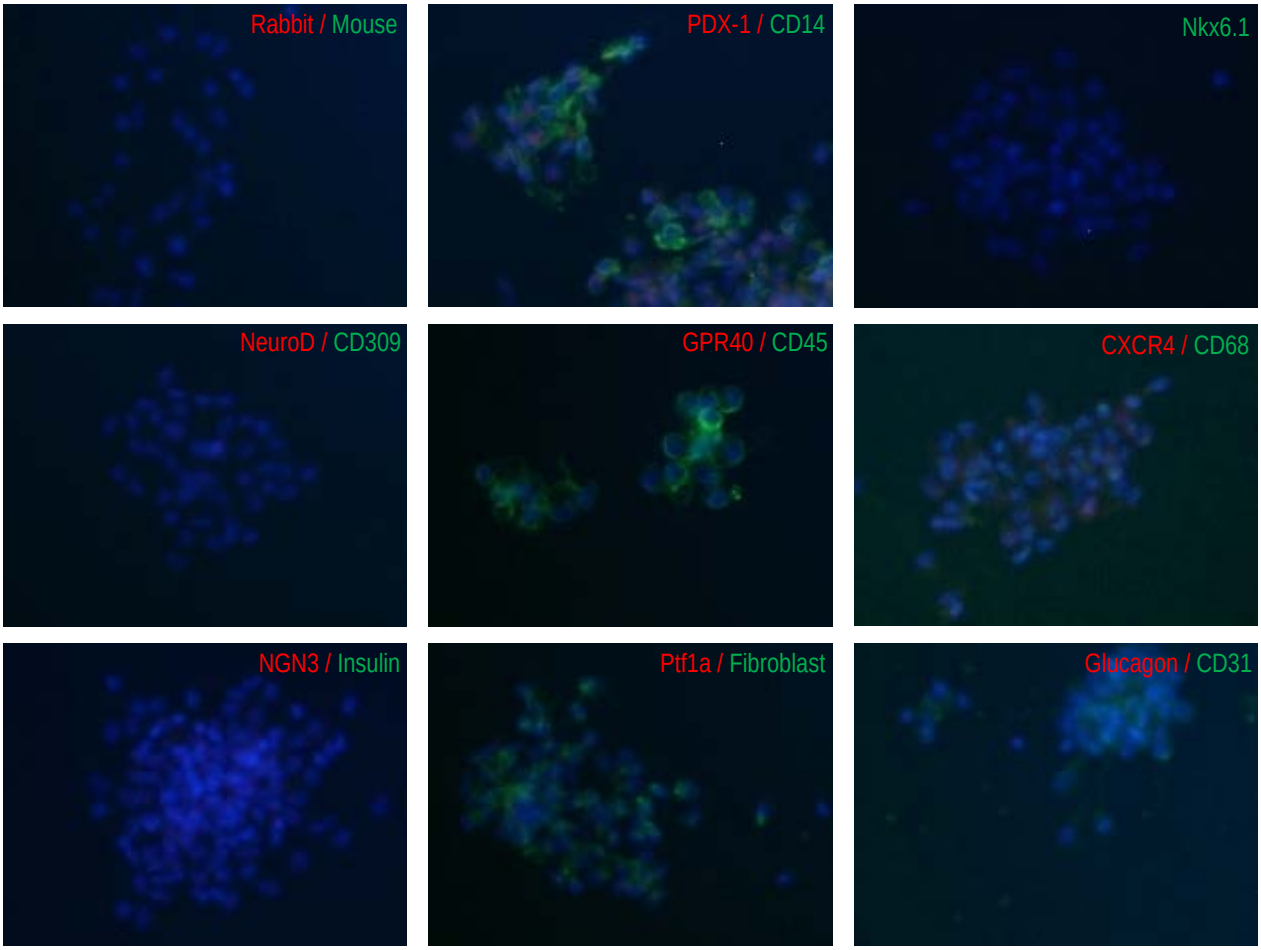


Figure 3.40 Phenotype of Pax4-treated PB-IPCs.

PB-IPCs (5×10^5 in 200 µL) were cultured for 1 week in full RPMI media containing 7% FBS with 1 µM additions of Pax4 being made on days 0, 3, and 6, together with 1 µL/µg protein of Pro-DeliverIN (n=1). Cells were stained with antibodies against various cell markers, and immunoreactivity was detected with a donkey anti-rabbit antibody (red) and with a donkey anti-mouse antibody (green). Cell nuclei were stained blue with DAPI. Images were taken at 200x magnification. The images are presented so that the staining obtained with each IgG control immediately precedes stainings with antibodies of the same host species.

Table 3.3 Summary of the phenotype of PB-IPCs transduced with PDX-1 and Pax4 proteins

		Control	PDX-1	Pax4
Pancreatic	PDX-1	x x	x x	x
	CXCR4	x	x	x
	Nkx6.1			
	NeuroD			
	GPR40			
	Neurogenin3			
	Ptf1a			
	Insulin			
	Glucagon*			
Other lineage	Fibroblast	x x	x x	x x
	CD31*	x x	x	x
	CD309			
Peripheral Blood Cells	CD14	x	x	x x x
	CD68	x x	x x	x
	CD45	x x x	x x x	x x x

						% Positive
0	0.1-20	21-40	41-60	61-80	81-100	

x	x x	x x x	Intensity of staining – weak/moderate/strong

*Note: Expression levels of CD31 and glucagon for the Control cells were obtained from Figure 3.7 (Table 3.1).

3.10 Are PB-IPCs immunosuppressive?

Zhao *et al.* (2012) had reported that CB-SCs with a phenotype similar to PB-IPCs were immunosuppressive and able to convert naive T cells into Tregs (Zhao *et al.* 2012). The finding that PB-IPCs expressed FOXP3 (Figure 3.9, Figure 3.12 and Figure 3.13), suggested that PB-IPCs might have immunosuppressive properties. To test this notion, cultured PB-IPCs and monocytes were cocultured with a combination of freshly isolated autologous and allogeneic PBMCs. Thus, PB-IPCs and monocytes from 2 different donors each were cultured for 1 week in full RPMI media containing 7% FBS in a hydrophobic or tissue culture dish, respectively, and then incubated with the two donor PBMC populations to establish a mixed lymphocyte response (see Figure 3.41 for a diagram of the experimental design). The lymphocytes from the two donors were expected to attack one another causing extensive cell apoptosis. If the PB-IPCs were immunosuppressive then they would be expected to inhibit the mixed lymphocyte response. PB-IPCs and monocytes were omitted from controls i.e. the PBMCs form the two donors were simply mixed and added to untreated culture dishes. Cells in suspension were stained with Annexin-V to detect apoptosis and were phenotyped for the expression of hematopoietic markers.

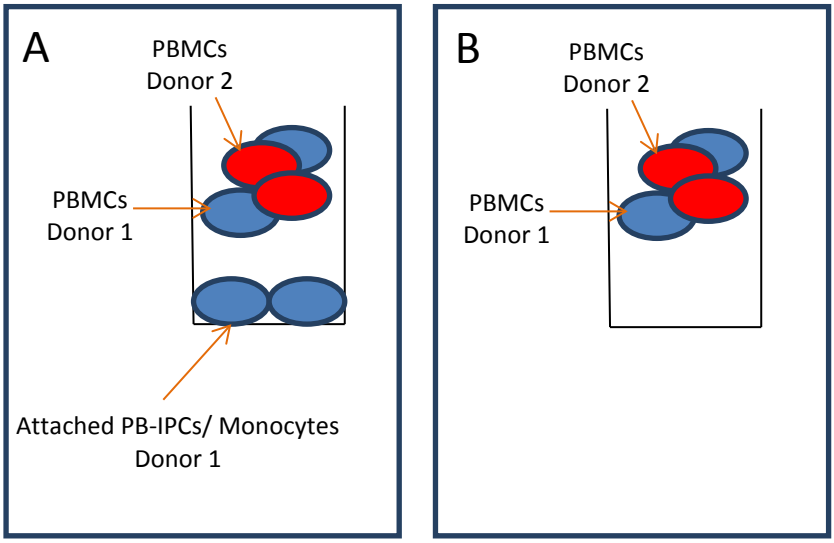


Figure 3.41 Diagram detailing the mixed lymphocyte response experimental design.

PB-IPCs or monocytes (Donor 1) were cultured for 1 week in 96 well tissue culture or hydrophobic dishes, respectively in full RPMI media containing 7% FBS. PBMCs from Donor 1 and Donor 2 were cocultured with (A) or without (B) attached PB-IPCs or monocytes from Donor 1 for up to 120 h in the same media (n=2).

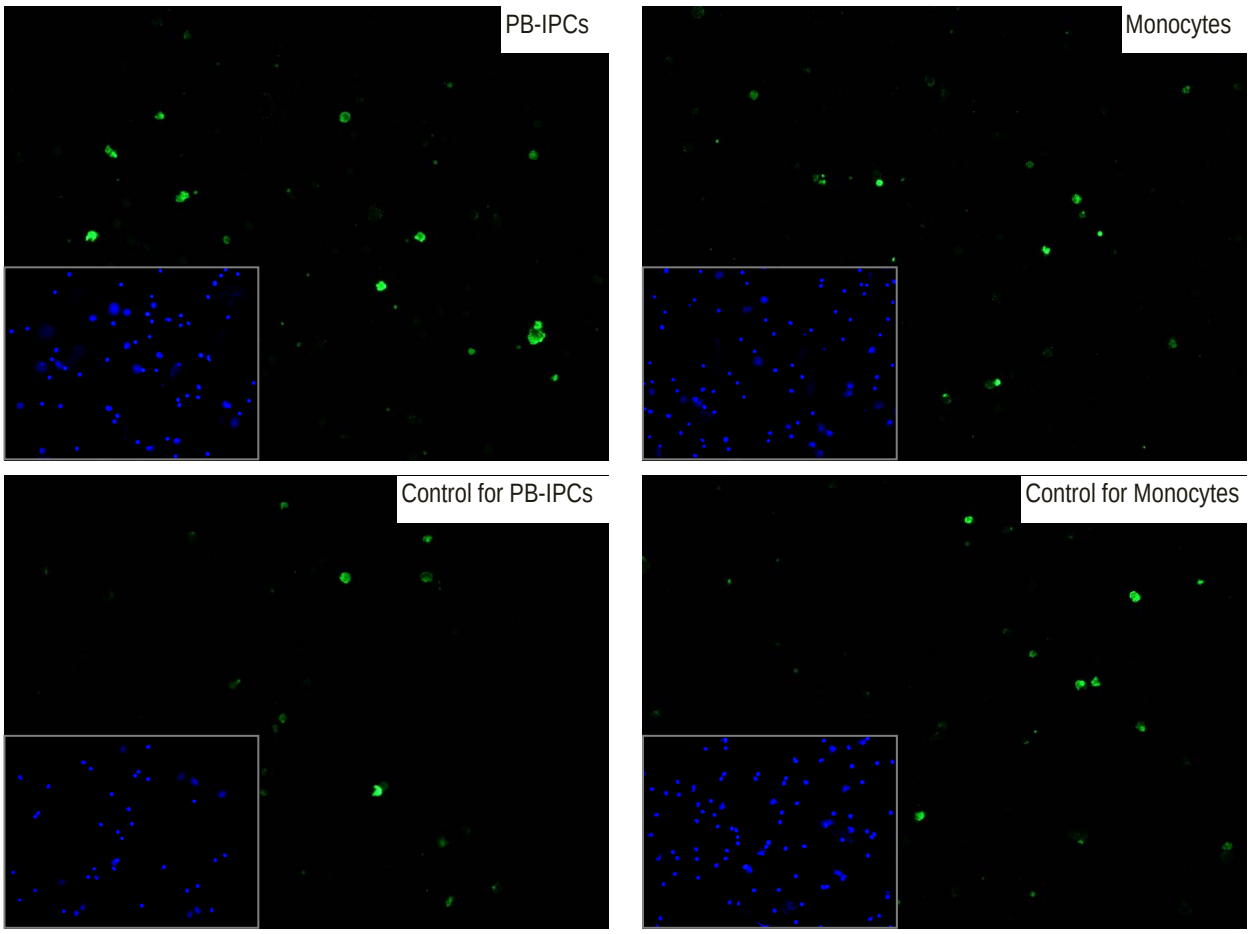


Figure 3.42 PB-IPCs and monocytes do not significantly alter the mixed lymphocyte response at 48 h.

PBMCs from two different donors were overlaid onto PB-IPCs and monocytes that had been cultured for 1 week in full RPMI media containing 7% FBS (n=2). The PB-IPCs and monocytes were omitted from controls. The suspension cells were stained with Annexin-V (green) after 24 h of incubation of the mixed lymphocyte response. Cell nuclei were stained blue with DAPI (inset). Images were taken at 200x magnification; Annexin-V image is displayed 2.4 x larger than DAPI inset.

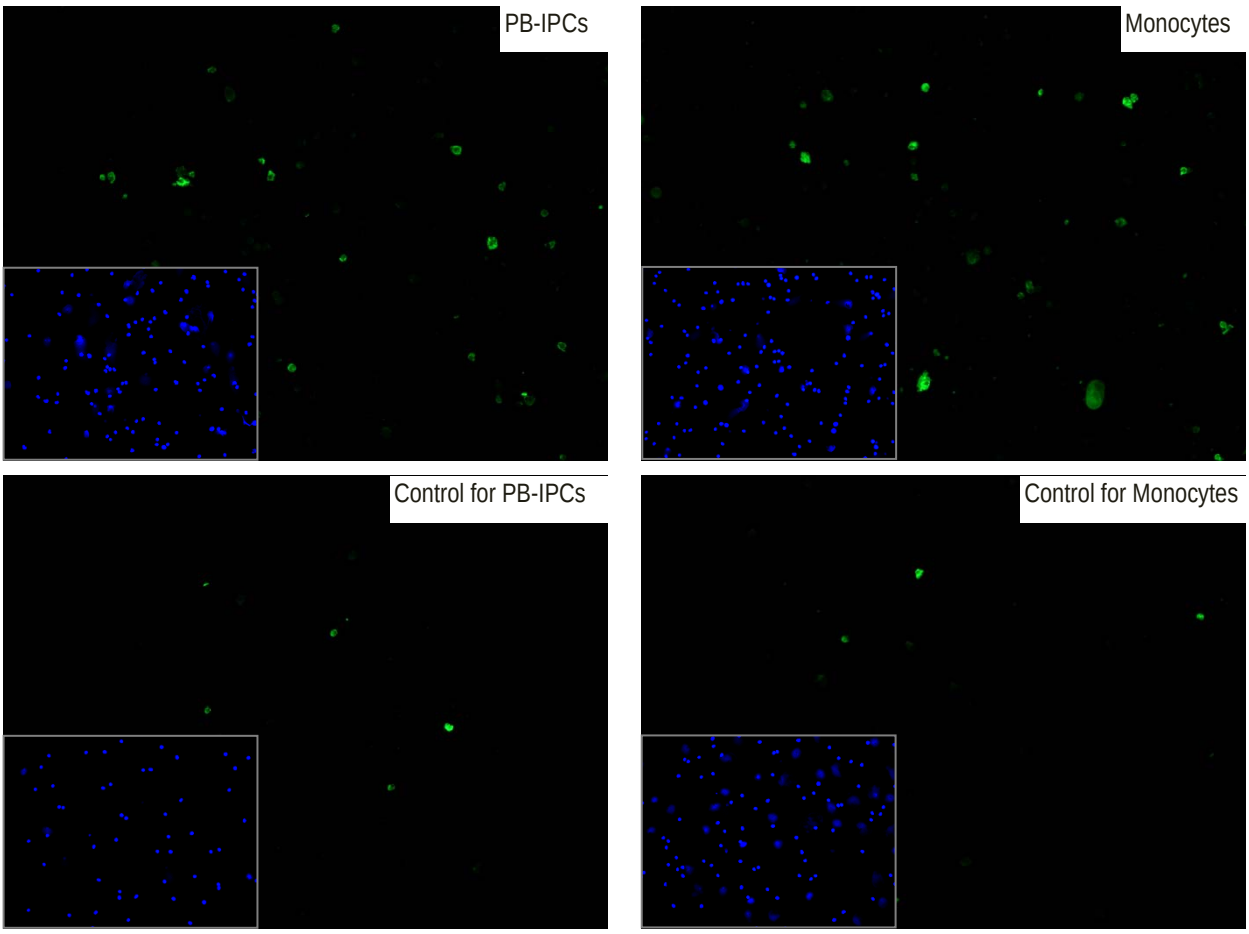


Figure 3.43 PB-IPCs and monocytes increased the level of apoptosis in the mixed lymphocyte response at 72 h, but only the effect of the monocytes was significant.

PBMCs from two different donors were overlaid onto PB-IPCs and monocytes that had been cultured for 1 week in full RPMI media containing 7% FBS (n=2). The PB-IPCs and monocytes were omitted from controls. The suspension cells were stained with Annexin-V (green) after 24 h of incubation of the mixed lymphocyte response. Cell nuclei were stained blue with DAPI (inset). Images were taken at 200x magnification; Annexin-V image is displayed 2.4 x larger than DAPI inset.

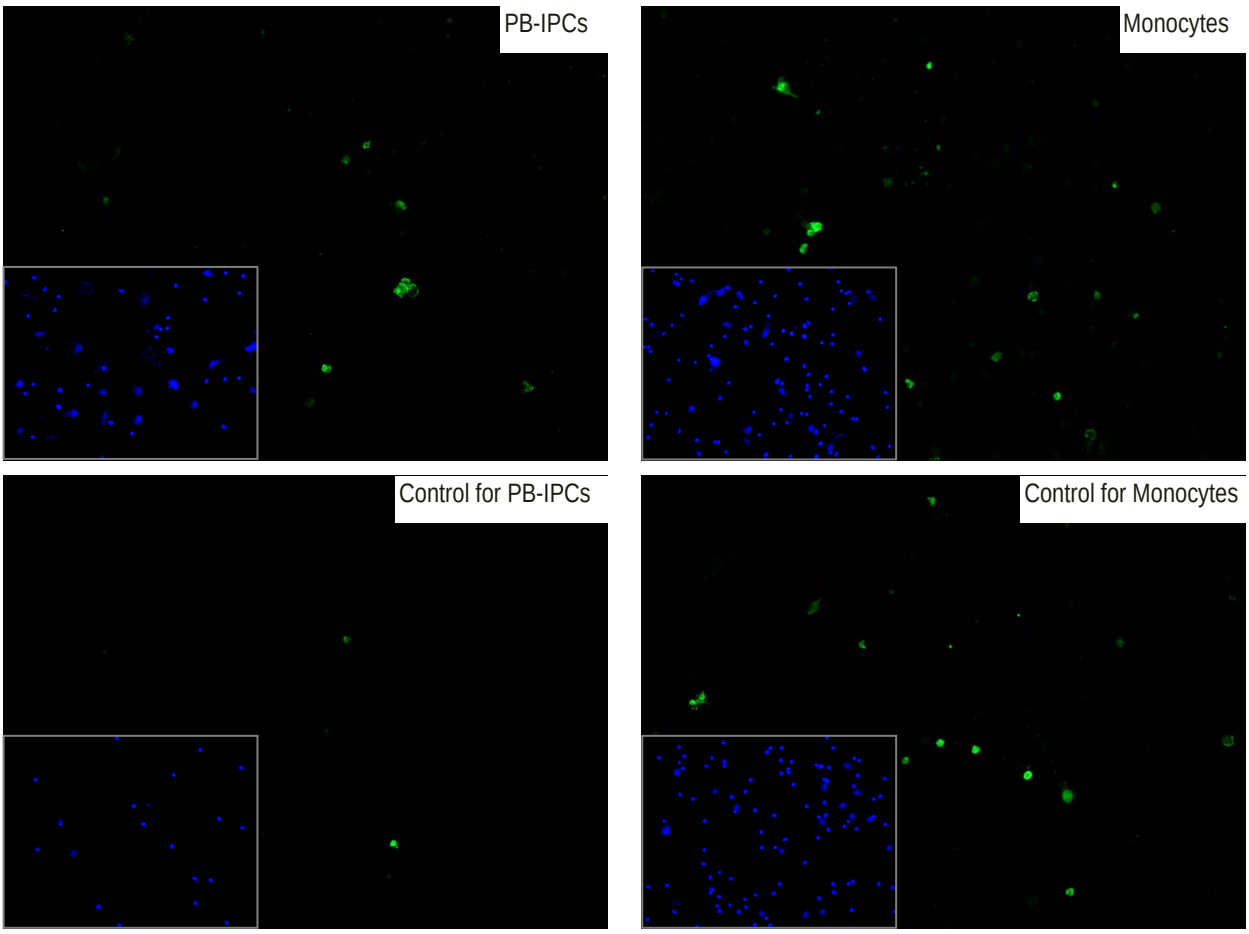


Figure 3.44 PB-IPCs significantly increased the mixed lymphocyte response at 96 h, while monocytes did not significantly alter the response.

PBMCs from two different donors were overlaid onto PB-IPCs and monocytes that had been cultured for 1 week in full RPMI media containing 7% FBS (n=2). The PB-IPCs and monocytes were omitted from controls. The suspension cells were stained with Annexin-V (green) after 24 h of incubation of the mixed lymphocyte response. Cell nuclei were stained blue with DAPI (inset). Images were taken at 200x magnification; Annexin-V image is displayed 2.4 x larger than DAPI inset.

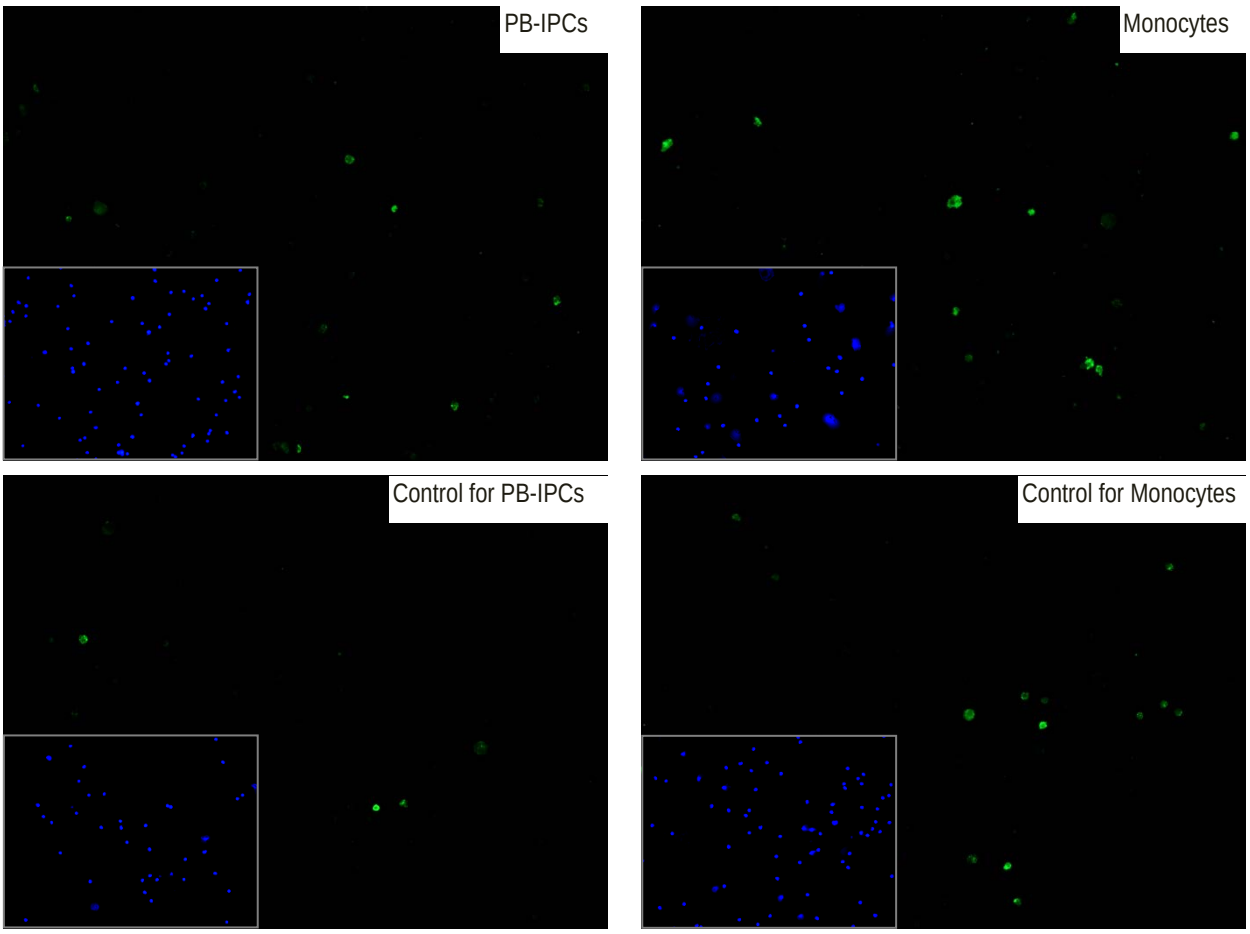


Figure 3.45 PB-IPCs and monocytes increased the level of apoptosis in the mixed lymphocyte response at 120 h, but the results were non-significant.

PBMCs from two different donors were overlaid onto PB-IPCs and monocytes that had been cultured for 1 week in full RPMI media containing 7% FBS (n=2). The PB-IPCs and monocytes were omitted from controls. The suspension cells were stained with Annexin-V (green) after 24 h of incubation of the mixed lymphocyte response. Cell nuclei were stained blue with DAPI (inset). Images were taken at 200x magnification; Annexin-V image is displayed 2.4 x larger than DAPI inset.

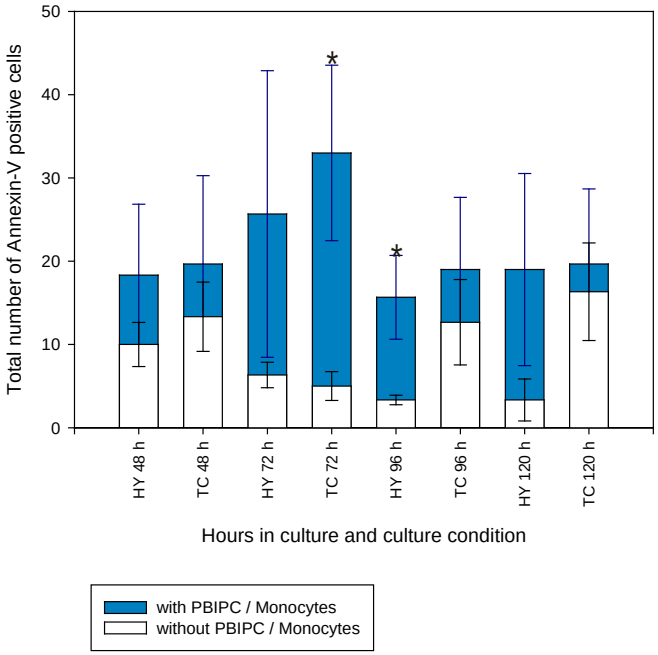


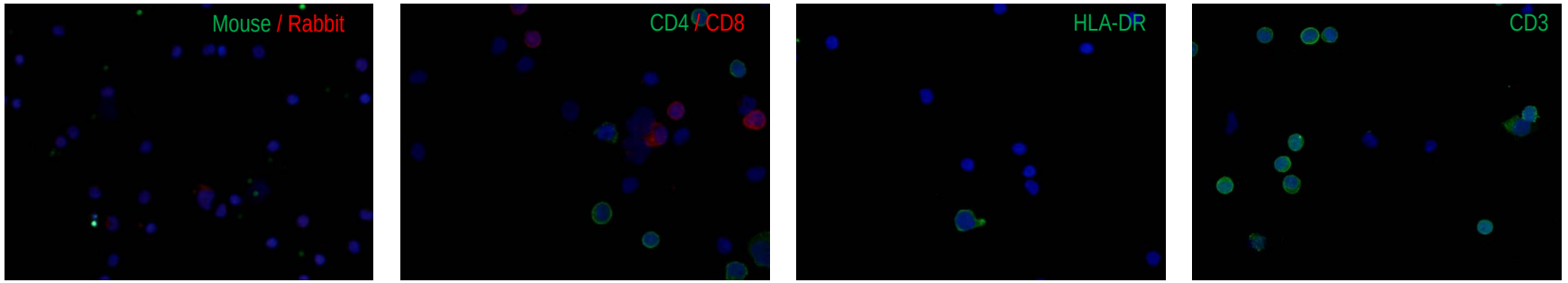
Figure 3.46 Summary of the number of apoptotic cells present at different times during the mixed lymphocyte response.

The experiment is as described in Figure 3.42 to Figure 3.45. Results are presented as the mean (n=3) ± SD of cells in 3 wells. * Significant difference between the presence and absence of PB-IPCs or monocytes: 72 h TC: p = 0.010, 96 h HY: p = 0.014.

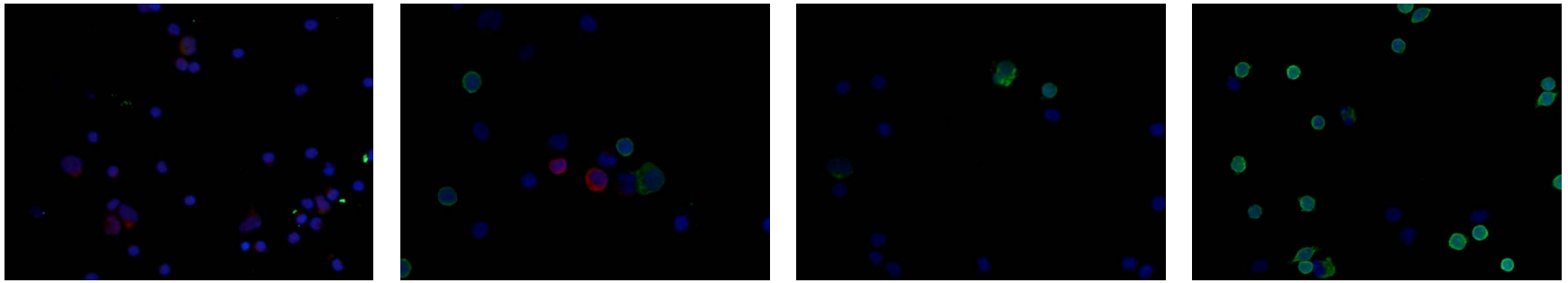
Only small numbers of apoptotic cells were present in the mixed lymphocyte response after 24 h, hence were not quantified (data not shown). One week cultures of PB-IPCs and monocytes did not significantly alter the number of apoptotic cells in the mixed lymphocyte response up to 48 h. In contrast, both the monocytes and PB-IPCs increased the response at 72 h but only the effect of the monocytes was significant (p = 0.010, n=3) compared with the control. PB-IPCs significantly increased the response at 96 h (p = 0.014, n=3) compared with the control, whereas the monocytes did not significantly alter the response. Similarly, at 120 h both PB-IPCs and monocytes increased the response, but none of the results were significant. Thus PB-IPCs appear to be immunostimulatory at the later stages of the mixed lymphocyte response, but the results were only significant at the 96 h time-point.

3.10.1 Phenotypes of cells present in the mixed lymphocyte response at different time-points

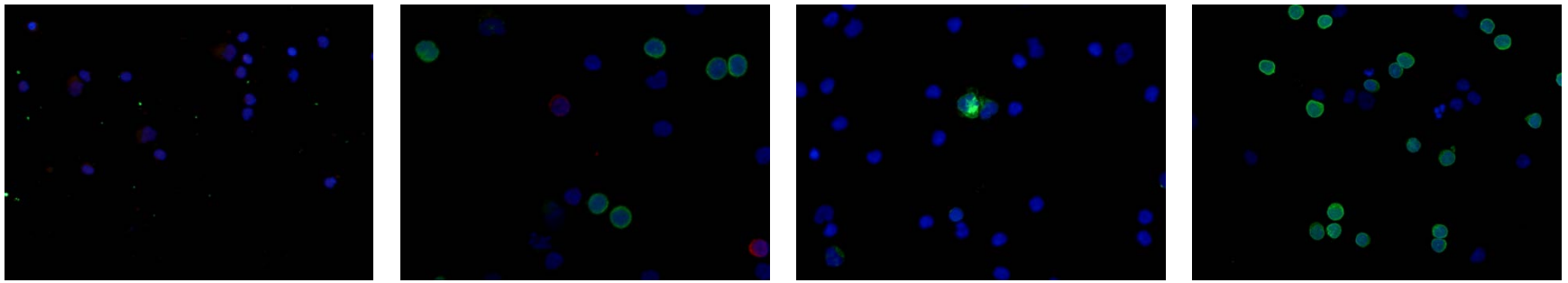
The suspension cells present in the mixed lymphocyte response (MLR) were predominantly $CD3^+$ T cells as expected (Figure 3.47 to Figure 3.51). Cells that were $CD4^+$, $CD8^+$, or HLA-DR^+ were clearly detectable. The percentage of $CD4^+$ cells varied throughout the mixed lymphocyte response with 13-50% of cells expressing this marker (Figure 3.52). In contrast, the number of $CD8^+$ cells increased over time, irrespective of the presence or absence of PB-IPCs and monocytes, potentially reflecting an increase in the number of cytotoxic T cells (Figure 3.47 to Figure 3.52). The number of cells expressing HLA-DR was strikingly upregulated at 72 h, reflecting cell activation (Figure 3.49 to Figure 3.51). Note that the photographs of the cells are not representative of the entire numbers of cells in the well. The average fraction of each cell type recorded in one part of the field from each of three wells is summarized in Figure 3.52.



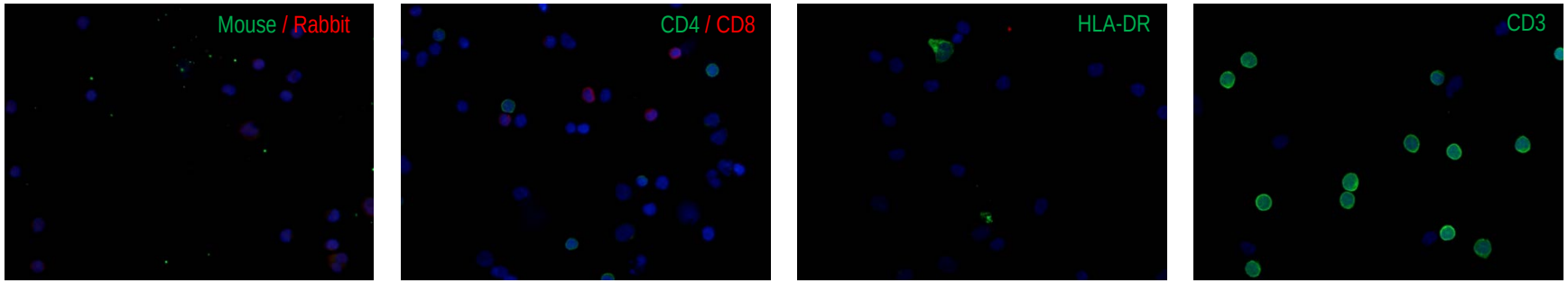
24 h PB-IPCs MLR



24 h Monocytes MLR



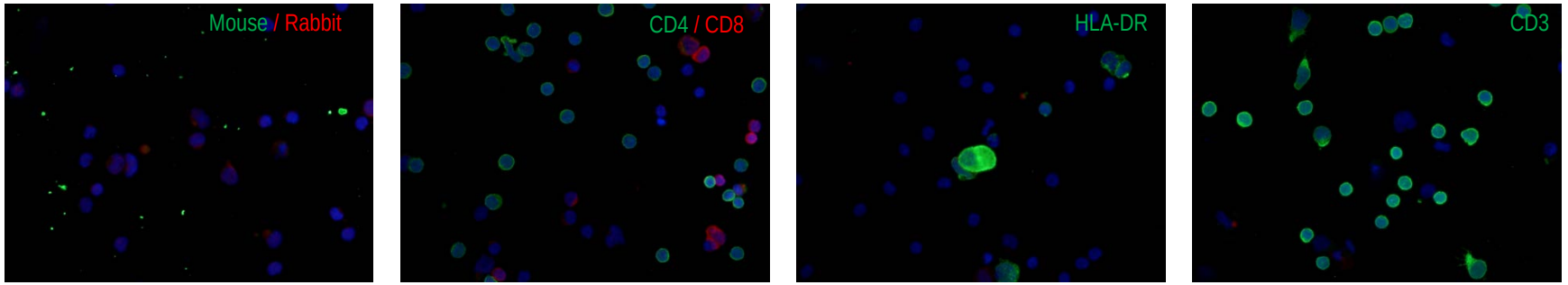
24 h MLR control for PB-IPCs



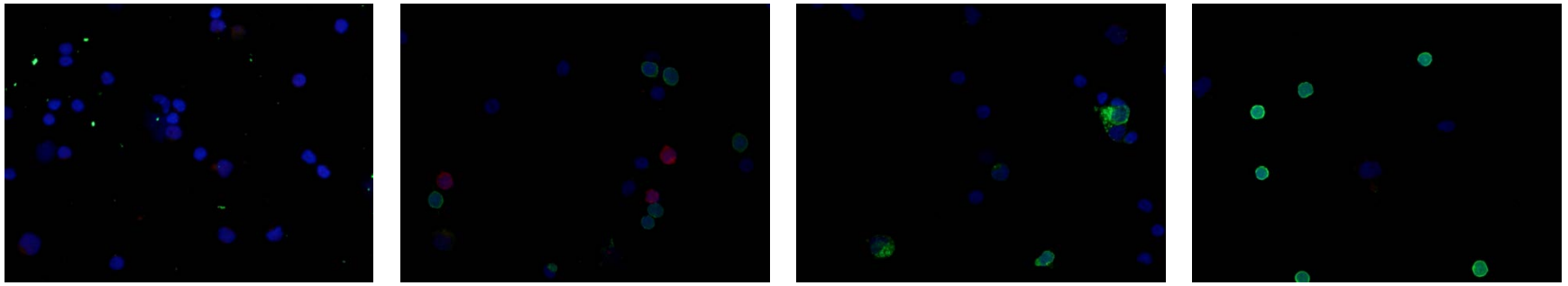
24 h MLR control for monocytes

Figure 3.47 Phenotype of cells in the mixed lymphocyte response at 24 h.

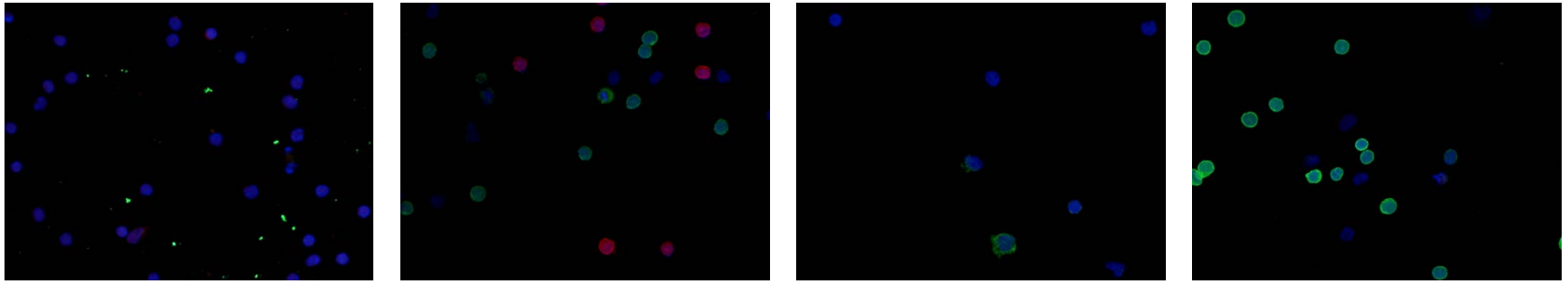
Refer to Figure 3.41 legend for experimental setup. Cells were stained with antibodies against various cell markers. Immunoreactivity was detected with a donkey anti-rabbit antibody (red) and with a donkey anti-mouse antibody (green). Cell nuclei were stained blue with DAPI. Images were taken at 200x magnification. The images are presented so that the staining obtained with each IgG control immediately precedes stainings with antibodies of the same host species.



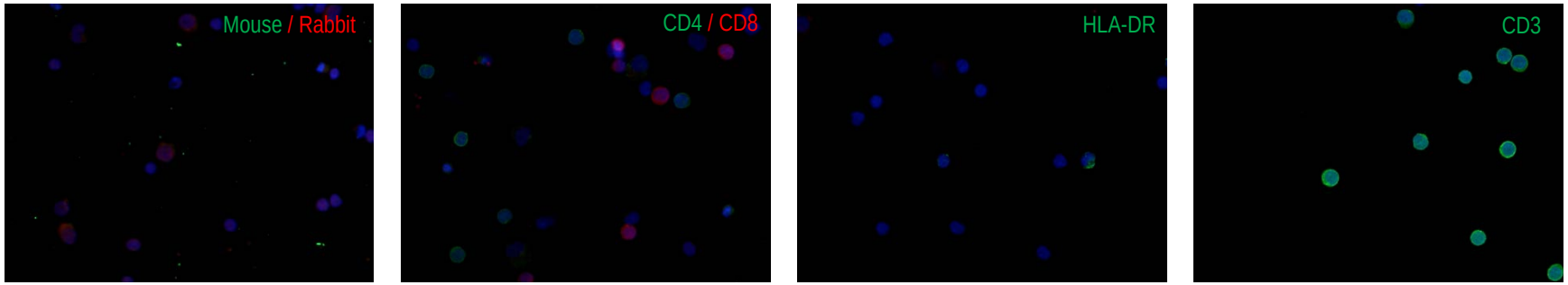
48 h PB-IPCs MLR



48 h Monocytes MLR



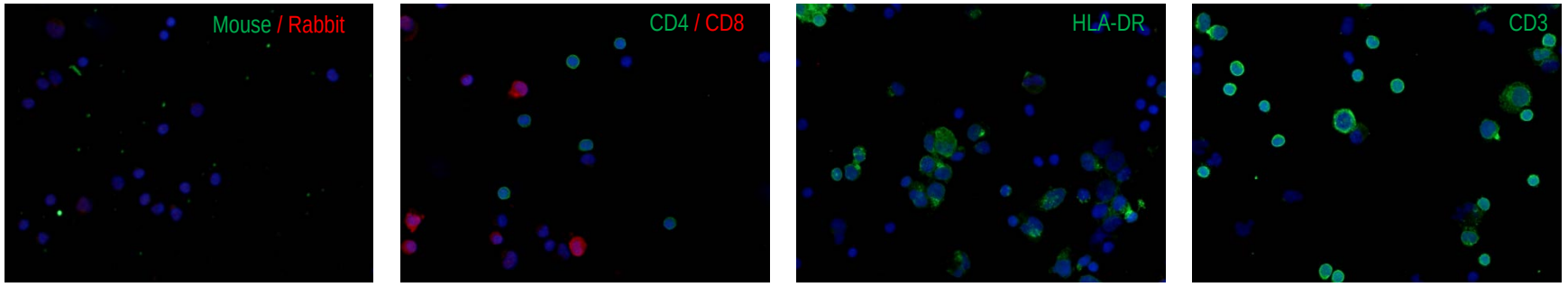
48 h MLR control for PB-IPCs



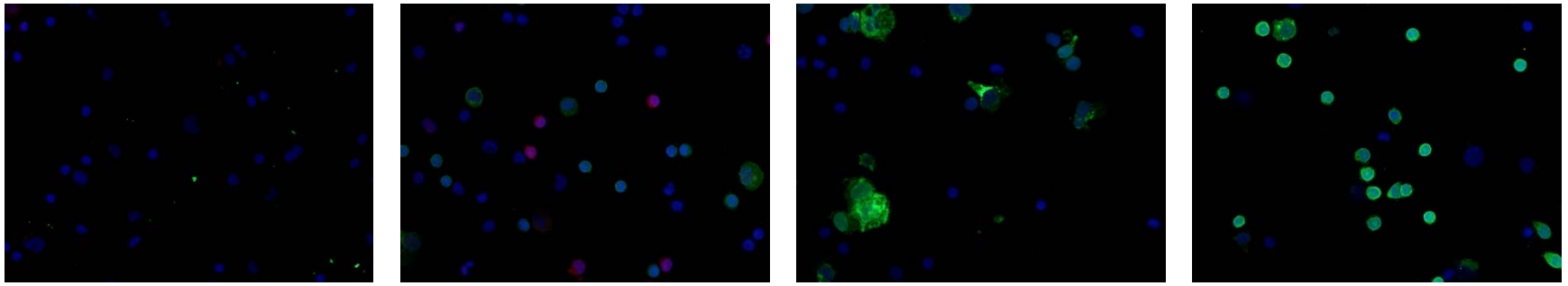
48 h MLR control for monocytes

Figure 3.48 Phenotype of cells in the mixed lymphocyte response at 48 h.

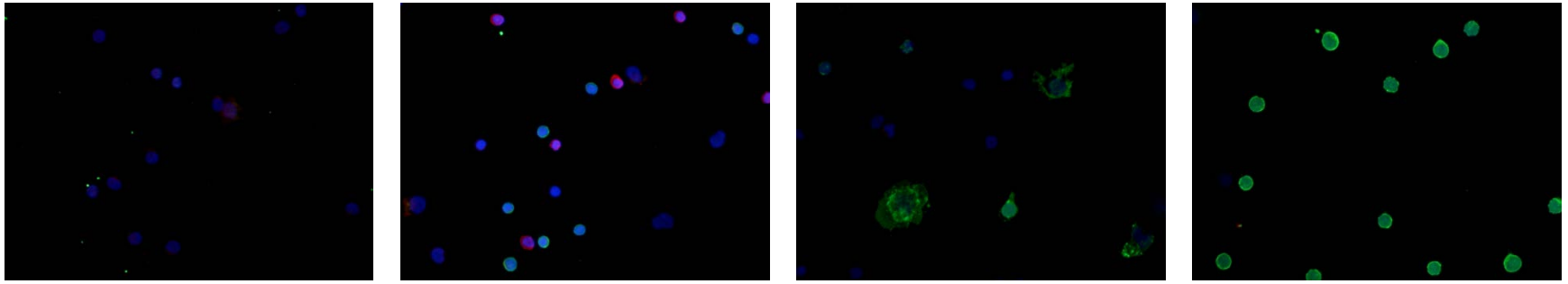
Refer to Figure 3.41 legend for experimental setup. Cells were stained with antibodies against various cell markers. Immunoreactivity was detected with a donkey anti-rabbit antibody (red) and with a donkey anti-mouse antibody (green). Cell nuclei were stained blue with DAPI. Images were taken at 200x magnification. The images are presented so that the staining obtained with each IgG control immediately precedes stainings with antibodies of the same host species.



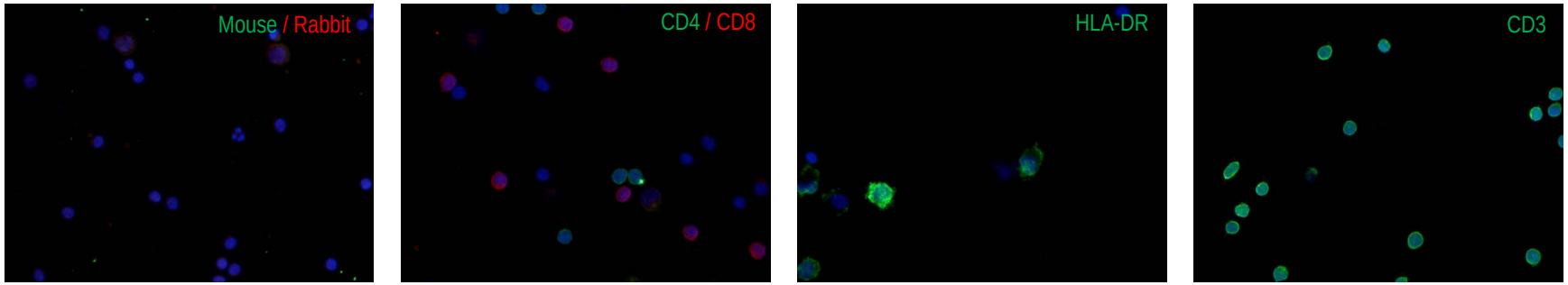
72 h PB-IPCs MLR



72 h Monocytes MLR



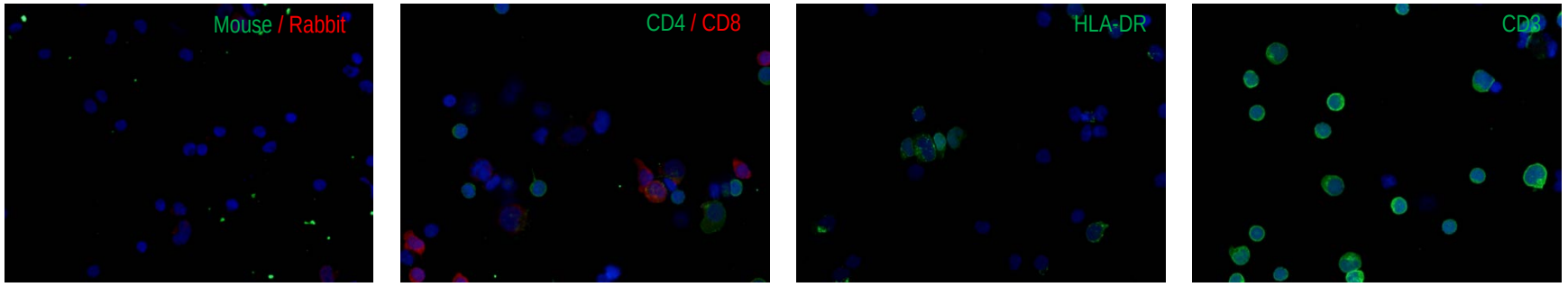
72 h MLR control for PB-IPCs



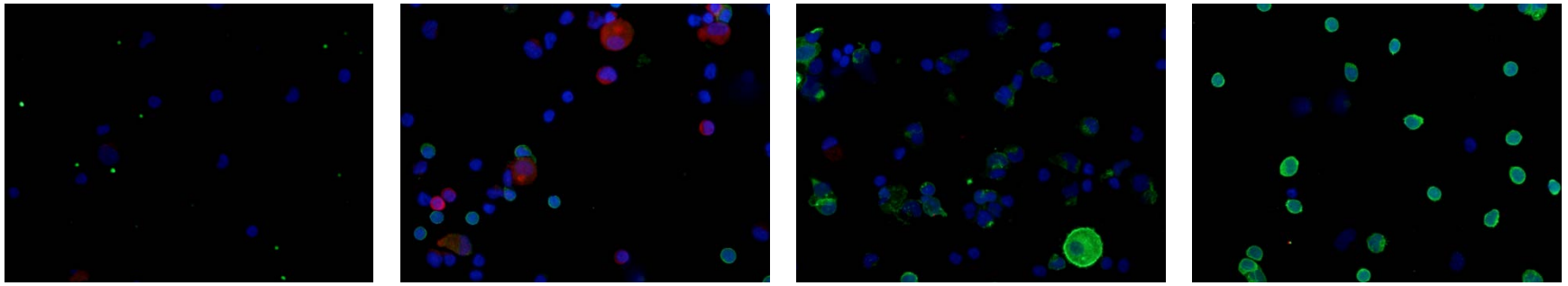
72 h MLR control for monocytes

Figure 3.49 Phenotype of cells in the mixed lymphocyte response at 72 h.

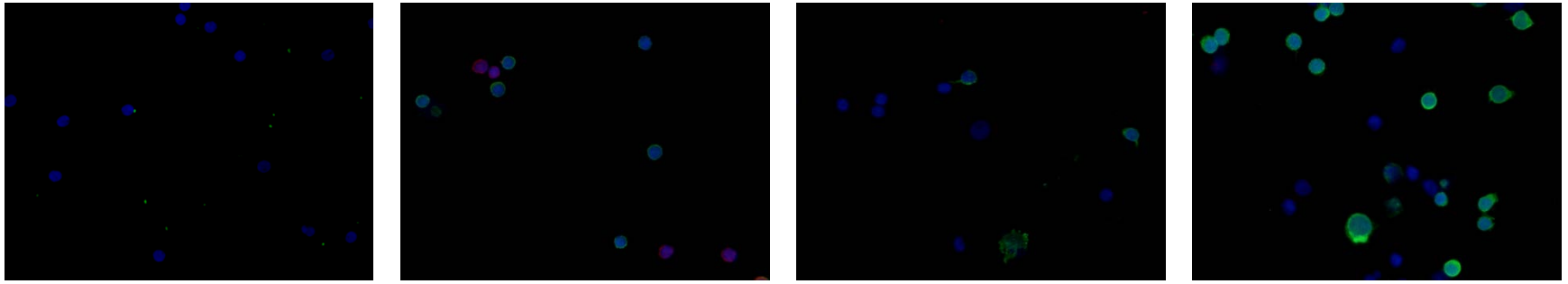
Refer to Figure 3.41 legend for experimental setup. Cells were stained with antibodies against various cell markers. Immunoreactivity was detected with a donkey anti-rabbit antibody (red) and with a donkey anti-mouse antibody (green). Cell nuclei were stained blue with DAPI. Images were taken at 200x magnification. The images are presented so that the staining obtained with each IgG control immediately precedes stainings with antibodies of the same host species.



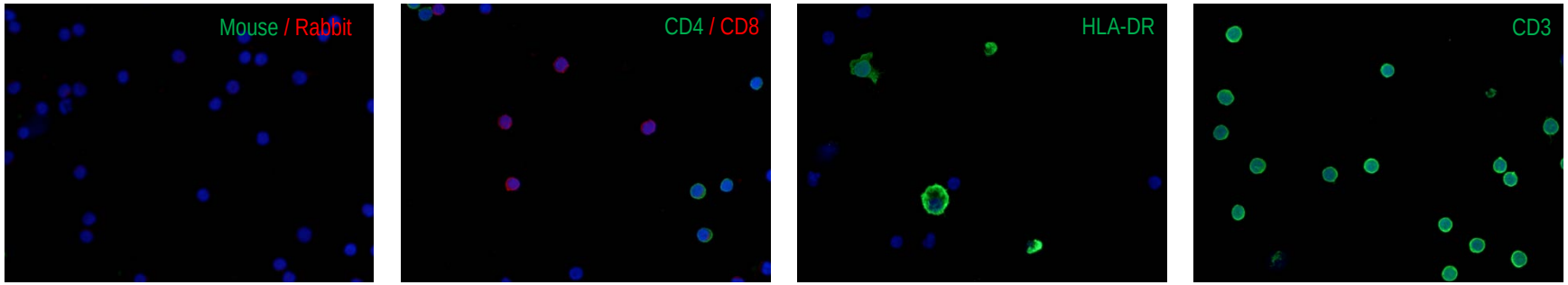
96 h PB-IPCs MLR



96 h Monocytes MLR



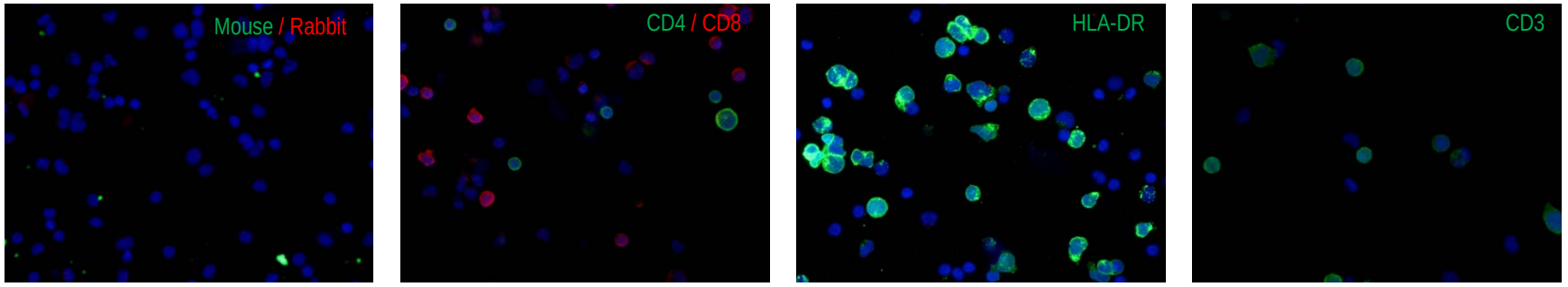
96 h MLR control for PB-IPCs



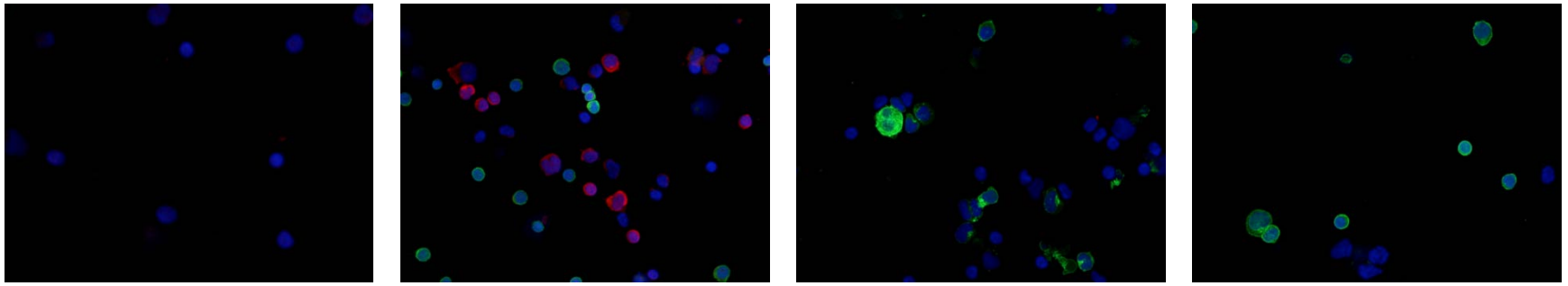
96 h MLR control for monocytes

Figure 3.50 Phenotype of cells in the mixed lymphocyte response at 96 h.

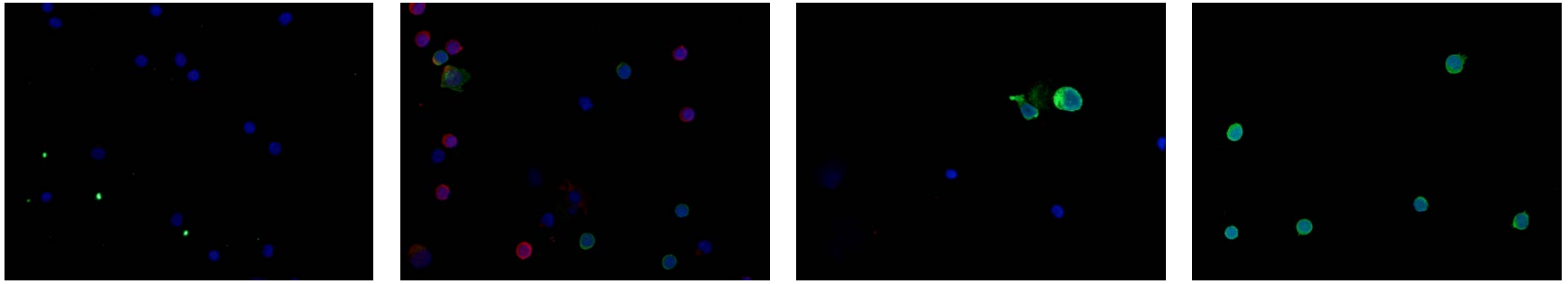
Refer to Figure 3.41 legend for experimental setup. Cells were stained with antibodies against various cell markers. Immunoreactivity was detected with a donkey anti-rabbit antibody (red) and with a donkey anti-mouse antibody (green). Cell nuclei were stained blue with DAPI. Images were taken at 200x magnification. The images are presented so that the staining obtained with each IgG control immediately precedes stainings with antibodies of the same host species.



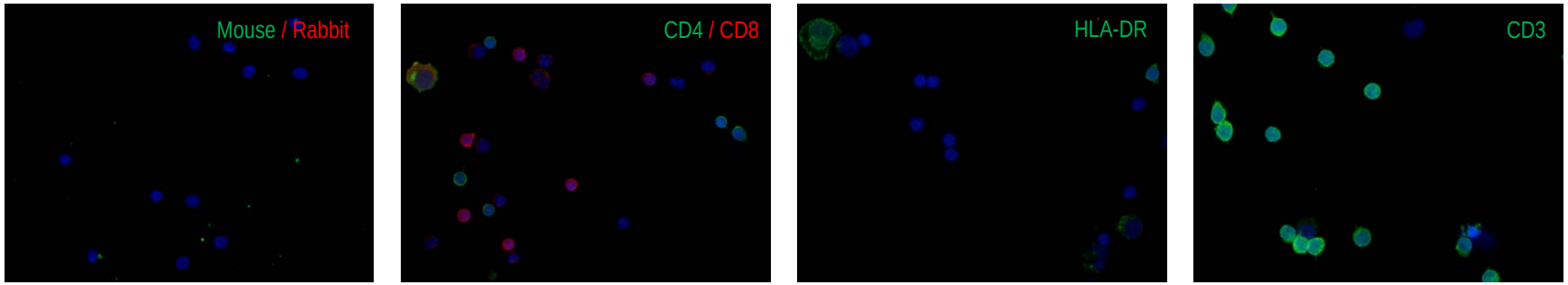
120 h PB-IPCs MLR



120 h Monocytes MLR



120 h MLR control for PB-IPCs



120 h MLR control for monocytes

Figure 3.51 Phenotype of cells in the mixed lymphocyte response at 120 h.

Refer to Figure 3.41 legend for experimental setup. Cells were stained with antibodies against various cell markers. Immunoreactivity was detected with a donkey anti-rabbit antibody (red) and with a donkey anti-mouse antibody (green). Cell nuclei were stained blue with DAPI. Images were taken at 200x magnification. The images are presented so that the staining obtained with each IgG control immediately precedes stainings with antibodies of the same host species.

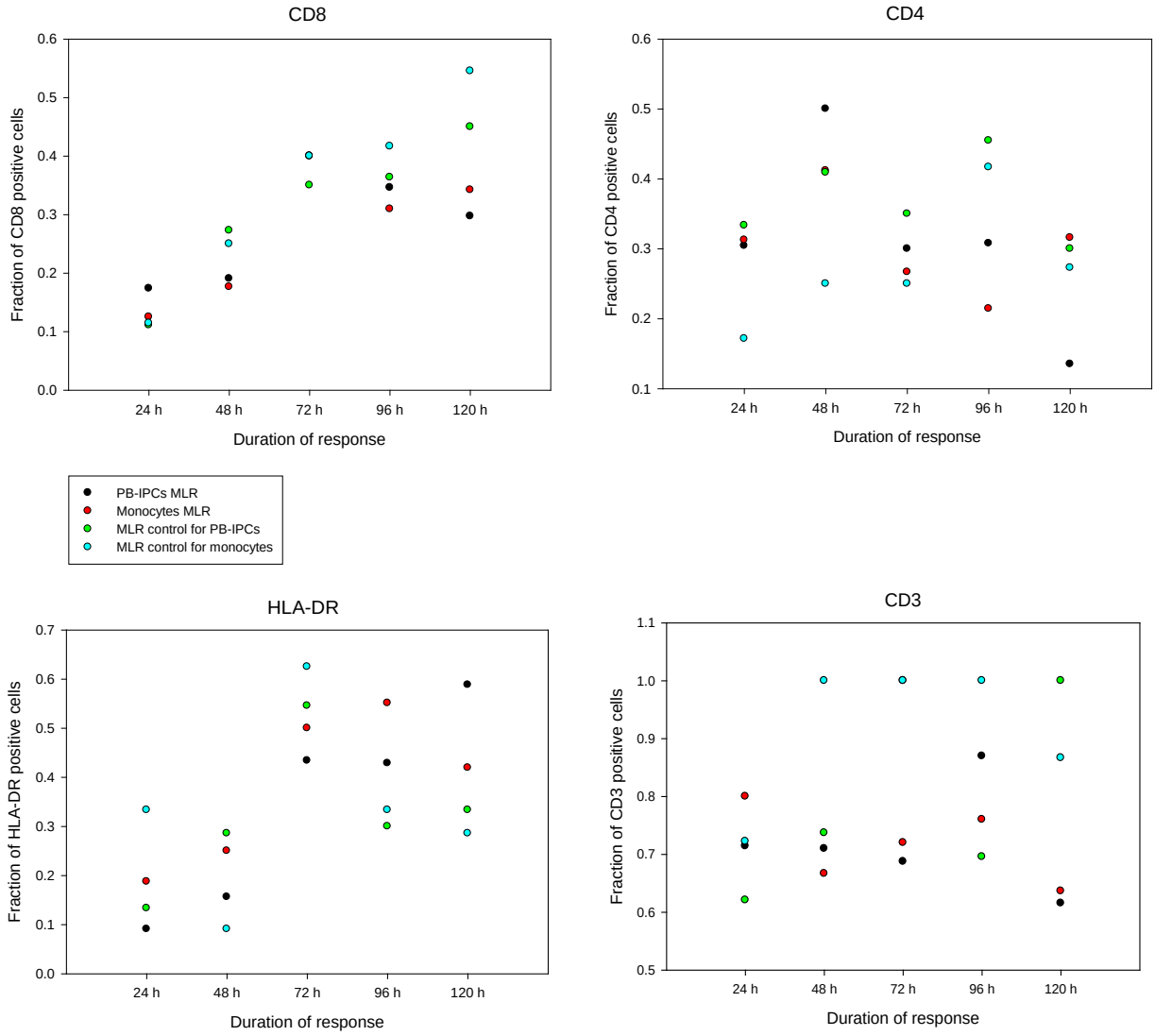


Figure 3.52 Summary of the phenotypes of the suspension cells present during the mixed lymphocyte reactions.

The fractions of cells expressing CD4, CD8, HLA-DR or CD3 at each time-point are shown. The average fraction of each cell type recorded in one part of the field from each of three wells is presented.

3.11 Inhibiting the effects of endotoxins on cell function

Bacterial endotoxins such as LPS have been shown to inhibit β-cell function, as demonstrated in rats where stimulation of β-cells with LPS inhibits insulin secretion in response to high concentrations of glucose (Osterbye *et al.* 2010). LPS stimulation of isolated human islets resulted in the upregulation of CD14 and toll-like receptor 4 (TLR4) mRNAs, which may be significant as the β-cells of type 1 diabetics that displayed a significant loss of viability expressed TLR4 (Garay-Malpartida *et al.* 2011).

In contrast, it has been reported that immune stimulation may be required for pancreatic regeneration within the liver (Wang *et al.* 2007). The delivery of non-toxic viruses capable of expressing PDX-1 and NGN3 into the liver of diabetic mice did not result in regeneration of insulin-producing cells (Wang *et al.* 2007). However, the levels of serum insulin were restored when an immune response was stimulated by including an irrelevant adenoviral vector (Wang *et al.* 2007).

Many recombinant proteins used to induce cellular differentiation are produced in *Escherichia coli*, and are contaminated with LPS (Cardoso *et al.* 2007). LPS was present in preparations of recombinant *Schistosoma mansoni* proteins produced in *Escherichia coli* (Cardoso *et al.* 2007). The recombinant proteins stimulated PBMCs to release the cytokines TNF-α and IL-10 (Cardoso *et al.* 2007).

Spermine is a ubiquitous biogenic polyamine that reversibly suppresses the synthesis of monocyte proinflammatory cytokines, and thereby inhibits monocyte activation (Zhang *et al.* 1999). It is naturally released at sites of inflammation by injured cells to restrain monocyte activation, and prevent further destruction of tissues (Zhang *et al.* 1999). Exposure of attached monocytes to spermine inhibits LPS-induced expression and secretion of TNF (Zhang *et al.* 1997).

Here experiments were designed to test whether spermine-mediated repression of monocyte activation would enhance the differentiation of PB-IPCs towards the pancreatic lineage. It was hypothesized that spermine would inhibit the inflammatory activation of PB-IPCs and prevent their loss of function as seen with rat β-cells (Osterbye *et al.* 2010), and enhance their response to differentiation factors. Control and LPS-stimulated cultures of PB-IPCs strongly expressed the activation antigen HLA-DR and CD68 (Figure 3.53). It was found that spermine (35 μM) inhibited the expression of HLA-DR and CD68 by PB-IPCs at day 3 of culture (Figure 3.53). Spermine was also able to inhibit the expression of HLA-DR and CD68 seen in the presence of LPS (100 ng/mL) (Figure 3.53). Spermine-treated cells appeared to be slightly smaller and darker as viewed by phase contrast microscopy (Figure 3.53).

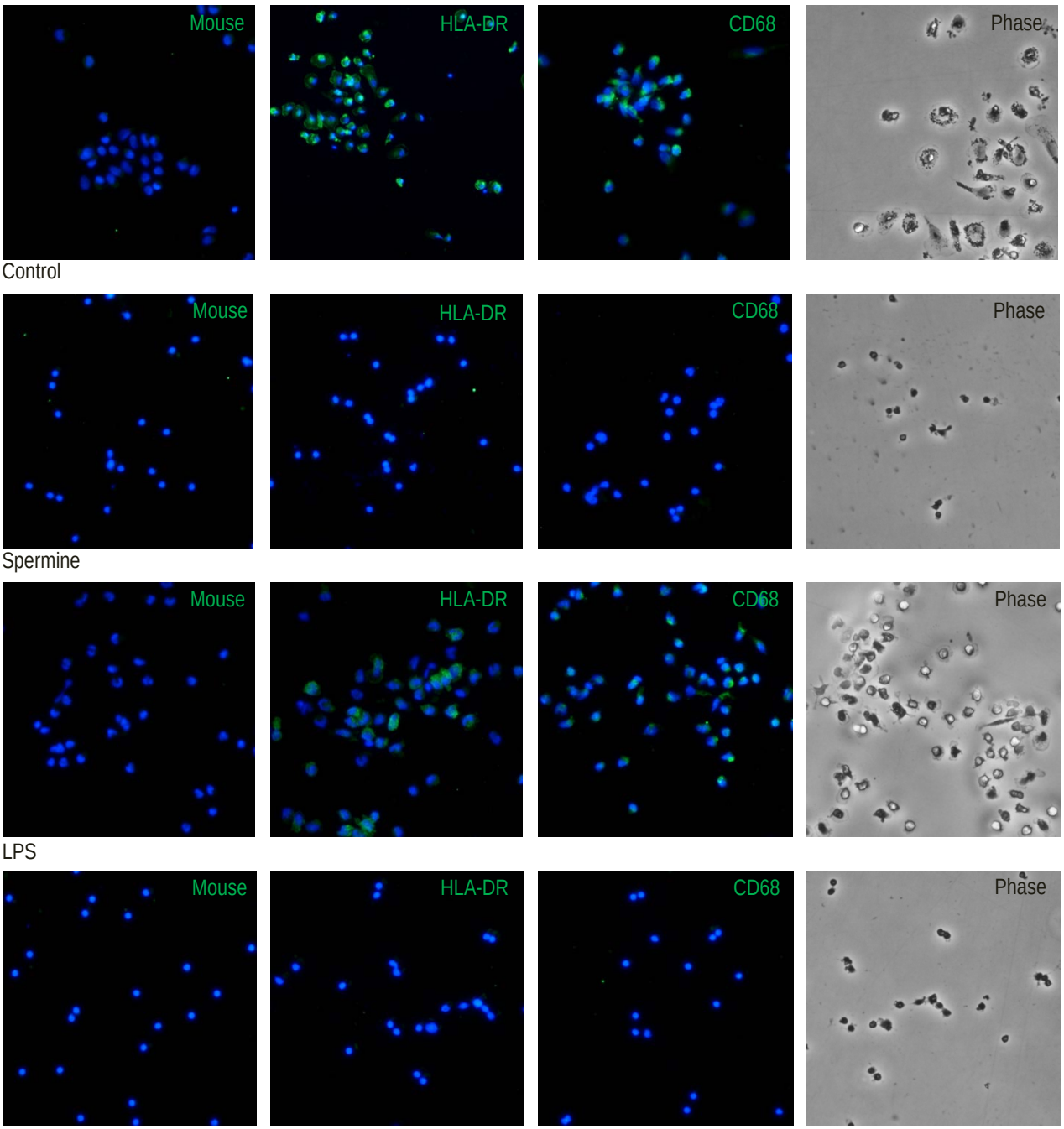


Figure 3.53 Spermine inhibits the expression of CD68 and HLA-DR by PB-IPCs.

PBMCs were allowed to attach to a hydrophobic dish for 2 h, followed by incubation for 3 days in the absence or presence of 100 ng/mL of LPS and 35 μM spermine in full RPMI media containing 7% FBS, as indicated (n=1). Cells were stained with antibodies against various cell markers. Immunoreactivity was detected with a donkey anti-mouse antibody (green). Cell nuclei were stained blue with DAPI. Representative phase contrast images are also shown. Images were taken at 200x magnification. The images are presented so that the staining obtained with the IgG control immediately precedes stainings with antibodies of the same host species.

Spermine (35 μM) was included in Zhao's protocol described in Section 3.8.1, to discover whether suppression of monocyte activation would enhance the pancreatic differentiation of PB-IPCs. It was included in either a pre-incubation step so that the PB-IPCs would not express CD68 and HLA-DR prior to differentiation (Figure 3.55), or included during pre-incubation and the subsequent differentiation (Figure 3.56). Spermine prevented expression of CD68, and caused HLA-DR to become downregulated in both treatment protocols, compared to the control cells (compare Figure 3.54, Figure 3.55, and Figure 3.56). Unfortunately, inclusion of spermine did not promote the expression of insulin (Figure 3.55 and Figure 3.56). Rather, inclusion of spermine appeared to inhibit pancreatic differentiation as PDX-1 or HNF6, which were normally upregulated during Zhao's protocol, were absent (Figure 3.55 and Figure 3.56). The markers SOX-17, Nestin, CD58, HLA-DR, and CD14 were downregulated (Figure 3.55 and Figure 3.56). Several of the cells that were positively stained for cell markers appeared to lack nuclei suggesting a loss of cell viability (Figure 3.55 and Figure 3.56). In accord, approximately 50% of the cells stained with trypan blue indicating they had not survived the prolonged exposure to spermine (data not shown).

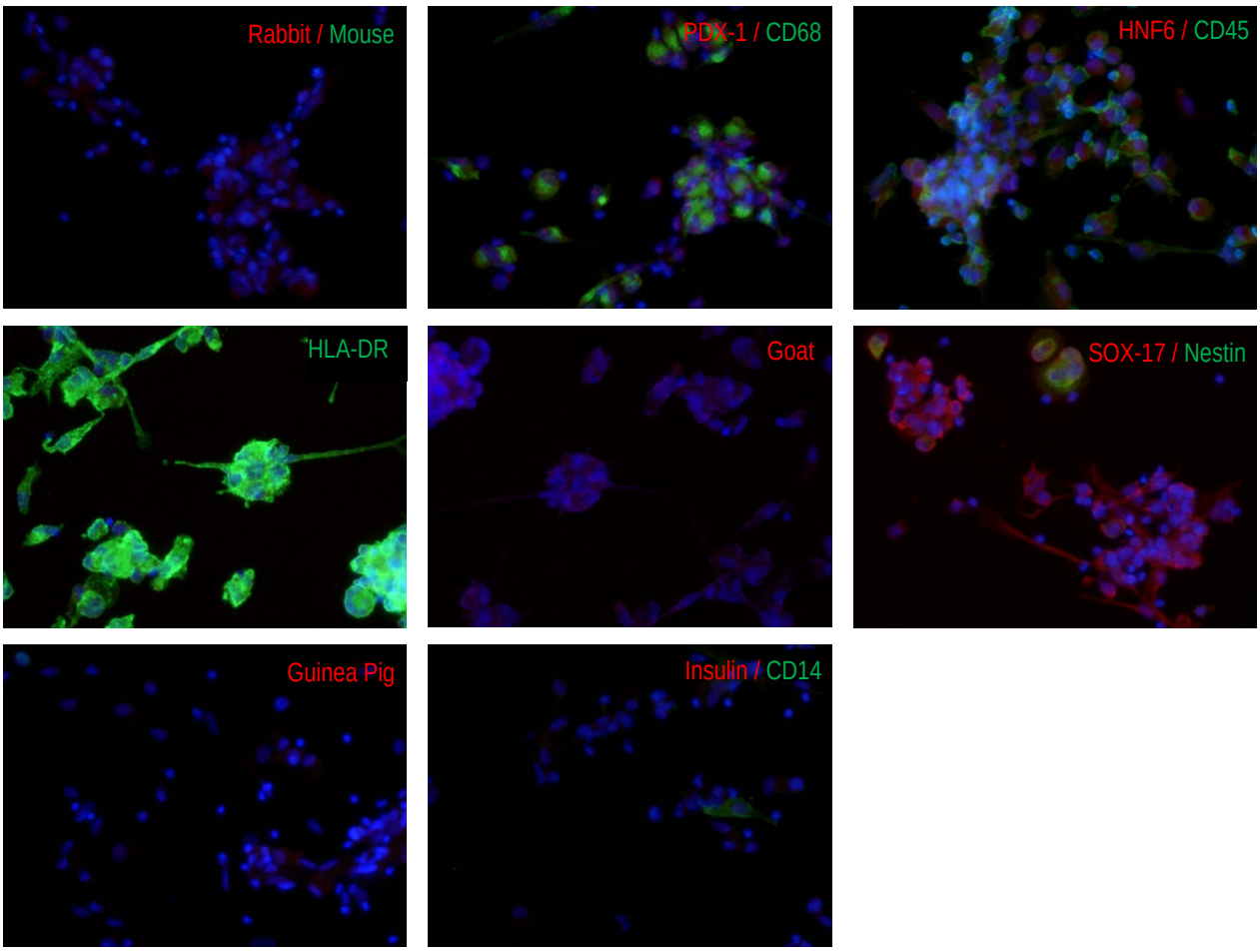


Figure 3.54 Control PB-IPC populations cultured in the absence of spermine.

PB-IPCs were cultured for 3 days in full RPMI media containing 7% FBS. The medium was then changed to Zhao's protocol differentiation medium (DMEM medium containing 10 nM Ex4, 10 ng/mL GM-CSF, 25 mM glucose, 7% FBS, and 1% PSG), followed by incubation for 5 days (n=1). Cells were stained with antibodies against various cell markers. Immunoreactivity was detected with donkey anti-rabbit, donkey anti-goat, and goat anti-guinea pig antibodies (red) and with a donkey anti-mouse antibody (green). Cell nuclei were stained blue with DAPI. Images were taken at 200x magnification. The images are presented so that the staining obtained with each IgG control immediately precedes stainings with antibodies of the same host species.

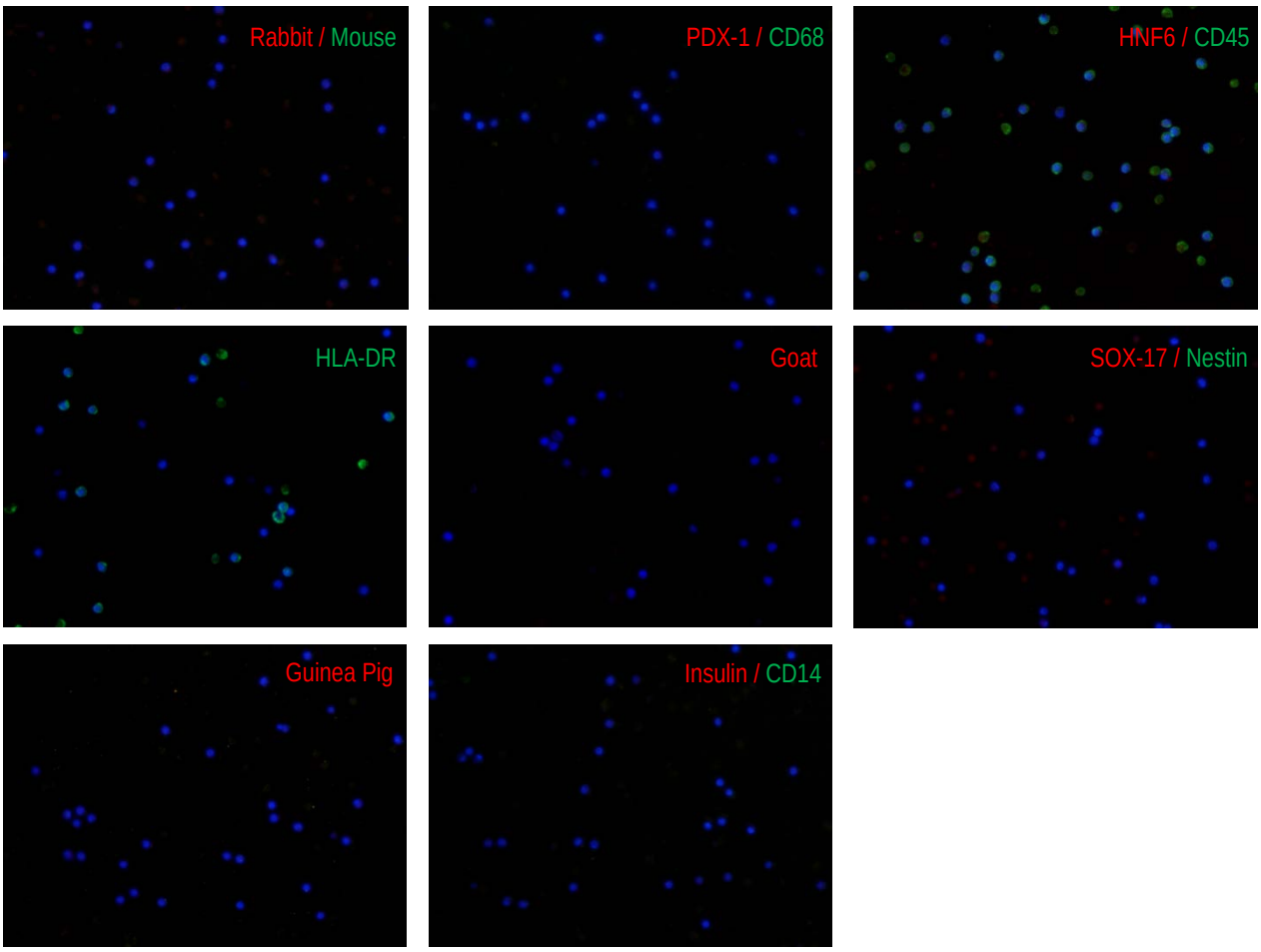


Figure 3.55 Pre-treatment of PB-IPCs with spermine inhibits their activation, but does not enhance pancreatic differentiation.

PB-IPCs were cultured for 3 days in full RPMI media containing 7% FBS, and 35 μM spermine. The medium was then changed to Zhao's protocol differentiation medium (DMEM medium containing 10 nM Ex4, 10 ng/mL GM-CSF, 25 mM glucose, 7% FBS, and 1% PSG), followed by incubation for 5 days (n=1). Cells were stained with antibodies against various cell markers. Immunoreactivity was detected with donkey anti-rabbit, donkey anti-goat, and goat anti-guinea pig antibodies (red) and with a donkey anti-mouse antibody (green). Cell nuclei were stained blue with DAPI. Images were taken at 200x magnification. The images are presented so that the staining obtained with each IgG control immediately precedes stainings with antibodies of the same host species.

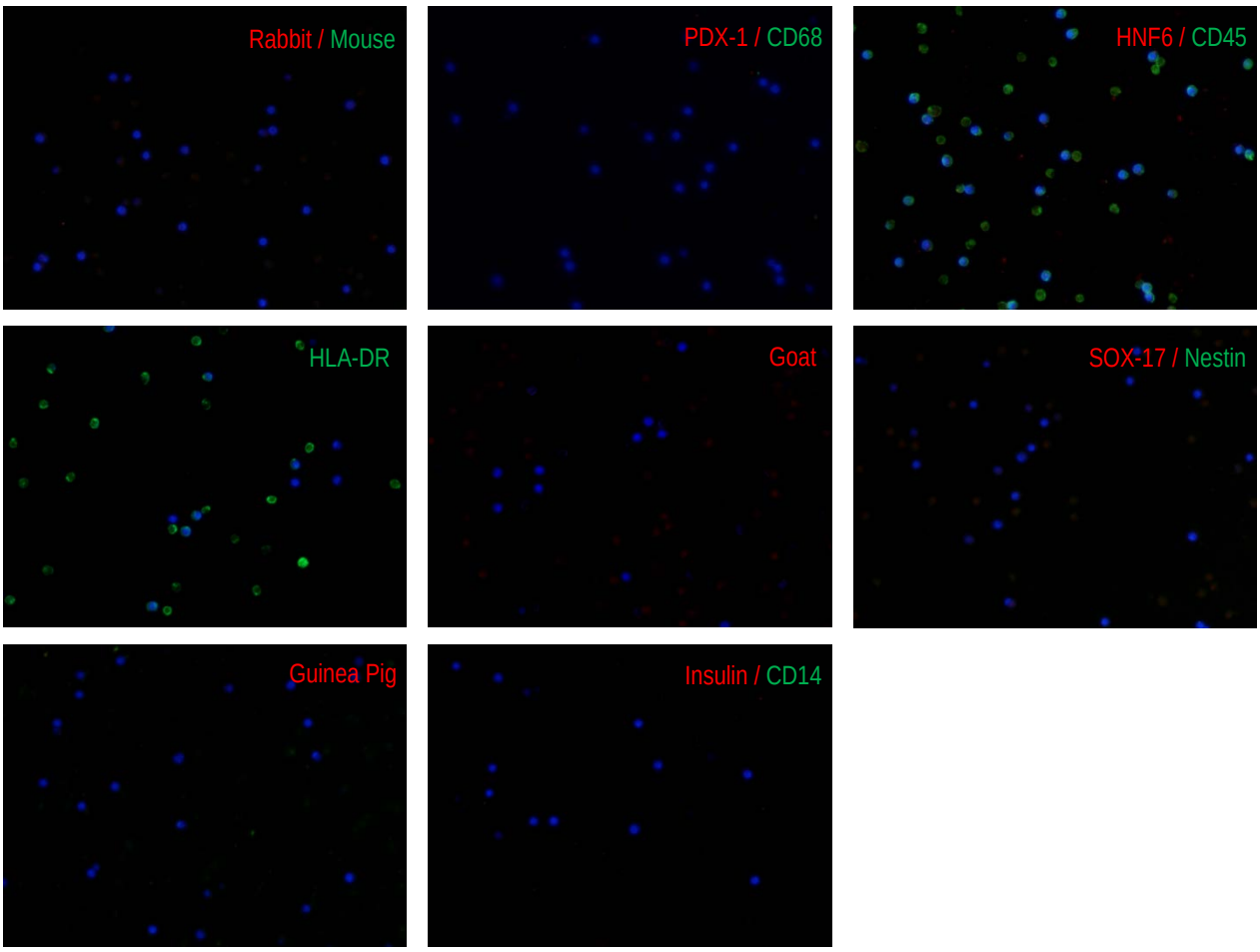


Figure 3.56 Inclusion of spermine during pretreatment and differentiation steps does not enhance the pancreatic differentiation of PB-IPCs.

PB-IPCs were cultured for 3 days full RPMI media containing 7% FBS, and 35 μM spermine. The medium was then changed to Zhao's protocol differentiation medium (DMEM medium containing 10 nM Ex4, 10 ng/mL GM-CSF, 25 mM glucose, 7% FBS, and 1% PSG) with the addition of 35 μM spermine, followed by incubation for 5 days (n=1). Cells were stained with antibodies against various cell markers. Immunoreactivity was detected with donkey anti-rabbit, donkey anti-goat, and goat anti-guinea pig antibodies (red) and with a donkey anti-mouse antibody (green). Cell nuclei were stained blue with DAPI. Images were taken at 200x magnification. The images are presented so that the staining obtained with each IgG control immediately precedes stainings with antibodies of the same host species.

3.12 Discussion

The present study was undertaken to further characterise the PB-IPC population in terms of their stem cell-like properties, and also to investigate their plasticity, and ability to be differentiated towards the pancreatic lineage. A direct comparison was made between PB-IPCs and monocytes, the only other spontaneously adherent blood cell population. The study has shown that PB-IPCs express several pancreatic cell markers, as discussed below, and yet they are very similar to monocytes in terms of their morphology, phenotype, and function. They appear to be a population of cells very closely related to monocytes that uniquely possess the ability to spontaneously adhere to hydrophobic rather than hydrophilic surfaces.

3.12.1 Phenotype of PB-IPCs

Zhao *et al.* (2007) reported that PB-IPCs cultured in the absence of additional factors other than FBS expressed insulin, C-peptide, MafA, Nkx6.1, PDX-1, NeuroD, HNF6, PC1/3, PC2, CXCR4, CD45, Oct-4, and Nanog. The present study replicated the culture of PB-IPCs, revealing that during culture they expressed PDX-1, CXCR4, HNF6, SOX-17, CD45, Nestin, vWF, CD31, fibroblast factor (prolyl 4-hydroxylase or disulphide-isomerase), FOXP3, CD68, CD11b, CD11c, CD14, CD40, HLA-DR, and AIRE, but not insulin, C-peptide, MafA, Nkx6.1, NeuroD, PC1/3, or PC2 as reported by Zhao *et al.* (2007). These findings indicate that the populations of PB-IPCs isolated by Zhao *et al.* (2007) are different from those isolated during this study. The reason for the differences between the two studies is not obvious.

Whilst immunocytochemistry is not quantitative, it does allow for an estimate of the prevalence of cells expressing a particular marker. HNF6 was weakly expressed by both PB-IPCs and monocytes after three days in culture, indicating that differentiation along the pancreatic lineage had begun. In the mouse, HNF6 is expressed by epithelial cells and is required for the development of endocrine cells within the pancreas (Jacquemin *et al.* 2000). It is also a marker of the formation of the posterior foregut during pancreatic differentiation (D'Amour *et al.* 2006). By one week equal numbers of PB-IPCs and monocytes expressed HNF6, and by two weeks slightly more monocytes expressed HNF6 than did PB-IPCs. These results indicate that the dynamics of PB-IPC and monocyte differentiation towards the pancreatic lineage are different.

After one week in culture both PB-IPCs and monocytes expressed PDX-1. PDX-1, like HNF6, is a marker of posterior foregut differentiation, and is upregulated during pancreatic development (Soria 2001; D'Amour *et al.* 2006). After one week of culture PDX-1 was expressed by a higher proportion of monocytes than PB-IPCs and more strongly, but after two weeks both populations showed moderate PDX-1 nuclear expression in the majority of cells. PDX-1 was expressed as two forms of 31 kDa and 46 kDa. It has been reported that the 31 kDa protein is an inactive cytoplasmic form, whereas the 46 kDa protein is the sumoylated active form of PDX-1 that is translocated into the nucleus (Kishi *et al.* 2003). The PB-IPCs isolated by Zhao *et al.* (2007) expressed the 31 kDa inactive form of PDX-1, indicating that these cells should not have been able to differentiate into insulin-expressing cells unless the 46 kDa form was present but not reported (Kishi *et al.* 2003; Noguchi *et al.* 2003; Kaneto *et al.* 2005).

PB-IPCs isolated by Zhao *et al.* (2007) strongly expressed CXCR4. In the present study, PB-IPCs weakly expressed CXCR4 after two weeks of culture, whilst monocytes weakly expressed CXCR4 after just one week of culture. CXCR4 is expressed during the definitive endoderm stage of pancreatic development (D'Amour *et al.* 2006), and is also associated with hematopoietic stem cell localization or homing where it binds with SDF-1α on bone marrow endothelium (Kayali *et al.* 2003). CXCR4 is also expressed by T cells, B cells and macrophages (Buckley *et al.* 2000), which is not in disagreement with the notion that PB-IPCs are a population of unique monocytes. The induction of expression of CXCR4 by both PB-IPCs and monocytes coincided with the expression of SOX-17. SOX-17 expression could indicate definitive endoderm differentiation along the pancreatic lineage (D'Amour *et al.* 2006), or differentiation towards a number of different cell lineages as SOX-17 is more widely distributed than is often appreciated (Sohn *et al.* 2006; Lange *et al.* 2009; Nakajima-Takagi *et al.* 2013). However, the expression of a combination of pancreatic development markers by PB-IPCs and monocytes including HNF6, PDX-1, CXCR4, and SOX-17 suggests these cells are undergoing early development towards a pancreatic cell precursor.

PB-IPCs expressed Nestin from as early as day three of culture, with most cells expressing this marker by two weeks. Surprisingly, Nestin was also expressed by monocytes, which are not thought to have stem cell-like qualities. Nestin is a marker of precursor cells capable of being differentiated into pancreatic β-cells (Yue *et al.* 2006; Milanesi *et al.* 2011). Nestin was used as a marker to select rat bone marrow stem cells prior their differentiation into pancreatic endocrine and ductal cells (Milanesi *et al.* 2011). Nestin is also considered to be a neural stem cell marker (Keyoung *et al.* 2001), in accord with the notion that neuronal cells and pancreatic β-cells share a common early pathway of differentiation. Approximately 50% of PB-IPCs also expressed CD31, which was often co-expressed with Nestin after one week of culture, indicating that the PB-IPC population could also contain endothelial progenitor cells. However, PB-IPCs did not express CD34, a marker for both vascular endothelial cells and hematopoietic stem cells (Klein *et al.* 2003). Another endothelial cell marker vWF was detected on a few cells after initial attachment, which could reflect endogenous expression or the binding of fragments of activated platelets (Krissansen *et al.* 1990; Schmeisser *et al.* 2001). Half of the monocytes cultured for one week were labelled by the anti-vWF antibody, and by two weeks the majority of PB-IPCs and monocytes were labelled with this marker. The role of vWF is to bind collagen exposed on endothelial cells to enable the adhesion of platelets during blood clotting, and also to carry the blood clotting factor VIII in the circulation (Sadler 1998). $CD34^{-}CD14^{+}$ monocytes cultured on fibronectin in an angiogenic medium containing VEGF, bFGF, and IGF-1 displayed upregulated vWF expression over time, and after two weeks of culture approximately half of the monocytes expressed vWF (Schmeisser *et al.* 2001). They formed tubular-like structures on Matrigel®, suggesting they had differentiated into endothelial cells capable of forming venules (Schmeisser *et al.* 2001). Like PB-IPCs, they expressed CD68 after two weeks of culture (Schmeisser *et al.* 2001). Macrophages have been shown to take up circulating vWF and degrade it *in vivo*, suggesting that they play a prominent role in the clearance of the VWF/FVIII complex (van Schooten *et al.* 2008). Therefore, late-stage upregulation of vWF by the PB-IPCs or monocytes in the present study could either be uptake of vWF from the serum, or platelet membrane fragments, or differentiation of these cells into endothelial-like cells which also express CD31 despite not using forced endothelial differentiation with angiogenic factors.

The isolated PB-IPCs did not express the stem cell factor Oct-4, which is at variance with the study by Zhao *et al.* (2007). Nevertheless, potential stem-ness was evidenced by the presence of alkaline phosphatase activity in a very small percentage of cells after three days of culture. Human ESCs are categorized as undifferentiated if they possess alkaline phosphatase activity, however, unlike PB-IPCs, they also express Oct-4 (O'Connor *et al.* 2008). Alkaline phosphatase is also expressed by partially reprogrammed iPSCs that do not co-express all the necessary markers of an induced stem cell (Chan *et al.* 2009). Therefore the presence of alkaline phosphatase activity and Nestin expression by PB-IPCs is likely not sufficient proof that those PB-IPCs that express alkaline phosphatase are “true” stem cells.

The interpretation of the expression of pancreatic and stem cell markers requires caution as the PB-IPCs also highly expressed immunoregulatory markers such as CD68, HLA-DR, CD11c, and, AIRE. The cells have a confusing phenotype. They could be transitioning from a monocyte-like cell into pancreatic cells, or into antigen presenting cells capable of presenting pancreatic antigens. It is important to note that CD68 is not entirely restricted to macrophages (Gottfried *et al.* 2008; La Rocca *et al.* 2009). In accord, the anti-CD68 antibody EMB11 used in this study has been previously shown to recognise macrophages, but also acini and islets of Langerhans, connective tissue and endothelium (Pulford *et al.* 1990). In the present study, the antibody strongly stained both PB-IPCs and monocytes. The strong expression of HLA-DR by PB-IPCs is in sharp contrast to the findings by Zhao *et al.* (2007), where the expression of this activation marker was not observed. The PB-IPCs expressed HLA-DR throughout the entire culture period. HLA-DR is known to be expressed by monocytes, B cells, dendritic cells, and by a large number of other cell types that are in a state of activation (McCarthy *et al.* 1997). Thus, HLA-DR expression by PB-IPCs indicates either that they are activated, or they are related to one of the latter hematopoietic cells types, in particular monocytes. Accordingly, the PB-IPCs strongly expressed the dendritic cell marker CD11c. In contrast, CD11c was not expressed by the PB-IPCs reported by Zhao *et al.* (2008).

AIRE was moderately expressed by the majority of monocytes and by about half of the PB-IPCs after two weeks of culture. AIRE is a transcription factor that induces the expression of extra-thymic tissue-specific antigens within the thymus, which is critical for the development of central immune tolerance (Kont *et al.* 2008). It is expressed by $CD14^{+}$ monocytes and differentiated dendritic cells cultured *in vitro* (Kogawa *et al.* 2002). The expression of HLA-DR, CD11c, and AIRE by PB-IPCs indicates at that least some PB-IPCs are dendritic cell-like. Occasional PB-IPCs expressed CD11b/Mac-1 indicating they were related to macrophages. At variance, the PB-IPCs reported by Zhao *et al.* (2007) did not express CD11b, CD14, and CD40. A large number of PB-IPCs expressed CD14 during the early stages of culture, however their numbers gradually decreased with time and were replaced by cells expressing CD11c, suggesting perhaps that these monocyte-like cells had differentiated into dendritic-like cells. In accord, a few PB-IPCs moderately expressed CD40, a marker of immature dendritic cells (Banchereau *et al.* 2000), after one week of culture.

PB-IPCs expressed a variety of cell markers which are commonly expressed by monocytes, macrophages, and fibrocytes (monocyte-derived cells that have features of both macrophages and fibroblasts) such as CD45, CD11b, CD11c, CD31, CD68, and CXCR4 (Pilling *et al.* 2009). Fibrocytes express several hematopoietic cell markers, including CD45, the adhesion proteins CD11b, CD11c and CD11d, antigen-presenting factors such as MHC class I and II molecules, CD80 and CD86, and CD34 which is expressed by pluripotent cells (Reilkoff *et al.* 2011). Expression of CD34 allows fibrocytes to be distinguished from macrophages and fibroblasts, which only weakly express CD34 (Reilkoff *et al.* 2011). Thus, PB-IPCs do not appear to be fibrocytes as they lack CD34. PB-IPCs and monocytes both strongly expressed the fibroblast factor prolyl 4-hydroxylase (β-subunit, P4HB, EC 1.14.11.2). However, the β-subunit of prolyl 4-hydroxylase (the Fibroblast antibody immunogen) and protein disulphide-isomerase are products of the same gene and have the same epitopes and therefore antibodies cannot detect the difference between them (Koivu *et al.* 1987; Pihlajaniemi *et al.* 1987; Galligan and Petersen 2012). Protein disulphide-isomerase is a luminal protein widely expressed in the endoplasmic reticulum of mammalian cells including the pancreas, liver, lymph nodes, brain, and spleen (Bjelland 1987). CD68 is not only expressed by monocytes/macrophages, but also weakly expressed by fibroblasts (Pilling *et al.* 2009), and as mentioned above an array of other cell types (Pulford *et al.* 1990; Gottfried *et al.* 2008). Monocytes isolated from a mouse with a schistosome-infection (trematode worm) expressed the fibroblast marker procollagen and CD11b, representing a population of monocytes that were transdifferentiating into fibroblasts (Bertrand *et al.* 1992).

3.12.2 PB-IPCs are not immunosuppressive

The immunosuppressive potential of the PB-IPCs was investigated by determining whether they were capable of inhibiting a mixed lymphocyte response. The PB-IPCs did not appear to be capable of inhibiting a mixed lymphocyte response, but rather the presence of either monocytes or PB-IPCs significantly increased the amount of cell death at later time-points. Previous research has shown that monocytes which express HLA-DR are critical to the mixed lymphocyte response, and increasing the fraction of monocytes present increases cell proliferation during a mixed lymphocyte response (Mann and Abelson 1980). The number of HLA-DR-expressing cells in suspension during the mixed lymphocyte assay increased dramatically indicating cell activation. The increased number of HLA-DR-expressing cells coincided with significant increases in cell death in the mixed lymphocyte response. Initial characterization of PB-IPCs and monocytes in normal culture revealed they strongly express HLA-DR and this would likely have enhanced the mixed lymphocyte response. The presence of PB-IPCs appeared to increase the number of $CD8^+$ cells, whereas the number of $CD4^+$ cells was not altered dramatically, potentially indicating that a cytotoxic T cell response was induced, and conversely that the population of helper T cells and Tregs was not generated or expanded.

FOXP3 was expressed by both the PB-IPCs and monocytes in this study, however, as discussed, neither population were immunosuppressive during an allogeneic mixed lymphocyte response. Therefore the expression of FOXP3 does not promote tolerogenicity, which may require additional factors. $FOXP3^+$ mesenchymal stem cells treated with siRNA to knockdown FOXP3 by 50-70% maintained their immunosuppressive potential during a mixed lymphocyte response, indicating that FOXP3 was not totally responsible for their immunosuppressive potential (Sundin *et al.* 2011). Nevertheless, MSCs with high FOXP3 expression were more immunosuppressive than those with low expression (Sundin *et al.* 2011). Tregs are characterized by their expression

of 3 markers, namely CD4, CD25, and FOXP3 (Zhao *et al.* 2009; Haller *et al.* 2011). The majority of PB-IPCs cannot be considered to be Treg cells as they did not express CD4. In summary, the PB-IPCs generated in the study according to a published procedure are not immunosuppressive, and do not bear the triplet of cell markers that would characterize them as Tregs.

The lack of immune suppression by adult blood PB-IPCs during the mixed lymphocyte response is in marked contrast to the immunosuppressive ability of CB-SCs, which were isolated by Zhao *et al.* (2006) from cord blood using an identical procedure i.e. by attachment to hydrophobic dishes. The researchers discovered that CB-SCs like the PB-IPCs they isolated from adult blood expressed Oct-4, Nanog, CD9, CD45, CD117, and did not express CD34, CD11b, CD14 (Zhao *et al.* 2006; Zhao *et al.* 2007a). A major difference was the fact that only 5% of CB-SCs expressed HLA-ABC, whereas all PB-IPCs strongly expressed this marker (Zhao *et al.* 2006; Zhao *et al.* 2007a). The PB-IPCs isolated in the present study strongly expressed HLA-DR, which may be responsible for the loss of immunosuppressive ability during a mixed lymphocyte response.

The striking similarity of PB-IPCs to cultured monocytes extended to their appearance whereby both populations had similar morphologies, consisting of mostly rounded cells, with the occasional elongated cell that became progressively more flattened during culture. PB-IPCs could be isolated from both healthy control subjects and from diabetic subjects. Therefore if this population of cells could somehow be modified to act like CB-SCs then the subjects own PB-IPCs could be incorporated into Stem Cell Educator therapy. PB-IPCs produced in the present study would pose a potential danger for patients, given their potential to enhance rather than suppress immune responses. They closely resemble monocytes, as evidenced by their phagocytic ability (Aderem and Underhill 1999), and sensitivity to the monocyte killer L-leucine methyl ester (Thiele *et al.* 1983). The phagocytic and lysosomal functionality of PB-IPCs confirms they are a unique population of monocyte-derived cells.

3.12.3 PB-IPCs do not proliferate in the absence of growth factors

The fact that PB-IPCs did not proliferate significantly in the absence of growth factors is also at variance with the findings of Zhao *et al.* (2007), who reported they readily proliferated in hydrophobic dishes. Further support for the lack of proliferation was revealed when it was discovered that the PB-IPCs were senescent after only four days in culture. This study found that as with cancer cells, senescence could be inhibited with PKC (Paget *et al.* 2012). The addition of PKC caused cell clustering which is what would be expected of monocytes after activation of cell-surface integrin cell adhesion molecules (Xue *et al.* 2012). These findings provide further evidence that PB-IPCs are not suitable for stem cell therapy, as they do not self-renew like a true stem cell population, but rather have a very limited lifespan.

3.12.4 Phenotype of differentiated PB-IPCs

Differentiation of PB-IPCs towards the pancreatic lineage into mature insulin-producing cells was not achieved in this study. Replication of the isolation and differentiation protocol published by Zhao *et al.* (2008) did not result in the expression by PB-IPCs of mature pancreatic markers such as insulin, C-peptide, and amylin as reported by Zhao *et al.* Since the paper by Zhao *et*

al. was published in 2008 there has not been a single independent publication in support of the published data. Attempts to prevent the PB-IPCs from becoming senescent prior to differentiation with the Zhao *et al.* (2008) protocol did not improve their ability to be differentiated to insulin-producing cells. They maintained their monocyte-like characteristics despite this pretreatment.

GLP-1 has previously been shown to induce the differentiation of Nestin$^+$ ESCs from primates into insulin-producing cells, by a mechanism involving the upregulation of PDX-1 (Yue *et al.* 2006). In contrast, PDX-1 was not upregulated by PB-IPCs cultured with GLP-1, and the resulting cells did not express insulin. The combination of GLP-1 with EX-4 and nicotinamide did not improve the differentiation of PB-IPCs. Serum-free/low conditions may be required, as reported for the differentiation of hESCs to definitive endoderm with activin A (McLean *et al.* 2007). Alternatively, the successful differentiation of PB-IPCs to insulin-producing cells may require additional factors. An exhaustive study of all potential factors that could drive the differentiation of PB-IPCs towards the β-cell lineage is beyond the scope of the present study.

Attempts to differentiate PB-IPCs towards the pancreatic lineage by the addition of recombinant forms of PDX-1 (naturally cell-permeable) and Pax4 (assisted entry with Pro-DeliverIN) were unsuccessful. Activated virally-expressed forms of PDX-1 successfully transdifferentiated mature hepatocytes into insulin-producing cells (Yamada *et al.* 2006). Liew *et al.* (2008) reported that ESCs transfected with Pax4 differentiated along the pancreatic pathway and expressed proinsulin. Rat epithelial stem-like WB-F344 cells derived from liver expressed NeuroD, Pax4, Nkx6.1, and insulin when cultured for two weeks with high glucose alone, and showed heightened expression of these markers after the addition of PDX-1 protein (Delisle *et al.* 2009). It is possible the PB-IPCs require a prolonged period to transdifferentiate into mature pancreatic cells. Pancreatic gene expression was not seen at earlier time-points (day 6 and 9 of treatment) in the above study by Delisle *et al.* (2009). However, since freshly isolated and plated PB-IPCs already expressed PDX-1, HNF6, CXCR4, and SOX-17, it was hypothesized that differentiation would occur over a short time-frame. PDX-1 caused an increase in the number of CD68 positive cells suggesting an increase in the number of macrophage-like cells, whereas in contrast Pax4 treatment decreased the expression of CD68 and PDX-1, but increased the number of CD14 cells. The expression of Pax4 was not studied as the anti-Pax4 antibody purchased (Abcam, ab42450) was not specific (data not shown), and therefore the results were not included. The treated cells moderately expressed prolyl 4-hydroxylase or disulphide-isomerase. If strong pancreatic differentiation factors are not able to promote the differentiation of PB-IPCs towards β-cells, the approach of combining this strategy with knock down of transcription factors that maintain the monocytic characteristics of PB-IPCs may be required. Thus, a colleague reported that knock down of the transcription factor Ptf1a which maintains the acinar phenotype was able to transform mouse acinar cells into insulin-producing cells when combined with EGF, LIF and nicotinamide (unpublished, Liu *et al.* 2012). Alternatively, higher concentrations of recombinant PDX-1 and Pax4 may be required, as overall the transcription factors had only a slight effect on the differentiation of the PB-IPCs.

3.12.5 Phenotype of spermine-treated PB-IPCs

The addition of spermine successfully downregulated the expression of the immunoregulatory cell activation marker HLA-DR on PB-IPCs and monocytes. However, spermine treatment also downregulated the expression of PDX-1, HNF6, SOX-17, and Nestin. This could indicate that PB-IPC activation is required prior to the induction of pancreatic differentiation, rather than deactivation.

3.12.6 PB-IPCs – a mixed population of cells

Taken together the PB-IPC population is complex, containing cells which express pancreatic differentiation markers, endothelial markers, a stem cell marker, immunoregulatory and monocyte markers, fibrocyte and fibroblast markers. They have the ability to stimulate a mixed lymphocyte response, are phagocytic, are non-proliferative, do not readily differentiate towards the pancreatic lineage, and downregulation of their monocyte-like markers resulted in a concomitant decrease in pancreatic cell markers. Therefore the PB-IPC population contains a mixed population of cells. The entire PB-IPC population strongly expresses a number of different monocyte markers, so they are at least monocyte-like, potentially in the process of transdifferentiation along a number of different cell lineages. However, it was not possible to perform directed differentiation of PB-IPCs towards the pancreatic lineage with the protocol published by Zhao *et al.* (2008), and with the in-house differentiation protocols trialled. The results suggest that PB-IPCs represent a unique population of monocytes capable of adhering to hydrophobic surfaces that may play a role in presenting tissue-specific antigens including pancreatic antigens. Cell sorting based on particular cell markers may lead to a population of cells that alone can be differentiated towards the pancreatic lineage, as it has not been possible to differentiate these cells as a heterogeneous population of cells. The very rare subpopulation of alkaline phosphatase positive cells warrant further investigation as they may most closely resemble stem cells. The only concern here is that they did not express alkaline phosphatase activity until day three which does not support them being stem cells, unless they were spontaneously dedifferentiating.

Chapter 4 Programmable Cells of Monocytic Origin and Fibroblast-resembling-macrophages

4.1 Scope of chapter

PBMCs have been dedifferentiated into PCMOs and f-MOs, which are plastic and can be differentiated towards the pancreatic cell lineage and other cell lineages (Zhao *et al.* 2003; Ruhnke *et al.* 2005). Here, attempts were made to replicate these findings, and to improve the differentiation protocols. Attempts were made to differentiate PCMOs and/or f-MOs to pancreatic cells with islet cell conditioning medium (ICM), to endothelial cells with $VEGF_{165}$, to neural cells with NGFβ, and to T lymphocytes with IL-2.

4.2 Generation of PCMOs, and attempts to differentiate them towards the pancreatic cell lineage

4.2.1 Dedifferentiation of PBMC to PCMOs

Monocytes from 2 different donors were dedifferentiated to form PCMOs according to the protocol published by Ruhnke *et al.* (2005). PBMCs were resuspended at 1-2 x 10^6 cells/mL in full RPMI media containing 7% FBS and allowed to attach to conventional and hydrophobic culture dishes for 2 h at 37°C in 5% CO_2. The medium was then removed and the wells were washed thrice with full RPMI media containing 7% FBS to remove remaining unattached cells such as lymphocytes. The resulting attached cell populations were dedifferentiated into PCMOs over 6 days in the same dishes in full RPMI media containing 140 μM β-mercaptoethanol, 5 ng/mL M-CSF, 0.4 ng/mL IL-3 (CYT-417, ProSpec-TechnoGene Ltd.), and 7% FBS. The results presented below are representative of 2 separate experiments.

Morphologically the cells cultured in the hydrophobic dishes were mostly aggregated, whereas cells cultured in the tissue culture dishes formed both cell aggregates and monolayers (Figure 4.1 and Figure 4.2). The resulting cells strongly expressed CD14 and CD68 (Figure 4.1 and Figure 4.2). In comparison, only 20% of PB-IPCs had expressed CD14 (see Chapter 3). The PCMOs expressed PDX-1, which appeared to be located within the cell nuclei (Figure 4.1 and Figure 4.2). SOX-17 expression was weakly detectable (Figure 4.1 and Figure 4.2). As expected, the pancreatic markers amylin, GPR40, insulin, Nkx6.1 and Wnt-3 were not expressed (Figure 4.1 and Figure 4.2). The T cell activation marker CD154 and the dendritic (or cortical thymic epithelial) cell marker CD205 were also not expressed (Figure 4.1 and Figure 4.2). A summary of these findings is presented in Table 4.1.

Culture on hydrophobic dishes

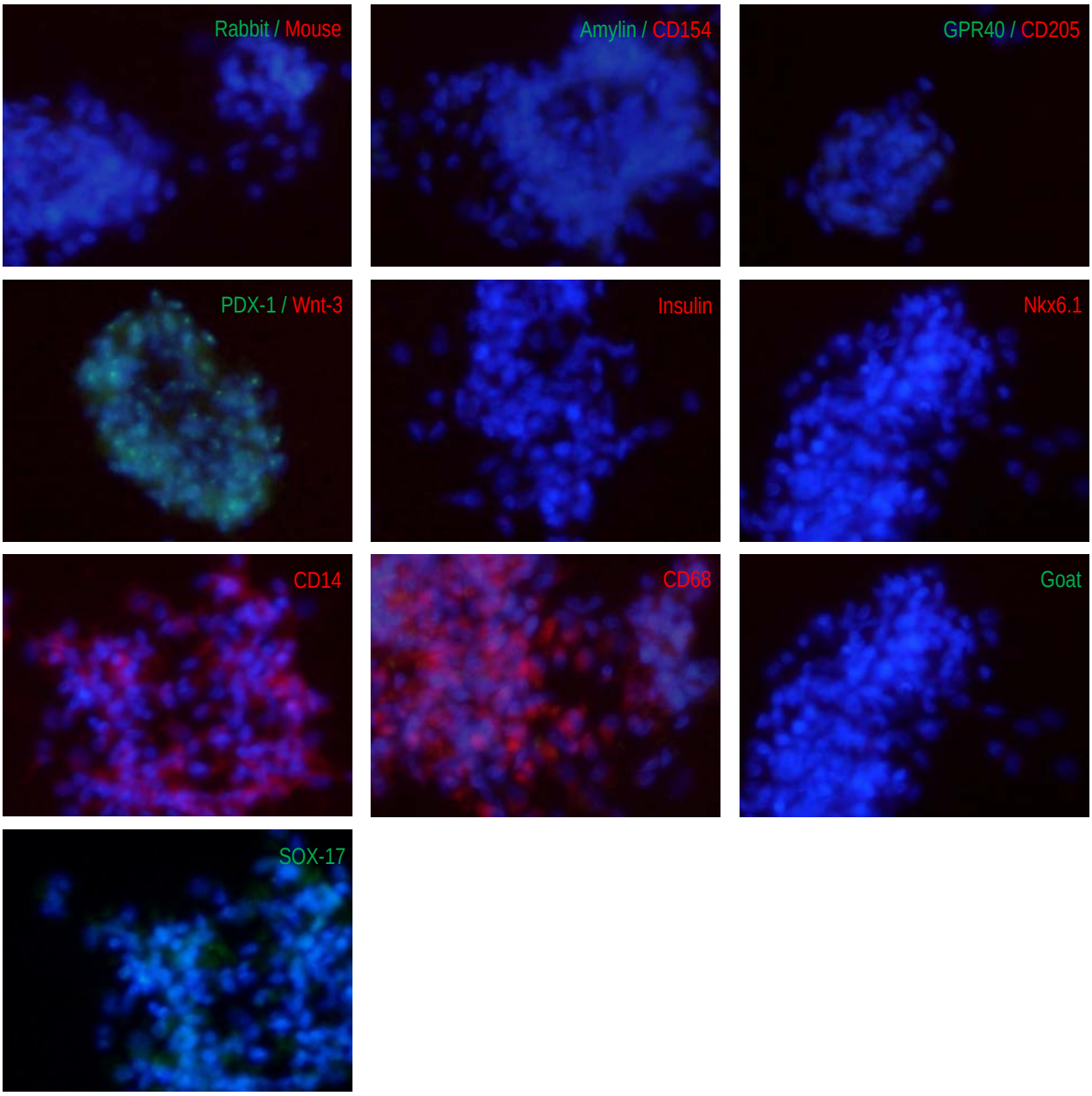


Figure 4.1 Dedifferentiation of PBMCs into PCMOs in hydrophobic dishes.

PBMCs adherent to hydrophobic dishes were cultured for 6 days in the same dishes in full RPMI media containing 140 μM β-mercaptoethanol, 5 ng/mL M-CSF, 0.4 ng/mL IL-3, and 7% FBS (n=2). Cells were stained for the expression of various cell markers. Immunoreactivity was detected with donkey anti-rabbit and donkey anti-goat antibodies (green) and with a donkey anti-mouse antibody (red). Cell nuclei were stained blue with DAPI. Images were taken at 200x magnification. The images are presented so that the staining obtained with each IgG control immediately precedes stainings with antibodies of the same host species.

Culture on tissue culture dishes

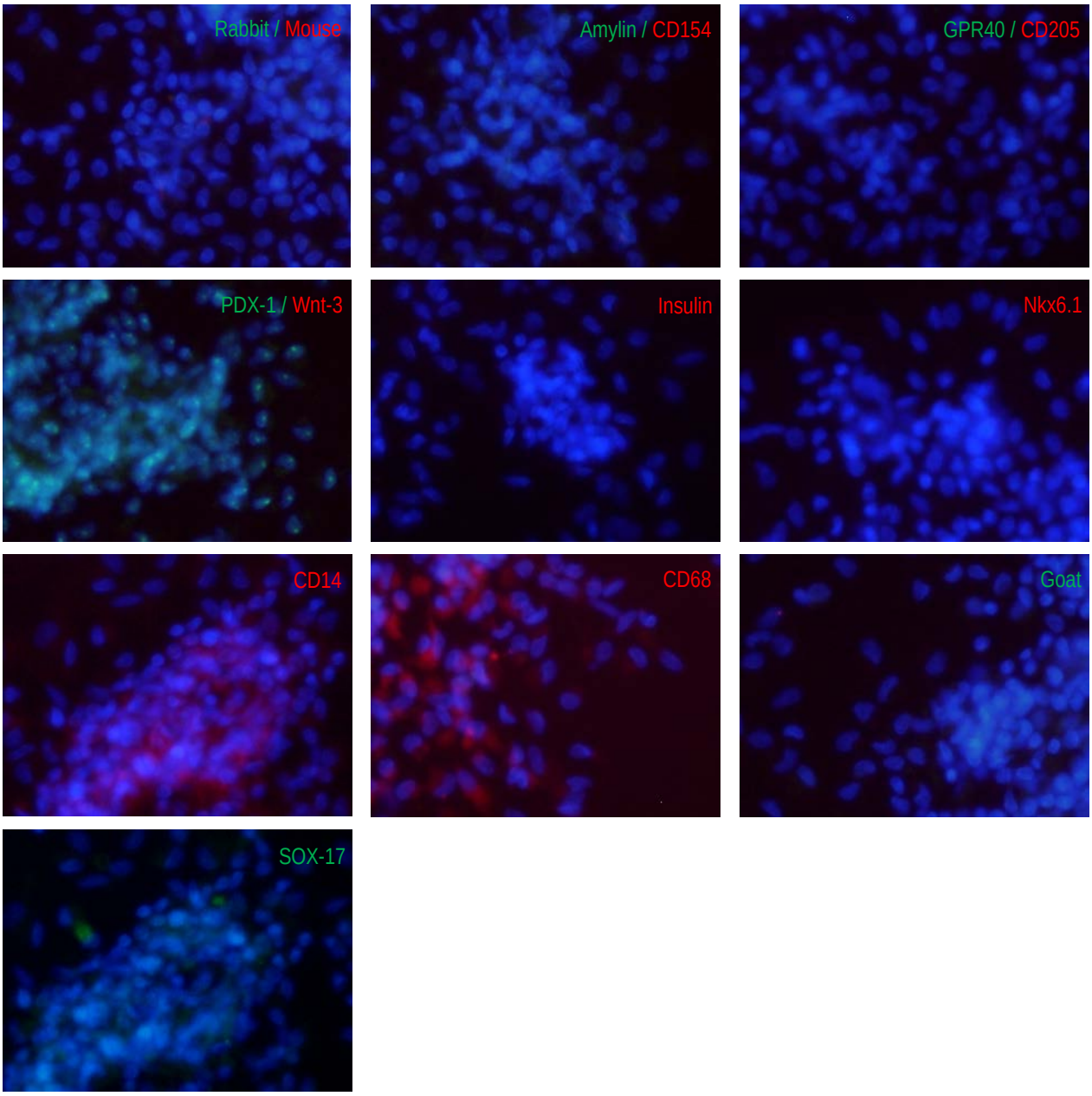


Figure 4.2 Dedifferentiation of PBMCs into PCMOs in tissue culture dishes.

PBMCs adherent to tissue culture dishes were cultured for 6 days in the same dishes in full RPMI media containing 140 μM β-mercaptoethanol, 5 ng/mL M-CSF, 0.4 ng/mL IL-3, and 7% FBS (n=2). Cells were stained for the expression of various cell markers. Immunoreactivity was detected with donkey anti-rabbit and donkey anti-goat antibodies (green) and with a donkey anti-mouse antibody (red). Cell nuclei were stained blue with DAPI. Images were taken at 200x magnification. The images are presented so that the staining obtained with each IgG control immediately precedes stainings with antibodies of the same host species.

Table 4.1 Summary of the phenotyping of PBMCs dedifferentiated into PCMOs

	HY	TC
CD14	x x x	x x x
SOX-17	x	x
CD68	x x x	x x x
CD154		
Amylin		
CD205		
GPR40		
Insulin		
Nkx6-1		
Wnt-3		
PDX-1	x x	x x

0	0.1-20	21-40	41-60	61-80	81-100

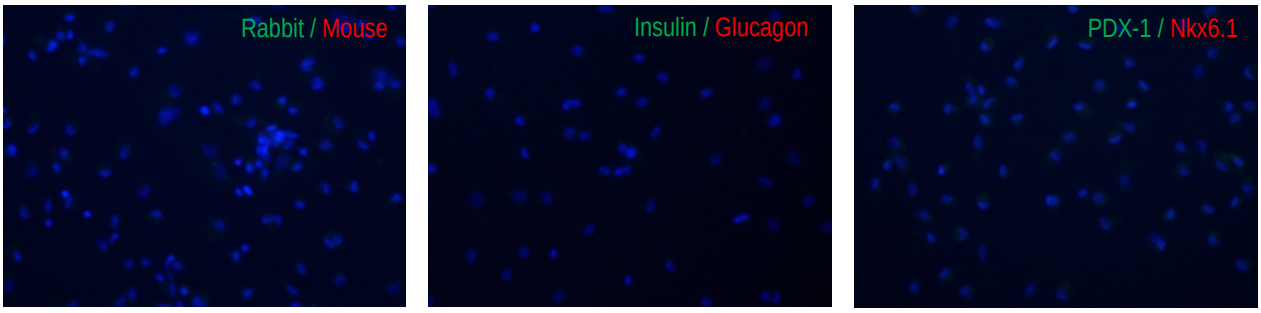
x	x x	x x x

Intensity of staining – weak/moderate/strong

Abbreviations: HY: culture in hydrophobic dishes, TC: culture in tissue culture dishes.

4.2.2 Islet cell conditioning medium is not able to differentiate PCMOs into pancreatic cells

PCMO from 1 donor were cultured for 1 week in either ICM or control medium (full RPMI media containing 10% FBS) in tissue culture dishes. ICM is RPMI1640 media (11879-020, Gibco) containing 10 ng/mL EGF (PHG0314, Invitrogen), 20 ng/mL HGF (294-HG/CF, R&D Systems), 10 mmol/L nicotinamide (N5535, Sigma), and 5 mmol/L glucose (G8270, Sigma) (Ruhnke *et al.* 2005). The majority of the cells cultured in ICM (Figure 4.4) continued to strongly express HLA-DR and CD14 albeit HLA-DR expression was reduced compared to cells cultured in control medium (Figure 4.3). Unfortunately the ICM-treated PCMO did not express PDX-1, insulin, glucagon, Nkx6.1, NeuroD, Pax6, NGN3 or Glut-2 (Figure 4.3 and Figure 4.4). A summary of these findings compared with the published results (Ruhnke *et al.* 2005) is presented in Table 4.2.



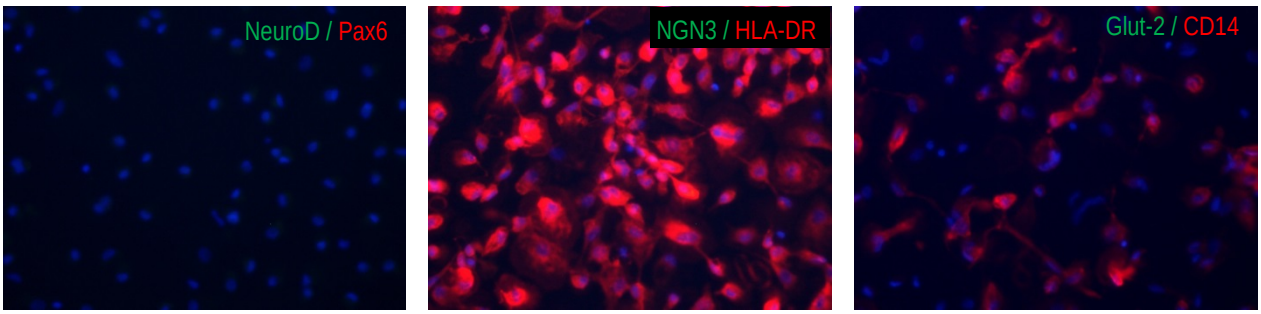


Figure 4.3 Dedifferentiation of PBMCs into PCMOs, followed by culture in control medium.

PBMCs were cultured for 6 days in PCMO dedifferentiation medium (full RPMI media containing 140 μM β-mercaptoethanol, 5 ng/mL M-CSF, 0.4 ng/mL IL-3, and 7% FBS), followed by culture for 1 week in control medium (full RPMI media containing 10% FBS) (n=1). Cells were stained for the expression of various cell markers. Immunoreactivity was detected with donkey anti-rabbit, and donkey anti-goat antibodies (green) and with a donkey anti-mouse antibody (red). Cell nuclei were stained blue with DAPI. Images were taken at 200x magnification. The images are presented so that the staining obtained with each IgG control immediately precedes stainings with antibodies of the same host species.

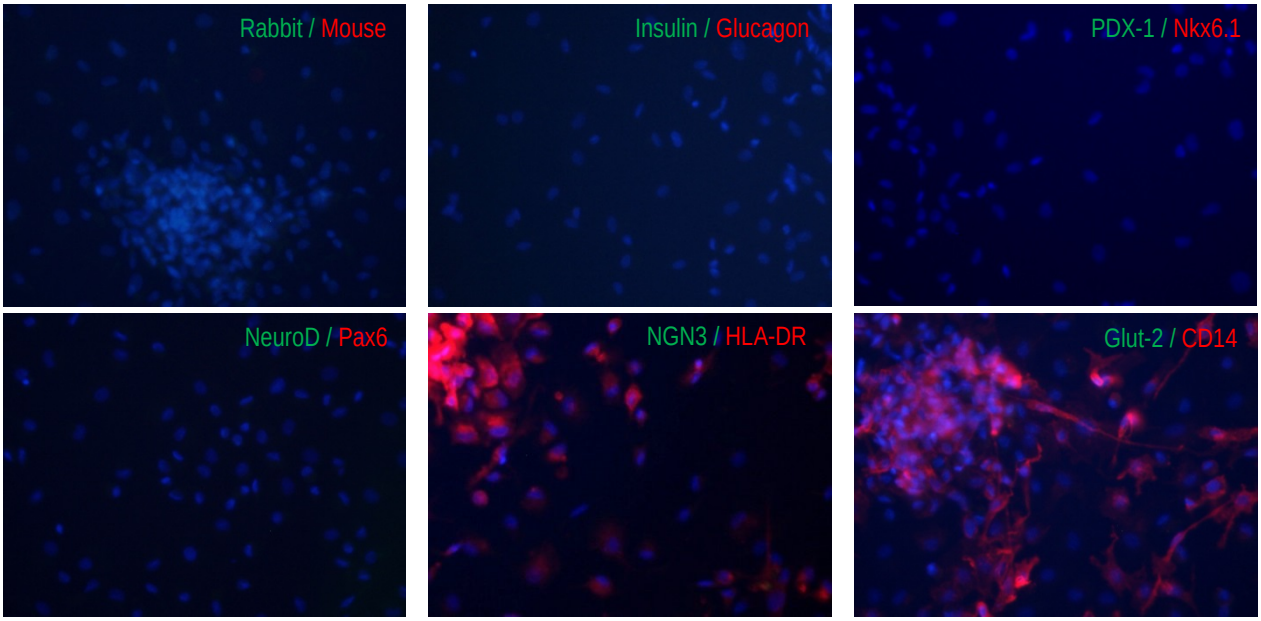


Figure 4.4 Attempt to differentiate PCMOs into pancreatic cells using islet cell conditioning medium.

PBMCs were cultured for 6 days in PCMO dedifferentiation medium (full RPMI media containing 140 μM β-mercaptoethanol, 5 ng/mL M-CSF, 0.4 ng/mL IL-3, and 7% FBS), followed by culture for 1 week in ICM (full RPMI medium containing 10 ng/mL EGF, 20 ng/mL HGF, 10 mM nicotinamide, and 5 mM glucose) (n=1). Cells were stained for the expression of various cell markers. Immunoreactivity was detected with donkey anti-rabbit and donkey anti-goat antibodies (green) and with a donkey anti-mouse antibody (red). Cell nuclei were stained blue with DAPI. Images were taken at 200x magnification. The images are presented so that the staining obtained with each IgG control immediately precedes stainings with antibodies of the same host species.

Table 4.2 Summary of the phenotyping of PCMO differentiated with islet cell conditioning medium (ICM) or control medium[a]

Condition for first 6 days	Condition for 1 week	Insulin	Glucagon	PDX-1	Nkx6.1	NeuroD	Pax6	NGN3	HLA-DR	Glut-2	CD14
PCMO (IL-3 + M-CSF in 10% FBS)	ICM	N	N	N	N	N	N	N	94% strong	N	84%
PCMO (IL-3 + M-CSF in 10% FBS)	Control medium	N	N	N	N	N	N	N	100% v strong	N	77%
Ruhnke (IL-3 + M-CSF in 7% FBS)	ICM	45%	34%	60%	mRNA	mRNA	mRNA	mRNA	-	mRNA	-

[a]The results are presented as the percentage of cells that express a particular marker. N - negative, no expression of cell marker. The published results of Ruhnke *et al.* (2005) are shown in the bottom row. The results are presented as the percentage of cells that express a particular marker, as determined by flow cytometry; mRNA, expression of mRNA encoding a particular marker was detected; "-"represents not tested.

4.3 Generation of f-MOs, and attempts to differentiate them towards the pancreatic cell lineage

4.3.1 Dedifferentiation of PBMCs to f-MOs

Monocytes from 2 different donors were induced to form f-MOs according to a protocol developed by Zhao *et al.* (2003). PBMCs were allowed to attach to tissue culture plates for 2 h in full RPMI media containing 10% FBS. Non-adherent cells were removed by washing the cells thrice with full medium. The attached monocytes were then induced to become f-MOs by culture for 11 days in the same dishes with full RPMI media containing 10% FBS and 50 ng/mL M-CSF. The medium containing M-CSF was refreshed every 2-3 days. PBMCs from 2 different donors cultured in the absence of M-CSF remained mostly round in shape, whereas cells cultured in the presence of M-CSF adopted the spindle-shaped morphology characteristic of f-MOs (Figure 4.5).

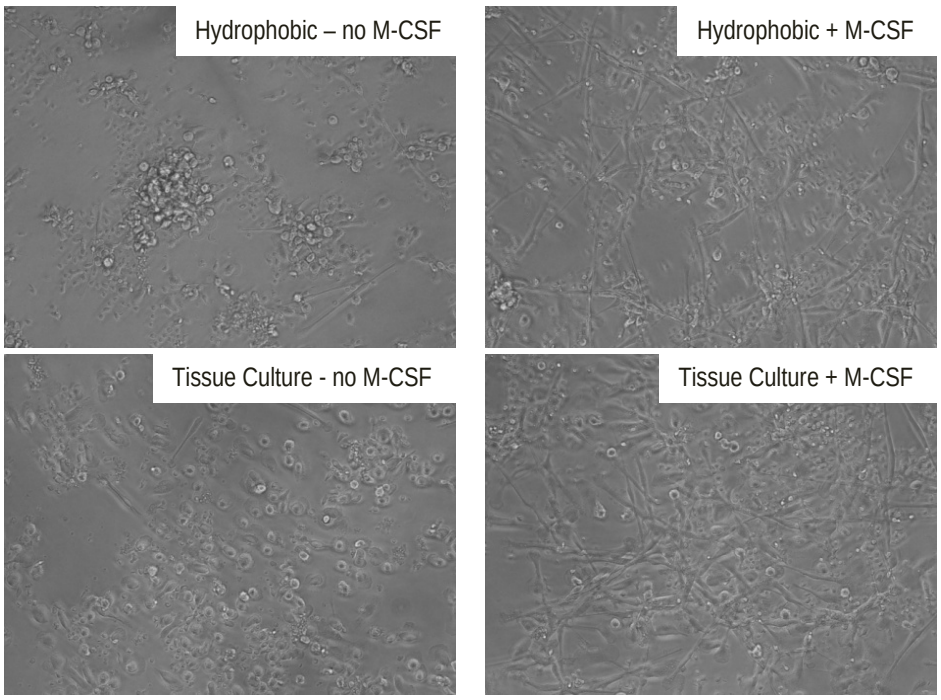


Figure 4.5 M-CSF-induced differentiation of PBMCs into f-MOs.

PBMCs that adhered to tissue culture and hydrophobic dishes were cultured for 11 days in the same dishes in full RPMI media containing 10% FBS, with and without 50 ng/mL M-CSF (n=2). Phase contrast images were taken at 200x magnification.

4.3.2 Islet cell conditioning medium is not able to differentiate f-MOs into pancreatic cells

f-MOs from different 2 donors generated as above in tissue culture dishes were cultured for 1 week in ICM to induce pancreatic differentiation, or in control medium (full RPMI media containing 10% FBS). A control population of PBMCs (monocytes) that attached to tissue culture dishes were cultured for 18 days in control medium. Half of the f-MOs cultured in ICM continued to express CD14, as did the f-MOs cultured in control medium, whereas only 32% of monocytes expressed this antigen (Figure 4.6, Figure 4.7, and Figure 4.8). Over half of the f-MOs cultured in ICM and control medium appeared to express PDX-1 in their nuclei (Figure 4.6 and Figure 4.7). Fewer f-MOs (64%) cultured for 1 week in control medium expressed PDX-1 compared to the monocytes (100%) cultured for 18 days in control medium (Figure 4.6 and Figure 4.8). The undifferentiated f-MOs, differentiated f-MO, and the monocytes did not express the pancreatic markers NeuroD or insulin (Figure 4.6, Figure 4.7, and Figure 4.8).

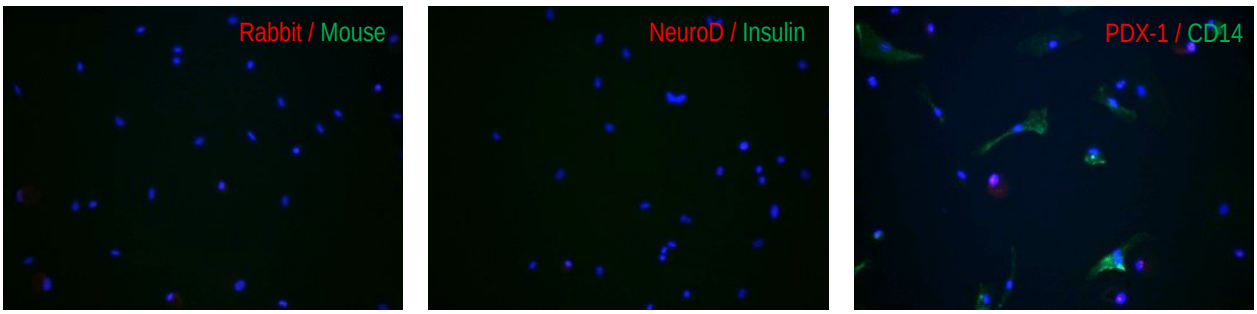


Figure 4.6 Differentiation of PBMCs to f-MOs and their culture in control medium.

PBMCs that adhered to tissue culture dishes were cultured for 11 days in the same dishes in full RPMI media containing 10% FBS, and 50 ng/mL M-CSF, and then for 1 week in the same medium lacking M-CSF (n=2). f-MOs were stained for the expression of various cell markers. Immunoreactivity was detected with a donkey anti-rabbit antibody (red), and a donkey anti-mouse antibody (green). Cell nuclei were stained blue with DAPI. Images were taken at 200x magnification. The images are presented so that the staining obtained with each IgG control immediately precedes stainings with antibodies of the same host species.

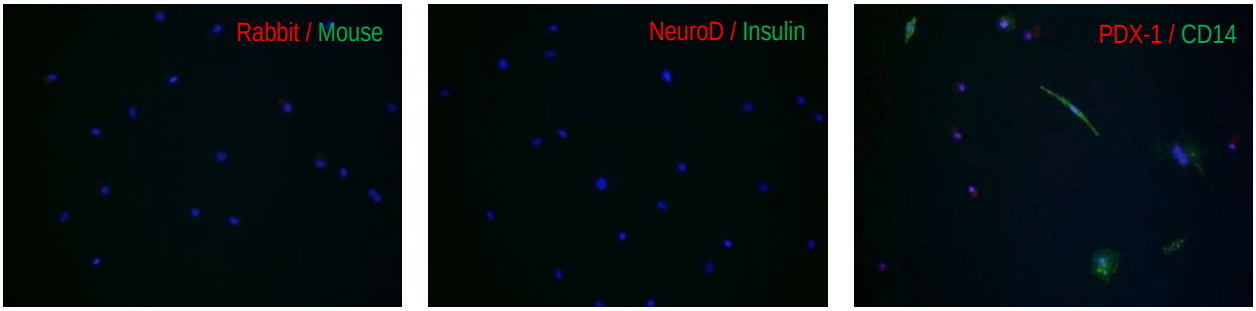


Figure 4.7 Differentiation of f-MOs with islet cell conditioning medium.

PBMCs that adhered to tissue culture dishes were cultured for 11 days in the same dishes in full RPMI media containing 10% FBS, and 50 ng/mL M-CSF. The f-MOs were then cultured for 1 week in ICM (full RPMI media containing 10 ng/mL EGF, 20 ng/mL HGF, 10 mM nicotinamide, and 5 mM glucose) (n=2). Cells were stained for the expression of various cell markers. Immunoreactivity was detected with a donkey anti-rabbit antibody (red), and a donkey anti-mouse antibody (green). Cell nuclei were stained blue with DAPI. Images were taken at 200x magnification. The images are presented so that the staining obtained with each IgG control immediately precedes stainings with antibodies of the same host species.

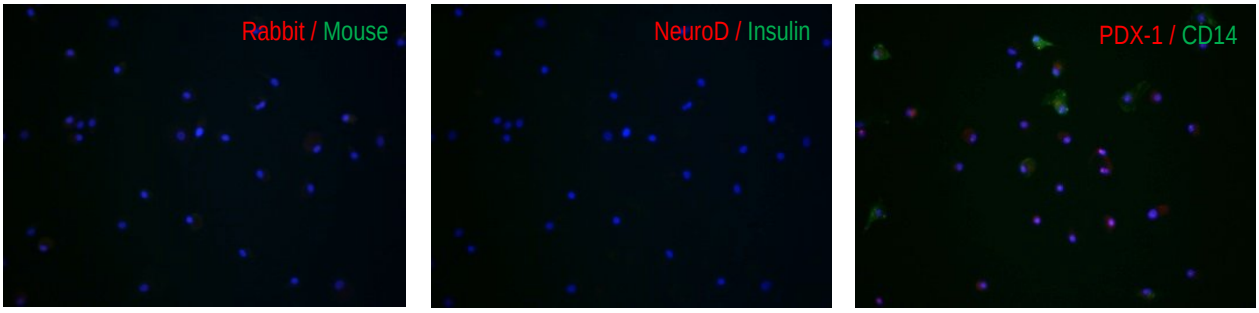


Figure 4.8 Culture of monocytes for 18 days in control medium.

PBMC-derived monocytes that adhered to tissue culture dishes were cultured for 18 days in the same dishes in control medium (full RPMI media containing 10% FBS) (n=2). Monocytes were stained for the expression of various cell markers.

Immunoreactivity was detected with a donkey anti-rabbit antibody (red), and a donkey anti-mouse antibody (green). Cell nuclei were stained blue with DAPI. Images were taken at 200x magnification. The images are presented so that the staining obtained with each IgG control immediately precedes stainings with antibodies of the same host species.

4.3.3 Differentiation of f-MOs to other cell lineages

Attempts were made to differentiate f-MOs prepared from 1 donor to other cell lineages including endothelial cells, neural cells, and T lymphocytes. f-MOs were obtained by culture of monocytes with M-CSF for 11 days. They were then cultured for 5 days in control medium (full RPMI media containing 10% FBS) containing a lineage-specific differentiation factor. They were compared with monocytes that were cultured in control medium for 16 days.

4.3.3.1 Endothelial differentiation with $VEGF_{165}$

Zhao *et al.* (2003) reported that f-MOs differentiated with $VEGF_{165}$ became 70% endothelial and 30% neuronal. To test whether the f-MOs isolated here also showed this plasticity they were cultured for 5 days with full RPMI media containing 10% FBS and 50 ng/mL $VEGF_{165}$ (ab56620, Abcam Inc.). The resulting cells strongly expressed HLA-DR (Figure 4.9). The endothelial marker vWF was only weakly expressed by a subpopulation of cells, whereas the neuronal maker NSE was not detected. The culture was contaminated by T cells as evidenced by expression of CD3 and CD4 by several cells (Figure 4.9). As expected, the pancreatic cell markers Glut-2 and glucagon were not detected (Figure 4.9).

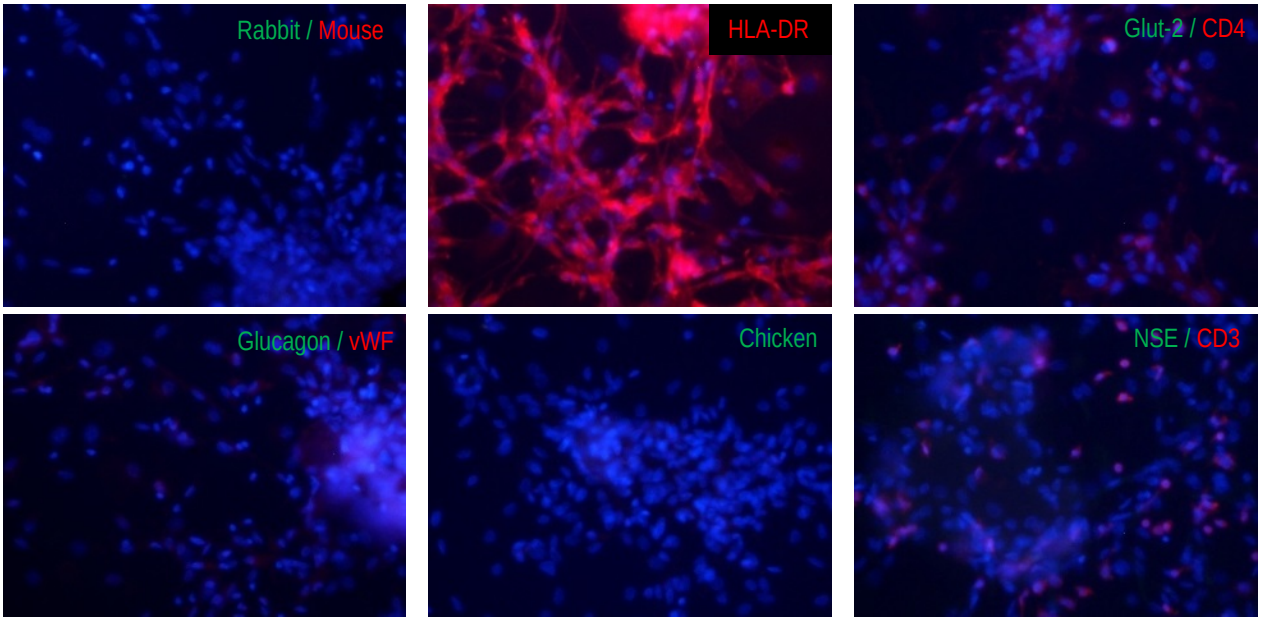


Figure 4.9 Attempt to differentiate f-MOs to endothelial cells with $VEGF_{165}$.

Monocytes that adhered to tissue culture dishes were cultured for 11 days in the same dishes in full RPMI media containing 10% FBS, and 50 ng/mL M-CSF (n=1). The f-MOs were then cultured for 5 days in full RPMI media containing 10% FBS, and 50 ng/mL $VEGF_{165}$. Cells were stained for the expression of various cell markers. Immunoreactivity was detected with donkey anti-rabbit and goat anti-chicken antibodies (green), and with a donkey anti-mouse antibody (red). Cell nuclei were stained blue with DAPI. Images were taken at 200x magnification. The images are presented so that the staining obtained with each IgG/IgY control immediately precedes stainings with antibodies of the same host species.

4.3.3.2 Neuronal differentiation with NGFβ

Zhao *et al.* (2003) reported that f-MOs differentiated with NGFβ became 90% neuronal. f-MOs were cultured for 5 days in full RPMI media containing 10% FBS and 200 ng/mL of NGFβ (N1408, R&D Systems) to determine whether they would form cells with a neural-like phenotype. Culture of f-MOs with NGFβ led to expression of the neural marker NSE by just 6% of the cells (Figure 4.10). HLA-DR was strongly expressed by most cells, whereas vWF was weakly expressed by a small number of cells. Staining with antibodies against CD4 and CD3 revealed that the cultures were contaminated with T cells (Figure 4.10). As expected, expression of Glut-2 and glucagon was not detected (Figure 4.10).

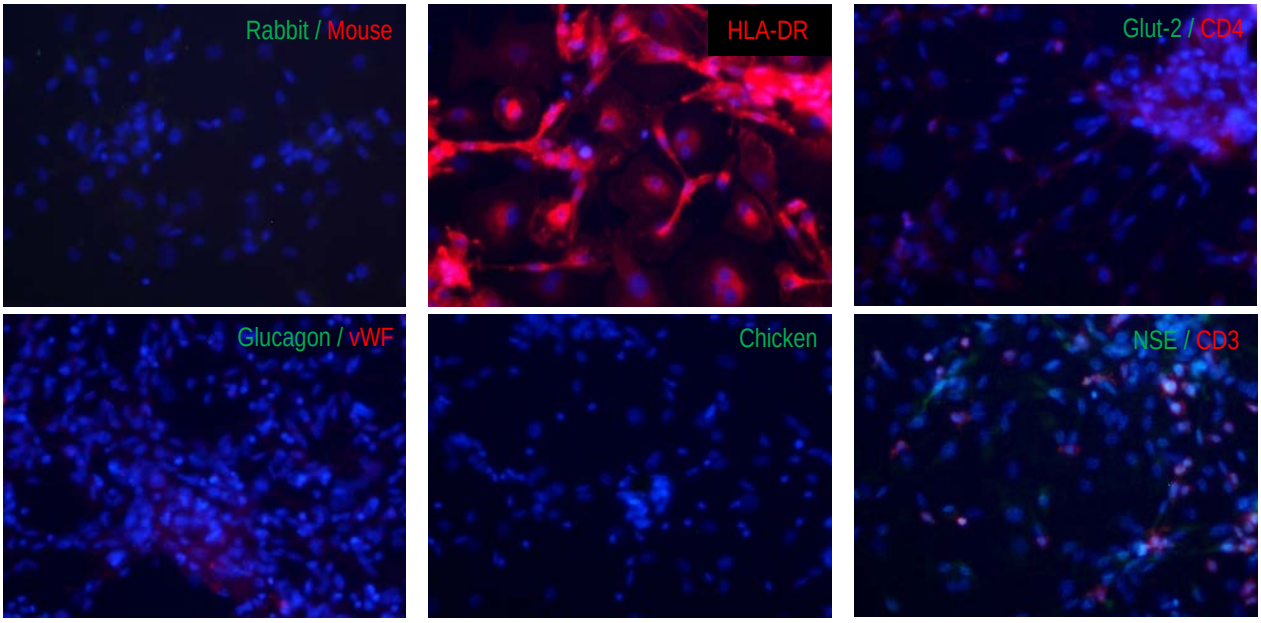


Figure 4.10 Attempt to differentiate f-MOs to neural cells with NGFβ.

Monocytes that adhered to tissue culture dishes were cultured for 11 days in the same dishes in full RPMI media containing 10% FBS, and 50 ng/mL M-CSF (n=1). The f-MOs were then cultured for 5 days in full RPMI media containing 10% FBS, and 200 ng/mL NGFβ. Cells were stained for the expression of various cell markers. Immunoreactivity was detected with donkey anti-rabbit and goat anti-chicken antibodies (green), and with a donkey anti-mouse antibody (red). Cell nuclei were stained blue with DAPI. Images were taken at 200x magnification. The images are presented so that the staining obtained with each IgG/IgY control immediately precedes stainings with antibodies of the same host species.

4.3.3.3 T lymphocyte differentiation with IL-2

Zhao *et al.* (2003) reported that f-MOs form T lymphocytes after differentiation with IL-2. f-MOs were cultured for 5 days in full RPMI media containing 10% FBS and 1,200 U/mL of IL-2 (CYT-095, ProSpec-TechnoGene Ltd.) to determine whether they would form cells with a T lymphocyte phenotype. The majority of the resulting cells very strongly expressed HLA-DR, and a few cells weakly expressed vWF (Figure 4.11). As expected, the numbers of CD3 and CD4 expressing T cells were expanded, due either to proliferation of contaminating T cells, or due to differentiation of f-MOs into T cells (Figure 4.11). Expression of Glut-2, glucagon and NSE was not detected (Figure 4.11). A summary of the phenotyping of f-MOs following their differentiation with the above differentiation factors is shown in Table 4.3.

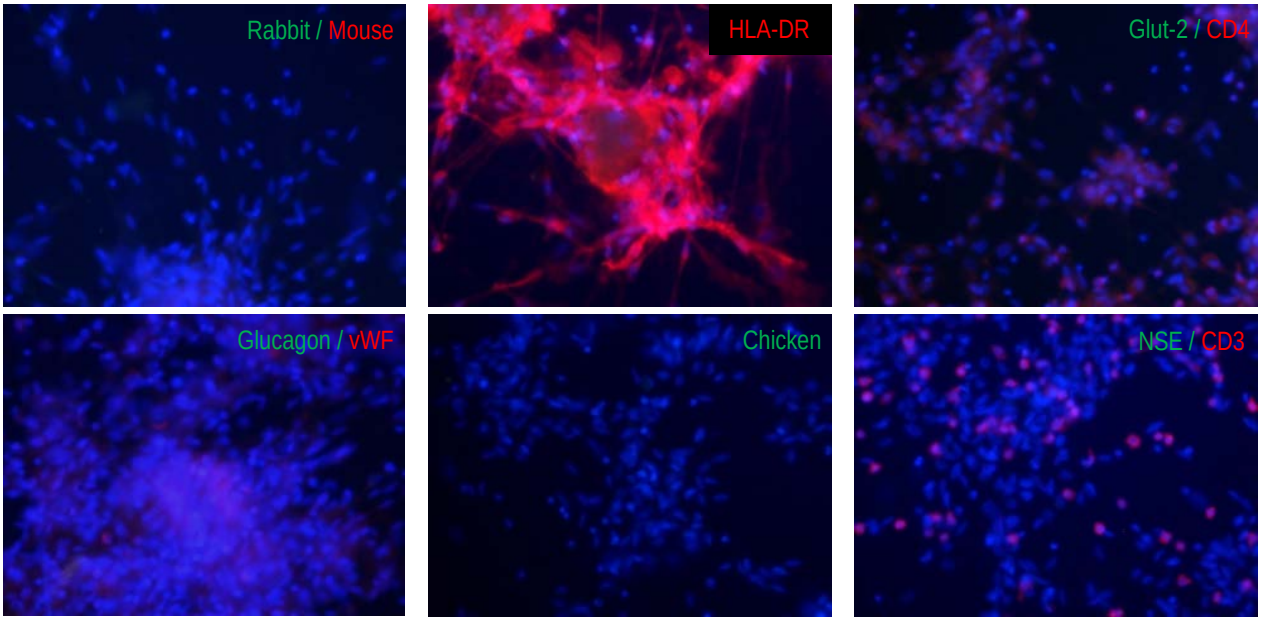


Figure 4.11 Attempt to differentiate f-MOs to T lymphocytes with IL-2.

Monocytes that adhered to tissue culture dishes were cultured for 11 days in the same dishes in full RPMI media containing 10% FBS, and 50 ng/mL M-CSF (n=1). The f-MOs were then cultured for 5 days in full RPMI media 10% FBS, and 1,200 units/mL of IL-2. Cells were stained for the expression of various cell markers. Immunoreactivity was detected with donkey anti-rabbit and goat anti-chicken antibodies (green), and with a donkey anti-mouse antibody (red). Cell nuclei were stained blue with DAPI. Images were taken at 200x magnification. The images are presented so that the staining obtained with each IgG/IgY control immediately precedes stainings with antibodies of the same host species.

4.3.3.4 Phenotype of monocytes cultured for 16 days in control medium

Monocytes that adhered to tissue culture dishes were cultured for 16 days in the same dishes in control medium (full RPMI media containing 10% FBS). The resulting cells strongly expressed HLA-DR (Figure 4.12). Some cells weakly expressed vWF, and occasional CD4 and CD3 contaminating T cells were present (Figure 4.12). Expression of Glut-2, glucagon and NSE was not detected (Figure 4.12).

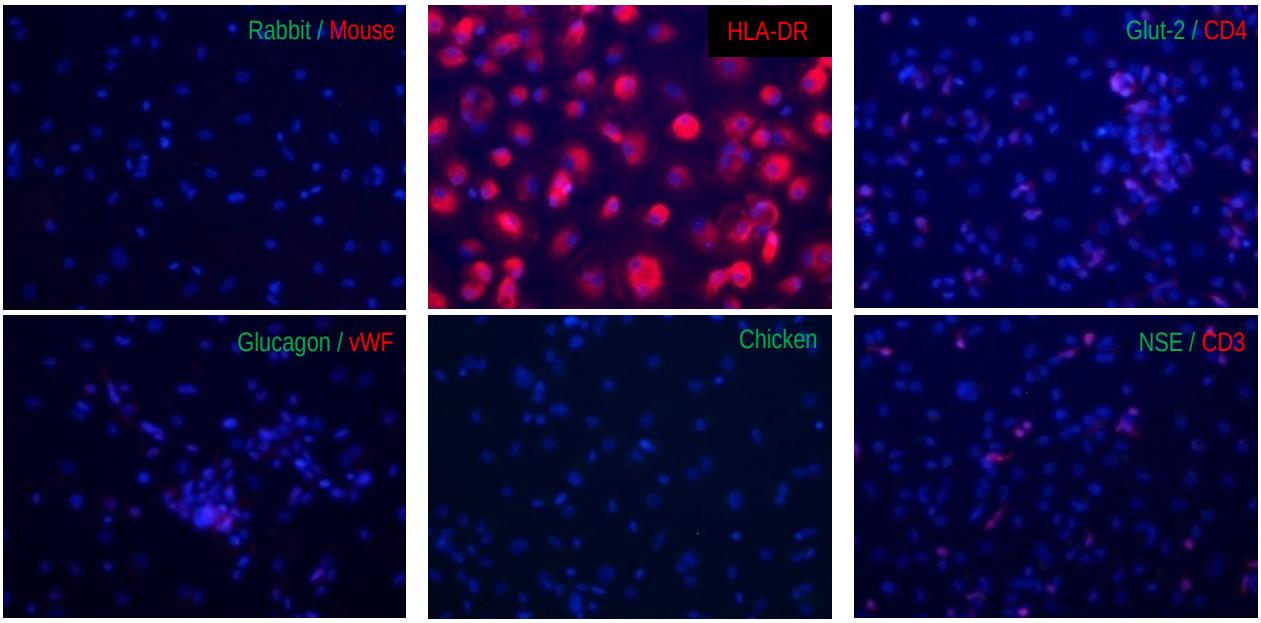


Figure 4.12 Phenotyping of monocytes cultured for 16 days in control medium.

Monocytes that adhered to tissue culture dishes were cultured for 16 days in the same dishes in full RPMI media containing 10% FBS (n=1). Cells were stained for the expression of various cell markers. Immunoreactivity was detected with donkey anti-rabbit and goat anti-chicken antibodies (green), and with a donkey anti-mouse antibody (red). Cell nuclei were stained blue with DAPI. Images were taken at 200x magnification. The images are presented so that the staining obtained with each IgG/IgY control immediately precedes stainings with antibodies of the same host species.

Table 4.3 Summary of the phenotype of differentiated f-MOs

	Condition 1	Condition 2	HLA-DR	Glut-2	CD4	Glucagon	vWF	NSE	CD3
	Control	Control	x x x		x		x		x x
Zhao*	Control	Control			x x x		x x x	x x x	x x x
	M-CSF	$VEGF_{165}$	x x x		x x		x		x x
Zhao*	M-CSF	$VEGF_{165}$					x x x	x x x	
	M-CSF	NGFβ	x x x		x x		x	x	x x
Zhao*	M-CSF	NGFβ						x x x	
	M-CSF	IL-2	x x x		x x		x		x x
Zhao*	M-CSF	IL-2			x x x				x x x

0	0.1-20	21-40	41-60	61-80	81-100	% Positive

x	x x	x x x	Intensity of staining - weak/moderate/strong

Not tested by Zhao *et al.* (2003)

*The results by Zhao *et al.* have been interpreted form their paper (Zhao *et al.* 2003).

4.3.3.5 Morphologies of differentiated f-MOs

f-MOs have a fibroblast-like (Zhao *et al.* 2003) or filamentous appearance (Figure 4.5), hence it was of interest to learn whether the above differentiated f-MOs would retain this appearance. f-MOs treated with $VEGF_{165}$ were mostly elongated cells with some round-shaped cells present (Figure 4.13). f-MOs treated with NGFβ were mostly elongated cells which appeared to form linkages reminiscent of neural networks, in accord with the fact that some of the cells expressed the neural marker NSE (Figure 4.13). f-MOs cultured with IL-2 formed both elongated cells and round-shaped cells in tight clusters (Figure 4.13). The clusters appeared to be CD4+ cells, as seen in Figure 4.11. As expected, monocytes cultured in the absence of added growth factors had a rounded morphology (Figure 4.13).

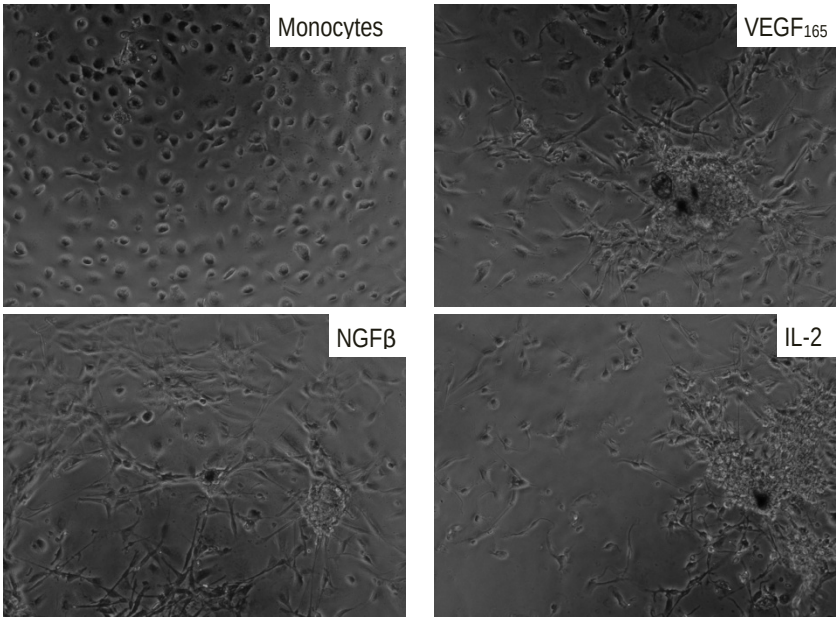


Figure 4.13 Phase contrast images of differentiated f-MOs.

Phase contrast images of f-MOs differentiated for 5 days with $VEGF_{165}$, NGFβ, and IL-2, respectively (n=1). Monocytes are shown for comparison. Images were taken at 200x magnification.

4.4 PCMOs and f-MOs rapidly become senescent

The resistance of PCMOs and f-MOs to differentiation towards the pancreatic lineage as observed here suggested the cells may be undergoing senescence. PCMOs and f-MOs were generated from 2 separate donors as above using tissue culture dishes, and cultured for 4 and 11 days, and their state of senescence was investigated by incubating the cells with X-gal to detect senescence-associated β-galactosidase. The images in Figure 4.14 are representative of the results obtained. Both the PCMOs and f-MOs were senescent at days 4 and 11 (Figure 4.14). They were tested for the expression of stem cell associated alkaline

phosphatase activity at day 11 of culture, and were found to be lacking this stem-cell-associated activity (Figure 4.15). Cultured monocytes were also senescent at days 4 and 11 (Figure 4.14), and did not express alkaline phosphatase activity (Figure 4.15).

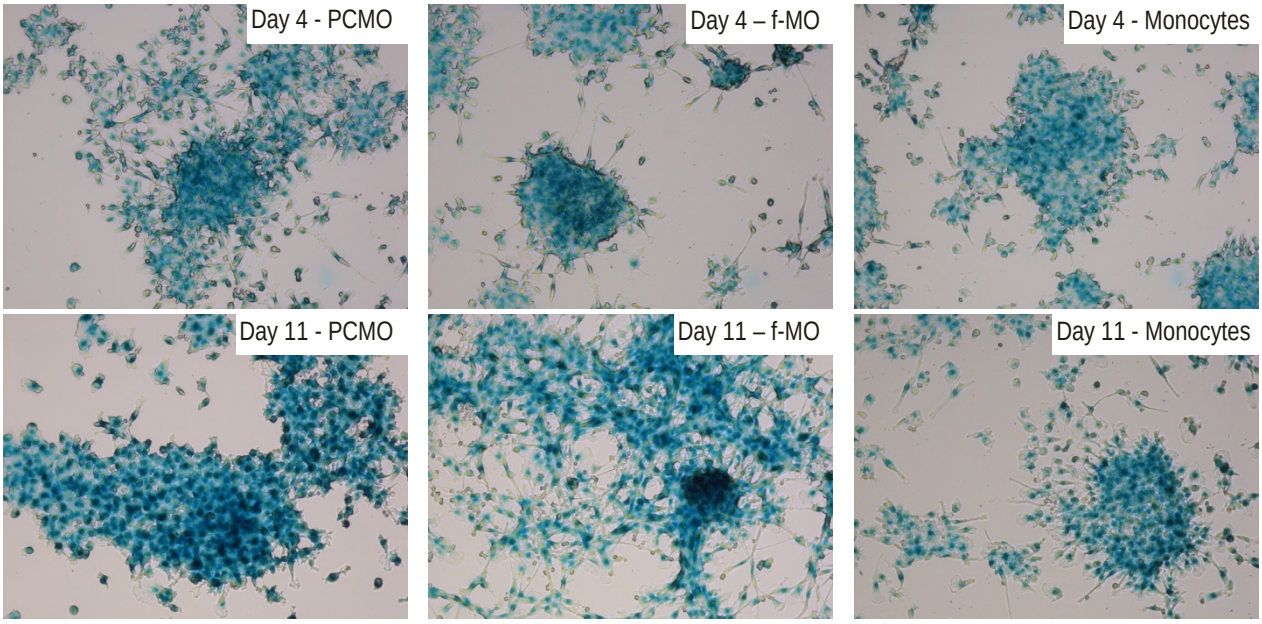


Figure 4.14 PCMOs and f-MOs are senescent after 4 days of culture.

Monocytes that adhered to tissue culture dishes were cultured for up to 11 days in the same dishes in control media, in PCMO dedifferentiation medium (full RPMI media containing 140 μM β-mercaptoethanol, 5 ng/mL M-CSF, 0.4 ng/mL IL-3, and 7% FBS) to form PCMOs, or in full RPMI media containing 10% FBS, and 50 ng/mL M-CSF to form f-MOs (n=2). PCMOs, f-MO, and monocytes were stained with X-gal (blue) to detect senescence-associated β-galactosidase at days 4 and 11. Bright field images were taken at 200x magnification.

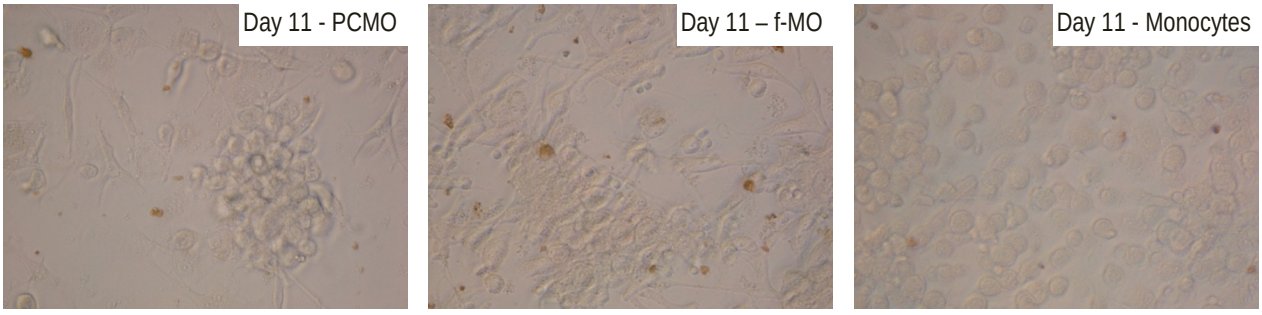


Figure 4.15 PCMOs and f-MOs do not express alkaline phosphatase activity that characterizes stem cells.

PCMOs, f-MOs, and monocytes cultured for 11 days (refer to Figure 4.14) were stained for the presence of alkaline phosphatase activity (denoted by purple colouration) (n=2). Note the orange colouration of some cells is debris present in the culture. Bright field images were taken at 400x magnification.

4.5 Discussion

4.5.1 PCMOs

Ruhnke *et al.* (2005) reported that PBMCs can be dedifferentiated into PCMOs which display plasticity, and can be differentiated into insulin-expressing cells. In the present study attempts to reproduce the dedifferentiation of PBMCs into PCMOs followed by their differentiation into insulin-producing Neoislets was not achievable. The PBMCs maintained their viability after culture on both hydrophobic and tissue culture surfaces in PCMO generating medium. The only difference in phenotype between cells cultured on either surface was an increase in cell clustering observed on the hydrophobic surface. Removal of M-CSF and IL-3 from the medium decreased the size and number of cell clusters indicating that the presence of these factors induces the clustering of PCMOs.

PBMCs cultured in PCMO medium maintained their expression of CD14 (macrophage marker), which was in agreement with the original PCMO publication (Ruhnke *et al.* 2005). However, this contrasts with the results of a more recent study on PCMOs which showed that CD14 expression decreased (Ungefroren *et al.* 2010), as it does in the cultured PB-IPC population (Chapter 3). PCMOs produced in the present study expressed the pancreatic marker SOX-17, in contrast to the two published studies (Ruhnke *et al.* 2005; Ungefroren *et al.* 2010). The presence of SOX-17 could indicate that PCMOs are undergoing dedifferentiation to a pancreatic precursor cell type. Ruhnke *et al.* (2005) reported that PCMOs express mRNAs encoding pancreatic markers such as Glut-2, NeuroD, NGN3, Nkx6.1, and MafA. In contrast to the two previous studies on PCMOs, the PCMOs in the present study did not express Nkx6.1. This could either indicate that either the mRNAs detected by Ruhnke *et al.* (2005) did not result in protein production, or that the level of protein produced is too low to be detected by immunocytochemistry.

The PCMOs produced in the present study cannot be regarded as stem cells as they quickly became senescent, similar to monocytes. Also they did not express alkaline phosphatase activity which characterizes stem cells. Previous reports revealed that PCMOs express Oct-4 and Nanog (Ungefroren *et al.* 2010), however since the PCMOs in the present study were senescent, the expression of these stem cell markers was not tested.

As mentioned above, PCMO clusters cultured in control media in the absence of M-CSF and IL-3 became disaggregated and grew as a monolayer and may have become terminally differentiated. On the other hand PCMOs cultured in ICM remained as clusters reminiscent of islet-like cells seen in the pancreas. HGF which is present in the ICM has previously been shown to induce clustering of acinar cells whilst promoting pancreatic differentiation (Mashima *et al.* 1996). However, PCMOs cultured in ICM did not express pancreatic markers, despite Ruhnke's report that PCMOs express PDX-1, insulin, glucagon, Nkx6.1, NeuroD, Pax6, NGN3, and Glut-2. HLA-DR expression was decreased after PCMOs were cultured in ICM medium, indicating that the PCMOs had become less activated, which either could be beneficial or unfavourable for pancreatic differentiation.

4.5.2 f-MOs

As expected, most PBMCs formed spindle-shaped f-MOs after attachment and culture with M-CSF in tissue culture dishes (Zhao *et al.* 2003). As reported here for the first time, they also formed f-MOs when cultured with M-CSF on a hydrophobic surface. Thus both monocyte types can be dedifferentiated to f-MOs by culture on their respective hydrophilic and hydrophobic surface. In contrast, and as expected, PBMCs cultured in the absence of M-CSF generated few spindle-shaped cells (Finnin *et al.* 1999). f-MOs quickly became senescent, suggesting they had not dedifferentiated into a stem-like state capable of being redifferentiated. Accordingly, they did not possess stem cell-associated alkaline phosphatase activity. Therefore, this thesis provides no support for the stem-ness of f-MOs or for their potential ability to be differentiated along other cell lineages.

Nevertheless, attempts were made to differentiate the cells along several different lineages, as f-MOs have previously been shown to differentiate into endothelial and neuronal cells and T cells (Zhao *et al.* 2003). An attempt to differentiate f-MOs into mature pancreatic cells using ICM, which had been devised for PCMO differentiation into insulin-producing cells (Ruhnke *et al.* 2005), was not effective. Approximately half to two-thirds of f-MOs and monocytes cultured in ICM and control media expressed CD14, indicating that f-MOs had maintained their monocytic character. Cells either expressed CD14 or PDX-1, but not both, suggesting two populations of cells had formed. One population retained its monocytic character, whereas the other had lost it and had gained characteristics of a pancreatic cell progenitor. f-MOs cultured with either ICM or control medium did not express insulin and NeuroD, indicating the cells were not particularly pancreatic-like.

Attempts were also made to differentiate f-MOs towards the endothelial, neuronal, and T lymphocyte cell lineages using published protocols. A subset of f-MOs exposed to $VEGF_{165}$, weakly expressed vWF, demonstrating that f-MOs either already expressed this endothelial cell marker, or could be differentiated to express it. They maintained an elongated morphology and highly expressed HLA-DR suggesting they were in a state of activation. Zhao *et al.* (2003) reported that the expression of HLA-DR by f-MOs was weaker than that of s-MO, suggesting that f-MOs were not as activated. They reported that most $VEGF_{165}$ treated f-MOs expressed vWF, and some even expressed the neuronal marker NSE. The appearance of NSE-expressing cells was not observed in the present study.

An attempt to differentiate f-MOs towards the neuronal cell lineage was more successful as a small subpopulation of differentiated f-MOs weakly expressed the neuronal marker NSE. However, they also expressed the endothelial marker vWF, and expressed HLA-DR. Most of the cells adopted an elongated neuronal-like morphology similar to that of f-MOs. Again the present study was unable to repeat Zhao's results, which reported that most f-MOs expressed NSE after treatment with NGFβ. They did not assess the expression of HLA-DR. Thus, it seems that the f-MOs isolated in the present study were less prone to neuronal differentiation, as there were less neuronal cells present after NGFβ induced differentiation compared with the previous study by Zhao *et al.* (2003).

In contrast to the above, an attempt to differentiate f-MOs with IL-2 into T lymphocytes appeared to be more successful in that the number of CD3 and CD4 T cells was enhanced. However, as mentioned earlier (Section 4.3.3.3), it is not possible to know from these experiments whether the CD3 and CD4 T cells were differentiated from the f-MOs or whether the IL-2 caused the proliferation of contaminating CD3 and CD4 cells. Zhao *et al.* (2003) reported that treatment of f-MOs with IL-2 produced CD3 T cells, some of which expressed CD4.

4.5.3 Comparison of the shared and unique properties of PCMOs and f-MOs

Both the PCMO or f-MO populations were senescent, and did not have stem-cell associated alkaline phosphatase activity. Neither population was able to be differentiated into insulin-producing cells with ICM, but PCMOs expressed PDX-1 which indicates a similarity to pancreatic progenitors. The significance of PDX-1 expression in PCMOs is uncertain as further attempts to induce pancreatic differentiation were not successful. f-MOs differentiated with ICM formed two different cell populations. One monocyte-like population retained CD14 expression, whereas the other population had lost CD14 expression, forming pancreatic-progenitor-like cells that expressed PDX-1. In summary, attempts at using current dedifferentiation protocols, and steps to improve them, have not been successful at differentiating PCMOs and f-MOs towards the pancreatic pathway. More effective dedifferentiation protocols incorporating agents that downregulate transcription factors associated with the monocyte lineage need to be developed to allow for greater cell plasticity.

The limited differentiation of f-MOs towards the endothelial and neuronal lineages demonstrates that f-MOs show some plasticity, but the percentage of cells that underwent transdifferentiation was low. Another potential use of f-MOs may lie in their ability to be differentiated into Tregs with specificity for pancreatic antigens, which could be employed to suppress diabetes-associated autoimmunity. Such cells could be used to halt the immune destruction of residual β-cells during the onset of type 1 diabetes and to protect islet grafts. The population of f-MO-derived CD4 cells requires further investigation to determine whether they are contaminants, or derived from transdifferentiation, and whether they are effector T cells or Treg cells.

Chapter 5 Human Amniotic Stem Cells

5.1 Introduction

Human amniotic stem cells (HASCs) are reported to be very plastic and can be differentiated into all 3 germ layers including the endoderm, suggesting they could be employed for pancreatic development (Miki *et al.* 2005). Commercially obtained HASCs express the stem cell markers Oct-4 and Nanog (Sharma *et al.* 2003), and those freshly isolated express PDX-1 RNA (Miki *et al.* 2005). HASCs have been differentiated along the pancreatic lineage by culturing them with Celprogen Inc.'s pancreatic differentiation kit (Sharma *et al.* 2003). The resulting cells expressed insulin RNA, but the expression of insulin protein was not reported (Sharma *et al.* 2003). HASCs have been differentiated along the pancreatic lineage with nicotinamide alone in the culture medium (Miki *et al.* 2005). Nicotinamide induced the expression of glucagon protein, and insulin RNA, but not insulin protein (Miki *et al.* 2005). Human amnion-derived fibroblast-like cells (HADFILs) have been differentiated into insulin (protein) expressing cells by a 3 step differentiation protocol that required culturing the cells in Matrigel to induce islet-like clusters (Tamagawa *et al.* 2009). It is not known whether these insulin-producing cells are functional *in vivo* in response to changes in glucose (Tamagawa *et al.* 2009). The differentiation of HASCs into insulin-producing cells warranted further investigation.

5.2 Scope of chapter

The aim here was to determine whether HASCs obtained from Celprogen Inc. (1 batch) could be differentiated towards the pancreatic lineage using Celprogen Inc.'s pancreatic differentiation media in the presence or absence of different extracellular matrices. Pancreatic differentiation of the commercially obtained HASCs was also trialled in tissue culture plates with differentiation agents such as Ex4, nicotinamide, and GLP-1. The parental cells and the resulting differentiated cells were phenotyped for expression of stem cell and pancreatic markers, including alkaline phosphatase activity.

5.3 Characterization of HASCs

5.3.1 Phenotyping of HASCs for expression of cell markers

HASCs from 1 batch were cultured for 2 days in Human ESC Media containing serum (M36101-28S, Celprogen Inc.) on plates coated with Human ESC Extra-cellular Matrix (E36101-28, Celprogen Inc.). The cells formed a monolayer, with most of the cells being elongated (Figure 5.1). In a separate experiment they were cultured for 3 days and then characterized for the expression of stem cell and pancreatic cell markers (n=2) (Figure 5.2). The HASCs weakly expressed the stem cell markers Nestin and Oct-4 and strongly expressed SOX-17, as judged by the level of intensity of the immunostaining (Figure 5.2). They did not express CD34 or Nanog (Figure 5.2). A small number of HASCs weakly expressed PDX-1, whereas expression of the pancreatic markers NGN3, glucagon, CXCR4 and NeuroD was not detectable (Figure 5.2). The occasional expression of PDX-1 indicates the HASCs are a heterogenous population of cells. The results of phenotyping the HASCs are summarized in Table 5.1.

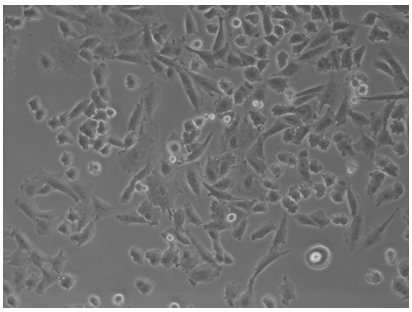
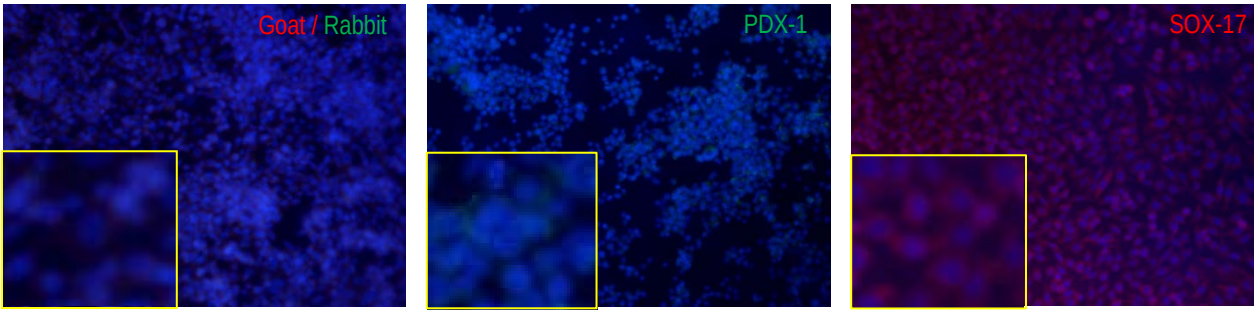


Figure 5.1 Phase contrast image of a 2 day culture of HASCs.

HASCs were cultured for 2 days in human ESC media containing serum on dishes coated with human ESC extracellular matrix. The image was taken at 200x magnification.



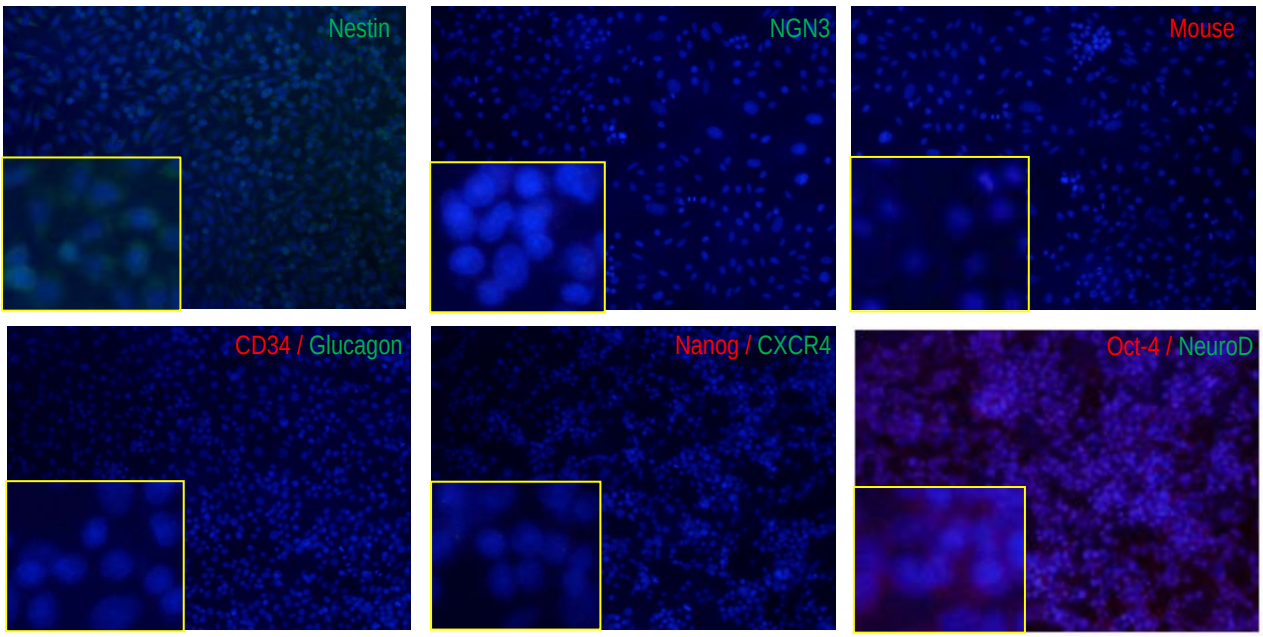


Figure 5.2 Phenotyping of HASCs for stem and pancreatic cell markers.

HASCs were cultured for 3 days in human embryonic stem cell media containing 10% FBS in dishes coated with human embryonic stem cell extracellular matrix. Cells were immunostained for the expression of various cell markers. Immunoreactivity was detected with donkey anti-goat and anti-mouse antibodies (red) and with a donkey anti-rabbit antibody (green). Cell nuclei were stained blue with DAPI. Images were taken at 200x magnification; inset is a higher magnification of each image. The images are presented so that the staining obtained with each IgG control immediately precedes stainings with antibodies of the same host species.

5.3.1.1 Summary of the phenotype of HASCs

Table 5.1 Summary of the phenotype of HASCs

	HASCs
PDX-1	x
SOX-17	x x x
Nestin	x
NGN3	
CD34	
Glucagon	
Nanog	
CXCR4	
Oct-4	x
NeuroD	

0	0.1-20	21-40	41-60	61-80	81-100	% Positive

x	x x	x x x	Intensity of staining - weak/moderate/strong

5.3.2 HASCs do not display alkaline phosphatase activity

Phenotyping of the HASCs (Figure 5.2) revealed that HSCs express Nestin and Oct-4, suggesting they are stem cell-like. The stem-ness of the HASCs was further characterised by investigating whether they expressed stem-cell-associated alkaline phosphatase activity (n=2) (Figure 5.3). The HASCs did not give the characteristic purple colour following staining with X-Phos and NBT that would indicate alkaline phosphatase activity (Figure 5.3).

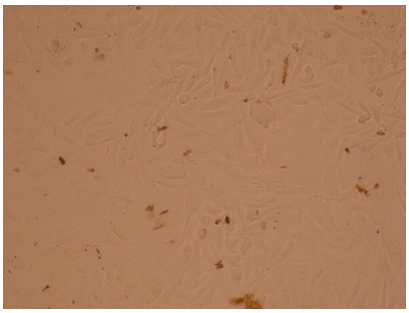


Figure 5.3 HASCs do not display alkaline phosphatase activity.

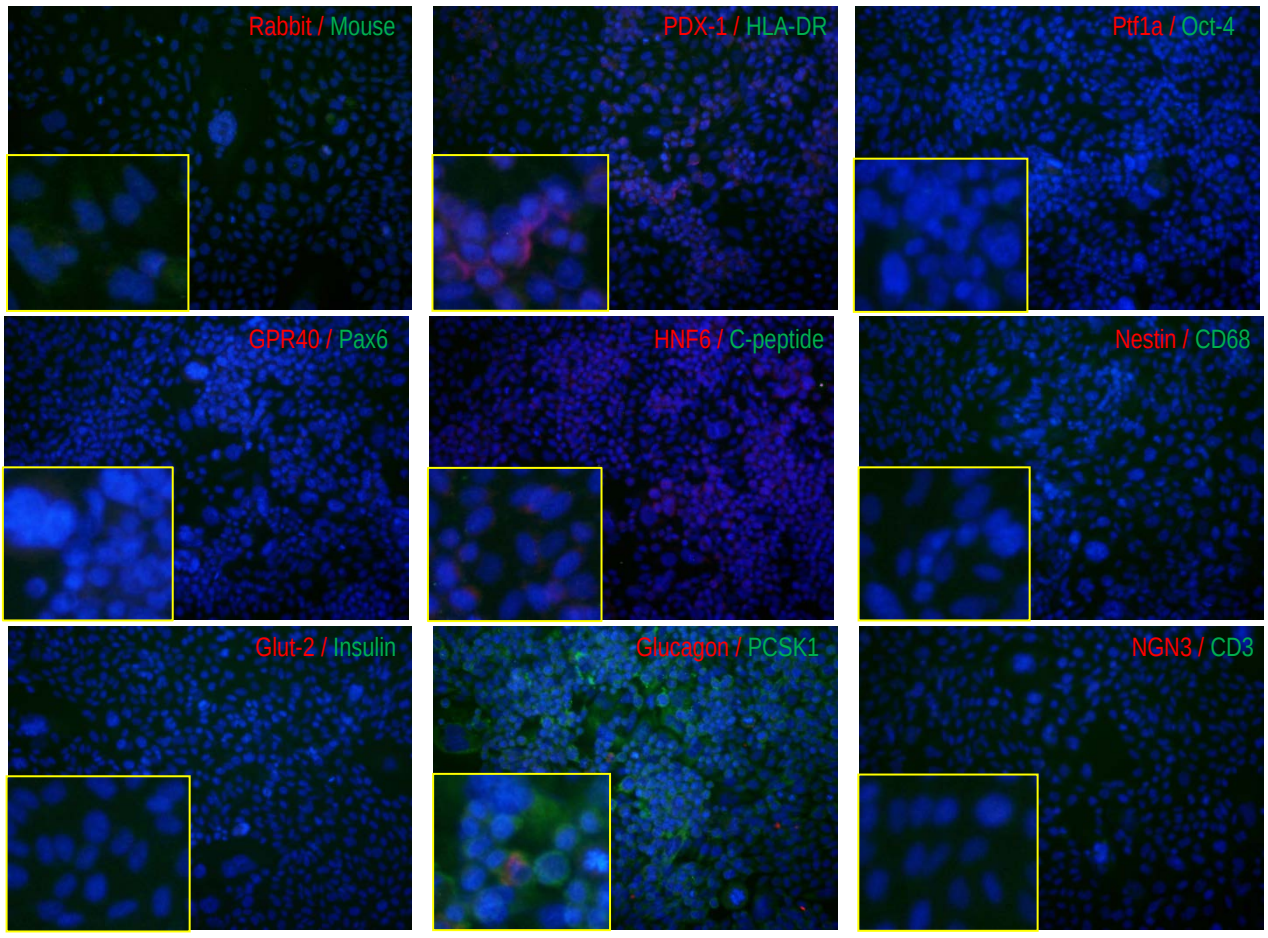
HASCs were cultured for 1 week, as described above, prior to testing for alkaline phosphatase activity. They were tested for alkaline phosphatase activity at pH 6.0 by staining with X-Phos and NBT, where a purple-red colouration would indicate activity. The image was taken at 200x magnification.

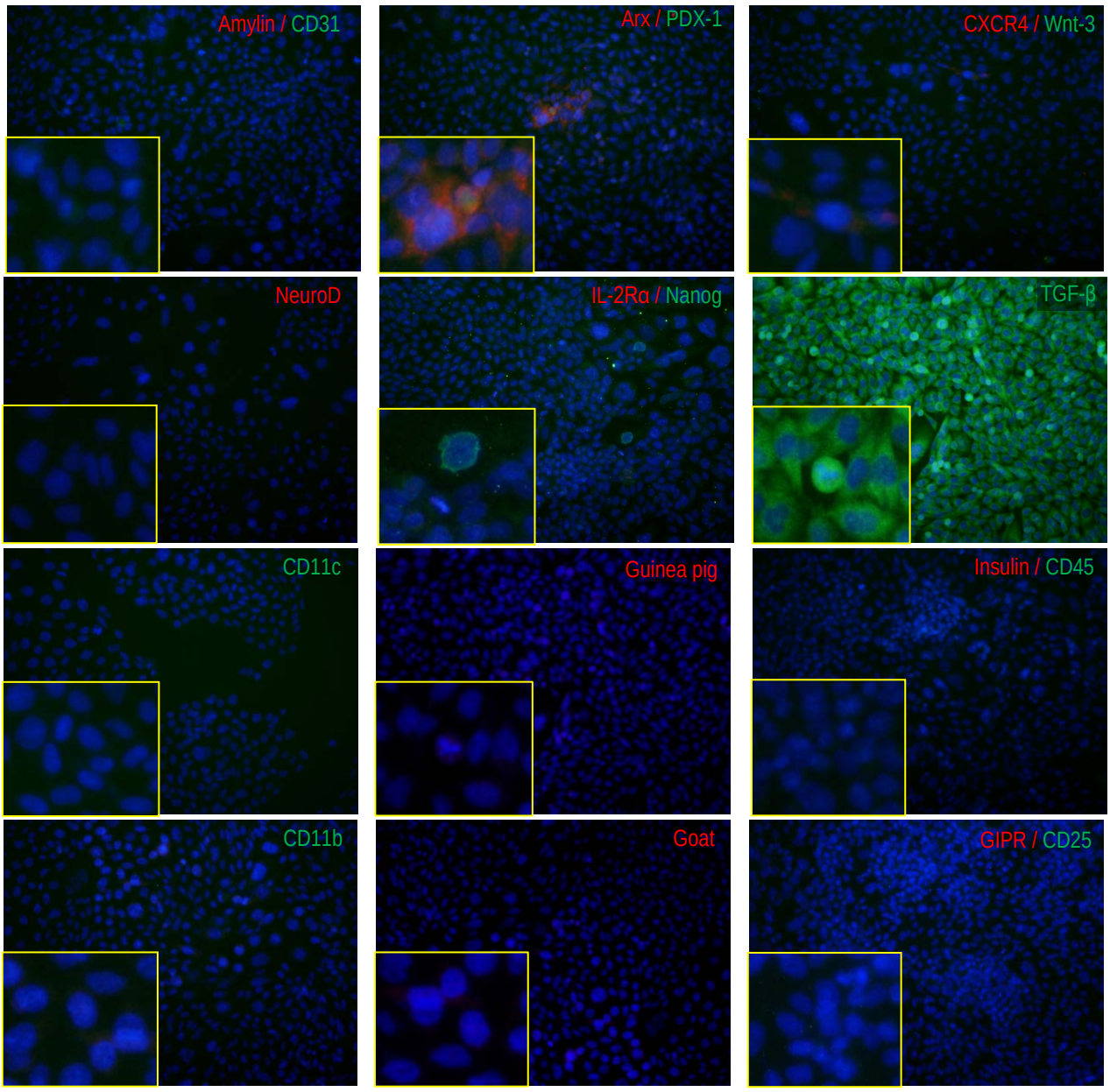
5.4 Can HASCs be differentiated into pancreatic cells?

5.4.1 Phenotype of HASCs differentiated with pancreatic differentiation matrices

The aim here was to determine whether HASCs could be differentiated toward the pancreatic lineage by culture for 1 week in Celprogen Inc.'s human pancreatic differentiation media and matrices. HASCs were cultured for 1 week in Human Pancreatic Cancer Stem Cell Culture Differentiation Media with Serum (M36004-05DS, Celprogen Inc.) on plates coated with Human Pancreatic Cancer Stem Cell Culture Extracellular Differentiation Matrix (D36115-42, Celprogen Inc.) (n=2). In another approach they were cultured for 1 week in Human Pancreatic (Trans-Differentiated) Stem Cell Culture Differentiation Medium with Serum (D36004-05, Celprogen Inc.) on plates coated with Human Pancreatic (Trans-Differentiated) Stem Cell Extracellular Differentiation Matrix (D36004-05, Celprogen Inc.) (n=2). Both resulting cell populations were phenotyped for stem cell and pancreatic cell markers (Figure 5.4 and Figure 5.5). Repeats of these experiments showed that the HASCs differentiated on each Celprogen matrix formed populations having a similar phenotype. The cells cultured on the pancreatic cancer stem cell differentiation matrix were termed differentiated HASCs (dHASCs) (Figure 5.4), whereas the cells cultured on the pancreatic trans-differentiation matrix were termed trans-differentiated HASCs (tdHASCs) (Figure 5.5).

Most dHASCs strongly expressed SOX-17, and small numbers expressed Nanog and/or glucagon (Figure 5.4). Unlike undifferentiated HASCs (Figure 5.2) they did not express Oct-4 or Nestin (Figure 5.4). A few cells co-expressed PDX-1 and Arx (Figure 5.4). PDX-1 was expressed more strongly than seen with undifferentiated HASCs (compare Figure 5.2 and Figure 5.4). Most cells strongly expressed PCSK1 (Figure 5.4). The latter results together along with the weak expression of HNF6 and CXCR4 signalled that some of the dHASCs had developed characteristics of pancreatic cells (Figure 5.4). All of the dHASCs very strongly expressed TGF-β, suggesting they would be immunosuppressive (Figure 5.4). They strongly expressed AIRE (Figure 5.4). They did not express the pancreatic markers Ptf1a, GPR40, Pax6, C-peptide, Glut-2, insulin, NGN3, amylin, Wnt-3, NeuroD, GIPR, or MafA, the immunological markers HLA-DR, CD68, CD3, IL-2Rα, CD45, CD11b, CD11c, CD25, and CD20, and the endothelial marker CD31 (Figure 5.4). The results of phenotyping the HASCs are summarized in Table 5.2.




Amylin / CD31
Arx / PDX-1
CXCR4 / Wnt-3
NeuroD
IL-2Rα / Nanog
TGF-β
CD11c
Guinea pig
Insulin / CD45
CD11b
Goat
GIPR / CD25

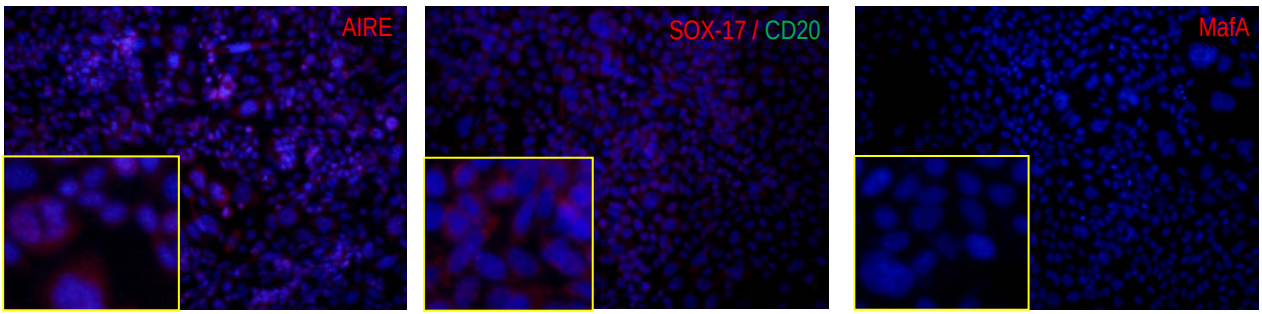
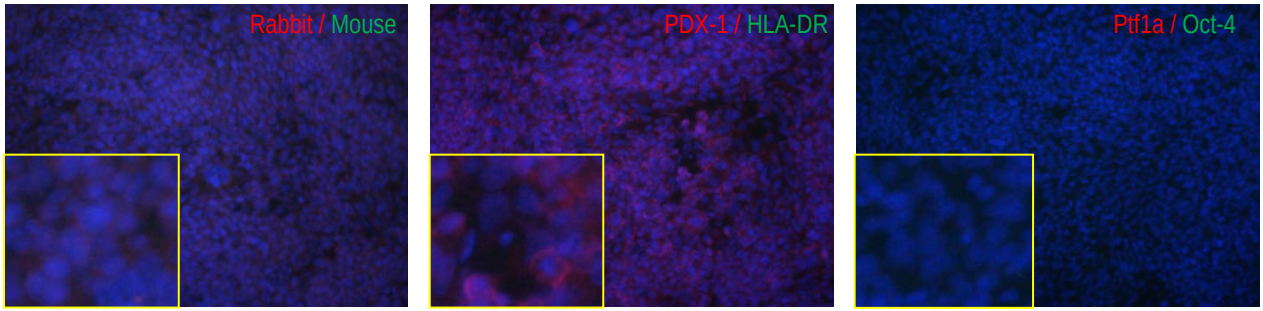
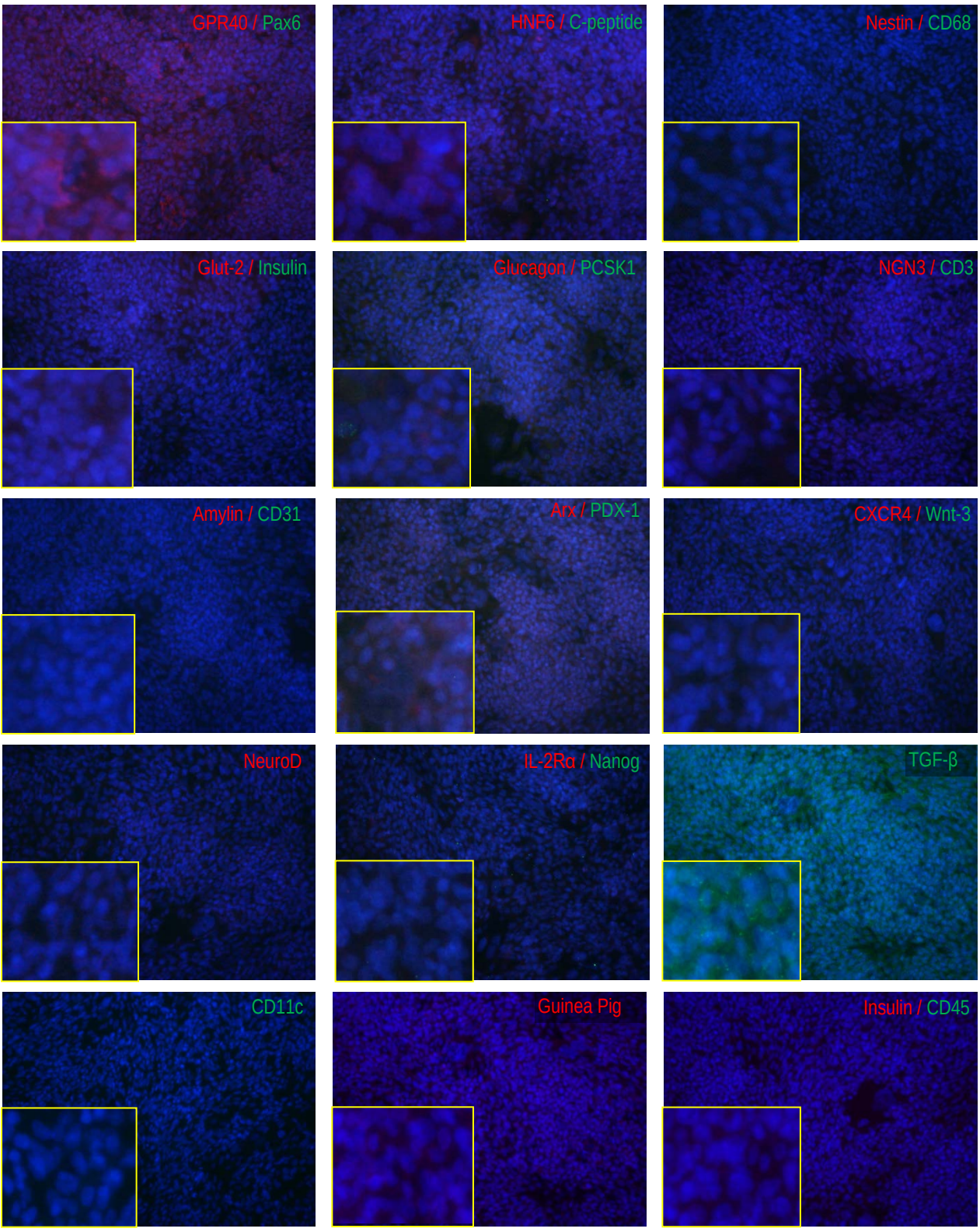


Figure 5.4 Phenotyping of HASCs after differentiation towards the pancreatic lineage by culture on pancreatic cancer stem cell differentiation matrix.

HASCs were cultured for 1 week in human pancreatic cancer stem cell culture differentiation medium containing serum in dishes coated with the human pancreatic cancer stem cell differentiation matrix. Cells were immunostained for the expression of various cell markers. Immunoreactivity was detected with donkey anti-rabbit and anti-goat antibodies (red), goat anti-guinea pig antibody (red), and with a donkey anti-mouse antibody (green). Cell nuclei were stained blue with DAPI. Images were taken at 200x magnification; inset is a higher magnification of each image. The images are presented so that the staining obtained with each IgG control immediately precedes stainings with antibodies of the same host species.

HASCs were cultured on the human pancreatic trans-differentiation differentiation matrix to form tdHASCs. The resulting cells very strongly expressed PDX-1 and GPR40 (Figure 5.5). PDX-1 appeared to be confined to the cytoplasm of cells (Figure 5.5). A few tdHASCs weakly expressed PSCK1, and GIPR (Figure 5.5). Unfortunately the donkey antibody used to detect the rabbit antibodies gave a high background level of staining; hence it is not known whether the weak expression of Arx, HNF6, and glucagon is authentic or just background staining (Figure 5.5). Most tdHASCs strongly expressed AIRE, and SOX-17, and moderately expressed TGF-β (Figure 5.5). They did not express Oct-4 or Nestin, the pancreatic markers Ptf1a, Pax6, HNF6, C-peptide, Glut-2, insulin, HNF6, NGN3, amylin, Arx, CXCR4, Wnt-3, NeuroD, or MafA, the immunological markers HLA-DR, CD68, CD3, IL-2Rα, CD45, CD11b, CD11c, CD25, and CD20, and the endothelial marker CD31 (Figure 5.5). The results of phenotyping the HASCs are summarized in Table 5.2.




GPR40 / Pax6
HNF6 / C-peptide
Nestin / CD68
Glut-2 / Insulin
Glucagon / PCSK1
NGN3 / CD3
Amylin / CD31
Arx / PDX-1
CXCR4 / Wnt-3
NeuroD
IL-2Rα / Nanog
TGF-β
CD11c
Guinea Pig
Insulin / CD45

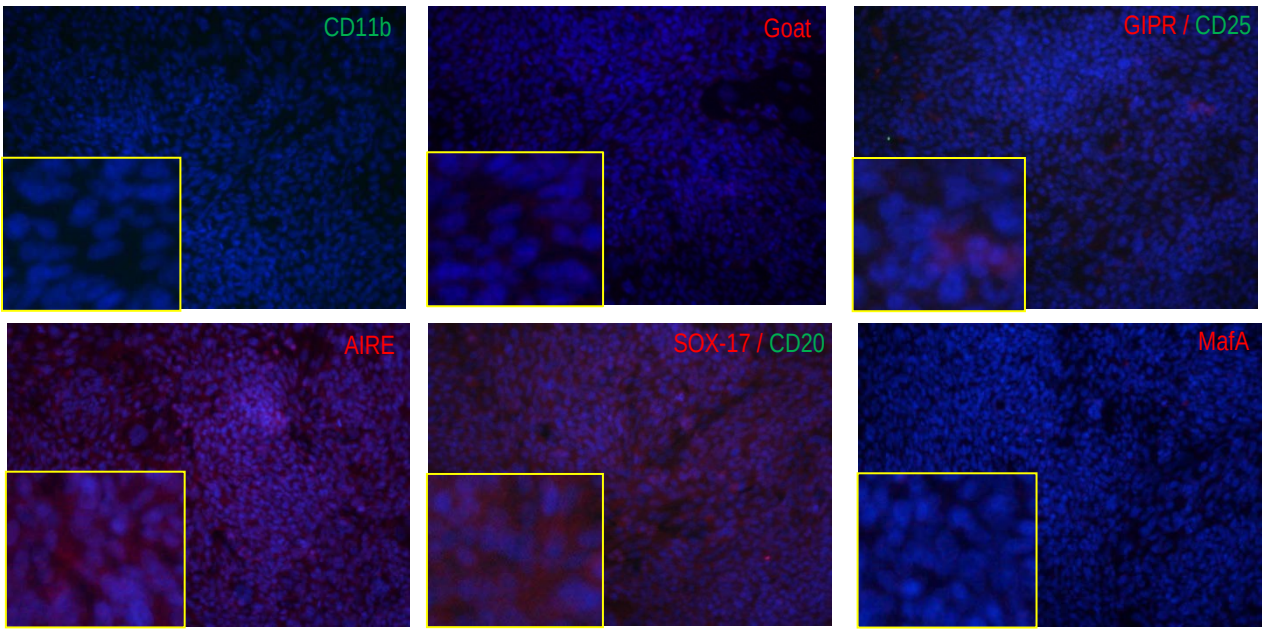


Figure 5.5 Phenotyping of HASCs after differentiation towards the pancreatic lineage by culture on pancreatic trans-differentiation stem cell differentiation matrix.

HASCs were cultured for 1 week human pancreatic (trans-differentiated) stem cell culture differentiation medium containing serum in dishes coated with the human pancreatic (trans-differentiation) stem cell differentiation matrix. Cells were immunostained for the expression of various cell markers. Immunoreactivity was detected with donkey anti-rabbit and anti-goat antibodies (red), goat anti-guinea pig antibody (red), and with a donkey anti-mouse antibody (green). Cell nuclei were stained blue with DAPI. Images were taken at 200x magnification; inset is a higher magnification of each image. The images are presented so that the staining obtained with each IgG control immediately precedes stainings with antibodies of the same host species.

5.4.1.1 Summary of the phenotype of differentiated HASCs

Table 5.2 Summary of the phenotype of HASCs cultured with two different differentiation media on two different pancreatic differentiation matrices

	dHASC	tdHASC
PDX-1	x x x	x x x
HLA-DR		
Ptf1a		
Oct-4		
GPR40		x x x
Pax6		
HNF6	x	
C-peptide		
Nestin		
CD68		
Glut-2		
Insulin		
Glucagon	x x x	
PCSK1	x x x	x
NGN3		
CD3		
Amylin		

	dHASC	tdHASC
CD31		
Arx	x x x	
CXCR4	x	
Wnt-3		
NeuroD		
IL-2Rα		
Nanog	x x x	
TGF-β	x x x	x x
CD45		
CD11b		
CD11c		
GIPR		x
CD25		
AIRE	x x x	x x x
SOX-17	x x x	x x x
CD20		
MafA		

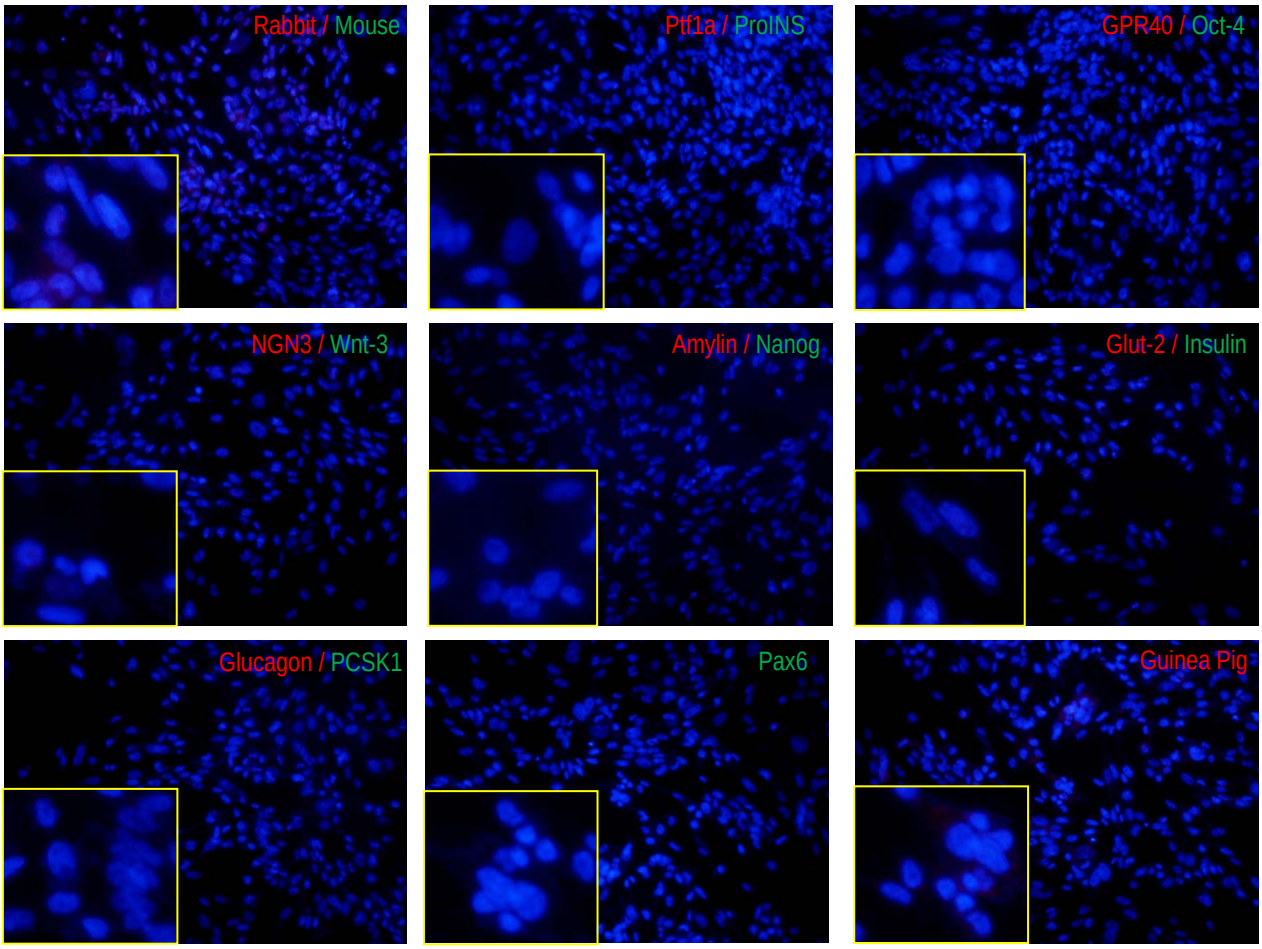
0	0.1-20	21-40	41-60	61-80	81-100	% Positive

x	x x	x x x	Intensity of staining - weak/moderate/strong

5.4.2 Phenotype of HASCs differentiated on tissue culture plates with differentiation agents

Further attempts were made to induce HASCs to differentiate towards the pancreatic lineage by culturing the cells in tissue culture plates with DMEM medium containing a variety of different pancreatic differentiation agents. The resulting populations were then phenotyped for stem cell and pancreatic cell markers (Figure 5.7 to Figure 5.9).

In the first study, HASCs were cultured for 1 week in DMEM medium containing 10 nM Ex4 + 10 ng/mL GM-CSF + 25 mM glucose + 7% FBS + 1% PSG, which had been used by Zhao *et al.* to induce pancreatic differentiation (Zhao and Mazzone 2008) (n=1). Many of the resulting cells weakly expressed SOX-17 (Figure 5.6). The differentiation medium did not induce expression of the pancreatic markers Ptf1a, ProINS, GPR40, NGN3, Wnt-3, amylin, Nanog, Glut-2, insulin, glucagon, PCSK1, Pax6, C-peptide, or PDX-1, the stem cell markers Nestin, Oct-4, or Nanog, or TGF-β (Figure 5.6). A summary of the phenotype of the HASCs treated with this differentiation medium is presented in Table 5.3.



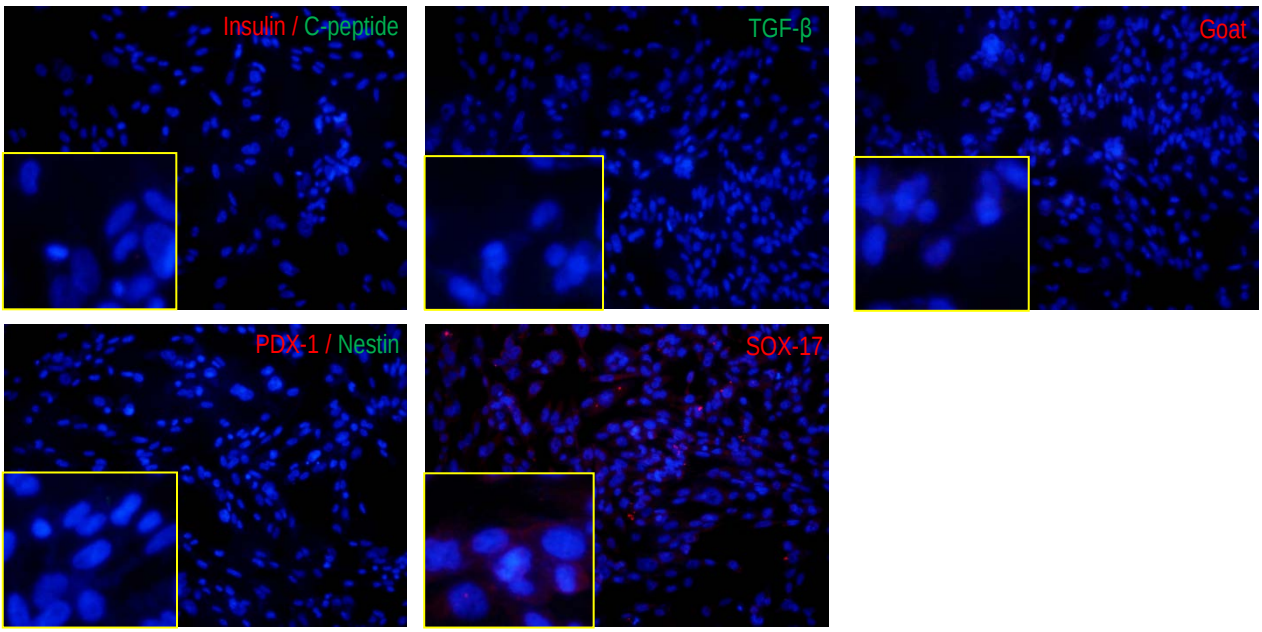
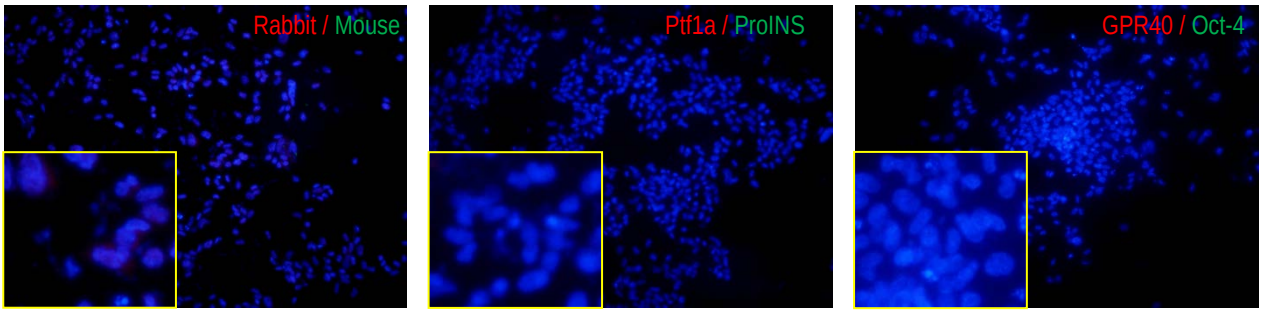


Figure 5.6 Phenotyping of HASCs differentiated towards the pancreatic lineage with a medium containing Ex4 and GM-CSF.

HASCs were cultured for 1 week in DMEM medium containing 10 nM Ex4 + 10 ng/mL GM-CSF + 25 mM glucose + 7% FBS + 1% PSG in tissue culture plates. Cells were immunostained for the expression of various cell markers. Immunoreactivity was detected with donkey anti-rabbit and anti-goat antibodies (red), goat anti-guinea pig antibody (red) and a donkey anti-mouse antibody (green). Cell nuclei were stained blue with DAPI. Images were taken at 200x magnification; inset is a higher magnification of each image. The images are presented so that the staining obtained with each IgG control immediately precedes stainings with antibodies of the same host species.

In a second study, the HASCs were cultured for 1 week in DMEM medium containing 10 mM nicotinamide + 25 mM D-glucose + N2 supplement + 1% PSG (here termed NGN) (n=1). The NGN-treated population of cells moderately expressed SOX-17, but did not express any of the other pancreatic and stem cell markers tested (Figure 5.7). A summary of the phenotype of the HASCs treated with this differentiation medium is presented in Table 5.3.



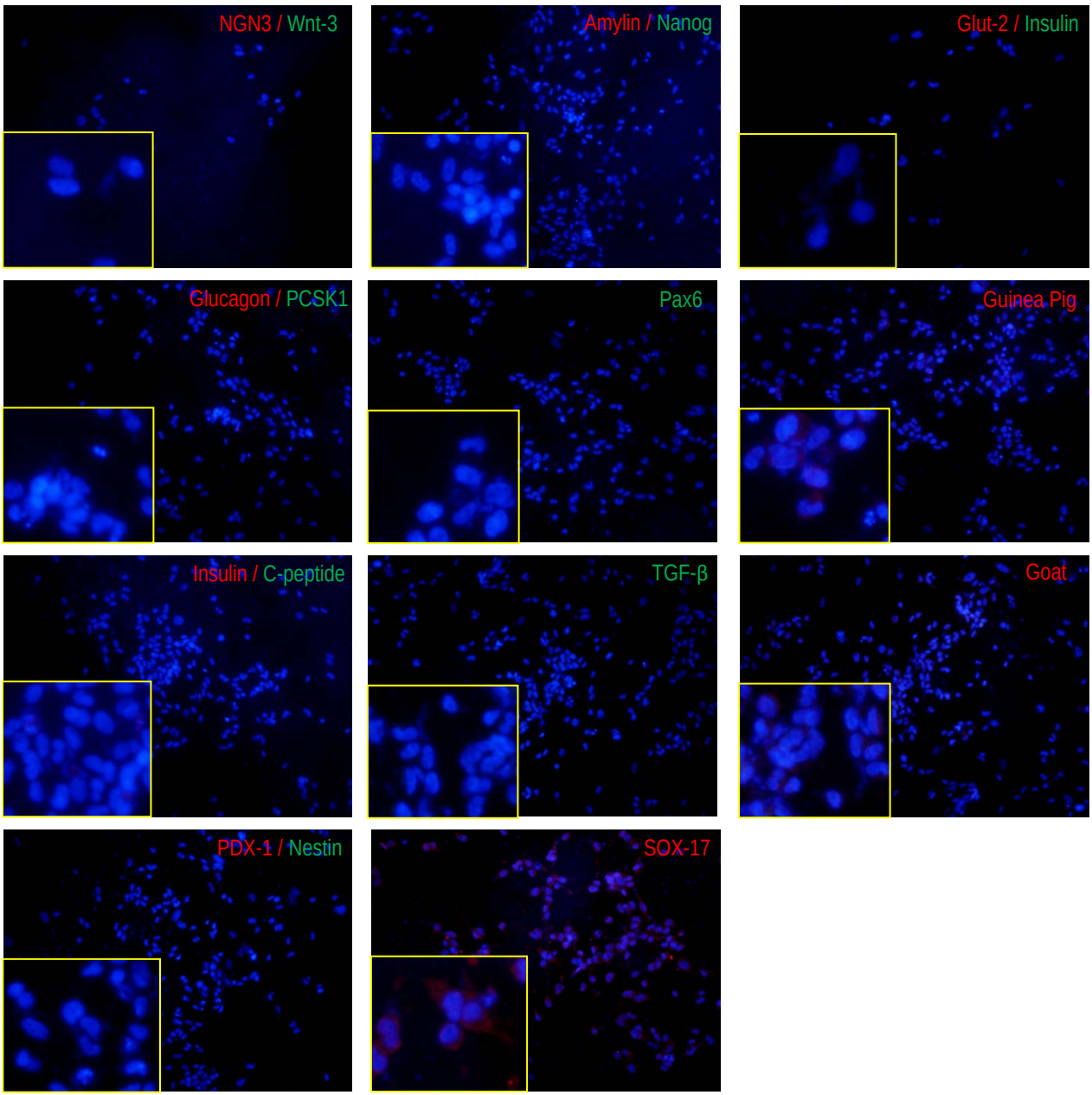
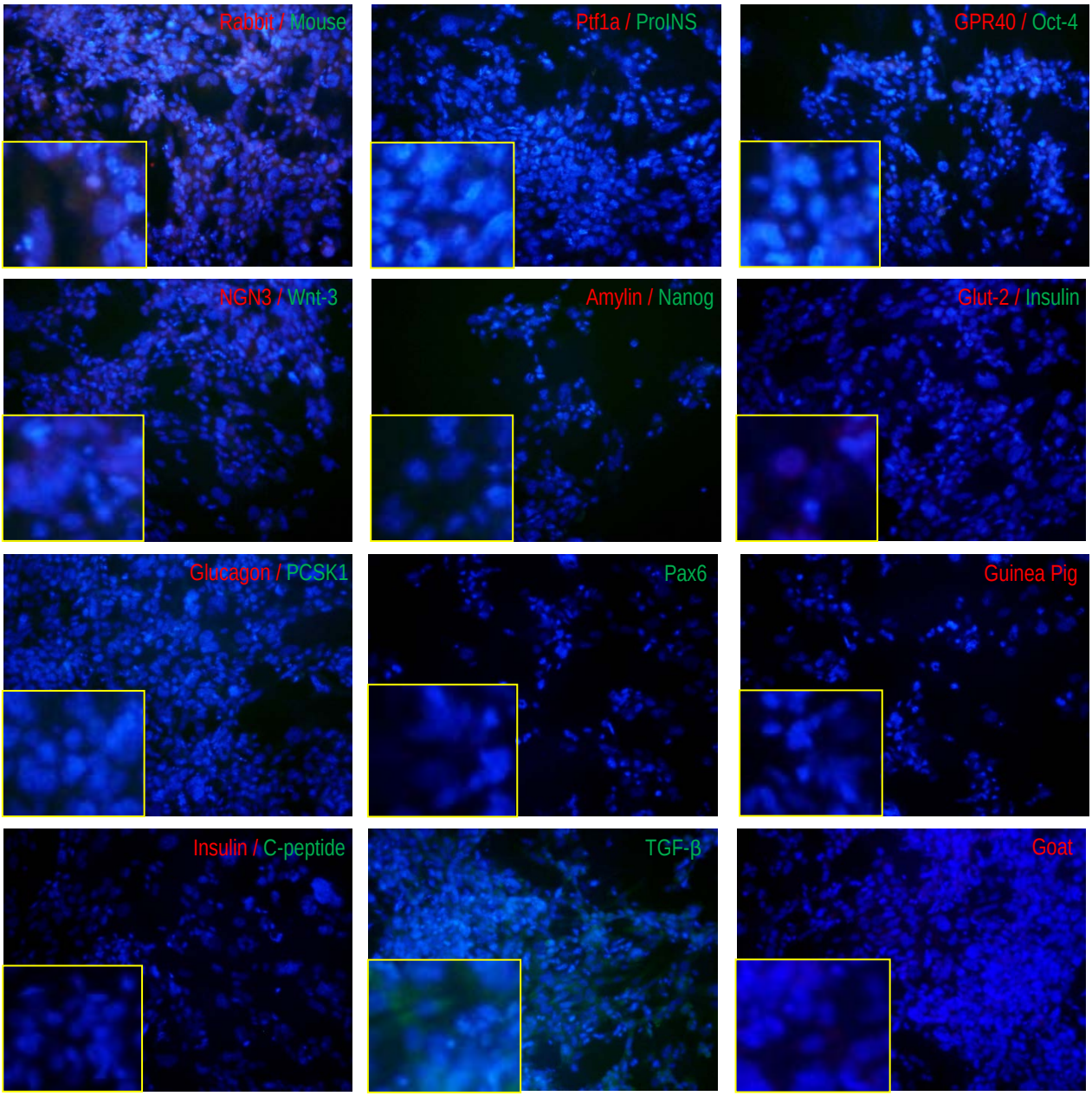


Figure 5.7 Phenotyping of HASCs differentiated along the pancreatic lineage with a medium containing nicotinamide and high glucose.

HASCs were cultured for 1 week in DMEM medium containing 10 mM nicotinamide + 25 mM D-glucose + N2 supplement + 1% PSG in tissue culture dishes. Cells were immunostained for the expression of various cell markers. Immunoreactivity was detected with donkey anti-rabbit and anti-goat antibodies (red), goat anti-guinea pig antibody (red), and a donkey anti-mouse antibody (green). Cell nuclei were stained blue with DAPI. Images were taken at 200x magnification; inset is a higher magnification of each image. The images are presented so that the staining obtained with each IgG control immediately precedes stainings with antibodies of the same host species.

In a third study, HASCs were cultured for 2 weeks in DMEM medium containing 100 nM GLP-1 + 7% FBS + 1% PSG (here termed GLP-1) (n=1). The resulting cells expressed TGF-β and SOX-17 (Figure 5.8). The GLP-1-treated HASCs did not express Ptf1a, ProINS, GPR40, NGN3, Wnt-3, amylin, Nanog, Glut-2, insulin, glucagon, PCSK1, Pax6, C-peptide, or PDX-1, or the stem cell markers Nestin, Oct-4, or Nanog (Figure 5.8). A summary of the phenotype of the HASCs treated with this differentiation medium is presented in Table 5.3.



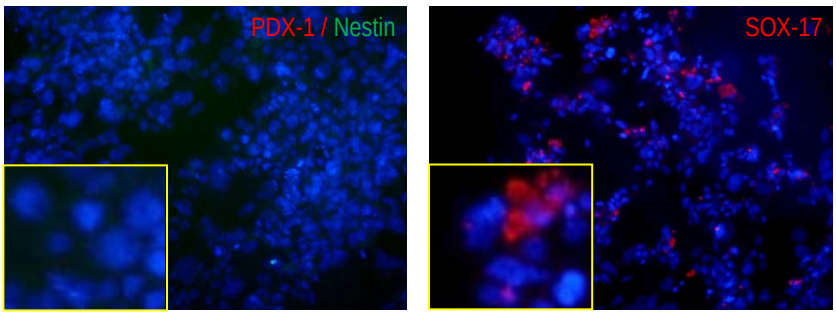
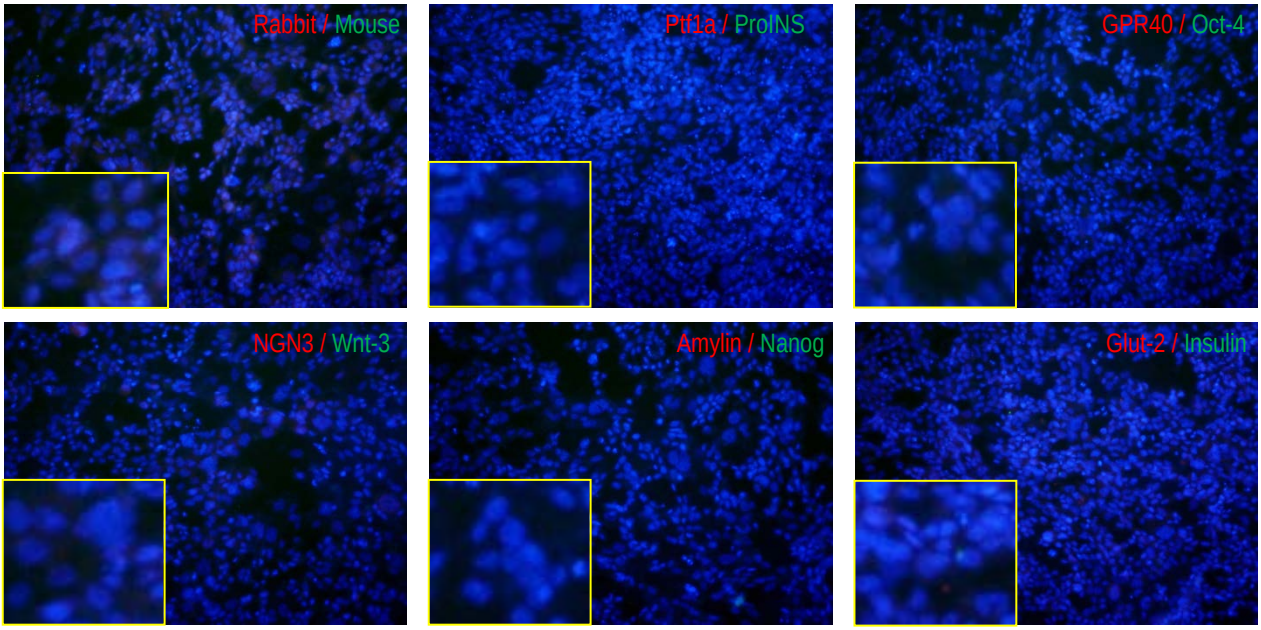


Figure 5.8 Phenotyping of HASCs differentiated towards the pancreatic lineage with GLP-1.

HASCs were cultured for 2 weeks in DMEM medium containing 100 nM GLP-1 + 7% FBS + 1% PSG in tissue culture plates. Cells were immunostained for the expression of various cell markers. Immunoreactivity was detected with donkey anti-rabbit and goat antibodies (red), a goat anti-guinea pig antibody (red), and a donkey anti-mouse antibody (green). Cell nuclei were stained blue with DAPI. Images were taken at 200x magnification; inset is a higher magnification of each image. The images are presented so that the staining obtained with each IgG control immediately precedes stainings with antibodies of the same host species.

In a fourth study, HASCs were treated for 2 weeks with DMEM medium containing 100 nM GLP-1 + 10 nM Ex4 + 7% FBS + 1% PSG (here termed GLP-1/Ex4) (n=1). Some of the resulting cells strongly expressed SOX-17 and weakly expressed TGF-β (Figure 5.9). They did not express Ptf1a, ProINS, GPR40, NGN3, Wnt-3, amylin, Nanog, Glut-2, insulin, glucagon, PCSK1, Pax6, C-peptide, or PDX-1, or the stem cell markers Nestin, Oct-4, and Nanog (Figure 5.9). A summary of the phenotype of the HASCs treated with this differentiation medium is presented in Table 5.3.



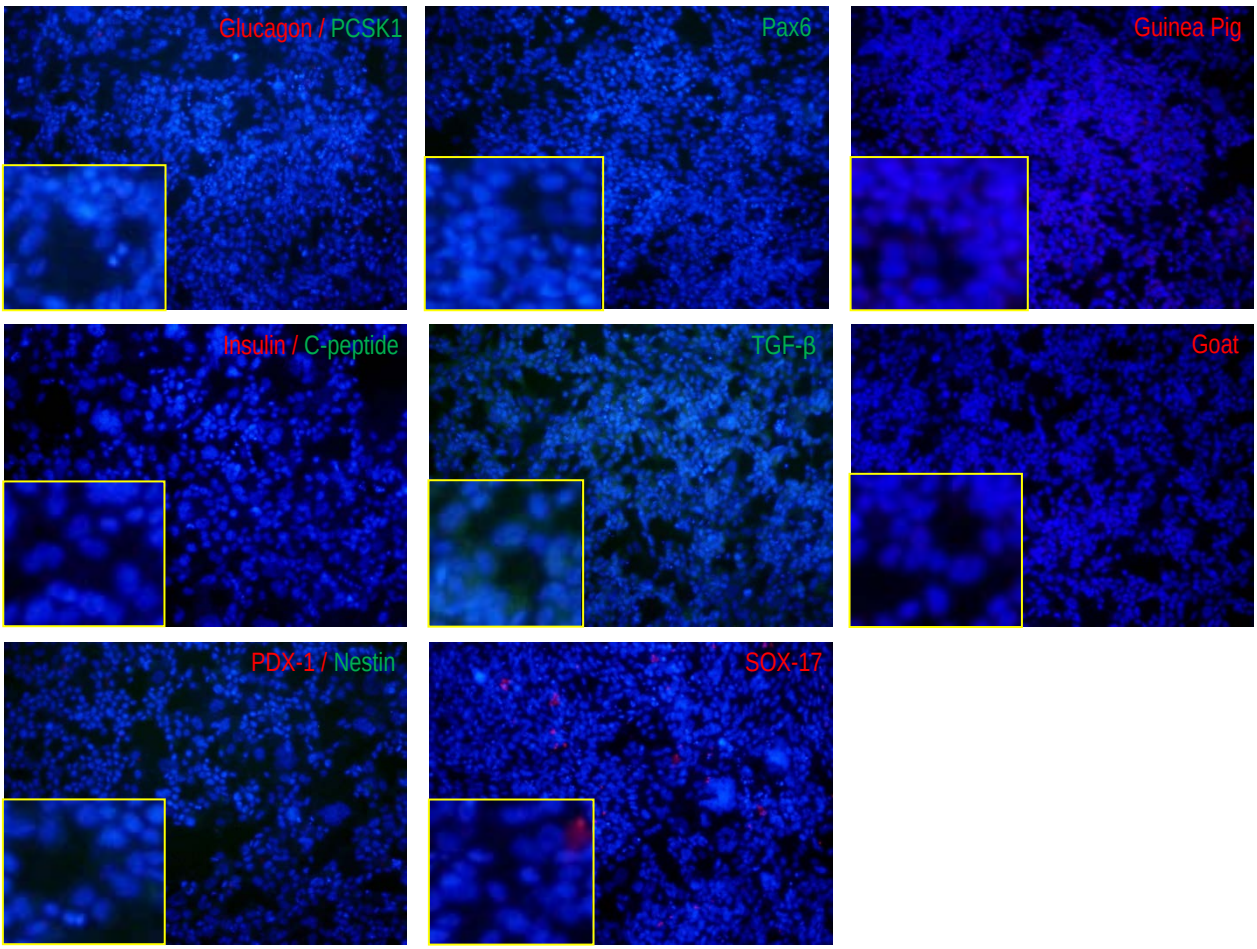


Figure 5.9 Phenotyping of HASCs differentiated along the pancreatic lineage with a medium containing GLP-1 and Ex4.

HASCs were cultured for 2 weeks in DMEM medium containing 100 nM GLP-1 + 10 nM Ex4 + 7% FBS + 1% PSG. Cells were immunostained for the expression of various cell markers. Immunoreactivity was detected with donkey anti-rabbit and goat antibodies (red), a goat anti-guinea pig antibody (red), and a donkey anti-mouse antibody (green). Cell nuclei were stained blue with DAPI. The images are presented so that the staining obtained with each IgG control immediately precedes stainings with antibodies of the same host species.

5.4.2.1 Summary of the phenotype of HASCs cultured with differentiation agents

Table 5.3 Summary of the phenotype of HASCs cultured with differentiation agents

	Zhao	NGN	GLP-1	GLP-1 /Ex4
Ptf1a				
ProINS				
GPR40				
Oct-4				
NGN3				
Wnt-3				
Amylin				
Nanog				
Glut-2				
Insulin				
Glucagon				
PCSK1				
Pax6				
C-peptide				
TGF-β			x	x
PDX-1				
Nestin				
SOX-17	x	x x	x x x	x x x

0	0.1-20	21-40	41-60	61-80	81-100	% Positive

x	x x	x x x	Intensity of staining – weak/moderate/strong

5.5 Discussion

Stem cells from the human amniotic fluid and membrane are easily obtainable from a full-term placenta (Miki *et al.* 2007), which makes them a promising source of stem cells for type 1 diabetes therapy. In this study, undifferentiated HASCs were characterized and several protocols were employed to investigate their ability to differentiate towards the pancreatic lineage. Derived cell populations were screened for the expression of pancreatic and immunogenic markers that were previously assessed, including additional markers to help ascertain the cell phenotypes. The results are discussed in comparison to previously characterized populations of undifferentiated and differentiated HASCs, HAESCs, and HADFILs (Sharma *et al.* 2003; Miki *et al.* 2005; Tamagawa *et al.* 2009).

5.5.1 Phenotype of HASCs

HASCs commercially obtained from Celprogen Inc. have been reported to express Oct-4 and Nanog (Sharma *et al.* 2003). However, here the HASCs from Celprogen Inc. only weakly expressed Oct-4, and Nanog was not detected. The differences seen may be due to batch variations or could be typical, but only a single batch of HASCs was obtained from Celprogen Inc., and they were not contacted to discuss the differences between the reported phenotype and the results obtained here. HAESCs downregulate their stem cell marker expression when cultured in monolayers (Miki *et al.* 2005), and this could have occurred in the present study. Despite the weak Oct-4 expression and lack of Nanog expression, the undifferentiated HASCs expressed the stem cell marker Nestin, the definitive endoderm marker SOX-17, and a small number of cells expressed PDX-1. The non-uniform expression of some markers indicates that the HASCs are a heterogenous population of cells. They did not display alkaline phosphatase activity, which may indicate they were no longer completely stem-like and had begun to differentiate, potentially along the pancreatic lineage as judged by the expression of SOX-17 and PDX-1 protein. Nestin expressing cells reportedly exist within human islets where they may be responsible for neogenesis within the islet, and can undergo pancreatic differentiation *ex vivo* (Zulewski *et al.* 2001). Therefore the HASCs could be viewed as having the potential to be differentiated towards the β-cell lineage. Undifferentiated HADFILs also express SOX-17 and Nestin RNA (Tamagawa *et al.* 2009), and undifferentiated HAESCs (Miki *et al.* 2005) and HASCs (Sharma *et al.* 2003) express PDX-1 RNA. However, the latter cells have yet to be analysed for expression of SOX-17 or PDX-1 protein. This thesis followed the protocols recommended by Celprogen Inc. to differentiate the HASCs into insulin-producing cells. The protocols involved culturing the cells as a monolayer on specific matrices.

5.5.2 Phenotype of differentiated HASCs

5.5.2.1 dHASCs

HASCs differentiated by culture on pancreatic cancer stem cell differentiation matrix in human pancreatic cancer stem cell culture differentiation medium containing serum did not express Nestin, but a few cells expressed Nanog. Thus, Nestin was downregulated upon induction of differentiation of HASCs towards the pancreatic cell lineage as expected. The small number of

Nanog positive cells was not expected, but may reflect small numbers of similar cells in the undifferentiated cell population that went unobserved. The expression of SOX-17 was slightly weaker after the differentiation of HASCs into dHASCs. This is in agreement with a study where HADFILs differentiated along the pancreatic lineage showed a decrease in SOX-17 expression compared to undifferentiated HADFILs (Tamagawa *et al.* 2009). However, in that case the cells were more fully differentiated as they also expressed insulin (Tamagawa *et al.* 2009), whereas the dHASCs in the present study did not express insulin. Another study which used the same method for HASC differentiation reported expression of insulin mRNA, but did not analyse the expression of insulin protein (Sharma *et al.* 2003).

PDX-1 expression was upregulated on a few cells upon HASC differentiation into dHASCs. In two previous reports, HASCs did not show a difference in PDX-1 RNA expression before and after pancreatic differentiation (Sharma *et al.* 2003; Miki *et al.* 2005). However, variations in PDX-1 expression levels are seen during different stages of pancreatic development (Soria 2001; D'Amour *et al.* 2006), so the increase in PDX-1 expression here is not an unexpected phenomenon.

HNF6 was expressed by dHASCs. This result is in contrast to undifferentiated HADFIL which express HNF6 expression, and then lose expression after differentiation (Tamagawa *et al.* 2009). HNF6 is a marker for endocrine tissue and formation of the posterior foregut during embryogenesis (Jacquemin *et al.* 2000; D'Amour *et al.* 2006), therefore the upregulation of HNF6 in response to the induction of pancreatic differentiation is expected. HNF6 positively regulates NGN3 expression (Jacquemin *et al.* 2000), but expression of NGN3 was not detected at the end-point of the differentiation protocol, but may have occurred with prolonged culture.

Arx was expressed by a few dHASCs cells and co-localized with PDX-1. Arx has a role in α-cell development in the mouse, such that mice which lack Arx do not form α-cells within their pancreas (Collombat *et al.* 2007). These mice also have a larger β-cell mass indicating that Arx is a negative regulator of β-cell mass (Collombat *et al.* 2009). It is possible that Arx^{+} cells may have inhibited the β-cell differentiation of neighbouring cells. HASCs differentiated with the protocol used here were reported to express glucagon protein and mRNA, and insulin mRNA, but not protein (Sharma *et al.* 2003). This thesis did not analyse mRNA expression. In the mouse, differentiation of α- and β-cells occurs simultaneously, with some cells expressing both glucagon and insulin (Slack 1995). However, it appears the differentiation protocol used in this thesis is more efficient at differentiating HASCs towards α-cells rather than β-cells.

PCSK1 (also known as PC1/3) is co-expressed with glucagon during pancreatic development in the mouse, whereas in contrast α-cells of adult mice do not express this marker (Wilson *et al.* 2002). In the pancreas of adult mice it is the β-cells which express PCSK1 instead, where PCSK1 has a role in cleaving proinsulin (Wilson *et al.* 2002). L cells in the gut that express proglucagon also express PCSK1 which cleaves proglucagon into GLP-1 and GLP-2 (Wilson *et al.* 2002). It is predicted that in the developing pancreas PCSK1 also cleaves proglucagon into GLP-1 (and GLP-2) to induce β-cell development (Wilson *et al.* 2002). The upregulation of PCSK1 in the dHASCs which occasionally expressed glucagon could therefore potentially be used to aid the

development of insulin-expressing β-cells. It appears that the *in vitro* differentiation of HASCs is mimicking pancreatic differentiation seen *in vivo*.

The dHASCs also expressed AIRE which has a role in immune tolerance (Kont *et al.* 2008). The expression of AIRE along with TGF-β indicates that dHASCs may be involved in antigen presentation or are directly immunosuppressive, respectively. As expected, the dHASCs did not express the immune cell markers CD68, CD3, CD45, CD11b, CD11c, and CD20. They also did not express HLA-DR suggesting they are not activated, and may have low immunogenicity. CB-HSCs are immunosuppressive and have been used to induce the proliferation of Tregs ($CD4^+CD62L^+$) in a population of spleen-derived lymphocytes (Zhao *et al.* 2009). Treating diabetic mice with the Tregs resulted in upregulation of TGF-β around the islets which formed a protective barrier against immune attack (Zhao *et al.* 2009). Residual β-cells were stimulated to proliferate and β-cell mass increased (Zhao *et al.* 2009). More recently CB-HSCs have been used within the Stem Cell Educator to treat human patients with type 1 diabetes (Zhao *et al.* 2012), as discussed in Section 1.14.2.1. There is currently a grant offered from the JDRF (JDRF.org) to replicate this ground breaking research, and further analyse the clinical outcomes. The expression of AIRE and TGF-β by dHASCs indicates they may have the potential to stimulate the proliferation of Tregs for the treatment of patients with type 1 diabetes, though the exciting α-cell-like character of dHASCs renders this notion less likely.

5.5.2.2 tdHASCs

Culture of HASCs on pancreatic transdifferentiation matrix in pancreatic (trans-differentiated) stem cell culture differentiation medium containing serum produced transdifferentiated HASCs (tdHASCs) which strongly expressed PDX-1, GPR40, SOX-17, and AIRE, moderately expressed TGF-β, and weakly expressed PCSK1, and GIPR. The expression of Oct-4, Nestin and Nanog was not detectable, indicating that all cells had downregulated their stem cell markers upon differentiation. The expression of PDX-1, GPR40, SOX-17, and GIPR indicates that tdHASCs are mostly a population of pancreatic progenitors. GPR40 is a membrane-bound receptor found on insulin-producing cells (Salehi *et al.* 2005). GIPR is a seven-transmembrane protein receptor expressed by cells in the pancreas, upper intestinal tract, adrenal gland, adipose tissue, and the brain (Brubaker and Drucker 2002). GIPR binds GIP which is an insulinotropic peptide (Brubaker and Drucker 2002). Therefore tdHASCs express several key factors required for insulin secretion, and yet did not secrete insulin indicating they have not yet fully matured. The tdHASCs may have expressed HNF6, Arx, and glucagon, but their expression was much weaker than expressed by dHASCs and the results are confounded by the high background levels of staining of the donkey anti-rabbit secondary antibody. Overall the above results suggest that the majority of tdHASCs are pancreatic progenitors that have not fully matured into hormone producing cells.

Importantly, the tdHASCs like dHASCs also expressed TGF-β and AIRE which means that they are also potentially immunosuppressive, or could potentially act as antigen-presenting cells capable of expressing a variety of different lineage-specific markers. However, as with the dHASCs, no other immunological markers were detected, and HLA-DR was absent

suggesting they may have low immunogenicity. The expression of TGF-β and AIRE by undifferentiated HASCs was not assessed; however it is possible that the undifferentiated cells also express these cell markers.

One of the future problems with progressing with these potentially promising findings arises from the fact that the compositions of the differentiation media and extracellular matrices are proprietary to Celprogen Inc.

5.5.2.3 Differentiation of HASCs on tissue culture plates

The differentiation of HASCs on tissue culture plates did not result in the upregulation of a number of pancreatic markers including PDX-1, GPR40, insulin and C-peptide. The protocol devised by Zhao *et al.* (2008) only resulted in cells weakly expressing SOX-17, indicating potential differentiation to cells representing definitive endoderm. Stem cell markers (e.g. Nestin) were not expressed by these cells, indicating that differentiation had begun, and the cells were no longer stem-like. The cells did not express TGF-β.

The NGN protocol (active ingredients being nicotinamide and high glucose) produced cells with a phenotype similar to that obtained with Zhao's protocol in that the cells failed to express any pancreatic markers. They displayed slightly stronger expression of SOX-17. HASCs cultured with nicotinamide have been reported to express glucagon protein and insulin, HNF6, and Nkx2.2 RNA (Miki *et al.* 2005). However, those HASCs were cultured on plates coated with type 1 collagen (Miki *et al.* 2005), suggesting the type of culture surface has a profound effect on the resulting cell phenotype. The HASCs cells cultured in NGN on tissue culture dishes also did not express TGF-β.

Differentiation of HASCs with GLP-1 in tissue culture dishes yielded a population of cells that strongly expressed SOX-17. The GLP-1 differentiated HASCs weakly expressed TGF-β, indicating they were potentially immunosuppressive. The addition of Ex4 to the GLP-1 protocol (GLP-1/Ex4) did not alter the GLP-1 treated HASC phenotype, and hence did not appear to be beneficial.

Due to the lack of favourable differentiation on tissue culture plates these protocols were not repeated.

5.5.3 HASCs potential for therapeutic treatment of type 1 diabetics

HASCs are non-tumorigenic when transplanted into NOD or SCID mice (Sharma *et al.* 2003; Miki *et al.* 2005), suggesting they could be useful for clinical therapy in humans if they can be successfully differentiated to an insulin-producing cell type. Kadam *et al.* managed to successfully differentiate human amnion-derived mesenchymal stromal cells into islet-like clusters that express insulin (Kadam *et al.* 2010). Encapsulation and transplantation of the insulin-expressing cells into diabetic mice restored normoglycemia (Kadam *et al.* 2010). The dHASCs and tdHASCs have the phenotype of pancreatic progenitors. Further research will be necessary to promote these pancreatic progenitors into mature endocrine insulin-expressing cells. They express high

levels of TGF-β which would help protect the graft from immune attack. The fully differentiated β-cells would hopefully exhibit low immunogenicity once matured and have value in treating treat type 1 diabetics. The differentiated HASC population used in therapy would need to contain no undifferentiated stem cells, since even though the HASCs do not form tumours it is still dangerous to treat a patient with undifferentiated stem cells as their lineage development cannot be controlled.

Chapter 6 Cord Blood Hematopoietic Stem Cells

6.1 Introduction

Opposite-sex cord blood infusion of patients for hematopoietic rescue after high-dose chemoradiotherapy for the treatment of a marrow failure syndrome or lympho-haematopoietic malignancy provided an opportunity to determine whether cord blood hematopoietic stem cells (CB-HSCs) have the capacity to differentiate into insulin-expressing β-cells in humans (Huang *et al.* 2011). Some of the infused cord blood cells managed to find their way to the pancreas, and formed insulin-expressing cells within the islets (Huang *et al.* 2011). The study did not establish whether the cells had the functional properties of β-cells (Huang *et al.* 2011). Therefore the ability of cord blood cells to be differentiated along the pancreatic lineage warrants further investigation.

6.2 Scope of chapter

CB-HSCs obtained from Celprogen Inc. were characterized for their stem and pancreatic properties. A population of cells trans-differentiated from cord blood into pancreatic-like cells, termed P-HSCs, were also obtained from Celprogen Inc., and characterized. The CB-HSCs were trialled for their ability to differentiate along the pancreatic lineage by culturing them in a commercially obtained human pancreatic trans-differentiation medium and on a human pancreatic stem cell differentiation extracellular matrix.

6.3 Characterisation of CB-HSCs

CB-HSCs from 1 batch provided by Celprogen Inc. were cultured according to the manufacturer's recommendations in Human Stem Cell Culture Media with serum (M36001-02S, Celprogen Inc.) on 96-well plates precoated with Human Stem Cell Extracellular Matrix (E36001-02-96Well, Celprogen Inc.) up to passage 6. They formed a monolayer having a cobblestone appearance (Figure 6.1). They were phenotyped for the expression of stem cell and pancreatic markers and the images are representative of the findings (n=2) (Figure 6.2). Immunocytochemistry revealed small numbers of cells strongly expressed the stem cell marker Nestin and the definitive endoderm marker SOX-17 (Figure 6.2). CB-HSCs also occasionally showed moderate expression of GPR40 (Figure 6.2). CB-HSCs were proliferative in culture as evidenced by weak nuclear expression of PCNA (Figure 6.2). They did not express the stem cell markers Oct-4 and CD34 (Figure 6.2), the pancreatic markers insulin, glucagon, amylin, Glut-2, PDX-1, Pax6, PCKS1, NeuroD, GIPR, MafA, NGN3, Nkx6.1, Wnt-3, Arx, Glut-1, HNF6 and CXCR4, the immune markers HLA-DR and AIRE, and the endothelial markers CD31 or vWF (Figure 6.2). A summary of the phenotyping of the CB-HSCs is shown in Table 6.1.

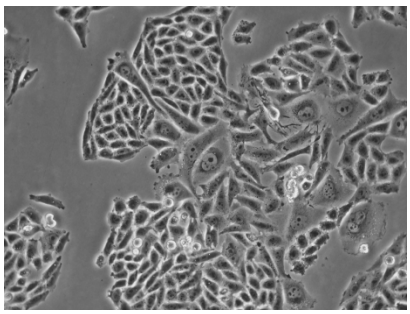
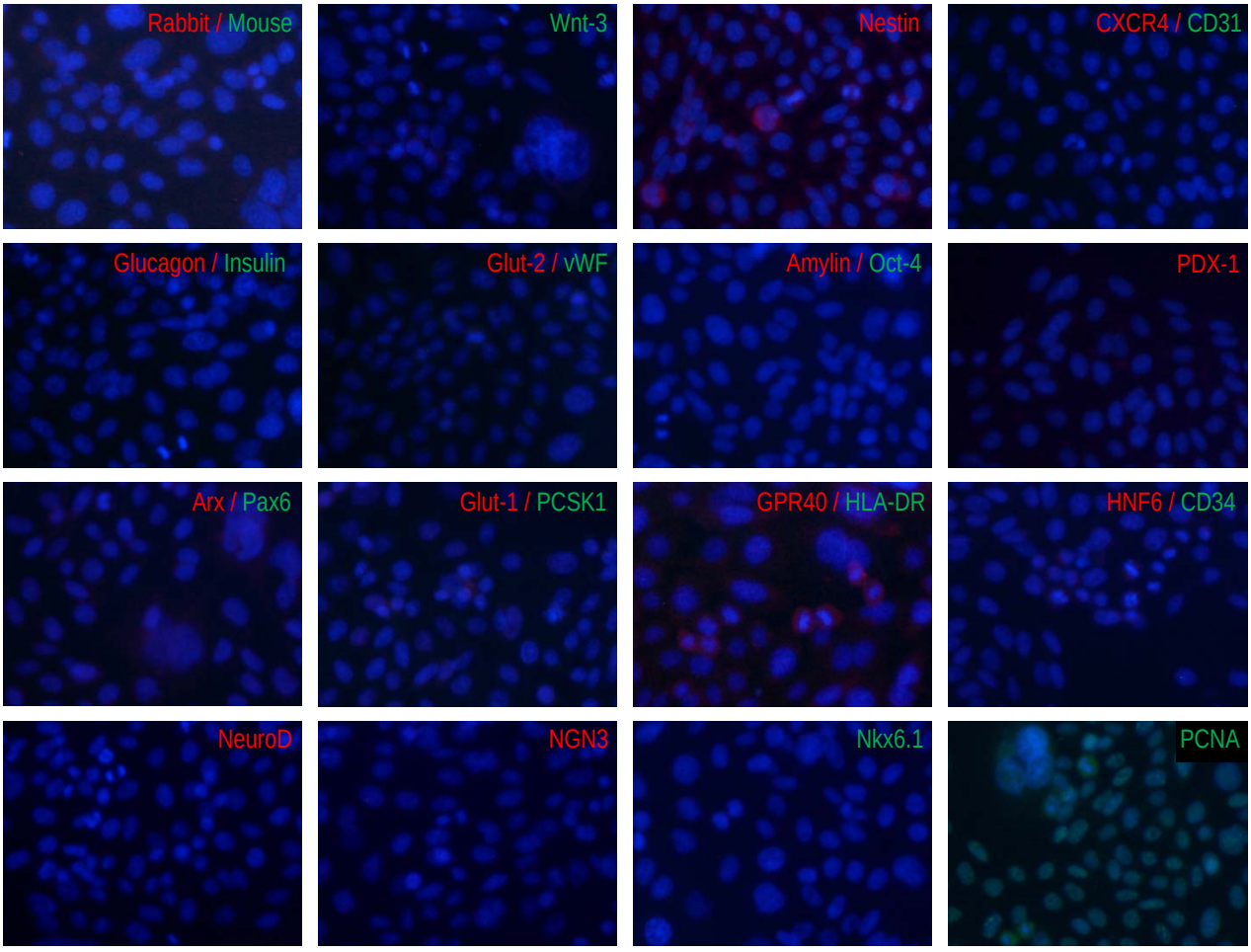


Figure 6.1 Phase contrast image of a culture of CB-HSCs.

CB-HSCs were cultured for 4 days in human stem cell culture medium containing serum on a human stem cell extracellular matrix. The phase contrast image was taken at 200x magnification.



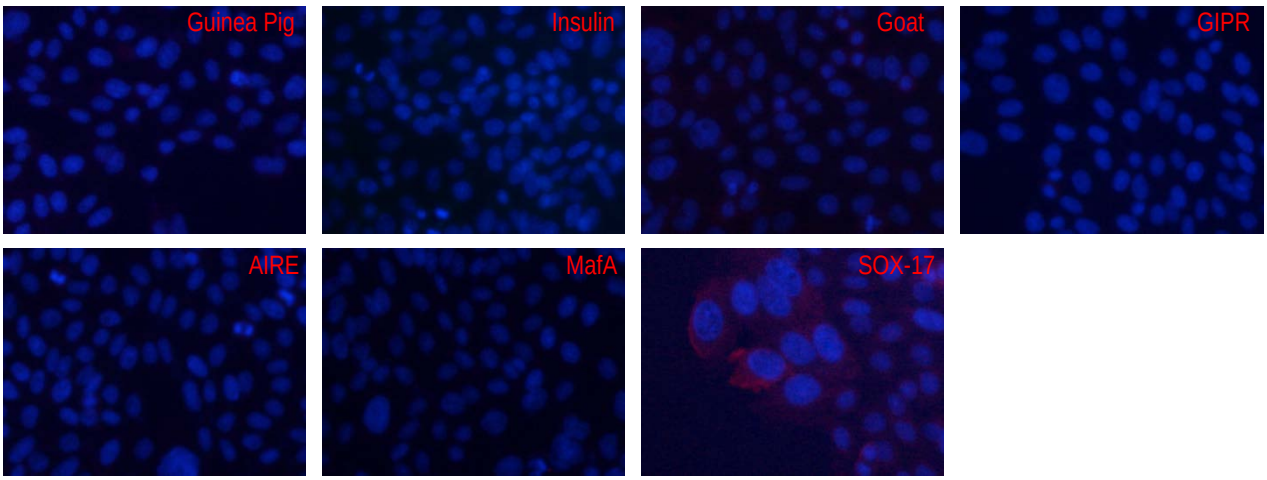


Figure 6.2 Phenotyping of CB-HSCs for stem and pancreatic markers.

CB-HSCs were cultured for 4 days in human stem cell culture medium containing serum on a human stem cell extracellular matrix. Cells were immunostained for the expression of various cell markers. Immunoreactivity was detected with a donkey anti-rabbit, goat anti-guinea pig and donkey anti-goat antibodies (red) and with a donkey anti-mouse antibody (green). Cell nuclei were stained blue with DAPI. Images were taken at 200x magnification. The images are presented so that the staining obtained with each IgG control immediately precedes stainings with antibodies of the same host species.

6.4 Characterisation of P-HSCs

6.4.1 Phenotyping of P-HSCs for cell markers

P-HSCs were cultured according to the manufacturer's recommendations in Human Pancreatic (Trans-Differentiated) Stem Cell Media with serum (M36004-05S, Celprogen Inc.) on 96-well plates precoated with Human Pancreatic Stem Cell Extra-cellular Matrix (E36004-05, Celprogen Inc.). They formed a monolayer with a cobblestone appearance (Figure 6.3). They were phenotyped for the expression of stem cell and pancreatic markers, and found to have a phenotype similar to that of CB-HSCs (Figure 6.4). The experiment was conducted twice with the same batch of P-HSCs, and the images are representative of these findings (Figure 6.4). A sub-set of P-HSCs strongly expressed Nestin (Figure 6.4). Small numbers of P-HSCs moderately expressed the pancreatic markers GPR40, and GIPR (Figure 6.4). Most P-HSCs moderately expressed the proliferation cell marker PCNA (Figure 6.4). They did not express the stem cell markers Oct-4 or CD34, the pancreatic markers insulin, glucagon, amylin, Glut-2, Glut-1, PDX-1, Pax6, PCKS1, NeuroD, HNF6, MafA, Arx, NGN3, Nkx6.1, Wnt-3, SOX-17 or CXCR4, the immune markers HLA-DR or AIRE, and the endothelial markers CD31 and vWF (Figure 6.2). A summary of the phenotyping of the P-HSCs is shown in Table 6.1.

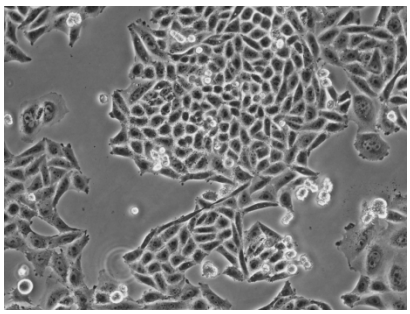
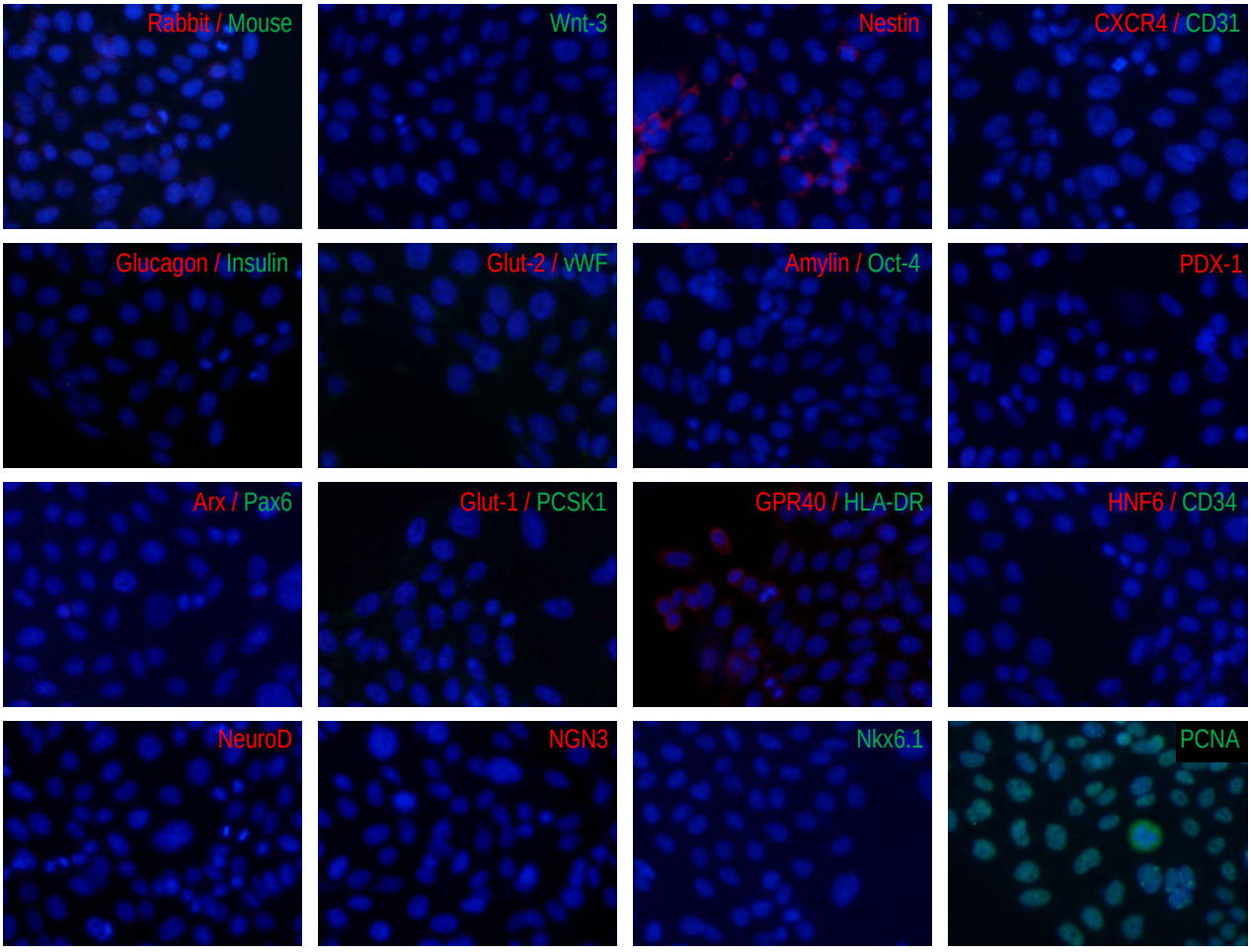


Figure 6.3 Phase contrast image of a culture of P-HSCs.

P-HSCs were cultured for 4 days in human pancreatic (trans-differentiated) stem cell medium containing serum on a human pancreatic stem cell extracellular matrix. The phase contrast image was taken at 200x magnification.



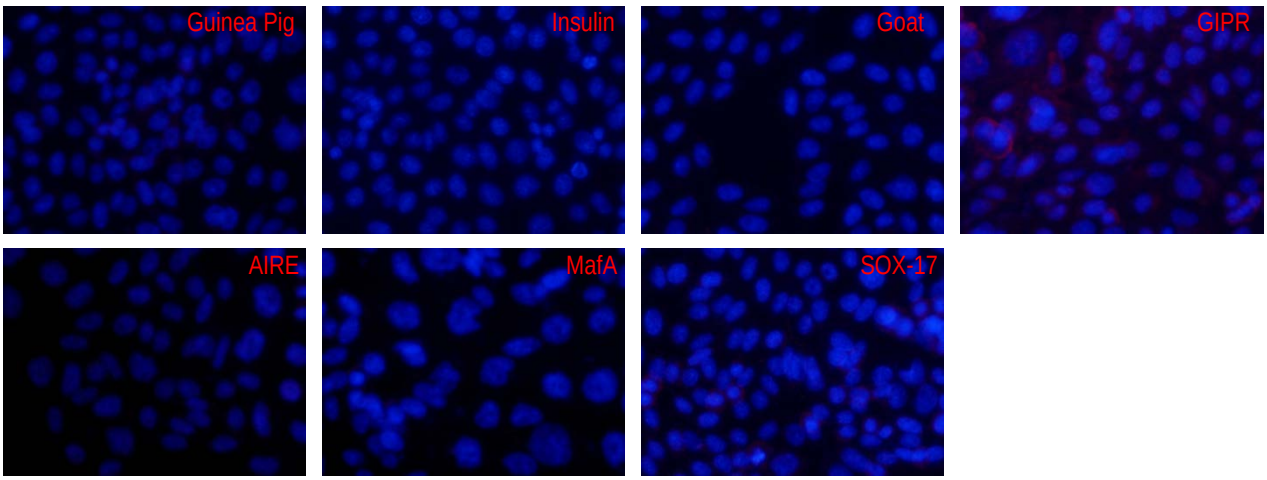


Figure 6.4 Phenotyping of P-HSCs for stem and pancreatic markers.

P-HSCs were cultured for 4 days in human pancreatic (trans-differentiated) stem cell medium containing serum on a human pancreatic stem cell extracellular matrix. Cells were immunostained for the expression of various cell markers. Immunoreactivity was detected with a donkey anti-rabbit, goat anti-guinea pig and donkey anti-goat antibodies (red) and with a donkey anti-mouse antibody (green). Cell nuclei were stained blue with DAPI. Images were taken at 200x magnification. The images are presented so that the staining obtained with each IgG control immediately precedes stainings with antibodies of the same host species.

6.4.2 Summary of the phenotyping of CB-HSCs and P-HSCs

Table 6.1 Summary of the phenotyping of CB-HSCs and P-HSCs for pancreatic and stem cell markers

	CB-HSCs	P-HSCs
Wnt-3		
Nestin	x x x	x x x
CD31		
CXCR4		
Insulin		
Glucagon		
vWF		
Glut-2		
Oct-4		
Amylin		
PDX-1		
Pax6		
Arx		
PCSK1		

	CB-HSCs	P-HSCs
Glut-1		
HLA-DR		
GPR40	x x	x x
CD34		
HNF6		
NeuroD		
NGN3		
Nkx6.1		
PCNA	x	x x
Insulin (GP)		
GIPR		x x
AIRE		
MafA		
SOX-17	x x x	

0	0.1-20	21-40	41-60	61-80	81-100	% Positive

x	x x	x x x	Intensity of staining - weak/moderate/strong

6.4.3 Western blot analysis confirms that P-HSCs do not express insulin

Phenotyping by immunocytochemistry showed that P-HSCs do not express insulin (Figure 6.4). This is at variance with the claims of the manufacturer. Lysates of P-HSCs containing the cytoplasmic and nuclear fractions were subjected to Western blot analysis with the same guinea pig anti-insulin antibody in order to validate the immunocytochemistry findings. The P-HSCs were cultured for 1 week in human pancreatic (trans-differentiated) stem cell medium containing serum on a human pancreatic stem cell extracellular matrix prior to cell lysis. Insulin was not detected in either the cytoplasmic or nuclear fractions of P-HSCs cells (n=2). In contrast, recombinant insulin which was included to confirm the immunoreactivity of the anti-insulin antibody was detectable at 0.1 μg (Figure 6.5). The membrane was stripped and reprobed with an anti-actin antibody, which confirmed that the P-HSC proteins had not been degraded (Figure 6.5).

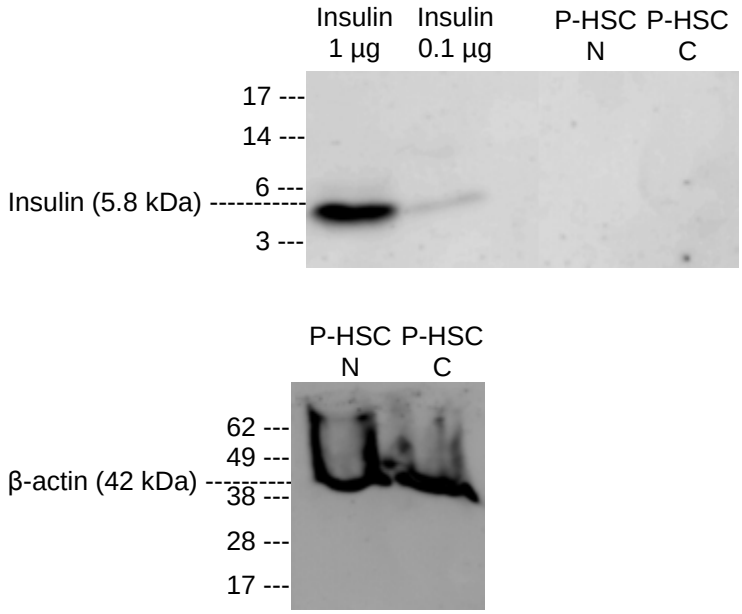


Figure 6.5 Western blot analysis confirms that P-HSCs do not express insulin.

P-HSCs were cultured for 1 week in human pancreatic (trans-differentiated) stem cell medium containing serum on a human pancreatic stem cell extracellular matrix. Cell lysates (1 x 10^6 cell equivalents) containing the cytoplasmic and nuclear fractions were resolved on an SDS-polyacrylamide gel under reducing conditions, and Western blotted with a guinea pig anti-insulin (5.8 kDa) (upper blot) and a rabbit anti-β-actin (42 kDa) (lower blot). Immunoreactivity was detected with a donkey anti-guinea pig HRP-conjugated antibody. Recombinant insulin protein (1 μg and 0.1 μg) was included as a positive control. Abbreviations: P-HSC N: nuclear lysate, P-HSC C: cytoplasmic lysate.

6.5 CB-HSCs and P-HSCs do not display alkaline phosphatase activity

The results in Figure 6.2 and Figure 6.4 showed that CB-HSCs and P-HSCs expressed Nestin, suggesting the cells may have stem cell-like properties. The stem-ness of CB-HSCs and P-HSCs was further investigated by analysing for expression of stem-cell-associated alkaline phosphatase activity (n=2) (Figure 6.6). Neither the CB-HSCs nor the P-HSCs gave the characteristic purple colour following staining with X-Phos and NBT that would indicate alkaline phosphatase activity (Figure 6.6).

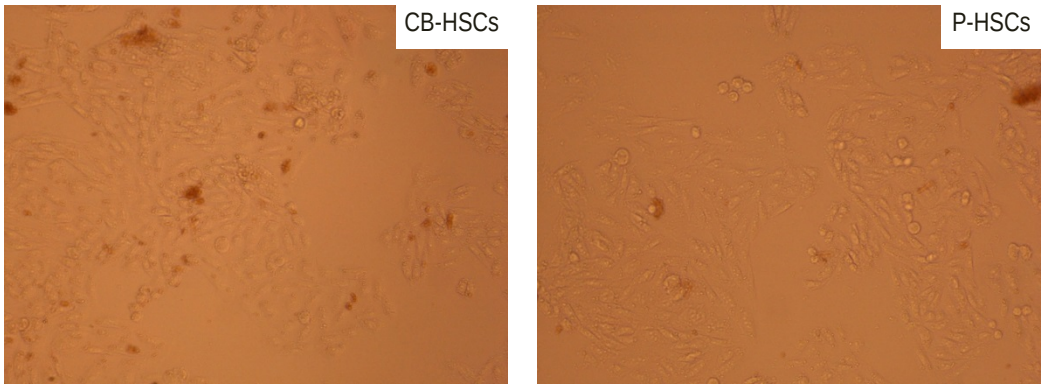
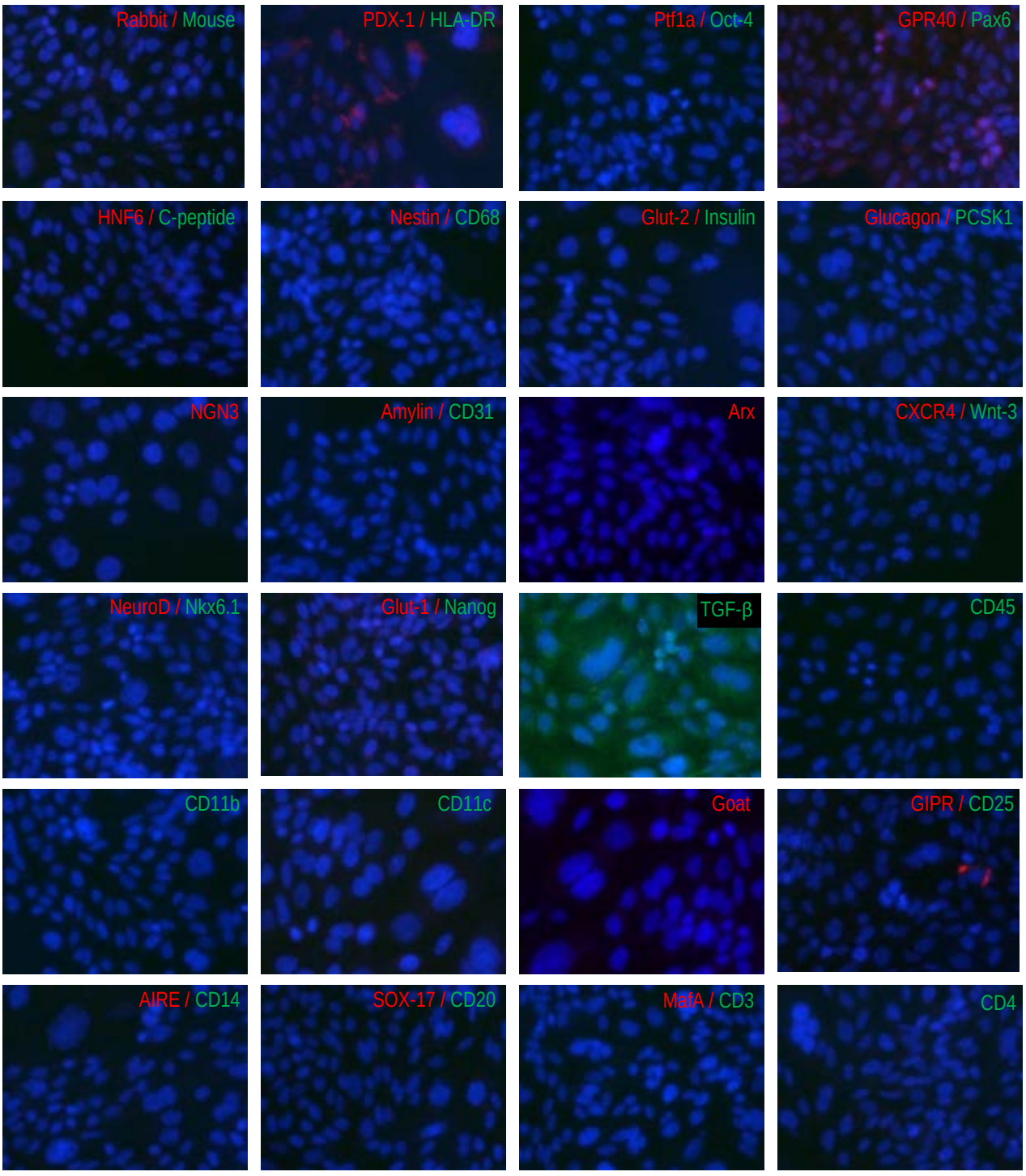


Figure 6.6 CB-HSCs and P-HSCs do not display alkaline phosphatase activity.

CB-HSCs and P-HSCs were cultured for 1 week, as described above, prior to testing for alkaline phosphatase activity. They were tested for alkaline phosphatase activity at pH 6.0 by staining with X-Phos and NBT, where a purple-red colouration would indicate activity.

6.6 Can CB-HSCs be differentiated into pancreatic cells?

Here the aim was to determine whether the Celprogen Inc. trans-differentiation protocol would be able to differentiate CB-HSCs into pancreatic cells, termed here differentiated CB-HSCs (dCB-HSCs). CB-HSCs were cultured for 1 week in Human Pancreatic (Trans-Differentiated) Stem Cell Culture Differentiation Medium with serum (M36004-05DS, Celprogen Inc.) on plates coated with Human Pancreatic Cancer Stem Cell Differentiation Matrix (D36115-42, Celprogen Inc.) (n=2). The medium was refreshed every 24-48 h. The cells were then phenotyped for the expression of stem cell and pancreatic markers (Figure 6.7). The images are representative of the results of 2 separate experiments (Figure 6.7). The dCB-HSCs did not express the stem cell marker Nestin (Figure 6.7). Like the P-HSCs (Figure 6.4), they expressed GIPR and although the expression was stronger, it was expressed by very few cells (Figure 6.7). The dCB-HSCs strongly expressed PDX-1, and moderately expressed GPR40 (Figure 6.7). They strongly expressed TGF-β (Figure 6.7). They did not express the pancreatic markers insulin, glucagon, amylin, C-peptide, Ptf1a, Pax6, HNF6, Glut-2, PCSK1, NGN3, Arx, CXCR4, Wnt-3, NeuroD, Nkx6.1, Glut-1, SOX-17 or MafA, the stem cell marker Oct-4, the immune cell markers HLA-DR, CD68, CD45, CD11b, CD11c, CD25, AIRE, CD14, CD20, CD3, or CD4, and the endothelial marker CD31 (Figure 6.7). A summary of the phenotyping of the dCB-HSCs is shown in Table 6.2.


Rabbit / Mouse
PDX-1 / HLA-DR
Ptf1a / Oct-4
GPR40 / Pax6
HNF6 / C-peptide
Nestin / CD68
Glut-2 / Insulin
Glucagon / PCSK1
NGN3
Amylin / CD31
Arx
CXCR4 / Wnt-3
NeuroD / Nkx6.1
Glut-1 / Nanog
TGF-β
CD45
CD11b
CD11c
Goat
GIPR / CD25
AIRE / CD14
SOX-17 / CD20
MafA / CD3
CD4

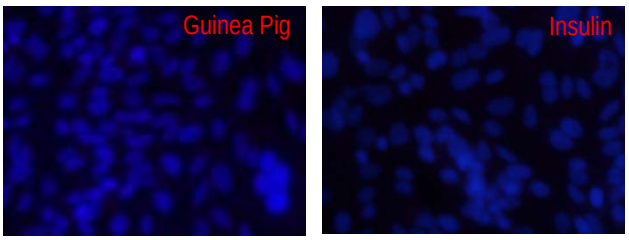


Figure 6.7 Phenotyping of dCB-HSCs for stem and pancreatic markers.

CB-HSCs were cultured for 1 week in human pancreatic (trans-differentiated) stem cell culture differentiation medium containing serum on a human pancreatic stem cell culture differentiation matrix. Cells were immunostained for the expression of various cell markers. Immunoreactivity was detected with donkey anti-rabbit, goat anti-guinea pig and donkey anti-goat antibodies (red) and with a donkey anti-mouse antibody (green). Cell nuclei were stained blue with DAPI. Images were taken at 200x magnification. The images are presented so that the staining obtained with each IgG control immediately precedes stainings with antibodies of the same host species.

Table 6.2 Summary of the phenotyping of dCB-HSCs

	dCB-HSCs
PDX-1	x x x
HLA-DR	
Ptf1a	
Oct-4	
GPR40	x x
Pax6	
HNF6	
C-peptide	
Nestin	
CD68	
Glut-2	
Insulin	
Glucagon	

	dCB-HSCs
PCSK1	
NGN3	
CD3	
Amylin	
CD31	
Arx	
CXCR4	
Wnt-3	
NeuroD	
Nkx6.1	
Glut-1	
Nanog	
TGF-β	x x x

	dCB-HSCs
CD45	
CD11b	
CD11c	
GIPR	x x x
CD25	
AIRE	
CD14	
SOX-17	
CD20	
MafA	
CD4	
Insulin	

0	0.1-20	21-40	41-60	61-80	81-100	% Positive

x	x x	x x x	Intensity of staining - weak/moderate/strong

6.7 Discussion

6.7.1 Phenotype of CB-HSCs

The phenotype of CB-HSCs sourced from Celprogen Inc. differed from that reported by the manufacturer. These differences were not discussed further with Celprogen Inc. and it is not known whether the variation seen is specific to the batch of CB-HSCs obtained or is typical of CB-HSCs cultured under these conditions. The CB-HSCs were expected to express the stem cell marker Nestin and the HSC marker CD34. In this study it was found while the CB-HSCs expressed Nestin as predicted, they did not express CD34. Nestin expression has been used as a marker of cells capable of pancreatic differentiation in primate ESCs (Yue *et al.* 2006). Nestin-selected ESCs differentiate into insulin-producing cells after exposure to GLP-1 (Yue *et al.* 2006). Therefore CB-HSCs expressing Nestin might be expected to have the ability to differentiate into pancreatic cells. In terms of CD34 expression, it was reported that the prevalence of $CD34^+$ stem cells in isolated cord blood is only ~1% (Nimgaonkar *et al.* 1995). It is possible that Celprogen Inc. failed to recheck the expression of CD34 on every batch of CB-HSCs distributed to purchasers. Alternatively, CD34 may have been expressed at such low levels that it was undetectable in the present study, or perhaps it was downregulated during expansion of the cells.

The expression of PCNA by the CB-HSCs indicates the cell population is proliferative, but they did not express alkaline phosphatase which is characteristic of stem cell populations.

Expression of the definitive endoderm marker SOX-17 (D'Amour *et al.* 2006) by the CB-HSCs cultured in Human Stem Cell Culture Media with Serum on Human Stem Cell Extracellular Matrix plates could indicate that they have spontaneously begun to differentiate towards the pancreatic lineage. Conversely, the expression of SOX-17 by undifferentiated HADFILs (human amnion-derived fibroblast-like cells) is reduced after induction of pancreatic differentiation (Tamagawa *et al.* 2009). It is often not appreciated that SOX-17 is not necessarily a marker of endoderm, being quite widely expressed on different cell types such as neuronal, epithelial, and hematopoietic cells (Sohn *et al.* 2006; Lange *et al.* 2009; Nakajima-Takagi *et al.* 2013).

The membrane-bound receptor GPR40 is expressed on insulin-producing cells (Salehi *et al.* 2005). The moderate expression of GPR40 supports the notion that the CB-HSCs in the present study were undergoing pancreatic differentiation. However, no cells expressed insulin indicating the cells were still immature or had not adopted a proper β-cell phenotype.

6.7.2 Phenotype of differentiated CB-HSCs (dCB-HSCs)

CB-HSCs that were differentiated into dCB-HSCs by culture in human pancreatic (trans-differentiated) stem cell culture differentiation medium containing serum on a human pancreatic stem cell culture differentiation matrix expressed the pancreatic marker PDX-1. This *de novo* expression of PDX-1 indicates the cells had differentiated towards the pancreatic lineage at least as

far as formation of the posterior foregut (D'Amour *et al.* 2006). PDX-1 is expressed from the point of posterior foregut differentiation and is then continuously expressed as β-cells mature (D'Amour *et al.* 2006).

As with the CB-HSCs and P-HSCs, dCB-HSCs also expressed GPR40 to a similar extent. In contrast, GIPR was only expressed by dCB-HSCs and P-HSCs, but by only a few cells. Taken together, the fact that the dCB-HSCs expressed PDX-1, GPR40, and GIPR provides evidence of pancreatic differentiation, and yet the cells should be regarded as progenitor cells as they did not express the mature endocrine β-cell markers insulin and amylin.

The finding that the dCB-HSCs strongly expressed TGF-β could indicate that they are immunosuppressive. Such a property could be beneficial for patients with type 1 diabetes if the differentiated cells retain TGF-β expression and form an immunosuppressive barrier after transplantation into the pancreas. Haller *et al.* (2011) reported that the infusion of undifferentiated autologous cord blood into children with type 1 diabetes leads to a small increase in the frequency of Tregs, however there was no long-term change in C-peptide levels (Haller *et al.* 2011). A subpopulation of CB-HSCs termed CB-SCs can be isolated from whole cord blood by their unique ability to attach to hydrophobic dishes, and have the ability to induce the proliferation of Tregs (Zhao *et al.* 2012). The system is called the Stem Cell Educator where a patient's lymphocytes are allowed to flow over attached CB-SCs, and the lymphocytes which differentiate into Tregs are then returned to the patient (Zhao *et al.* 2012). An earlier study (2009) had shown that CB-SC-expanded Tregs transplanted into mice cause an upregulation of TGF-β around islets forming an immunosuppressive barrier allowing for regeneration of β-cell mass (Zhao *et al.* 2009). Human type 1 diabetes subjects treated with lymphocytes subjected to the Stem Cell Educator had increased frequencies of $CD4^+CD25^+FOXP3^+$ Tregs, and heightened levels of TGF-β after 4 weeks of treatment (Zhao *et al.* 2012). Treated patients with moderate or severe type 1 diabetes showed improved fasting C-peptide levels at 12 and 24 weeks (Zhao *et al.* 2012), indicating the pancreas may be undergoing regeneration. Therefore the use of CB-HSCs and CB-SCs to produce Tregs capable of counteracting the immune destruction associated with type 1 diabetes, and the dependence on TGF-β, warrants further investigation.

6.7.3 Phenotype of P-HSCs

The P-HSCs differentiated from CB-HSCs by Celprogen Inc. were reported by the provider to express insulin, PDX-1, CD117, and GAD. The cells purchased in the present study expressed several pancreatic markers (GPR40 and GIPR), and retained Nestin expression like the parental cells. However, they did not express insulin and PDX-1 as expected. Nestin is co-expressed with PDX-1, and occasionally with insulin, during the pancreatic differentiation of ESCs, but is downregulated when islet-like clusters are formed (Yue *et al.* 2006). The P-HSCs moderately expressed PCNA indicating they are a proliferative population, but were not stem-like as they did not express alkaline phosphatase activity.

Expression of SOX-17 was lost after the P-HSCs had been induced to undergo pancreatic differentiation, in accord with the finding by Tamagawa *et al.* (2009) that SOX-17 RNA levels decrease after the pancreatic differentiation of HADFILs.

The differentiated P-HSCs moderately expressed GPR40, which as mentioned above is present on insulin-producing cells (Salehi *et al.* 2005). The pancreatic receptor GIPR, which is involved in insulin secretion, but which is also expressed by cells in the upper intestinal tract, adrenal gland, adipose tissue, and the brain (Brubaker and Drucker 2002) was moderately expressed by a few P-HSCs, whereas it was absent from the parental cells.

6.7.4 Potential of CB-HSCs, dCB-HSCs, and P-HSCs

The expression of pancreatic markers by differentiated CB-HSCs provides evidence of their potential to undergo pancreatic differentiation. Furthermore the increased expression of pancreatic markers by dCB-HSCs and P-HSCs suggests that it may be possible with additional approaches to promote their maturation to insulin-producing cells for the treatment of type 1 diabetes. The immunosuppressive capabilities of the dCB-HSCs warrants further investigation of their potential as a tolerogenic cell type for generating Tregs to prevent graft destruction associated with β-cell replacement therapies.

Chapter 7 Adipose Stem Cells

7.1 Introduction

The ease in obtaining adipose stem cells (ASCs) directly from lipoaspirate means that type 1 diabetes patients could donate some of their excess fat stores to provide stem cells for their own treatment (Locke *et al.* 2011). Several research groups have shown that ASCs can be differentiated towards the pancreatic lineage (Timper *et al.* 2006; Lin *et al.* 2009; Chandra *et al.* 2011; Kang *et al.* 2011). ASCs have been differentiated to produce insulin mRNA in just 3 days (Timper *et al.* 2006). ASCs have also been differentiated using a multi-step process to form insulin-producing cells that express a range of different pancreatic mRNAs (Chandra *et al.* 2011). However, the level of insulin mRNA expression was 10^5 times lower than that of the cells of a human foetal pancreas (12 week) (Chandra *et al.* 2011). The differentiated ASCs expressed insulin, C-peptide, PDX-1, somatostatin, and Glut-2 in islet-like cell aggregate (ICAs) (Chandra *et al.* 2011). Transplantation of encapsulated ICAs and undifferentiated ASCs into STZ-induced diabetic Swiss albino mice lowered their levels of blood glucose, but not to normoglycemic levels (Chandra *et al.* 2011). Therefore current ASC differentiation protocols need to be enhanced to increase the ability of differentiated ASCs to control blood glucose.

7.2 Scope of chapter

This chapter describes the characterisation and differentiation of 1 batch of commercial ASCs obtained from Invitrogen™. The ASCs were cultured in conventional tissue culture plates, in ultra-low attachment plates, and in hydrophobic petri dishes. Stem cell properties such as expression of the stem cell markers, aldehyde dehydrogenase (ALDH), and alkaline phosphatase were investigated. The ability of the ASCs to be forced to differentiate into adipocytes was investigated. The ASCs were also tested for their ability to differentiate towards the pancreatic lineage by subjecting them to different differentiation protocols, including stage-specific protocols in which they were successively differentiated to definitive endoderm, primitive gut tube, and posterior foregut. Both current ASC differentiation protocols and combinations of protocols previously used to differentiate other stem cell populations were trialled in order to increase pancreatic marker expression by the differentiating ASCs.

7.3 Characterisation of ASCs for adipose stem cell markers

ASCs were cultured for 2 weeks in conventional tissue culture plates with expansion medium (n=2) (Figure 7.1). All cells strongly expressed the ASC markers CD29 (integrin β1 subunit) and CD90 (Thy-1) (Figure 7.1), and weakly expressed the definitive endoderm marker SOX-17 (Figure 7.2). They did not express insulin (Figure 7.2). These experiments were conducted twice and the images are representative of the findings (Figure 7.2). A summary of the phenotype of ASCs is presented in Table 7.1.

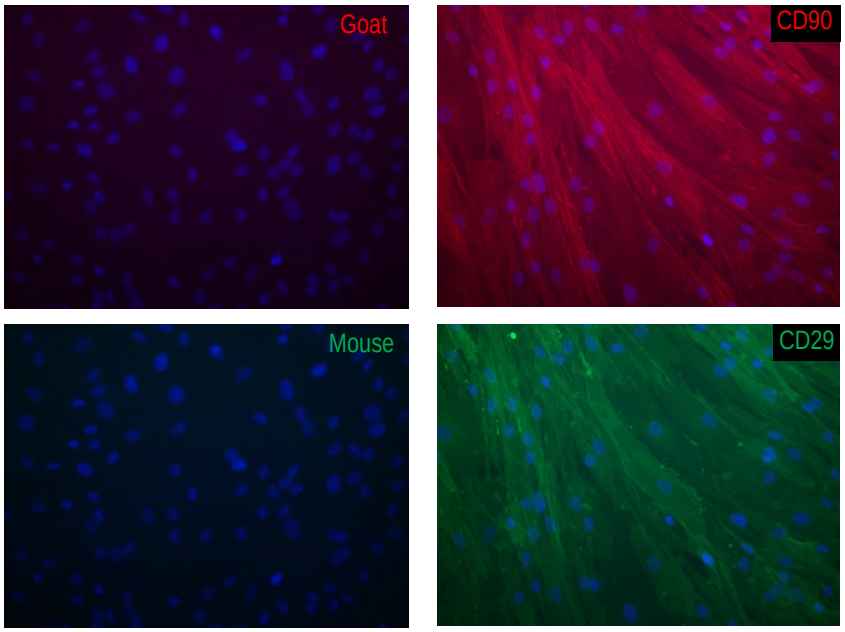


Figure 7.1 Phenotyping of ASCs for adipose stem cell markers.

ASCs were cultured for 2 weeks in expansion medium. They were immunostained for the expression of CD90 and CD29. Immunoreactivity was detected with donkey anti-goat (red) and donkey anti-mouse (green) antibodies. Cell nuclei were stained blue with DAPI. Images were taken at 400x magnification. The images are presented so that the staining obtained with each IgG control immediately precedes stainings with antibodies of the same host species.

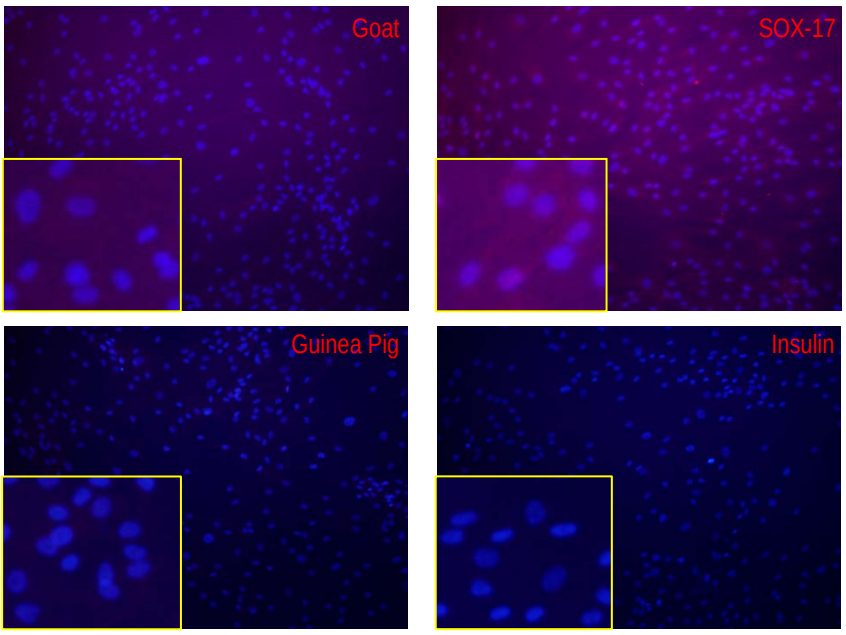


Figure 7.2 Phenotyping of ASCs for stem and pancreatic cell markers.

ASCs were cultured for 2 weeks in expansion medium. Cells were immunostained for the expression of stem cell and pancreatic cell markers. Immunoreactivity was detected with donkey anti-goat (red), donkey anti-mouse (green), goat anti-guinea pig (red), and donkey anti-rabbit (green) antibodies. Cell nuclei were stained blue with DAPI. Images were taken at 200x magnification; inset is a 4x magnification of part of the image. The images are presented so that the staining obtained with each IgG control immediately precedes stainings with antibodies of the same host species.

7.4 Induced adipogenesis of ASCs

ASCs were cultured In conventional tissue culture dishes for 2 days in expansion medium and then the medium was aspirated and replaced with STEMPRO® Adipocyte Differentiation Basal Medium and 1x STEMPRO® Adipogenesis Supplement (A10070-01, Gibco), which was refreshed every 3 days (n=2). Cells were analysed for expression of lipid by Oil Red O staining after 1, 2, and 3 weeks of culture (Figure 7.3). The ASCs rapidly developed an adipocyte character characterised by an increase in the appearance of lipid droplets within the cell (Zuk *et al.* 2002). The differentiated cells contained lipid-containing vacuoles which stained particularly brightly (Figure 7.3). The number and size of the lipid-containing vacuoles steadily increased during the time in culture (Figure 7.3). In contrast, the adipose stem cells maintained in expansion medium did not stain red with Oil Red O (Figure 7.3). These results were representative of 2 separate experimentss.

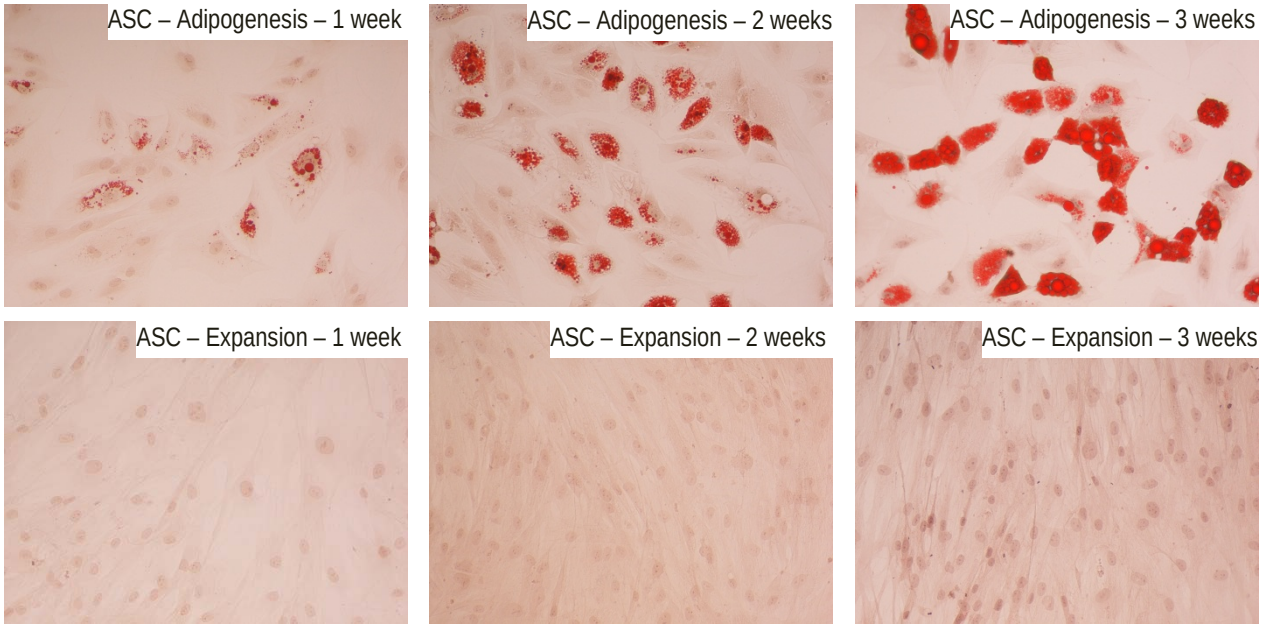


Figure 7.3 Induced adipogenesis of ASCs.

ASCs were cultured for 1, 2, and 3 weeks in StemPro® Adipogenesis Differentiation medium (upper panel of photos) or expansion medium (lower panel of photos). They were stained for the presence of lipid with Oil Red O, which stains lipids red. Cells were co-stained with hematoxylin (brown). Abbreviations: Adipogenesis, StemPro® Adipogenesis Differentiation medium; Expansion, expansion medium. Images were taken at 200x magnification.

7.4.1 Phenotyping of ASCs for adipose stem cell markers after induced adipogenesis

All ASCs cultured for 2 weeks in StemPro® Adipogenesis Differentiation medium continued to express the adipose stem cell markers CD90 and CD29 (Figure 7.4), and weakly expressed the definitive endoderm marker SOX-17 (n=2) (Figure 7.5). They did not express insulin (Figure 7.5). A summary of the phenotype of ASCs undergoing adipogenesis is presented in Table 7.1.

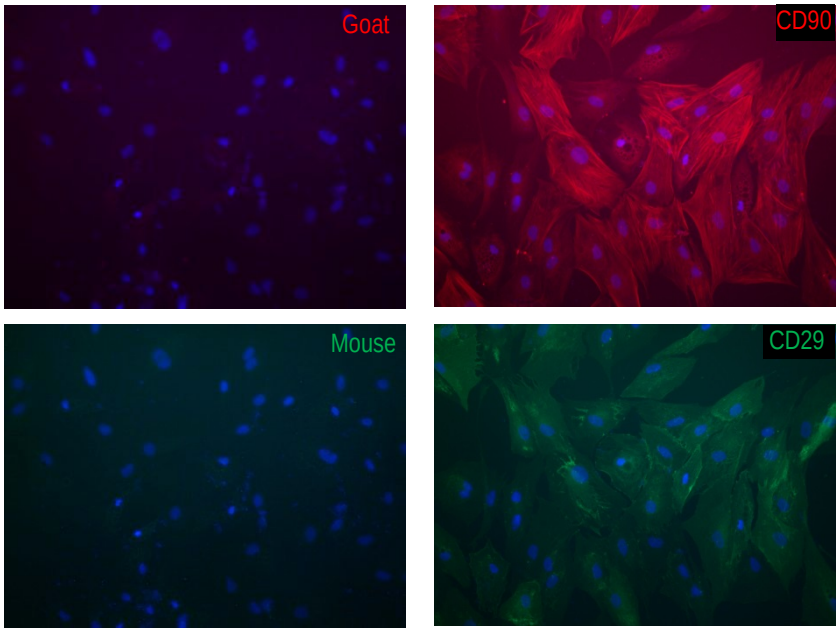
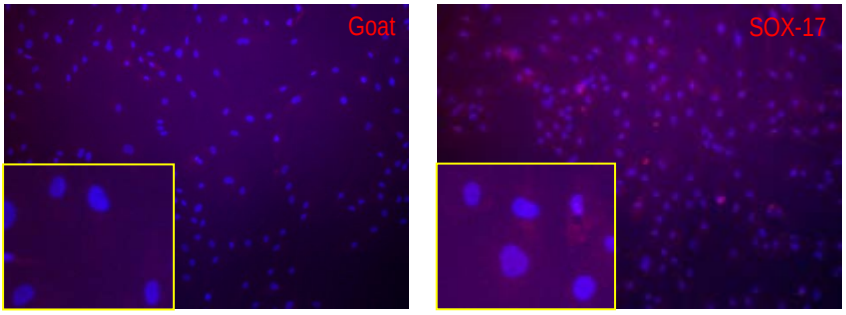


Figure 7.4 ASCs forced to undergo adipogenesis and phenotyped for the expression of adipose stem cell markers.

ASC were cultured for 2 weeks in StemPro® Adipogenesis Differentiation medium, and immunostained for the expression of CD90 and CD29. Immunoreactivity was detected with donkey anti-goat (red) and donkey anti-mouse (green) antibodies. Cell nuclei were stained blue with DAPI. Images were taken at 400x magnification. The images are presented so that the staining obtained with each IgG control immediately precedes stainings with antibodies of the same host species.



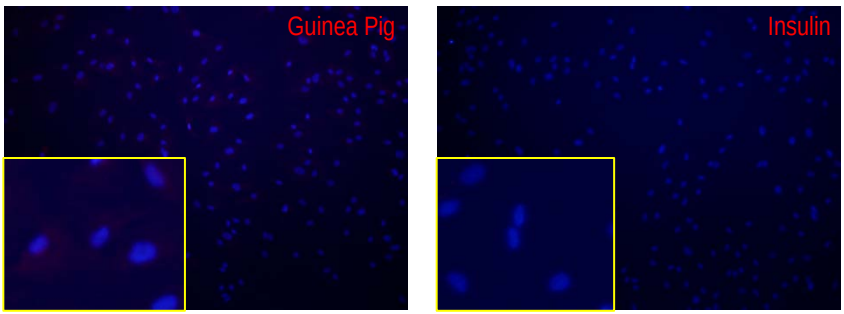


Figure 7.5 Phenotyping of ASCs for stem and pancreatic markers after adipogenesis.

ASCs were cultured for 2 weeks in StemPro® Adipogenesis Differentiation medium and immunostained for the expression of stem cell and pancreatic cell markers. Immunoreactivity was detected with donkey anti-goat (red), donkey anti-mouse (green), goat anti-guinea pig (red), and donkey anti-rabbit (green) antibodies. Cell nuclei were stained blue with DAPI. Images were taken at 200x magnification; inset is a 4x magnification of part of the image. The images are presented so that the staining obtained with each IgG control immediately precedes stainings with antibodies of the same host species.

Table 7.1 Summary of markers expressed by ASC after expansion or adipogenesis

	Expansion	Adipogenesis
CD29	x x x	x x x
CD90	x x x	x x x
SOX-17	x	x
Insulin		

0	0.1-20	21-40	41-60	61-80	81-100	% Positive

x	x x	x x x	Intensity of staining - weak/moderate/strong

7.5 ASCs display aldehyde dehydrogenase activity

ASCs were analysed further for stem cell properties, given that they express the adipose stem cell markers CD90 and CD29 (Figure 7.1). They were cultured for 1 week in tissue culture plates in expansion medium and screened for ALDH enzyme activity (Figure 7.6). The ALDEFLUOR® assay revealed that a subpopulation (6.5%) of ASCs displayed a high level of ALDH expression ($ALDH^+$), as shown by a strong green fluorescent signal (Figure 7.6 and Figure 7.7). RINm5F cells used as controls were not stained green by the ALDEFLUOR® assay (Figure 7.6). The ASCs were also cultured for 10 weeks in tissue culture plates in expansion medium and passaged weekly prior to analysis. ADLH expression was quantified by flow cytometry up to passage 10 (P10) to investigate whether ASCs lose this stem and progenitor cell marker with increasing passage number. There was no loss in the proportion of $ALDH^+$ cells between passages P3 to P10 (Figure 7.7).

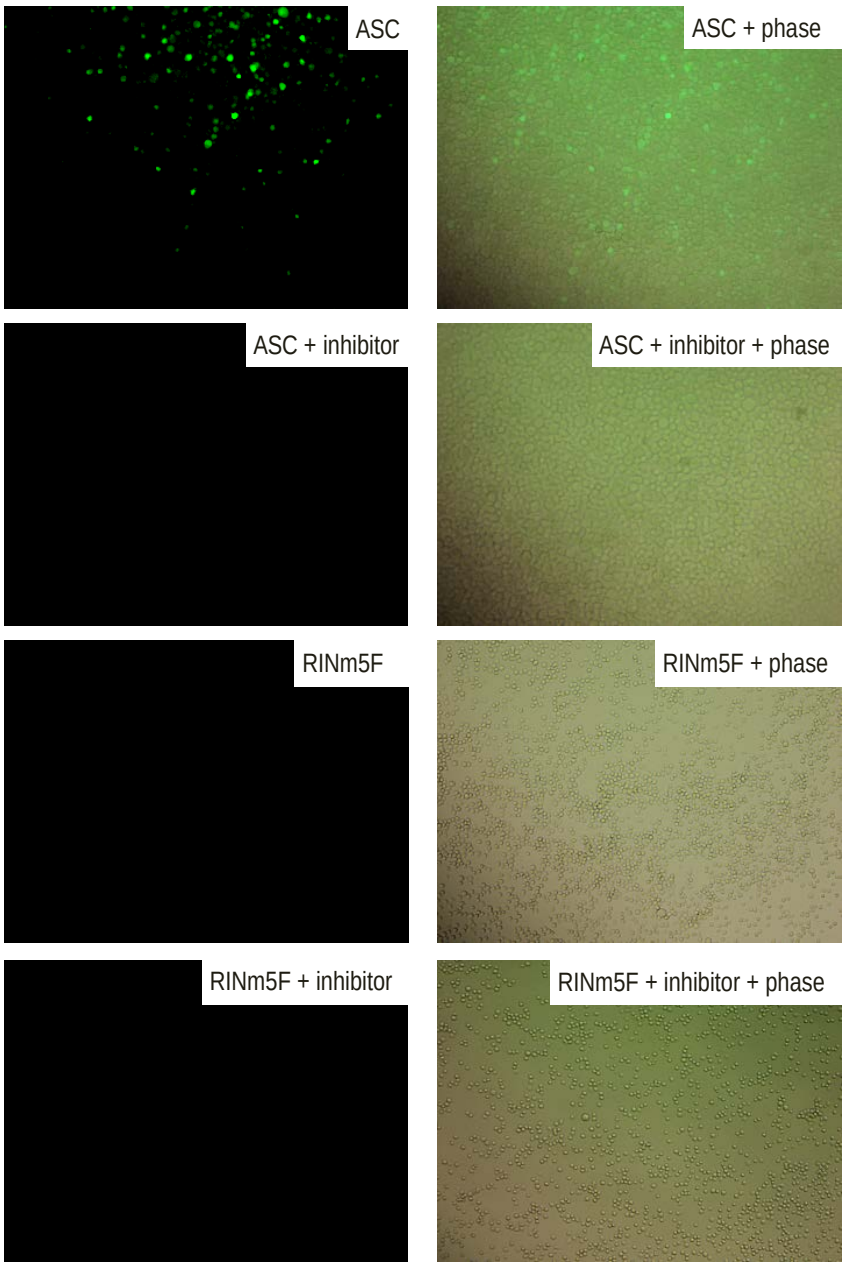


Figure 7.6 A subpopulation of ASCs display ALDH activity.

ASCs were cultured in expansion medium in tissue culture dishes for 1 week prior to analysis. They were tested for ALDH activity by incubating them with the substrate BAAA which fluoresces bright green after modification by ALDH. An ALDH inhibitor and the RINm5F cell line were used as negative controls. The cells were viewed by phase contrast and fluorescence microscopy. Images were taken at 100x magnification.

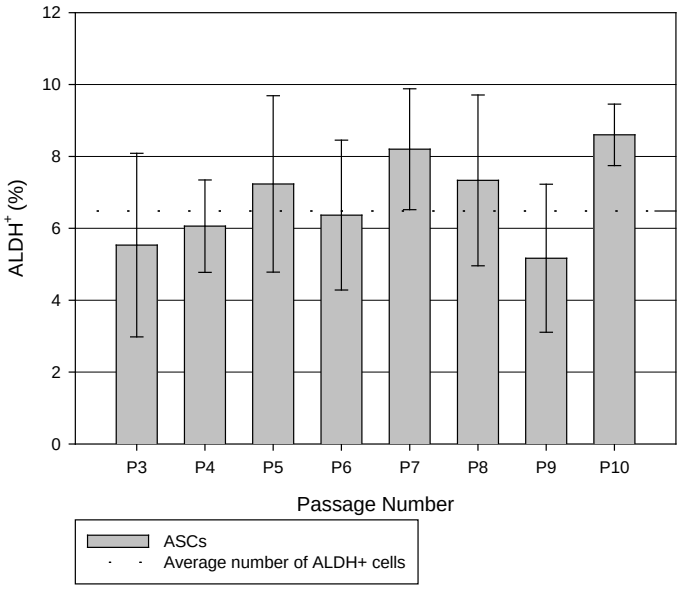


Figure 7.7 ASC retain ALDH enzyme expression for at least 10 passages.

ASCs were cultured for 10 weeks in expansion medium in tissue culture plates and passaged weekly. They were analysed for ALDH activity by flow cytometry (n=3-7).

7.6 ASCs do not display alkaline phosphatase activity

As above, ASCs express CD90 and CD29, and a subpopulation highly express the ALDH enzyme. They were stained with Naphthol/Fast Red Violet solution to determine whether they expressed stem-cell associated alkaline phosphatase activity (Figure 7.8). They did not display the characteristic purple colour that would indicate alkaline phosphatase activity (Figure 7.8).

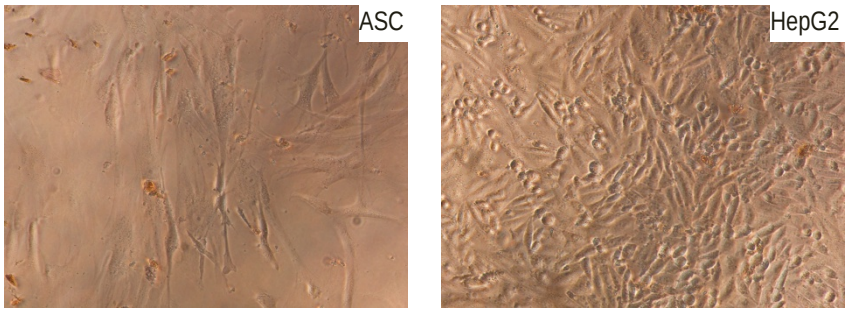


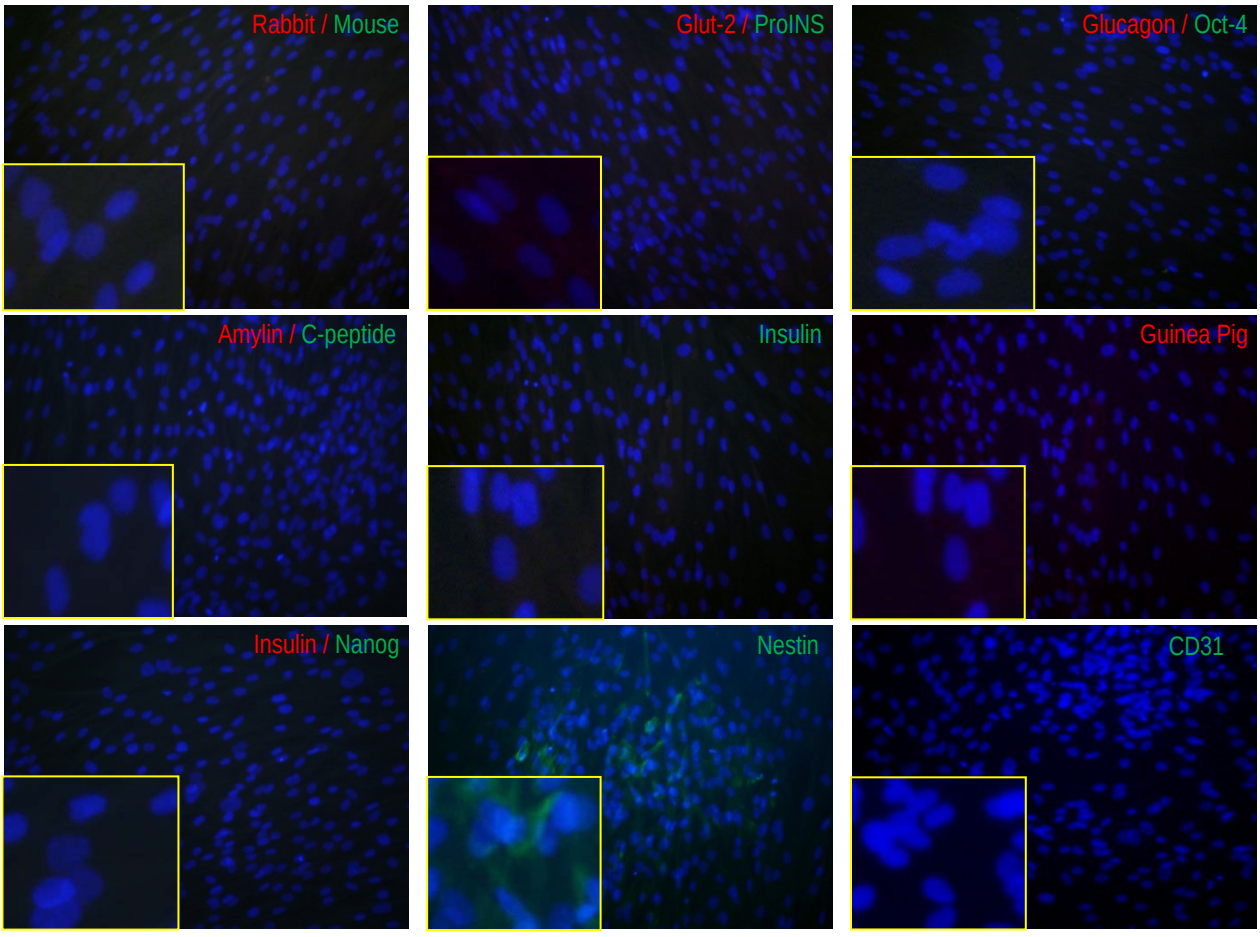
Figure 7.8 ASCs do not display alkaline phosphatase activity.

ASCs were cultured for 3 days in expansion medium prior to testing for alkaline phosphatase activity at pH 6.0 with Naphthol/Fast Red Violet solution, where a purple-red colouration would indicate activity (n=2). HepG2 was included as a negative control cell line as it does not have alkaline phosphatase activity. Images were taken at 200x magnification.

7.7 Trials to differentiate attached ASCs towards the pancreatic lineage

7.7.1 Trials to differentiate ASCs into hormone-expressing endocrine cells

The commercial ASCs had stem and progenitor cell associated ALDH expression (Figure 7.6), which suggested they should be plastic. They were cultured in expansion medium in tissue culture dishes and further phenotyped at days 3, 7 and 14 for both stem cell and pancreatic markers to determine their features when cultured without forced differentiation (n=2) (Figure 7.9 to 15). The images below are representative of 2 separate epxeriments. After 3 days of culture the ASCs weakly expressed the definitive endoderm marker SOX-17 (Figure 7.9), as above, and some cells strongly expressed the stem cell marker Nestin indicating the population of cells was heterogenous (Figure 7.9). They did not express the stem cell markers Oct-4 or Nanog, the pancreatic markers Glut-2, proinsulin, glucagon, amylin, C-peptide, insulin, the monocyte marker CD14 or the endothelial cell marker CD31 (Figure 7.9). A summary of these findings is presented in Table 7.3.



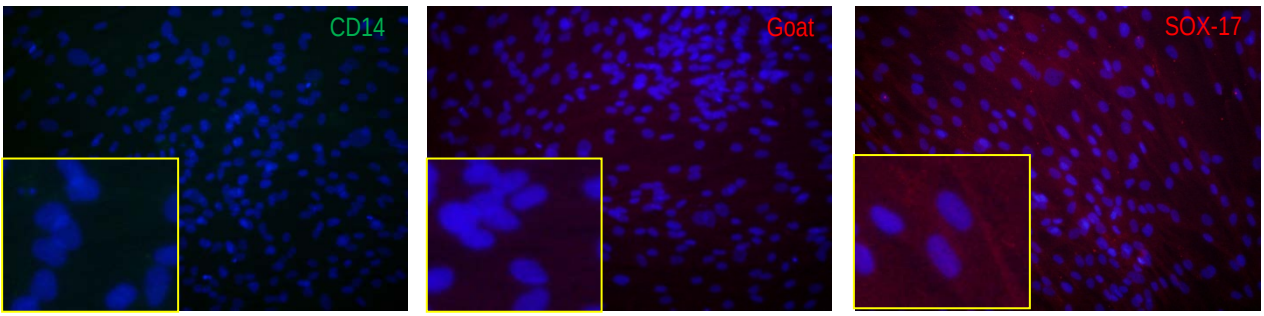
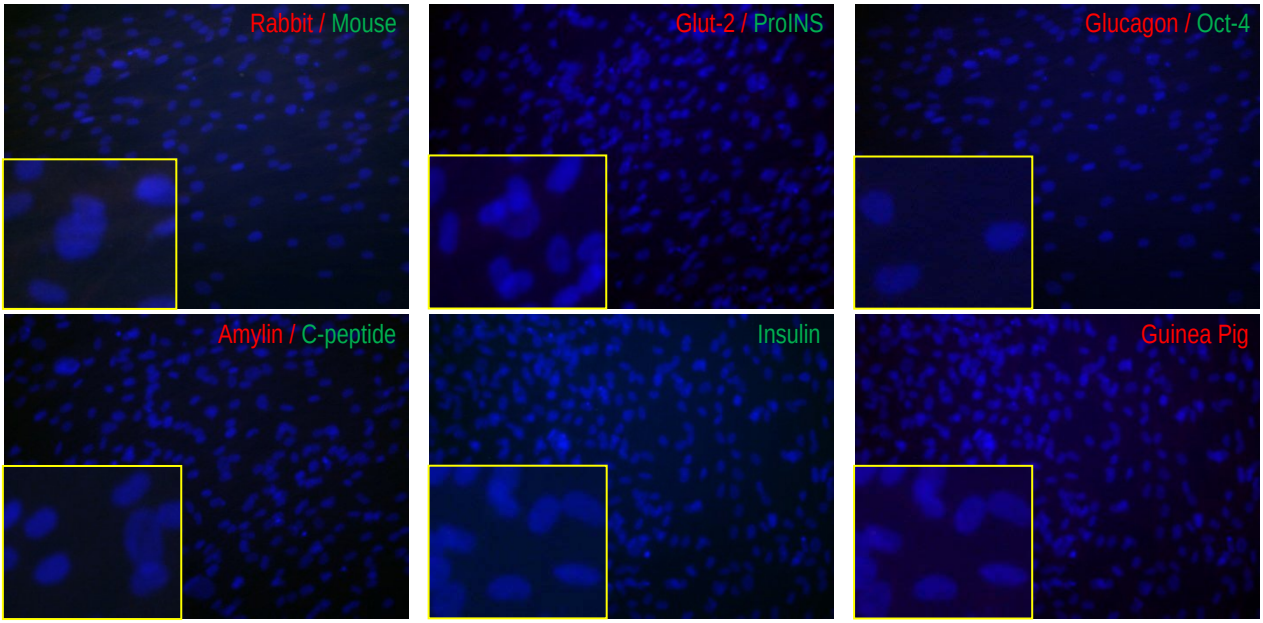


Figure 7.9 Phenotyping of ASCs cultured for 3 days in tissue culture plates for stem and pancreatic markers.

ASCs were cultured for 3 days in expansion medium in tissue culture plates, and immunostained for the expression of stem cell and pancreatic cell markers. Immunoreactivity was detected with donkey anti-rabbit (red), donkey anti-mouse (green), goat anti-guinea pig (red), and donkey anti-goat (red) antibodies. Cell nuclei were stained blue with DAPI. Images were taken at 200x magnification; inset is a 4x magnification of part of the image. The images are presented so that the staining obtained with each IgG control immediately precedes stainings with antibodies of the same host species.

After seven days in expansion medium the ASCs continued to express the definitive endoderm marker SOX-17, and fewer cells expressed Nestin, and still did not express Oct-4 or Nanog (Figure 7.10). They did not express other pancreatic markers tested including Glut-2, proinsulin, glucagon, amylin, C-peptide, and insulin (Figure 7.10). They did not express either CD14 or CD31 (Figure 7.10). A summary of these findings is presented in Table 7.3.



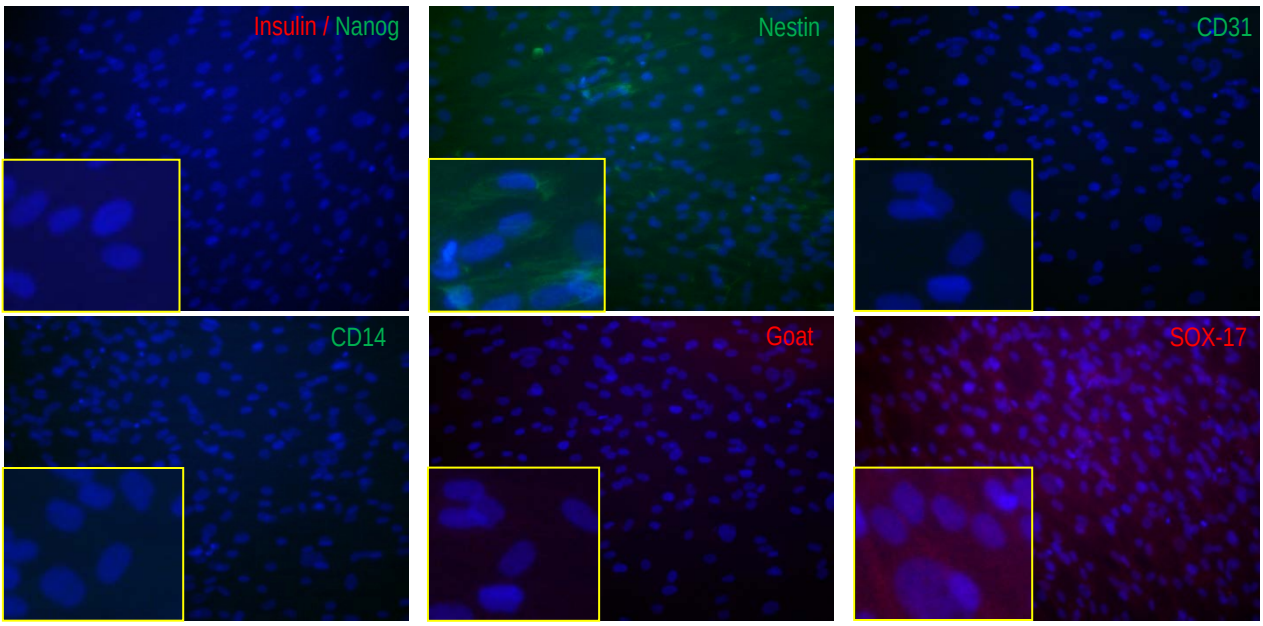
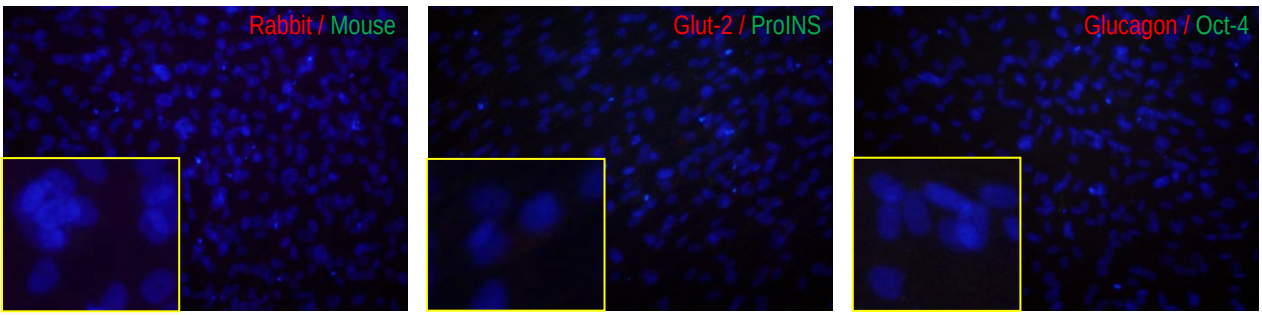


Figure 7.10 Phenotyping of ASCs cultured for 1 week in tissue culture plates for stem and pancreatic markers.

ASCs were cultured for 1 week in expansion medium in tissue culture plates. Cells were immunostained for the expression of stem cell and pancreatic markers. Immunoreactivity was detected with donkey anti-rabbit (red), donkey anti-mouse (green), goat anti-guinea pig (red), and donkey anti-goat (red) antibodies. Cell nuclei were stained blue with DAPI. Images were taken at 200x magnification; inset is a 4x magnification of part of the image. The images are presented so that the staining obtained with each IgG control immediately precedes stainings with antibodies of the same host species.

After fourteen days in expansion medium the ASCs weakly expressed the definitive endoderm marker SOX-17, and a small number of Nestin positive ASCs were present (Figure 7.11). They did not express Oct-4 or Nanog (Figure 7.11). The ASCs did not express other pancreatic markers tested including Glut-2, proinsulin, glucagon, amylin, C-peptide, and insulin (Figure 7.11). They did not express either CD14 or CD31 (Figure 7.11). A summary of these findings is presented in Table 7.3.



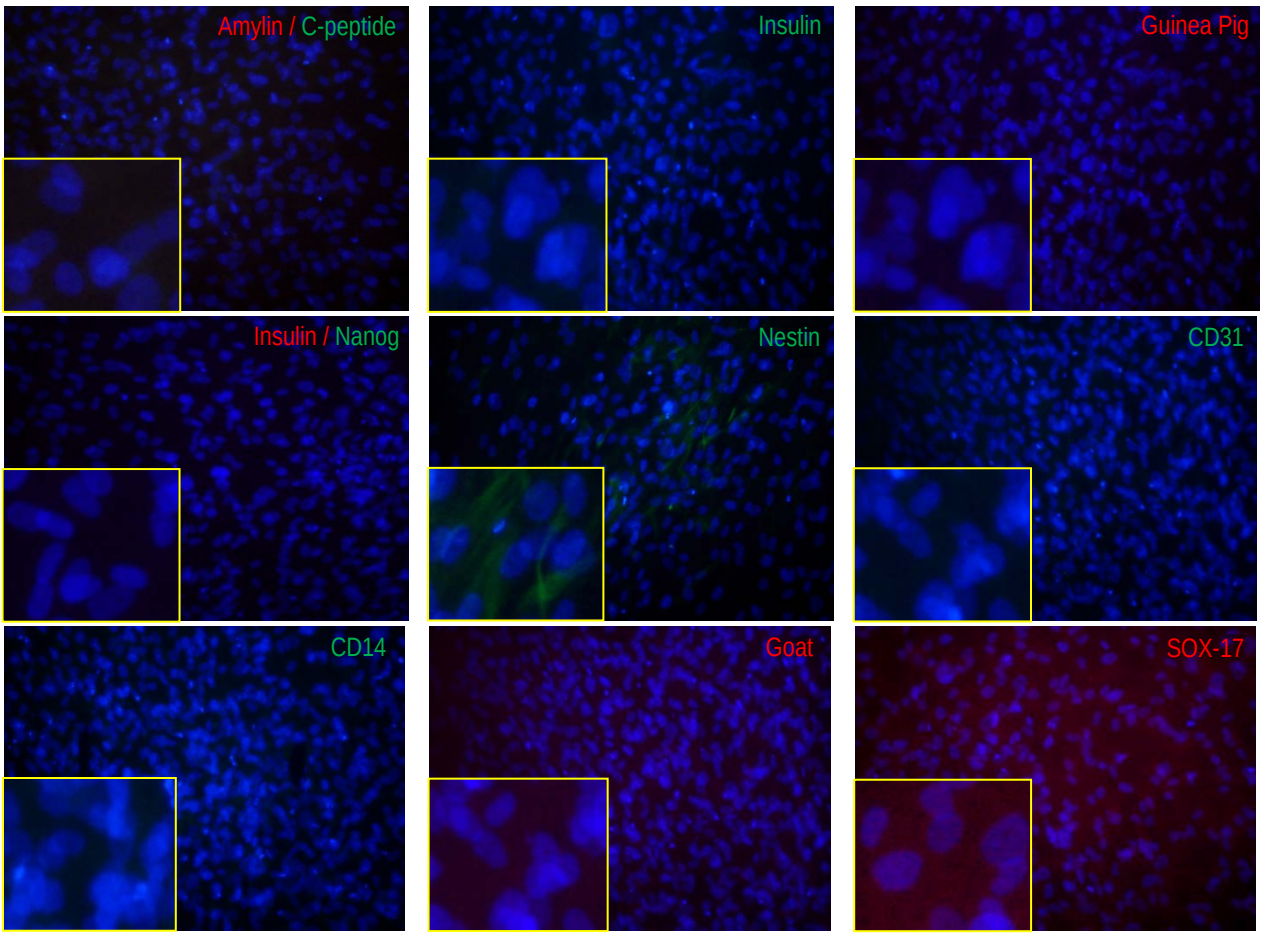


Figure 7.11 Phenotyping of ASCs cultured for 2 weeks in tissue culture plates for stem and pancreatic markers.

ASCs were cultured for 2 weeks in expansion medium in tissue culture plates. They were immunostained for the expression of stem cell and pancreatic cell markers. Immunoreactivity was detected with donkey anti-rabbit (red), donkey anti-mouse (green), goat anti-guinea pig (red), and donkey anti-goat (red) antibodies. Cell nuclei were stained blue with DAPI. Images were taken at 200x magnification; inset is a 4x magnification of part of the image. The images are presented so that the staining obtained with each IgG control immediately precedes stainings with antibodies of the same host species.

7.7.1.1 Differentiation of ASCs using the Chandra protocol

ASCs were differentiated with a multi-stage protocol developed by Chandra *et al.* (2011) and analysed at various time-points (n=2). The protocol was performed in conventional tissue culture plates. Chandra's protocol is outlined in Table 7.2. ASCs were seeded in serum-free medium-A (SFM-A) and cultured for 2 days. They were then cultured for an additional 2 days in SFM-B, and then cultured for 10 days in SFM-C. The composition of the different media is detailed in Table 7.2. The results below are representative of 2 separate expriments.

The agents used in Chandra's media are intended to promote pancreatic differentiation in 3 stages. BSA (Cohn Fraction V) is a common cell culture additive that helps protect cells from oxidative damage and to help stabilize the other protein components in the medium. ITS and β-mercaptoethanol are included in SFM-A to protect the ASCs from stress induced by culturing the cells in a serum free medium (Chandra *et al.* 2009). Sodium butyrate is used to induce chromatin rearrangements (Goicoa *et al.* 2006). It has a concentration and time-dependent effect on the differentiation of ESCs into either pancreatic progenitors or hepatocytes (Goicoa *et al.* 2006). Activin A is commonly used to induce definitive endoderm formation (D'Amour *et al.* 2006; Chandra *et al.* 2011). The growth factor bFGF is included to promote proliferation and survival of the ASCs (Chandra *et al.* 2011). Taurine is included as an essential amino acid required for the development of functional β-cells (Cherif *et al.* 1998; Boujendar *et al.* 2003; Chandra *et al.* 2009). The inclusion of NEAAs, taurine, and GLP-1 at the final stage promote ASC survival and pancreatic lineage differentiation (Yue *et al.* 2006; Chandra *et al.* 2009).

Table 7.2 Chandra's differentiation protocol and composition of media

Timing	Media	Composition	Differentiation stage
Days 1-2	SFM-A	DMEM/F12 + 1% BSA (Cohn Fraction V) (A8806, Sigma) + 1 x ITS (51500-056, Gibco) + 4 nM activin A (CYT-414, ProSpec-TechnoGene Ltd.) + 1 mM sodium butyrate (B5887, Sigma-Aldrich) + 50 μM β-mercaptoethanol + 2 ng/mL bFGF	Definitive endoderm
Days 3-4	SFM-B	DMEM/F12 + 1% BSA + 1x ITS + 0.3 mM taurine (T8691, Sigma)	Pancreatic endoderm
Days 5-14	SFM-C	DMEM/F12 + 1.5% BSA + 1x ITS + 3 mM taurine + 100 nM GLP-1 (G8147, Sigma Aldrich) + 10 mM nicotinamide + 1x NEAA (11140-050, Gibco)	Pancreatic maturation

Abbreviations: SFM - serum free medium, BSA – bovine serum albumin, ITS – insulin/transferrin/selenium, GLP-1 – glucagon-like peptide-1, NEAA – non-essential amino acids.

ASCs were cultured with Chandra's media and immunostained for cell markers after 3 days. They weakly expressed SOX-17, but did not express Nestin, Oct-4, and Nanog (Figure 7.12). They did not express other pancreatic markers tested including proinsulin, C-peptide, and insulin (Figure 7.12). They did not express Glut-2, glucagon and amylin, albeit staining was

confounded by the high background staining of the donkey anti-rabbit antibody (Figure 7.12). They also did not express either CD14 or CD31 (Figure 7.12). A summary of these findings is presented in Table 7.3.

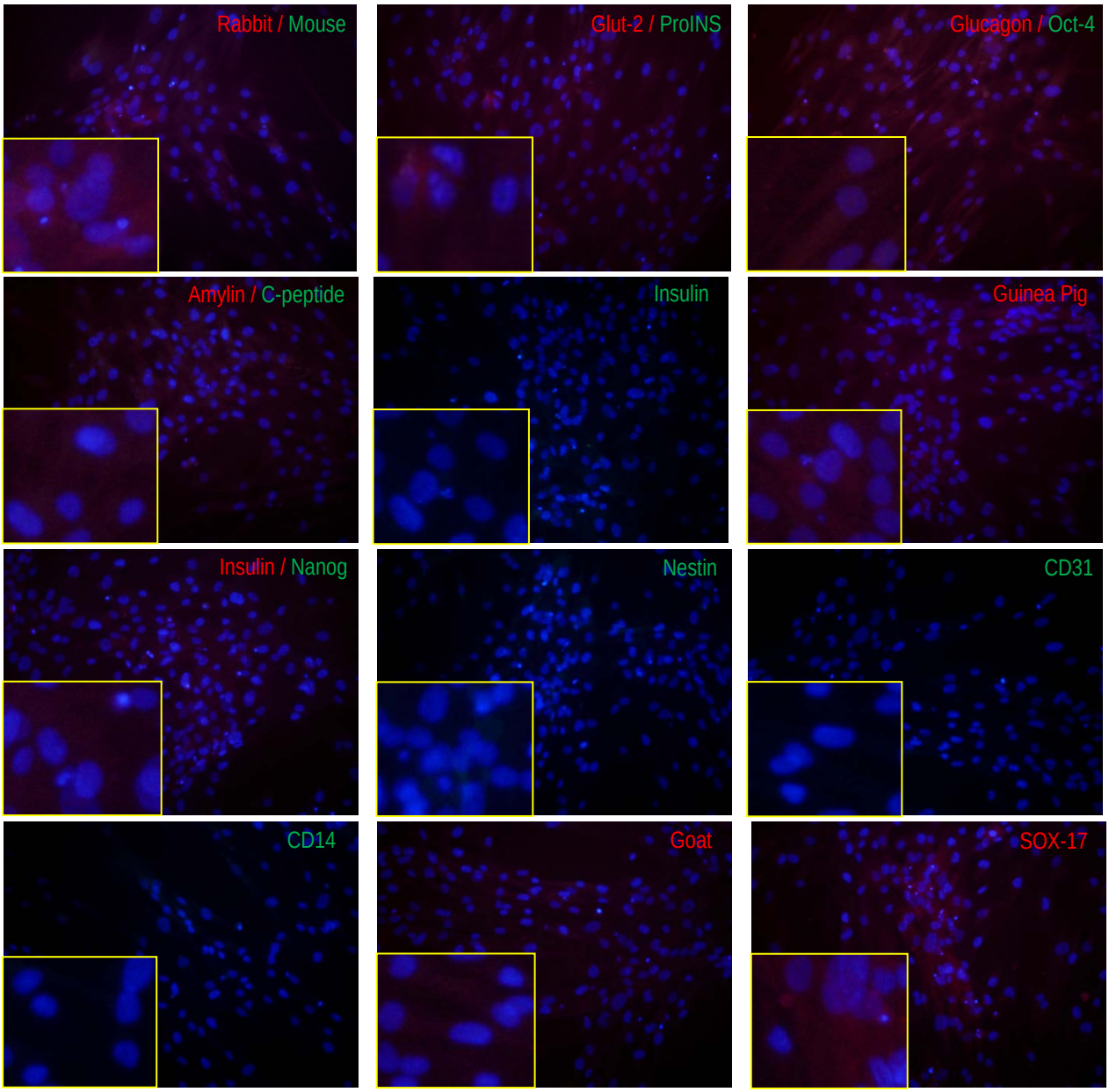
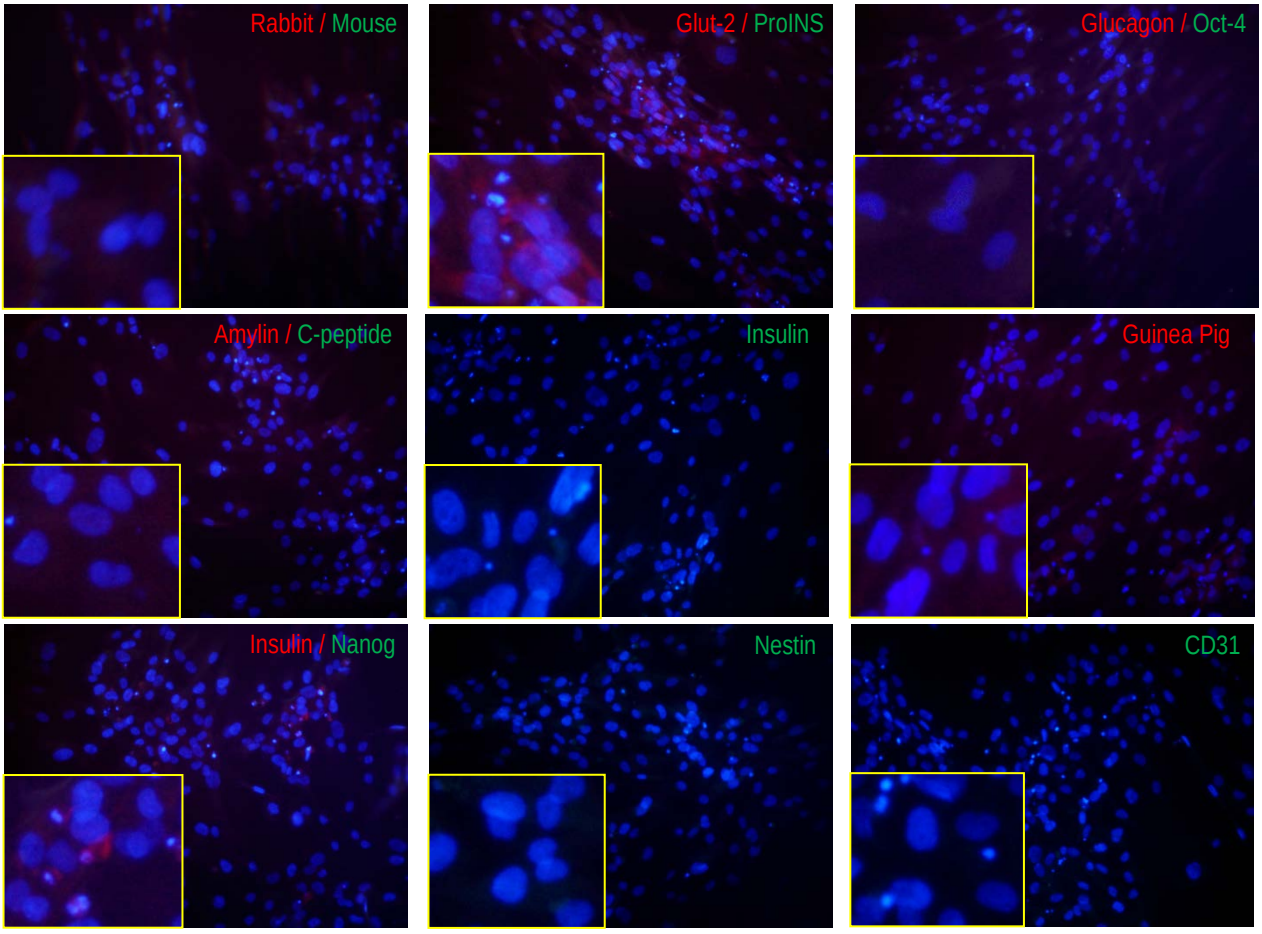


Figure 7.12 Phenotyping of ASCs cultured for 3 days according to the Chandra protocol.

ASCs were cultured according to the Chandra protocol in tissue culture plates, and immunostained for the expression of stem cell and pancreatic cell markers after 3 days. Immunoreactivity was detected with donkey anti-rabbit (red), donkey anti-mouse (green), goat anti-guinea pig (red), and donkey anti-goat (red) antibodies. Cell nuclei were stained blue with DAPI. Images were taken at 200x magnification; inset is a 4x magnification of part of the image. The images are presented so that the staining obtained with each IgG control immediately precedes stainings with antibodies of the same host species.

ASCs cultured in the Chandra protocol differentiation medium for seven days displayed only weak expression of SOX-17 and did not express Nestin, Oct-4, or Nanog (Figure 7.13). They expressed Glut-2 and insulin; however insulin was detected with the guinea pig anti-insulin antibody but not the mouse anti-insulin antibody (Figure 7.13). Both the donkey anti-rabbit and goat anti-guinea pig antibodies used to detect Glut-2 and insulin, respectively, gave high background staining, rendering the latter results uncertain (Figure 7.13). The other pancreatic markers tested (proinsulin, glucagon, amylin, or C-peptide) were not expressed (Figure 7.13). The ASCs also did not express either CD14 or CD31 (Figure 7.13). A summary of these findings is presented in Table 7.3.



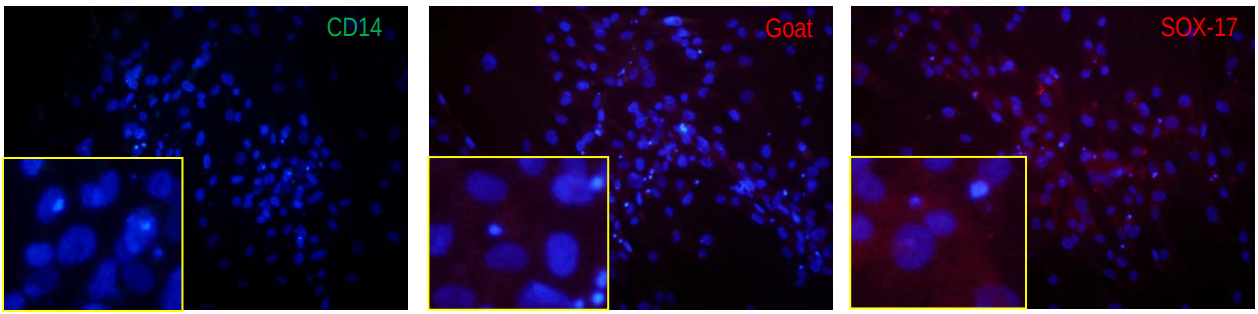
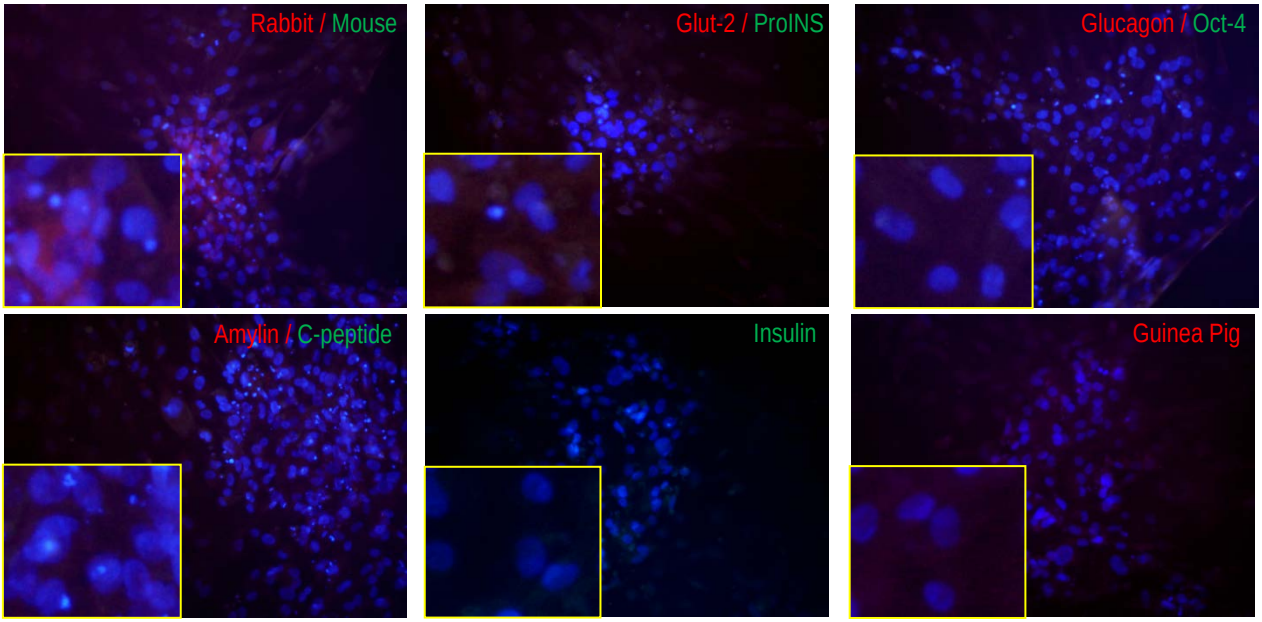


Figure 7.13 Phenotyping of ASCs cultured for 1 week according to the Chandra protocol.

ASCs were cultured according to the Chandra protocol in tissue culture plates, and immunostained for the expression of stem cell and pancreatic cell markers after 1 week. Immunoreactivity was detected with donkey anti-rabbit (red), donkey anti-mouse (green), goat anti-guinea pig (red), and donkey anti-goat (red) antibodies. Cell nuclei were stained blue with DAPI. Images were taken at 200x magnification; inset is a 4x magnification of part of the image. The images are presented so that the staining obtained with each IgG control immediately precedes stainings with antibodies of the same host species.

ASCs cultured in the Chandra protocol differentiation medium for fourteen days did not express insulin, Glut-2, glucagon, and amylin. However, the results are equivocable due to the high background staining of the control antibodies in each instance. They weakly expressed SOX-17 (Figure 7.14). The other markers tested (proinsulin, glucagon, amylin, C-peptide, Nestin, Oct-4, CD14, and CD31) were also not expressed (Figure 7.14). A summary of these findings is presented in Table 7.3.



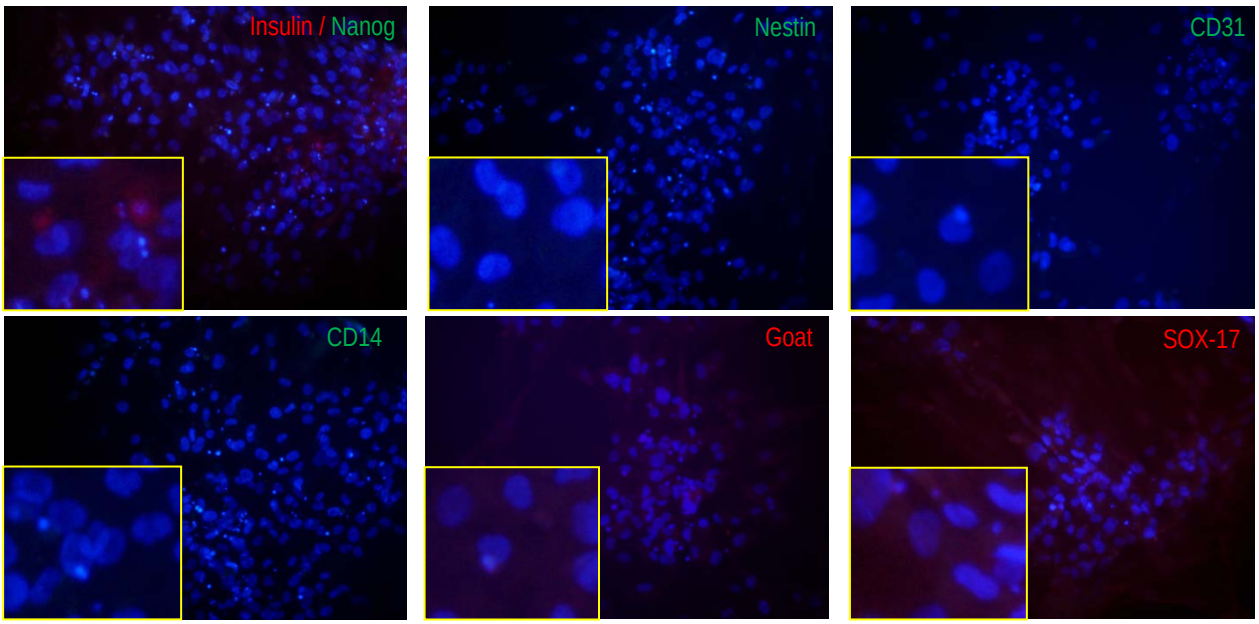


Figure 7.14 Phenotyping of ASCs cultured for 2 weeks according to the Chandra protocol.

ASCs were cultured according to the Chandra protocol in tissue culture plates, and immunostained for the expression of stem cell and pancreatic cell markers after 2 weeks. Immunoreactivity was detected with donkey anti-rabbit (red), donkey anti-mouse (green), goat anti-guinea pig (red), and donkey anti-goat (red) antibodies. Cell nuclei were stained blue with DAPI. Images were taken at 200x magnification; inset is a 4x magnification of part of the image. The images are presented so that the staining obtained with each IgG control immediately precedes stainings with antibodies of the same host species.

7.7.1.2 Differentiation of ASCs using the Timper protocol with IGF-2

Timper *et al.* (2006) reported that ASCs could be differentiated into pancreatic cells that express insulin, somatostatin, or glucagon in as little as 3 days in a defined medium. Here ASCs were cultured in tissue culture plates for 3 days in a differentiation medium based on the Timper protocol which was modified to contain IGF-2 instead of pentagastrin (n=2). The modified Timper's medium contained DMEM/F12 (17.5 mM glucose), 10 mM nicotinamide, 2 nM activin-A, 10 nM Ex4, 100 pM HGF, 50 ng/mL IGF-2, 1x B27 supplement, 1x N2 supplement, and 1% PSG. The resulting cells were immunostained for the expression of cell markers. The results are representative of 2 separate experiments. They showed weak expression of SOX-17 and Glut-2, and moderate expression of amylin, but did not express Nestin, Oct-4, and Nanog, where interpretation of the results was slightly confounded by the high level of background staining by the donkey anti-rabbit, goat anti-guinea pig, and donkey anti-goat antibodies. For this reason the expression of glucagon also cannot be judged with certainty (Figure 7.15). However, insulin, proinsulin, and C-peptide were not detected (Figure 7.15). They also did not express CD14 or CD31 (Figure 7.15). A summary of these findings is presented in Table 7.3.

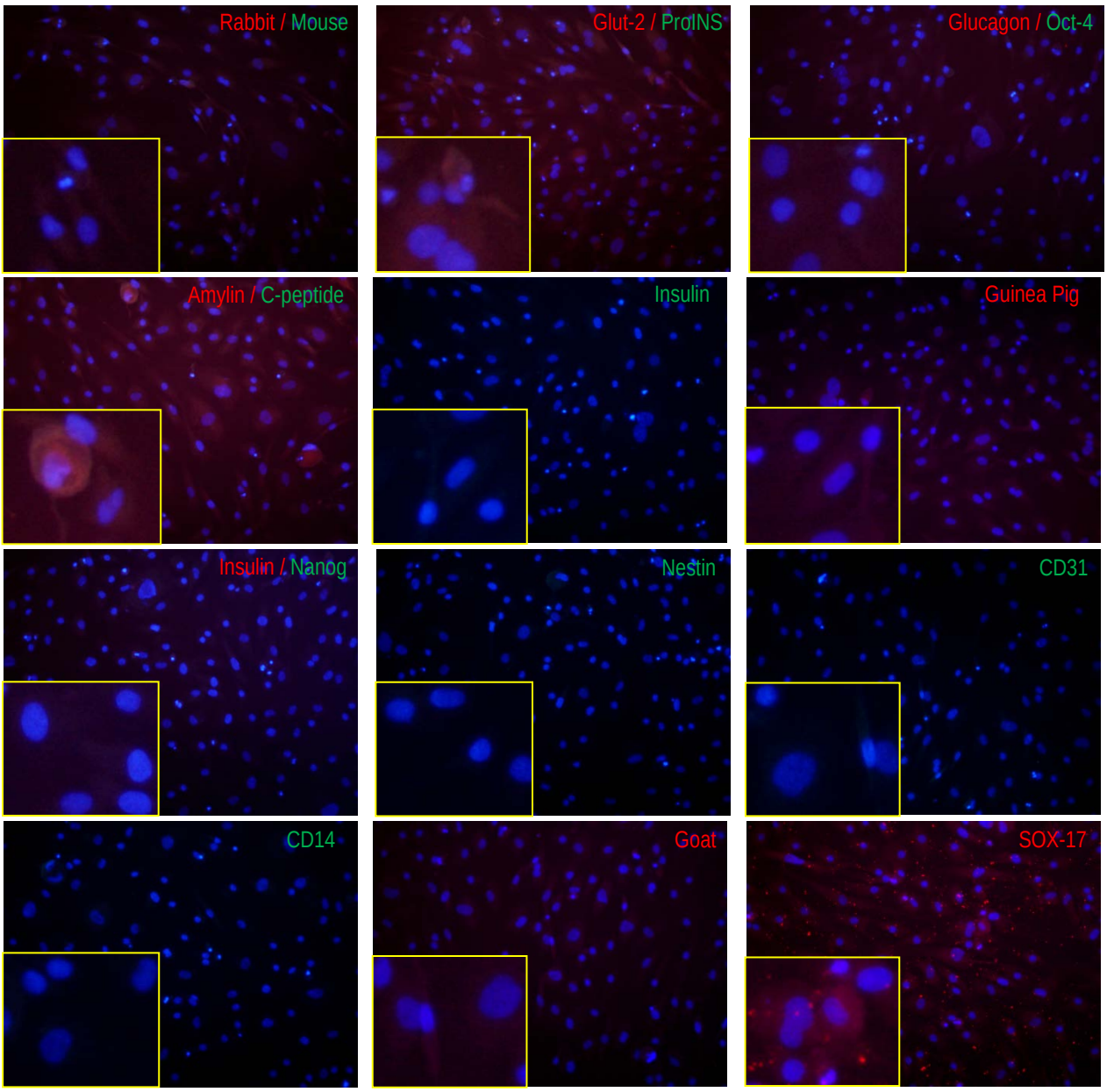


Figure 7.15 Phenotyping of ASCs cultured for 3 days in a modified version of the Timper protocol.

ASCs were cultured for 3 days in a modified version of the Timper protocol, and immunostained for the expression of stem cell and pancreatic cell markers. Immunoreactivity was detected with donkey anti-rabbit (red), donkey anti-mouse (green), goat anti-guinea pig (red), and donkey anti-goat (red) antibodies. Cell nuclei were stained blue with DAPI. Images were taken at 200x magnification; inset is a 4x magnification of part of the image. The images are presented so that the staining obtained with each IgG control immediately precedes stainings with antibodies of the same host species.

Table 7.3 Summary of the phenotype of ASCs after differentiation in either expansion media, or according to Chandra's and Timper's (+IGF-2, -pentagastrin) protocols

	Day 3	Day 7	Day 14	Day 3	Day 7	Day 14	Day 3
	Expansion			Chandra			Timper (IGF-2)
Glut-2				x*	x x x*	x*	x*
Glucagon				x*		x*	x*
Amylin				x*		x*	x x*
Insulin					x x x*	x*	
SOX-17	x	x	x	x	x	x	x*
ProINS							
Oct-4							
C-peptide							
Nanog							
Nestin	x x x	x x x	x x x				
CD14							
CD31							

0	0.1-20	21-40	41-60	61-80	81-100	% Positive

x	x x	x x x	Intensity of staining - weak/moderate/strong

* Equivocable due to the high background staining of the control antibodies.

7.7.2 Stage-specific differentiation of ASCs

Multi-stage pancreatic differentiation of whole ASC populations was trialled in an attempt to replicate the natural differentiation of stem cells to β-cells that occurs during embryogenesis (Table 7.4). Various agents were selected which induce the differentiation of stem cells to definitive endoderm, primitive gut tube, and posterior foregut (n=2). The cells were also cultured for 10 days in tissue culture dishes with expansion medium to serve as controls for comparison. The results presented below are representative of 2 separate experiments. The majority of cells cultured in expansion medium strongly expressed Nestin (Figure 7.16). They did not express FOXA2, CXCR4, SOX-17, PDX-1, HNF6, HNF4a, and Nkx2.2 (Figure 7.16). The lack of expression of SOX-17 as detected with a mouse anti-SOX-17 antibody contradicts the expression of SOX-17 detected with a goat anti-SOX-17 antibody at day 7 (Figure 7.10). See Table 7.5, column E for a summary of the phenotype of the ASCs differentiated in expansion medium.

Table 7.4 Stage-specific differentiation protocols

		Days in culture									
Differentiation media	Label	1	2	3	4	5	6	7	8	9	10
Expansion	E	DMEM/F12 + 10% FBS + 2 ng/mL bFGF + 1% PSG									
IDE-1 (100 nM). DE - Borowiak *et al.* (2009), PG & PF - D'Amour *et al.* (2006), Talavera-Adame *et al.* (2011)	A	Advanced RPMI + 1x Glutamax + 0.2% FBS + 100 nM IDE-1				Advanced RPMI + 2% FBS + 0.25 µM KAAD-CYC + 50 ng/mL FGF10		DMEM + 1% B27 + 0.25 µM KAAD-CYC + 50 ng/mL FGF10 + 2 µM RA			
	Ab	Advanced RPMI + 1x Glutamax + 0.2% FBS + 100 nM IDE-1				Advanced RPMI + 2% FBS + 0.25 µM KAAD-CYC + 50 ng/mL FGF10 + BMP-2		DMEM + 1% B27 + 0.25 µM KAAD-CYC + 50 ng/mL FGF10 + 2 µM RA + BMP-2			
IDE-1 (400 nM). DE - Borowiak *et al.* (2009), PG & PF - D'Amour *et al.* (2006), Talavera-Adame *et al.* (2011)	B	Advanced RPMI + 1x Glutamax + 0.2% FBS + 400 nM IDE-1				Advanced RPMI + 2% FBS + 0.25 µM KAAD-CYC + 50 ng/mL FGF10		DMEM + 1% B27 + 0.25 µM KAAD-CYC + 50 ng/mL FGF10 + 2 µM RA			
	Bb	Advanced RPMI + 1x Glutamax + 0.2% FBS + 400 nM IDE-1				Advanced RPMI + 2% FBS + 0.25 µM KAAD-CYC + 50 ng/mL FGF10 + BMP-2		DMEM + 1% B27 + 0.25 µM KAAD-CYC + 50 ng/mL FGF10 + 2 µM RA + BMP-2			
activin A + Wnt3a, activin A. DE - D'Amour *et al.* (2006), PG & PF - D'Amour *et al.* (2006), Talavera-Adame *et al.* (2011)	C	Advanced RPMI + 100 ng/mL activin A + 25 ng/mL Wnt3a		Advanced RPMI + 100 ng/mL activin A				Advanced RPMI + 2% FBS + 0.25 µM KAAD-CYC + 50 ng/mL FGF10		DMEM + 1% B27 + 0.25 µM KAAD-CYC + 50 ng/mL FGF10 + 2 µM RA	
	Cb	Advanced RPMI + 100 ng/mL activin A + 25 ng/mL Wnt3a		Advanced RPMI + 100 ng/mL activin A				Advanced RPMI + 2% FBS + 0.25 µM KAAD-CYC + 50 ng/mL FGF10 + BMP-2		DMEM + 1% B27 + 0.25 µM KAAD-CYC + 50 ng/mL FGF10 + 2 µM RA + BMP-2	
activin A + Wnt3a. DE - Borowiak *et al.* (2009), PG & PF - D'Amour *et al.* (2006), Talavera-Adame *et al.* (2011)	D	Advanced RPMI + 50 ng/mL activin A + 25 ng/mL Wnt3a						Advanced RPMI + 2% FBS + 0.25 µM KAAD-CYC + 50 ng/mL FGF10		DMEM + 1% B27 + 0.25 µM KAAD-CYC + 50 ng/mL FGF10 + 2 µM RA	
	Db	Advanced RPMI + 50 ng/mL activin A + 25 ng/mL Wnt3a						Advanced RPMI + 2% FBS + 0.25 µM KAAD-CYC + 50 ng/mL FGF10 + BMP-2		DMEM + 1% B27 + 0.25 µM KAAD-CYC + 50 ng/mL FGF10 + 2 µM RA + BMP-2	

		Days in culture									
Differentiation media	Label	1	2	3	4	5	6	7	8	9	10
IDE-2 (200 nM). DE - Borowiak *et al.* (2009), PG & PF - D'Amour *et al.* (2006), Talavera-Adame *et al.* (2011)	F	Advanced RPMI + 1x Glutamax + 0.2% FBS + 200 nM IDE-2				Advanced RPMI + 2% FBS + 0.25 µM KAAD-CYC + 50 ng/mL FGF10		DMEM + 1% B27 + 0.25 µM KAAD-CYC + 50 ng/mL FGF10 + 2 µM RA			
	Fb	Advanced RPMI + 1x Glutamax + 0.2% FBS + 200 nM IDE-2				Advanced RPMI + 2% FBS + 0.25 µM KAAD-CYC + 50 ng/mL FGF10 + BMP-2		DMEM + 1% B27 + 0.25 µM KAAD-CYC + 50 ng/mL FGF10 + 2 µM RA + BMP-2			

Definitive endoderm – stage 1
Primitive gut tube – stage 2
Posterior foregut – stage 3

Abbreviations: DE: definitive endoderm, PG: primitive gut tube, PF: posterior foregut, IDE: induce definitive endoderm, KAAD-CYC: KAAD-cyclopamine, RA: all trans-retinoic acid.

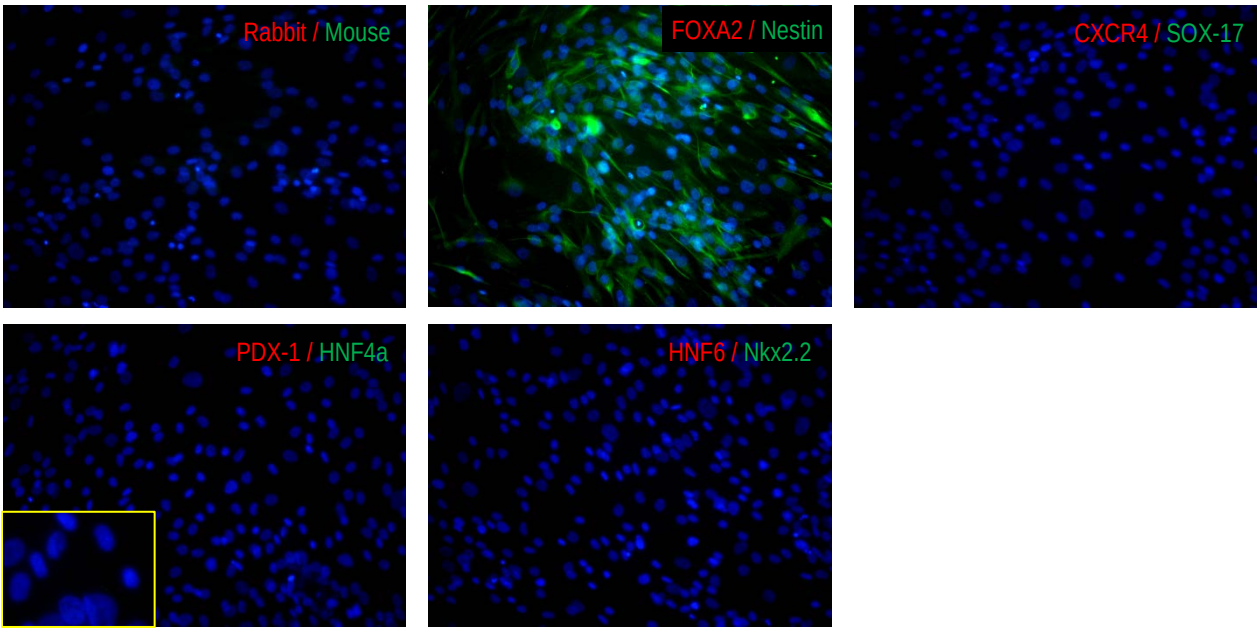


Figure 7.16 Phenotyping of ASCs cultured for 10 days in expansion medium.

Cells were immunostained for the expression of stem cell and pancreatic cell markers. Immunoreactivity was detected with donkey anti-rabbit (red) and donkey anti-mouse (green) antibodies. Cell nuclei were stained blue with DAPI. Images were taken at 200x magnification; inset is a 4x magnification of part of the image. The images are presented so that the staining obtained with each IgG control immediately precedes stainings with antibodies of the same host species.

7.7.2.1 Stage 1 – formation of definitive endoderm

Factors capable of inducing definitive endoderm formation in hESCs were trialled on ASCs including IDE-1, activin-A and Wnt3a (D'Amour *et al.* 2005; D'Amour *et al.* 2006; Borowiak *et al.* 2009). These factors upregulate the expression of the definitive endoderm markers such as SOX-17, FOXA2, and CXCR4 (D'Amour *et al.* 2005; D'Amour *et al.* 2006; Borowiak *et al.* 2009). Two concentrations of IDE-1 were trialled as it had been shown with mouse ESCs that IDE-1 dose-dependently induces SOX-17 expression (EC_{50} of 125 nM) (Borowiak *et al.* 2009).

In the first trial, ASCs were cultured for 4 days according to a procedure published by Borowiak *et al.* (2009) to induce definitive endoderm where the media used was comprised of advanced RPMI (12633012, Gibco), 1x Glutamax (35050-061, Gibco), 0.2% FBS, and 100 nM IDE-1 (04-0026, Stemgent) (Figure 7.17). The ASCs continued to strongly express Nestin (Figure 7.17). The definitive endoderm marker SOX-17 was weakly expressed by a few cells, but the other definitive endoderm markers CXCR4 and FOXA2 were not detected (Figure 7.17). A few cells moderately expressed the primitive gut tube marker PDX-1 but HNF6 could not be detected above background (Figure 7.17). The ASCs did not express HNF4a, or Nkx2.2 (Figure 7.17). See Table 7.5, stage 1; column A for a summary of the phenotype of the ASCs differentiated with 100 nM IDE.

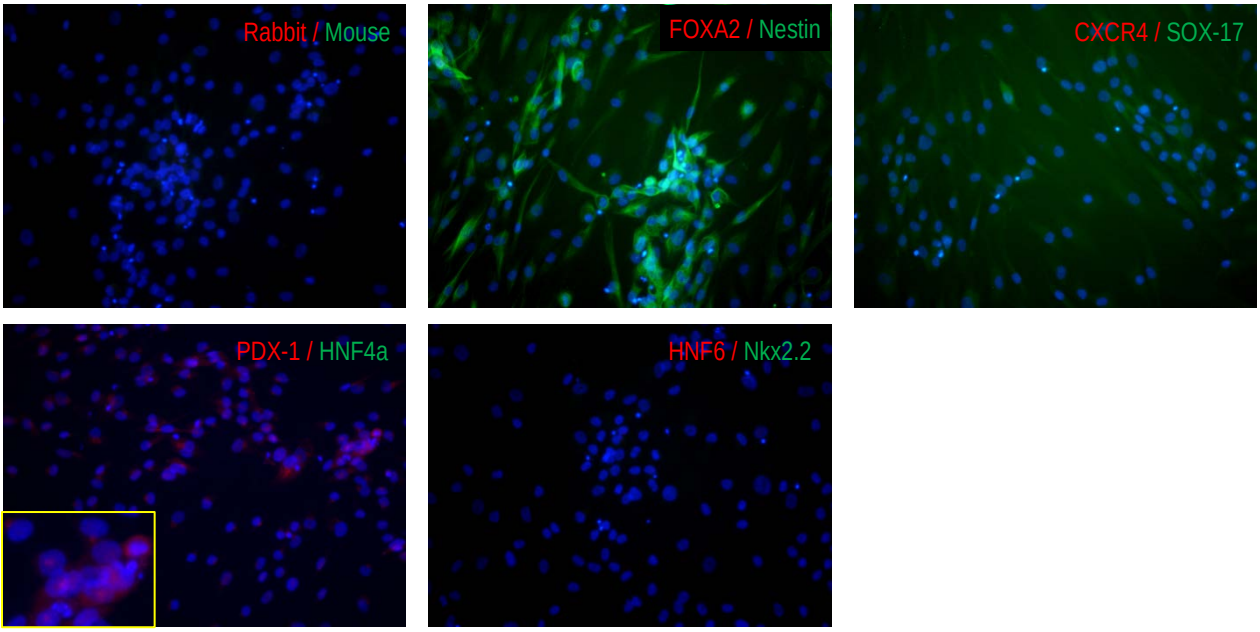


Figure 7.17 Phenotyping of ASCs differentiated with 100 nM IDE-1 towards definitive endoderm (Stage 1).

Cells were cultured for 4 days with 100 nM IDE in tissue culture dishes, and immunostained for the expression of stem cell and pancreatic cell markers. Immunoreactivity was detected with donkey anti-rabbit (red) and donkey anti-mouse (green) antibodies. Cell nuclei were stained blue with DAPI. Images were taken at 200x magnification; inset is a 4x magnification of part of the image. The images are presented so that the staining obtained with each IgG control immediately precedes stainings with antibodies of the same host species.

In the second trial, the concentration of IDE-1 was increased to 400 nM to determine whether there would be a greater change in the expression of cell markers (Borowiak *et al.* 2009) (Figure 7.18). The ASCs cultured for 4 days with 400 nM IDE continued to strongly express Nestin (Figure 7.18). They did not express CXCR4, FOXA2, SOX-17, PDX-1, HNF4a, HNF6 and Nkx2.2 (Figure 7.18). See Table 7.5, stage 1; column B for a summary of the phenotype of the ASCs differentiated with 400 nM IDE.

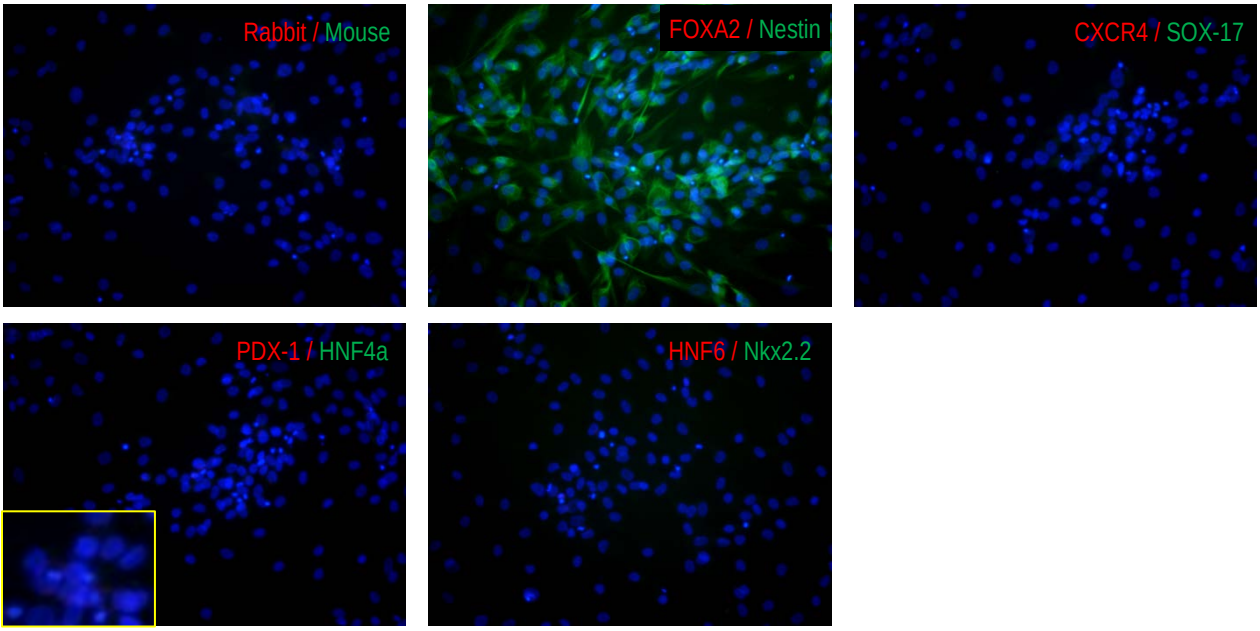


Figure 7.18 Phenotyping of ASCs differentiated with 400 nM IDE-1 towards definitive endoderm (Stage 1).

Cells were cultured for 4 days with 400 nM IDE and immunostained for the expression of stem cell and pancreatic cell markers. Immunoreactivity was detected with donkey anti-rabbit (red) and donkey anti-mouse (green) antibodies. Cell nuclei were stained blue with DAPI. Images were taken at 200x magnification; inset is a 4x magnification of part of the image. The images are presented so that the staining obtained with each IgG control immediately precedes stainings with antibodies of the same host species.

In the third trial, ASCs were cultured for 2 days according to D'Amour *et al.* (2006) using a media comprised of advanced RPMI, 100 ng/mL activin A, and 25 ng/mL Wnt3a (ab81484, Abcam Inc.), followed by 4 days in advanced RPMI containing 100 ng/mL activin A to induce definitive endoderm (D'Amour *et al.* 2006) (Figure 7.19). Some cells weakly expressed SOX-17 and HNF4a, and strongly expressed Nestin (Figure 7.19). A few cells weakly expressed the posterior foregut marker HNF6 (Figure 7.19). PDX-1 was weakly expressed by most cells; often within the nucleus (Figure 7.19).The remaining definitive endoderm markers FOXA2 and CXCR4 were not detected (Figure 7.19). The posterior foregut marker Nkx2.2 was also not detected (Figure 7.19). See Table 7.5, stage 1; column C for a summary of the phenotype of the ASCs differentiated with activin A + Wnt3a followed by activin A alone.

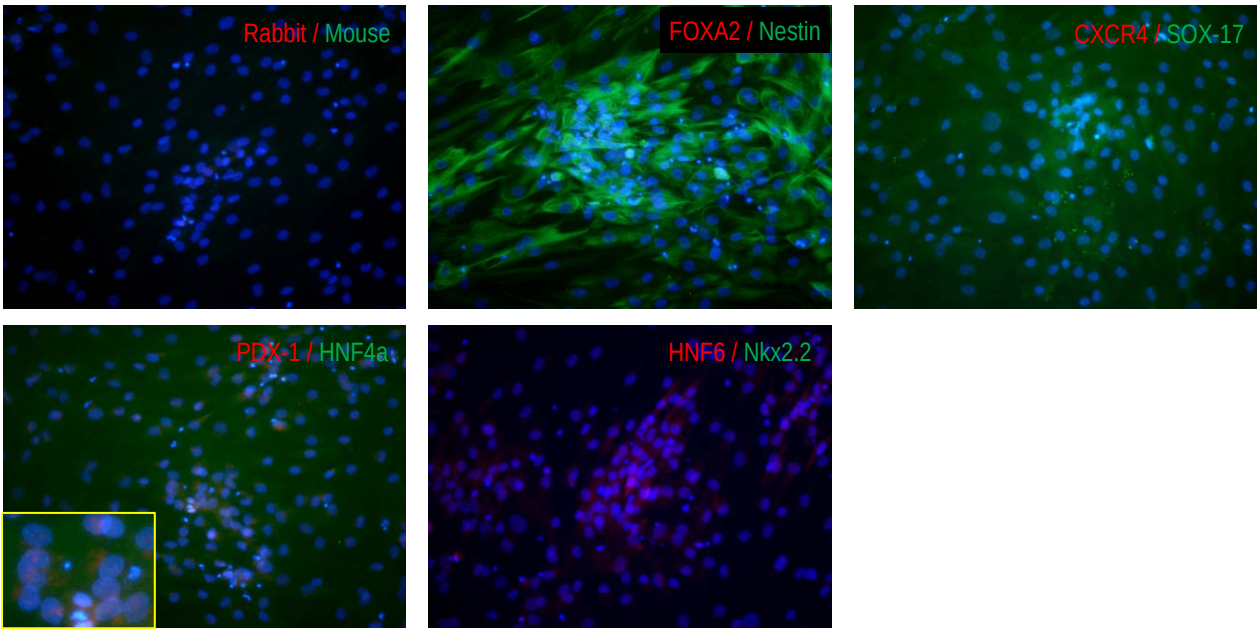


Figure 7.19 Phenotyping of ASCs differentiated with activin A + Wnt3a followed by activin A alone towards definitive endoderm (Stage 1).

ASCs were cultured for 2 days with 100 ng/mL activin A + 25 ng/mL Wnt3a, followed by 4 days with 100 ng/mL activin A alone, and immunostained for the expression of stem cell and pancreatic cell markers. Immunoreactivity was detected with donkey anti-rabbit (red) and donkey anti-mouse (green) antibodies. Cell nuclei were stained blue with DAPI. Images were taken at 200x magnification; inset is a 4x magnification of part of the image. The images are presented so that the staining obtained with each IgG control immediately precedes stainings with antibodies of the same host species.

In a fourth and final trial, ASCs were cultured for 6 days according to Borowiak *et al.* (2009) in a medium comprised of advanced RPMI + 50 ng/mL activin A + 25 ng/mL Wnt3a to induce definitive endoderm (Borowiak *et al.* 2009) (Figure 7.20). The cells strongly expressed Nestin and most cells weakly expressed SOX-17 (Figure 7.20). They weakly expressed HNF4a, PDX-1 (some nuclear) and HNF6 (Figure 7.20). They did not express FOXA2, CXCR4, or Nkx2.2 (Figure 7.20). See Table 7.5, stage 1; column D for a summary of the phenotype of the ASCs differentiated with activin A + Wnt3a.

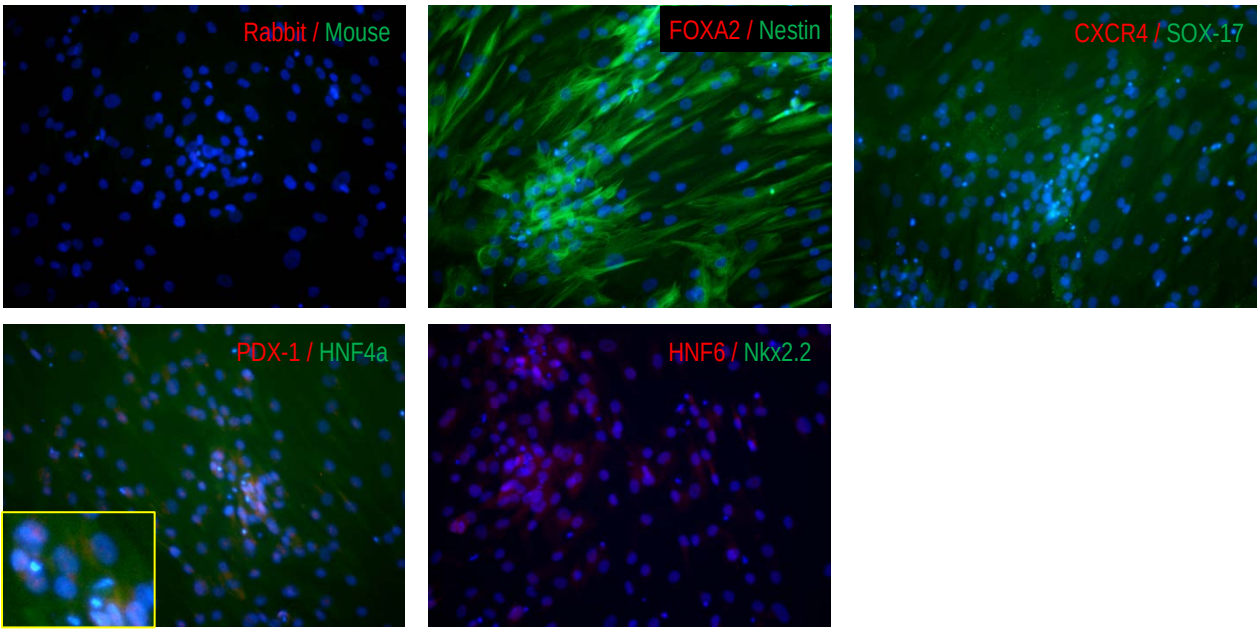


Figure 7.20 Phenotyping of ASCs differentiated with activin A + Wnt3a towards definitive endoderm (Stage 1).

Cells were cultured for 6 days with 100 ng/mL activin A + 25 ng/mL Wnt3a in tissue culture dishes, and immunostained for the expression of stem cell and pancreatic cell markers. Immunoreactivity was detected with donkey anti-rabbit (red) and donkey anti-mouse (green) antibodies. Cell nuclei were stained blue with DAPI. Images were taken at 200x magnification; inset is a 4x magnification of part of the image. The images are presented so that the staining obtained with each IgG control immediately precedes stainings with antibodies of the same host species.

7.7.2.2 Stage 2 – formation of primitive gut tube

The next stage of differentiation (Stage 2) required that the ASCs that had been differentiated to form definitive endoderm be induced to form primitive gut tube (D'Amour *et al.* 2006). It was reported that culture of definitive endoderm differentiated hESCs for 2 to 4 days in advanced RPMI containing 2% FBS, 0.25 μM KAAD-cyclopamine, and 50 ng/mL FGF10 leads to the upregulation of expression of HNF4a and HNF1B that typify primitive gut tube (D'Amour *et al.* 2006). Here ASCs were cultured for 2 days in the same medium. In addition some ASCs were also cultured with the further addition of 100 ng/mL bone morphogenic protein-2 (BMP-2) (CYT-261, ProSpec-TechnoGene Ltd.). Culturing mouse ESC embryoid bodies with endothelial cells causes pancreatic differentiation (Talavera-Adame *et al.* 2011). BMP-2 released by endothelial cells was reported to

stimulate ESCs to undergo pancreatic differentiation and express PDX-1, Nkx6.1, insulin and amylin (Talavera-Adame *et al.* 2011). Each of the four differentiation protocols used to form definitive endoderm was thus followed with the combination of agents developed by D'Amour *et al.* (2006) in the presence or absence of BMP-2 to induce primitive gut tube formation. See Table 7.4 for a detailed description of the protocols and composition of media used.

For trial 1, ASCs cultured for 4 days with 100 nM IDE-1 were subsequently cultured for 2 days with 0.25 μM KAAD-cyclopamine (sc-221448, Santa Cruz Biotechnology Inc.) + 50 ng/mL FGF10 (345-FG, R&D Systems) (D'Amour *et al.* 2006) (Figure 7.21). Most of the resulting cells strongly expressed Nestin, weakly expressed SOX-17, PDX-1, and HNF4a. They did not express FOXA2, CXCR4, HNF6, and Nkx2.2 (Figure 7.21). See Table 7.5, stage 2; column A for a summary of the phenotype of the ASCs differentiated with KAAD-cyclopamine + FGF10.

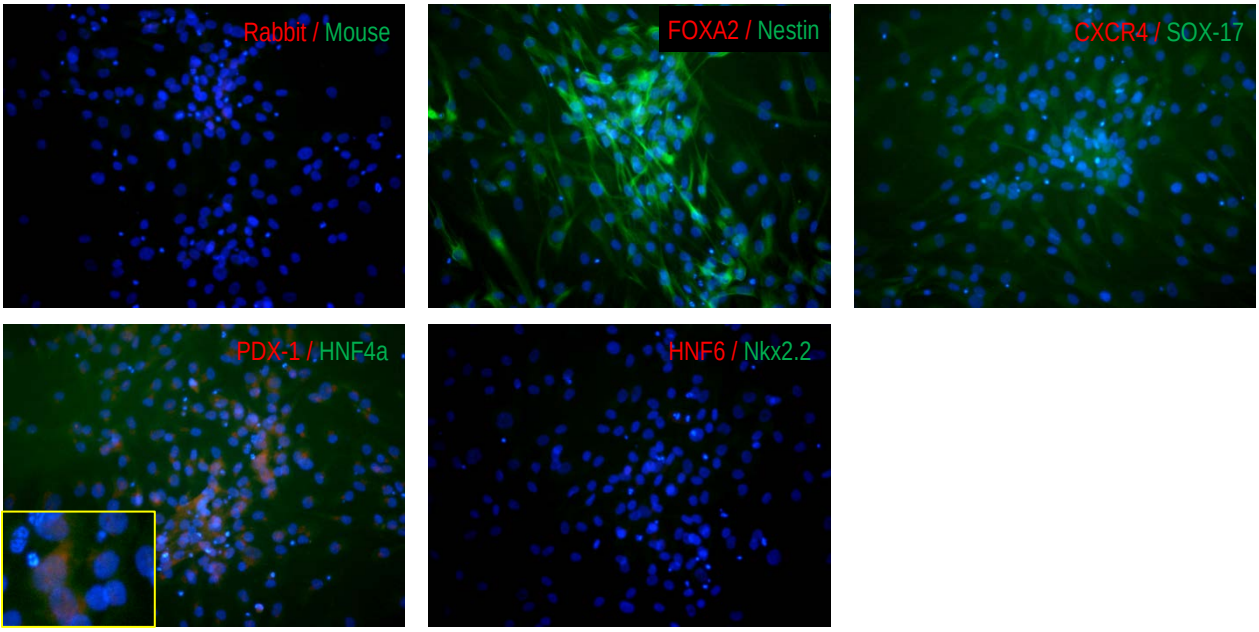


Figure 7.21 Phenotyping of ASCs differentiated with 100 nM IDE-1, followed by KAAD-cyclopamine + FGF10 towards the formation of primitive gut tube (Stage 2).

Cells that had been differentiated for 4 days with 100 nM IDE-1 were cultured for 2 days with 0.25 μM KAAD-cyclopamine + 50 ng/mL FGF10 and immunostained for the expression of stem cell and pancreatic cell markers. Immunoreactivity was detected with donkey anti-rabbit (red) and donkey anti-mouse (green) antibodies. Cell nuclei were stained blue with DAPI. Images were taken at 200x magnification; inset is a 4x magnification of part of the image. The images are presented so that the staining obtained with each IgG control immediately precedes stainings with antibodies of the same host species.

For trial 2, ASCs cultured for 4 days with 100 nM IDE-1 were subsequently cultured for 2 days with 0.25 μM KAAD-cyclopamine + 50 ng/mL FGF10 + 100 ng/mL BMP-2, to determine whether the inclusion of BMP-2 would help promote differentiation (D'Amour *et al.* 2006; Talavera-Adame *et al.* 2011) (Figure 7.22). The resulting cells strongly expressed Nestin, and weakly expressed SOX-17 and HNF6 (Figure 7.22). More than half of the cells moderately expressed PDX-1 in both the cytoplasm and the nucleus (Figure 7.22). They did not express FOXA2, CXCR4, HNF4a, or Nkx2.2 (Figure 7.22). See Table 7.5, stage 2; column A-b for a summary of the phenotype of the ASCs differentiated with 100 nM IDE-1, then with KAAD-cyclopamine, FGF10, and BMP-2.

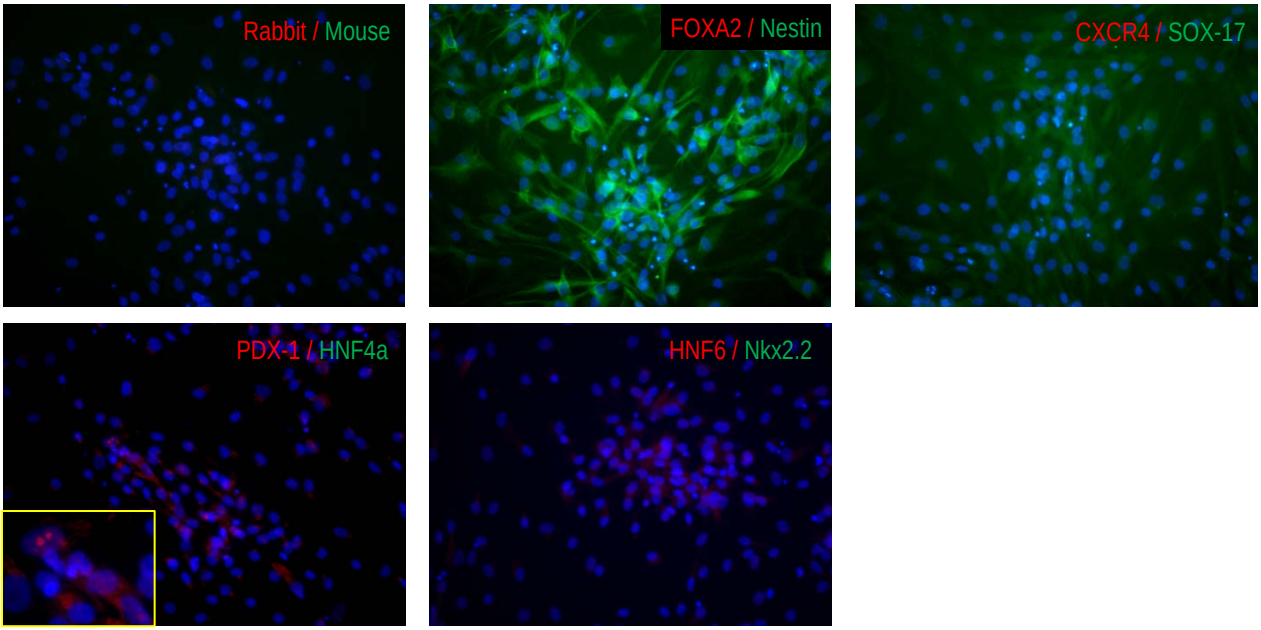


Figure 7.22 Phenotyping of ASCs differentiated with 100 nM IDE-1, followed by KAAD-cyclopamine + FGF10 + BMP-2 towards formation of primitive gut tube (Stage 2).

Cells that had been differentiated for 4 days with 100 nM IDE were cultured for 2 days with 0.25 μM KAAD-cyclopamine + 50 ng/mL FGF10 + 100 ng/mL BMP-2 and immunostained for the expression of stem cell and pancreatic cell markers. Immunoreactivity was detected with donkey anti-rabbit (red) and donkey anti-mouse (green) antibodies. Cell nuclei were stained blue with DAPI. Images were taken at 200x magnification; inset is a 4x magnification of part of the image. The images are presented so that the staining obtained with each IgG control immediately precedes stainings with antibodies of the same host species.

For trial 3, ASCs cultured for 4 days in 400 nM IDE-1 were subsequently cultured for 2 days in 0.25 μM KAAD-cyclopamine + 50 ng/mL FGF10 (D'Amour *et al.* 2006) (Figure 7.23). The resulting cells strongly expressed Nestin, and weakly expressed PDX-1 (cytoplasmic and nuclear) (Figure 7.23). A subpopulation of cells moderately expressed SOX-17 and weakly expressed HNF6 (Figure 7.23). The ASCs did not express FOXA2, CXCR4, HNF4a, and Nkx2.2 (Figure 7.23). See Table 7.5, stage 2; column B for a summary of the phenotype of the ASCs differentiated with 400 nM IDE-1, then with KAAD-cyclopamine + FGF10.

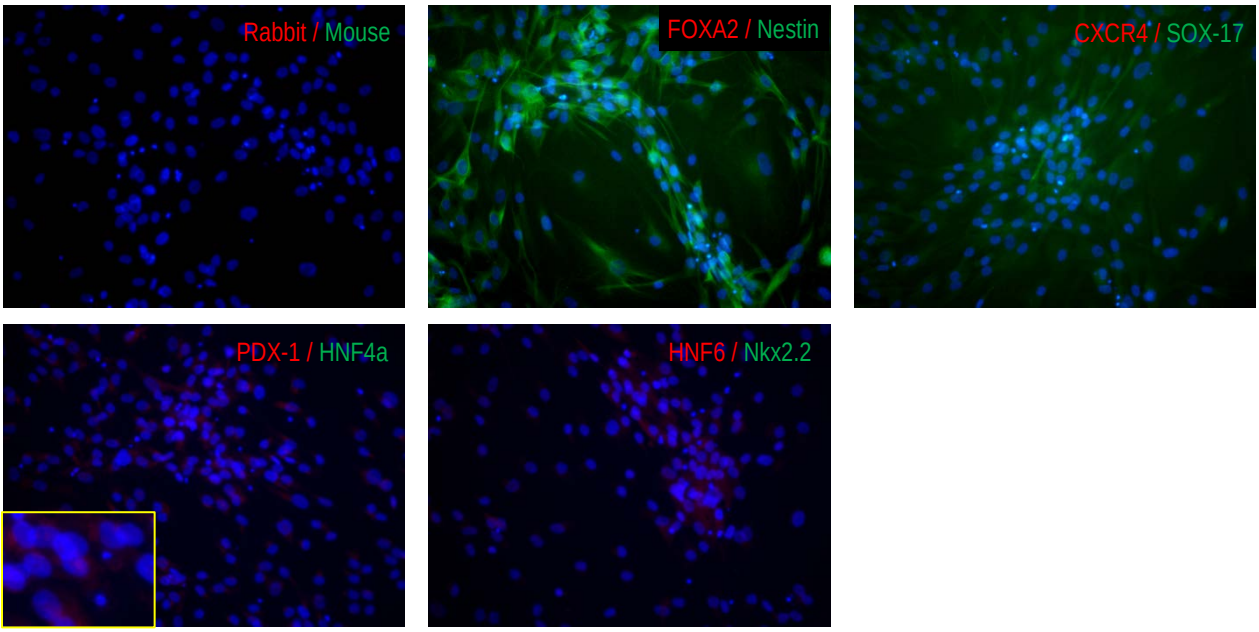


Figure 7.23 Phenotyping of ASCs differentiated with 400 nM IDE-1, followed by KAAD-cyclopamine + FGF10 towards the formation of primitive gut tube (Stage 2).

Cells that had been differentiated for 4 days with 400 nM IDE were cultured for 2 days with 0.25 μM KAAD-cyclopamine + 50 ng/mL FGF10 and immunostained for the expression of stem cell and pancreatic cell markers. Immunoreactivity was detected with donkey anti-rabbit (red) and donkey anti-mouse (green) antibodies. Cell nuclei were stained blue with DAPI. Images were taken at 200x magnification; inset is a 4x magnification of part of the image. The images are presented so that the staining obtained with each IgG control immediately precedes stainings with antibodies of the same host species.

For trial 4, ASCs cultured for 4 days with 400 nM IDE-1 were subsequently cultured for 2 days with 0.25 μM KAAD-cyclopamine + 50 ng/mL FGF10 + 100 ng/mL BMP-2 (D'Amour *et al.* 2006; Talavera-Adame *et al.* 2011) (Figure 7.24). The resulting cells strongly expressed Nestin, and weakly expressed SOX-17, PDX-1, and HNF6 (Figure 7.24). Expression of FOXA2, CXCR4, HNF4a, and Nkx2.2 was not detected (Figure 7.24). See Table 7.5, stage 2; column B-b for a summary of the phenotype of the ASCs differentiated with 400 nM IDE-1 and then with KAAD-cyclopamine + FGF10 + BMP-2.

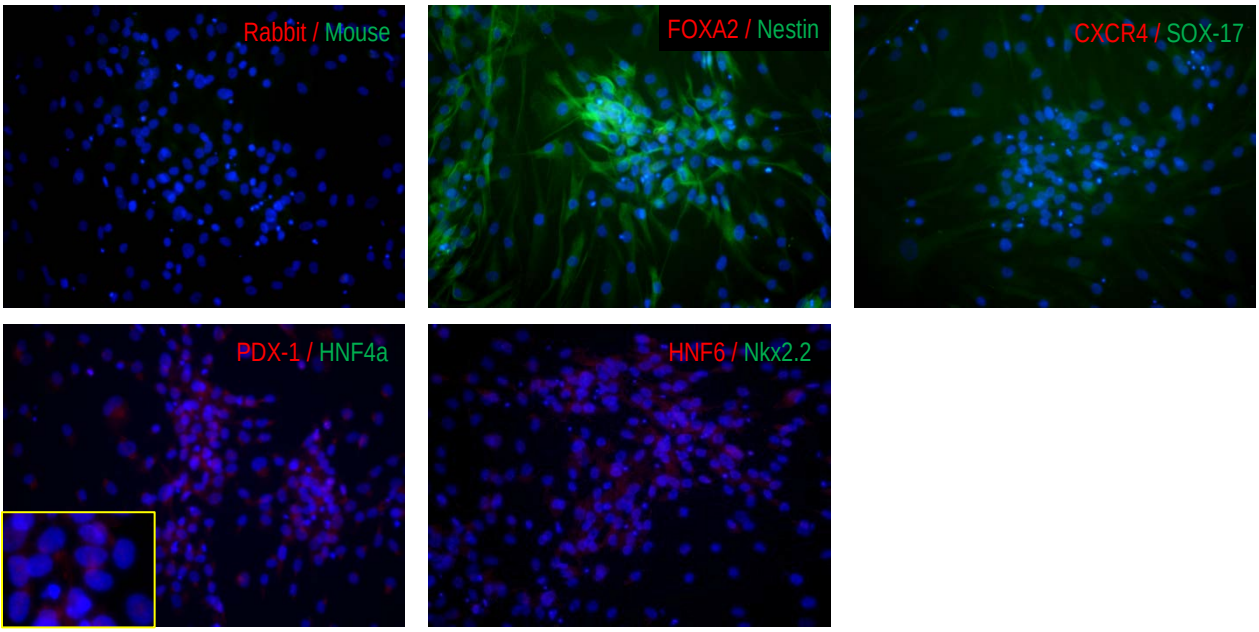


Figure 7.24 Phenotyping of ASCs differentiated with 400 nM IDE-1, followed by KAAD-cyclopamine + FGF10 + BMP-2 towards the formation of primitive gut tube (Stage 2).

Cells that had been differentiated for 4 days with 400 nM IDE were cultured for 2 days with 0.25 μM KAAD-cyclopamine + 50 ng/mL FGF10 + 100 ng/mL BMP-2, and immunostained for the expression of stem cell and pancreatic cell markers. Immunoreactivity was detected with donkey anti-rabbit (red) and donkey anti-mouse (green) antibodies. Cell nuclei were stained blue with DAPI. Images were taken at 200x magnification; inset is a 4x magnification of part of the image. The images are presented so that the staining obtained with each IgG control immediately precedes stainings with antibodies of the same host species.

For trial 5, ASCs cultured for 2 days in activin A + Wnt3a and 4 days in activin A only were subsequently cultured for 2 days with 0.25 μM KAAD-cyclopamine + 50 ng/mL FGF10 (D'Amour *et al.* 2006) (Figure 7.25). The resulting cells strongly expressed Nestin, and weakly expressed SOX-17, and PDX-1 (nuclear and cytoplasmic) (Figure 7.25). The cells did not express FOXA2, CXCR4, HNF4a, HNF6, and Nkx2.2 (Figure 7.25). See Table 7.5, stage 2; column C for a summary of the phenotype of the ASCs differentiated with activin A + Wnt3a followed by activin A only, and then with KAAD-cyclopamine + FGF10.

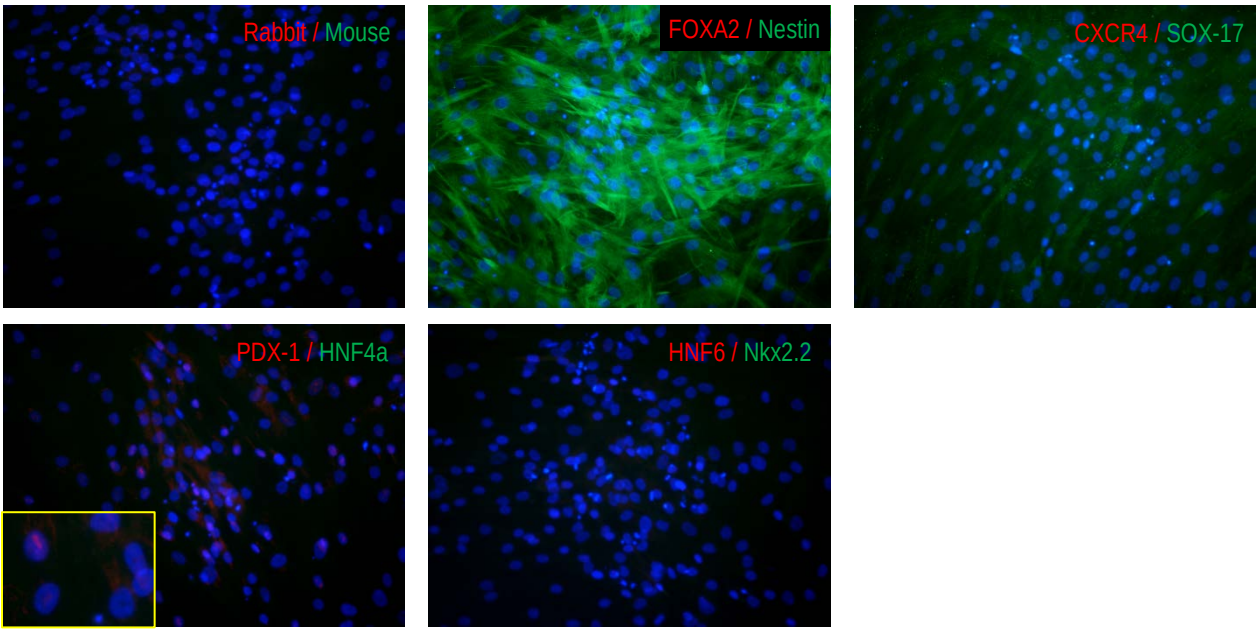


Figure 7.25 Phenotyping of ASCs differentiated with activin A + Wnt3a followed by activin A only, followed by KAAD-cyclopamine + FGF10 towards formation of primitive gut tube (Stage 2).

Cells that had been differentiated for 2 days with activin A + Wnt3a, followed by 4 days with activin A only were cultured for 2 days with 0.25 μM KAAD-cyclopamine + 50 ng/mL FGF10 and immunostained for the expression of stem cell and pancreatic cell markers. Immunoreactivity was detected with donkey anti-rabbit (red) and donkey anti-mouse (green) antibodies. Cell nuclei were stained blue with DAPI. Images were taken at 200x magnification; inset is a 4x magnification of part of the image. The images are presented so that the staining obtained with each IgG control immediately precedes stainings with antibodies of the same host species.

For trial 6, ASCs cultured for 2 days in activin A + Wnt3a, followed by 4 days with activin A only were subsequently cultured for 2 days with 0.25 μM KAAD-cyclopamine + 50 ng/mL FGF10 + 100 ng/mL BMP-2 (D'Amour *et al.* 2006; Talavera-Adame *et al.* 2011) (Figure 7.26). The resulting cells strongly expressed Nestin and weakly expressed SOX-17, and PDX-1 (Figure 7.26). They did not express FOXA2, CXCR4, HNF4a, HNF6, and Nkx2.2 (Figure 7.26). See Table 7.5, stage 2; column C-b for a summary of the phenotype of the ASCs differentiated with activin A + Wnt3a, followed by activin A only, and then with KAAD-cyclopamine + FGF10 + BMP-2.

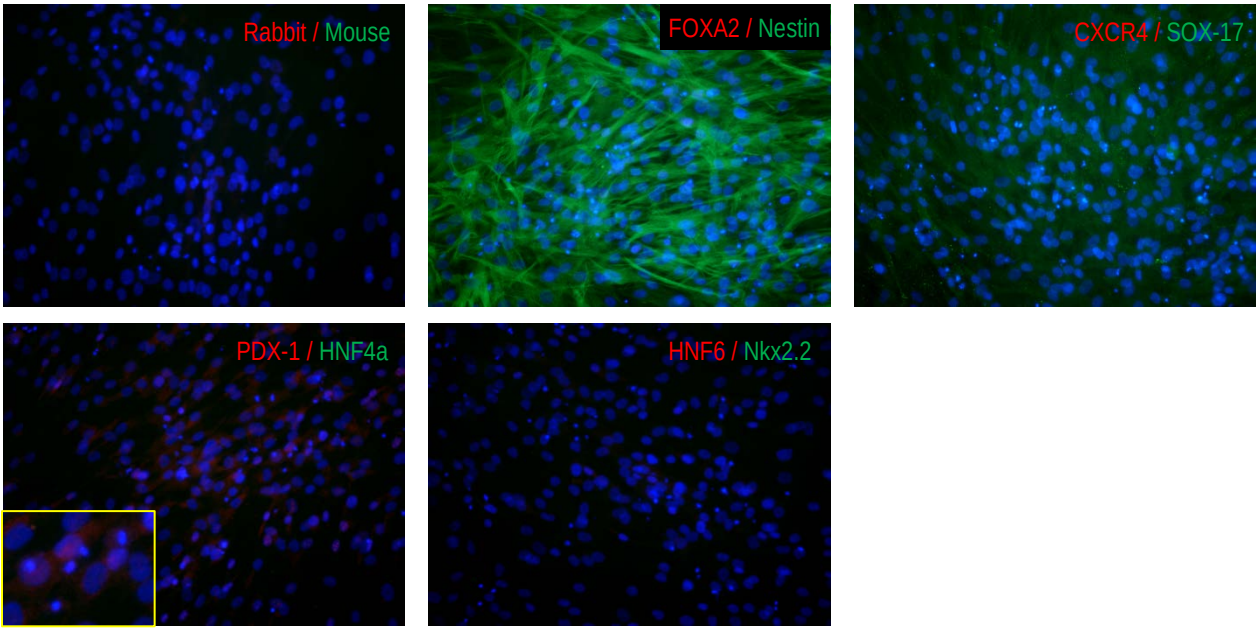


Figure 7.26 Phenotyping of ASCs differentiated with activin A + Wnt3a, followed by activin A only, followed by KAAD-cyclopamine + FGF10 + BMP-2 towards the formation of primitive gut tube (Stage 2).

Cells that had been differentiated for 2 days with activin A + Wnt3a, followed by 4 days with activin A only were cultured for 2 days with 0.25 μM KAAD-cyclopamine + 50 ng/mL FGF10 + 100 ng/mL BMP-2 and immunostained for the expression of stem cell and pancreatic cell markers. Immunoreactivity was detected with donkey anti-rabbit (red) and donkey anti-mouse (green) antibodies. Cell nuclei were stained blue with DAPI. Images were taken at 200x magnification; inset is a 4x magnification of part of the image. The images are presented so that the staining obtained with each IgG control immediately precedes stainings with antibodies of the same host species.

For trial 7, ASCs cultured for 6 days in activin A + Wnt3a, were subsequently cultured for 2 days in 0.25 μM KAAD-cyclopamine + 50 ng/mL FGF10 (D'Amour *et al.* 2006) (Figure 7.27). The resulting cells strongly expressed Nestin, and some cells weakly expressed SOX-17, and PDX-1 in their cytoplasm (Figure 7.27). Expression of FOXA2, CXCR4, HNF4a, HNF6, and Nkx2.2 could not be detected (Figure 7.27). See Table 7.5, stage 2; column D for a summary of the phenotype of the ASCs cultured with activin A + Wnt3a, and then with KAAD-cyclopamine + FGF10.

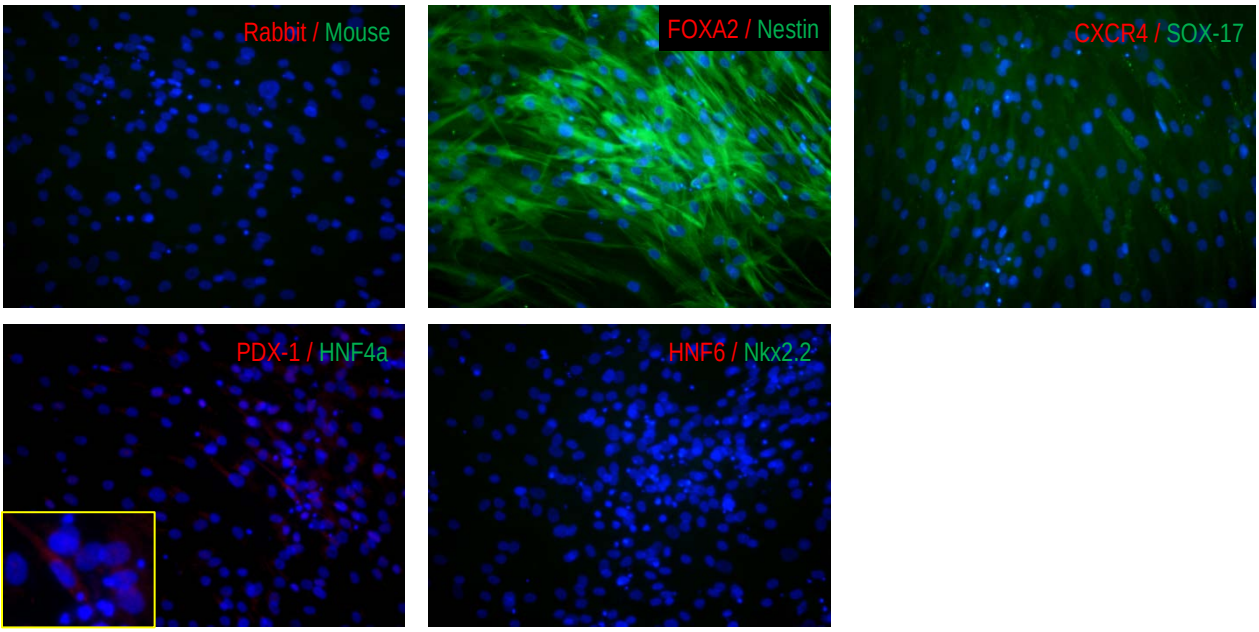


Figure 7.27 Phenotyping of ASCs differentiated with activin A + Wnt3a, followed by KAAD-cyclopamine + FGF10 towards formation of primitive gut tube (Stage 2).

Cells that had been differentiated for 6 days with activin A + Wnt3a were cultured for 2 days with 0.25 μM KAAD-cyclopamine + 50 ng/mL FGF10, and immunostained for the expression of stem cell and pancreatic cell markers. Immunoreactivity was detected with donkey anti-rabbit (red) and donkey anti-mouse (green) antibodies. Cell nuclei were stained blue with DAPI. Images were taken at 200x magnification; inset is a 4x magnification of part of the image. The images are presented so that the staining obtained with each IgG control immediately precedes stainings with antibodies of the same host species.

For trial 8, ASCs cultured for 6 days in activin A + Wnt3a, were subsequently cultured for 2 days in 0.25 μM KAAD-cyclopamine + 50 ng/mL FGF10 + 100 ng/mL BMP-2 (D'Amour *et al.* 2006; Borowiak *et al.* 2009) (Figure 7.28). The resulting cells strongly expressed Nestin and weakly expressed SOX-17 (Figure 7.28). Expression of FOXA2, CXCR4, PDX-1, HNF4a, HNF6, and Nkx2.2 was not detected (Figure 7.28). See Table 7.5, stage 2; column D-b for a summary of the phenotype of the ASCs cultured with activin A + Wnt3a, and then with KAAD-cyclopamine + FGF10 + BMP-2.

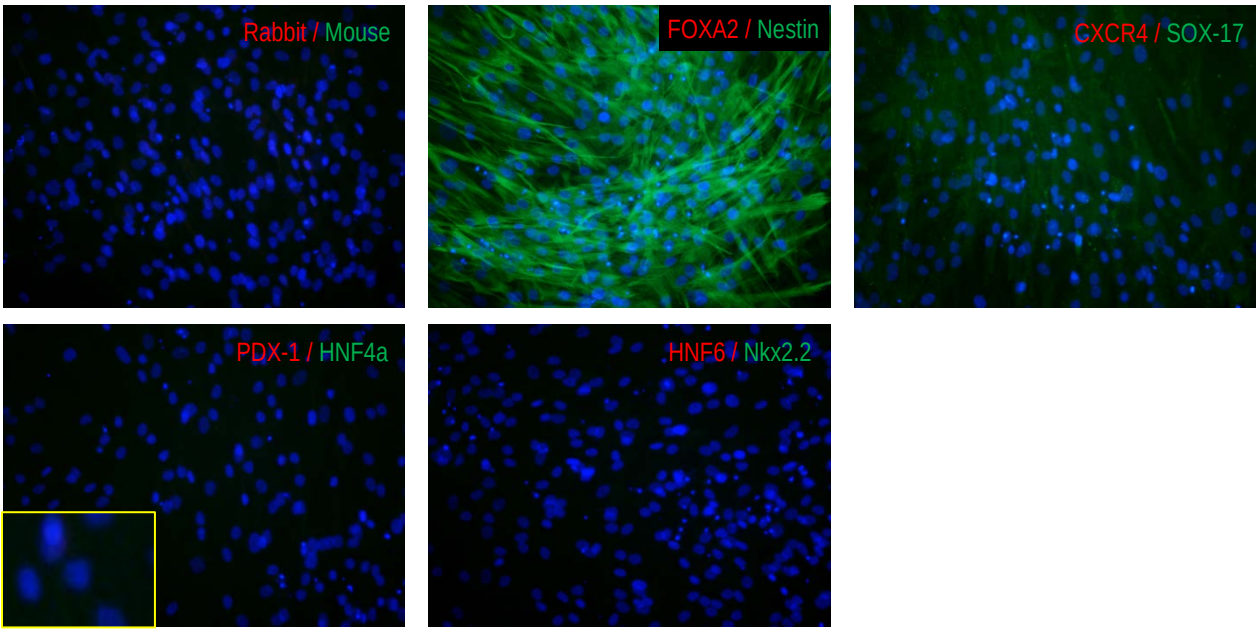


Figure 7.28 Phenotyping of ASCs differentiated with activin A + Wnt3a, followed by KAAD-cyclopamine + FGF10 + BMP-2 towards formation of primitive gut tube (Stage 2).

Cells that had been differentiated for 6 days with activin A + Wnt3a were cultured for 2 days with 0.25 μM KAAD-cyclopamine + 50 ng/mL FGF10 + 100 ng/mL BMP-2, and immunostained for the expression of stem cell and pancreatic cell markers. Immunoreactivity was detected with donkey anti-rabbit (red) and donkey anti-mouse (green) antibodies. Cell nuclei were stained blue with DAPI. Images were taken at 200x magnification; inset is a 4x magnification of part of the image. The images are presented so that the staining obtained with each IgG control immediately precedes stainings with antibodies of the same host species.

7.7.2.3 Stage 3 – formation of posterior foregut

The next stage of differentiation (Stage 3) required that the ASCs that had been differentiated to form primitive gut tube be induced to form posterior foregut (D'Amour *et al.* 2006). The procedure used to induce formation of posterior foregut was based on a protocol by D'Amour *et al.* (2006). D'Amour *et al*. (2006) reported that primitive gut tube differentiated hESCs cultured for 2 to 4 days in DMEM containing 1% B27, 0.25 μM KAAD-cyclopamine, 50 ng/mL FGF10, and 2 μM all trans-retinoic acid express the posterior foregut markers PDX-1 and HNF6. Each of the eight differentiation protocols tested during stage 2 to form primitive

gut tube was thus followed with the D'Amour *et al.* (2006) combination of agents in the presence or absence of 100 ng/mL BMP-2 to induce posterior foregut formation. See Table 7.4 for a detailed description of the protocols and composition of media used.

For trial 1, ASCs cultured for 4 days with 100 nM IDE-1, followed by 2 days with KAAD-cyclopamine + FGF10, were then cultured for 2 days with 0.25 KAAD-cyclopamine + 50 ng/mL FGF10 + 2 μM all trans-retinoic acid (R2625, Sigma) (D'Amour *et al.* 2006) (Figure 7.29). The resulting cells strongly expressed Nestin, weakly expressed PDX-1, and a few cells weakly expressed HNF6 (Figure 7.29). They did not express FOXA2, CXCR4, SOX-17, HNF4a, and Nkx2.2 (Figure 7.29). See Table 7.5, stage 3; column A for a summary of the phenotype of the ASCs cultured at Stage 3 with KAAD-cyclopamine + FGF10 + all trans-retinoic acid.

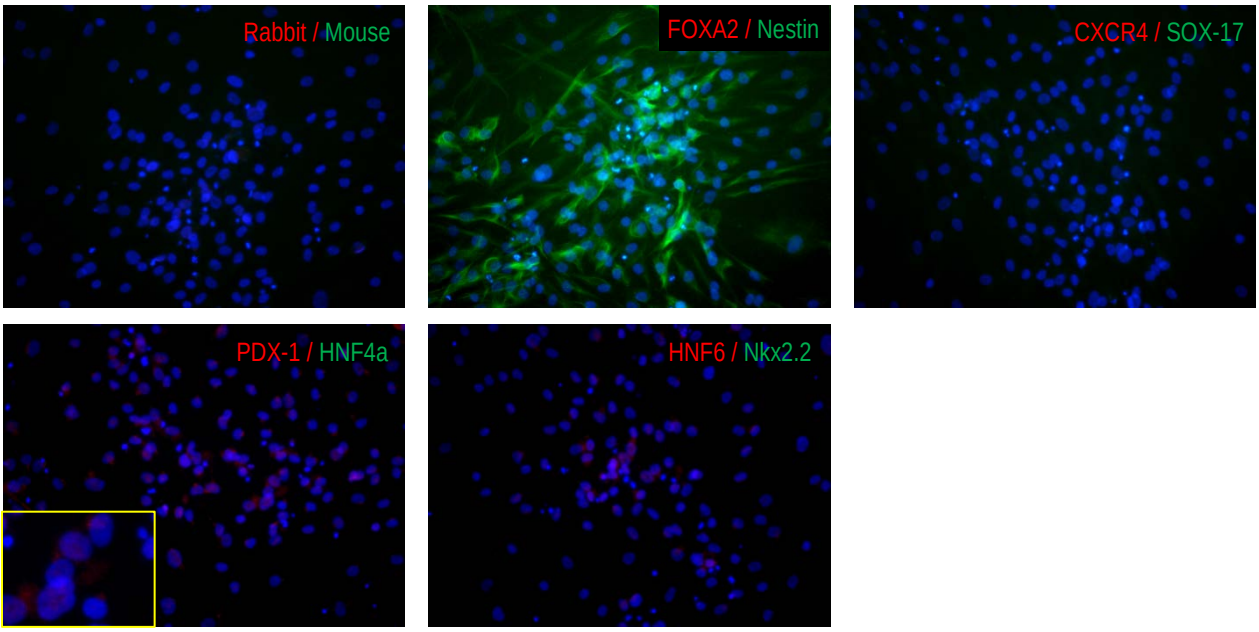


Figure 7.29 Phenotyping of ASCs differentiated with 100 nM IDE-1, followed with KAAD-cyclopamine + FGF10, and then with KAAD-cyclopamine + FGF10 + all trans-retinoic acid towards formation of posterior foregut (Stage 3).

Cells that had been differentiated for 4 days with 100 nM IDE-1 and 2 days with KAAD-cyclopamine + FGF10 were cultured for 2 days with 0.25 μM KAAD-cyclopamine + 50 ng/mL FGF10 + 2 μM all trans-retinoic acid and immunostained for the expression of stem cell and pancreatic cell markers. Immunoreactivity was detected with donkey anti-rabbit (red) and donkey anti-mouse (green) antibodies. Cell nuclei were stained blue with DAPI. Images were taken at 200x magnification; inset is a 4x magnification of part of the image. The images are presented so that the staining obtained with each IgG control immediately precedes stainings with antibodies of the same host species.

For trial 2, ASCs cultured for 4 days with 100 nM IDE-1, followed by 2 days with KAAD-cyclopamine + FGF10 + BMP-2, were then cultured for 2 days with 0.25 μM KAAD-cyclopamine + 50 ng/mL FGF10 + 2 μM all trans-retinoic acid + 100 ng/mL BMP-2 (D'Amour *et al.* 2006; Talavera-Adame *et al.* 2011) (Figure 7.30). The resulting cells strongly expressed Nestin, and weakly expressed PDX-1 (Figure 7.30). A few cells weakly expressed SOX-17, and HNF6 (Figure 7.30). The expression of FOXA2, CXCR4, HNF4a, and Nkx2.2 was not detected (Figure 7.30). See Table 7.5, stage 3; column A-b for a summary of the phenotype of the ASCs cultured at Stage 3 with KAAD-cyclopamine + FGF10 + all trans-retinoic acid + BMP-2.

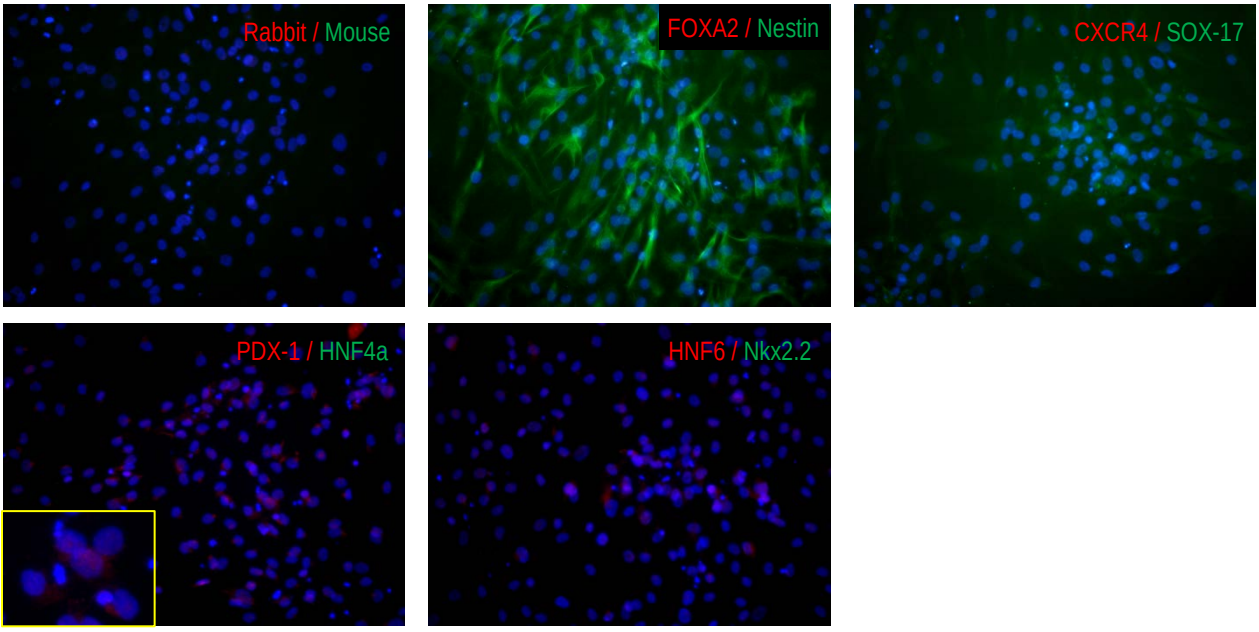


Figure 7.30 Phenotyping of ASCs cultured with 100 nM IDE-1, followed with KAAD-cyclopamine + FGF10 + BMP2, and then with KAAD-cyclopamine + FGF10 + all trans-retinoic acid + BMP-2 towards formation of posterior foregut (Stage 3).

Cells that had been differentiated for 4 days with 100 nM IDE-1 and 2 days with KAAD-cyclopamine + FGF10 + BMP-2 were cultured for 2 days with 0.25 μM KAAD-cyclopamine + 50 ng/mL FGF10 + 2 μM all trans-retinoic acid + 100 ng/mL BMP-2 and immunostained for the expression of stem cell and pancreatic cell markers. Immunoreactivity was detected with donkey anti-rabbit (red) and donkey anti-mouse (green) antibodies. Cell nuclei were stained blue with DAPI. Images were taken at 200x magnification; inset is a 4x magnification of part of the image. The images are presented so that the staining obtained with each IgG control immediately precedes stainings with antibodies of the same host species.

For trial 3, ASCs cultured for 4 days in a higher concentration of IDE-1 (400 nM), followed by 2 days with KAAD-cyclopamine + FGF10, were then cultured for 2 days with 0.25 μM KAAD-cyclopamine + 50 ng/mL FGF10 + 2 μM all trans-retinoic acid (D'Amour *et al.* 2006) (Figure 7.31). The resulting cells showed strong expression of Nestin. A few cells weakly expressed HNF4a, HNF6, and PDX-1 (in both the cytoplasm and the nucleus) (Figure 7.31). The expression of FOXA2, CXCR4, SOX-17, and Nkx2.2 was not detected (Figure 7.31). See Table 7.5, stage 3; column B for a summary of the phenotype of the ASCs cultured at Stage 3 with KAAD-cyclopamine + FGF10 + all trans-retinoic acid.

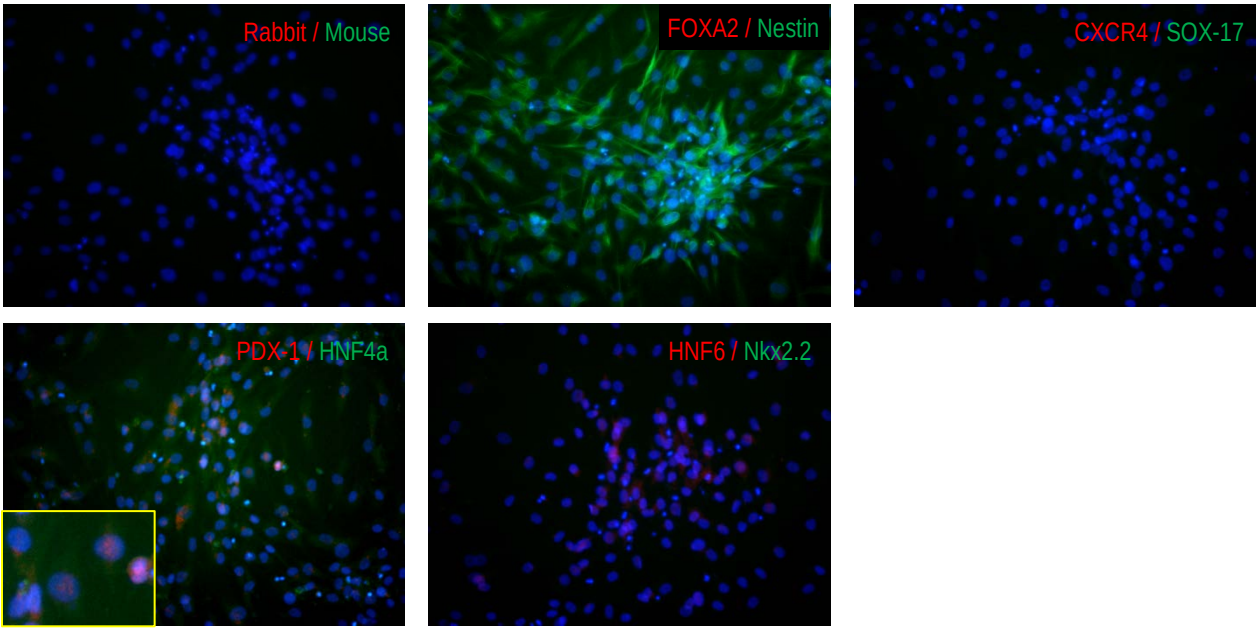


Figure 7.31 Phenotyping of ASCs differentiated with 400 nM IDE-1, followed by KAAD-cyclopamine + FGF10, and then with KAAD-cyclopamine + FGF10 + all trans-retinoic acid towards formation of posterior foregut (Stage 3).

Cells that had been differentiated for 4 days with 400 nM IDE-1 and 2 days with KAAD-cyclopamine + FGF10 were cultured for 2 days with 0.25 μM KAAD-cyclopamine + 50 ng/mL FGF10 + 2 μM all trans-retinoic acid and immunostained for the expression of stem cell and pancreatic cell markers. Immunoreactivity was detected with donkey anti-rabbit (red) and donkey anti-mouse (green) antibodies. Cell nuclei were stained blue with DAPI. Images were taken at 200x magnification; inset is a 4x magnification of part of the image. The images are presented so that the staining obtained with each IgG control immediately precedes stainings with antibodies of the same host species.

For trial 4, ASCs cultured for 4 days in the higher concentration of IDE-1 (400 nM), followed by 2 days with KAAD-cyclopamine + FGF10 with BMP-2, were then cultured for 2 days with 0.25 μM KAAD-cyclopamine + 50 ng/mL FGF10 + 2 μM all trans-retinoic acid + 100 ng/mL BMP-2 (D'Amour *et al.* 2006; Talavera-Adame *et al.* 2011) (Figure 7.32). The resulting cells strongly expressed Nestin, and weakly expressed HNF6 (Figure 7.32). A few cells weakly expressed SOX-17 and PDX-1 (cytoplasm and nucleus) (Figure 7.32). FOXA2, CXCR4, HNF4a, and Nkx2.2 were not detected (Figure 7.32). See Table 7.5, stage 3; column B-b for a summary of the phenotype of the ASCs cultured at Stage 3 with KAAD-cyclopamine + FGF10 + all trans-retinoic acid + BMP-2.

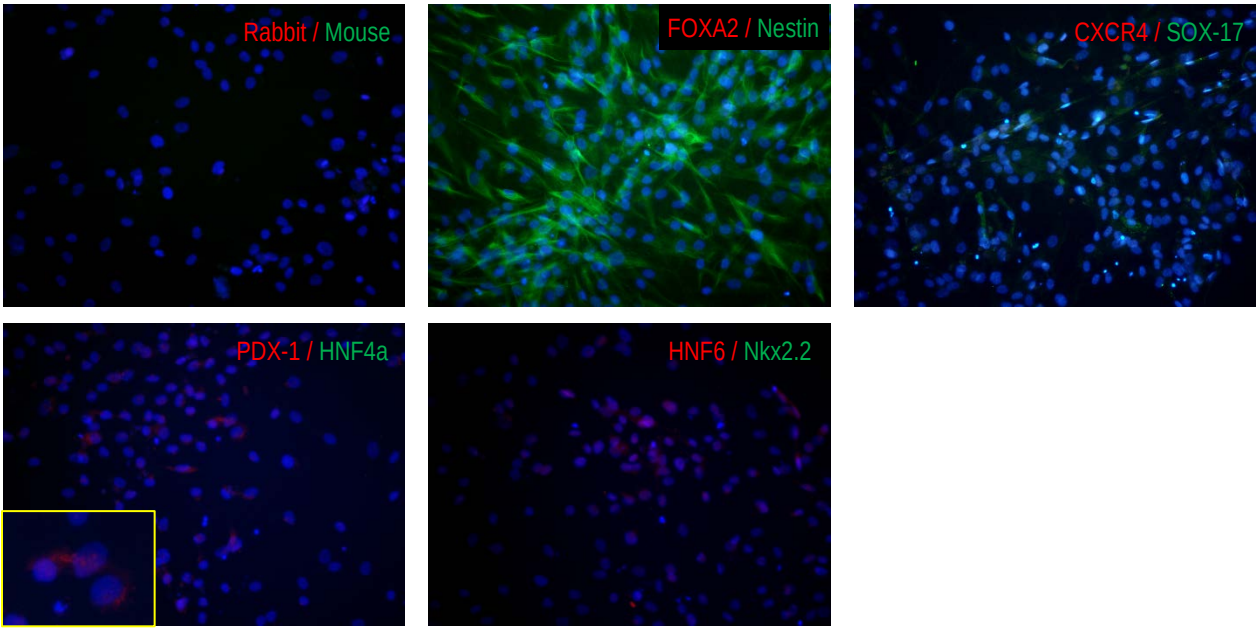


Figure 7.32 Phenotyping of ASCs differentiated with 400 nM IDE-1, followed by KAAD-cyclopamine + FGF10 + BMP-2, and then with KAAD-cyclopamine + FGF10 + retinoic acid + BMP-2 towards formation of posterior foregut (Stage 3).

Cells that had been differentiated for 4 days with 400 nM IDE-1 and 2 days with KAAD-cyclopamine + FGF10 + BMP-2 were cultured for 2 days with 0.25 μM KAAD-cyclopamine + 50 ng/mL FGF10 + 2 μM all trans-retinoic acid + 100 ng/mL BMP-2 and immunostained for the expression of stem cell and pancreatic cell markers. Immunoreactivity was detected with donkey anti-rabbit (red) and donkey anti-mouse (green) antibodies. Cell nuclei were stained blue with DAPI. Images were taken at 200x magnification; inset is a 4x magnification of part of the image. The images are presented so that the staining obtained with each IgG control immediately precedes stainings with antibodies of the same host species.

For trial 5, ASCs cultured for 2 days with activin A + Wnt3a, followed by 4 days with activin A only, followed by 2 days with KAAD-cyclopamine + FGF10, were then cultured for 2 days with 0.25 μM KAAD-cyclopamine + 50 ng/mL FGF10 + 2 μM all trans-retinoic acid (D'Amour *et al.* 2006) (Figure 7.33). The resulting cells strongly expressed Nestin and weakly expressed HNF4a (Figure 7.33). They did not express FOXA2, CXCR4, SOX-17, PDX-1, HNF6, and Nkx2.2 (Figure 7.33). See Table 7.5, stage 3; column C for a summary of the phenotype of the ASCs cultured at Stage 3 with KAAD-cyclopamine + FGF10 + all trans-retinoic acid.

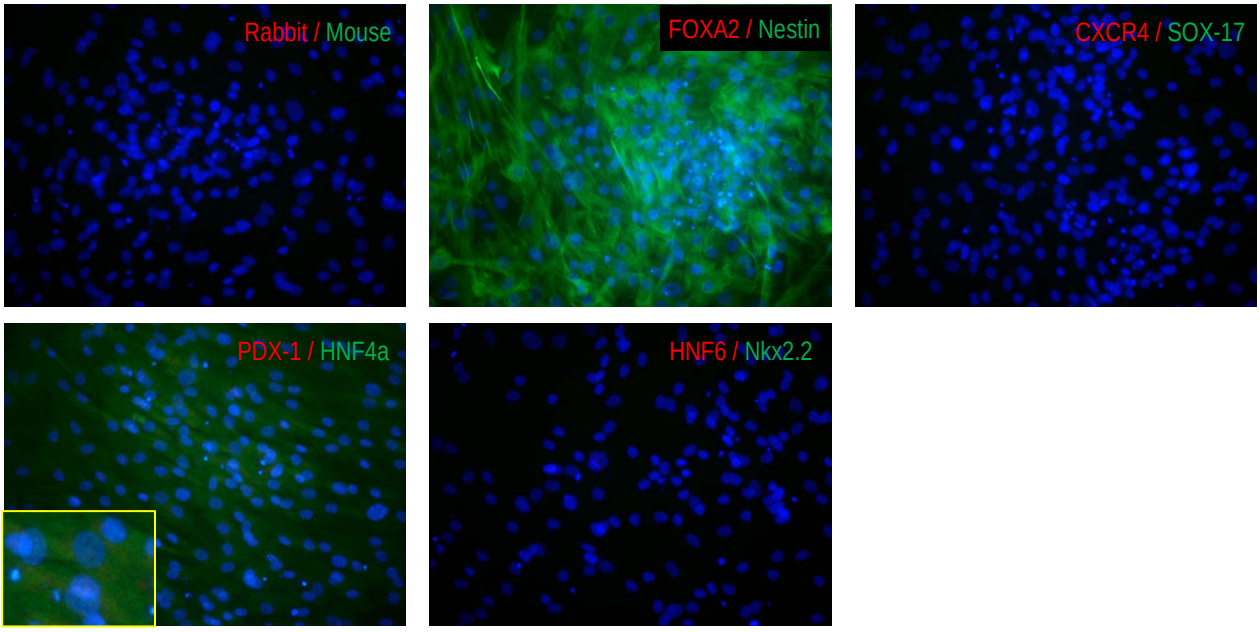


Figure 7.33 Phenotyping of ASCs differentiated with activin A + Wnt3a, followed by activin A only, followed by KAAD-cyclopamine + FGF10, and then with KAAD-cyclopamine + FGF10 + all trans-retinoic acid towards formation of posterior foregut (Stage 3).

Cells that had been differentiated for 2 days with activin A + Wnt3a, followed by 4 days with activin A only, and 2 days with KAAD-cyclopamine + FGF10 were cultured for 2 days with 0.25 μM KAAD-cyclopamine + 50 ng/mL FGF10 + 2 μM all trans-retinoic acid and immunostained for the expression of stem cell and pancreatic cell markers. Immunoreactivity was detected with donkey anti-rabbit (red) and donkey anti-mouse (green) antibodies. Cell nuclei were stained blue with DAPI. Images were taken at 200x magnification; inset is a 4x magnification of part of the image. The images are presented so that the staining obtained with each IgG control immediately precedes stainings with antibodies of the same host species.

For trial 6, ASCs cultured for 2 days with activin A + Wnt3a, followed by 4 days with activin A alone, followed by KAAD-cyclopamine + FGF10 + BMP-2, were then cultured for 2 days with 0.25 μM KAAD-cyclopamine + 50 ng/mL FGF10 + 2 μM all trans-retinoic acid + 100 ng/mL BMP-2 (D'Amour *et al.* 2006; Talavera-Adame *et al.* 2011) (Figure 7.34). The resulting cells strongly expressed Nestin and weakly expressed SOX-17. About half of the cells weakly expressed PDX-1 in the nucleus (Figure 7.34). The expression of FOXA2, CXCR4, HNF4a, HNF6, and Nkx2.2 was not detected (Figure 7.34). See Table 7.5, stage 3; column C-b for a summary of the phenotype of the ASCs cultured at Stage 3 in KAAD-cyclopamine + FGF10 + all trans-retinoic acid + BMP-2.

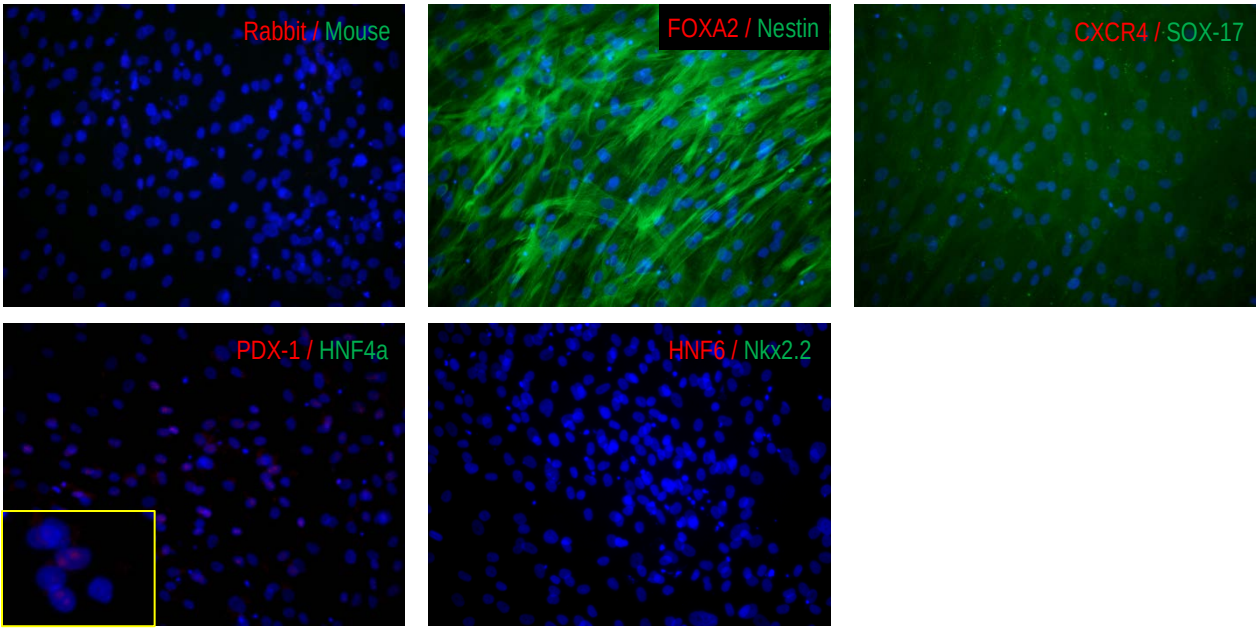


Figure 7.34 Phenotyping of ASCs differentiated with activin A + Wnt3a, followed by activin A alone, followed by KAAD-cyclopamine + FGF10 + BMP-2, and then with KAAD-cyclopamine + FGF10 + retinoic acid + BMP-2 towards formation of posterior foregut (Stage 3).

Cells that had been differentiated for 2 days with activin A + Wnt3a, followed by 4 days with activin A alone, and 2 days with KAAD-cyclopamine + FGF10 + BMP-2 were cultured for 2 days with 0.25 μM KAAD-cyclopamine + 50 ng/mL FGF10 + 2 μM all trans-retinoic acid + 100 ng/mL BMP-2 and immunostained for the expression of stem cell and pancreatic cell markers. Immunoreactivity was detected with donkey anti-rabbit (red) and donkey anti-mouse (green) antibodies. Cell nuclei were stained blue with DAPI. Images were taken at 200x magnification; inset is a 4x magnification of part of the image. The images are presented so that the staining obtained with each IgG control immediately precedes stainings with antibodies of the same host species.

For trial 7, ASCs cultured for 6 days with activin A + Wnt3a, followed by 2 days with KAAD-cyclopamine + FGF10, were then cultured for 2 days with 0.25 μM KAAD-cyclopamine + 50 ng/mL FGF10 + 2 μM all trans-retinoic acid to induce posterior foregut formation (D'Amour *et al.* 2006) (Figure 7.35). The resulting cells strongly expressed Nestin, and weakly expressed SOX-17 and HNF4a (Figure 7.35). A few cells weakly expressed PDX-1 in the nucleus (Figure 7.35). FOXA2, CXCR4, HNF6, and Nkx2.2 were not detected (Figure 7.35). See Table 7.5, stage 3; column D for a summary of the phenotype of the ASCs cultured at Stage 3 in KAAD-cyclopamine + FGF10 + all trans-retinoic acid.

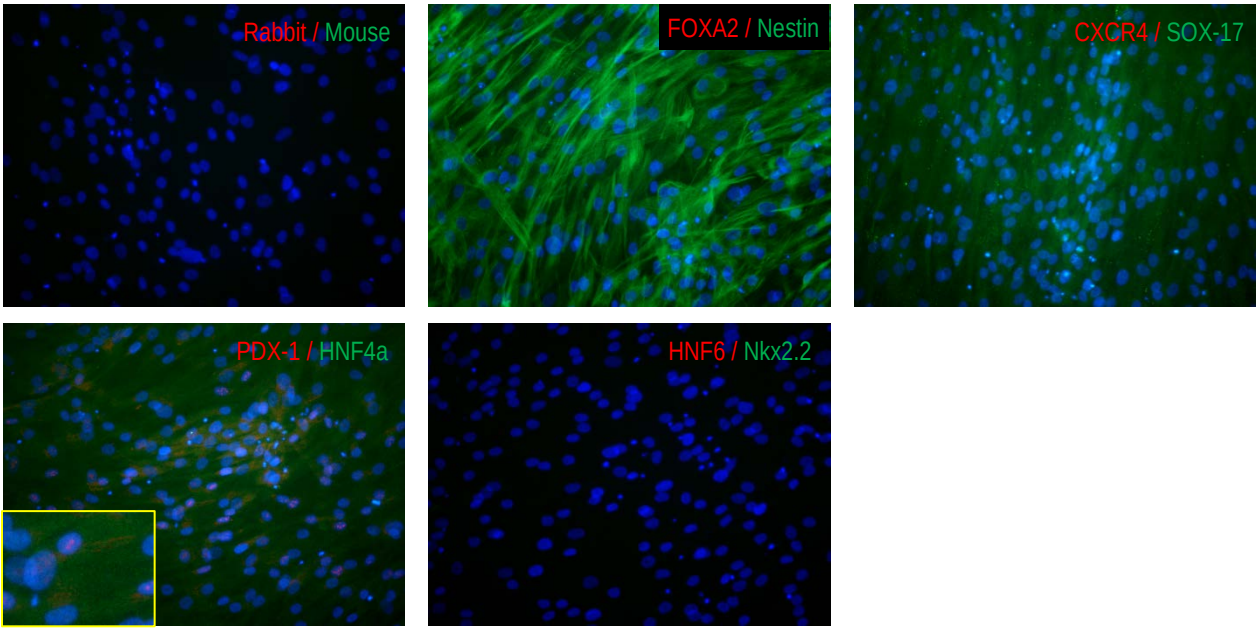


Figure 7.35 Phenotyping of ASCs differentiated with activin A + Wnt3a, followed by KAAD-cyclopamine + FGF10, and then with KAAD-cyclopamine + FGF10 + all trans-retinoic acid towards formation of posterior foregut (Stage 3).

Cells that had been differentiated for 6 days with activin A + Wnt3a, and 2 days with KAAD-cyclopamine + FGF10 were cultured for 2 days with 0.25 μM KAAD-cyclopamine + 50 ng/mL FGF10 + 2 μM all trans-retinoic acid and immunostained for the expression of stem cell and pancreatic cell markers. Immunoreactivity was detected with donkey anti-rabbit (red) and donkey anti-mouse (green) antibodies. Cell nuclei were stained blue with DAPI. Images were taken at 200x magnification; inset is a 4x magnification of part of the image. The images are presented so that the staining obtained with each IgG control immediately precedes stainings with antibodies of the same host species.

For trial 8, ASCs cultured for 6 days with activin A + Wnt3a, followed with KAAD-cyclopamine + FGF10 + BMP-2, were then cultured with 0.25 μM KAAD-cyclopamine + 50 ng/mL FGF10 + 2 μM all trans-retinoic acid + 100 ng/mL BMP-2 (D'Amour *et al.* 2006; Talavera-Adame *et al.* 2011) (Figure 7.36). The resulting cells strongly expressed Nestin and weakly expressed HNF4a (Figure 7.36). The expression of SOX-17, FOXA2, CXCR4, PDX-1, HNF6, and Nkx2.2 was not detected (Figure 7.36). See Table 7.5, stage 3; column D-b for a summary of the phenotype of the ASCs cultured at Stage 3 in KAAD-cyclopamine + FGF10 + all trans-retinoic acid + BMP-2.

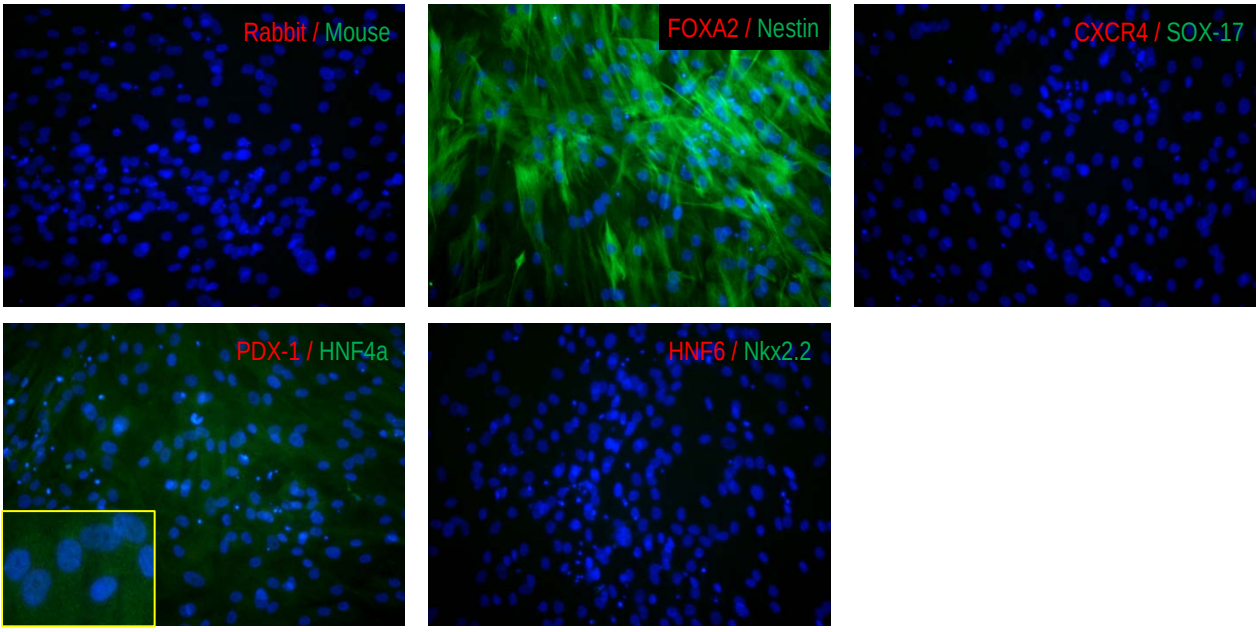


Figure 7.36 Phenotyping of ASCs differentiated with activin A + Wnt3a, followed by KAAD-cyclopamine + FGF10 + BMP-2, and then with KAAD-cyclopamine + FGF10 + all trans-retinoic acid + BMP-2 towards the formation of posterior foregut (Stage 3).

Cells that had been differentiated for 6 days with activin A + Wnt3a followed by 2 days with KAAD-cyclopamine + FGF10 + BMP-2 were cultured for 2 days with 0.25 μM KAAD-cyclopamine + 50 ng/mL FGF10 + 2 μM all trans-retinoic acid + 100 ng/mL BMP-2 and immunostained for the expression of stem cell and pancreatic cell markers. Immunoreactivity was detected with donkey anti-rabbit (red) and donkey anti-mouse (green) antibodies. Cell nuclei were stained blue with DAPI. Images were taken at 200x magnification; inset is a 4x magnification of part of the image. The images are presented so that the staining obtained with each IgG control immediately precedes stainings with antibodies of the same host species.

Table 7.5 Summary of the phenotyping of ASCs after their differentiation along embryonic pathways (Stage 1-3) that lead to the formation of the pancreas

		Stage 1				Stage 2								Stage 3							
	E	A	B	C	D	A	A-b	B	B-b	C	C-b	D	D-b	A	A-b	B	B-b	C	C-b	D	D-b
Nestin	x x x	x x x	x x x	x x x	x x x	x x x	x x x	x x x	x x x	x x x	x x x	x x x	x x x	x x x	x x x	x x x	x x x	x x x	x x x	x x x	x x x
FOXA2																					
SOX-17		x		x	x	x	x	x x	x	x	x	x	x		x		x		x	x	
CXCR4																					
HNF4a				x	x	x										x		x x		x	x
PDX-1		x x		x	x	x	x x	x	x	x	x	x		x	x	x	x		x	x	
HNF6				x	x		x	x	x					x	x	x	x				
Nkx2.2																					

0	0.1-20	21-40	41-60	61-80	81-100	% Positive

x	x x	x x x	Intensity of staining - weak/moderate/strong

Abbreviations: E – expansion medium; Stage 1 (definitive endoderm): A – 100 nM IDE-1, B – 400 nM IDE-1, C – activin A + Wnt3a then activin A alone, D – activin A + Wnt3a; Stage 2 (primitive gut tube): Stage 1 followed by KAAD-cyclopamine + FGF10 (A to D) or by KAAD-cyclopamine + FGF10 + BMP-2 (A-b to D-b) ; Stage 3 (posterior foregut): Stage 1, followed by Stage 2, and then by KAAD-cyclopamine + FGF10 + all trans-retinoic acid (A to D) or by KAAD-cyclopamine + FGF10 + BMP-2 (A-b to D-b).

7.7.2.3.1 Western Blot analysis of PDX-1 expression at stage 3 of differentiation

Cells in Section 7.7.2.3 were lysed and subjected to Western blot analysis with an anti-PDX-1 antibody. The blot was stripped and reblotted with an anti-β-actin antibody which served as a loading control. The analysis confirmed that ASCs express the posterior foregut marker PDX-1 of 46 kDa during stage 3 of differentiation along the pancreatic lineage (Figure 7.37). The blot was subjected to densitometry analysis by ImageJ, where the densities of the PDX-1 bands were normalized with respect to the β-actin bands (Figure 7.38). The analysis revealed that cells treated with 100 nM IDE-1, followed by KAAD-cyclopamine + FGF10, and then KAAD-cyclopamine + FGF10 + all trans-retinoic acid (A) had the highest level of PDX-1 expression (n=2). PDX-1 was detected in ASCs subjected to protocols C, Db, and expansion, whereas PDX-1 expression had not been detected by immunohistochemistry.

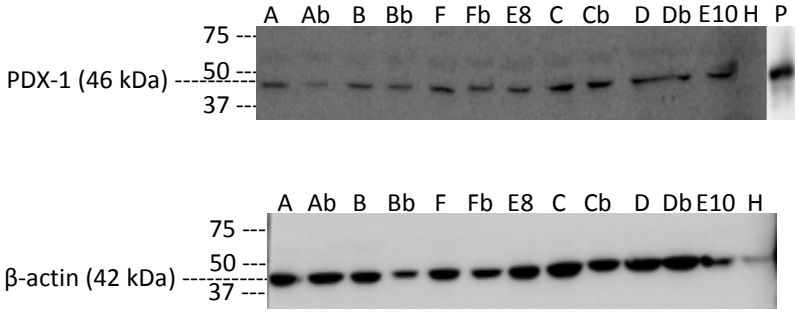


Figure 7.37 Western blot analysis confirms ASCs express PDX-1 when induced to differentiate to the posterior foregut stage of differentiation.

ASCs were cultured 8 or 10 days in expansion medium to represent cells that have not been subjected to forced differentiation (E8, E10). For differentiation ASCs were cultured for 4 days (A, Ab, B, Bb, F, Fb) or 6 days (C, Cb, D, Db) in definitive endoderm media (stage 1), followed by 2 days in primitive gut tube differentiation media (stage 2), and finally for an additional 2 days in posterior foregut differentiation (stage 3) (refer to Table 7.4). Whole cell lysates (1 x 10^4 cell equivalents) were resolved on an SDS-polyacrylamide gel under reducing conditions, and Western blotted with a rabbit anti-PDX-1 antibody (sc-25403) (upper blot), then stripped and blotted with a rabbit anti-β-actin (42 kDa) antibody (lower blot). Immunoreactivity was detected with a donkey anti-rabbit HRP-conjugated antibody. A recombinant human PDX-1 protein (100 ng) was included as a positive control. It was separately exposed for a lesser time to avoid over exposure. H: HepG2 control cell line that does not express PDX-1, P: recombinant human PDX-1.

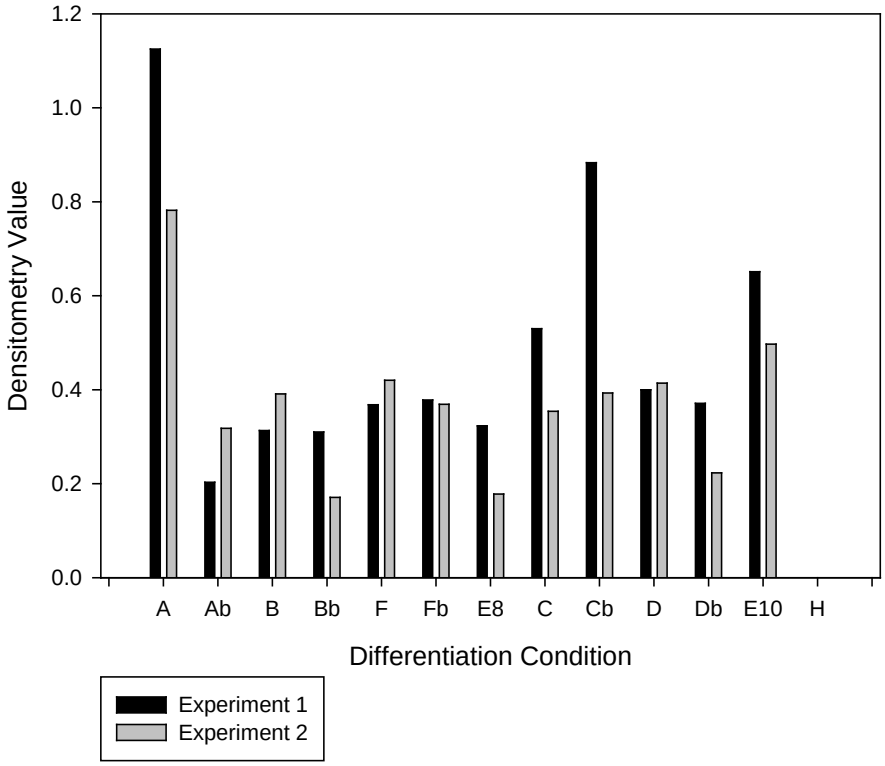


Figure 7.38 Analysis of the expression of PDX-1 by ASCs after differentiation into formation of the primitive gut tube.

ASCs were cultured in the differentiation media described in Table 7.4. SDS-gels in Figure 7.37 were subjected to densitometry analysis using Image J. The values for PDX-1 were normalized with respect to β-actin to allow for differences in the amount of sample loaded. Refer to Table 7.4 for description of labelling of differentiation conditions. E8/10: expansion medium day 8/10, H: HepG2 control cell line that does not express PDX-1.

7.7.3 Differentiation of ASCs that are sorted with respect to expression of ALDH

ASCs were separated by FACS into $ALDH^+$ and $ALDH^-$ populations to enrich for a cell population ($ALDH^+$) that might be expected to have greater stem cell-like properties, and thereby be more amenable to differentiation (n=1) (Figure 7.39). The original ASC population contained 3 x 10^6 cells, which yielded a total of 2 x 10^5 $ALDH^+$ ASCs with widely varying levels of ALDH activity. The separated populations were seeded into tissue culture plates and cultured for 4 days in expansion medium, 4 days in definitive endoderm differentiation medium, or 4 days in definitive endoderm medium followed by 2 days in primitive gut tube differentiation medium.

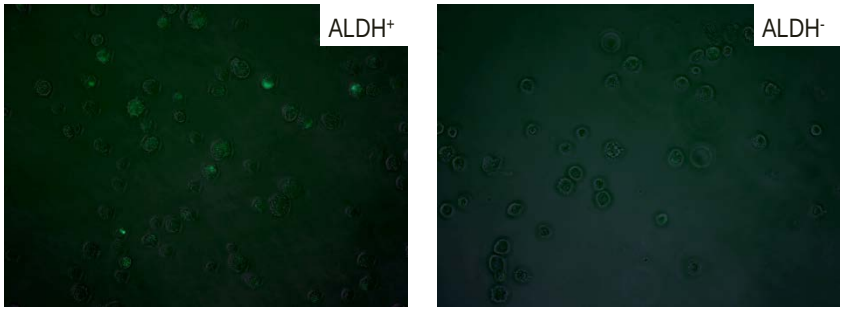
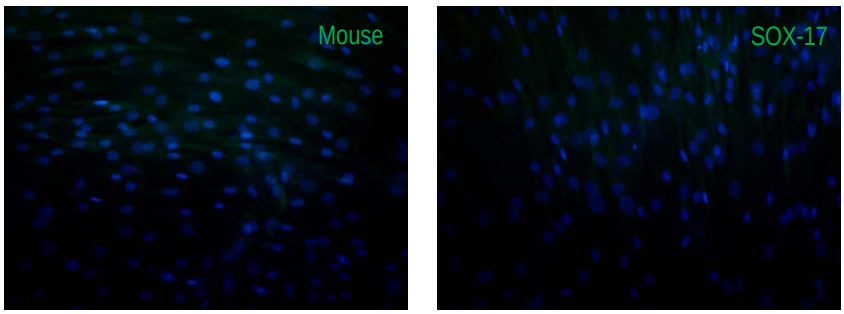


Figure 7.39 ASCs sorted according to their ALDH activity.

ASCs were incubated with the fluorescent ALDH substrate BAAA, and the green fluorescent $ALDH^+$ population was sorted and separated from the non-fluorescent $ALDH^-$ population by FACS. Images were taken at 200x magnification.

7.7.3.1 Expansion medium characterisation

$ALDH^+$ or $ALDH^-$ populations of ASCs were cultured in expansion medium for 4 days and phenotyped for stem cell, definitive endoderm, and primitive gut tube markers. Neither cell population expressed SOX-17 or HNF4, but moderately expressed Nestin (Figure 7.40 and Figure 7.41). A summary of the phenotypes of the $ALDH^+$ or $ALDH^-$ populations cultured in expansion medium is presented in Table 7.6.



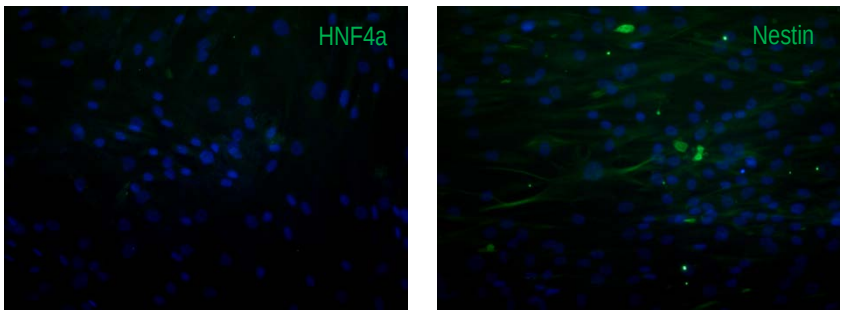


Figure 7.40 Phenotyping of ALDH$^+$ ASCs cultured for 4 days in expansion medium.

Cells were immunostained for the expression of stem cell and pancreatic cell differentiation markers. Immunoreactivity was detected with a donkey anti-mouse (green) antibody. Cell nuclei were stained blue with DAPI. Images were taken at 200x magnification. The images are presented so that the staining obtained with the IgG control immediately precedes stainings with antibodies of the same host species.

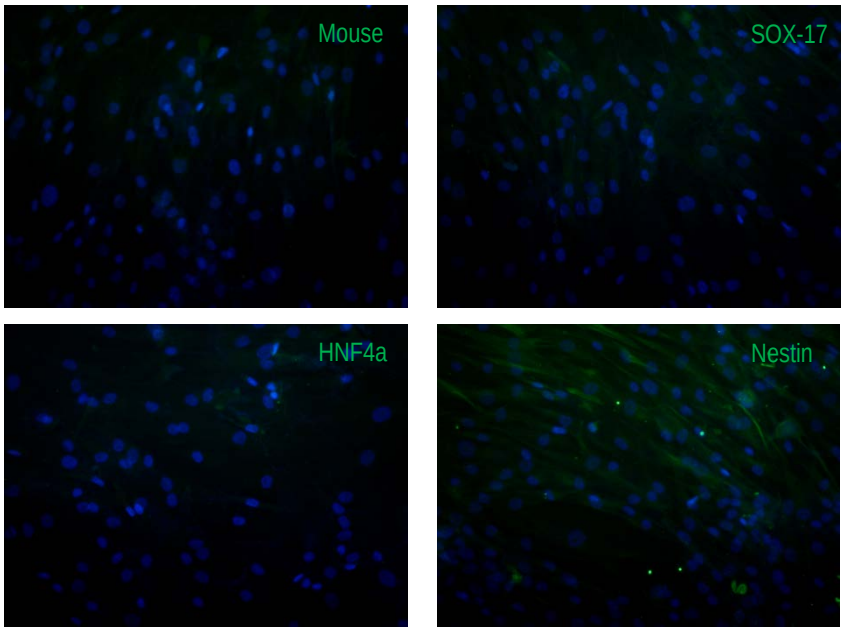


Figure 7.41 Phenotyping of ALDH- ASCs cultured for 4 days in expansion medium.

Cells were immunostained for the expression of stem cell and pancreatic cell differentiation markers. Immunoreactivity was detected with a donkey anti-mouse (green) antibody. Cell nuclei were stained blue with DAPI. Images were taken at 200x magnification. The images are presented so that the staining obtained with the IgG control immediately precedes stainings with antibodies of the same host species.

7.7.3.2 Definitive endoderm differentiation

To induce definitive endoderm differentiation the ALDH$^+$ and ALDH$^-$ sorted populations were separately cultured for 4 days in advanced RPMI medium containing 1x Glutamax, 0.2% FBS and 200 nM IDE-2 (04-0027, Stemgent) (Borowiak *et al.* 2009). Neither population expressed SOX-17 and HNF4a (Figure 7.42 and Figure 7.43). A summary of the phenotype of the ALDH$^+$ or ALDH$^-$ populations cultured in definitive endoderm differentiation medium is presented in Table 7.6.

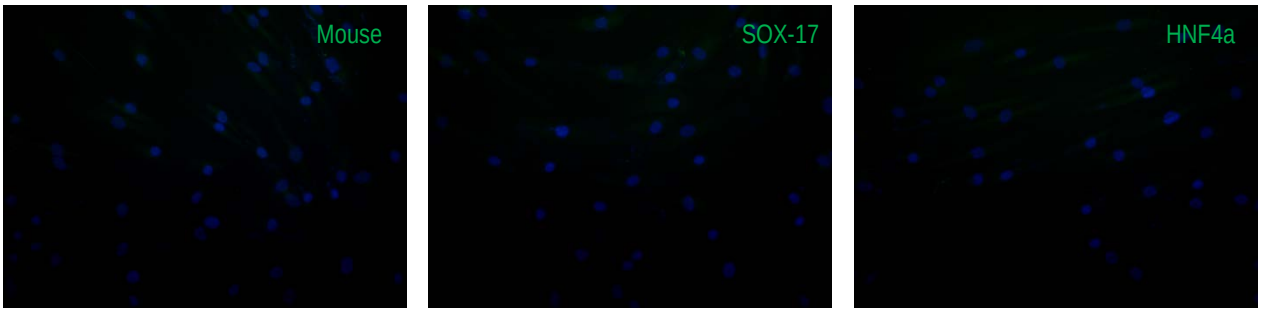


Figure 7.42 Phenotyping of ALDH$^+$ ASCs cultured in the presence of 200 nM IDE-2.

Cells were immunostained for the expression of pancreatic differentiation markers. Immunoreactivity was detected with a donkey anti-mouse (green) antibody. Cell nuclei were stained blue with DAPI. Images were taken at 200x magnification. The images are presented so that the staining obtained with the IgG control immediately precedes stainings with antibodies of the same host species.

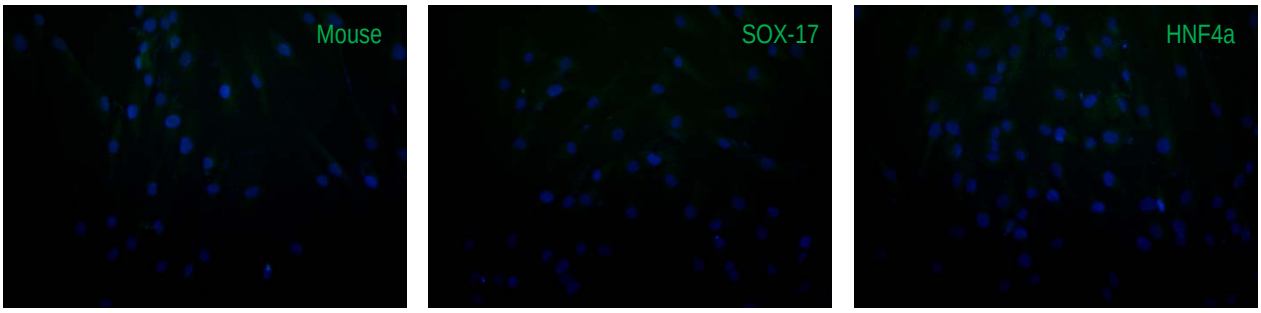


Figure 7.43 Phenotyping of ALDH- ASCs cultured in the presence of 200 nM IDE-2.

Cells were immunostained for the expression of pancreatic differentiation markers. Immunoreactivity was detected with a donkey anti-mouse (green) antibody. Cell nuclei were stained blue with DAPI. Images were taken at 200x magnification. The images are presented so that the staining obtained with the IgG control immediately precedes stainings with antibodies of the same host species.

7.7.3.3 Primitive gut tube differentiation

To induce primitive gut tube differentiation the ALDH$^+$ and ALDH$^-$ sorted populations were separately cultured with 200 nM IDE-2 for 4 days followed by culture with advanced RPMI containing 2% FBS, 0.25 μM KAAD-cyclopamine, 50 ng/mL FGF10 and 100 ng/mL BMP-2 for an additional 2 days (D'Amour *et al.* 2006; Talavera-Adame *et al.* 2011). Neither population expressed SOX-17 and HNF4a, but they both moderately expressed Nestin (Figure 7.44 and Figure 7.45). A summary of the phenotype of the ALDH$^+$ or ALDH$^-$ populations cultured in primitive gut tube differentiation medium is presented in Table 7.6.

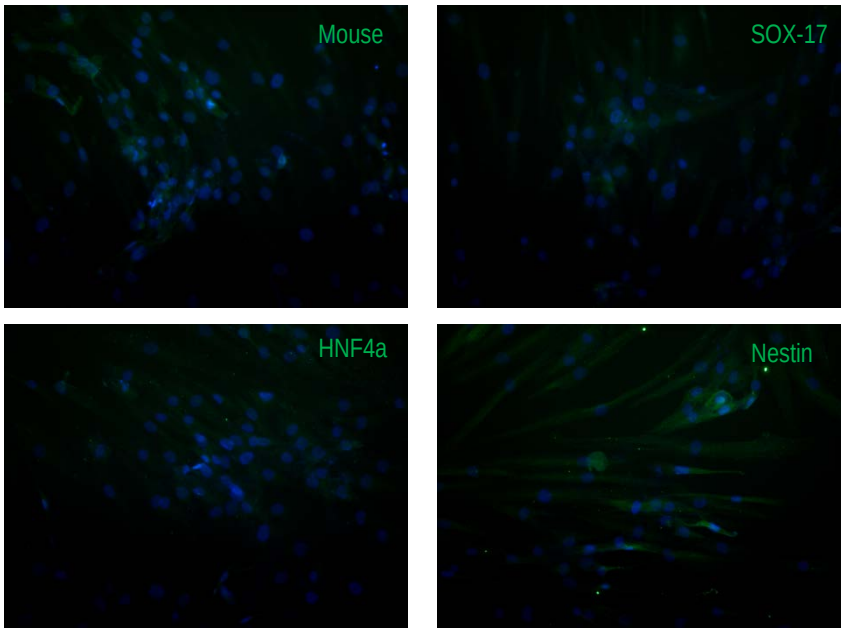
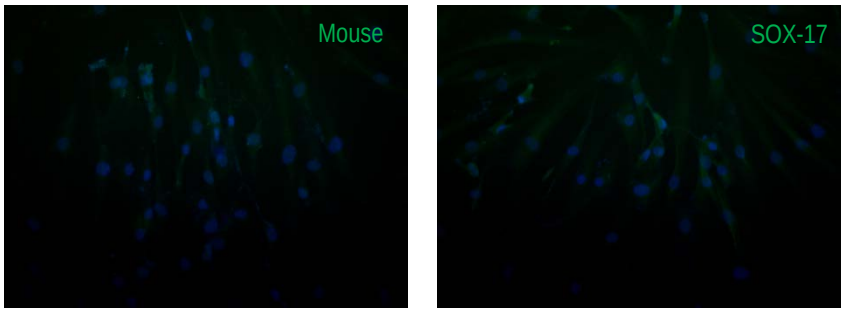


Figure 7.44 Phenotyping of ALDH$^+$ ASCs cultured in 200 nM IDE-2 followed by KAAD-cyclopamine + FGF10 + BMP-2.

Cells were immunostained for the expression of stem cell and pancreatic cell differentiation markers. Immunoreactivity was detected with a donkey anti-mouse (green) antibody. Cell nuclei were stained blue with DAPI. Images were taken at 200x magnification. The images are presented so that the staining obtained with the IgG control immediately precedes stainings with antibodies of the same host species.



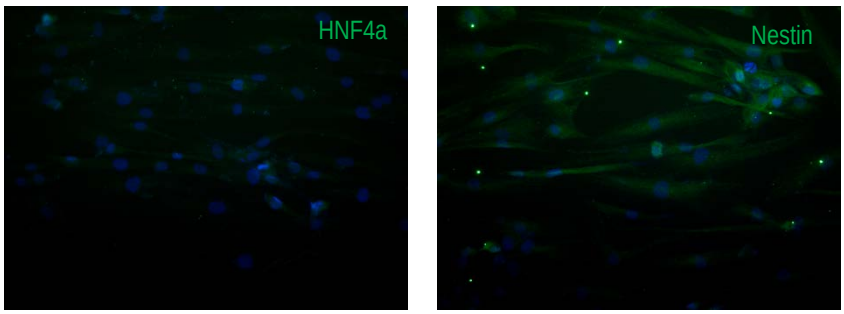


Figure 7.45 Phenotyping of ALDH$^-$ ASCs cultured in 200 nM IDE-2 followed by KAAD-cyclopamine + FGF10 + BMP-2.

Cells were immunostained for the expression of stem cell and pancreatic differentiation markers. Immunoreactivity was detected with a donkey anti-mouse (green) antibody. Cell nuclei were stained blue with DAPI. Images were taken at 200x magnification. The images are presented so that the staining obtained with the IgG control immediately precedes stainings with antibodies of the same host species.

Table 7.6 Summary of the phenotypes of differentiated ALDH$^+$ and ALDH$^-$ populations of ASCs

	E$^+$	E$^-$	DE$^+$	DE$^-$	PG$^+$	PG$^-$
SOX-17						
HNF4a						
Nestin	x x	x x	NT	NT	x x	x x

0	0.1-20	21-40	41-60	61-80	81-100	% Positive

x	x x	x x x	Intensity of staining - weak/moderate/strong

Abbreviations: $^+$: ALDH$^+$, $^-$: ALDH$^-$, E: expansion medium, DE: definitive endoderm differentiation medium, PG: primitive gut tube differentiation medium, NT: not tested.

7.8 Differentiation of ASCs cultured in suspension towards the pancreatic lineage

Chandra's protocol utilised ultra-low attachment plates to promote the formation of ASCs into islet-like cell aggregates (Chandra *et al.* 2011). These plates enabled the formation of compact clusters within 24-36 h of culture, and after 14 days the clusters resembled pancreatic islets which expressed endodermal markers (Chandra *et al.* 2011). Another study has shown that culture of ESCs in low glucose as suspension cells during pancreatic differentiation improves insulin secretion, compared with ESCs cultured in a monolayer (Segev *et al.* 2004). Therefore pancreatic differentiation of ASCs in suspension was also trialled here to enhance the ability of ASCs to differentiate along the pancreatic lineage. ASCs were cultured on either ultra-low attachment (CORN3471, Merck Millipore) (Figure 7.46) or hydrophobic (351146, BD) (data not shown) 6-well plates. They formed tight

clusters within 2 days when cultured in either expansion medium or Chandra's medium (SFM-A) (Figure 7.46). The ASCs remain clustered for at least 2 weeks when cultured in either medium in ultra-low attachment or hydrophobic plates (data not shown).

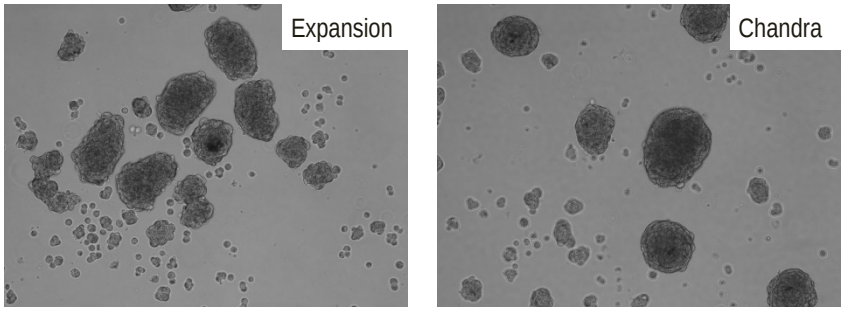
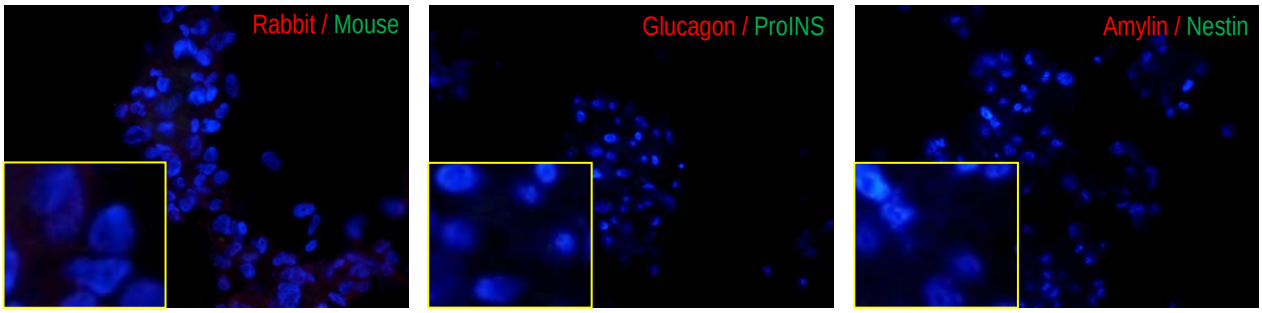


Figure 7.46 Phase contrast images of clustered ASCs after culture in ultra-low attachment plates.

ASCs were cultured for 2 days in either expansion medium (Expansion) or Chandra's medium (SFM-A). Images were taken at 100x magnification.

7.8.1 Differentiation in Chandra's media

ASCs cultured for 2 weeks in suspension with Chandra's media (see Table 7.2 for media details) in ultra-low attachment plates were phenotyped for stem cell and pancreatic markers (n=3) (Figure 7.47). Three separate experiments gave similar outcomes. Cells cultured in ultra-low attachment plates did not express the stem cell marker Nestin (Figure 7.47), as previously described for cells cultured in Chandra's media on tissue culture plates (Figure 7.14). Weak expression of insulin was detected with the guinea pig anti-insulin antibody, but not with the mouse anti-insulin antibody, but the result was equivocable due to the level of background staining by the guinea pig control antibody (Figure 7.47). The result is similar to that described for cells cultured in Chandra's media on tissue culture plates (Figure 7.13 and Figure 7.14). The cells in suspension did not express proinsulin, amylin, glucagon or Wnt-3 (Figure 7.47).



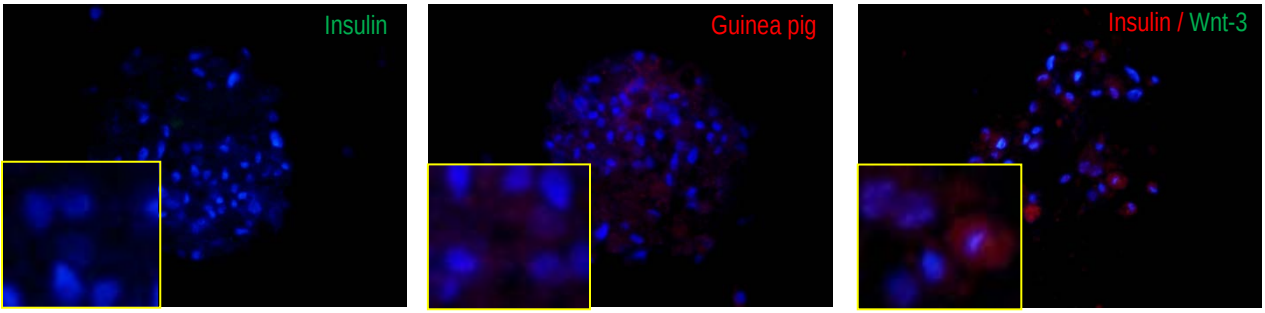


Figure 7.47 Phenotyping of ASCs cultured for 2 weeks with Chandra's media in ultra-low attachment plates.

ASCs were cultured for 2 days with SFM-A, followed by 2 days with SFM-B, and 10 days with SFM-C in ultra-low attachment plates and phenotyped for stem cell and pancreatic cell markers. Immunoreactivity was detected with donkey anti-rabbit (red), donkey anti-mouse (green), and goat anti-guinea pig (red) antibodies. Cell nuclei were stained blue with DAPI. Images were taken at 200x magnification; inset is a 4x magnification of part of the image. The images are presented so that the staining obtained with each IgG control immediately precedes stainings with antibodies of the same host species.

ASCs were cultured for 2 weeks in Chandra's media in hydrophobic plates (n=2). The resulting cells did not express Nestin, proinsulin, amylin, glucagon and Wnt-3 (Figure 7.48). They weakly expressed insulin as detected with the guinea pig anti-insulin antibody, but the expression of insulin could not be confirmed with the mouse anti-insulin antibody (Figure 7.48).

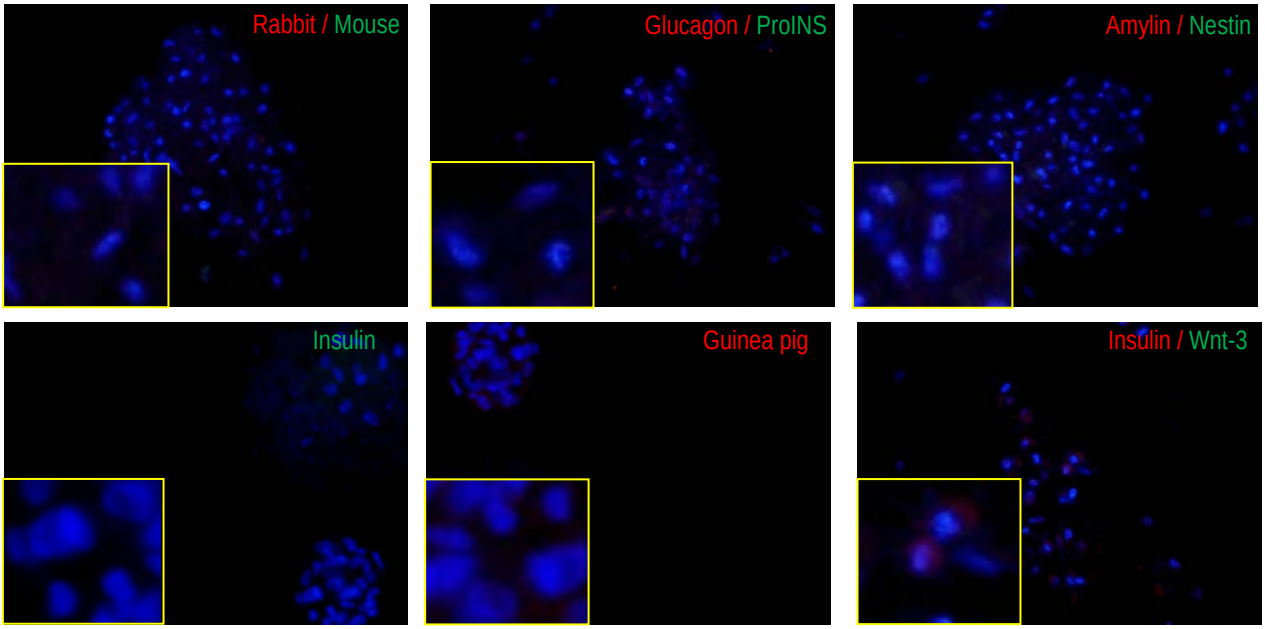


Figure 7.48 Phenotyping of ASCs cultured for 2 weeks with Chandra's media in hydrophobic plates.

ASCs were cultured for 2 days with SFM-A, followed by 2 days with SFM-B, and 10 days with SFM-C in hydrophobic plates, and phenotyped for stem cell and pancreatic cell markers. Immunoreactivity was detected with donkey anti-rabbit (red), donkey anti-mouse (green), and goat anti-guinea pig (red) antibodies. Cell nuclei were stained blue with DAPI. Images were taken at 200x magnification; inset is a 4x magnification of part of the image. The images are presented so that the staining obtained with each IgG control immediately precedes stainings with antibodies of the same host species.

7.8.2 Differentiation in Timper's medium

ASCs were cultured for 3 days on ultra-low attachment plates with Timper's medium which contains DMEM/F12 (17.5 mM glucose), 10 mM nicotinamide, 2 nM activin-A, 10 nM Ex4, 100 pM HGF, 10 nM pentagastrin, 1x B27 supplement, 1x N2 supplement, and 1% PSG (Timper *et al.* 2006). They formed cell clusters which did not express insulin, C-peptide, or amylin (n=2) (Figure 7.49).

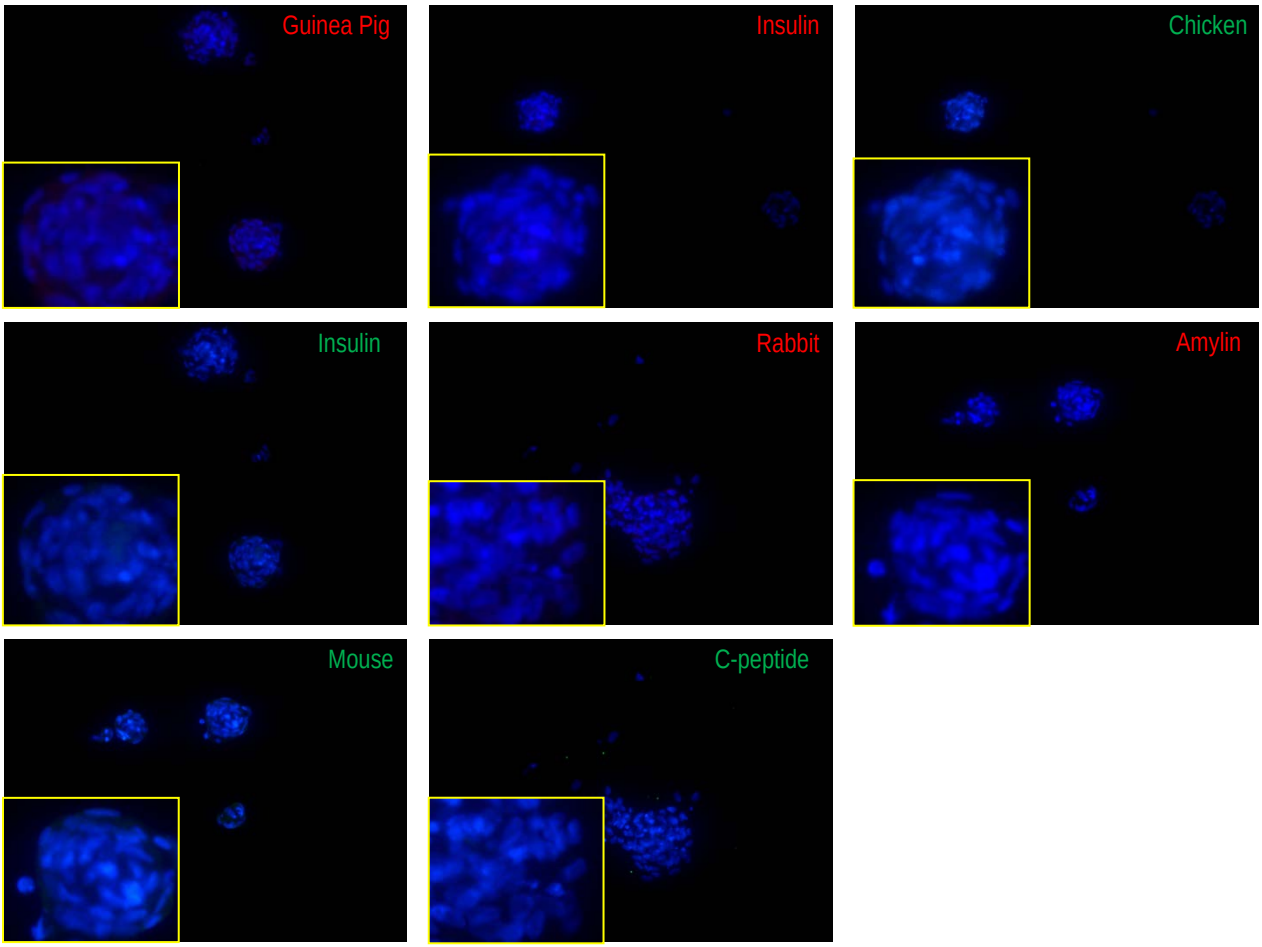


Figure 7.49 Phenotyping of ASCs cultured for 3 days with Timper's medium in ultra-low attachment plates.

ASCs were cultured for 3 days with Timper's medium in ultra-low attachment plates, and phenotyped for stem cell and pancreatic cell markers. Immunoreactivity was detected with goat anti-guinea pig (red), goat anti-chicken (green), donkey anti-rabbit (red), and donkey anti-mouse (green) antibodies. Cell nuclei were stained blue with DAPI. Images were taken at 200x magnification; inset is a 4x magnification of part of the image. The images are presented so that the staining obtained with each IgG/IgY control immediately precedes stainings with antibodies of the same host species.

7.8.3 Investigation of insulin expression by differentiated ASCs cultured in ultra-low attachment plates using a panel of anti-insulin antibodies

The above experiments showed that ASCs expressed insulin after differentiation with Chandra's media, but while insulin was detected with the anti-insulin guinea pig antibody, it was not detected with the mouse anti-insulin antibody (Figure 7.47). An antibody raised in chicken against insulin was purchased and tested for immunoreactivity to validate the results obtained with the guinea pig antibody (n=2). Unfortunately, the chicken anti-insulin antibody did not detect insulin expression by the differentiated ASCs despite very strong staining by the guinea pig anti-insulin antibody (Figure 7.50). Further, once again the expression of C-peptide and amylin was not detected (Figure 7.50). ASCs cultured in expansion medium did not express insulin, C-peptide, and amylin, and served as negative controls (Figure 7.51).

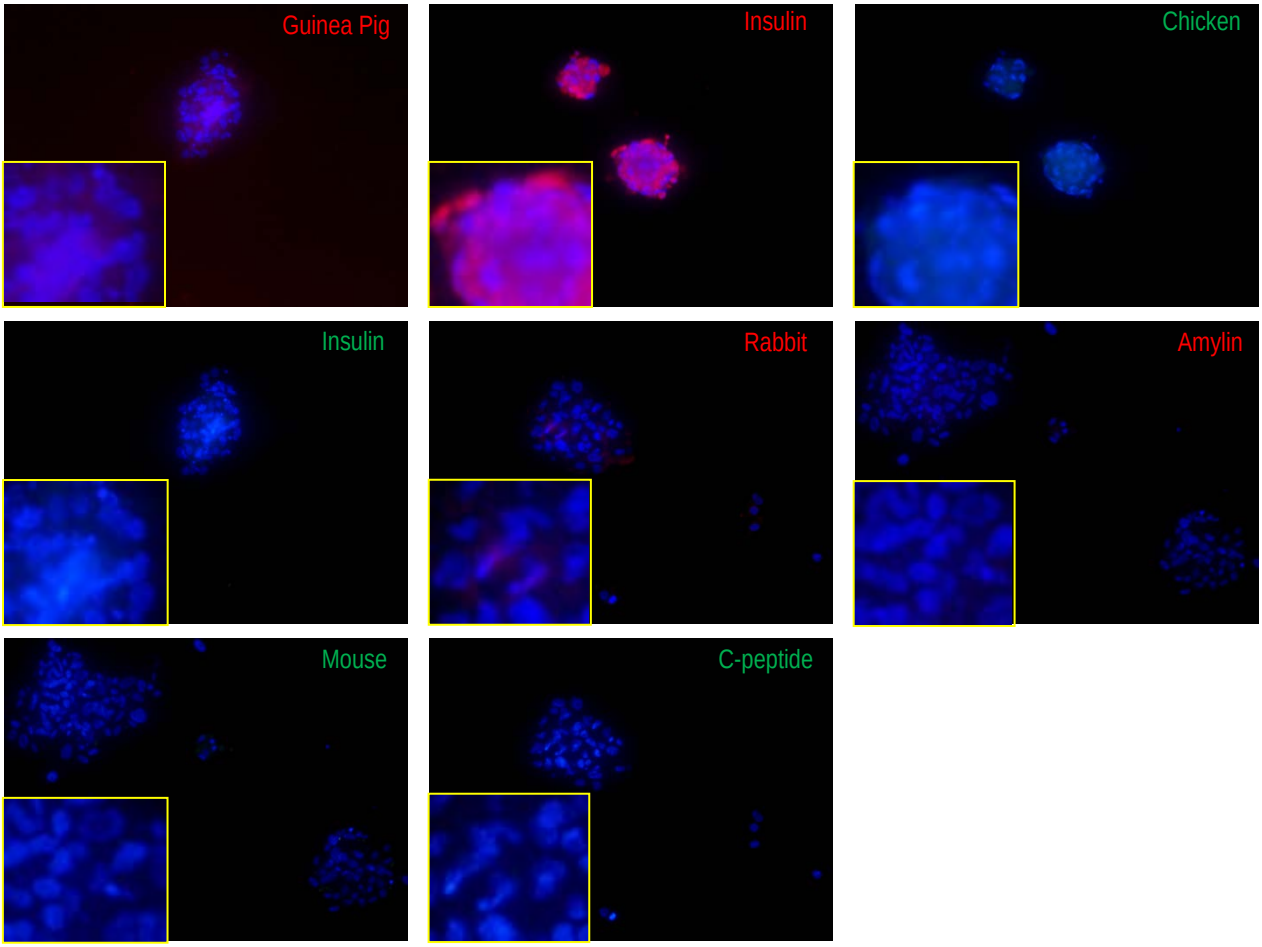


Figure 7.50 Phenotyping of ASCs cultured for 2 weeks with Chandra's media in ultra-low attachment plates.

ASCs were cultured for 2 days with SFM-A, followed by 2 days with SFM-B, and 10 days with SFM-C in ultra-low attachment plates, and phenotyped for stem cell and pancreatic cell markers. Immunoreactivity was detected with goat anti-guinea pig (red), goat anti-chicken (green), donkey anti-rabbit (red), and donkey anti-mouse (green) antibodies. Cell nuclei were stained blue with DAPI. Images were taken at 200x magnification; inset is a 4x magnification of part of the image. The images are presented so that the staining obtained with each IgG/IgY control immediately precedes stainings with antibodies of the same host species.

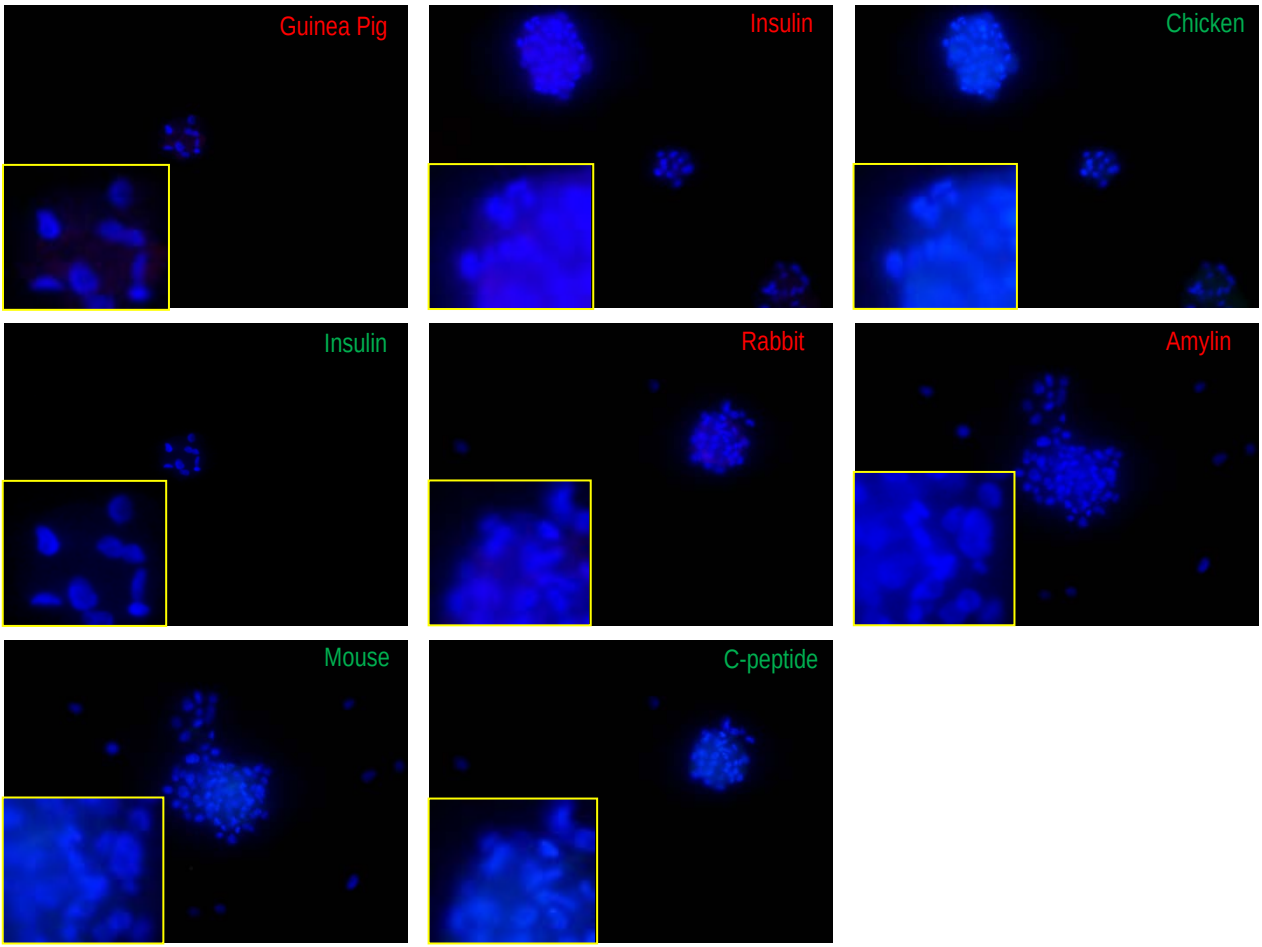


Figure 7.51 Phenotyping of ASCs cultured for 2 weeks with expansion medium in ultra-low attachment plates.

ASCs were cultured for 2 weeks in expansion medium in ultra-low attachment plates, and phenotyped for stem cell and pancreatic cell markers. Immunoreactivity was detected with goat anti-guinea pig (red), goat anti-chicken (green), donkey anti-rabbit (red), and donkey anti-mouse (green) antibodies. Cell nuclei were stained blue with DAPI. Images were taken at 200x magnification; inset is a 4x magnification of part of the image. The images are presented so that the staining obtained with each IgG/IgY control immediately precedes stainings with antibodies of the same host species.

7.8.3.1 Is the guinea pig anti-insulin antibody specific for insulin?

The failure of the mouse and chicken anti-insulin antibodies to recognize insulin expressed by the differentiated ASCs raised concerns over the authenticity of the insulin staining detected by the guinea-pig anti-insulin antibody. Was the guinea-pig anti-insulin antibody specific for insulin? Guinea-pig anti-insulin antibodies are reported to cross-react with insulin from several mammalian species, with 100% specificity for human insulin, and less than 0.01-0.05% cross-reactivity with glucagon and human growth hormone (see www.dako.com, www.sigma.com). Insulin is most closely related to insulin-like 3, insulin-like growth factor

I, and insulin-like growth factor II, hence a dot blot was performed to investigate the possibility that the guinea pig anti-insulin antibody is binding these insulin homologues (n=1) (Figure 7.52). Pure insulin, insulin-like 3, insulin-like growth factor I, and insulin-like growth factor II proteins were blotted onto a nitrocellulose membrane and probed with the guinea pig anti-insulin antibody. The antibody only detected insulin on the dot blot i.e. there was no reactivity with the insulin homologues (Figure 7.52).

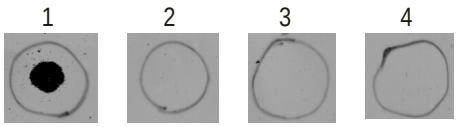


Figure 7.52 The guinea pig anti-human insulin antibody only detects insulin and not insulin homologues.

Pure recombinant forms (1 μg of each) of insulin (spot 1), insulin-like 3 (spot 2), insulin-like growth factor I (spot 3), and insulin-like growth factor II (spot 4) in PBS were spotted onto a nitrocellulose membrane. The position of each protein is denoted by a circle. The dot blot was probed with a guinea pig anti-insulin antibody, and immunoreactivity was detected with a donkey anti-guinea pig HRP-conjugated secondary antibody, and developed by chemiluminescence.

7.8.3.2 Can Western blot analysis confirm insulin expression by ASCs differentiated by Chandra's media?

The ASCs differentiated according to the Chandra protocol were analysed for the expression of insulin by Western blot analysis using the guinea pig anti-insulin antibody (Figure 7.53). It was hoped that the guinea pig anti-insulin antibody would either recognize insulin, or a cross-reactive protein which might be identifiable due to its molecular size. The ASCs were cultured in ultra-low attachment plates for 2 weeks in either expansion medium or Chandra's media. The cells were then lysed, separated into cytoplasmic and nuclear fractions, the cell proteins separated by electrophoresis on a Tris-Tricine gel under reducing conditions, and Western blot analysis performed (Figure 7.53). Recombinant insulin was included as a positive control. The guinea pig anti-insulin antibody detected 0.1 μg of recombinant insulin, but no band corresponding to insulin at was detected in the ASC lysates (Figure 7.53). The presence of β-actin was readily detected with an anti-β-actin antibody, indicating that the protein lysates had not been degraded (Figure 7.53).

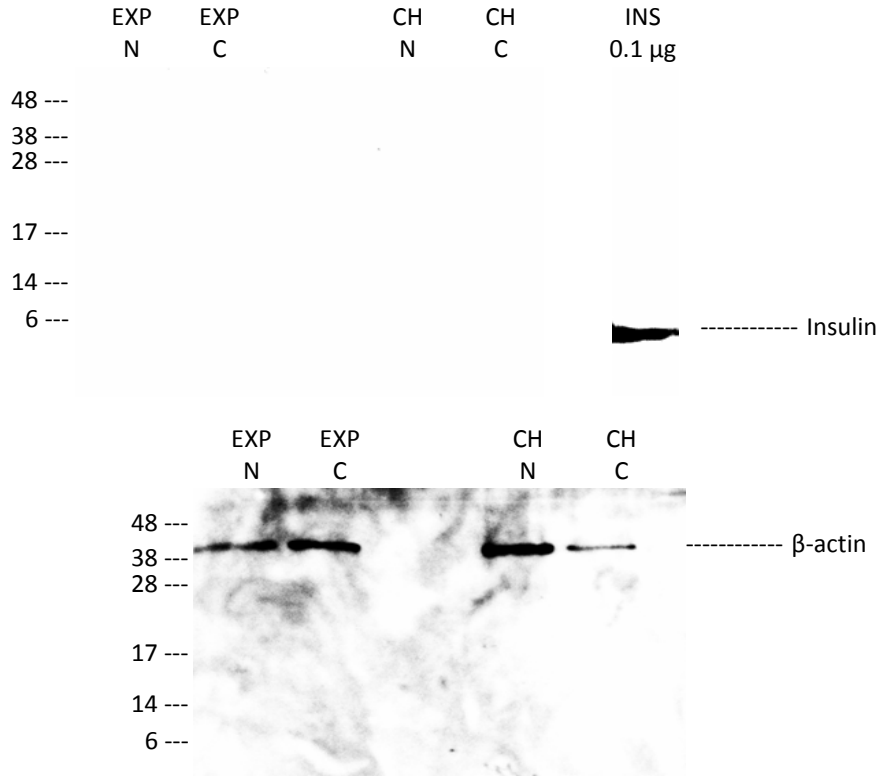


Figure 7.53 Insulin expressed by ASCs differentiated with Chandra's media is not detected by Western blot analysis.

ASCs were cultured for 2 weeks in either expansion medium (EXP) or Chandra's media (CH) in ultra-low attachment plates. They were lysed and the nuclear (N) and cytoplasmic (C) fractions were separated on a Tris-tricine gel, and Western blotted with a guinea pig anti-insulin antibody (upper blot). The membrane was stripped and reprobed with an anti-β-actin antibody (lower blot). Recombinant insulin (INS) was included as a positive control. Immunoreactivity was developed with a donkey anti-guinea pig HRP-conjugated antibody (n=2). The positions of insulin (5.8 kDa) and β-actin (42 kDa) are shown in the right-hand margin. Molecular weight markers are shown in the left-hand margin.

7.8.4 Are definitive endoderm markers expressed prior to insulin expression by ASCs cultured in ultra-low attachment plates?

Differentiating stem cells express definitive endoderm markers such as SOX-17 and CXCR4 during the early stages of stem cell differentiation towards the pancreatic lineage (D'Amour *et al.* 2006). Here the aim was to determine whether insulin-expressing ASCs cultured in Chandra-based media in ultra-low attachment plates expressed definitive endoderm markers at an early stage of differentiation. ASCs were cultured for up to 4 days in 4 different differentiation media combinations with 3 media based on Chandra's media and 1 media based on D'Amour *et al.'s* (2006) media as described in Table 7.7 (n=1).

The differentiated ASCs were analysed for expression of definitive endoderm markers after 2 and 4 days of culture. ASCs cultured in Chandra-based differentiation media did not express the definitive endoderm markers SOX-17 or CXCR4 at either

time-point, and retained the stem cell marker Nestin at day 4 (Figure 7.54 to Figure 7.58). PDX-1 was not expressed at day 4, indicating the cells had not passed the posterior foregut stage (Figure 7.56 to Figure 7.58) (D'Amour *et al.* 2006). ASCs cultured in D'Amour's differentiation medium for 4 days strongly expressed Nestin, but did not express Nanog, or other pancreatic markers to indicate pancreatic differentiation into insulin-producing cells including SOX-17 or CXCR4, PDX-1, HNF-6, and NeuroD (Figure 7.59). They did not express Wnt-3 (Figure 7.59), which is expressed by cells in the mesoendoderm stage of differentiation, which occurs prior to definitive endoderm formation (D'Amour *et al.* 2006). A summary of these findings is presented in Table 7.8.

Table 7.7 Compositions of ASC differentiation media

	Timeline	Medium name	Base medium	Added Components
i	Days 1-2	SFM-A	DMEM/F12	1% BSA + 1 x ITS + 4 nM Activin A + 1 mM Sodium butyrate + 50 µM 2-mercaptoethanol + 2ng/mL bFGF
	Days 3-4	SFM-B	DMEM/F12	1% BSA + 1 x ITS + 0.3 mM Taurine
ii	Days 1-2	SFM-A + mix	DMEM/F12	1% BSA + 1 x ITS + 4 nM Activin A + 1 mM Sodium butyrate + 50 µM 2-mercaptoethanol + 2 ng/mL bFGF + 100 ng/mL BMP-2 + 100 nM IDE-1 +200 nM IDE-2
	Days 3-4	SFM-B + mix	DMEM/F12	1% BSA + 1 x ITS + 0.3 mM Taurine + 100 ng/mL BMP-2 + 1 µM PDX-1 + 25 ng/mL FGF10 + 300 nM (-)-Indolactam V
iii	Days 1-2	SFM-A + long-mix	DMEM/F12	1% BSA + 1 x ITS + 4 nM Activin A + 1 mM Sodium butyrate + 50 µM 2-mercaptoethanol + 2 ng/mL bFGF + 100 ng/mL BMP-2 + 100 nM IDE-1 +200 nM IDE-2
	Days 3-4	SFM-A + long-mix	DMEM/F12	1% BSA + 1 x ITS + 4 nM Activin A + 1 mM Sodium butyrate + 50 µM 2-mercaptoethanol + 2 ng/mL bFGF + 100 ng/mL BMP-2 + 100 nM IDE-1 +200 nM IDE-2
iv	Days 1-2	D'Amour	RPMI	100 ng/mL Activin A + 25 ng/mL Wnt3a (serum free)
	Days 3-4	D'Amour	RPMI	100 ng/mL Activin A + 0.25% FBS

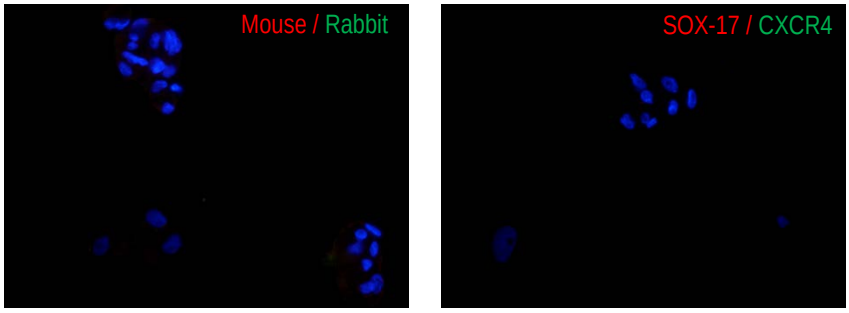


Figure 7.54 Phenotyping of ASCs cultured for 2 days in Chandra's SFM-A medium in ultra-low attachment plates for markers of definitive endoderm.

ASCs were cultured for 2 days in Chandra's SFM-A in ultra-low attachment plates, and phenotyped for the expression of definitive endoderm markers SOX-17 and CXCR4. Immunoreactivity was detected with donkey anti-mouse (red) and donkey anti-rabbit (green) antibodies. Cell nuclei were stained blue with DAPI. Images were taken at 400x magnification. The images are presented so that the staining obtained with each IgG control immediately precedes stainings with antibodies of the same host species.

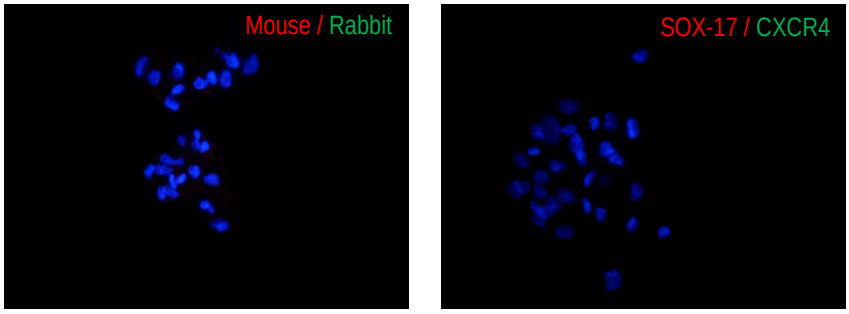


Figure 7.55 Phenotyping of ASCs cultured for 2 days in Chandra's SFM-A + mix medium in ultra-low attachment plates for markers of definitive endoderm.

ASCs were cultured for 2 days in Chandra's SFM-A + mix medium in ultra-low attachment plates, and phenotyped for the expression of definitive endoderm markers SOX-17 and CXCR4. Immunoreactivity was detected with donkey anti-mouse (red) and donkey anti-rabbit (green) antibodies. Cell nuclei were stained blue with DAPI. Images were taken at 400x magnification. The images are presented so that the staining obtained with each IgG control immediately precedes stainings with antibodies of the same host species.

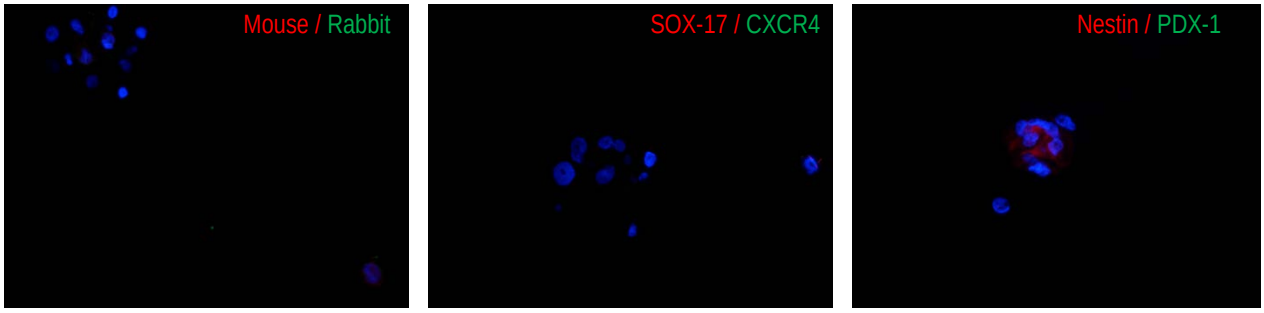


Figure 7.56 Phenotyping of ASCs cultured for 2 days in Chandra's SFM-A medium, followed by 2 days in Chandra's SFM-B medium in ultra-low attachment plates for markers of definitive endoderm.

ASCs were cultured for 2 days in Chandra's SFM-A medium, followed by 2 days in Chandra's SFM-B medium in ultra-low attachment plates and phenotyped for the expression of definitive endoderm, stem cell and posterior foregut markers. Immunoreactivity was detected with donkey anti-mouse (red) and donkey anti-rabbit (green) antibodies. Cell nuclei were stained blue with DAPI. Images were taken at 400x magnification. The images are presented so that the staining obtained with each IgG control immediately precedes stainings with antibodies of the same host species.

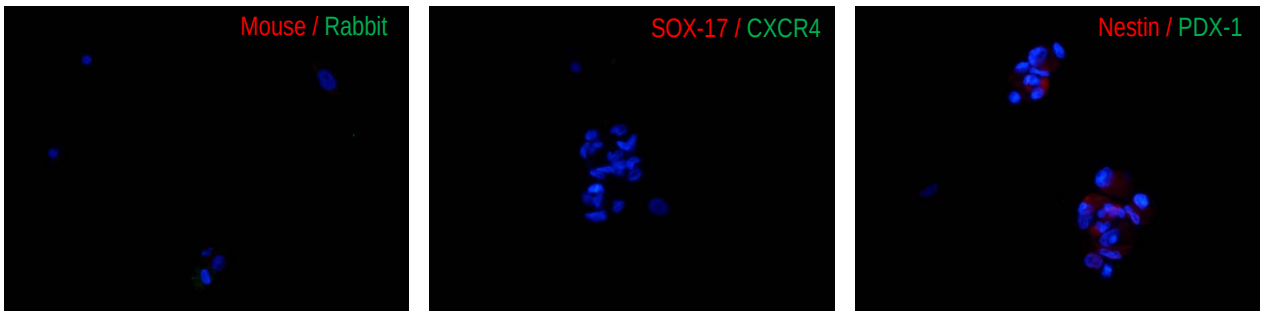


Figure 7.57 Phenotyping of ASCs cultured for 2 days in Chandra's SFM-A + mix medium followed by 2 days in Chandra's SFM-B + mix medium in ultra-low attachment plates for markers of definitive endoderm.

ASCs were cultured for 2 days in Chandra's SFM-A + mix medium, followed by 2 days in Chandra's SFM-B + mix medium in ultra-low attachment plates, and phenotyped for the expression of definitive endoderm, stem cell and posterior foregut markers. Immunoreactivity was detected with donkey anti-mouse (red) and donkey anti-rabbit (green) antibodies. Cell nuclei were stained blue with DAPI. Images were taken at 400x magnification. The images are presented so that the staining obtained with each IgG control immediately precedes stainings with antibodies of the same host species.

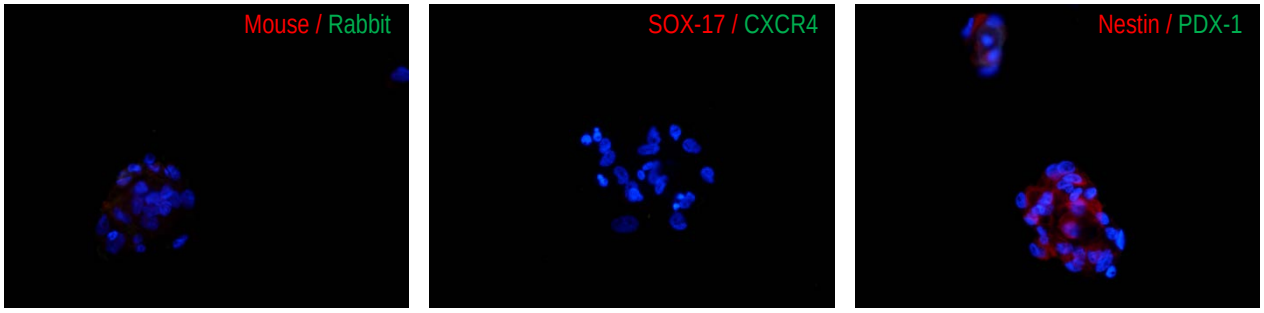


Figure 7.58 Phenotyping of ASCs cultured for 4 days in Chandra's SFM-A + long-mix medium in ultra-low attachment plates for markers of definitive endoderm.

ASCs were cultured for 4 days in Chandra's SFM-A + long-mix medium in ultra-low attachment plates, and phenotyped for expression of definitive endoderm, stem cell and posterior foregut markers. Immunoreactivity was detected with donkey anti-mouse (red) and donkey anti-rabbit (green) antibodies. Cell nuclei were stained blue with DAPI. Images were taken at 400x magnification. The images are presented so that the staining obtained with each IgG control immediately precedes stainings with antibodies of the same host species.

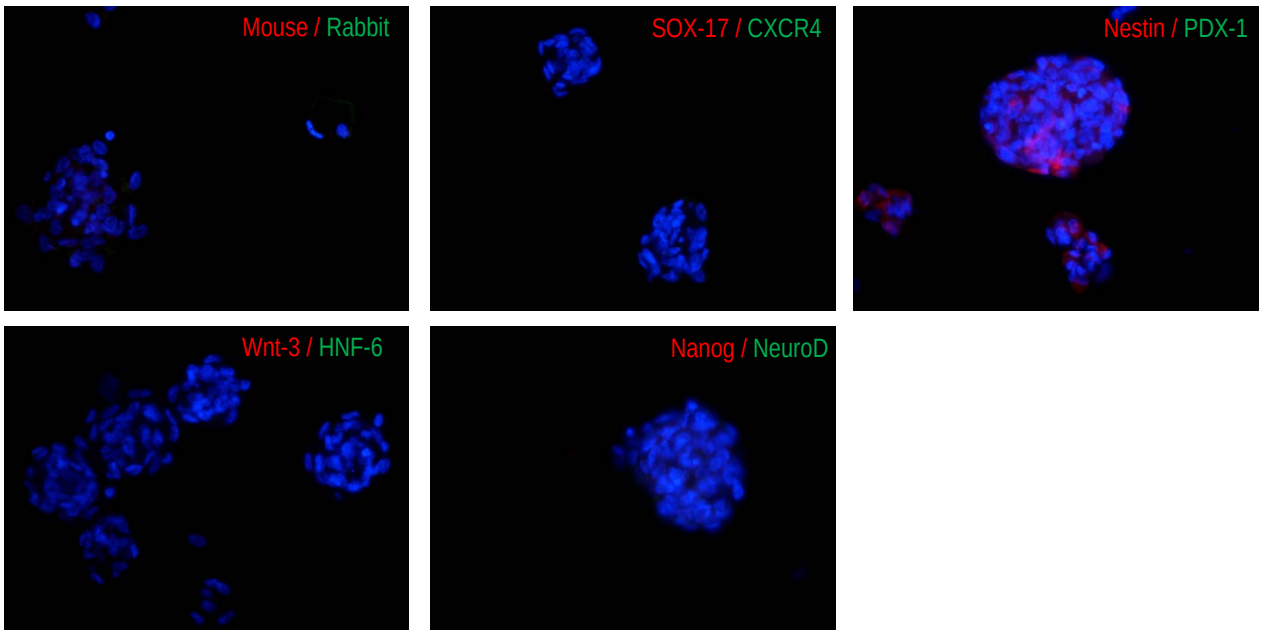


Figure 7.59 Phenotyping of ASCs cultured for 4 days in D'Amour's medium in ultra-low attachment plates for markers of definitive endoderm.

ASCs were cultured for 4 days in D'Amour's medium in ultra-low attachment plates, and phenotyped for expression of definitive endoderm, stem cell and posterior foregut markers. Immunoreactivity was detected with donkey anti-mouse (red) and donkey anti-rabbit (green) antibodies. Cell nuclei were stained blue with DAPI. Images were taken at 400x magnification. The images are presented so that the staining obtained with each IgG control immediately precedes stainings with antibodies of the same host species.

Table 7.8 Summary of expression by ASCs of markers of definitive endoderm after 2-4 days of differentiation with Chandra and D'Amour's media

	2 days		4 days			
	SFM-A	SFM-A + mix	SFM-A then SFM-B	SFM-A + mix then SFM-B + mix	SFM-A + long-mix	D'Amour
SOX-17						
CXCR4						
Nestin			x x x	x x x	x x x	x x x
PDX-1						
Wnt-3						
HNF-6						
Nanog						
NeuroD						

0	0.1-20	21-40	41-60	61-80	81-100	% Positive

x	x x	x x x	Intensity of staining - weak/moderate/strong

7.9 Discussion

7.9.1 Phenotype of ASCs

The ASCs from Invitrogen™ were adult stem cells as they express the mesenchymal and adipose stem cell markers CD90 and CD29. They weakly expressed SOX-17 which is expressed by cells differentiating along the pancreatic lineage from the definitive endoderm stage (D'Amour *et al.* 2006). However, other studies reported that undifferentiated ASCs do not express SOX-17 (Lee *et al.* 2008; Chandra *et al.* 2009). Undifferentiated human amnion-derived fibroblast-like cells express SOX-17 (Tamagawa *et al.* 2009), in accord with the fact that SOX-17 is not a specific marker of pancreatic differentiation, but rather is expressed by many different cell types including cells of the heart, lung, spleen, ovary, placenta, foetal lung, kidney, and gastrointestinal tract (Katoh 2002). SOX-17 is also expressed by blood vessels and positively regulates both tumour angiogenesis and haemogenic endothelial development (Clarke *et al.* 2013; Yang *et al.* 2013). Therefore, SOX-17 expression alone without additional lineage-specific markers does not provide enough evidence to define a particular the cell type, given that it is expressed by so many different cell types. SOX-17 may be naturally expressed by the purchased population of undifferentiated stem cells, or it may become expressed *de novo* after differentiation of the cells in expansion medium.

ASCs are reported to be able to differentiate along the adipogenic, osteogenic, myogenic, and chondrogenic pathways (Zuk *et al.* 2002; Locke *et al.* 2011). As expected, the ASCs in this study differentiated to become adipocytes when cultured with StemPro® Adipogenesis Differentiation medium, producing cells that contained large lipid vesicles. They did not spontaneously differentiate into adipocytes when cultured in expansion medium.

Only ~6% of the ASCs expressed aldehyde dehydrogenase activity ($ALDH^+$) at passage 3 (P3), and this proportion did not decrease up to P10. The earliest passage number analysed was P3 as cell stocks were at P2. In contrast, Mitchell *et al.* (2006) reported that >70% of ASCs were $ALDH^+$ at P4, but this proportion decreased to 10% by P9. The only difference between the expansion media used in the two studies was the inclusion of bFGF in the present study as bFGF was reported to enhance the proliferation of ASCs (Timper *et al.* 2006; Chandra *et al.* 2011). It is not known why so few of the ASCs our laboratory purchased were $ALDH^+$, but in accord they did not express stem cell-associated alkaline phosphatase. The low number of $ALDH^+$ cells provides further evidence they are a heterogenous population of cells.

Some expanded ASCs strongly expressed the stem cell marker Nestin for at least two weeks. Nestin positive ESCs can be differentiated into pancreatic cells (Yue *et al.* 2006), and Nestin is marker of pancreatic cell precursors within rodent ductal stem cells (Kim *et al.* 2010). However, Nestin is not necessarily a maker for pancreatic development as it is also expressed by cells capable of differentiating along the neuronal lineage (Lumelsky *et al.* 2001). The fact that the ASCs expressed Nestin is only a potential indicator that they are a source of pancreatic progenitors that might have the potential to differentiate towards the

pancreatic lineage. As expected, the ASCs did not spontaneously differentiate into mature β-cells in expansion medium as they did not express other pancreatic markers including insulin, amylin and C-peptide.

7.9.2 Differentiation of attached ASCs

7.9.2.1 Chandra's protocol

Chandra's protocol was originally designed to be performed in ultra-low attachment plates (Chandra *et al.* 2011), but was initially employed here using conventional tissue culture plates to investigate the potential of attached ASCs to undergo differentiation towards the pancreatic lineage. The differentiated cells no longer expressed Nestin from as early as day three indicating they had lost their stem-ness and had begun to differentiate. Like the ASCs here, bone marrow stem cells quickly lose their expression of Nestin after culture in a pancreatic differentiation medium (Milanesi *et al.* 2011). The expression of Glut-2 was induced after three days, and maintained for two weeks of culture, but the results were equivocable due to the high level of background staining of the control antibody. A key outcome was the expression of insulin after one week of culture, but again the results were confounded by the background staining of the control antibody. Of note, the presence of insulin was detected with the guinea pig anti-insulin antibody, but not with a mouse anti-insulin antibody. Further, the expression of C-peptide was not detected. C-peptide is a by-product released during insulin processing and is therefore commonly used to measure insulin secretion and prove the insulin is genuine and not taken up from the media (Hansson *et al.* 2004). Therefore the lack of C-peptide detected casts doubt over whether the insulin expression seen in these conditions is genuine. In contrast, Chandra *et al.* (2011) reported that ASCs differentiated by culture in ultra-low attachment plates differentiate into cells expressing insulin and C-peptide. These conflicting results suggest culturing ASCs in suspension may be required to enhance their ability to mature into insulin expressing β-cells.

7.9.2.2 Timper's protocol with IGF-2

Timper's protocol was developed using ultra-low attachment plates, but was initially trialled here using conventional tissue culture plates as a low cost option. IGF-2 was included as a supplement as it was reported to enhance the differentiation of ASCs towards the pancreatic lineage (Kang *et al.* 2011). Culture of the ASCs in Timper's medium with IGF-2 instead of pentagastrin for three days resulted in a loss of the stem cell marker Nestin confirming that differentiation had been induced. The cells showed signs of pancreatic differentiation as they expressed SOX-17, Glut-2, and amylin albeit the results were again potentially confounded by the high level of background staining of the control antibodies. In the mouse, amylin is expressed on its own or co-expressed with proglucagon or proinsulin during early pancreatic development, and then later co-expressed with insulin by matured β-cells (Wilson *et al.* 2002). The fact that the differentiated ASCs did not express either glucagon or insulin indicated they had not matured. In contrast, Timper *et al.* (2006) reported their differentiated ASCs expressed C-peptide and PDX-1 protein, along with insulin, glucagon and somatostatin mRNA. Therefore additional factors such as pentagastrin, and potentially the use of ultra-low attachment plates are required for β-cell maturation.

7.9.2.3 Stage-specific differentiation of ASCs

7.9.2.3.1 Stage 1 – formation of definitive endoderm

All the agents used here to induce the formation of definitive endoderm failed to downregulate the expression of Nestin indicating the cells retained their precursor phenotype. Differentiation of ASCs with 100 nM IDE-1, activin A and Wnt3a followed by activin A alone, and activin A and Wnt3a led to the upregulation of SOX-17 suggesting the formation of definitive endoderm. These findings are in agreement with the induced definitive endoderm differentiation seen with these factors in ESCs by other research groups (D'Amour *et al.* 2006; Borowiak *et al.* 2009).

However, in contrast to the finding with ESCs by Borowiak *et al.* (2009), SOX-17 was not expressed when the concentration of IDE-1 was increased to 400 nM indicating that lower concentrations of IDE-1 are required to produce definitive endoderm in ASCs. However, as mentioned above SOX-17 is also expressed by other cell types including those of the heart, lung, spleen, ovary, placenta, foetal lung, kidney, and gastrointestinal tract (Katoh 2002).

Further proof these cells were differentiating towards the pancreatic lineage with activin A and Wnt3a followed by activin A alone, and activin A and Wnt3a came from expression of the posterior foregut markers PDX-1 and HNF6 (D'Amour *et al.* 2006), being localized to the nucleus. PDX-1 is known to be synthesized in the cytoplasm and then translocated to the nucleus, where it increases insulin gene expression (Kishi *et al.* 2003).

The primitive gut tube marker HNF4a (D'Amour *et al.* 2006) was weakly expressed in response to differentiation with the combination of activin A and Wnt3a followed by activin A alone, and with activin A and Wnt3a. The weak expression of HNF4a may represent the early stages of differentiation into formation of the primitive gut tube when the marker is first upregulated.

The remaining definitive endoderm markers tested, namely FOXA2 and CXCR4, were not expressed suggesting additional reagents may be required to induce the formation of proper definitive endoderm. Nevertheless, the expression of SOX-17, FOXA2 and/or CXCR4 were observed in ESCs differentiating into definitive endoderm with these factors (D'Amour *et al.* 2006; Borowiak *et al.* 2009). Therefore there are differences in the way ASCs and ESCs respond to the definitive endoderm differentiation factors trialled here.

7.9.2.3.2 Stage 2 – formation of primitive gut tube

The weak expression of SOX-17 by the differentiating ASCs indicated they were entering the pancreatic pathway (at least weakly). It is also important to note that immunocytochemistry only gives an indication of expression and is not a tool to measure expression levels. Also, there could be additional pancreatic markers expressed by these newly differentiating cells which were

not screened for in these experiments which would further confirm their pancreatic progenitor status. Therefore attempts were made to further induce their pancreatic differentiation.

Nestin was not downregulated during the formation of primitive gut tube indicating the differentiated cells retained their stem-like qualities. In support, the expression of SOX-17 was either maintained or weakly induced. SOX-17 was most strongly expressed following induction of definitive endoderm with 400 nM IDE-1, and induction of primitive gut tube with KAAD-cyclopamine and FGF10. Nevertheless, only a few cells showed moderate expression of SOX-17, with the majority showing only weak expression. SOX-17 expression is known to vary throughout the pancreatic differentiation of embryonic stem cells (D'Amour *et al.* 2006), and is therefore not a good indicator of the stages of pancreatic differentiation.

KAAD-cyclopamine is a sonic hedgehog inhibitor which promotes primitive gut tube and posterior foregut differentiation of iPSCs and ESCs (D'Amour *et al.* 2006; Maehr *et al.* 2009). The addition of FGF10 at this stage is to mimic that normally seen *in vivo* during pancreatic development where FGF10 is produced by the pancreatic mesenchyme (Bhushan *et al.* 2001). In the present study culturing the ASCs with 100 nM IDE-1 to induce definitive endoderm followed by KAAD-cyclopamine and FGF10 induced the expression of the primitive gut tube marker HNF4a. This is in accord with the result obtained by D'Amour *et al.* (2006) where ESCs treated with KAAD-cyclopamine and FGF10 showed upregulation of HNF4a. D'Amour *et al.* (2006) also reported a decrease in CXCR4 and maintenance of SOX-17 expression. Therefore like ESC pancreatic differentiation (D'Amour *et al.* 2006), the expression of CXCR4 is not expected during formation of the primitive gut tube.

In this present study the expression of PDX-1 was upregulated or maintained in all culture conditions tested except for culture in activin A and Wnt3a, followed by the KAAD-cyclopamine and FGF10 ± BMP-2 combination. PDX-1 was most strongly expressed after culture with 100 nM IDE-1, followed by KAAD-cyclopamine and FGF10 with BMP-2, indicating BMP-2 is beneficial for ASC differentiation in this combination. In accord, mouse embryoid bodies cultured with BMP-2 undergo pancreatic differentiation as seen by the upregulation of PDX-1, Nkx6.1, insulin, and amylin (Talavera-Adame *et al.* 2011). Mouse studies have shown the presence of PDX-1 is required for the development of the pancreas (Jonsson *et al.* 1994), and PDX-1 positive cells develop into all the cell types of the pancreas, including β-cells (Gu *et al.* 2003).

The other posterior foregut marker HNF6 was weakly detected following culture with 100 nM IDE-1 followed by KAAD-cyclopamine, FGF10 and BMP-2, and 400 nM IDE-1 followed by KAAD-cyclopamine, FGF10 ± BMP-2. In agreement the D'amour *et al.* (2006) study also reported a low level of expression of HNF6 mRNA by ESCs following their differentiation to primitive gut tube cells.

The expression of HNF4a, PDX-1, and SOX-17 by ASCs treated with 100 nM IDE-1 followed by KAAD-cyclopamine and FGF10, and the expression of PDX-1, SOX-17, and HNF6 by ASCs treated with 100 nM IDE-1 followed by KAAD-cyclopamine, FGF10

and BMP-2, and 400 nM IDE-1 followed by KAAD-cyclopamine, FGF10 ± BMP-2 is promising for lineage transdifferentiation of ASCs into pancreatic cells.

7.9.2.3.3 Stage 3 – formation of posterior foregut

The upregulation of pancreatic markers on ASCs during the induction of definitive endoderm and primitive gut tube indicated that the ASCs were showing the potential to be differentiated towards the pancreatic lineage. However, they still continued to strongly express Nestin even after the differentiation towards posterior foregut, indicating they were still stem-like.

Retinoic acid is a positive regulator of PDX-1 expression by both mouse and human ESCs (Micallef *et al.* 2005; D'Amour *et al.* 2006). After treatment with IDE-1, followed by the combination of KAAD-cyclopamine, FGF10 ± BMP2, followed by all trans-retinoic acid, KAAD-cyclopamine, FGF10 ± BMP2 promoted the expression of the posterior foregut markers PDX-1 and HNF6 in ASCs. ESCs cultured with this combination also express PDX-1 and HNF6, but in contrast, they also expressed HNF4a (D'Amour *et al.* 2006). A higher concentration of IDE-1, followed by the combination of KAAD-cyclopamine and FGF10, followed by all trans-retinoic acid, KAAD-cyclopamine and FGF10 resulted in cells that also expressed the primitive gut tube marker HNF4a, whereas SOX-17 was not detectable in agreement with continued maturation.

HNF4a was the only pancreatic marker expressed after culture of cells with activin A and Wnt3a followed by activin A alone, followed by combinations of KAAD-cyclopamine, FGF10 and all trans-retinoic acid indicating that this particular protocol developed by D'Amour *et al.* (2006) was not effective in inducing and maintaining the formation of the posterior foregut. At this stage ESCs are induced to express PDX-1, upregulate the expression of HNF-6, and maintain the expression of HNF4a (D'Amour *et al.* 2006). Including BMP-2 with this combination allowed for the maintenance of SOX-17 and PDX-1, but not HNF6, indicating further factors are required for progressive differentiation.

The induction of formation of posterior foregut with activin A and Wnt3a followed by combinations of KAAD-cyclopamine, FGF10 and all trans-retinoic acid did not result in the expression of HNF6. However, the differentiated ASCs did express PDX-1, SOX-17, and HNF4a. Inclusion of BMP-2 only resulted in the cells expressing HNF4a indicating that the inclusion of BMP-2 was not beneficial for pancreatic differentiation in this combination.

Immunocytochemistry showed that most of the culture conditions used to induce formation of posterior foregut produced cells that expressed PDX-1. Western blot analysis was used to quantify the level of expression of PDX-1, and revealed that the various culture conditions induced a similar level of PDX-1 expression after combinations of media. The protocol that was consistently the most effective at upregulating PDX-1 expression was 100 nM IDE-1, followed by KAAD-cyclopamine and FGF10, and then KAAD-cyclopamine, FGF10 and all trans-retinoic acid. This is in agreement with the finding by Borowiak *et al.* (2009) who reported a higher incidence of PDX-1 expressing cells when differentiating IDE-1 treated ESCs with the combination of all trans-retinoic acid, KAAD-cyclopamine and FGF10, compared with activin A-treated ESCs.

7.9.2.4 Differentiation of ALDH$^+$ and ALDH$^-$ ASCs

Both ALDH$^+$ and ALDH$^-$ populations of ASCs expressed Nestin, suggesting they might both have the potential to be differentiated to insulin-producing cells, as seen with ESCs (Yue *et al.* 2006). Like ASCs, ALDH$^+$ cells isolated from centroacinar/terminal ductal cells in an adult mouse pancreas express Nestin and form spheres when cultured in ultra-low attachment plates (Rovira *et al.* 2010). These mouse ALDH$^+$ cells also have the ability to spontaneously differentiate into endocrine cells which express insulin and C-peptide (Rovira *et al.* 2010). The ALDH$^+$ or ALDH$^-$ ASCs in this present study did not express SOX-17 or HNF4a when treated with IDE-2 to induce definitive endoderm differentiation. In contrast, ESCs treated with IDE-2 express SOX-17 (Borowiak *et al.* 2009). ASCs differentiated with KAAD-cyclopamine, FGF10 and BMP-2 to induce primitive gut tube differentiation did not express SOX-17 or HNF4a. Thus, additional programming is required. Western blot analysis revealed unfractionated ASC populations cultured with IDE-2 to induce definitive endoderm, followed by primitive gut tube and posterior foregut differentiation media were capable of differentiating into PDX-1-expressing cells. A previous report showed that ESCs upregulate PDX-1 in response to these agents (Borowiak *et al.* 2009). Here the ALDH-sorted ASCs cultured in differentiation media were only differentiated up to the primitive gut tube stage and therefore PDX-1 expression was not analysed.

7.9.3 Differentiation of ASCs in suspension

7.9.3.1 Chandra's protocol

ASCs cultured in Chandra's media on ultra-low attachment or hydrophobic plates formed tight clusters, similar to those reported by Chandra *et al.* (2011). The cell seeding density (2 x 10^5/cm^2) that best mimicked the appearance of these clusters was 5x less than the reported optimal seeding density of 1 x 10^6/cm^2 noted in Chandra's 2009 and 2011 publications (Chandra *et al.* 2009; Chandra *et al.* 2011). A volume of 2 ml of cells at a density of 4.8 x 10^6 cells/mL would need to have been plated to achieve the seeding density used by Chandra, given that 6-well plates were used here having a growth area of 9.5 cm^2. In our laboratory, higher seeding densities resulted in the formation of a single giant cell cluster (data not shown). Personal correspondence with Dr Vikash Chandra (National Centre for Cell Science, Ganeshkhind, Pune, India) resulted in a recommendation to pipette these large clusters to help break them up. However, in practice it was found that the giant clusters quickly reformed. Therefore in order to form clusters suitable for analysis the lower cell seeding density was used for these experiments. The phenotype of the ASCs revealed they no longer expressed Nestin after culture for two weeks indicating they were no longer stem-like. The clusters varied in insulin expression from weak to very strong, as detected by the guinea pig anti-insulin antibody; however this expression could not be confirmed with the mouse and chicken anti-insulin antibodies. Further, expression of proinsulin, C-peptide, and amylin was not detected. It is plausible that insulin expression may reflect uptake of insulin from the medium which is supplemented with insulin/transferrin/selenium. In agreement previous studies of insulin expression with ESCs have been proven not to be genuine as the ESCs lacked other pancreatic proteins such as C-peptide, PDX-1, and glucagon, or mRNA encoding these proteins (Hansson *et al.* 2004). Alternatively, the guinea pig anti-insulin antibody in this study is binding to a homologous region of an insulin-related protein. In contrast Chandra *et al.* (2011) reported that ASCs cultured for two weeks in

Chandra's media expressed insulin, C-peptide, PDX-1, Glut-2, and somatostatin. The variation in the results between the two laboratories may reflect ASC donor population differences, differences in cell techniques, or that the differentiation protocol is not reproducible. Correspondence between Dr Vikash Chandra (National Centre for Cell Science, Ganeshkhind, Pune, India) was not fruitful, as Dr Chandra relayed that no additional steps were required to achieve β-cell differentiation.

7.9.3.2 Timper's protocol

Replication of the Timper protocol (Timper *et al.* 2006) did not result in pancreatic differentiation of ASCs. Here ASCs cultured for three days in Timper's medium did not express insulin, C-peptide, or amylin. There is only one medium required for the Timper protocol which contains DMEM/F12 (high glucose), nicotinamide, activin A, exendin-4, hepatocyte growth factor, and pentagastrin (Timper *et al.* 2006). This medium reportedly induces the pancreatic differentiation and maturation of ASCs in one step in just three days, resulting in C-peptide and somatostatin secretion, and the expression of mRNA for ISL-1, PDX-1, NGN3 insulin, glucagon, and somatostatin (Timper *et al.* 2006). In comparison, other protocols require about two weeks for differentiation in various differentiation media (D'Amour *et al.* 2006; Chandra *et al.* 2011; Kang *et al.* 2011). Longer protocols with stage-specific media might be expected to be more effective as they more closely mimic pancreatic differentiation.

7.9.3.3 Insulin authenticity

The absence of expression of pancreatic-related markers such as amylin and C-peptide following differentiation of ASCs with Chandra's protocol in conventional dishes or ultra-low attachment plates suggests that insulin detected was not synthesized by the cells or not authentic. A mouse anti-insulin antibody and a chicken anti-insulin antibody could not confirm the results obtained with the guinea-pig anti-insulin antibody, suggesting the insulin present was not authentic. A dot blot analysis to determine antibody specificity revealed that the guinea pig anti-insulin antibody binds to insulin and does not bind to the closely-related insulin homologue proteins insulin-like 3, IGF-1, or IGF-2. The manufacturer reports that the guinea pig anti-insulin antibody displays less than 0.01-0.05% cross-reactivity with glucagon. A colleague has used the batch of guinea pig anti-insulin antibody employed in this study on human pancreatic sections, and found strong immunoreactivity with insulin and no cross-reactivity with glucagon (unpublished, Shiva Reddy). Western blot experiments with the guinea pig anti-insulin antibody, which recognised recombinant human insulin, showed that ASCs cultured according to the Chandra protocol in ultra-low attachment plates did not express insulin. It is possible that very small amounts of insulin are taken up into the cells from the media, which are below the level of detection with this method. However, as the other two anti-insulin antibodies failed to detect the expressed insulin, it seems likely that the guinea pig antibody recognises insulin, but is cross-reacting with an undefined insulin-related protein. Cross-reactivity could occur with the sharing of just a single epitope of less than 15 amino acid residues (Frank 2002). The fact that the guinea-pig anti-insulin antibody is widely used by researchers studying diabetes is cause for concern.

7.9.3.4 Formation of definitive endoderm by ASCs cultured in suspension

ASCs cultured in ultra-low attachment plates did not express the definitive endoderm markers SOX-17 or CXCR4 during the first stages (day 2 and 4) of culture in Chandra's media, suggesting they had not begun to differentiate towards the pancreatic lineage. This is in contrast to the publication by Chandra *et al.* (2011) which reported that the ASCs expressed SOX-17 after 2 days of culture. Attempts to upregulate definitive endoderm and primitive gut tube markers with the assistance of BMP-2, IDE-1, IDE-2, FGF10 and ILV were also not successful. Therefore the combinations of agents used in this study are not recommended to induce the formation of definitive endoderm and primitive gut tube by ASCs cultured in ultra-low attachment plates. The protocol by D'Amour *et al.* (2006) was also not effective for promoting the pancreatic differentiation of ASCs cultured in ultra-low attachment plates as the cells maintained their stem-ness as judged by the continued expression of Nestin, and failed to express pancreatic markers.

7.9.4 Differentiation potential of ASCs towards pancreatic cell lineages

ASCs display potential for pancreatic differentiation into mature β-cells. Firstly they are Nestin positive, secondly they display aldehyde dehydrogenase activity, both of which are characteristic of stem cells, and thirdly they express the endoderm marker SOX-17. ESCs have previously been preselected based on their Nestin expression prior to pancreatic differentiation in order to increase the differentiation potential of the cell population (Yue *et al.* 2006). However, ASCs are not ESCs and express different markers including the adipose stem cell markers CD29 and CD90. The differentiation protocols trialled in this study showed that ASCs could be differentiated to express SOX-17, Glut-2, amylin, HNF4a, PDX-1, and HNF6. The most matured pancreatic-like cells in this study expressed PDX-1 and HNF6 when attached to conventional dishes, representing cells of the posterior foregut.

Chapter 8 Induced Pluripotent Stem Cells

8.1 Introduction

Human newborn fibroblasts (HNFs) were transformed into induced pluripotent stem cells (iPSCs) by treating them with the four stem cell transcription factors Oct-4, SOX-2, KLF4, and c-Myc that had been rendered cell-permeable by fusion to a polyarginine peptide (Kim *et al.* 2009). The stem cell transcription factors were produced by transfecting the cell line HEK293 with a plasmid encoding each factor (Kim *et al.* 2009). HNFs were treated with protein extracts of the transfectants (Kim *et al.* 2009). The cell permeable transcription factors were taken up into the nucleus and cytoplasm of cells within 8 hours (Kim *et al.* 2009). For the first 6 weeks the HNFs were treated once a week with the whole cell protein extracts of the transcription factor transfectants in DMEM medium containing L-glutamine, β-mercaptoethanol, NEAA, FBS, PSG, and LIF (ES media 1) (Kim *et al.* 2009). For the 7th week of treatment the HNFs were transferred onto mouse embryonic fibroblast (MEF) feeder cells with 1 part ES media 1 to 3 parts ES media 3 (ES media 3: DMEM containing L-glutamine, β-mercaptoethanol, NEAA, knock-out serum replacement, and PSG) (Kim *et al.* 2009). For the final week of treatment the cells were cultured on MEFs with ES media 3 alone (Kim *et al.* 2009). The iPSCs expressed alkaline phosphatise, and readily differentiated into all 3 germ layers when cultured either in suspension where they form EBs or on gelatin-coated plates (Kim *et al.* 2009).

8.2 Scope of chapter

In this chapter attempts were made to produce the four iPSC-inducing transcription factor proteins Oct-4, c-Myc, KLF4, and SOX-2 for subsequent iPSC generation. Initially, two cell lines were trialled for their transfection efficiency and ability to produce the transcription factors. Transfection of the selected cell line was then optimized for each of the four plasmids encoding the four transfection factors.

8.3 Selection of a cell line for producing stem cell transcription factors

The two cell lines 266-6 and CHO-K1 were tested for their ability to be transfected to produce the pluripotent stem cell inducing factors. The 266-6 cell line is a pancreatic acinar tumour cell line, and the CHO-K1 cell line is an ovarian cancer cell line. CHO-K1 cell line is highly transfectable with both Lipofectamine LTX (Invitrogen™) and magnetic systems such as Polymag (OZ Biosciences) (Scherer *et al.* 2002; Sato *et al.* 2007). The 266-6 cell line is also transfectable (http://atcc.org/Products/All/CRL-2151.aspx, ATCC®). Both cell lines were transfected with 3 μg of an Oct-4 plasmid for 3 h using the Lipofectamine LTX transfection reagent system. The transfection medium was then replaced with the respective cell culture media, and the cells cultured for 2 days. The cells were stained for Oct-4 expression with an anti-Oct-4 antibody, revealing that CHO-K1 cells were more efficiently transfected with Lipofectamine LTX to produce Oct-4 than were 266-6 cells (n=3) (Figure 8.1).

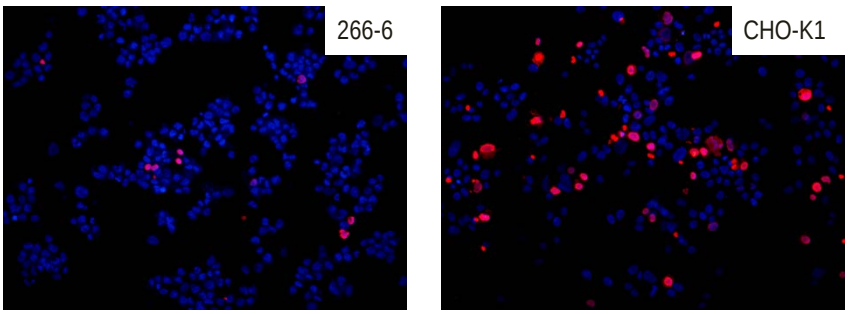


Figure 8.1 CHO-K1 cells are more efficiently transfected with Lipofectamine LTX to produce Oct-4 than are 266-6 cells.

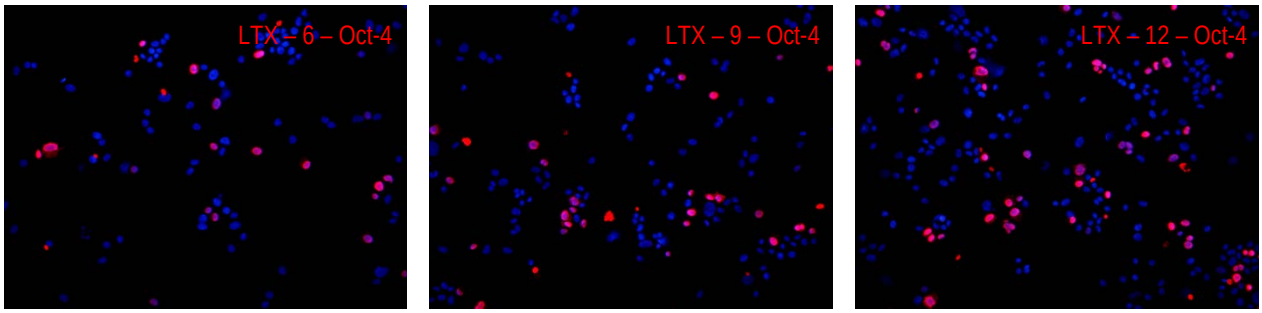
CHO-K1 and 266-6 cells were each transfected for 3 h with 3 μg of an Oct-4 plasmid using the Lipofectamine LTX transfection reagent. The transfection medium was removed and the cells cultured for 2 days. The cells were immunostained with a mouse anti-Oct-4 antibody. Immunoreactivity was detected with a donkey anti-mouse antibody (red). Cell nuclei were stained blue with DAPI. Images were taken at 200x magnification.

8.4 Optimization of transfection of CHO-K1 cells

The Lipofectamine LTX and Polymag transfection reagents were compared for their ability to transfect CHO-K1 cells to express Oct-4.

8.4.1 Oct-4

The transfection protocol was optimized for Lipofectamine LTX-mediated transfection by increasing the volume of transfection agent used while at the same time keeping the amount (3 μg) of Oct-4 plasmid constant. The protocol was relatively insensitive to the volume of transfection agent used as increasing the volume of transfection agent from 6 to 15 μL had no marked effect on the numbers of transfectants expressing Oct-4, with approximately 35% of CHO-K1 cells expressing this antigen (n=1) (Figure 8.2). Approximately 10% or less CHO-K1 cells were transfected to express Oct-4 by using the Polymag transfection reagent, with the lowest volume (3 μL) of reagent used producing the highest level of transfection (n=1) (Figure 8.3). In summary, in comparison the Lipofectamine LTX transfection reagent gave a higher efficiency of transfection than did the Polymag reagent (Figure 8.2 and Figure 8.3).



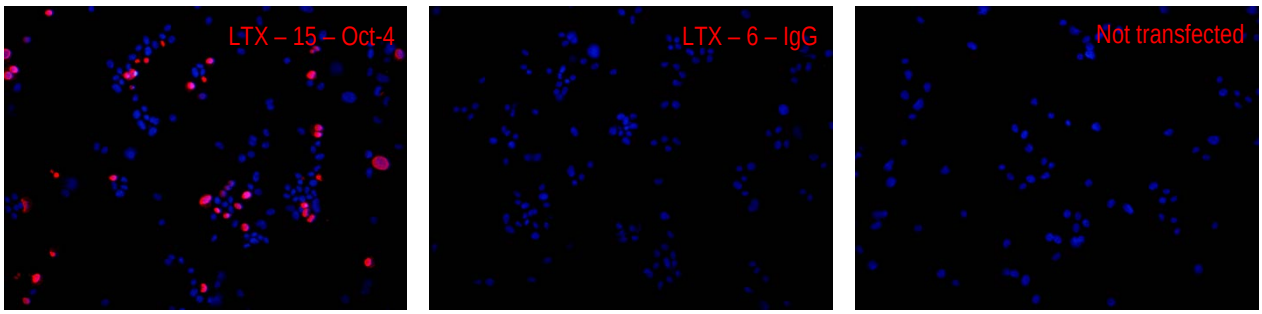


Figure 8.2 Transfection of CHO-K1 cells with an Oct-4 plasmid using Lipofectamine LTX.

CHO-K1 cells were transfected for 3 h with 3 μg of an Oct-4 plasmid using increasing volumes (6, 9, 12, and 15 μL) of the Lipofectamine LTX transfection reagent in OPTI-MEM medium. The cells were then cultured in tissue culture medium for 2 days. They were immunostained for Oct-4 expression where immunoreactivity was detected with a donkey anti-mouse (red) antibody. Cell nuclei were stained blue with DAPI. LTX: Lipofectamine LTX, Oct-4: stained with an anti-Oct-4 antibody; IgG: stained with a mouse IgG control antibody, Not transfected: cells immunostained with Oct-4 to show that non-transfected CHO-K1 do not express Oct-4. Images were taken at 200x magnification.

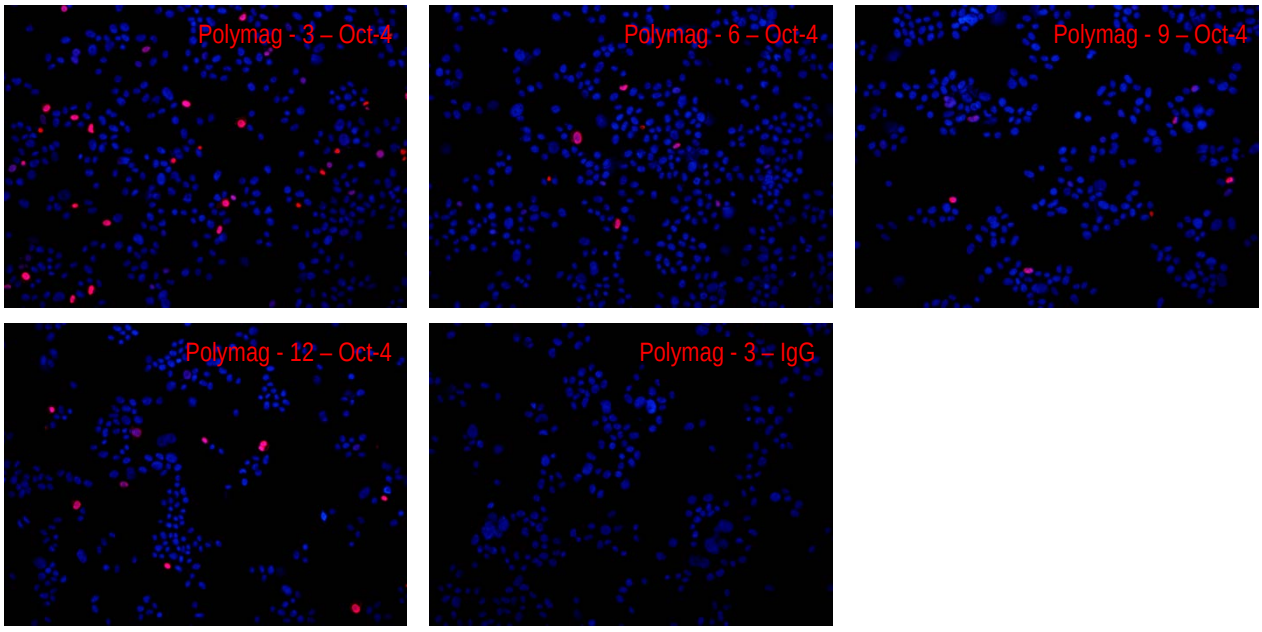


Figure 8.3 Transfection of CHO-K1 cells with an Oct-4 plasmid using Polymag.

CHO-K1 cells were transfected for 3 h with 3 μg of an Oct-4 plasmid using increasing volumes (3, 6, 9, 12 μL) of the Polymag transfection reagent in OPTI-MEM medium. The cells were then cultured in tissue culture medium for 2 days. They were immunostained for Oct-4 expression with immunoreactivity detected with a donkey anti-mouse (red) antibody. Cell nuclei were stained blue with DAPI. Polymag: Polymag transfection reagent, Oct-4: stained with an anti-Oct-4 antibody; IgG: stained with a mouse IgG control antibody. Images were taken at 200x magnification.

Western blot analysis was used to compare the amount of Oct-4 expressed in response to the varying volumes of transfection reagent employed (n=1) (Figure 8.4). Cells were harvested 2 days following transfection and the proteins extracted in protein

extraction buffer. The protein extracts were resolved by SDS-PAGE, transferred onto nitrocellulose, and Western blotted with an anti-Oct-4 antibody. The western blot revealed a band at 44 kDa which is the expected size for Oct-4 (Figure 8.4). Quantification of the Oct-4 bands by densitometry and normalization compared with β-actin indicated that 6 μL was the optimal volume of LTX required for transfection of the Oct-4 plasmid into CHO-K1 cells (Figure 8.5). Increasing the amount of LTX used decreased the transfection efficiency (Figure 8.5). Western blot analysis of lysates of the Polymag transfected CHO-K1 cells showed that 3 μL of Polymag resulted in expression of Oct-4, whereas expression of Oct-4 could not be detected when using increased volumes of Polymag (Figure 8.6).

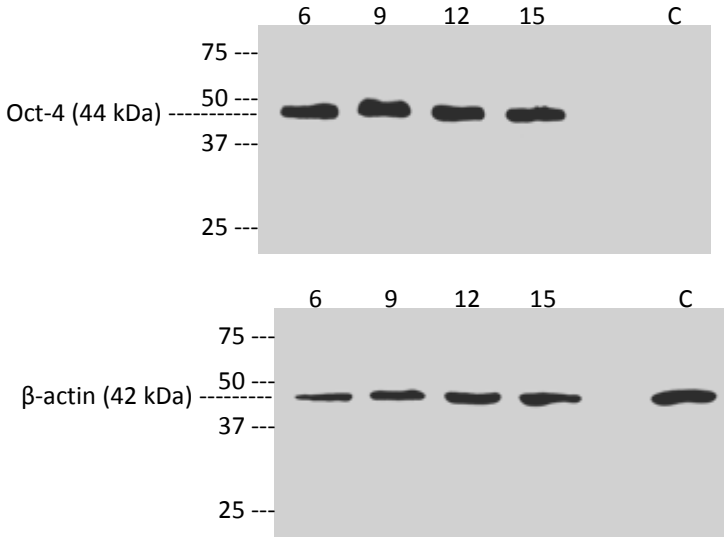


Figure 8.4 Western blot analysis of CHO-K1 cells transfected to express Oct-4 using Lipofectamine LTX.

CHO-K1 cells were transfected for 3 h with 3 μg of Oct-4 plasmid mixed with increasing volumes (6 to 15 μL) of Lipofectamine LTX in OPTI-MEM medium. The cells were then cultured in full medium for an additional 2 days prior to protein extraction, and Western blot analysis. Upper blot: protein extracts of CHO-K1 cells transfected with the Oct-4 plasmid using varying amounts of LTX (6-15 μL), and control cells (C) which were not transfected were Western blotted with an antibody against Oct-4, and immunoreactivity detected with a goat anti-mouse HRP-conjugated antibody. The position of Oct-4 at 44 kDa is indicated in the left-hand margin. Lower blot: The blot was stripped and reprobed with an antibody against human β-actin, with immunoreactivity detected with a donkey anti-rabbit HRP-conjugated antibody. The position of β-actin at 42 kDa is indicated in the left-hand margin.

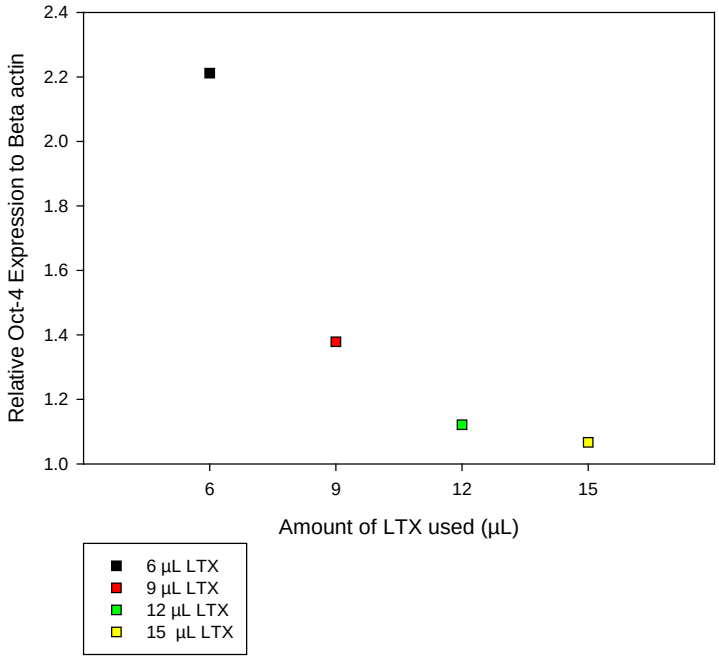


Figure 8.5 Quantification of Oct-4 expression by transfectants.

The densities of the Oct-4 bands relative to the β-actin bands in the Western blot in Figure 8.4 were determined with Image J. The analysis revealed that 6 µL of LTX gave optimal transfection efficiency.

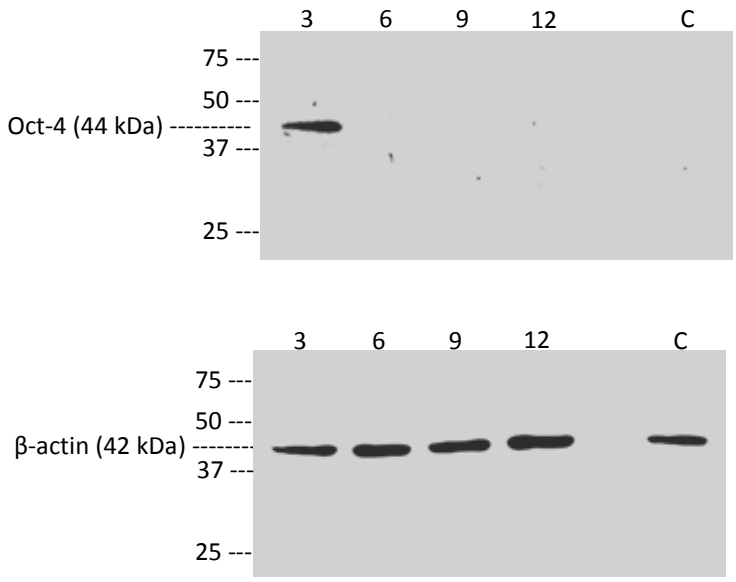


Figure 8.6 Western blot analysis of CHO-K1 cells transfected to express Oct-4 using Polymag.

CHO-K1 cells were transfected for 3 h with 3 μg of Oct-4 plasmid using the Polymag transfection reagent in OPTI-MEM medium. The cells were then cultured in full medium for an additional 2 days prior to protein extraction, and Western blot analysis. Upper blot: protein extracts of CHO-K1 cells transfected with the Oct-4 plasmid using varying amounts of Polymag (3-12 μL), and control cells (C) which were not transfected were Western blotted with an antibody against Oct-4, and immunoreactivity detected with a goat anti-mouse HRP-conjugated antibody. The position of Oct-4 at 44 kDa is indicated in the left-hand margin. Lower blot: The blot was reprobed with an antibody against human β-actin, with immunoreactivity detected with a donkey anti-rabbit HRP-conjugated antibody. The position of β-actin at 42 kDa is indicated in the left-hand margin.

8.4.2 c-Myc

Western blot analysis confirmed that the c-Myc protein at 41 kDa was expressed by the CHO-K1 cells following transfection with the c-Myc plasmid using any of the four volumes of LTX trialled (n=1) (Figure 8.7). Quantification of the c-Myc bands by densitometry and normalization compared with β-actin indicated that 15 μL of LTX was optimal for transfection of the c-Myc plasmid (Figure 8.8).



Figure 8.7 Western blot analysis of CHO-K1 cells transfected to express c-Myc using Lipofectamine LTX.

CHO-K1 cells were transfected for 3 h with 3 μg of c-Myc plasmid mixed with increasing volumes (6 to 15 μL) of Lipofectamine LTX in OPTI-MEM medium. The cells were then cultured in full medium for an additional 2 days prior to protein extraction, and Western blot analysis. Left blot: protein extracts of CHO-K1 cells transfected with the c-Myc plasmid using varying amounts of LTX (6-15 μL) were Western blotted with an antibody against c-Myc, and immunoreactivity detected with a goat anti-mouse HRP-conjugated antibody. The position of Oct-4 at 44 kDa is indicated in the left-hand margin. Right blot: The blot was stripped and reprobed with an antibody against human β-actin, with immunoreactivity detected with a donkey anti-rabbit HRP-conjugated antibody. The position of β-actin at 42 kDa is indicated in the left-hand margin.

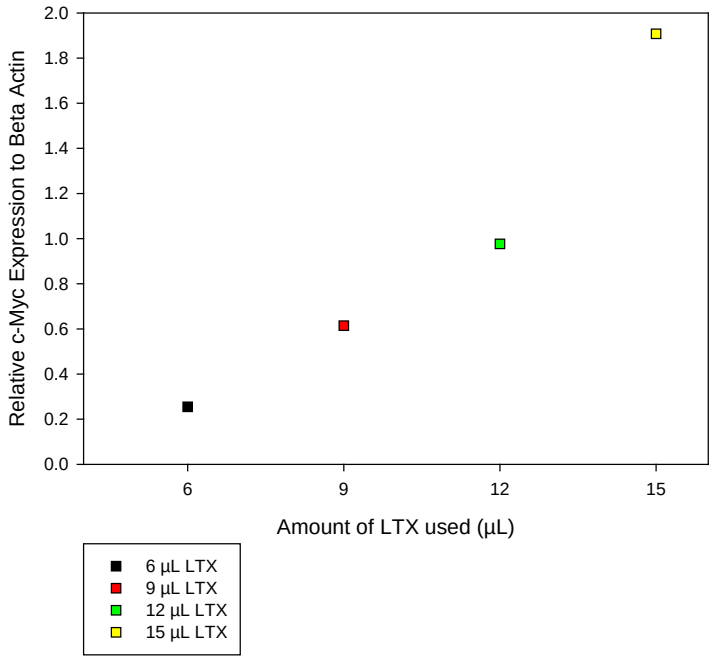


Figure 8.8 Quantification of c-Myc expression by transfectants.

The densities of the c-Myc bands relative to the β-actin bands in the Western blot in Figure 8.7 were determined with Image J. The analysis revealed that 15 μL of LTX gave optimal transfection efficiency.

8.4.3 KLF4

Western blot analysis confirmed that the KLF4 protein at ~65 kDa was expressed by CHO-K1 cells following transfection with the KLF4 plasmid using any of the four volumes of LTX (n=1) (Figure 8.9). The size of the KLF4 protein at 65 kDa is in agreement with the published size (Piccinni *et al.* 2004; Kim *et al.* 2009) (Figure 8.9). The apparently non-specific bands that migrate below the main KLF4 band are likely due to proteolytic degradation of KLF4 (Figure 8.9). Quantification of KLF4 expression by densitometry and normalization compared with β-actin indicated that 9 μL of LTX was optimal for KLF4 plasmid transfection (Figure 8.10).

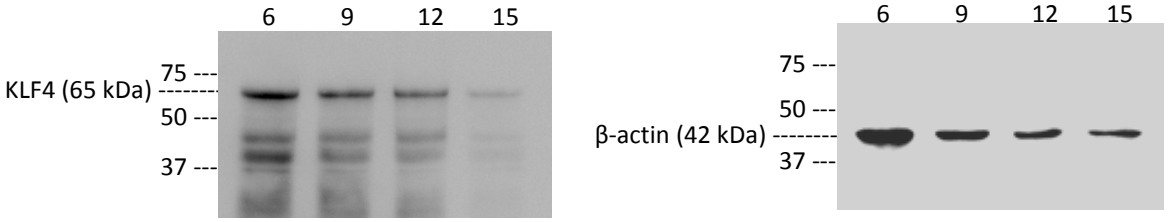


Figure 8.9 Western blot analysis of CHO-K1 cells transfected to express KLF4 using Lipofectamine LTX.

CHO-K1 cells were transfected for 3 h with 3 μg of KLF4 plasmid mixed with increasing volumes (6 to 15 μL) of Lipofectamine LTX in OPTI-MEM medium. The cells were then cultured in full medium for an additional 2 days prior to protein extraction, and Western blot analysis. Left blot: protein extracts of CHO-K1 cells transfected with the KLF4 plasmid using varying amounts of LTX (6-15 μL) were Western blotted with an antibody against KLF4, and immunoreactivity detected with a goat anti-mouse HRP-conjugated antibody. The position of KLF4 at 65 kDa is indicated in the left-hand margin. Right blot: The blot was stripped and reprobed with an antibody against human β-actin, with immunoreactivity detected with a donkey anti-rabbit HRP-conjugated antibody. The position of β-actin at 42 kDa is indicated in the left-hand margin.

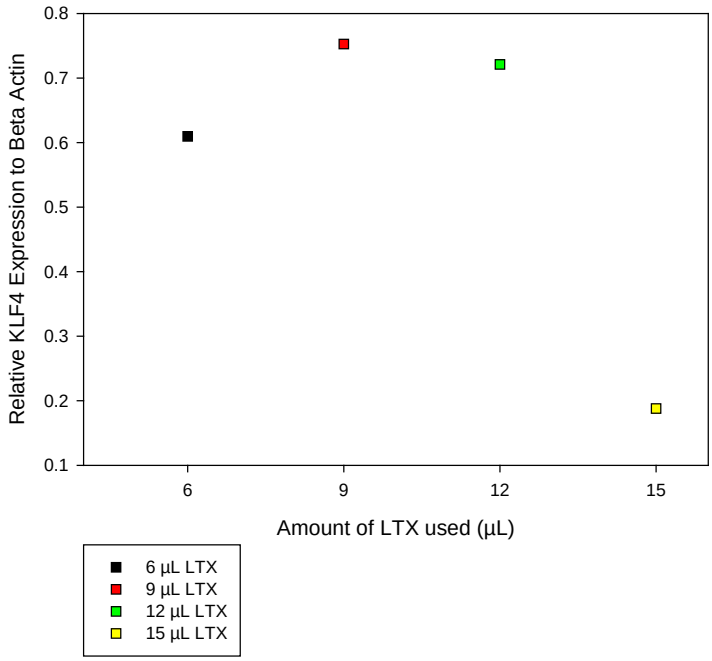


Figure 8.10 Quantification of KLF4 expression by transfectants.

The densities of the KLF4 bands relative to the β-actin bands in the Western blot in Figure 8.9 were determined with Image J. The analysis revealed that 9 µL of LTX gave optimal transfection efficiency.

8.4.4 SOX-2

Western blot analysis confirmed that SOX-2 at 40 kDa was expressed by CHO-K1 cells following transfection with the SOX-2 plasmid using any of the four volumes of LTX (n=1) (Figure 8.11). Quantification of the SOX-2 band by densitometry and normalization compared with β-actin indicated that 9 µL of Lipofectamine LTX was optimal for SOX-2 expression (Figure 8.12).

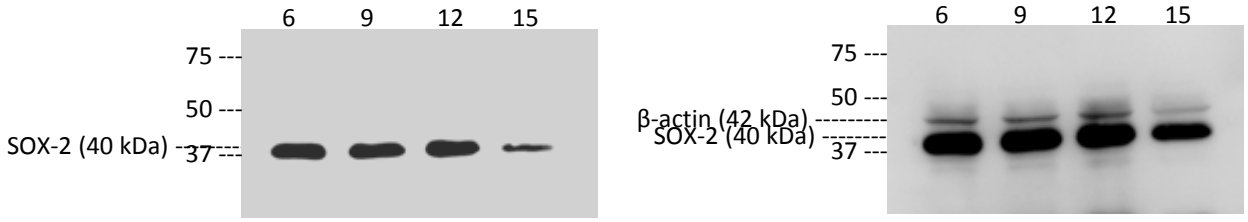


Figure 8.11 Western blot analysis of CHO-K1 cells transfected to express SOX-2 using Lipofectamine LTX.

CHO-K1 cells were transfected for 3 h with 3 μg of SOX-2 plasmid mixed with increasing volumes (6 to 15 μL) of Lipofectamine LTX in OPTI-MEM medium. The cells were then cultured in full medium for an additional 2 days prior to protein extraction, and Western blot analysis. Left blot: protein extracts of CHO-K1 cells transfected with varying amounts of the SOX-2 plasmid using LTX (6-15 μL) were Western blotted with an antibody against SOX-2, and immunoreactivity detected with a goat anti-mouse HRP-conjugated antibody. The position of SOX-2 at 40 kDa is indicated in the left-hand margin. Right blot: The blot was stripped and reprobed with an antibody against human β-actin (42 kDa), with immunoreactivity detected with a donkey anti-rabbit HRP-conjugated antibody. Stripping was incomplete and hence a SOX-2 band at 40 kDa was detected as indicated in the left-hand margin. The position of β-actin at 42 kDa is also indicated in the left-hand margin.

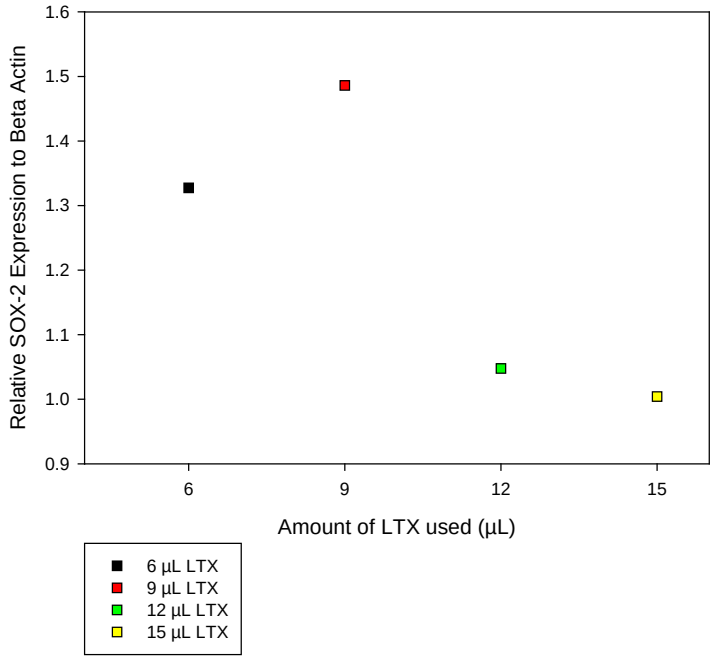


Figure 8.12 Quantification of SOX-2 expression by transfectants.

The densities of the KLF4 bands relative to the β-actin bands in the Western blot in Figure 8.11 were determined with Image J. The analysis revealed that 9 μL of LTX gave optimal transfection efficiency.

8.5 Discussion

8.5.1 Production of recombinant stem cell transcription factors

The four stem cell transcription factors Oct-4, c-Myc, KLF4 and SOX-2 were each successfully expressed using the CHO-K1 cell expression system. Each of the latter factors was obtained by transfecting 1 x 10^6 cells with 3 μg of expression plasmid. Optimal transfection required use of the Lipofectamine LTX reagent system. Less than half of each transfected cell population expressed the factors. The yield could potentially be increased by creating stably transfected cell lines using antibiotic selection with blasticidin. A variety of protease inhibitors will need to be screened for their ability to protect KLF4 from protease degradation.

8.5.2 Potential uses for the stem cell transcription factors

The transcription factor-encoding plasmids were not tested for their ability to penetrate cells and induce the formation of iPSCs as time did not allow for the continuation of this particular project. A previous study used the protein extracts of whole cell lysates of transfectants, like those developed here, to create an iPSC line from human newborn fibroblasts (HNFs) (Kim *et al.* 2009). iPSC generation required 6 weeks of treatment with the transcription factors, followed by 2 weeks of culture on MEF feeder cells (Kim *et al.* 2009). iPSCs could potentially be developed from almost any cell type, including human adipose stem cells, and an individual's donor cells for personal treatment. A feeder-free culture system would be beneficial for establishing iPSC lines for clinical use as it would avoid the potential health risks associated with mouse feeder cells. Plates coated with vitronectin have been proven to effectively support the generation of iPSCs from fibroblasts following electroporation with plasmids (Chen *et al.* 2011). Vitronectin supports human ESC and iPSC attachment, proliferation and pluripotency (Braam *et al.* 2008; Chen *et al.* 2011).

Chapter 9 General Discussion, Conclusions, and Future Directions

9.1 General discussion

The adult stem cell populations investigated in this study did not differentiate into mature insulin-producing cells as expected using the published protocols. Further attempts with additional differentiation agents and novel procedures also did not produce mature β-cells. It is not known whether the variance between the present studies and the published literature are due to differences in the initial adult stem cell populations that were either isolated or purchased, or whether the published results are not sufficiently robust and hence are difficult to independently reproduce, or if it is a combination of both explanations. The principles of scientific inquiry require that research results should be able to be reproduced by independent groups. There are many examples of findings published in scientific journals that cannot be repeated independently, which is a huge concern for the research community, and funding agencies (Ioannidis *et al.* 2012; Landis *et al.* 2012). The complexity of stem cell differentiation, which can be affected by the nature and shape of the surface upon which cells are grown (Valamehr *et al.* 2008; Reilly and Engler 2009), subtle changes in media composition, and environmental conditions means that results obtained in the stem cell field may be more prone to irreproducibility.

The peripheral blood insulin-producing cell (PB-IPC) population was discovered 6 years ago in 2007 by Zhao *et al.*, and yet there has been no subsequent independent published study which has confirmed the existence of this population of cells as described. The initial publication has been cited several times. The earliest citation is in a review article where the publication was cited during a description of HSC markers (Markel *et al.* 2008).The following two citations were from the same laboratory group, which reported that a cell population similar or identical to PB-IPCs can be isolated from cord blood (Zhao *et al.* 2010; Zhao *et al.* 2012). The later publication described the development of the Stem Cell Educator system which employs CB-SCs to stimulate the production of Tregs that are capable of preventing and potentially reversing autoimmunity (Zhao *et al.* 2012). Therefore, this present study is the first to question the reproducibility of the results reported by Zhao *et al.* in 2007.

Some members of the initial publishing group that reported the transdifferentiation of PCMOs into NeoHepatocytes and NeoIslets questioned whether transdifferentiation had actually taken place (Ruhnke *et al.* 2005; Riquelme *et al.* 2009). Further investigation revealed that the NeoHepatocytes express hepatocyte genes during normal macrophage differentiation, and therefore the expression of hepatocyte genes is unlikely to indicate transdifferentiation into true hepatocyte-like cells (Riquelme *et al.* 2009). An independent publication by Schmitt *et al.* (2012) questioned the validity of programmable cells of monocytic origin (PCMOs). No differences in phenotype could be found between monocytes in culture and PCMOs (Schmitt *et al.* 2012). Schmitt *et al.* (2012) also reported that transdifferentiation of monocytes into proper osteoblasts was not achievable with a classic osteoblast differentiation medium (Schmitt *et al.* 2012). Rather the PCMOs retained their hematopoietic markers and became activated

monocytes retaining classic macrophage morphology (Schmitt *et al.* 2012). In agreement with the findings reported here, Schmitt *et al.* (2012) also reported that PCMOs express the monocyte marker CD68. PCMOs cultured in osteoblast differentiation medium retained expression of CD68, which is not expressed by true osteoblasts (Schmitt *et al.* 2012). Nevertheless, the differentiated PCMOs did express osteoblast-related markers such as osteonectin and osteopontin (Schmitt *et al.* 2012). However, these markers are not tissue-specific, and were found to be expressed by monocytes as well as osteoblasts (Schmitt *et al.* 2012). It can be difficult to determine using simple cell-lineage markers whether stem cells have been differentiated into the intended cell type, but they should at least express several of the cell-lineage markers associated with the intended cell type, and have lost the cell-lineage markers that defined the parental cell type. In this present study, monocytes were dedifferentiated into f-MOs, and then cultured in pancreatic differentiation media where some cells displayed the pancreatic marker PDX-1 and others retained the monocytic marker CD14. There was a lack of other pancreatic markers expressed by these cells which means they require further differentiation to adopt a true pancreatic phenotype. PCMOs cultured in the same conditions also retained CD14 expression but downregulated PDX-1. Therefore these cells must be considered to be in a state of transition, having features of both monocytes and pancreatic progenitors. Chapari *et al.* (2012) recently independently reported that PCMOs cultured in fibroblast conditioned media containing a combination of HGF, EGF, nicotinamide differentiated into insulin-producing cells (Chapari *et al.* 2012). However, whether these cells retained the expression of monocytic markers was not determined, and hence more work is required to validate these cells as mature β-cells.

There have been no previously published attempts to differentiate f-MOs into insulin-producing cells. $CD14^+$ monocytes have been differentiated into endothelial cells by culture with FBS on fibronectin-coated plates without prior dedifferentiation into f-MOs (Kuwana *et al.* 2003; Sharifi *et al.* 2006). In another study, monocytes cultured in the presence of pleiotrophin, which is expressed by monocytes/macrophages, differentiated into endothelial cells (Sharifi *et al.* 2006). Therefore, dedifferentiation of monocytes to f-MOs may not be required to induce the transdifferentiation of monocytes, at least with some protocols. In contrast, Zhao *et al.* (2003) reported the differentiation of f-MOs into endothelial cells in the presence of $VEGF_{165}$. In this present study subpopulations of cells were able to be differentiated with $VEGF_{165}$ into endothelial-like cells which expressed vWF and with NGFβ into neuronal-like cells which expressed NSE. The number of CD3 and CD4 T cells increased in f-MOs populations in response to culture with IL-2, which may have been due to transdifferentiation of f-MOs or the proliferation of contaminating T cells.

Human amniotic stem cells (HASCs) and cord blood hematopoietic stem cells (CB-HSCs) were reported to differentiate into pancreatic cells with the use of specialized pancreatic differentiation matrices and media available from Celprogen Inc. (Sharma *et al.* 2003; J.P. Sharma, personal correspondence, January 18, 2011). It was reported that the differentiated HASCs did not express insulin protein, only insulin mRNA, but glucagon protein was expressed (Sharma *et al.* 2003), indicating this protocol alone is not effective at inducing the formation of pancreatic β-cells. This present study confirmed that HASCs and CB-HSCs do not express insulin protein, but have the potential to undergo pancreatic differentiation. HASCs can be induced to express GPR40, Arx, CXCR4, HNF6, glucagon, PCSK1, GIPR, PDX-1, and SOX-17. CB-HSCs can be induced to express GPR40,

GIPR, and PDX-1. Additional combinations of agents are required to induce their commitment and maturation to the β-cell lineage. The composition of the Celprogen Inc. media and matrices used in this study are proprietary, which is a problem as the specific factors responsible for enhanced differentiation are unknown.

Differentiation of ASCs into insulin-producing cells according to the Chandra protocol (Chandra *et al.* 2011) has not been independently validated. This is the first study to report that the Chandra protocol is not sufficiently robust in that human ASCs, either attached or in suspension, could not be differentiated using the protocol into cells capable of producing genuine insulin. In this study ASCs cultured according to the Chandra protocol expressed insulin, as detected with the guinea pig anti-insulin antibody, but the insulin was not genuine as it could not be detected with mouse or chicken anti-insulin antibodies and the cells did not co-express other key β-cell related proteins such as C-peptide and amylin. Chandra *et al.* (2009) had earlier reported that the same protocol was able to differentiate mouse ASCs to cells expressing insulin. Zhang *et al.* (2011) confirmed these findings by demonstrating that the protocol differentiated mouse ASCs to express insulin, C-peptide, PDX-1, Glut-2, NeuroD and other pancreatic markers (Zhang *et al.* 2011). Therefore, the Chandra protocol has at least been validated for mouse ASCs. The reason for the discrepancy between the two human studies is not known, but may relate to differences in the adipose stem cell populations contained in our laboratory stock and that of Chandra's group.

The Timper protocol was independently validated in 3 publications from Trivedi's research group (Trivedi *et al.* 2008; Vanikar *et al.* 2010; Dave *et al.* 2012). The publications by Trivedi *et al.* (2008) and Vanikar *et al.* (2010) describe the cotransplantation of adipose tissue-derived insulin-secreting mesenchymal stem cells and HSCs to treat type 1 diabetes in human patients. The ASCs employed were differentiated in a medium identical to that described by Timper *et al.* (2006). The derived cells expressed Pax6, PDX-1, Isl-1, and also insulin and C-peptide (Vanikar *et al.* 2010). Patients followed-up after an average of 23 months had decreased exogenous insulin requirements (from 1.14 units/kg/day to 0.63 units/kg/day), increased C-peptide levels (from 0.1 ng/mL to 0.38 ng/mL), no longer suffered from diabetic ketoacidosis, and experienced no adverse effects due to treatment (Vanikar *et al.* 2010). The most recent publication by this group reported that ASCs differentiated for three days according to the Timper protocol are capable of responding to changes in glucose by secreting insulin and C-peptide (Dave *et al.* 2012). In the present study, ASCs cultured according to the Timper protocol did not express insulin, amylin or C-peptide protein. Again, there is no simple explanation as to why the results of the Timper and Trivedi groups could not be reproduced. Perhaps there are differences between the parental ASC populations, the initial isolation and expansion techniques, or essential details are missing from the methodology described in the publications.

The present study suggested, as expected, that different stem cell types respond differently to the same pancreatic differentiation agents. For example, while Borowiak *et al.* (2009) reported that the majority of hESCs cultured with the definitive endoderm-inducing agent IDE-1 expressed SOX-17, only a few of the ASCs cultured with IDE-1 in the present study expressed SOX-17. ASCs appear to be less responsive than hESCs to IDE-1. In the experiments by Borowiak *et al.* (2009), the hESCs cells were cultured on a mouse embryonic fibroblast feeder layer which may release factors that influence cell differentiation. In addition,

hESCs differentiated with activin A and Wnt3a form definitive endoderm cells that express FOXA2, CXCR4, SOX-17 (D'Amour *et al.* 2006), whereas in the present study ASCs cultured under identical conditions expressed only SOX-17 and not FOXA2 and CXCR4. Therefore, each stem cell type requires a different set of differentiation agents in order to be induced to form the same cell lineage.

The transdifferentiation protocol that resulted in a cell-type most closely resembling mature insulin-producing β-cells employed HASCs, which were cultured for 1 week in human pancreatic cancer stem cell culture differentiation media with serum on plates coated with human pancreatic cancer stem cell culture extracellular differentiation matrix (both from Celprogen Inc.). The parental HASC population expressed Nestin, Oct-4, SOX-17, and PDX-1, hence already possessed features of pancreatic progenitors. Upon differentiation the expression of Nestin and Oct-4 was downregulated, whereas the expression of SOX-17 was maintained. Other pancreatic markers were upregulated including PDX-1, Arx, CXCR4, HNF6, glucagon, and PCSK1. There were a few Nanog-expressing stem cells present which indicated that the cell population as a whole had not completely differentiated. This cell population also expressed TGF-β and AIRE indicating that they cells may be immunosuppressive or tolerogenic, respectively. PCSK1 is expressed alongside glucagon during pancreas development in the mouse, and is thought to induce β-cell development (Wilson *et al.* 2002). The expression of Arx may indicate that the glucagon-expressing α-cell phenotype is emerging (Collombat *et al.* 2007), which indicates definite differentiation along the pancreatic lineage. The expression of these markers alongside the definitive endoderm markers CXCR4 and SOX-17, and the primitive gut tube markers HNF6 and PDX-1 demonstrates a population of cells undergoing pancreatic maturation. Further differentiation agents are required to induce the formation of the mature β-cell phenotype. Alternatively, high level expression of the promiscuous transcription factor AIRE might mean the cells are capable of expressing a wide-range of cell-lineage factors, and hence could resemble any number of different cell types.

ASCs cultured according to Chandra's protocol, either attached to tissue culture dishes or cultured in suspension, displayed expression of insulin, and hence could be regarded as β-cells. However it is not known whether the insulin is genuine as the cells failed to express C-peptide, and also did not express amylin. The guinea pig anti-insulin antibody, which was mostly used in the study to detect insulin, has been used in many published studies (Gittes *et al.* 1996; Schwitzgebel *et al.* 2000; Kawahira *et al.* 2003; Vats *et al.* 2012). It detects insulin-expressing β-cells in human and foetal/adult mouse pancreases (Gittes *et al.* 1996; Schwitzgebel *et al.* 2000; Kawahira *et al.* 2003; Vats *et al.* 2012). In the present study it detected insulin expressed by the rat INS-1E and RINm5f pancreatic β-cell lines by immunocytochemistry, detected insulin expressed by the INS-1E cell line by dot blot analysis, and detected insulin expressed by the RINm5F cell line by Western blot analysis. Specificity of the antibody for insulin and not related proteins was confirmed with a series of dot blots of the insulin homologues insulin-like 3, insulin-like growth factor I, and insulin-like growth factor II. It is an enigma why several differentiated cells in the present study could be stained for insulin expression with the guinea-pig antibody, but not with mouse and chicken anti-insulin antibodies.

A variety of different techniques were used to phenotype the stem cell populations and their derived cell populations examined in this study. Immunocytochemistry was the main technique used. Often comparisons were made between the efficacy of the different differentiation conditions in terms of the number of cells expressing a particular cell lineage marker, or the strength of the immunostaining and protein expression. These comparisons cannot be considered absolute and only give a crude indication of protein expression. Immunostaining intensity is influenced by antibody concentration, incubation time, the nature of the secondary antibody, and the fluorophore. Changes noted can only be relative to cells tested with the same antibody and immunocytochemistry technique at the same time. Different antibodies detecting the same cell marker can give different strengths of signal. This was noted during testing for SOX-17 expression by ASCs in that the mouse anti-SOX-17 antibody gave a weaker signal than did the goat anti-SOX-17 antibody. Antibody specificity was judged by a stronger signal observed with the primary antibody compared to an isotype-matched control antibody (e.g. mouse IgG, chicken IgY), and/or by the size of the antigen detected on Western blots. Western blot analysis was employed when more precise protein quantification was required, where protein expression was calculated relative to the total amount of protein loaded.

9.2 Conclusions

The results obtained in this study have established that peripheral blood insulin-producing cells (PB-IPCs), programmable cells of monocytic origin (PCMOs), f-macrophages (f-MOs), human amniotic stem cells (HASCs), cord blood hematopoietic stem cells (CB-HSCs), and adipose stem cells (ASCs) display limited plasticity towards the pancreatic lineage. All of these cell populations are easily obtained, and apart from the amniotic and cord blood stem cells can be isolated from adult donors (Zhao *et al.* 2003; Ruhnke *et al.* 2005; Miki *et al.* 2007; Zhao *et al.* 2007a; Haller *et al.* 2011; Locke *et al.* 2011).

Investigation of the PB-IPC population showed they have the potential for pancreatic differentiation as they express PDX-1, HNF6, CXCR4, and SOX-17, but they also express monocytic markers and possess phagocytic function. The cells stubbornly maintained their expression of monocytic markers despite efforts to transdifferentiate them into β-cells. In particular, in this study the protocol published by Zhao *et al.* (2008) did not result in the transdifferentiation of PB-IPCs into insulin-producing cells, and therefore the protocol is deemed to be either irreproducible, or insufficiently robust. Whilst PB-IPCs expressed the markers FOXP3 and AIRE that characterize immunosuppressive cells and tolerogenic cells, they did not inhibit a mixed lymphocyte response and are therefore unlikely to be an immunosuppressive population.

Similarly, PCMOs dedifferentiated from PBMCs maintained their monocytic character as seen by the continued expression of CD14, but also showed pancreatic potential as they expressed PDX-1 and SOX-17. However, these cells were senescent and did not display alkaline phosphatase activity. Culturing the PCMOs in the islet cell conditioning medium (ICM) (Ruhnke *et al.* 2005), decreased the expression of PDX-1 and HLA-DR and did not upregulate additional pancreatic markers. These results contrast with the publication by Ruhnke *et al.* (2005), which reported that PCMOs expressed insulin and C-peptide. In summary, the PCMOs in this present study did not express insulin, which raises questions as to the validity of PCMOs as questioned by Schmitt *et al.* (2012), and the reproducibility and robustness of the published protocol.

Monocytes cultured with M-CSF formed f-MOs that have a characteristic spindle shape, as published (Zhao *et al.* 2003). They were a senescent cell population and did not display alkaline phosphatase activity. f-MOs cultured in ICM maintained their monocytic characteristics, as evidenced by continued expression of CD14. The population contained less PDX-1-expressing cells compared with fresh monocytes, and could not be further differentiated into pancreatic cells with ICM, but instead showed limited plasticity towards the endothelial, and neuronal cell lineages. Of all the adult stem cells studied, the f-MOs show the greatest plasticity towards the T lymphocyte lineage and therefore represent a potential source for the generation of these cells in the future.

The HASCs purchased for this study are considered to be stem cells as they express Nestin and Oct-4, and yet resembled pancreatic progenitors as they expressed PDX-1 and SOX-17. Nestin-positive ESCs have been differentiated into insulin-producing cells (Yue *et al.* 2006). This present investigation revealed that Nestin-positive HASCs have pancreatic differentiation potential, as their culture on defined pancreatic differentiation matrices led to the downregulation of expression of Nestin, and upregulation of expression of CXCR4, HNF6, Arx, glucagon, and PCSK1. However, they did not express insulin, and therefore further approaches are needed to induce their maturation towards the β-cell lineage. They showed signs of being an immunosuppressive or tolerogenic population as evidenced by their expression of TGF-β and AIRE, respectively. This feature could be exploited to prevent the rejection of transplanted insulin-producing cells during the treatment of type 1 diabetes.

CB-HSCs purchased for this study expressed Nestin, indicating that like HASCs they may have potential to undergo pancreatic differentiation. Indeed the undifferentiated CB-HSCs also expressed SOX-17 and GPR40. Their differentiation on a defined transdifferentiation matrix resulted in expression of PDX-1, GIPR, and expression of GPR40 was retained. Like HASCs, they also expressed TGF-β, which could be exploited to enhance graft retention.

The ASCs purchased for this study expressed the adipose stem cell markers CD29 and CD90, the stem cell marker Nestin, and for the first time it was discovered that ASCs express SOX-17. They displayed stem cell-specific aldehyde dehydrogenase activity indicating they are indeed stem cells. Stage-specific differentiation of ASCs with 100 nM IDE-1 (definitive endoderm), followed by KAAD-cyclopamine and FGF10 (primitive gut tube), and then KAAD-cyclopamine, FGF10 and all trans-retinoic acid (posterior foregut) was the most efficient protocol at upregulating PDX-1 expression, as seen by Western blot analysis. This result indicates that ASCs are capable of being differentiated to the posterior foregut stage of pancreatic differentiation in a defined media. D'Amour *et al.* (2006) reported that further differentiation of these cells may be possible by extending the protocol for a further 2 days with KAAD-cyclopamine, FGF10, all trans-retinoic acid, DAPT (γ-secretase inhibitor), and Ex4 to induce pancreatic endoderm where the cells express Nkx6.1, NGN3, Pax4, and Nkx2.2, and then for 3+ additional days with KAAD-cyclopamine, FGF10, all trans-retinoic acid, Ex4, IGF-1, and HGF to induce endocrine precursor insulin, glucagon, and somatostatin expressing cells (D'Amour *et al.* 2006). The protocol could potentially be improved by including betacellulin and

nicotinamide during the last two phases (Cho *et al.* 2008). Therefore the final stages of maturation of ASCs into insulin-producing cells might require particular combinations of pancreatic maturation agents.

In this study, AIRE was expressed by cultured PB-IPCs, monocytes, dHASCs, and tdHASCs. In accord, Kogawa *et al.* (2002) reported that AIRE is expressed by cultured monocytes and differentiated $CD11c^+$ dendritic cells. AIRE is expressed by antigen-presenting cells in the thymus where it promiscuously upregulates the expression of normal tissue-specific antigens for presentation to enable selection of T effector cell and Tregs in the development of central and peripheral immune tolerance (Kont *et al.* 2008). The significance of AIRE in the above cell stem cell types is not known. AIRE has been reported to promote the self-renewal of ESCs (Bin *et al.* 2012). It is hypothesised that stem cell populations which express AIRE may be able to induce peripheral immune tolerance after transplantation *in vivo*, as they may be able to present tissue-specific antigens which are not expressed in the thymus (Metzger and Anderson 2011). This may be a way of inducing tolerance of β-cell associated antigens in sufferers of type 1 diabetes.

The recombinant transcription factors Oct-4, c-Myc, KLF4 and SOX-2 that are required to induce the formation of iPSCs were produced by transfection of CHO-K1 cells with plasmids encoding these factors. They can now be used to develop an iPSC line, which could be subjected to the pancreatic differentiation protocols trialled in this study.

In conclusion, this study has shown that PB-IPCs, PCMOs, f-MOs, HASCs, CB-HSCs, and ASCs are capable of being transdifferentiated to express pancreatic lineage markers. Interestingly, several of the cell populations employed in this study expressed pancreatic progenitor markers prior to exposure to pancreatic differentiation agents. A number of pancreatic differentiation media proved to be effective at upregulating the expression of additional pancreatic markers by these cell populations. Further studies will be needed to develop robust approaches to complete the pancreatic differentiation process in order to produce cells that express insulin, and respond to glucose by upregulating insulin expression.

9.3 Future directions

The ability of the different adult stem cell populations investigated in this study to be differentiated into insulin-producing cells should be further studied to discover reliable and robust methods of differentiation. Parameters that could be altered include different differentiation factor combinations and concentrations, length of culture, and attachment matrices (Evans *et al.* 2009). Attempts to induce cell differentiation *in vivo* should also be investigated. Cells labelled with a fluorophore or bearing an X/Y chromosome mismatch with the recipient could be injected intravenously or directly into the pancreas. Their establishment within the pancreas could be monitored by measuring the retention of fluorescently labelled cells or by screening pancreatic sections with an X/Y chromosome probe (Zhao *et al.* 2007a). In order for the cells to fully commit to the pancreatic lineage they could be forced to lose the character of the parental cell lineage. Hesselson *et al.* (2011) reported that forced suppression of the transcription factor Ptf1a, which maintains the acinar phenotype, induced the *in vivo* transformation of acinar cells into insulin-producing endocrine cells in a zebrafish model. Further, Qiliang Liu (2012), a lab colleague, demonstrated that forced

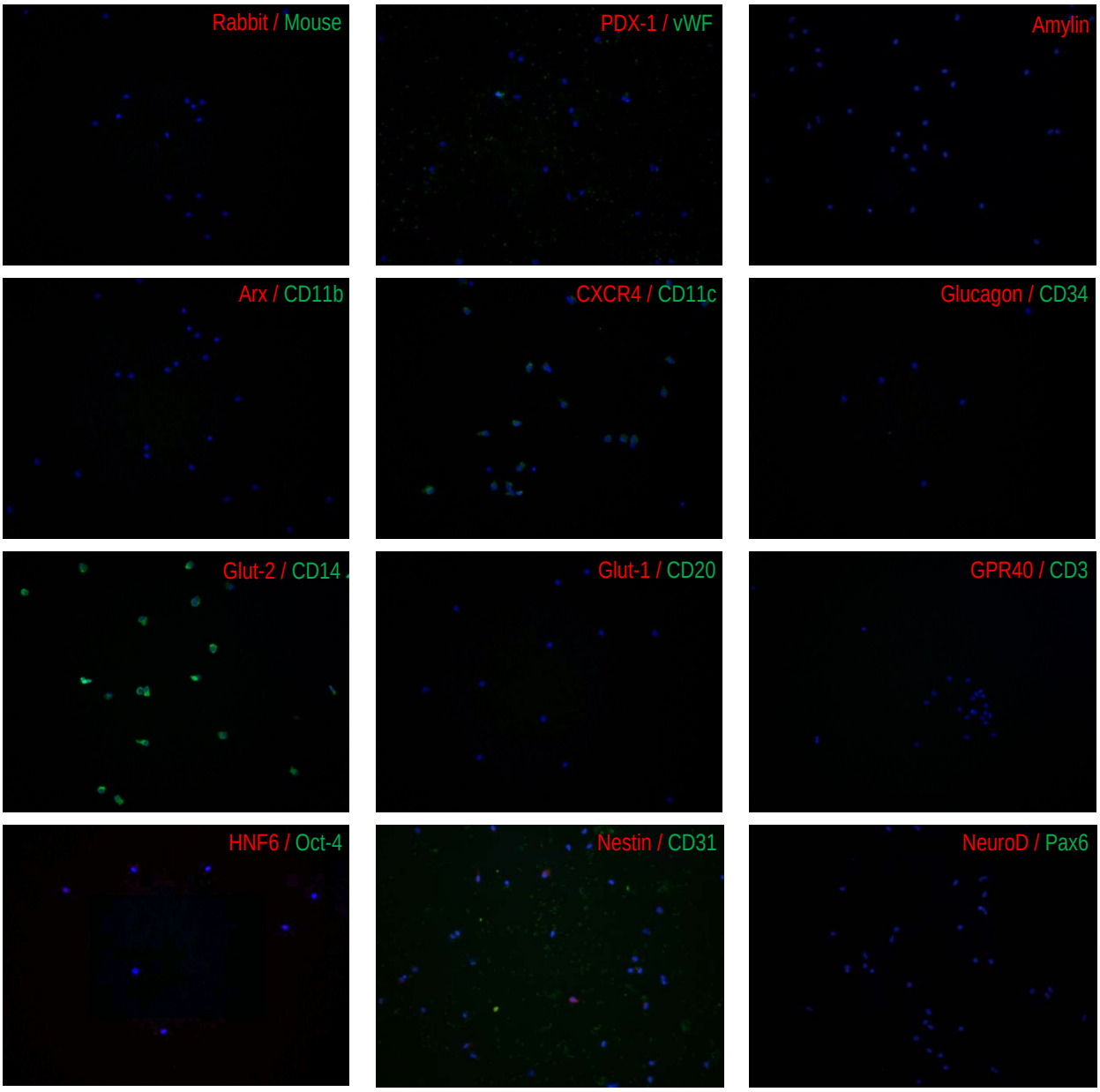
downregulation of Pft1a in combination with stimulation with pancreatic differentiation factors transformed mouse acinar cells into insulin-producing cells. Talchai *et al.* (2012) reported that somatic ablation of the transcription factor Foxo1 in $NGN3^{+}$ enteroendocrine progenitor cells induced the formation of insulin-expressing cells in the intestines of mice that expressed C-peptide in response to glucose. The latter approaches are particularly promising and warrant further application. For the treatment of type 1 diabetes it is vitally important that the insulin cells produced must be able to respond to changes in glucose concentration.

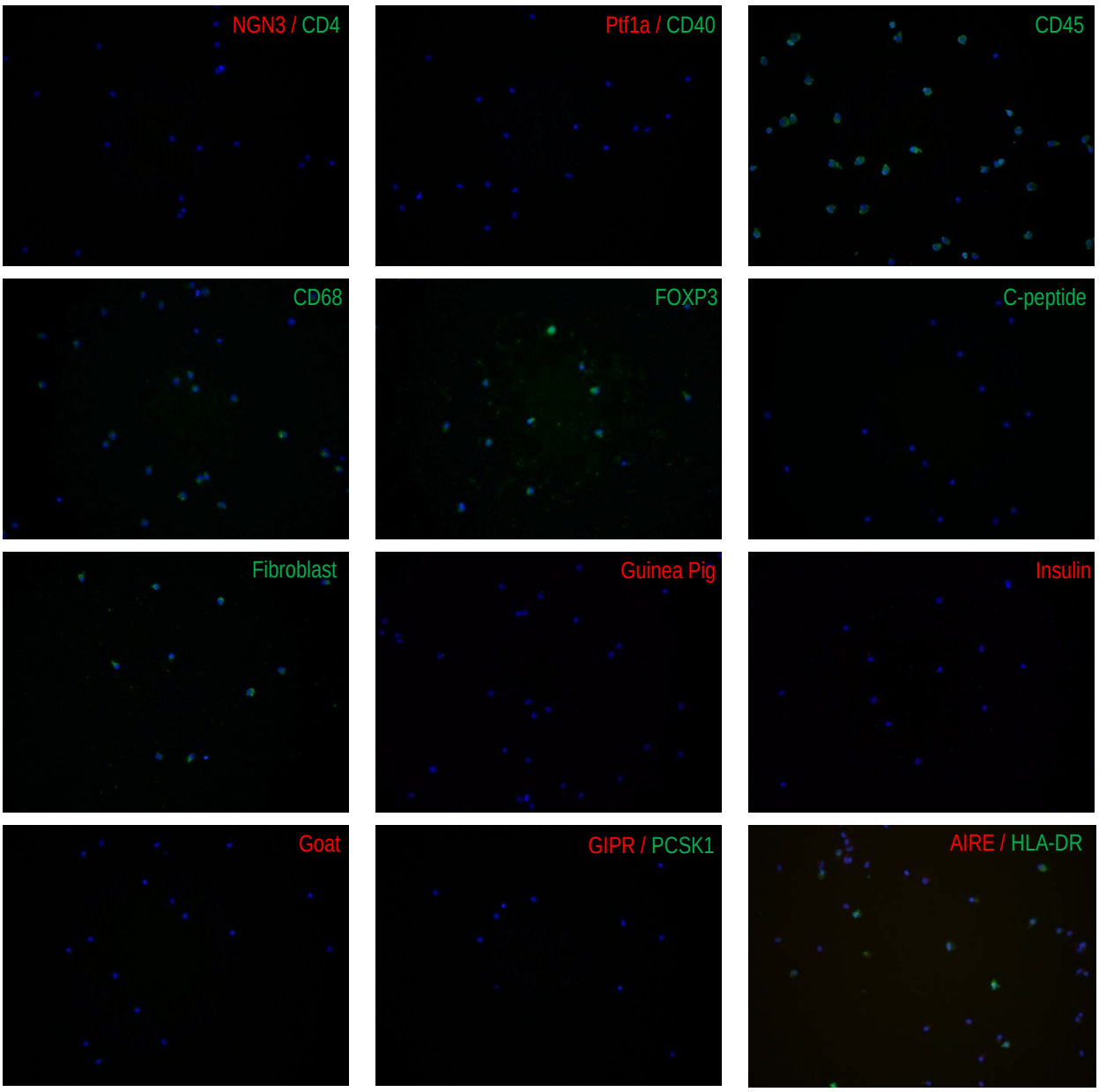
The expression of TGF-β by the CB-HSCs, dHASCs, and tdHASCs could indicate that these cells are capable of suppressing a local immune attack after transplantation by forming an immunosuppressive barrier around the differentiated cells. Zhao *et al.* (2009) reported that transplantation of Tregs formed by the coculture of mouse lymphocytes with CB-SCs led to increased expression of TGF-β in the pancreatic islets of mice (Zhao *et al.* 2009). The upregulation of TGF-β surrounding the islets was hypothesized to protect newly formed islets against immune attack (Zhao *et al.* 2009). Therefore, transplantation of undifferentiated CB-HSCs, dHASCs, and tdHASCs into the pancreas should be investigated as an approach to inhibit diabetes-associated autoimmunity. These cell populations may be able to stimulate the generation of Tregs *in vivo*. Alternatively, they could be used to generate Tregs *ex vivo* using the Stem Cell Educator system as described by Zhao *et al.* (2012), which would then be transplanted into a patient with type 1 diabetes to reverse autoimmunity. Future experiments should be undertaken to compare the effectiveness of the hydrophobic surface selected CB-SCs with that of the CB-HSCs, dHASCs, and tdHASCs at inducing immune suppression and tolerance by performing a mixed lymphocyte response assay and trialling the cells in the Stem Cell Educator system developed by Zhao *et al.* (2012).

When working with commercially produced stem cell populations it might be worthwhile to enrich for those cells that best express stem cell features, and then to expand them to provide a sufficient number of cells for subsequent experiments in order to decrease subsequent variability of results. It will be interesting to observe whether results obtained using iPSCs suffer from irreproducibility problems given that such stem cell populations are induced in a controlled laboratory setting with a specific set of differentiation proteins.

This study has clearly brought attention to the need for independent evaluation of the published stem cell differentiation protocols. It will be important to ensure that key findings presented in this thesis are published so that researchers are made aware that many of the published protocols in the adult stem cell field are not as robust as they first seem.

Appendix A


Rabbit / Mouse
PDX-1 / vWF
Amylin
Arx / CD11b
CXCR4 / CD11c
Glucagon / CD34
Glut-2 / CD14
Glut-1 / CD20
GPR40 / CD3
HNF6 / Oct-4
Nestin / CD31
NeuroD / Pax6


NGN3 / CD4
Ptf1a / CD40
CD45
CD68
FOXP3
C-peptide
Fibroblast
Guinea Pig
Insulin
Goat
GIPR / PCSK1
AIRE / HLA-DR

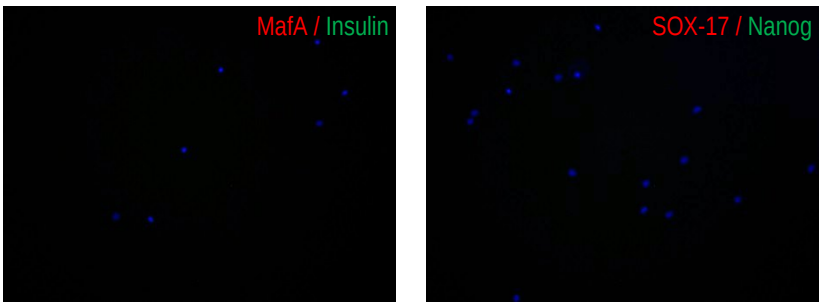


Figure A. 1 Phenotyping of monocytes cultured in tissue culture dishes for 3 days.

Adherent monocytes were cultured in full RPMI media containing 7% FBS. Cells were stained for the expression of various cell markers. Immunoreactivity was detected with donkey anti-rabbit, goat anti-guinea pig, and donkey anti-goat (red) antibodies and with a donkey anti-mouse antibody (green). Nuclei were stained blue with DAPI. Images were taken at 200x magnification. The images are presented so that the staining obtained with each IgG control immediately precedes stainings with antibodies of the same host species.

References

Adeghate, E., P. Schattner and E. Dunn (2006). "An update on the etiology and epidemiology of diabetes mellitus." Ann N Y Acad Sci 1084: 1-29.

Aderem, A. and D. M. Underhill (1999). "Mechanisms of phagocytosis in macrophages." Annu Rev Immunol 17: 593-623.

Arntfield, M. E. and D. van der Kooy (2011). "beta-Cell evolution: How the pancreas borrowed from the brain: The shared toolbox of genes expressed by neural and pancreatic endocrine cells may reflect their evolutionary relationship." Bioessays 33(8): 582-587.

Asfari, M., D. Janjic, P. Meda, G. Li, P. A. Halban and C. B. Wollheim (1992). "Establishment of 2-mercaptoethanol-dependent differentiated insulin-secreting cell lines." Endocrinology 130(1): 167-178.

Banchereau, J., F. Briere, C. Caux, J. Davoust, S. Lebecque, Y. J. Liu, B. Pulendran and K. Palucka (2000). "Immunobiology of dendritic cells." Annu Rev Immunol 18: 767-811.

Bertrand, S., M. Godoy, P. Semal and P. Van Gansen (1992). "Transdifferentiation of macrophages into fibroblasts as a result of Schistosoma mansoni infection." Int J Dev Biol 36(1): 179-184.

Bhushan, A., N. Itoh, S. Kato, J. P. Thiery, P. Czernichow, S. Bellusci and R. Scharfmann (2001). "Fgf10 is essential for maintaining the proliferative capacity of epithelial progenitor cells during early pancreatic organogenesis." Development 128(24): 5109-5117.

Bin, G., Z. Jiarong, W. Shihao, S. Xiuli, X. Cheng, C. Liangbiao and Z. Ming (2012). "Aire promotes the self-renewal of embryonic stem cells through Lin28." Stem Cells Dev 21(15): 2878-2890.

Bjelland, S. (1987). "Tissue distribution and molecular heterogeneity of bovine thiol:protein-disulphide oxidoreductase (disulphide interchange enzyme)." Comp Biochem Physiol B 87(4): 907-914.

Bongso, A. and E. H. Lee (2005). Stem cells: from bench to bedside, World Scientific.

Borowiak, M., R. Maehr, S. Chen, A. E. Chen, W. Tang, J. L. Fox, S. L. Schreiber and D. A. Melton (2009). "Small molecules efficiently direct endodermal differentiation of mouse and human embryonic stem cells." Cell Stem Cell 4(4): 348-358.

Boujendar, S., E. Arany, D. Hill, C. Remacle and B. Reusens (2003). "Taurine supplementation of a low protein diet fed to rat dams normalizes the vascularization of the fetal endocrine pancreas." J Nutr 133(9): 2820-2825.

Braam, S. R., L. Zeinstra, S. Litjens, D. Ward-van Oostwaard, S. van den Brink, L. van Laake, F. Lebrin, P. Kats, R. Hochstenbach, R. Passier, A. Sonnenberg and C. L. Mummery (2008). "Recombinant vitronectin is a functionally defined substrate that supports human embryonic stem cell self-renewal via alphavbeta5 integrin." Stem Cells 26(9): 2257-2265.

Brubaker, P. L. and D. J. Drucker (2002). "Structure-function of the glucagon receptor family of G protein-coupled receptors: the glucagon, GIP, GLP-1, and GLP-2 receptors." Receptors Channels 8(3-4): 179-188.

Buckley, C. D., N. Amft, P. F. Bradfield, D. Pilling, E. Ross, F. Arenzana-Seisdedos, A. Amara, S. J. Curnow, J. M. Lord, D. Scheel-Toellner and M. Salmon (2000). "Persistent induction of the chemokine receptor CXCR4 by TGF-beta 1 on synovial T cells contributes to their accumulation within the rheumatoid synovium." J Immunol 165(6): 3423-3429.

Buteau, J., S. Foisy, E. Joly and M. Prentki (2003). "Glucagon-like peptide 1 induces pancreatic beta-cell proliferation via transactivation of the epidermal growth factor receptor." Diabetes 52(1): 124-132.

Cai, J., M. L. Weiss and M. S. Rao (2004). "In search of "stemness"." Exp Hematol 32(7): 585-598.

Cardoso, L. S., M. I. Araujo, A. M. Goes, L. G. Pacifico, R. R. Oliveira and S. C. Oliveira (2007). "Polymyxin B as inhibitor of LPS contamination of Schistosoma mansoni recombinant proteins in human cytokine analysis." Microb Cell Fact 6: 1.

Chan, E. M., S. Ratanasirintrawoot, I. H. Park, P. D. Manos, Y. H. Loh, H. Huo, J. D. Miller, O. Hartung, J. Rho, T. A. Ince, G. Q. Daley and T. M. Schlaeger (2009). "Live cell imaging distinguishes bona fide human iPS cells from partially reprogrammed cells." Nat Biotechnol 27(11): 1033-1037.

Chandra, V., S. G, S. Phadnis, P. D. Nair and R. R. Bhonde (2009). "Generation of pancreatic hormone-expressing islet-like cell aggregates from murine adipose tissue-derived stem cells." Stem Cells 27(8): 1941-1953.

Chandra, V., G. Swetha, S. Muthyala, A. K. Jaiswal, J. R. Bellare, P. D. Nair and R. R. Bhonde (2011). "Islet-like cell aggregates generated from human adipose tissue derived stem cells ameliorate experimental diabetes in mice." PLoS One 6(6): e20615.

Chao, S. H., J. N. Harada, F. Hyndman, X. Gao, C. G. Nelson, S. K. Chanda and J. S. Caldwell (2004). "PDX1, a cellular homeoprotein, binds to and regulates the activity of human cytomegalovirus immediate early promoter." J Biol Chem 279(16): 16111-16120.

Chapari, H., F. Farokhi, N. Delirezh, S. Javadi and F. Tanhaye Kalate Sabz (2012). "Effects of fibroblasts conditioned media on differentiation of programmable cells of monocytic origin to insulin-producing cells." Tehran Univ Med J 69(11): 695-702.

Chen, G., D. R. Gulbranson, Z. Hou, J. M. Bolin, V. Ruotti, M. D. Probasco, K. Smuga-Otto, S. E. Howden, N. R. Diol, N. E. Propson, R. Wagner, G. O. Lee, J. Antosiewicz-Bourget, J. M. Teng and J. A. Thomson (2011). "Chemically defined conditions for human iPSC derivation and culture." Nat Methods 8(5): 424-429.

Chen, S., M. Borowiak, J. L. Fox, R. Maehr, K. Osafune, L. Davidow, K. Lam, L. F. Peng, S. L. Schreiber, L. L. Rubin and D. Melton (2009). "A small molecule that directs differentiation of human ESCs into the pancreatic lineage." Nat Chem Biol 5(4): 258-265.

Cherif, H., B. Reusens, M. T. Ahn, J. J. Hoet and C. Remacle (1998). "Effects of taurine on the insulin secretion of rat fetal islets from dams fed a low-protein diet." J Endocrinol 159(2): 341-348.

Chick, W. L., S. Warren, R. N. Chute, A. A. Like, V. Lauris and K. C. Kitchen (1977). "A transplantable insulinoma in the rat." Proc Natl Acad Sci U S A 74(2): 628-632.

Cho, Y. M., J. M. Lim, D. H. Yoo, J. H. Kim, S. S. Chung, S. G. Park, T. H. Kim, S. K. Oh, Y. M. Choi, S. Y. Moon, K. S. Park and H. K. Lee (2008). "Betacellulin and nicotinamide sustain PDX1 expression and induce pancreatic beta-cell differentiation in human embryonic stem cells." Biochem Biophys Res Commun 366(1): 129-134.

Clanchy, F. I., A. C. Holloway, R. Lari, P. U. Cameron and J. A. Hamilton (2006). "Detection and properties of the human proliferative monocyte subpopulation." J Leukoc Biol 79(4): 757-766.

Clarke, R. L., A. D. Yzaguirre, Y. Yashiro-Ohtani, A. Bondue, C. Blanpain, W. S. Pear, N. A. Speck and G. Keller (2013). "The expression of Sox17 identifies and regulates haemogenic endothelium." Nat Cell Biol 15(5): 502-510.

Collombat, P., J. Hecksher-Sorensen, J. Krull, J. Berger, D. Riedel, P. L. Herrera, P. Serup and A. Mansouri (2007). "Embryonic endocrine pancreas and mature beta cells acquire alpha and PP cell phenotypes upon Arx misexpression." J Clin Invest 117(4): 961-970.

Collombat, P., X. Xu, P. Ravassard, B. Sosa-Pineda, S. Dussaud, N. Billestrup, O. D. Madsen, P. Serup, H. Heimberg and A. Mansouri (2009). "The ectopic expression of Pax4 in the mouse pancreas converts progenitor cells into alpha and subsequently beta cells." Cell 138(3): 449-462.

D'Amour, K. A., A. D. Agulnick, S. Eliazer, O. G. Kelly, E. Kroon and E. E. Baetge (2005). "Efficient differentiation of human embryonic stem cells to definitive endoderm." Nat Biotechnol 23(12): 1534-1541.

D'Amour, K. A., A. G. Bang, S. Eliazer, O. G. Kelly, A. D. Agulnick, N. G. Smart, M. A. Moorman, E. Kroon, M. K. Carpenter and E. E. Baetge (2006). "Production of pancreatic hormone-expressing endocrine cells from human embryonic stem cells." Nat Biotechnol 24(11): 1392-1401.

Daneman, D. (2006). "Type 1 diabetes." Lancet 367(9513): 847-858.

Danke, N. A., D. M. Koelle, C. Yee, S. Beheray and W. W. Kwok (2004). "Autoreactive T cells in healthy individuals." J Immunol 172(10): 5967-5972.

Dave, S. D., A. V. Vanikar and H. L. Trivedi (2012). "Ex vivo generation of glucose sensitive insulin secreting mesenchymal stem cells derived from human adipose tissue." Indian J Endocrinol Metab 16 Suppl 1: S65-69.

Debacq-Chainiaux, F., J. D. Erusalimsky, J. Campisi and O. Toussaint (2009). "Protocols to detect senescence-associated beta-galactosidase (SA-betagal) activity, a biomarker of senescent cells in culture and in vivo." Nat Protoc 4(12): 1798-1806.

Delisle, J. C., L. Martignat, L. Dubreil, P. Sai, J. M. Bach, V. Louzier and S. Bosch (2009). "PDX-1 or PDX-1-VP16 protein transduction induces beta-cell gene expression in liver-stem WB cells." BMC Res Notes 2: 3.

Devaskar, S. U., S. J. Giddings, P. A. Rajakumar, L. R. Carnaghi, R. K. Menon and D. S. Zahm (1994). "Insulin gene expression and insulin synthesis in mammalian neuronal cells." J Biol Chem 269(11): 8445-8454.

Elliott, R. B., L. Escobar, P. L. Tan, M. Muzina, S. Zwain and C. Buchanan (2007). "Live encapsulated porcine islets from a type 1 diabetic patient 9.5 yr after xenotransplantation." Xenotransplantation 14(2): 157-161.

Eubank, T. D., M. Galloway, C. M. Montague, W. J. Waldman and C. B. Marsh (2003). "M-CSF induces vascular endothelial growth factor production and angiogenic activity from human monocytes." J Immunol 171(5): 2637-2643.

Evans, N. D., C. Minelli, E. Gentleman, V. LaPointe, S. N. Patankar, M. Kallivretaki, X. Chen, C. J. Roberts and M. M. Stevens (2009). "Substrate stiffness affects early differentiation events in embryonic stem cells." Eur Cell Mater 18: 1-13; discussion 13-14.

Finnin, M., J. A. Hamilton and S. T. Moss (1999). "Characterization of a CSF-induced proliferating subpopulation of human peripheral blood monocytes by surface marker expression and cytokine production." J Leukoc Biol 66(6): 953-960.

Frank, S. A. (2002). Specificity and cross-reactivity. Immunology and Evolution of Infectious Disease, Princeton (NJ): Princeton University Press.

Galligan, J. J. and D. R. Petersen (2012). "The human protein disulfide isomerase gene family." Hum Genomics 6: 6.

Gao, F., D. Q. Wu, Y. H. Hu, G. X. Jin, G. D. Li, T. W. Sun and F. J. Li (2008). "In vitro cultivation of islet-like cell clusters from human umbilical cord blood-derived mesenchymal stem cells." Transl Res 151(6): 293-302.

Garay-Malpartida, H. M., R. F. Mourao, M. Mantovani, I. A. Santos, M. C. Sogayar and A. C. Goldberg (2011). "Toll-like receptor 4 (TLR4) expression in human and murine pancreatic beta-cells affects cell viability and insulin homeostasis." BMC Immunol 12(18): 18.

Garcia, C. A., K. R. Prabakar, J. Diez, Z. A. Cao, G. Allende, M. Zeller, R. Dogra, A. Mendez, E. Rosenkranz, U. Dahl, C. Ricordi, D. Hanahan and A. Pugliese (2005). "Dendritic cells in human thymus and periphery display a proinsulin epitope in a transcription-dependent, capture-independent fashion." J Immunol 175(4): 2111-2122.

Gazdar, A. F., W. L. Chick, H. K. Oie, H. L. Sims, D. L. King, G. C. Weir and V. Lauris (1980). "Continuous, clonal, insulin- and somatostatin-secreting cell lines established from a transplantable rat islet cell tumor." Proc Natl Acad Sci U S A 77(6): 3519-3523.

Gee, K. R., Z. L. Zhou, D. Ton-That, S. L. Sensi and J. H. Weiss (2002). "Measuring zinc in living cells. A new generation of sensitive and selective fluorescent probes." Cell Calcium 31(5): 245-251.

Gittes, G. K., P. E. Galante, D. Hanahan, W. J. Rutter and H. T. Debase (1996). "Lineage-specific morphogenesis in the developing pancreas: role of mesenchymal factors." Development 122(2): 439-447.

Goicoa, S., S. Alvarez, C. Ricordi, L. Inverardi and J. Dominguez-Bendala (2006). "Sodium butyrate activates genes of early pancreatic development in embryonic stem cells." Cloning and Stem Cells 8(3): 140-149.

Gottfried, E., L. A. Kunz-Schughart, A. Weber, M. Rehli, A. Peuker, A. Muller, M. Kastenberger, G. Brockhoff, R. Andreesen and M. Kreutz (2008). "Expression of CD68 in non-myeloid cell types." Scand J Immunol 67(5): 453-463.

Gu, G., J. R. Brown and D. A. Melton (2003). "Direct lineage tracing reveals the ontogeny of pancreatic cell fates during mouse embryogenesis." Mech Dev 120(1): 35-43.

Haller, M. J., C. H. Wasserfall, M. A. Hulme, M. Cintron, T. M. Brusko, K. M. McGrail, T. M. Sumrall, J. R. Wingard, D. W. Theriaque, J. J. Shuster, M. A. Atkinson and D. A. Schatz (2011). "Autologous umbilical cord blood transfusion in young children with type 1 diabetes fails to preserve C-peptide." Diabetes Care 34(12): 2567-2569.

Hansson, M., A. Tonning, U. Frandsen, A. Petri, J. Rajagopal, M. C. Englund, R. S. Heller, J. Hakansson, J. Fleckner, H. N. Skold, D. Melton, H. Semb and P. Serup (2004). "Artifactual insulin release from differentiated embryonic stem cells." Diabetes 53(10): 2603-2609.

Hassan, N. F., J. Chehimi, W. Z. Ho, D. E. Campbell and S. D. Douglas (1994). "Effect of hematopoietic growth factors on human blood monocytes/macrophages in in vitro culture." Clin Diagn Lab Immunol 1(6): 620-625.

Hesselson, D., R. M. Anderson and D. Y. Stainier (2011). "Suppression of Ptf1a activity induces acinar-to-endocrine conversion." Curr Biol 21(8): 712-717.

Huang, C. J., A. E. Butler, A. Moran, P. N. Rao, J. E. Wagner, B. R. Blazar, R. A. Rizza, J. C. Manivel and P. C. Butler (2011). "A low frequency of pancreatic islet insulin-expressing cells derived from cord blood stem cell allografts in humans." Diabetologia 54(5): 1066-1074.

Hume, D. A. (2006). "The mononuclear phagocyte system." Curr Opin Immunol 18(1): 49-53.

Ioannidis, J. P., B. Nosek and E. Iorns (2012). "Reproducibility concerns." Nat Med 18(12): 1736-1737.

Issa, F., J. Hester, R. Goto, S. N. Nadig, T. E. Goodacre and K. Wood (2010). "Ex vivo-expanded human regulatory T cells prevent the rejection of skin allografts in a humanized mouse model." Transplantation 90(12): 1321-1327.

Jacquemin, P., S. M. Durviaux, J. Jensen, C. Godfraind, G. Gradwohl, F. Guillemot, O. D. Madsen, P. Carmeliet, M. Dewerchin, D. Collen, G. G. Rousseau and F. P. Lemaigre (2000). "Transcription factor hepatocyte nuclear factor 6 regulates pancreatic endocrine cell differentiation and controls expression of the proendocrine gene ngn3." Mol Cell Biol 20(12): 4445-4454.

Jaiswal, S. and I. L. Weissman (2009). "Hematopoietic stem and progenitor cells and the inflammatory response." Ann N Y Acad Sci.

Jiang, W., Y. Shi, D. Zhao, S. Chen, J. Yong, J. Zhang, T. Qing, X. Sun, P. Zhang, M. Ding, D. Li and H. Deng (2007). "In vitro derivation of functional insulin-producing cells from human embryonic stem cells." Cell Res 17(4): 333-344.

Jonsson, J., L. Carlsson, T. Edlund and H. Edlund (1994). "Insulin-promoter-factor 1 is required for pancreas development in mice." Nature 371(6498): 606-609.

June, C. H., J. A. Ledbetter, P. S. Linsley and C. B. Thompson (1990). "Role of the CD28 receptor in T-cell activation." Immunol Today 11(6): 211-216.

Kadam, S. S., M. Sudhakar, P. D. Nair and R. R. Bhonde (2010). "Reversal of experimental diabetes in mice by transplantation of neo-islets generated from human amnion-derived mesenchymal stromal cells using immuno-isolatory macrocapsules." Cytotherapy 12(8): 982-991.

Kaneto, H., Y. Nakatani, T. Miyatsuka, T. A. Matsuoka, M. Matsuhisa, M. Hori and Y. Yamasaki (2005). "PDX-1/VP16 fusion protein, together with NeuroD or Ngn3, markedly induces insulin gene transcription and ameliorates glucose tolerance." Diabetes 54(4): 1009-1022.

Kang, H. M., S. Park and H. Kim (2011). "Insulin-like growth factor 2 enhances insulinogenic differentiation of human eyelid adipose stem cells via the insulin receptor." Cell Prolif 44(3): 254-263.

Katoh, M. (2002). "Molecular cloning and characterization of human SOX17." Int J Mol Med 9(2): 153-157.

Kawahira, H., N. H. Ma, E. S. Tzanakakis, A. P. McMahon, P. T. Chuang and M. Hebrok (2003). "Combined activities of hedgehog signaling inhibitors regulate pancreas development." Development 130(20): 4871-4879.

Kayali, A. G., K. Van Gunst, I. L. Campbell, A. Stotland, M. Kritzik, G. Liu, M. Flodstrom-Tullberg, Y. Q. Zhang and N. Sarvetnick (2003). "The stromal cell-derived factor-1alpha/CXCR4 ligand-receptor axis is critical for progenitor survival and migration in the pancreas." J Cell Biol 163(4): 859-869.

Keyoung, H. M., N. S. Roy, A. Benraiss, A. Louissaint, Jr., A. Suzuki, M. Hashimoto, W. K. Rashbaum, H. Okano and S. A. Goldman (2001). "High-yield selection and extraction of two promoter-defined phenotypes of neural stem cells from the fetal human brain." Nat Biotechnol 19(9): 843-850.

Kim, D., C. H. Kim, J. I. Moon, Y. G. Chung, M. Y. Chang, B. S. Han, S. Ko, E. Yang, K. Y. Cha, R. Lanza and K. S. Kim (2009). "Generation of human induced pluripotent stem cells by direct delivery of reprogramming proteins." Cell Stem Cell 4(6): 472-476.

Kim, S. K. and D. A. Melton (1998). "Pancreas development is promoted by cyclopamine, a hedgehog signaling inhibitor." Proc Natl Acad Sci U S A 95(22): 13036-13041.

Kim, S. Y., S. Lee, S. W. Hong, B. H. Min, K. U. Lee, M. Bendayan and I. S. Park (2010). "Nestin action during insulin-secreting cell differentiation." J Histochem Cytochem 58(6): 567-576.

Kishi, A., T. Nakamura, Y. Nishio, H. Maegawa and A. Kashiwagi (2003). "Sumoylation of Pdx1 is associated with its nuclear localization and insulin gene activation." Am J Physiol Endocrinol Metab 284(4): E830-840.

Klein, T., Z. Ling, H. Heimberg, O. D. Madsen, R. S. Heller and P. Serup (2003). "Nestin is expressed in vascular endothelial cells in the adult human pancreas." J Histochem Cytochem 51(6): 697-706.

Kodama, H., T. Inoue, R. Watanabe, D. Yasutomi, Y. Kawakami, S. Ogawa, K. Mikoshiba, Y. Ikeda and M. Kuwana (2006). "Neurogenic potential of progenitors derived from human circulating CD14+ monocytes." Immunol Cell Biol 84(2): 209-217.

Kogawa, K., S. Nagafuchi, H. Katsuta, J. Kudoh, S. Tamiya, Y. Sakai, N. Shimizu and M. Harada (2002). "Expression of AIRE gene in peripheral monocyte/dendritic cell lineage." Immunol Lett 80(3): 195-198.

Koivu, J., R. Myllyla, T. Helaakoski, T. Pihlajaniemi, K. Tasanen and K. I. Kivirikko (1987). "A single polypeptide acts both as the beta subunit of prolyl 4-hydroxylase and as a protein disulfide-isomerase." J Biol Chem 262(14): 6447-6449.

Kojima, H., M. Fujimiya, T. Terashima, H. Kimura and L. Chan (2006). "Extrapancreatic proinsulin/insulin-expressing cells in diabetes mellitus: is history repeating itself?" Endocr J 53(6): 715-722.

Kont, V., M. Laan, K. Kisand, A. Merits, H. S. Scott and P. Peterson (2008). "Modulation of Aire regulates the expression of tissue-restricted antigens." Mol Immunol 45(1): 25-33.

Krissansen, G. W., C. M. Lucas, F. C. Stomski, M. J. Elliott, M. C. Berndt, A. W. Boyd, M. A. Horton, D. A. Cheresh, M. A. Vadas and G. F. Burns (1990). "Blood leukocytes bind platelet glycoprotein (IIb-IIIa)' but do not express the vitronectin receptor." Int Immunol 2(3): 267-277.

Kronenberg, M. and A. Rudensky (2005). "Regulation of immunity by self-reactive T cells." Nature 435(7042): 598-604.

Kuwana, M., Y. Okazaki, H. Kodama, K. Izumi, H. Yasuoka, Y. Ogawa, Y. Kawakami and Y. Ikeda (2003). "Human circulating CD14+ monocytes as a source of progenitors that exhibit mesenchymal cell differentiation." J Leukoc Biol 74(5): 833-845.

La Rocca, G., R. Anzalone and F. Farina (2009). "The expression of CD68 in human umbilical cord mesenchymal stem cells: new evidences of presence in non-myeloid cell types." Scand J Immunol 70(2): 161-162.

Landis, S. C., S. G. Amara, K. Asadullah, C. P. Austin, R. Blumenstein, E. W. Bradley, R. G. Crystal, R. B. Darnell, R. J. Ferrante, H. Fillit, R. Finkelstein, M. Fisher, H. E. Gendelman, R. M. Golub, J. L. Goudreau, R. A. Gross, A. K. Gubitz,

S. E. Hesterlee, D. W. Howells, J. Huguenard, K. Kelner, W. Koroshetz, D. Krainc, S. E. Lazic, M. S. Levine, M. R. Macleod, J. M. McCall, R. T. Moxley, 3rd, K. Narasimhan, L. J. Noble, S. Perrin, J. D. Porter, O. Steward, E. Unger, U. Utz and S. D. Silberberg (2012). "A call for transparent reporting to optimize the predictive value of preclinical research." Nature 490(7419): 187-191.

Lange, A. W., A. R. Keiser, J. M. Wells, A. M. Zorn and J. A. Whitsett (2009). "Sox17 promotes cell cycle progression and inhibits TGF-beta/Smad3 signaling to initiate progenitor cell behavior in the respiratory epithelium." PLoS One 4(5): e5711.

Lee, J., D. J. Han and S. C. Kim (2008). "In vitro differentiation of human adipose tissue-derived stem cells into cells with pancreatic phenotype by regenerating pancreas extract." Biochem Biophys Res Commun 375(4): 547-551.

Leonard, J., B. Peers, T. Johnson, K. Ferreri, S. Lee and M. R. Montminy (1993). "Characterization of somatostatin transactivating factor-1, a novel homeobox factor that stimulates somatostatin expression in pancreatic islet cells." Mol Endocrinol 7(10): 1275-1283.

Levesque, J. P. and I. G. Winkler (2008). "Mobilization of hematopoietic stem cells: state of the art." Curr Opin Organ Transplant 13(1): 53-58.

Li, M. O. and R. A. Flavell (2008). "TGF-beta: a master of all T cell trades." Cell 134(3): 392-404.

Liew, C. G., N. N. Shah, S. J. Briston, R. M. Shepherd, C. P. Khoo, M. J. Dunne, H. D. Moore, K. E. Cosgrove and P. W. Andrews (2008). "PAX4 enhances beta-cell differentiation of human embryonic stem cells." PLoS One 3(3): e1783.

Lin, G., G. Wang, G. Liu, L. J. Yang, L. J. Chang, T. F. Lue and C. S. Lin (2009). "Treatment of Type 1 Diabetes with Adipose Tissue-Derived Stem Cells Expressing Pancreatic Duodenal Homeobox 1." Stem Cells Dev 18(10): 1399-1406.

Locke, M., V. Feisst and P. R. Dunbar (2011). "Concise review: human adipose-derived stem cells: separating promise from clinical need." Stem Cells 29(3): 404-411.

Lukowiak, B., B. Vandewalle, R. Riachy, J. Kerr-Conte, V. Gmyr, S. Belaich, J. Lefebvre and F. Pattou (2001). "Identification and purification of functional human beta-cells by a new specific zinc-fluorescent probe." J Histochem Cytochem 49(4): 519-528.

Lumelsky, N., O. Blondel, P. Laeng, I. Velasco, R. Ravin and R. McKay (2001). "Differentiation of embryonic stem cells to insulin-secreting structures similar to pancreatic islets." Science (New York, N.Y.) 292(5520): 1389-1394.

Maehr, R., S. Chen, M. Snitow, T. Ludwig, L. Yagasaki, R. Goland, R. L. Leibel and D. A. Melton (2009). "Generation of pluripotent stem cells from patients with type 1 diabetes." Proc Natl Acad Sci U S A 106(37): 15768-15773.

Mann, D. L. and L. Abelson (1980). "Monocyte function in mixed lymphocyte reactions." Cell Immunol 56(2): 357-364.

Markel, T. A., P. R. Crisostomo, T. Lahm, N. M. Novotny, F. J. Rescorla, J. Tector and D. R. Meldrum (2008). "Stem cells as a potential future treatment of pediatric intestinal disorders." J Pediatr Surg 43(11): 1953-1963.

Masharani, U. B. and J. Becker (2010). "Teplizumab therapy for type 1 diabetes." Expert Opin Biol Ther 10(3): 459-465.

Mashima, H., H. Shibata, T. Mine and I. Kojima (1996). "Formation of insulin-producing cells from pancreatic acinar AR42J cells by hepatocyte growth factor." Endocrinology 137(9): 3969-3976.

McCarthy, D. A., M. G. Macey, P. A. Bedford, S. C. Knight, D. C. Dumonde and K. A. Brown (1997). "Adhesion molecules are upregulated on dendritic cells isolated from human blood." Immunology 92(2): 244-251.

McCluskey, J. T., M. Hamid, H. Guo-Parke, N. H. McClenaghan, R. Gomis and P. R. Flatt (2011). "Development and functional characterization of insulin-releasing human pancreatic beta cell lines produced by electrofusion." J Biol Chem 286(25): 21982-21992.

McLean, A. B., K. A. D'Amour, K. L. Jones, M. Krishnamoorthy, M. J. Kulik, D. M. Reynolds, A. M. Sheppard, H. Liu, Y. Xu, E. E. Baetge and S. Dalton (2007). "Activin a efficiently specifies definitive endoderm from human embryonic stem cells only when phosphatidylinositol 3-kinase signaling is suppressed." Stem Cells 25(1): 29-38.

Medina, A., E. Brown, N. Carr and A. Ghahary (2009). "Circulating monocytes have the capacity to be transdifferentiated into keratinocyte-like cells." Wound Repair Regen 17(2): 268-277.

Merglen, A., S. Theander, B. Rubi, G. Chaffard, C. B. Wollheim and P. Maechler (2004). "Glucose sensitivity and metabolism-secretion coupling studied during two-year continuous culture in INS-1E insulinoma cells." Endocrinology 145(2): 667-678.

Metzger, T. C. and M. S. Anderson (2011). "Control of central and peripheral tolerance by Aire." Immunol Rev 241(1): 89-103.

Micallef, S. J., M. E. Janes, K. Knezevic, R. P. Davis, A. G. Elefanty and E. G. Stanley (2005). "Retinoic acid induces Pdx1-positive endoderm in differentiating mouse embryonic stem cells." Diabetes 54(2): 301-305.

Miki, T., T. Lehmann, H. Cai, D. B. Stolz and S. C. Strom (2005). "Stem cell characteristics of amniotic epithelial cells." Stem Cells 23(10): 1549-1559.

Miki, T., F. Marongiu, E. Ellis and C. S. S (2007). "Isolation of amniotic epithelial stem cells." Curr Protoc Stem Cell Biol Chapter 1: Unit 1E 3.

Milanesi, A., J. W. Lee, Q. Xu, L. Perin and J. S. Yu (2011). "Differentiation of nestin-positive cells derived from bone marrow into pancreatic endocrine and ductal cells in vitro." J Endocrinol 209(2): 193-201.

Mitchell, J. B., K. McIntosh, S. Zvonic, S. Garrett, Z. E. Floyd, A. Kloster, Y. Di Halvorsen, R. W. Storms, B. Goh, G. Kilroy, X. Wu and J. M. Gimble (2006). "Immunophenotype of human adipose-derived cells: temporal changes in stromal-associated and stem cell-associated markers." Stem Cells 24(2): 376-385.

Nakajima-Takagi, Y., M. Osawa, M. Oshima, H. Takagi, S. Miyagi, M. Endoh, T. A. Endo, N. Takayama, K. Eto, T. Toyoda, H. Koseki, H. Nakauchi and A. Iwama (2013). "Role of SOX17 in hematopoietic development from human embryonic stem cells." Blood 121(3): 447-458.

Nestle, F. O., C. Thompson, Y. Shimizu, L. A. Turka and B. J. Nickoloff (1994). "Costimulation of superantigen-activated T lymphocytes by autologous dendritic cells is dependent on B7." Cell Immunol 156(1): 220-229.

Nichols, J. and A. Cooke (2009). "Overcoming self-destruction in the pancreas." Curr Opin Biotechnol 20(5): 511-515.

Nimgaonkar, M. T., R. A. Roscoe, J. Persichetti, W. B. Rybka, A. Winkelstein and E. D. Ball (1995). "A unique population of CD34+ cells in cord blood." Stem Cells 13(2): 158-166.

Noguchi, H., H. Kaneto, G. C. Weir and S. Bonner-Weir (2003). "PDX-1 protein containing its own antennapedia-like protein transduction domain can transduce pancreatic duct and islet cells." Diabetes 52(7): 1732-1737.

O'Connor, M. D., M. D. Kardel, I. Iosfina, D. Youssef, M. Lu, M. M. Li, S. Vercauteren, A. Nagy and C. J. Eaves (2008). "Alkaline phosphatase-positive colony formation is a sensitive, specific, and quantitative indicator of undifferentiated human embryonic stem cells." Stem Cells 26(5): 1109-1116.

Offield, M. F., T. L. Jetton, P. A. Labosky, M. Ray, R. W. Stein, M. A. Magnuson, B. L. Hogan and C. V. Wright (1996). "PDX-1 is required for pancreatic outgrowth and differentiation of the rostral duodenum." Development 122(3): 983-995.

Ohlsson, H., K. Karlsson and T. Edlund (1993). "IPF1, a homeodomain-containing transactivator of the insulin gene." EMBO J 12(11): 4251-4259.

Ohmura, Y., M. Tanemura, N. Kawaguchi, T. Machida, T. Tanida, T. Deguchi, H. Wada, S. Kobayashi, S. Marubashi, H. Eguchi, Y. Takeda, N. Matsuura, T. Ito, H. Nagano, Y. Doki and M. Mori (2010). "Combined transplantation of pancreatic islets and adipose tissue-derived stem cells enhances the survival and insulin function of islet grafts in diabetic mice." Transplantation 90(12): 1366-1373.

Onkamo, P., S. Vaananen, M. Karvonen and J. Tuomilehto (1999). "Worldwide increase in incidence of Type I diabetes--the analysis of the data on published incidence trends." Diabetologia 42(12): 1395-1403.

Osterbye, T., D. P. Funda, P. Fundova, J. E. Mansson, H. Tlaskalova-Hogenova and K. Buschard (2010). "A subset of human pancreatic beta cells express functional CD14 receptors: a signaling pathway for beta cell-related glycolipids, sulfatide and beta-galactosylceramide." Diabetes Metab Res Rev 26(8): 656-667.

Paget, J. A., I. J. Restall, M. Daneshmand, J. A. Mersereau, M. A. Simard, D. A. Parolin, S. J. Lavictoire, M. S. Amin, S. Islam and I. A. Lorimer (2012). "Repression of cancer cell senescence by PKCiota." Oncogene 31(31): 3584-3596.

Pease, S., P. Braghetta, D. Gearing, D. Grail and R. L. Williams (1990). "Isolation of embryonic stem (ES) cells in media supplemented with recombinant leukemia inhibitory factor (LIF)." Dev Biol 141(2): 344-352.

Peng, Y., Y. Laouar, M. O. Li, E. A. Green and R. A. Flavell (2004). "TGF-beta regulates in vivo expansion of Foxp3-expressing CD4+CD25+ regulatory T cells responsible for protection against diabetes." Proc Natl Acad Sci U S A 101(13): 4572-4577.

Perez-Villamil, B., P. T. Schwartz and M. Vallejo (1999). "The pancreatic homeodomain transcription factor IDX1/IPF1 is expressed in neural cells during brain development." Endocrinology 140(8): 3857-3860.

Piccinni, S. A., A. L. Bolcato-Bellemin, A. Klein, V. W. Yang, M. Kedinger, P. Simon-Assmann and O. Lefebvre (2004). "Kruppel-like factors regulate the Lama1 gene encoding the laminin alpha1 chain." J Biol Chem 279(10): 9103-9114.

Pihlajaniemi, T., T. Helaakoski, K. Tasanen, R. Myllyla, M. L. Huhtala, J. Koivu and K. I. Kivirikko (1987). "Molecular cloning of the beta-subunit of human prolyl 4-hydroxylase. This subunit and protein disulphide isomerase are products of the same gene." EMBO J 6(3): 643-649.

Pilling, D., T. Fan, D. Huang, B. Kaul and R. H. Gomer (2009). "Identification of markers that distinguish monocyte-derived fibrocytes from monocytes, macrophages, and fibroblasts." PLoS One 4(10): e7475.

Praz, G. A., P. A. Halban, C. B. Wollheim, B. Blondel, A. J. Strauss and A. E. Renold (1983). "Regulation of immunoreactive-insulin release from a rat cell line (RINm5F)." Biochem J 210(2): 345-352.

Prokhorova, T. A., L. M. Harkness, U. Frandsen, N. Ditzel, H. D. Schroder, J. S. Burns and M. Kassem (2009). "Teratoma formation by human embryonic stem cells is site dependent and enhanced by the presence of Matrigel." Stem Cells Dev 18(1): 47-54.

Pugliese, A., M. Zeller, A. Fernandez, Jr., L. J. Zalcberg, R. J. Bartlett, C. Ricordi, M. Pietropaolo, G. S. Eisenbarth, S. T. Bennett and D. D. Patel (1997). "The insulin gene is transcribed in the human thymus and transcription levels correlated with allelic variation at the INS VNTR-IDDM2 susceptibility locus for type 1 diabetes." Nat Genet 15(3): 293-297.

Pulford, K. A., A. Sipos, J. L. Cordell, W. P. Stross and D. Y. Mason (1990). "Distribution of the CD68 macrophage/myeloid associated antigen." Int Immunol 2(10): 973-980.

Qian, W. J., J. L. Peters, G. M. Dahlgren, K. R. Gee and R. T. Kennedy (2004). "Simultaneous monitoring of Zn2+ secretion and intracellular Ca2+ from islets and islet cells by fluorescence microscopy." Biotechniques 37(6): 922-924, 926, 928-930 passim.

Reilkoff, R. A., R. Bucala and E. L. Herzog (2011). "Fibrocytes: emerging effector cells in chronic inflammation." Nat Rev Immunol 11(6): 427-435.

Reilly, G. C. and A. J. Engler (2009). "Intrinsic extracellular matrix properties regulate stem cell differentiation." J Biomech 43(1): 55-62.

Ren, J., P. Jin, E. Wang, E. Liu, D. M. Harlan, X. Li and D. F. Stroncek (2007). "Pancreatic islet cell therapy for type I diabetes: understanding the effects of glucose stimulation on islets in order to produce better islets for transplantation." J Transl Med 5: 1.

Riquelme, P., J. Wundt, J. A. Hutchinson, M. Brulport, Y. Jun, A. Sotnikova, U. Girreser, F. Braun, F. Govert, B. Soria, A. Nussler, B. Clement, J. G. Hengstler and F. Fandrich (2009). "A refined characterisation of the NeoHepatocyte phenotype necessitates a reappraisal of the transdifferentiation hypothesis." Differentiation 77(3): 263-276.

Rovira, M., S. G. Scott, A. S. Liss, J. Jensen, S. P. Thayer and S. D. Leach (2010). "Isolation and characterization of centroacinar/terminal ductal progenitor cells in adult mouse pancreas." Proc Natl Acad Sci U S A 107(1): 75-80.

Ruhnke, M., H. Ungefroren, A. Nussler, F. Martin, M. Brulport, W. Schormann, J. G. Hengstler, W. Klapper, K. Ulrichs, J. A. Hutchinson, B. Soria, R. M. Parwaresch, P. Heeckt, B. Kremer and F. Fandrich (2005). "Differentiation of in vitro-modified human peripheral blood monocytes into hepatocyte-like and pancreatic islet-like cells." Gastroenterology 128(7): 1774-1786.

Sadler, J. E. (1998). "Biochemistry and genetics of von Willebrand factor." Annu Rev Biochem 67: 395-424.

Salehi, A., E. Flodgren, N. E. Nilsson, J. Jimenez-Felstrom, J. Miyazaki, C. Owman and B. Olde (2005). "Free fatty acid receptor 1 (FFA1R/GPR40) and its involvement in fatty-acid-stimulated insulin secretion." Cell Tissue Res 322: 207-215.

Sato, T., T. S. Diehl, S. Narayanan, S. Funamoto, Y. Ihara, B. De Strooper, H. Steiner, C. Haass and M. S. Wolfe (2007). "Active gamma-secretase complexes contain only one of each component." J Biol Chem 282(47): 33985-33993.

Scherer, F., M. Anton, U. Schillinger, J. Henke, C. Bergemann, A. Kruger, B. Gansbacher and C. Plank (2002). "Magnetofection: enhancing and targeting gene delivery by magnetic force in vitro and in vivo." Gene Ther 9(2): 102-109.

Schmeisser, A., C. D. Garlichs, H. Zhang, S. Eskafi, C. Graffy, J. Ludwig, R. H. Strasser and W. G. Daniel (2001). "Monocytes coexpress endothelial and macrophagocytic lineage markers and form cord-like structures in Matrigel under angiogenic conditions." Cardiovasc Res 49(3): 671-680.

Schmitt, A., S. Ehnert, L. Schyschka, P. Buschner, A. Kuhnl, S. Dobele, S. Siebenlist, M. Lucke, U. Stockle and A. K. Nussler (2012). "Monocytes do not transdifferentiate into proper osteoblasts." ScientificWorldJournal 2012: 384936.

Schwitzgebel, V. M., D. W. Scheel, J. R. Conners, J. Kalamaras, J. E. Lee, D. J. Anderson, L. Sussel, J. D. Johnson and M. S. German (2000). "Expression of neurogenin3 reveals an islet cell precursor population in the pancreas." Development 127(16): 3533-3542.

Segev, H., B. Fishman, A. Ziskind, M. Shulman and J. Itskovitz-Eldor (2004). "Differentiation of human embryonic stem cells into insulin-producing clusters." Stem Cells 22(3): 265-274.

Shapiro, A. M., C. Ricordi, B. J. Hering, H. Auchincloss, R. Lindblad, R. P. Robertson, A. Secchi, M. D. Brendel, T. Berney, D. C. Brennan, E. Cagliero, R. Alejandro, E. A. Ryan, B. DiMercurio, P. Morel, K. S. Polonsky, J. A. Reems, R. G. Bretzel, F. Bertuzzi, T. Froud, R. Kandaswamy, D. E. Sutherland, G. Eisenbarth, M. Segal, J. Preiksaitis, G. S. Korbutt, F. B. Barton, L. Viviano, V. Seyfert-Margolis, J. Bluestone and J. R. Lakey (2006). "International trial of the Edmonton protocol for islet transplantation." N Engl J Med 355(13): 1318-1330.

Sharifi, B. G., Z. Zeng, L. Wang, L. Song, H. Chen, M. Qin, M. R. Sierra-Honigmann, S. Wachsmann-Hogiu and P. K. Shah (2006). "Pleiotrophin induces transdifferentiation of monocytes into functional endothelial cells." Arterioscler Thromb Vasc Biol 26(6): 1273-1280.

Sharma, J. P., H. Eran, F. Byhower, C. R. Sharma, M. R. Sharma, L. J. Byhower, K. A. Okbaok, N. J. Heidtbrink-Ramirez and N. Taw (2003). Human amniotic epithelial cells as an alternative source of human embryonic stem cells, Am Soc Cell Biol Ann Mtg.

Slack, J. M. (1995). "Developmental biology of the pancreas." Development 121(6): 1569-1580.

Sohn, J., J. Natale, L. J. Chew, S. Belachew, Y. Cheng, A. Aguirre, J. Lytle, B. Nait-Oumesmar, C. Kerninon, M. Kanai-Azuma, Y. Kanai and V. Gallo (2006). "Identification of Sox17 as a transcription factor that regulates oligodendrocyte development." J Neurosci 26(38): 9722-9735.

Sonksen, P. and J. Sonksen (2000). "Insulin: understanding its action in health and disease." Br J Anaesth 85(1): 69-79.

Soria, B. (2001). "In-vitro differentiation of pancreatic β-cells." Differentiation 68(4-5): 205-219.

Starr, T. K., S. C. Jameson and K. A. Hogquist (2003). "Positive and negative selection of T cells." Annu Rev Immunol 21: 139-176.

Steck, A. K. and M. J. Rewers (2011). "Genetics of type 1 diabetes." Clin Chem 57(2): 176-185.

Storms, R. W., A. P. Trujillo, J. B. Springer, L. Shah, O. M. Colvin, S. M. Ludeman and C. Smith (1999). "Isolation of primitive human hematopoietic progenitors on the basis of aldehyde dehydrogenase activity." Proc Natl Acad Sci U S A 96(16): 9118-9123.

Sundin, M., P. D'Arcy, C. C. Johansson, A. J. Barrett, H. Lonnies, B. Sundberg, S. Nava, R. Kiessling, D. Mougiakakos and K. Le Blanc (2011). "Multipotent mesenchymal stromal cells express FoxP3: a marker for the immunosuppressive capacity?" J Immunother 34(4): 336-342.

Takahashi, K. and S. Yamanaka (2006). "Induction of pluripotent stem cells from mouse embryonic and adult fibroblast cultures by defined factors." Cell 126(4): 663-676.

Talavera-Adame, D., G. Wu, Y. He, T. T. Ng, A. Gupta, S. Kurtovic, J. Y. Hwang, D. L. Farkas and D. C. Dafoe (2011). "Endothelial cells in co-culture enhance embryonic stem cell differentiation to pancreatic progenitors and insulin-producing cells through BMP signaling." Stem Cell Rev 7(3): 532-543.

Talchai, C., S. Xuan, T. Kitamura, R. A. DePinho and D. Accili (2012). "Generation of functional insulin-producing cells in the gut by Foxo1 ablation." Nat Genet 44(4): 406-412, S401.

Tamagawa, T., I. Ishiwata, K. Sato and Y. Nakamura (2009). "Induced in vitro differentiation of pancreatic-like cells from human amnion-derived fibroblast-like cells." Hum Cell 22(3): 55-63.

Tang, T. H., C. L. Li, X. Li, F. Q. Jiang, Y. K. Zhang, H. Q. Ren, S. S. Su and G. S. Jiang (2004). "Immune tolerance in pancreatic islet xenotransplantation." World J Gastroenterol 10(10): 1457-1461.

Thatava, T., T. J. Nelson, R. Edukulla, T. Sakuma, S. Ohmine, J. M. Tonne, S. Yamada, Y. Kudva, A. Terzic and Y. Ikeda (2010). "Indolactam V/GLP-1-mediated differentiation of human iPS cells into glucose-responsive insulin-secreting progeny." Gene Ther 18(3): 283-293.

Thiele, D. L., M. Kurosaka and P. E. Lipsky (1983). "Phenotype of the accessory cell necessary for mitogen-stimulated T and B cell responses in human peripheral blood: delineation by its sensitivity to the lysosomotropic agent, L-leucine methyl ester." J Immunol 131(5): 2282-2290.

Thiele, D. L. and P. E. Lipsky (1986). "The immunosuppressive activity of L-leucyl-L-leucine methyl ester: selective ablation of cytotoxic lymphocytes and monocytes." J Immunol 136(3): 1038-1048.

Thiele, D. L. and P. E. Lipsky (1990). "Mechanism of L-leucyl-L-leucine methyl ester-mediated killing of cytotoxic lymphocytes: dependence on a lysosomal thiol protease, dipeptidyl peptidase I, that is enriched in these cells." Proc Natl Acad Sci U S A 87(1): 83-87.

Timper, K., D. Seboek, M. Eberhardt, P. Linscheid, M. Christ-Crain, U. Keller, B. Muller and H. Zulewski (2006). "Human adipose tissue-derived mesenchymal stem cells differentiate into insulin, somatostatin, and glucagon expressing cells." Biochem Biophys Res Commun 341(4): 1135-1140.

Trivedi, H. L., A. V. Vanikar, U. Thakker, A. Firoze, S. D. Dave, C. N. Patel, J. V. Patel, A. B. Bhargava and V. Shankar (2008). "Human adipose tissue-derived mesenchymal stem cells combined with hematopoietic stem cell transplantation synthesize insulin." Transplant Proc 40(4): 1135-1139.

Ungefroren, H. and F. Fandrich (2010). "The programmable cell of monocytic origin (PCMO): a potential adult stem/progenitor cell source for the generation of islet cells." Adv Exp Med Biol 654: 667-682.

Ungefroren, H., S. Groth, A. Hyder, N. Thomsen, H. Hinz, N. Reiling, E. Grage-Griebenow, J. Held-Feindt, M. Schulze, A. K. Nussler and F. Fandrich (2010). "The generation of programmable cells of monocytic origin involves partial repression of monocyte/macrophage markers and reactivation of pluripotency genes." Stem Cells Dev 19(11): 1769-1780.

Valamehr, B., S. J. Jonas, J. Polleux, R. Qiao, S. Guo, E. H. Gschweng, B. Stiles, K. Kam, T. J. Luo, O. N. Witte, X. Liu, B. Dunn and H. Wu (2008). "Hydrophobic surfaces for enhanced differentiation of embryonic stem cell-derived embryoid bodies." Proc Natl Acad Sci U S A 105(38): 14459-14464.

van Schooten, C. J., S. Shahbazi, E. Groot, B. D. Oortwijn, H. M. van den Berg, C. V. Denis and P. J. Lenting (2008). "Macrophages contribute to the cellular uptake of von Willebrand factor and factor VIII in vivo." Blood 112(5): 1704-1712.

Vanikar, A. V., S. D. Dave, U. G. Thakkar and H. L. Trivedi (2010). "Cotransplantation of adipose tissue-derived insulin-secreting mesenchymal stem cells and hematopoietic stem cells: a novel therapy for insulin-dependent diabetes mellitus." Stem Cells Int 2010: 582382.

Varol, C., S. Yona and S. Jung (2009). "Origins and tissue-context-dependent fates of blood monocytes." Immunol Cell Biol 87(1): 30-38.

Vats, D., H. Wang, D. Esterhazy, K. Dikaiou, C. Danzer, M. Honer, F. Stuker, H. Matile, C. Migliorini, E. Fischer, J. Ripoll, R. Keist, W. Krek, R. Schibli, M. Stoffel and M. Rudin (2012). "Multimodal imaging of pancreatic beta cells in vivo by targeting transmembrane protein 27 (TMEM27)." Diabetologia 55(9): 2407-2416.

Vermes, I., C. Haanen, H. Steffens-Nakken and C. Reutelingsperger (1995). "A novel assay for apoptosis. Flow cytometric detection of phosphatidylserine expression on early apoptotic cells using fluorescein labelled Annexin V." J Immunol Methods 184(1): 39-51.

Wang, A. Y., A. Ehrhardt, H. Xu and M. A. Kay (2007). "Adenovirus transduction is required for the correction of diabetes using Pdx-1 or Neurogenin-3 in the liver." Mol Ther 15(2): 255-263.

Wang, S. Y., K. L. Mak, L. Y. Chen, M. P. Chou and C. K. Ho (1992). "Heterogeneity of human blood monocyte: two subpopulations with different sizes, phenotypes and functions." Immunology 77(2): 298-303.

Wild, S., G. Roglic, A. Green, R. Sicree and H. King (2004). "Global prevalence of diabetes: estimates for the year 2000 and projections for 2030." Diabetes Care 27(5): 1047-1053.

Wilson, M. E., J. A. Kalamaras and M. S. German (2002). "Expression pattern of IAPP and prohormone convertase 1/3 reveals a distinctive set of endocrine cells in the embryonic pancreas." Mech Dev 115(1-2): 171-176.

Winnier, G. E., B. S. Newsom, D. R. Rill and J. C. Williams (2010a). Monocyte-Dervied Stem Cells. US. US 2010/0047908.

Winnier, G. E., B. S. Newsom, D. R. Rill and J. C. Williams (2010b). Pancreatic Islet-like Cells. US. US 2010/0021435.

Winnier, G. E., J. Sciarrotta, M. Wallace-Shannon, B. S. Newsom and J. C. Williams (2007). Diabetic patients' monocyte derived insulin-producing islet-like clusters offer promise of autologous beta-cell replacement thereapy for Type 1 and 2 diabetes. International Society for Cellular Therapy.

Xue, Z. H., C. Q. Zhao, G. L. Chua, S. W. Tan, X. Y. Tang, S. C. Wong and S. M. Tan (2012). "Integrin alphaMbeta2 clustering triggers phosphorylation and activation of protein kinase C delta that regulates transcription factor Foxp1 expression in monocytes." J Immunol 184(7): 3697-3709.

Yamada, S., Y. Yamamoto, M. Nagasawa, A. Hara, T. Kodera and I. Kojima (2006). "In vitro transdifferentiation of mature hepatocytes into insulin-producing cells." Endocr J 53(6): 789-795.

Yanez, R., M. L. Lamana, J. Garcia-Castro, I. Colmenero, M. Ramirez and J. A. Bueren (2006). "Adipose tissue-derived mesenchymal stem cells have in vivo immunosuppressive properties applicable for the control of the graft-versus-host disease." Stem Cells 24(11): 2582-2591.

Yang, H., S. Lee, S. Lee, K. Kim, Y. Yang, J. H. Kim, R. H. Adams, J. M. Wells, S. J. Morrison, G. Y. Koh and I. Kim (2013). "Sox17 promotes tumor angiogenesis and destabilizes tumor vessels in mice." J Clin Invest 123(1): 418-431.

Yang, J. H., S. H. Lee, Y. T. Heo, S. J. Uhm and H. T. Lee (2010). "Generation of insulin-producing cells from gnotobiotic porcine skin-derived stem cells." Biochem Biophys Res Commun 397(4): 679-684.

Yue, F., L. Cui, K. Johkura, N. Ogiwara and K. Sasaki (2006). "Glucagon-like peptide-1 differentiation of primate embryonic stem cells into insulin-producing cells." Tissue Eng 12(8): 2105-2116.

Zangrossi, S., M. Marabese, M. Broggini, R. Giordano, M. D'Erasmo, E. Montelatici, D. Intini, A. Neri, M. Pesce, P. Rebulla and L. Lazzari (2007). "Oct-4 expression in adult human differentiated cells challenges its role as a pure stem cell marker." Stem Cells 25(7): 1675-1680.

Zhang, M., L. V. Borovikova, H. Wang, C. Metz and K. J. Tracey (1999). "Spermine inhibition of monocyte activation and inflammation." Mol Med 5(9): 595-605.

Zhang, M., T. Caragine, H. Wang, P. S. Cohen, G. Botchkina, K. Soda, M. Bianchi, P. Ulrich, A. Cerami, B. Sherry and K. J. Tracey (1997). "Spermine inhibits proinflammatory cytokine synthesis in human mononuclear cells: a counter regulatory mechanism that restrains the immune response." J Exp Med 185(10): 1759-1768.

Zhang, S., H. Dai, N. Wan, Y. Moore and Z. Dai (2011). "Promoting long-term survival of insulin-producing cell grafts that differentiate from adipose tissue-derived stem cells to cure type 1 diabetes." PLoS One 6(12): e29706.

Zhang, Y., W. Zhen, P. Maechler and D. Liu (2012). "Small molecule kaempferol modulates PDX-1 protein expression and subsequently promotes pancreatic beta-cell survival and function via CREB." J Nutr Biochem 2012: 20.

Zhao, Y., D. Glesne and E. Huberman (2003). "A human peripheral blood monocyte-derived subset acts as pluripotent stem cells." Proc Natl Acad Sci U S A 100(5): 2426-2431.

Zhao, Y., Z. Huang, P. Lazzarini, Y. Wang, A. Di and M. Chen (2007a). "A unique human blood-derived cell population displays high potential for producing insulin." Biochem Biophys Res Commun 360(1): 205-211.

Zhao, Y., Z. Huang, M. Qi, P. Lazzarini and T. Mazzone (2007b). "Immune regulation of T lymphocyte by a newly characterized human umbilical cord blood stem cell." Immunol Lett 108(1): 78-87.

Zhao, Y., Z. Jiang, T. Zhao, M. Ye, C. Hu, Z. Yin, H. Li, Y. Zhang, Y. Diao, Y. Li, Y. Chen, X. Sun, M. B. Fisk, R. Skidgel, M. Holterman, B. Prabhakar and T. Mazzone (2012). "Reversal of type 1 diabetes via islet beta cell regeneration following immune modulation by cord blood-derived multipotent stem cells." BMC Med 10(1): 3.

Zhao, Y., B. Lin, R. Darflinger, Y. Zhang, M. J. Holterman and R. A. Skidgel (2009). "Human cord blood stem cell-modulated regulatory T lymphocytes reverse the autoimmune-caused type 1 diabetes in nonobese diabetic (NOD) mice." PLoS One 4(1): e4226.

Zhao, Y., B. Lin, M. Dingeldein, C. Guo, D. Hwang and M. J. Holterman (2010). "New type of human blood stem cell: a double-edged sword for the treatment of type 1 diabetes." Transl Res 155(5): 211-216.

Zhao, Y. and T. Mazzone (2008). Embryonic-like Stem Cells Derived from Adult Human Peripheral Blood and Methods of Use. WO 2008/048671.

Zhao, Y., H. Wang and T. Mazzone (2006). "Identification of stem cells from human umbilical cord blood with embryonic and hematopoietic characteristics." Exp Cell Res 312(13): 2454-2464.

Zuk, P. A., M. Zhu, P. Ashjian, D. A. De Ugarte, J. I. Huang, H. Mizuno, Z. C. Alfonso, J. K. Fraser, P. Benhaim and M. H. Hedrick (2002). "Human adipose tissue is a source of multipotent stem cells." Mol Biol Cell 13(12): 4279-4295.

Zulewski, H., E. J. Abraham, M. J. Gerlach, P. B. Daniel, W. Moritz, B. Muller, M. Vallejo, M. K. Thomas and J. F. Habener (2001). "Multipotential nestin-positive stem cells isolated from adult pancreatic islets differentiate ex vivo into pancreatic endocrine, exocrine, and hepatic phenotypes." Diabetes 50(3): 521-533.